

USARTL-TR-78-25A

LEVEL

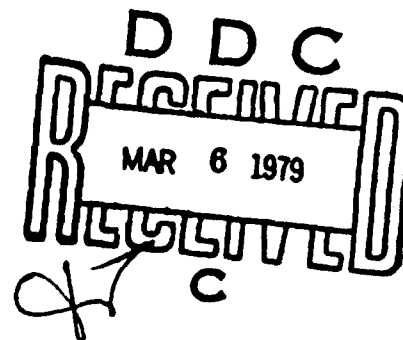


HELICOPTER TRANSPARENT ENCLOSURES
Volume I - Design Handbook

Bruce F. Kay
SIKORSKY AIRCRAFT DIVISION
United Technologies Corp.
Stratford, Conn. 06602

January 1979

Final Report



Approved for public release;
distribution unlimited.

Prepared for

APPLIED TECHNOLOGY LABORATORY

U. S. ARMY RESEARCH AND TECHNOLOGY LABORATORIES (AVRADCOM)

Fort Eustis, Va. 23604

79 63 01 069

AD A065268

DDC FILE COPY

APPLIED TECHNOLOGY LABORATORY POSITION STATEMENT

The high replacement cost of helicopter transparencies in terms of maintenance, aircraft availability, mission performance, and dollars is a serious problem. Recognizing this, the Applied Technology Laboratory funded PPG Industries and Good-year Aerospace Corporation to assess the problem and recommend remedial action. They reported that abrasion is a serious problem, and many windshields with degraded visibility are "lived with" in the field - partly because interchangeable parts are virtually nonexistent. Helicopter windshields are being replaced every 200 to 300 flight hours. This generally low reliability was largely attributed to the fact that the Army had neither specification nor any design guidelines addressing helicopter cockpit enclosures as a subsystem. Instead, each Army helicopter has its own Army/contractor negotiated model specification, giving rise to a generally low reliability. The needs were for: a specification with "teeth" in its qualification and acceptance criteria, together with a design handbook giving designers and procurement agencies alike insight into what is required for a better performing, more reliable product.

The objectives of this contract were to develop a draft specification and a comprehensive design handbook. The results are published in two reports: TR 78-26, Design, Test and Acceptance Criteria for Helicopter Transparent Enclosures; and TR 78-25A and B, Helicopter Transparent Enclosures, Volume I being the Design Handbook and Volume II being the General Specification.

In this program, emphasis was devoted to structural integrity, including the interactive effects of airframe stiffness, edge attachments, structural loads, thermal variations, vibration, and windshield manufacturing tolerances based on induced loads resulting from windshield/airframe contour mismatch. A NASTRAN finite element analysis of a windshield and its airframe support structure was used to analyze the structural interaction between fuselage deformation, airframe/cockpit enclosure loads, and windshield strains and deformations. Subsequent tests demonstrated the need for more refined NASTRAN modeling.

A General Specification has been developed with minimum performance levels stated for those characteristics/features considered common to all transparent enclosures, together with a set of qualification and acceptance test criteria to ensure conformance. The key aspect of the qualification and acceptance tests is the development of an integrated-endurance test. This test realistically combines operational loads and environmental extremes cyclically in a severely accelerated life cycle exposing failure modes, permitting an assessment of expected service life. This test puts "teeth" into the specification, and its implementation should afford a cost-effective means for substantiating windshield reliability. A realistic windshield wiper abrasion test has been embodied in the General Specification. At this time, there is insufficient data for relating results from this test to service life.

The General Specification and Design Handbook are responsive to the Army's need. Their implementation is encouraged.

This program was conducted under the technical cognizance of Joseph H. McGervey, Aeronautical Systems Division.

DISCLAIMERS

The findings in this report are not to be construed as an official Department of the Army position unless so designated by other authorized documents.

When Government drawings, specifications, or other data are used for any purpose other than in connection with a definitely related Government procurement operation, the United States Government thereby incurs no responsibility nor any obligation whatsoever; and the fact that the Government may have formulated, furnished, or in any way supplied the said drawings, specifications, or other data is not to be regarded by implication or otherwise as in any manner licensing the holder or any other person or corporation, or conveying any rights or permission, to manufacture, use, or sell any patented invention that may in any way be related thereto.

Trade names cited in this report do not constitute an official endorsement or approval of the use of such commercial hardware or software.

DISPOSITION INSTRUCTIONS

Destroy this report when no longer needed. Do not return it to the originator.

Unclassified

SECURITY CLASSIFICATION OF THIS PAGE (When Data Entered)

9 Fri 1979

19 REPORT DOCUMENTATION PAGE		READ INSTRUCTIONS BEFORE COMPLETING FORM	
18 1. REPORT NUMBER USARTL-TR-78-25A	2. GOVT ACCESSION NO.	3. RECIPIENT'S CATALOG NUMBER	
6 4. TITLE (and Subtitle) HELICOPTER TRANSPARENT ENCLOSURES. Volume I, Design Handbook.		5. TYPE OF REPORT & PERIOD COVERED Design Handbook	
7. AUTHOR(s) 13 Bruce F. Kay		14 8. PERFORMING ORG. REPORT NUMBER SER-58966	
9. PERFORMING ORGANIZATION NAME AND ADDRESS Sikorsky Aircraft Division United Technologies Corp. Stratford, Conn. 06602		15 10. PROGRAM ELEMENT, PROJECT, TASK AREA & WORK UNIT NUMBERS 62803A 1F262203AH86 03 009 ER	
11 CONTROLLING OFFICE NAME AND ADDRESS Applied Technology Laboratory, U.S. Army Research & Technology Laboratories (AVRADCOM) Fort Eustis, Va. 23604		12 REPORT DATE January 1979	
14 MONITORING AGENCY NAME & ADDRESS (if different from Controlling Office) 12 461 111		13 NUMBER OF PAGES 459	
		15. SECURITY CLASS. (of this report) Unclassified	
15a. DECLASSIFICATION/DOWNGRADING SCHEDULE			
6 9. DISTRIBUTION STATEMENT (of this Report) Approved for public release; distribution unlimited.			
17. DISTRIBUTION STATEMENT (of the abstract entered in Block 20, if different from Report)			
18. SUPPLEMENTARY NOTES Volume I of a two-volume report			
19. KEY WORDS (Continue on reverse side if necessary and identify by block number) Helicopter Design Optical Factors Maintenance Glint Transparent Enclosure Criteria Qualification Tests Inspection Transparent Materials Interlayers Abrasion Acceptance Tests Windshields Anti-Icing Ballistic Spall Canopy Visibility Structural Analysis Coatings Window			
20. ABSTRACT (Continue on reverse side if necessary and identify by block number) The Volume I design handbook is a comprehensive guide to the development of helicopter transparent enclosures. The handbook is structured in a manner that generally parallels the sequence of considerations used to develop helicopter transparencies. Separate chapters are devoted to subjects pertinent to the design, analysis and testing of transparent enclosures. Special characteristics and material properties are presented as applicable.			

DD FORM 1 JAN 73 1473

EDITION OF 1 NOV 65 IS OBSOLETE
S/N 0102-014-6601

Unclassified

SECURITY CLASSIFICATION OF THIS PAGE (When Data Entered)

323 800 SM
79 03 01 069

Unclassified

SECURITY CLASSIFICATION OF THIS PAGE(When Data Entered)

Volume II is a general specification and contains design, development, and and acceptance criteria. Guidelines for performing trade-offs between conflicting criteria are also given.

Para. 19 (Cont.)

Helicopter Egress
Fabrication
Laminates
Transparent Armor
Birdproofing

ACCESSION is-	
NTIS	W
DDC	C
UNANNOUNCED	
JUSTIFICATION	
BY	
DISTRIBUTION STATEMENT	
Date	

[Handwritten signature]

Unclassified

SECURITY CLASSIFICATION OF THIS PAGE(When Data Entered)

PREFACE

The work on this design handbook was performed under the supervision of Mr. B. F. Kay, Airframe Design and Development Section, who served in the capacity of Program Manager and Principal Investigator. The technical monitor for this program was Mr. J. H. McGarvey, Aeronautical Systems Division, Applied Technology Laboratory.

Grateful acknowledgement is extended to the following Sikorsky personnel, who contributed to the preparation of this handbook: R. Held, Dr. K. Rosen, R. DiGinova, D. Spacek and G. Parkinson. In addition, acknowledgement is given to the numerous sources of data, enumerated in the bibliographies, which include: the transparency industry, reports on Government-sponsored research, open literature, and periodic papers presented at various symposia.

TABLE OF CONTENTS

	<u>Page</u>
PREFACE	3
LIST OF ILLUSTRATIONS	12
LIST OF TABLES	27
1.0 INTRODUCTION	30
1.1 Transparent Enclosure Development Guide	30
1.2 Reference Information	31
2.0 VISIBILITY ENVELOPE	32
2.1 Side-by-Side Pilot	32
2.2 Single- and Tandem-Pilot Helicopters	34
2.3 Width of Structural Members	35
3.0 TRANSPARENCY SHAPE	39
3.1 Optical Effects of Obliquity	39
3.2 Optical Effects of Curvature	41
3.3 The Effect of Curvature on Enclosure Geometry	43
4.0 OPTICAL FACTORS	46
4.1 Definition of Optical Terms and their Effects on Vision	46
4.2 Optical Distortion	51
4.3 Haze	55
4.4 Light Transmission	57
4.5 Tinted Transparencies	59
4.6 Minor Optical Defects	61
4.7 Cracks	62
4.8 Reflections	62
4.9 Multiple Images	66
4.10 Antireflective Coatings	68
4.11 Head-Up Display	70
4.12 Analysis of Optical Deviation	75
5.0 RADAR CROSS SECTION REDUCTION	81
5.1 Reflection	81
5.2 Radar Reflecting Properties of Transparent Materials	81
5.3 Absorption	84

TABLE OF CONTENTS (Cont.)

	<u>Page</u>
6.0 EGRESS REQUIREMENTS	86
6.1 Mechanical Systems	86
6.2 Pyrotechnic Systems	87
6.3 Containment of Explosive Charge	90
6.4 Ballistic Initiation	91
6.5 System Safety	91
7.0 GLINT	93
7.1 Zone of Interest	93
7.2 Sun Positions	95
7.3 Glint Detection	95
7.4 Sun Glint	98
7.5 Glint Signature	98
7.6 Glint Signature Evaluation	99
7.7 Glint Countermeasures	113
8.0 ANTI-ICING	116
8.1 Definitions and Conditions	117
8.2 Heat Requirements	122
8.3 Analysis of Heat Requirements	123
8.4 Temperature Uniformity	135
8.5 Temperature Sensor Locations	141
8.6 Sample Problem	143
8.7 Windshield Temperature Profile	146
8.8 Defogging Requirements	149
8.9 Time to Warm Up	153
8.10 Hot Air Jet Blast	154
8.11 Air Temperature and Flow Requirements	155
9.0 ELECTRICAL HEATING SYSTEMS	159
9.1 Heated Area	159
9.2 Bus-Bar Spacing	159
9.3 Nominal Voltage	159
9.4 Phase Configuration	160
9.5 Phase Resistance and Applicable Tolerance	161
9.6 Permissible Phase Loading Unbalance	161
9.7 Electrical Terminations	162
9.8 Temperature Sensing Elements	165
9.9 Temperature Controller Switch Points	166
9.10 Power Control Modes	167
9.11 Fault Protection	170
9.12 Weight of Electrical Provisions	172

TABLE OF CONTENTS (Cont.)

	<u>Page</u>
10.0 RAIN REMOVAL SYSTEMS	174
10.1 Rain Intensities	174
10.2 Windshield Wipers	175
10.3 Jet Air Blast	176
10.4 Rain Repellents	177
10.5 Systems Comparison	178
11.0 TRANSPARENT ARMOR	181
11.1 Threat Specification	181
11.2 Transparent Armor Materials	182
11.3 Fragment Penetration Resistance	185
11.4 Installation	185
12.0 SPALL DESIGN REQUIREMENTS	187
12.1 Wound Criteria	187
12.2 Mechanisms of Spall	187
12.3 Major Parameters Influencing Spallation	191
12.4 Impact Conditions	191
12.5 Projectile Parameters	191
12.6 Target Parameters	192
12.7 Material Characteristics	192
12.8 Spall Fragment Energy	203
12.9 Blast Overpressure Hazards	204
13.0 BIRDPROOFING	210
13.1 Bird Hazards	210
13.2 Methods for Defeating Bird Strikes	210
13.3 Bird-Strike Capabilities of Transparent Materials	213
13.4 Bird Weight Relationships	219
13.5 Angle of Incidence	219
13.6 Temperature	220
13.7 Panel Size and Curvature	220
13.8 Impact Location	221
13.9 Edge Attachments	221
13.10 Bird Impact Forces	222
13.11 Structural Stiffness	222
13.12 Openable Hatches	222
13.13 Bird Impact Testing	223
14.0 LIGHTNING PROTECTION	227
15.0 STATIC ELECTRICITY	232

TABLE OF CONTENTS (Cont.)

	<u>Page</u>
16.0 FACE-PLY MATERIALS - PHYSICAL AND MECHANICAL PROPERTIES . .	235
16.1 Proprietary Products	235
16.2 Acrylic Plastic	235
16.3 Polycarbonate Sheet, MIL-P-83310	236
16.4 Glass, Monolithic, Aircraft-Glazing, MIL-G-25667 . .	237
16.5 Thermosetting Polyester, MIL-P-8257	239
16.6 Standard Gauges	239
16.7 Physical Properties	239
16.8 Mechanical Properties	245
16.9 Design Allowables	256
16.10 Material Attributes	259
17.0 INTERLAYERS-MECHANICAL AND PHYSICAL PROPERTIES	263
17.1 Interlayer Forms	263
17.2 Polyvinyl Butyral	264
17.3 Ethylene Terpolymer	265
17.4 Silicone-Base Interlayers	266
17.5 Polyurethane-Base Interlayers	266
18.0 COATINGS	270
18.1 Antireflective Coatings	270
18.2 Radar Cross Section Reduction Coatings	270
18.3 Electromagnetic Radiation Protection Coatings	270
18.4 Abrasion-Resistant Coatings	270
18.5 Rain Dispersion Coatings	271
18.6 Static Dissipation Coatings	271
18.7 Electrical Heating Films	271
18.8 Coating Resistivity	271
18.9 Solar and Infrared Shielding	275
19.0 ENVIRONMENTAL EFFECTS	278
19.1 Weathering	278
19.2 Moisture	278
19.3 Chemical Resistance	280
20.0 ABRASION	283
20.1 Effects of Abrasion	284
20.2 Abrasion Resistance	285
20.3 Abrasion Protection	285
20.4 Operational Durability	286
20.5 Abrasion Resistant Hardcoats	290

TABLE OF CONTENTS (Cont.)

	<u>Page</u>
21.0 IMPACT CHARACTERISTICS	296
21.1 Material Response to Low Energy Impacts	296
21.2 Temperature and Interlayer Effects on Laminates	299
21.3 Fail Safety	299
22.0 TRANSPARENCY SUPPORTS	302
22.1 Primary Structures	302
22.2 Secondary Structures	302
22.3 Tertiary Structures	304
23.0 EDGE ATTACHMENTS	307
23.1 Monolithic Panels	307
23.2 Laminated Panels	308
23.3 Flushness	310
23.4 Slip Planes	311
23.5 Joint Stiffness	311
23.6 Adhesives	314
23.7 Reinforcement Materials	315
23.8 Installation/Removal	315
23.9 Hole Size	320
23.10 Clamped-Edge Retainers	322
23.11 Sealing	324
24.0 INTERCHANGEABILITY	327
24.1 Thermal Expansion	328
24.2 Contour Conformity	329
25.0 STRUCTURAL LOADS	332
26.0 STRUCTURAL ANALYSIS	337
26.1 Aerodynamic Pressure Loading	337
26.2 Flat Plates (Bending Only)	337
26.3 Flat Plates (Bending with Membrane Action)	343
26.4 Curved Panels	345
26.5 Finite-Element Structural Analysis	347
26.6 Thermal Stress	354
26.7 Safety Factors	361
27.0 INTERLAYER DESIGN CONSIDERATIONS	363
27.1 Thermal Expansion/Contraction Differentials	363
27.2 Transverse Thermal Contraction due to Cold Edges	368
27.3 Interlayer Stress from Edge Loading	369

TABLE OF CONTENTS (Cont.)

	<u>Page</u>
27.0 INTERLAYER DESIGN CONSIDERATIONS (Continued)	
27.4 Manufacturing Stresses	370
27.5 Structural Coupling from Interlayers	371
27.6 Fail-Safe Criteria for Interlayers	376
27.7 Interlayer Adhesion Properties	379
28.0 WEIGHT	382
28.1 Weight Optimization	383
28.2 Transparency/Support Interactions	384
29.0 MANUFACTURING METHODS	386
29.1 Machinability	386
29.2 Drilling	387
29.3 Glass	388
29.4 Forming Techniques	389
29.5 Forming Stretched Acrylic	389
29.6 Forming Polycarbonate	390
29.7 Forming Methods	390
29.8 Forming Laminated Parts	391
29.9 Tolerances	393
29.10 Joining Transparent Materials - Solvent Cementing	393
29.11 Adhesive Bonding	394
29.12 Annealing	395
30.0 QUALIFICATION TESTS	397
30.1 Similarity	397
30.2 Test Methods	397
30.3 Material Specimen Tests	398
30.4 Abrasion Tests	400
30.5 Windshield-Wiper Test	400
30.6 Rubbing Abrasion Test	401
30.7 Weathering Tests	402
30.8 Component Tests	403
30.9 Birdproof Tests	403
30.10 Temperature Tests	403
30.11 Structural Integrity Tests	403
30.12 Fail-Safety Tests	404
30.13 Integrated Endurance Test	405
30.14 Windshield Endurance Test Facility	405
30.15 Endurance Test Load Spectrum	408
30.16 Environmental Conditions	408
30.17 Temperature Environment from Natural Climatic Conditions	408

TABLE OF CONTENTS (Cont.)

	<u>Page</u>
30.0 QUALIFICATION TESTS (Continued)	
30.18 Anti-Ice Heating	409
30.19 Cold Shock	410
30.20 Structural Loading Conditions	410
30.21 Load Spectra	410
30.22 Installation Preload	414
30.23 Miscellaneous Conditions	414
30.24 Systems Integration Tests	415
31.0 ACCEPTANCE TESTS	419
31.1 Acceptance Tests for Raw Materials	419
31.2 Test Methods	419
31.3 Finished Product Acceptance Tests	419
32.0 MAINTENANCE INSPECTION AND FAULT IDENTIFICATION	422
32.1 Storage	422
32.2 Cleaning	422
32.3 Precautions	423
32.4 Inspection	423
32.5 Malfunctions	423
32.6 Repairs	430
33.0 LIFE CYCLE COSTS	434
APPENDIXES	
A. APPLICABLE SPECIFICATIONS AND STANDARDS	439
B. HELICOPTER TRANSPARENCY CONFIGURATIONS	442
GLOSSARY	449

LIST OF ILLUSTRATIONS

<u>Figure</u>		<u>Page</u>
1-1	Flow Chart for Transparency Development	31
2-1	Side-by-Side Pilot Vision Plot	33
2-2	Single Pilot/Tandem Pilot Vision Plot	34
2-3	Areas Blocked by Windshield Frame Members That Are Narrower Than , Equal to, and Wider Than the Distance Between the Pupils	36
2-4	Effect of Canting Frames	37
3-1	Effects of Angle of Incidence on Optical Deviation .	40
3-2	Effects of Angle of Incidence on Surface Reflections and Transmission Loss	40
3-3	Optical Deviation Through a Curved Panel	41
3-4	Effects of the Thickness/Radius of Curvature Ratio on Optical Deviation at Three Angles of Incidence . . .	42
3-5	OH-13 Helicopter	43
3-6	Flat Versus Curved Panel Geometry	44
4-1	Five Types of Optical Distortion	52
4-2	Bull's-eye Distortion of a Grid Board Photo	53
4-3	Bull's-eye Distortion of an External Scene	53
4-4	Optical Grid Photograph	55
4-5	Typical Setup for Taking Grid Photographs	56
4-6	Measurement of Distortion	56
4-7	Effect of Luminance Level on Minimum Perceptible Visual Acuity and Maximum Sighting Range	58
4-8	Spectral Transmittance for Green/Grey Acrylic Plastic	59
4-9	Spectral Transmittance of Visible Wavelengths for Blue Acrylic Plastic	60

LIST OF ILLUSTRATIONS (Cont.)

<u>Figure</u>		<u>Page</u>
4-10	Sparse Crack Pattern	63
4-11	Dense Crack Pattern	63
4-12	Effect of Crack Density on Visual Response	64
4-13	Lateral Cracking vs. Angle of Incidence	54
4-14	Transparency Oriented to Reflect Instrument Lights Away From Rear Pilot	65
4-15	Windshield Reflections From Light Entering Cockpit Through Lower Window	66
4-16	Multiple Reflections From Monolithic Transparency . .	67
4-17	Multiple Reflections From Laminated Transparency With Conductive Coating	67
4-18	The Origin of Multiple Reflections in Double Glazing.	68
4-19	Destructive Interference of Reflected Light	69
4-20	Reflectance Curve of a Typical Antireflective Coating	69
4-21	Visible Light Reflectance versus Resistivity of Sierracote Metallic Coating	70
4-22	Fixed Head-Up Display	71
4-23	Movable Helmet-Mounted Display	71
4-24	Target Displacement Resulting From Optical Deviation	72
4-25	Deviation is a Function of Direction for a Curved Transparency	73
4-26	Lines of Sight Through a Curved Windshield	74
4-27	The Visual Parallax Problem	75
4-28	Refraction of Light	76

LIST OF ILLUSTRATIONS (Cont.)

<u>Figure</u>		<u>Page</u>
4-29	Geometrical Representation of the Deviation of a Line of Sight Through a Cylindrically Curved Transparent Panel of Uniform Thickness	77
5-1	Relationship Between Percent Reflection and Decibel Reduction in Echo	83
6-1	Separable Rubber Extrusion Mounting	86
6-2	Test Firing of an AH-1 Cobra Escape System	87
6-3	Cutting Sequence for Linear Explosive Charges	89
6-4	Explosive Cutting of Laminated Transparencies	90
6-5	Sikorsky S-72 Cutting Assembly	91
7-1	Zone of Interest for Glint Detection of Low- Flying Helicopters	94
7-2	Zone of Interest for Glint Detection as Related to the Helicopter	94
7-3	Contrast Discrimination Curve	96
7-4	Range of Possible Lighting Conditions	97
7-5	Snell's Law of Reflection	98
7-6	Visual Angle to Transparency and Sun	99
7-7	Sun Reflections From Surfaces of Different Curvature	100
7-8	Effective Area of Reflection for Curved Transparencies	101
7-9	Test Setup for Determining Canopy Sun-Glint Signature	101
7-10	Top View of Experiment Setup	104
7-11	Standard Format for Presenting Canopy Sun-Glint Signature	104
7-12	Illustration of Window Reflections	105

LIST OF ILLUSTRATIONS (Cont.)

<u>Figure</u>	<u>Page</u>
7-13 Basic Canopy Shape	106
7-14 Offending Sun Positions for Various Elevations of Front Sloped Window	107
7-15 Reflected Vectors That Correspond to the Offending Sun Positions in Figure 7-14	108
7-16 Offending Sun Positions for Various Elevations of Top Window	109
7-17 Reflected Vectors That Correspond to the Offending Sun Positions in Figure 7-16	110
7-18 Offending Sun Positions for Various Elevations of the Side Windows	111
7-19 Reflected Vectors That Correspond to the Offending Sun Positions in Figure 7-18	112
7-20 Downward Reflections From an Outward Canted Window .	113
7-21 Reflection Control With Fences	114
8-1 Anti-Icing of Main Windshields	116
8-2 Continuous (Stratiform Clouds) Atmospheric Icing Conditions, Liquid Water Content Versus Mean Effective Drop Diameter	118
8-3 Continuous (Stratiform Clouds) Atmospheric Icing Conditions, Ambient Temperature Versus Pressure Altitude	119
8-4 Continuous (Stratiform Clouds) Atmospheric Icing Conditions, Liquid Water Content Factor Versus Cloud Horizontal Distance	119
8-5 Intermittent (Cumuliform Clouds) Atmospheric Icing Conditions, Liquid Water Content Versus Mean Effective Drop Diameter	120
8-6 Intermittent (Cumuliform Clouds) Atmospheric Icing Conditions, Ambient Temperature Versus Pressure Altitude	121

LIST OF ILLUSTRATIONS (Cont.)

<u>Figure</u>		<u>Page</u>
8-7	Intermittent (Cumuliform Clouds) Atmospheric Icing Conditions, Liquid Water Content Factor Versus Cloud Horizontal Extent	122
8-8	Windshield Heating Requirement as Defined by MIL-T-5842A	123
8-9	A Model of a Windshield's Transverse Heat Flow . . .	124
8-10	Convection Heat Transfer Coefficient at Outside Surface of Windshield, Nomogram	127
8-11	Physical Significance of Collection Efficiency . . .	130
8-12	Curve of Droplet Catch Efficiency	133
8-13	Hot-Spot Film Temperature Versus Ambient Air Temperature	138
8-14	Variation in Airspeed at Windshield Surface	140
8-15	Transverse Temperature Sensor Location	141
8-16	Temperature Sensor Location Relative to Hot and Cold Spots	142
8-17	Windshield Cross Section and Temperature Profile . .	147
8-18	Psychrometric Chart for Obtaining the Dew Point at Temperatures Below 50°F	151
8-19	Psychrometric Chart for Obtaining the Dew Point, at Normal Temperatures	152
8-20	Biot and Fourier Relationships for Transient Heat Transfer Problems	153
8-21	Hot Air Jet Anti-Ice System	154
8-22	35°, Flat Windshield and Canopy	155
8-23	Relationship Between Jet Blast Velocity, Weight Flow, and Temperature Under Heavy Rain Conditions at 140 Knots	156

LIST OF ILLUSTRATIONS (Cont.)

<u>Figure</u>		<u>Page</u>
8-24	Windshield Surface Temperature as a Function of Air Temperature and Distance From Nozzle Under Moderate Rain Conditions at 140 Knots	157
9-1	Comparison of Y and Delta Electrical Systems	160
9-2	Unbalance Limits for Three-Phase Utilization Equipment	162
9-3	Windshield Electrical Terminals	163
9-4	Bus-Bars and Terminals for Three-Phase Electrically Heated Windshield	164
9-5	Typical Sensor Resistance/Temperature Characteristics	166
9-6	Power Modes for Windshield Temperature Controllers. .	167
9-7	Block Diagram of Typical Windshield Heating System	171
10-1	Windshield Wiper With Aerodynamic Deflector	175
10-2	View of Grid Through Sample Windshield Under Simulated Rainfall of 3 Inches per Hour	177
11-1	Ballistic Behavior of 38 oz/sq ft. Acrylic-Polycarbonate Laminates (17-Grain Fragment Simulators).	183
11-2	Abilities of .30-Caliber and .50-Caliber Projectiles to Penetrate Bullet-Resistant Glass, MIL-G-5485C . .	185
11-3	Transparent Armor Mounting Brackets	186
12-1	Wounding Model, Skin Laceration by Glass Fragments .	190
12-2	Monolithic .080-Inch Thick Polycarbonate Specimen After .30-Caliber Ball Ballistic Impact	193
12-3	Spall Penetration of Witness Sheet for Polycarbonate	194
12-4	Monolithic .080-Inch-Thick Stretched Acrylic Specimen After .30-Caliber Ball Ballistic Impact . .	195

LIST OF ILLUSTRATIONS (Cont.)

<u>Figure</u>		<u>Page</u>
12-5	Spall Penetration of Witness Sheet for Stretched Acrylic	195
12-6	Spall Produced by .30-Caliber Ball Ballistic Impact on Stretched Acrylic	196
12-7	0.080-Inch-Thick Cast Acrylic Specimen After .30-Caliber Ball Ballistic Impact	197
12-8	0.187-Inch-Thick Cast Acrylic Specimen After .30-Caliber Ball Ballistic Impact	197
12-9	Spall Penetration of Witness Sheet for Cast Acrylic	198
12-10	Spall Produced by .30-Caliber Ball Ballistic Impact on Cast Acrylic	198
12-11	Glass-Acrylic Laminated Specimen After .30-Caliber Ball Ballistic Impact	199
12-12	Spall Penetration of Witness Sheet for Glass-Acrylic Laminate	200
12-13	Spall Produced by .30-Caliber Ball Ballistic Impact on Glass-Acrylic Laminate	200
12-14	Laminated Glass Specimen After .30-Caliber Ball Ballistic Impact	201
12-15	Polyvinyl-Butyral Interlayer Fragment From a Laminated Glass Specimen	202
12-16	Spall Penetration of Witness Sheet for Laminated Glass Specimen	202
12-17	Spall Produced by .30-Caliber Ball Ballistic Impact on Laminated Glass	203
12-18	Spall Data Compared to Wounding Threshold	204
12-19	Critical Shatter Overpressure (Reflected) for Common Transparent Materials	205
12-20	Geometric Mean of the Fragment Velocity Versus the Peak Effective Overpressure	207

LIST OF ILLUSTRATIONS (Cont.)

<u>Figure</u>		<u>Page</u>
13-1	Bird Impact Damage at 122 Knots, Acrylic Windshield	211
13-2	Bird Impact Damage at 92 Knots, Glass-Faced Windshield	211
13-3	Manner in Which a Birdproof Windshield Panel Resists a Bird Strike	212
13-4	Safety Shield Laminated to Inboard Surface of Windshield to Reduce Spall	213
13-5	Windshield Sweepback Angle	215
13-6	Velocities of 4-lb Birds for Penetration of Flat Glass Windshields at 45° Impact Angles	217
13-7	Velocities of 4-lb Birds for Penetration of Flat Plastic Windshields at 45° Impact Angles.	218
13-8	Effect of PVB Temperature on Penetration Velocity . .	220
13-9	Edge Insert for Laminated Windshields	221
13-10	Bird Impact Test Facility	224
14-1	Crew Protection by Cockpit Frames	228
14-2	Shock Hazard due to Ungrounded Outside Air Temperature Gauge	230
16-1	Thermal Tempered Glass Residual Stress Distribution .	238
16-2	Chemical Tempered Glass Residual Stress Distribution	238
16-3	Tensile Stress-Strain Curves for Some Transparent Glazing Materials at Room Temperature	246
16-4	Effect of Temperature on Tensile Properties (Short-Time Test) of MIL-P-8184 Cast Acrylic Material	247
16-5	Effect of Temperature on Tensile Properties (Short-Time Test) of MIL-P-8457 Thermosetting Polyester Material	248

LIST OF ILLUSTRATIONS (Cont.)

<u>Figure</u>		<u>Page</u>
16-6	Effect of Temperature on Tensile Properties (Short-Time Test) of MIL-P-5425 Cast Acrylic Material	248
16-7	Effect of Temperature on Tensile Properties (Short-Time Test) of MIL-P-25690 Stretched Acrylic Material	249
16-8	Effect of Temperature on Tensile Properties (Short-Time Test) of MIL-P-83310 Polycarbonate Material	250
16-9	Effect of Duration of Loading on the Tensile Rupture Behavior of Plastic Glazing Materials at 80°F	252
16-10	Crazing of Plexiglas 55 Under Continuous Tensile Stress While Exposed to Natural Weather	252
16-11	The Effect of Sustained Loading on the Breaking Strength of Annealed Glass	253
16-12	Flexural Fatigue Curves for 0.25-Inch-Thick Plastic Glazing Materials at Room Temperature	253
16-13	Effect of Temperature on the K-Value of Glazing Materials	255
16-14	Coefficient of Linear Expansion Versus Temperature for Various Transparent Glazing Materials	257
17-1	Tensile Modulus of PVB Interlayer	265
17-2	Ultimate Strength versus Temperature for ETA, SS5272Y(HT) and PVB-3GH	267
17-3	Tensile Elongation Characteristics of ETA, SS5272Y (HT) and PVB as a Function of Temperature	268
18-1	Resistivity of a Square Shape	272
18-2	Sample Resistivity Calculations	273
18-3	Light Transmissions Versus Resistivity, Sierracin S-343 Coating	274

LIST OF ILLUSTRATIONS (Cont.)

<u>Figure</u>		<u>Page</u>
18-4	Spectral Distribution of Solar Radiant Power at Sea Level Perpendicular to the Sun's Rays	275
18-5	Visible Light Spectrum	276
18-6	Shielding of Solar Radiation for Sierracin S-343A . .	278
19-1	Humidity Expansion of Plexiglas 55	279
20-1	Windshield Wiper Abrasion Damage	283
20-2	Random Scratching of Transparent Plastic	284
20-3	Windshield Wiper Abrasion Test Results	287
20-4	Dry Rubbing Abrasion Test Results	288
20-5	Falling Sand Test Results	289
20-6	Effects of Outdoor Weathering on Coatings	293
21-1	0.080-Inch Stretched Acrylic After Low Temperature Dart Impact	297
21-2	Stretched Acrylic Fracture Surface	297
21-3	Glass-Glass Laminate After Room Temperature Dart Impact	298
21-4	0.080-Inch Cast Acrylic After Room Temperature Dart Impact	298
22-1	Typical Framing Members	302
22-2	Typical Box Members	303
22-3	Windshield In-Plane Stiffness Supports Roof Window .	304
22-4	Formed Hat Section Ribs on Door Window	305
22-5	Solid Acrylic Reinforcements on Sliding Window . . .	305
23-1	Laminar Splitting of Stretched Acrylic	307
23-2	Cast Acrylic Edge Reinforcements	308
.		

LIST OF ILLUSTRATIONS (Cont.)

<u>Figure</u>		<u>Page</u>
23-3	Laminated Transparency Edge Configurations	309
23-4	Function of Slip Planes	311
23-5	Edge Rotational Stiffness	312
23-6	Peel Stresses Due to Edge Rotation	312
23-7	Cleavage Test Setup	312
23-8	Stress Distribution in a Scarfed Adhesive Joint	314
23-9	Transparency Retention via Rubber Extrusions	317
23-10	Torquing Sequence for Closing Gap Between Transparency and Support	319
23-11	Riveted Installation	320
23-12	Spacer Used to Control Clamping Dimensions	321
23-13	Oversized Hole Installations for Flush Fasteners	321
23-14	Strain Compatibility Test	322
23-15	Single Glazing Clamp Retention	323
23-16	Double Glazing Clamp Retention	323
23-17	Lipped Window Retainer	324
23-18	Hollow-Bulb Seal and Pile Line	324
24-1	Master Mockup for Contoured Transparency	327
24-2	Differential Thermal Change in Length per Unit Length	328
24-3	Windshield Installation Preload, Induced Stress Versus Camber	330
26-1	Discontinuity Stresses due to Support Constraints	346
26-2	Stress Pattern for a Flat Windshield	348

LIST OF ILLUSTRATIONS (Cont.)

<u>Figure</u>		<u>Page</u>
26-3	NASTRAN Model of YUH60A Nose Section	351
26-4	Cathode Ray Tube Display	351
26-5	Temperature Profile of Heated Windshield	355
26-6	Tensile Stress at Edge of Semi-Infinite Glass Panel Produced by Cylindrical Hot Spot Located Near Edge .	356
26-7	Thermal Map of Typical Rectangular Windshield	357
26-8	Location and Direction of Maximum Tensile Stress Induced by Cold Edges	358
26-9	The Effect of Coupling on the Contraction of Different Materials	359
26-10	Interlayer Deformation due to Thermal Expansion Differences	361
27-1	Interlayer Shrinkage Forces During Conditions of Cold Soak	363
27-2	Cold Soak Forced Induced Into Unsymmetrical Laminates	364
27-3	Temperature Changes Used for Establishing Thermal Stress	364
27-4	Stress Distribution Along the Glass-Plastic Inter- face of a Three-Ply Laminate Subjected to a Uniform Temperature of -20°F, Obtained Photoelastically . .	366
27-5	Laminates Used to Obtain Facing Stresses	367
27-6	Cold Edge Contraction of Interlayer	368
27-7	Stress Distribution due to Cold Edges	368
27-8	Interlayer Strain Resulting From Flexural Loading of Laminate With Staggered Edge Restraint	369
27-9	Interlayer Strain Resulting From Application of Membrane Loads to Single Ply of Laminated Assembly .	370
27-10	Assembly-Induced Interlayer Bond Tension	370

LIST OF ILLUSTRATIONS (Cont.)

<u>Figure</u>		<u>Page</u>
27-11	Stress and Strain Distributions in a Fully Coupled Composite Beam with Equally Stiff Face Plies	371
27-12	Stress and Strain Distributions in an Uncoupled Composite Beam	372
27-13	Variation of Stiffness With Temperature, Glass/Plastic Laminate With PVB Interlayer	373
27-14	Variation of Stiffness with Temperature, Glass/Plastic Laminate With Ethylene Terpolymer Interlayer	374
27-15	Variation of Stiffness With Temperature of Plastic Laminate	375
27-16	Stress and Strain Distributions in a Fully Coupled Composite Beam With Face Plies of Unequal Stiffness	376
27-17	Interlayer Supports Aerodynamic Pressure Loads by Membrane Action	378
27-18	Fail-Safe Test of Fractured Glass Laminate	378
27-19	Shear Deformation of Interlayers	379
28-1	Deflection vs Pressure for Flat and Contoured 16-Inch Diameter, 1/4-Inch-Thick Acrylic Discs	383
29-1	Minimum Fillet Radius for Machined Undercuts	386
29-2	Diagram of Recommended Drill Geometry for Acrylic Plastics	387
29-3	Poorly Drilled Hole in Stretched Acrylic	388
29-4	Snap-Back Forming of Acrylic Sheet	391
29-5	Thinning of Free-Blown Acrylic Parts	392
29-6	Distinction Between Cohesion and Adhesion	394
30-1	Windshield Wiper Test Apparatus	401
30-2	Apparatus for the Dry-Rubbing Abrasion Test	402
30-3	Soft Rubber Patch Maintains Pressure for Fail-Safety Test	404

LIST OF ILLUSTRATIONS (Cont.)

<u>Figure</u>		<u>Page</u>
30-4	Typical Windshield Endurance Test Facility	406
30-5	Typical Schematic Diagram of an Endurance Test Facility	407
30-6	Aerodynamic Pressure Ground-Air-Ground Cycle	411
30-7	Hypothetical Distribution of Maximum Airspeed Versus Percentage of Flights	411
30-8	Schedule of Loading for Endurance Tests	412
30-9	Aerodynamic Pressures During Ground-Air-Ground Cycle With Multiple Load Peaks per Flight	414
30-10	Hypothetical Distribution of Maximum Airspeed Coupled With Load Factor	415
30-11	Icing Spray Rig Test	416
32-1	Crazed Acrylic Window	424
32-2	Laminated Glass Windshield Cracks From Excessive Installation Preload	425
32-3	Crack Originating at Delamination	425
32-4	Sliding Window Scratched by Sill	426
32-5	Windshield Scratched by Wiper	427
32-6	Delamination	423
32-7	Bubbles Formed in Interlayer of Laminated Windshield	428
32-8	Charred Heating Film Adjacent to Crack	429
32-9	Repaired Cracks	431
33-1	Simplified Life-Cycle Cost Model	435
33-2	Hypothetical Life-Cycle Costs for Heated Windshields	436
B-1	AH-1 Transparencies	442
B-2	UH-1 Transparencies	443

LIST OF ILLUSTRATIONS (Cont.)

<u>Figure</u>		<u>Page</u>
B-3	H-2 Transparencies	443
B-4	OH-6 Transparencies	444
B-5	CH-53 Transparencies	444
B-6	CH-47 Transparencies	445
B-7	CH-54 Transparencies	446
B-8	OH-58 Transparencies	446
B-9	UH-60 Transparencies	447
B-10	YAH-64 Transparencies	447

LIST OF TABLES

<u>Table</u>	<u>Page</u>
3-1 Acceptable Values of Optical Deviation	42
4-1 Typical Grid Slopes for Helicopter Transparencies . .	55
4-2 Recommended Light Transmission Values (%)	58
4-3 Allowable Minor Defects in Each Interlayer	62
5-1 Radar Attenuation Characteristics of Transparent Materials	82
7-1 Sun Elevation Occurrence for 20 ⁰ to 60 ⁰ North Latitude Locations	95
8-1 Temperature Versus Vapor Pressure of Saturated Air .	128
8-2 Altitude Versus Barometric Pressure	128
8-3 Temperature Versus Absolute Viscosity of Air	134
9-1 Typical Tolerance Analysis for Temperature Switch-off Point	168
10-1 Rain Intensities and Visiivility	174
10-2 Rain Removal Systems Comparison	179
11-1 Range Velocity Characteristics, Kinetic Energy (Solid Core) Ammunition	183
12-1 Fragment Data from UH-1 Helicopters Exposed to 500-lb TNT Airblasts	206
16-1 Standard Thicknesses and Tolerances of Cast Acrylic Sheet	240
16-2 Standard Thicknesses and Tolerances of MIL-P-8257 Thermosetting Plastic Sheet	241
16-3 Standard Thicknesses and Tolerances of MIL-P-83310 Polycarbonate Sheet	241

LIST OF TABLES (Cont.)

<u>Table</u>		<u>Page</u>
16-4	Standard Thicknesses and Tolerances of MIL-G-25667 Glass	242
16-5	Properties of Plastic Transparent Materials	243
16-6	Properties of Glass	244
16-7	Relative Crack Propagation Resistance of Various Materials	254
16-8	Allowable Tensile Stresses for Helicopter Transparent Enclosures	258
16-9	Summary of Transparent Glazing Material Attributes	259
17-1	Room Temperature Properties of Polyvinyl Butyral	265
17-2	Room Temperature Properties of Swedlow SS5272Y (HT) Silicone-Base Interlayer	266
18-1	Coating Resistivity	274
19-1	Chemicals That can Damage Plastic Glazing Materials	281
20-1	Ranking of Transparent Materials for Abrasion Resistance	285
20-2	Haze Level After 2000 Cycles of Windshield Wiper Abrasion for Various Hardcoated Materials	291
21-1	Effects of Temperature on Impact Strength of Laminated Glass	300
23-1	Factors Affecting Flushness of Edge Reinforcements for Laminated Windshields	310
23-2	Cleavage Strengths of Various Laminates	313
23-3	Coefficients of Thermal Expansion of Transparent Edge-Attachment Materials at Room Temperature	316
25-1	Loading Conditions	333
26-1	Stress and Deflection Formulas for Flat Plates	339
26-2	Stress and Deflection Coefficients for Circular Plates With Uniform Load Applied	340

LIST OF TABLES (Cont.)

<u>Table</u>		<u>Page</u>
26-3	Stress and Deflection Coefficients for Square or Rectangular Plates With Uniform Load Applied	341
26-4	Stress and Deflection Coefficients for Square Plate With Uniform Load Over Small Area of Radius r_0 . . .	342
26-5	Stress and Deflection Formulas for Circular Plates Under Uniform Loads That Produce Large Deflections .	343
26-6	Stress and Deflection Formulas for Rectangular Plates Under Uniform Loads That Produce Large Deflections .	344
27-1	Factors Governing Interlayer Stress in Laminated Transparencies From Thermal Expansion Differential .	365
27-2	Facing Stresses due to Differential Thermal Expansion/Contraction	367
27-3	Comparison of Stresses for Coupled and Uncoupled Composite Beams, Fixed Deflection	377
27-4	Typical Interlayer Adhesion Strength Properties . . .	380
28-1	Densities and Specific Strengths of Transparent Materials	382
28-2	Comparative Weights of Transparency Configurations .	384
29-1	Practical Tolerances for Transparent Components . . .	393
30-1	Qualification Tests for Raw Materials	399
30-2	Cold Climate Temperature Distribution	409
30-3	Hot Climate Temperature Distribution	409
30-4	Endurance Test Schedule (Example), Warm Climate, Airspeed Distribution From Figure 30-7	412
30-5	Endurance Test Schedule (Example), Cold Climate, Airspeed Distribution From Figure 30-7	413
30-6	Transparency Systems Integration Tests	415
31-1	Acceptance Tests for Raw Materials	420
33-1	Mean Time Between Removal-Replacement (MTBRR) for Helicopter Transparencies	434

1.0

INTRODUCTION

"Above all else, you must be able to see through it." This simple phrase embodies the essence of transparent enclosure design. To fulfill this need during extreme natural and induced environmental conditions, and still function as a weathertight structure, unique design features, materials, and ancillary systems are necessary.

Because of the complexity involved, collaborative efforts involving numerous disciplines are normally required to develop optimum designs. The coordination of such engineering activities is most effectively accomplished by specialists familiar with all systems.

To aid in these endeavors, this comprehensive design handbook has been prepared. This handbook provides pertinent design information that will enable engineers to address in a proficient manner all of the important attributes associated with helicopter transparent enclosures.

1.1 Transparent Enclosure Development Guide

This handbook is structured in a manner that roughly parallels the sequence of considerations used to develop helicopter transparent enclosures.

A flow chart illustrating a typical development program is shown in Figure 1-1. The orderly progression from preliminary design through final acceptance testing, with appropriate iterations, is necessary to achieve reliable, cost-effective products.

During preliminary design, the basic sizes, shapes and locations of the transparencies are determined. Careful considerations of major transparency attributes must be made at this time since subsequent changes to the basic configuration are usually difficult to make.

Next, special characteristics are extracted from the helicopter model specification, or customer requirements, and translated into specific transparency requirements.

Airframe interface and material selection is generally accomplished in parallel to optimize the design. Interaction with transparency manufacturers is appropriate at this time. After finalizing design and performance requirements, detail drawings and specifications are prepared.

As a final step prior to producing a new design, a comprehensive qualification program should be undertaken. Qualification testing is necessary because of complex interactions that occur that affect service life and which cannot be foretold by purely analytic means.

Acceptance testing and inspection are necessary to insure that production variables are maintained within acceptable limits. The last step, monitoring reliability under operational conditions, will confirm that original objectives are being met and will reveal any deficiencies that might otherwise escape detection during qualification.

1.2 Reference Information

Applicable standards and specifications for design are listed in Appendix A.

Transparent enclosure configurations for a number of different helicopter models are described in Appendix B.

A specification which consolidates design, acceptance and test criteria for helicopter transparent enclosures is presented in Volume II.

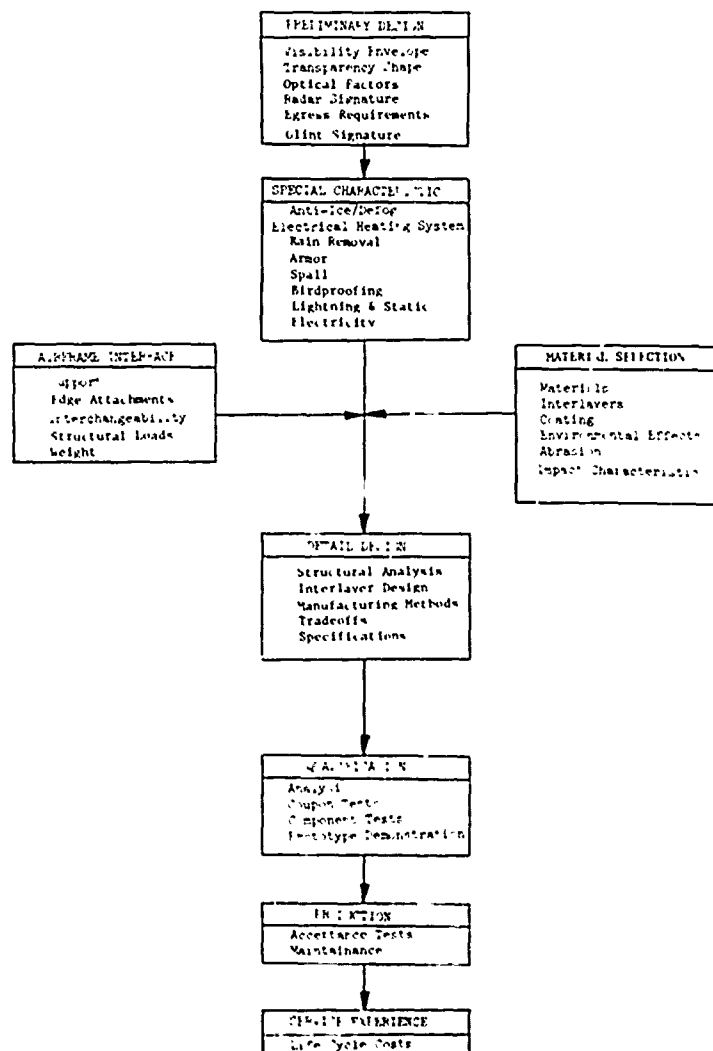


Figure 1-1. Flow Chart for Transparency Development.

2.0

VISIBILITY ENVELOPE

One of the first steps in designing a cockpit enclosure is to provide an acceptable field of vision for the flight crew. The maximum practical external vision should be provided for the pilots. MIL-STD-850B, "Aircrew Station Vision Requirements for Military Aircraft", specifies minimum requirements for side-by-side pilot, single-pilot and tandem-pilot helicopters. Particular consideration should be given in each case to the external vision provided in conjunction with the specified missions of the helicopter. It may be kept in mind that the total field, obtained by both head and eye movements that are performed easily and naturally, subtends about 75% of a sphere (155 degrees of either side, 91 degrees upward and 112 degrees downward).

The specific vision requirements from MIL-STD-850B are given relative to the longitudinal fuselage line and are as follows:

2.1 Side-by-Side Pilot

- a) Controls, consoles, and instrument panels shall be located so as not to restrict vision, with particular emphasis on adequate over-the-nose visibility. Insure that mounting and reinforcing frames or strips that divide transparent areas and form obstructions to vision are not more than 2 inches wide when projected onto a plane perpendicular to a line between the structure and the pilot's eyes at the design eye position. Distribute such obstructions to avoid critical vision areas.
- b) The following minimum angles of unimpaired vision shall be available to the pilot from the design eye position:
 - 1) At 0° azimuth, 25° down and 20° up shall be available.
 - 2) From 10° left azimuth to 10° right azimuth, downward vision shall increase from 20° to 30° .
 - 3) In the area between 10° right azimuth and 135° right azimuth, 50° of downward vision shall be available.
 - 4) From 0° to 80° right azimuth, upward vision shall increase from 20° to 40° .
 - 5) From 80° right azimuth to 100° right azimuth, upward vision shall be 40° .
 - 6) From 100° right azimuth to 135° right azimuth, upward vision requirements may decrease gradually from 40° to 20° .
 - 7) From 10° left azimuth to 100° left azimuth, 20° up and 20° down shall be available.

- c) There shall be no vertical obstruction between 20° right and 20° left of the longitudinal axis relative to the design eye position.
- d) There shall be no horizontal obstructions in the area extending 15° above the horizontal from 135° right to 40° left and decreasing to a point 10° above the horizontal at 100° left. No horizontal obstructions shall be in the area 15° below the horizon between 135° right and 100° left. If necessary, horizontal obstructions in this area shall be limited to one above the horizon and one below the horizon and shall be restricted to 4 inches in width.

The preceding requirements are plotted in Figure 2-1 as an Aitoff's equal area graph. The copilot's field of vision is a reverse image of Figure 2-1.

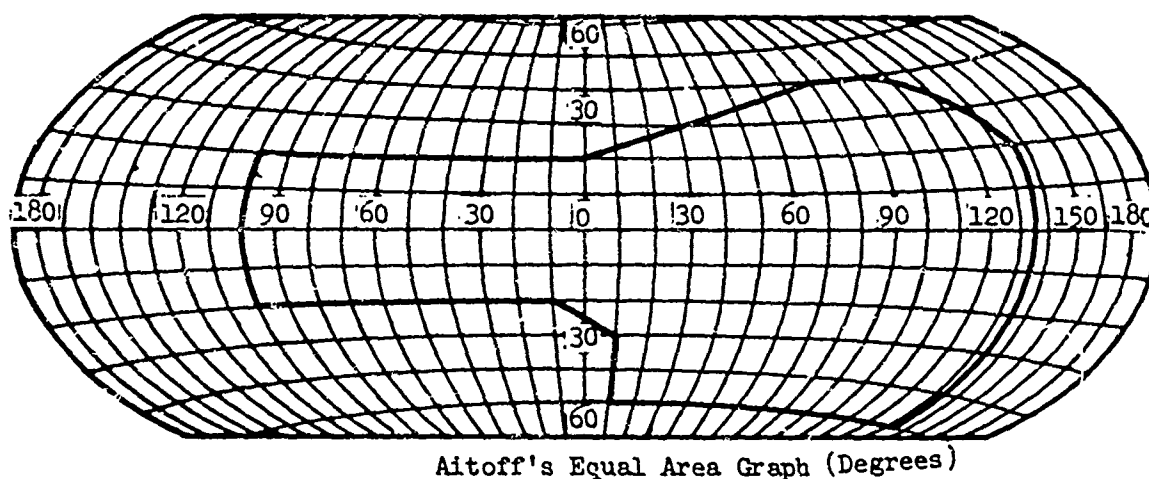


Figure 2-1. Side-by-Side Vision Plot.

2.2 Single- and Tandem-Pilot Helicopters

The vision requirements given below were excerpted from MIL-STD-850B and are applicable to single- and tandem-pilot helicopters with the pilot in either the forward or aft position. The forward cockpit position, if occupied by other than the primary pilot (i.e., gunner or observer), shall also comply with these requirements.

- a) The following shall be the minimum angles of unimpaired vision available to the pilot from the design eye position:
 - 1) At 0° azimuth, at least 25° down and 70° up.
 - 2) At 20° azimuth, left and right, 25° down and 70° up.
 - 3) At 30° azimuth, left and right, 30° down and 70° up.
 - 4) At 90° azimuth, left and right, 50° down and 70° up.
 - 5) At 135° azimuth, left and right, 34° down and 70° up.
- b) Visibility above the elevation specified in para. 2.2(a) of at least 90° shall be provided. Interruptions of vision by horizontal structure of not more than 2 inches of width along or above the elevation boundary of a and vertical structural members of not more than 2 inches in width located in accordance with para. 2.1(d) are permitted.

The preceding requirements are plotted in Figure 2-2 as an Aitoff's equal area graph.

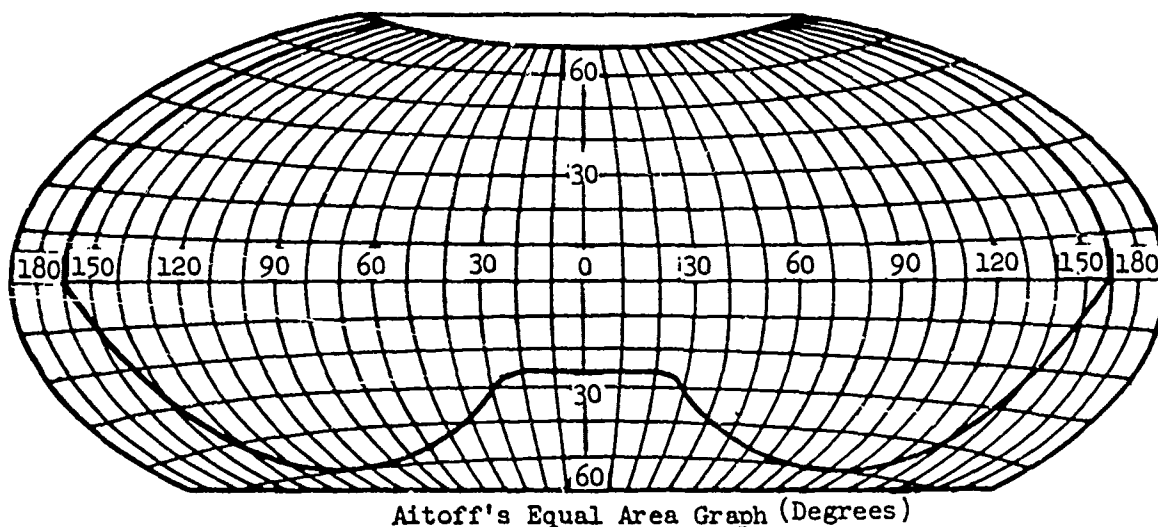


Figure 2-2. Single Pilot/Tandem Pilot Vision Plot.

2.3 Width of Structural Members

Structural members within the pilot's field of vision must be made as narrow as possible. A structural member will block off part of the field of vision for both eyes if it is wider than the distance between the pupils of the eyes; that is, if it is so wide that one eye will not "cover" for the other unless the pilot moves his head. The angle subtended by the blind area is proportional to the width of the frame member minus the interpupillary distance. These points are illustrated in Figure 2-3. In A, the frame is narrower than the effective interpupillary distance. The left eye can see any part of the field of vision that is blocked for the right eye and vice versa, except for a narrow triangular area just behind the frame. In B, the frame is just the width of the effective interpupillary distance - about 2-1/2 inches maximum. It creates a narrow blind area exactly as wide as the interpupillary distance, but the blind area gets no wider out into space; only a 2-1/2-inch strip will be blocked out whether an object is 5 inches or 5 miles behind the frame. Therefore, for practical purposes, in an aircraft, a frame 2-1/2 inches wide does not obstruct vision for both eyes. However, in C, the frame is wider than the interpupillary distance. The effective binocular blind area now increases with distance by a factor proportional to the excess in width over 2-1/2 inches and the distance of the frame member from the eyes.

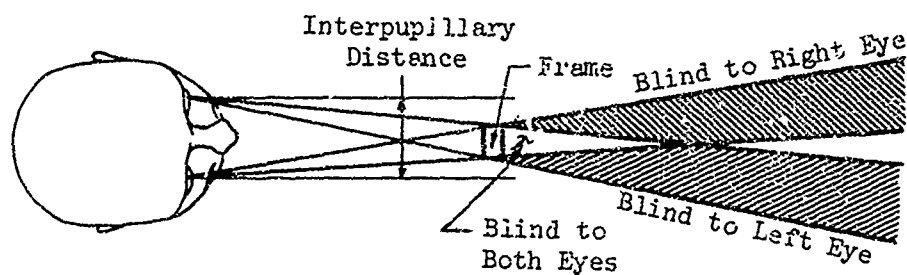
Note that for objects seen to one or the other side of the fore-and-aft vertical plane bisecting the head, the effective interpupillary distance (Figure 2-3C) decreases with the cosine of the angle between the line from eyes to object and the plane. In other words, a smaller obstruction to one side will block vision (provided the pilot does not turn his head). Therefore, obstructions should be less than the interpupillary distance: no more than 2 inches in width.

Horizontal obstructions should always be as narrow as possible since the eyes are in the same plane and therefore any obstruction will subtend an ever increasing area of vision.

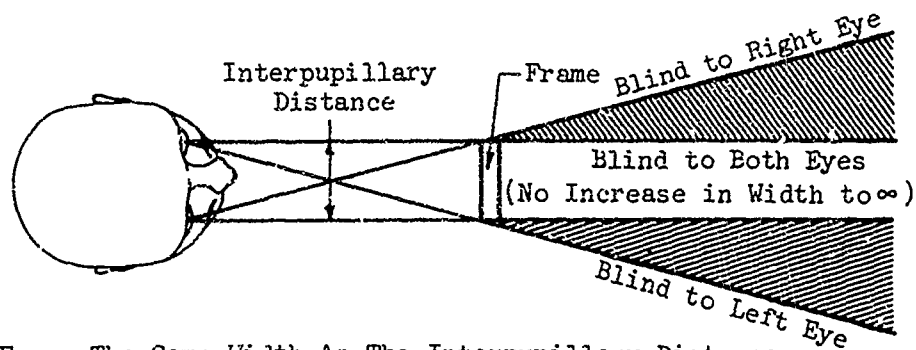
The importance of keeping obstructions as narrow as possible can be seen when one considers that large objects, such as an entire aircraft, can remain hidden behind structural members up to relatively close distances. Excessively wide structural members can therefore create potentially dangerous situations during combat, formation flying, nap-of-the-earth flight, and landing and ground operations.

It must be emphasized that obstruction width does not just include the structural framing member but also includes any opaque areas on the transparency itself that extend into the field of vision. This includes edge reinforcements, retention straps, and bus bars in the case of heated windshields.

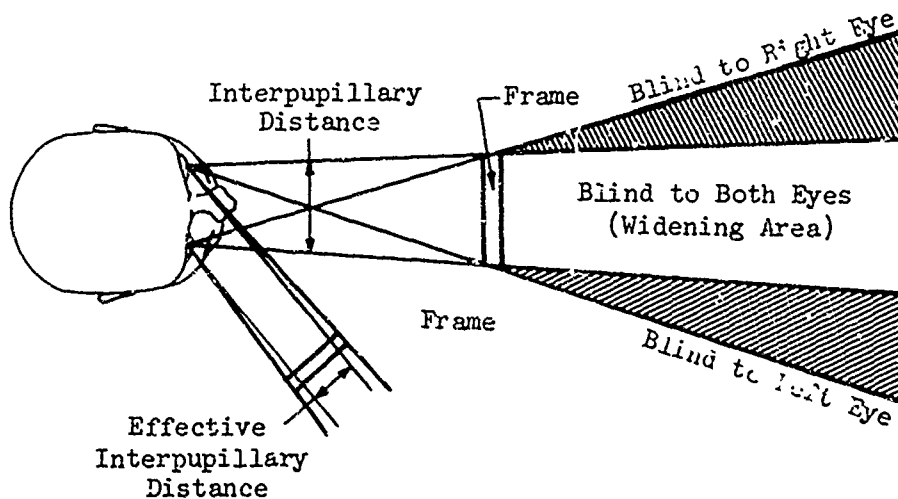
Reductions in projected areas can sometimes be obtained by canting or skewing the structural member, to align minimum dimensions with the lines of sight. This is illustrated in Figure 2-4.



A. Frame Narrower Than Interpupillary Distance



B. Frame The Same Width As The Interpupillary Distance



C. Frame Wider Than Interpupillary Distance

Figure 2-3. Areas Blocked by Windshield Frame Members That Are Narrower Than, Equal to, and Wider Than the Distance Between the Pupils.

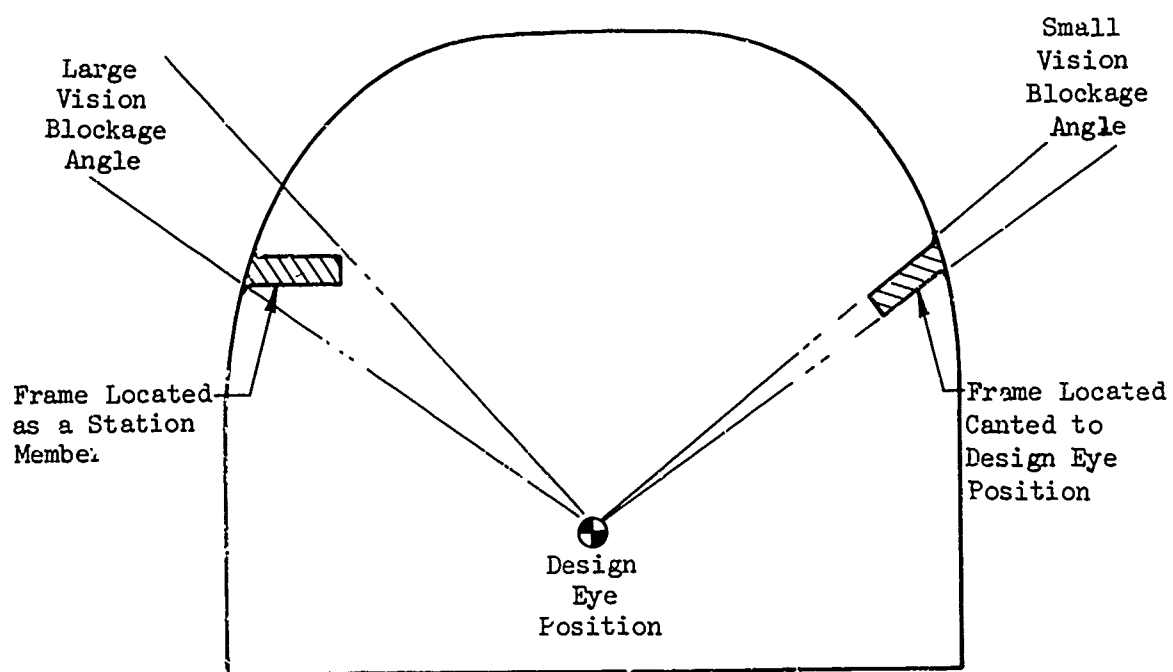


Figure 2-4. Effect of Canting Frames.

Bibliography

Grether, W. F., "Optical Factors in Aircraft Windshield Design as Related to Pilot Visual Performance," AMRL-TR-73-57, Aerospace Medical Research Laboratory, Wright-Patterson Air Force Base, Ohio, July 1973: - ...

Provines, W. F., and Kislin, B., "Transparencies Used in Military Aviation and their Effects on Vision," Journal of the American Optometric Association, Volume 42, Number 1, Jan. 1971.

3.0

TRANSPARENCY SHAPE

The size, shape and position of the transparent enclosure is determined early in the design stage because of its important relationship to the crew station and aerodynamic performance of the helicopter. This chapter provides information on the optical and structural effects of curvature and obliquity on enclosure geometry.

3.1 Optical Effects of Obliquity

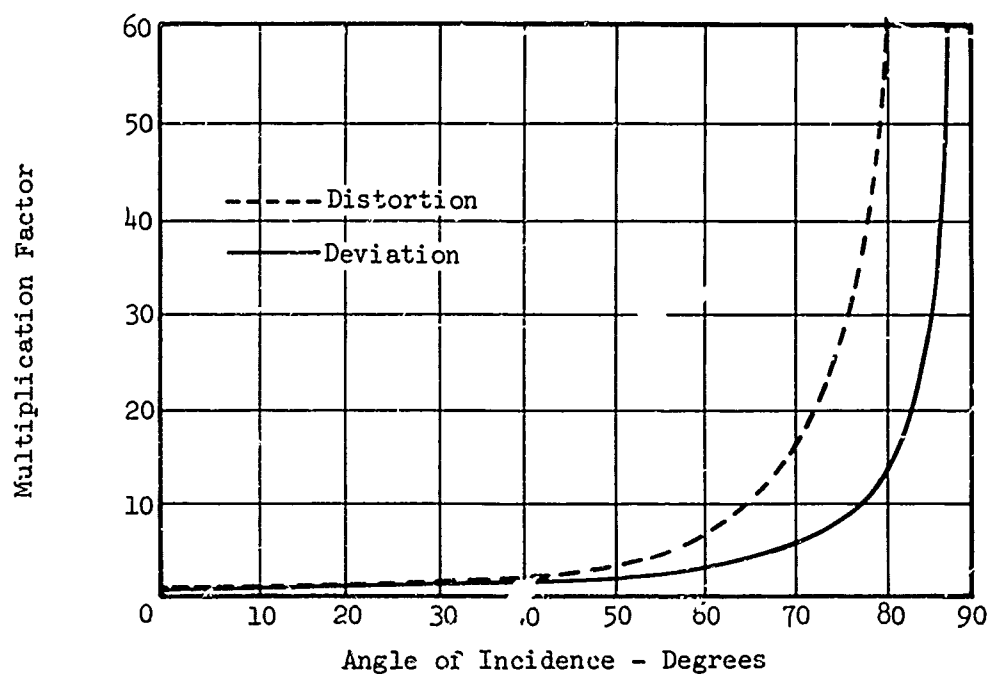
The angle of incidence is a very important parameter affecting the optical quality of transparency installations. Angle of incidence is defined as the angle between the line of sight and the normal (perpendicular) to the surface.

As the angle of incidence is increased, a number of optical effects occur that are unfavorable to vision. Some of these effects are caused by the increased thickness of the transparent material through which the light must pass. Other effects are due to greater portions of the light being reflected by the surfaces. However, most serious effects result from the magnification of deviations and distortions caused by nonparallelism and irregularity of the surfaces of the window.

Shown in Figure 3-1 are the changes in deviation and distortion resulting from angle of incidence. The curves show the multiplication factors by which the value at zero angle of incidence is increased. If, for example, a piece of glass caused a deviation of 10 minutes of arc at zero angle of incidence, this value would be increased to approximately 50 minutes of arc at 70°. For distortion, the curve is read in the same manner except that the measurement is in terms of maximum line slope change on a rectangular grid photographed through the test window.

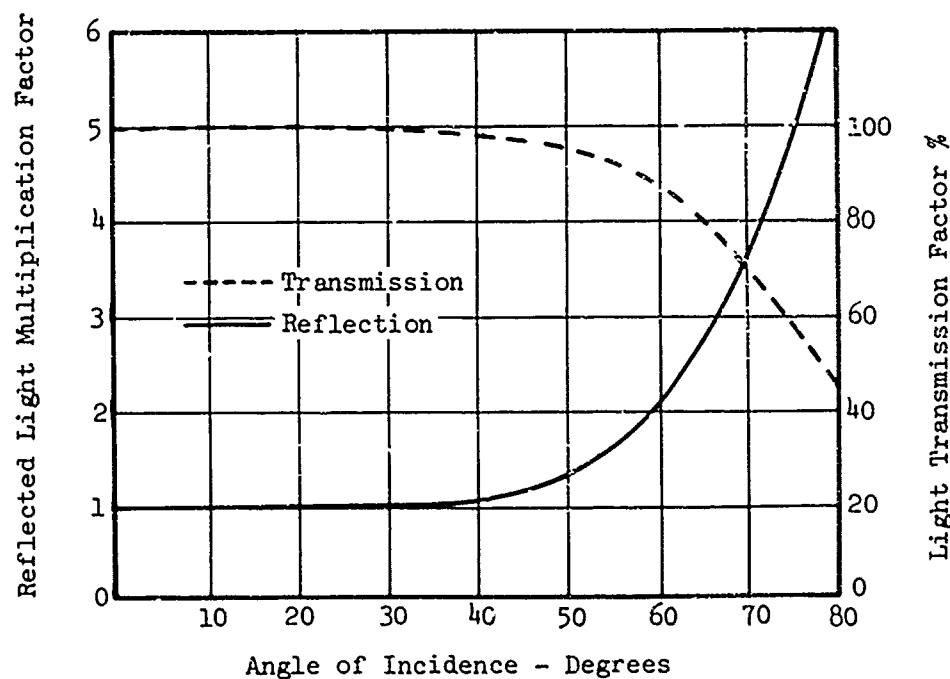
Similar data on the effects of angle of incidence are shown in Figure 3-2 for surface reflections and for light transmission through a window. The reflection data apply to the surface where light enters a window. The transmission losses shown in Figure 3-2 are due, in large part, to the light lost by reflection.

All four curves shown in Figures 3-1 and 3-2 have basically the same form and show that deviation, distortion, and transmission loss all increase rapidly as the angle of incidence exceeds 60°. For all curves the changes between 60° and 70° are greater than those between 0° and 60°. It is primarily from these data that the design standards were derived that set 60° as the maximum allowable angle of incidence for military aircraft windshields.



Data From Ref. 1

Figure 3-1. Effects of Angle of Incidence on Optical Deviation.



Data From Ref. 2

Figure 3-2. Effects of Angle of Incidence on Surface Reflections and Transmission Loss.

3.2 Optical Effects of Curvature

As shown in Figure 3-3, a light ray passing through a curved window at other than zero angle of incidence, with reference to the radius of curvature, will be given some angular deviation, even though there are no defects and the window surfaces are perfectly concentric. In addition to the angle of incidence, the amount of this deviation depends upon the radius of curvature, the thickness of the window, and the index of refraction. If a pilot's eye position is at the center of curvature for a circular windshield, he will experience no deviation caused by the curvature itself. Most likely, however, there will be some deviation from wedginess in the transparency since it is difficult to avoid such effects in curved panels.

The extent to which deviation can be affected by the radius of curvature is shown in Figure 3-4. This curve plots deviation as a function of the ratio of thickness to radius of curvature (thickness/curvature ratio) for various angles of incidence. The curve may also be used to calculate deviation for loft conic panels by approximating the radius of curvature tangent to the point being investigated. As seen from this curve, a combination of a thick window, a high angle of incidence, and a short radius of curvature can result in very high angles of deviation. To bring this curve into perspective, Table 3-1 lists values of acceptable optical deviation for different classes of transparencies. The values are tentative specifications obtained from Reference 4.

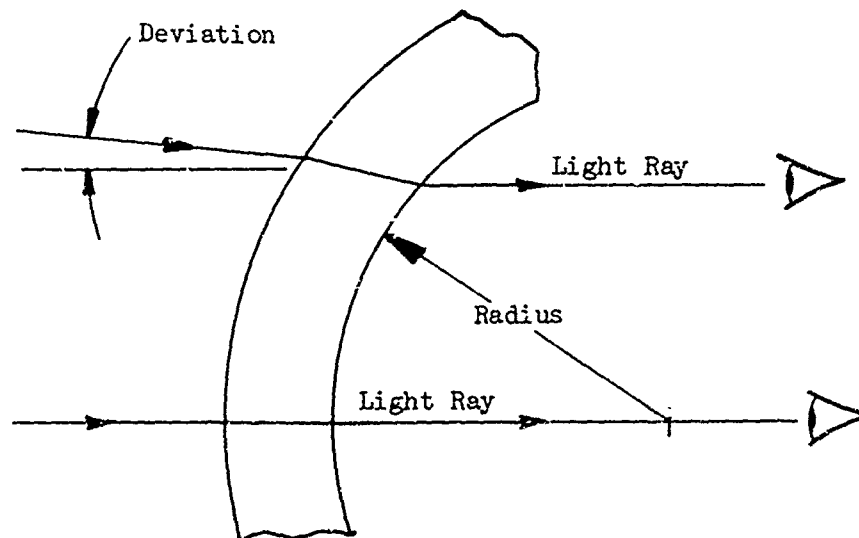
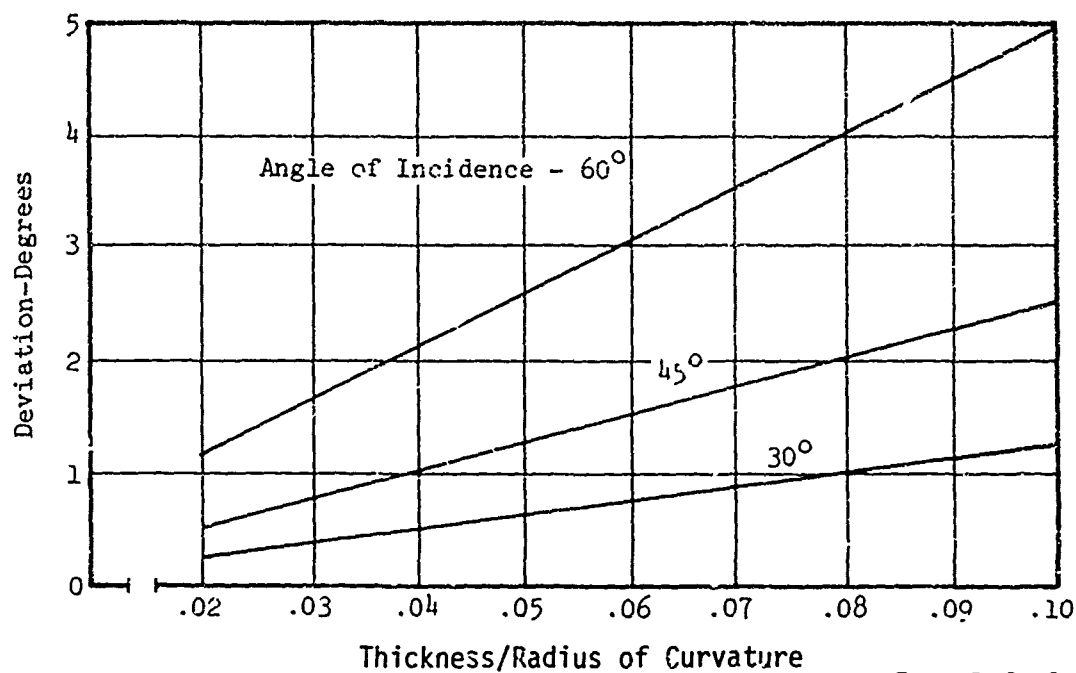


Figure 3-3. Optical Deviation Through a Curved Panel.

Binocular deviation limits are also presented to ensure that vision through the panel does not result in eye strain. Binocular deviation is the difference in deviation of two parallel incident rays, which, for this application, are considered to be 2.5 inches apart in a horizontal plane, this being the average spacing of the human's eyes.

TABLE 3-1. ACCEPTABLE VALUES OF OPTICAL DEVIATION

Type of Transparency	Optical Deviation (Minutes)	Binocular Deviation (Minutes)
Windshield gunsight area	± 1.8	-
Forward-facing windshield of the highest quality suitable for weapon aiming	5	10
Forward panels for non- combat aircraft	15	10
Side panels for non- combat aircraft, canopies	20	10



Data From Ref. 3

Figure 3-4. Effects of the Thickness/Radius of Curvature Ratio on Optical Deviation at Three Angles of Incidence.

3.3 The Effect of Curvature on Enclosure Geometry

Panel curvature has a direct bearing on the number and location of structural supports required in a cockpit enclosure. This stems from the fact that the primary loading condition used to design transparent enclosures is most often aerodynamic pressure loading. Since curved panels are the most efficient shapes used to support pressure loads, and flat panels are the least efficient, it should be expected that, for a given panel weight and pressure loading, the curved panels could be made larger than flat panels.

Although generalizations are difficult because of the number of variables involved, some practical size limitations for curved and flat helicopter transparencies have evolved over the years. Short-side dimensions for flat panels generally range from 18 inches to 24 inches, while the short-side dimensions for curved panels can be up to 30 to 40 inches. A classic example of how curvature can be used to minimize structural obstructions is the one-piece bubble enclosure used on the OH-13 helicopter (Figure 3-5).

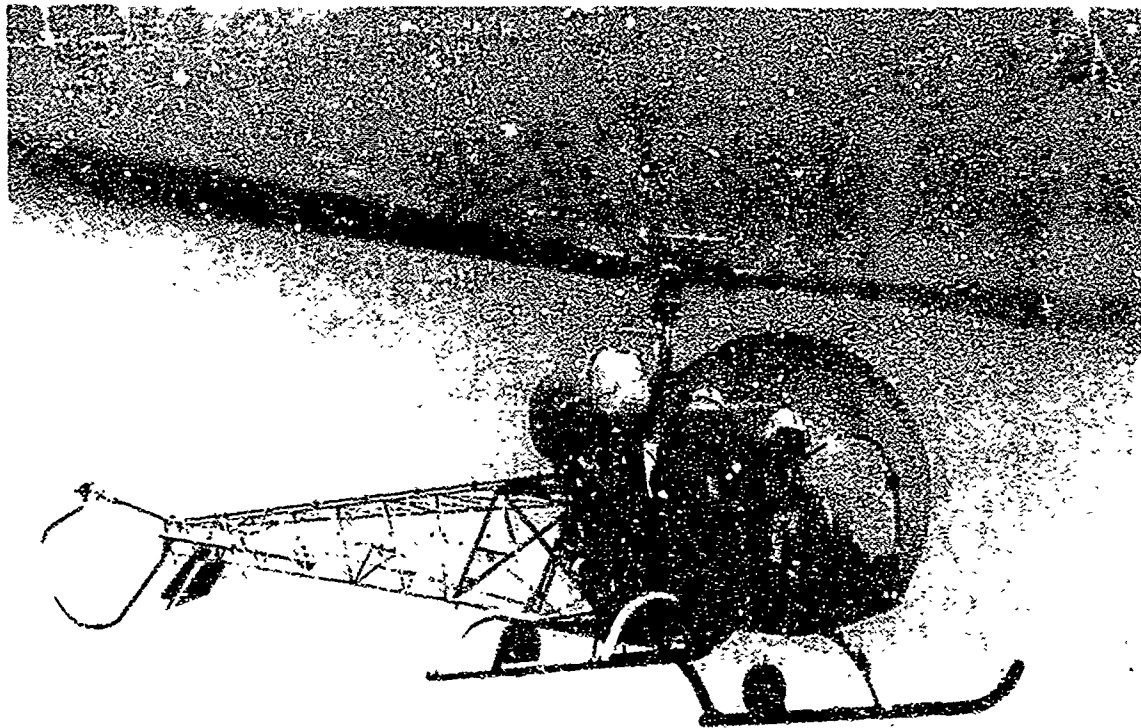


Figure 3-5. OH-13 Helicopter.

For side-by-side pilot helicopters, cockpits utilizing flat windshields as opposed to curved panels will invariably require additional support members. Figure 3-6 shows an example for a 68-inch-wide cockpit. On the left side of the illustration, two 29-inch curved panels are used to span the vision field from the center line of the aircraft to 45° aft of the pilot's design eye position. A total of three posts would be required for this installation; a center post, and left and right quarter posts.

On the right side of the illustration, flat panels are used to form the same basic shape. In this case, 29-inch flat panels would be excessively large, and the opening must be broken into two smaller 23-inch panels and a central 16-inch panel. An additional post is also necessary to support the smaller panels.

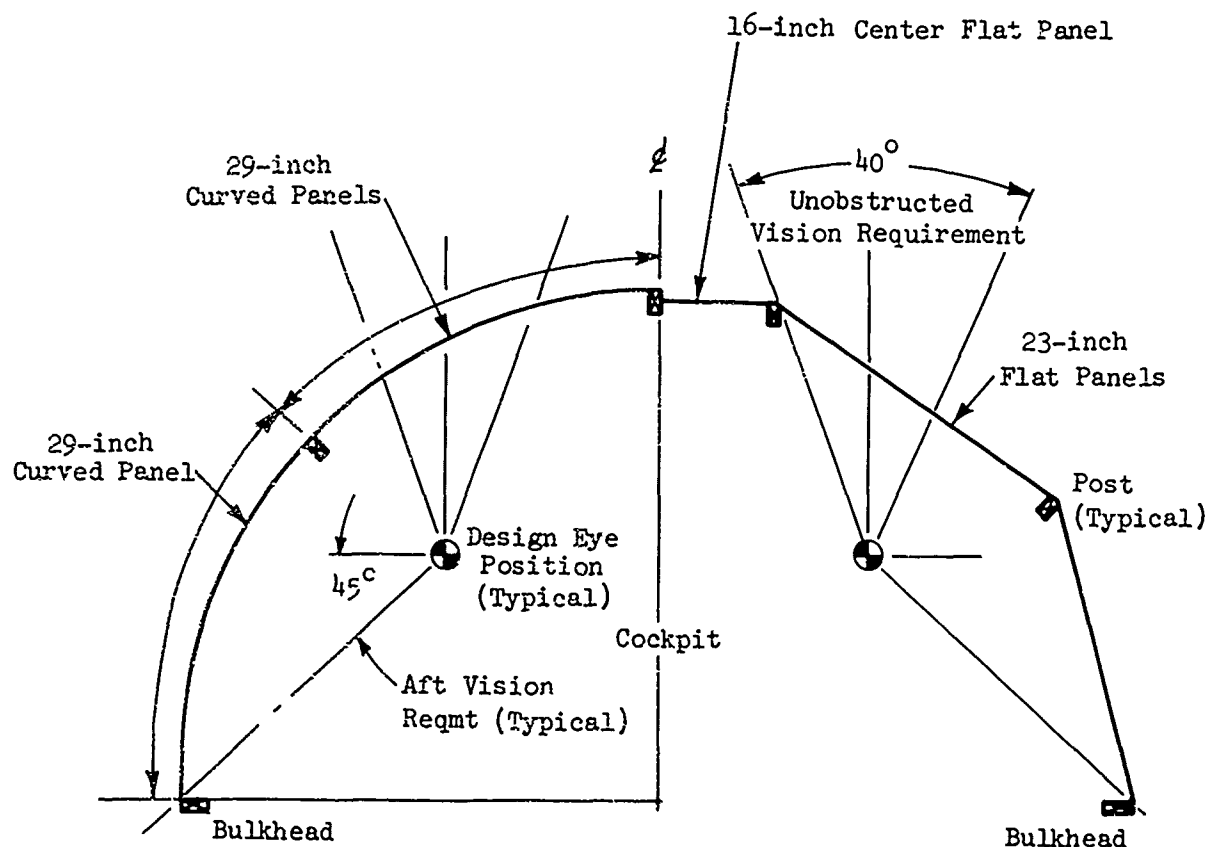


Figure 3-5. Flat Versus Curved Panel Geometry.

References

1. Grether, W. F., "Optical Factors in Aircraft Windshield Design as Related to Pilot Visual Performance," AMRL-TR-73-57, Aerospace Medical Research Laboratory, Wright-Patterson Air Force Base, Ohio, July 1973.
2. "Design Handbook," AFSC DH-2-1, Air Force System Command, Wright-Patterson Air Force Base, Ohio, Apr. 1973.
3. Holloway, R. A., "Survey of Optical Test Procedures for Aircraft Transparencies," LR-23771, Lockheed California Co., Sept. 1970, AD887715.
4. Corney, N. S., "Optical Requirements for Aircraft Transparencies," ARML-TR-126, Air Force Materials Laboratory, Wright-Patterson Air Force Base, Ohio, June 1973.

Bibliography

Wulfeck, J. W., et al, "Vision in Military Aircraft," WADC-TR-58-399, Wright Air Development Center, Wright-Patterson Air Force Base, Ohio, Nov. 1958.

Provines, W. F., and Kislin, B., "Transparencies used in Military Aviation and their Effects on Vision," Journal of the American Optometric Association Volume 42, Number 1, Jan. 1971.

Kohler, H., "Mathematical Method for Calculating the Optical Characteristics of Cone-shaped Cockpit Windscreens," Aircraft Engineering, June 1973.

"Plexiglas Handbook for Aircraft Engineering," Rohm & Haas Co., Philadelphia, Pa., 1951.

"Aircrew Station Vision Requirements for Military Aircraft," MIL-STD-850B, Department of Defense, Nov. 1970.

4.0

OPTICAL FACTORS

Good vision for flight crews is axiomatic. Aviators are carefully selected for maximum visual capability, and any significant degradation of this faculty will reduce flight safety and combat effectiveness. For Army helicopters, some of the tasks that require clear, uninterrupted vision through transparencies are listed below:

- Nap-of-the-earth flight
- Formation flight
- Detection and recognition of ground targets for navigation
- Reconnaissance, search and rescue
- Night flight
- Judging height and distances necessary for landing and takeoff
- Weapon guidance

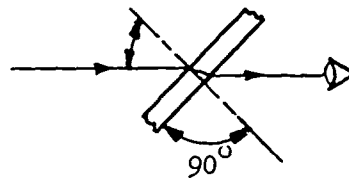
A certain amount of visual degradation will occur when looking through any transparent material. The minimization of such degradation should be the objective of all transparency specifications.

4.1 Definition of Optical Terms and Their Effects on Vision

Degradation of vision through transparencies can result from inherent optical properties of the transparent material, defects introduced during the manufacturing process, service-induced damage, or other factors determined by the geometry of the installation.

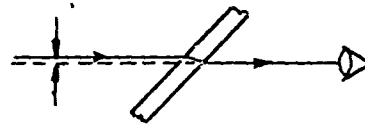
To provide a basis for the material that follows, this section describes the optical effects that will be discussed and shows how they interrelate with each other. For purposes of illustration, the effects are considerably exaggerated. All the effects are illustrated for simple, single-layer windows, rather than the laminated transparencies normally used in windshields. Each layer of a laminated transparency can contain any or all of the optical effects shown.

A. Angle of incidence



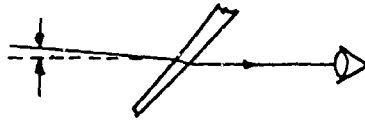
The angle of incidence is measured with respect to the pilot's line of sight and a line normal to the transparency surface. Optical defects are magnified as a function of increasing angle of incidence.

B. Displacement



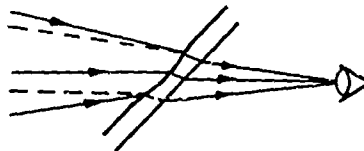
In passing through a window with parallel surfaces, light rays are bent and displaced as shown above. The displacement is zero for 0° angle of incidence and increases as the angle of incidence, thickness, or index of refraction is increased. The displacement is linear and usually measured in fractional inches. It does not increase with distance, and the effect on pilot vision is not significant.

C. Deviation



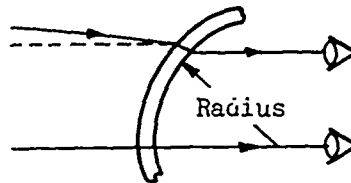
In passing through a window with nonparallel (wedge) surfaces the path of light is deviated angularly as shown above. The amount of deviation is expressed in terms of the angular change (degrees, minutes, or seconds). Deviation increases with the index of refraction of the window material, the angle between the surfaces, and the angle of incidence. Deviation causes objects to be seen at other than their true directions from the observer.

D. Distortion



If a window has minor variations in thickness or in the parallelism of the two surfaces, there will be variations in deviation for different parts of the window. This effect will cause straight lines to appear wavy and the shapes of objects to appear distorted. As moving objects are seen through different parts of the window, their motion and shapes will change irregularly. Distortion increases with the index of refraction and the angle of incidence. Also, curved windows normally cause much more distortion than flat windows.

E. Curvature

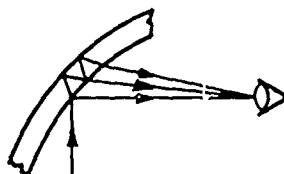


Light rays passing through a curved transparency at 0° angle of incidence to the radius of curvature will enter and exit with no deviation from the normal. For all other angles of incidence relative to the radius of curvature, the light will exit with some deviations, even though the surfaces are perfectly concentric. The deviation increases with the angle of incidence, the index of refraction, and the thickness of the transparency; it decreases with the radius of curvature.

F. Binocular Deviation

If there is a curvature in the horizontal plane, the deviation due to curvature will be different for the two eyes (as shown in E in exaggerated form), since they see through different parts of the curved window. This causes an effect called binocular deviation. It is believed that the eyes can readily adjust to small amounts of binocular deviation. However, when the collimated image of a gunsight or head-up display is superimposed over the view through a curved windshield, the binocular images may not be compatible. Curved windows are more difficult to manufacture than flat windows; therefore, they are more likely to have defects causing deviations and distortions, which will also cause binocular deviation effects. These will vary for different parts of the windshield.

G. Internal Reflections



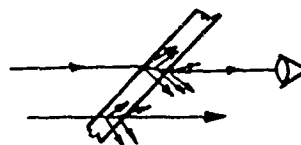
Light or bright objects inside the crew station can be reflected into the pilot's eyes from the inside surface of a window. Under many circumstances, ground lights, such as lights from a city, will also reflect from the inside windshield surface into the pilot's eyes. Such internally reflected images will appear superimposed over the area seen through the windshield and therefore will obscure vision for objects outside. These internally reflected images are normally troublesome only at night. Under certain conditions these reflections may be multiple, as in the case of multiple images discussed below.

H. Multiple Images



When light passes through a window, part is reflected at each surface as it enters and leaves. The proportion reflected is minimal at 0° angle of incidence, and increases to 100% as the angle approaches 90° . Under some optical conditions, the reflections inside the transparency may result in one or more secondary images, as illustrated above. For a laminated panel, there may be image reflections at each lamination. Since these secondary or ghost images are dimmer than the primary image, they are normally seen and become a problem only at night. The optical conditions most likely to produce multiple images are curved or flat panels with wedginess, combined with high angles of incidence. A metallic coating on the transparency increases the intensity of the secondary images. Such multiple images will occur with flat panels only if there is sufficient wedginess to reflect the displaced image(s) back to the observer's eyes, rather than along a path parallel to the exit path of the primary image. Multiple images can normally be avoided by use of high-quality flat panels.

I. Haze



As light enters or passes through a window, some of the light may be scattered or diffused, and may appear as haze or fog in the window. Haze is generally defined in terms of the percent of light scattered and therefore lost in passage through the window. The haze effect is increased as the angle of incidence is increased.

J. Transmission

This is defined as the intensity of light emerging from the transparency compared to the intensity of the light incident upon it. Losses are due to absorption within the materials involved and reflections at the various interfaces where there are changes of refractive index. High light transmission is of particular importance when flying under conditions of low light or when observing objects under conditions of low contrast.

K. Resolution

Resolution refers to visual acuity, or the ability of the observer to resolve fine detail. Under typical daytime conditions, using a rough rule of thumb, a person with normal vision can resolve lines separated by 1 minute of arc. A windshield may cause some loss of resolving power, particularly if dirty, scratched, or of poor quality material. Haze and reduced transmission are the major factors affecting visual acuity.

L. Minor Optical Defects

Minor optical defects, such as lint, dust, dirt particles, and bubbles, can exist within transparencies. Such inclusions can be distracting to the flight crew and mistaken for distant air traffic.

M. Cracks

Crack patterns resulting from structural failure or impact damage can interfere with vision due to prismatic effects on the light passing through the cracks. The severity of the vision blockage is primarily a function of crack density, obliquity, and the thickness of the transparency.

N. Dither

Transparency dither or shaking can occur as a result of aerodynamic or structure-borne vibrations. Dither is noticeable by the effects that it has on reflected or refracted light. This motion can cause optical distortions and reflections to become more pronounced, and thus become objectionable to flight crews.

4.2 Optical Distortion

Optical distortion is a result of nonuniformities in the material thickness or in the index of refraction. This causes rapid changes of deviation with changing lines of sight. Changes of the refractive index may be caused by temperature gradients.

4.2.1 Types of Distortion

Distortion can result in the following visual aberrations to objects viewed through the transparency:

1. Displaced
2. Deformed
3. Wavy
4. Contracted
5. Magnified
6. Locally Blurred

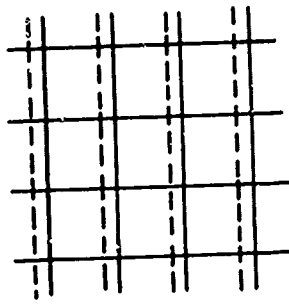
It is a common practice to evaluate distortion by means of photographs of square grid patterns taken through the transparency. Figure 4-1 shows how the first five preceding defects would appear in grid photographs. The sixth defect, local blurring, is caused by small depressions, such as bull's eyes. A bull's-eye defect is shown in a grid photograph in Figure 4-2, and the appearance of the same defect on an outside scene is shown in Figure 4-3. Combinations of defects are also possible.

4.2.2 Causes of Distortion

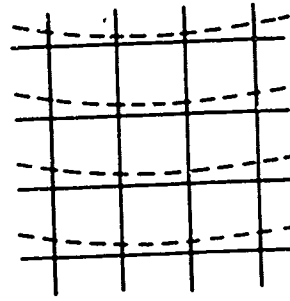
Optical distortion results from nonuniform material thickness or index of refraction. Transparent sheet materials procured to military specification have stringent optical deviation requirements and will be distortion-free if used without subsequent processing. However, operations such as forming invariably cause the material to thin out, and markoff from molds can create tiny surface depressions known as orange peel. Likewise, in producing curved multiple-ply transparencies, perfect congruence of facings is difficult to achieve during lamination, and thickness variations result.

Reworked transparencies in which scratches are blended out by material removal create local regions of distortion. Fluctuations in the thickness of transparent coatings can also bring about distortion.

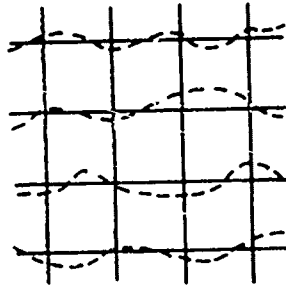
Indices of refraction for interlayer materials are temperature sensitive. Therefore, variations in temperature across the surface of a heated windshield will create distortion. This distortion assumes its worst form at low ambient temperatures when heat power demands and temperature gradients reach their peak values.



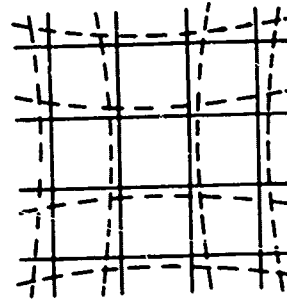
a) Type 1 - Line Displacement



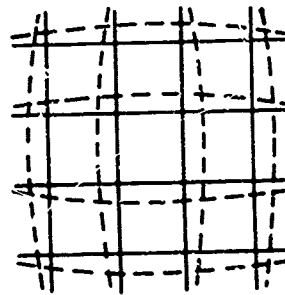
b) Type 2 - Curvature



c) Type 3 - Variable Displacement



d) Type 4 - Contraction (Pin Cushion)



e) Type 5 - Magnification (Barrel Distortion)

Figure 4-1. Five Types of Optical Distortion.

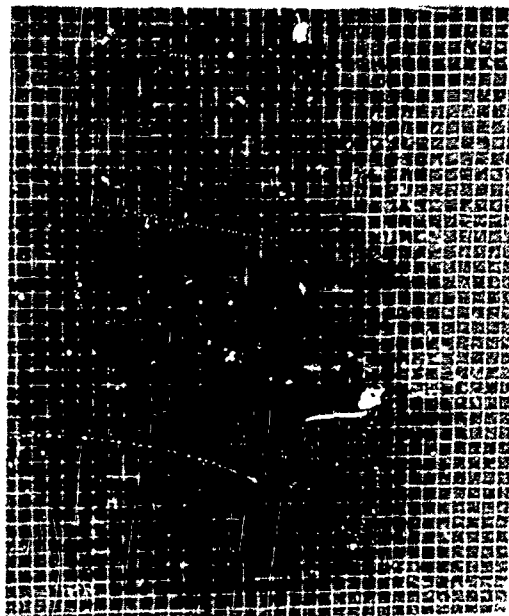


Figure 4-2. Bull's-eye Distortion of a Grid Board Photo.



Figure 4-3. Bull's-eye Distortion of an External Scene.

Discontinuities in a heating medium, such as deletion lines in a three-phase conductive coating, also give rise to distortions, since they are unheated. The localized effects on optical properties brought about from wire element heating systems are particularly severe and have led them to be termed "wobble-wires".

4.2.3 Effects of Optical Distortion

In the ordinary course of flying, minor optical distortions can be tolerated. Large distortions, however, can be expected to cause piloting errors and to annoy and fatigue the pilot, particularly after long periods of flight.

Some of the important cues in close-range distance judgement are binocular vision effects. These cues are based on the fact that the two eyes are separated as they view an object, and objects viewed with both eyes are viewed from slightly different angles and form slightly different images on the two retinas. Thus, distortion effects that cause convergence or divergence of the binocular lines of sight can cause errors in estimating distance.

External scenes appear to undulate when scanned through transparencies containing regions of local distortion. This effect is particularly noticeable along interfaces between curved and flat panels, where objects will appear to jump as they traverse the interface. Such defects can be a constant source of annoyance to flight crews, accelerate fatigue, and in extreme cases cause motion sickness.

4.2.4 Evaluating Distortion

There are several basic methods used to qualify the optical distortion of aircraft transparencies. Common to all methods is a setup similar to that shown in Figures 4-4 and 4-5 in which photographs are taken of a square grid pattern.

The distortion in the photograph can be quantified by measuring the slope of the grid lines as shown in Figure 4-6. This is a relatively simple method, since severe distortion can be readily detected and measured.

Table 4-1 lists typical grid slope values for helicopter transparencies. It should be noted that relaxation of windshield distortion requirements is sometimes necessary at specific locations within a panel because of manufacturing limitations.

TABLE 4-1. TYPICAL GRID SLOPES FOR HELICOPTER TRANSPARENCIES

Transparency	Grid Slope
Windshields	1:12
Other Cockpit Windows	1:8
Cabin Windows	1:4

A more precise method for measuring distortion uses calibrated grid boards to determine changes in optical deviation between grid lines. Such procedures entail measuring distances between grid lines, and are generally more laborious.

Differential methods that compare double-exposure photographs of grids taken through sample panels and master control panels are also used, but tend to rely on subjectivity.

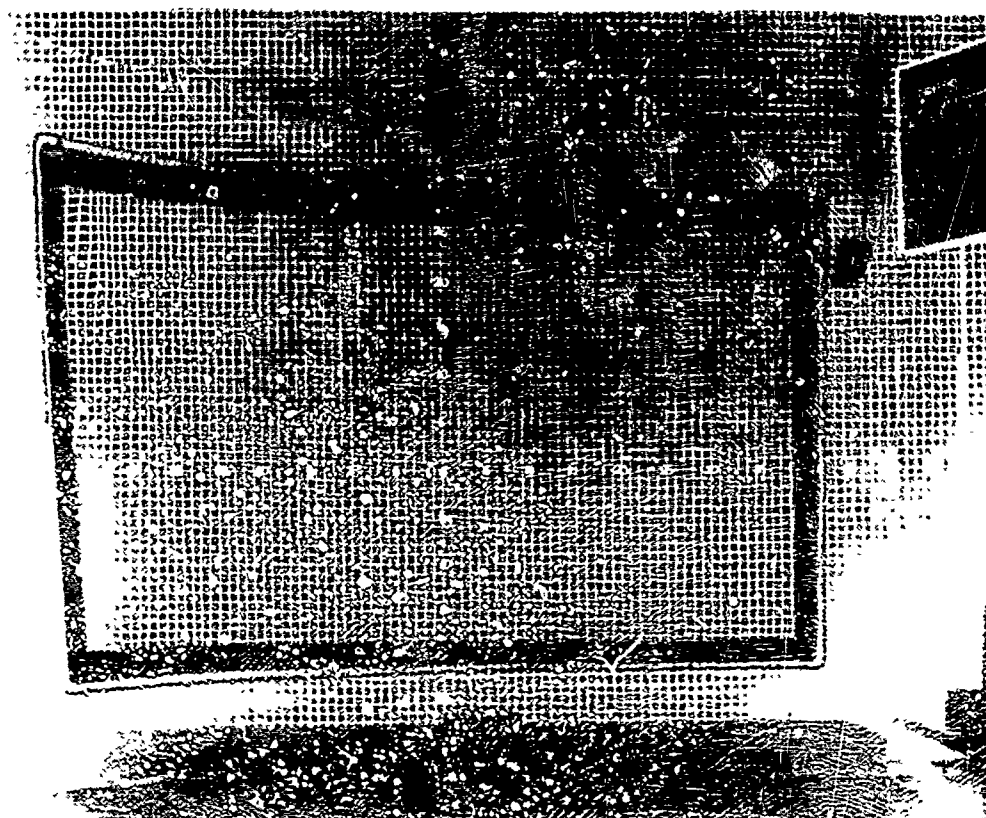


Figure 4-4. Optical Grid Photograph

4.3

Haze

A certain amount of haze is indigenous to most transparent materials. This haze occurs as a result of light being scattered by microscopic particles within the material. Such haze is usually

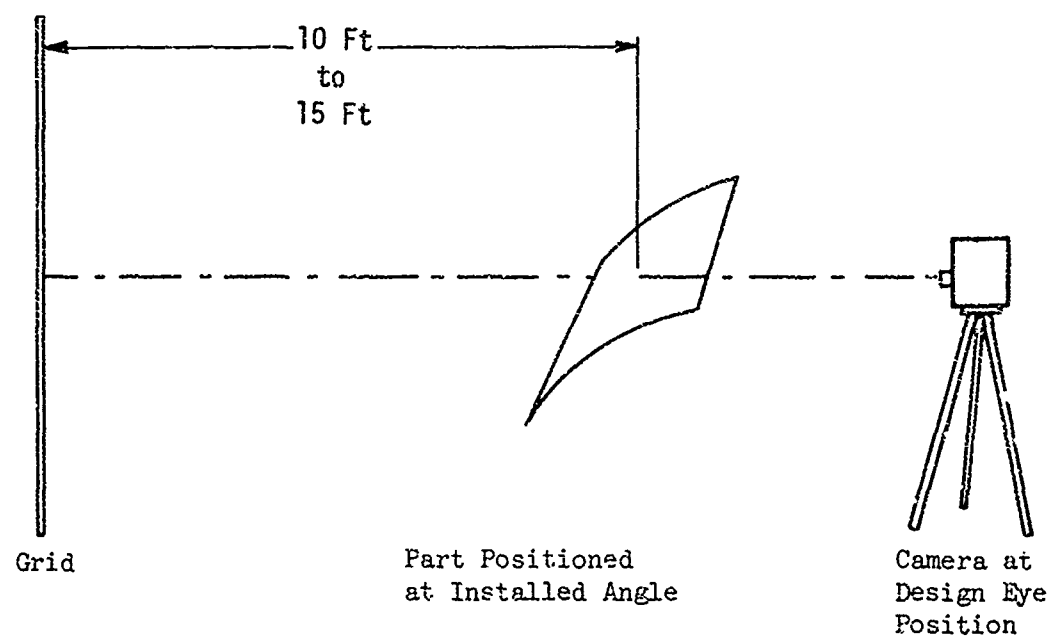
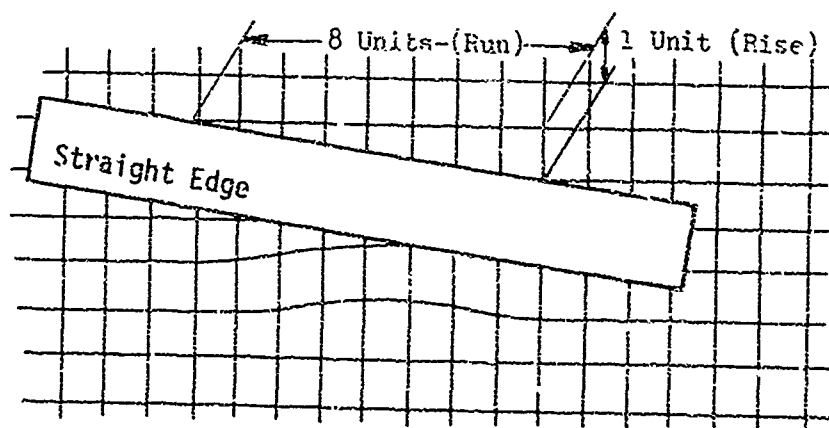


Figure 4-5. Typical Setup for Taking Grid Photographs .



In the Case of the Distortion Shown: Slope = Rise Over Run = 1:8

Figure 4-6. Measurement of Distortion.

minimal and should not exceed 2.5% for new materials. Objectionable haze occurs after the component is placed in service and can be created by a number of circumstances.

Internal haze can be caused by material transformations due to weathering, moisture absorption, or chemical attack. Surface haze can be caused by dirt, scratches, abrasion, or crazing.

The most serious consequence of haze is the transformation of the transparency into a sheet of glare when bright light strikes the surface at certain critical angles. The resultant loss of vision, which can be total in some cases, is a function of the haze level, external visibility conditions, and intensity and angle of incidence of the light source. Light sources can be direct sunlight during the day or miscellaneous illuminants during the night.

Unfortunately, the point at which maintenance actions are required because of excessive haze is made by operating personnel based on subjective opinions. Field surveys have indicated that abraded transparencies will be "lived with" until a level of about 15% haze is reached.

4.4 Light Transmission

Some light is always lost by absorption within transparent materials. For clear materials this is normally a small percentage of the total light and is a characteristic of the material and the angle of incidence. An additional quantity of light is lost by surface reflection. This occurs wherever there is a change in the index of reflection and will increase as a function of incidence angle.

For special applications, tinted materials and electrically conductive coatings are sometimes incorporated into the transparency. Tinted materials contain colorants that increase the absorption for specific wavelengths of light and have lower overall light transmission than clear materials.

The electrical conductive coatings used for windshield heating or radar reflective purposes are highly reflective and decrease overall light transmission by reflecting away a portion of the incident light. Further, if polarized light from the sky or from a runway falls upon the transparency, a change in plane or polarization may take place and dark patches may appear. If viewed obliquely, these patches interfere with vision.

During normal daylight conditions, reduced light transmission is quite tolerable, and, on a bright sunlight day, is even desirable. However, under poor lighting conditions, such as dusk, twilight, heavy overcast, and night time, the losses affect visual acuity and may be critical.

The effects of transmission losses can be estimated from human visual acuity data, such as shown in Figure 4-7. Also shown is the reduction in visual sighting range which results from the reduced acuity at the lower luminance levels. This curve shows that at daytime background luminance levels, 1.0 millilamberts and above, the luminance level has very little effect on visual acuity and visual sighting range. However, as luminance is reduced to nighttime levels, visual acuity falls off quite rapidly. Thus, during low ambient light conditions, any losses in transmission could be expected to reduce visual acuity and sighting range.

Recommended standards for light transmission are presented in Table 4-2.

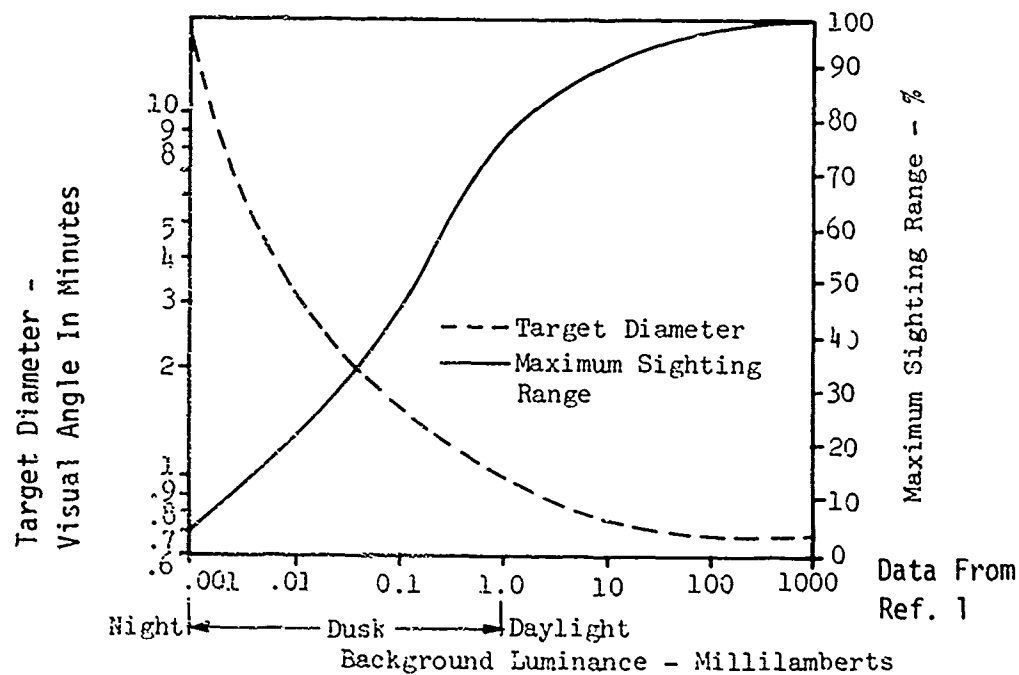


Figure 4-7. Effect of Luminance Level on Minimum Perceptible Visual Acuity and Maximum Sighting Range.

TABLE 4-2. RECOMMENDED LIGHT TRANSMISSION VALUES (%)

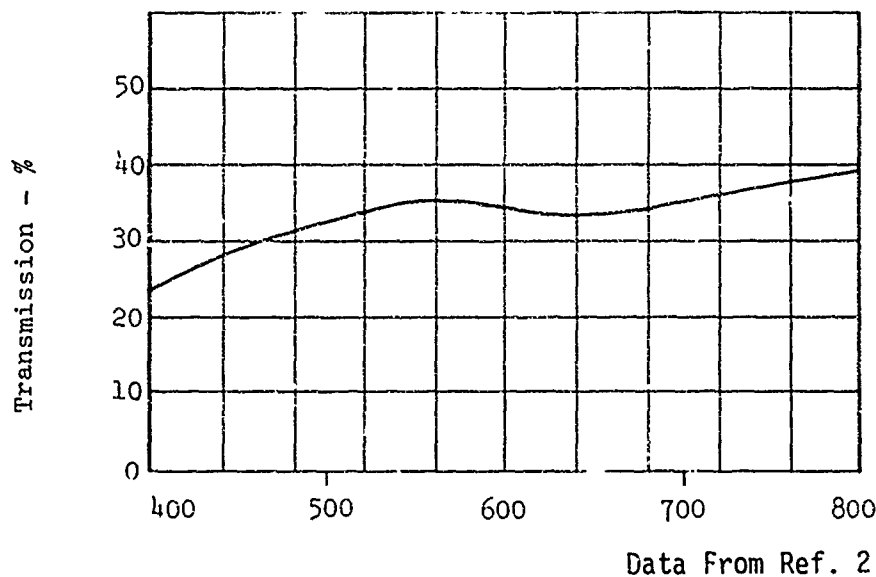
Rank	Windshield Incidence Angles (degrees)					Canopies
	0	55	60	65	70	
Highly Desirable	66	71	74	83	99	89
Acceptable		66	69	78	93	83
Minimum	60	64	67	75	89	77

Data from Ref. 1

4.5

Tinted Transparencies

Tinted transparent plastics have been used in helicopter overhead windows and canopies to reduce eye strain from bright sunlight and to reduce cockpit temperatures from solar radiation. Depending upon the manufacturer, roof windows have been tinted green/grey or blue with overall light transmissions falling in a range between about 16% and 76%. Figure 4-8 shows a typical light transmission curve for a green tinted material.



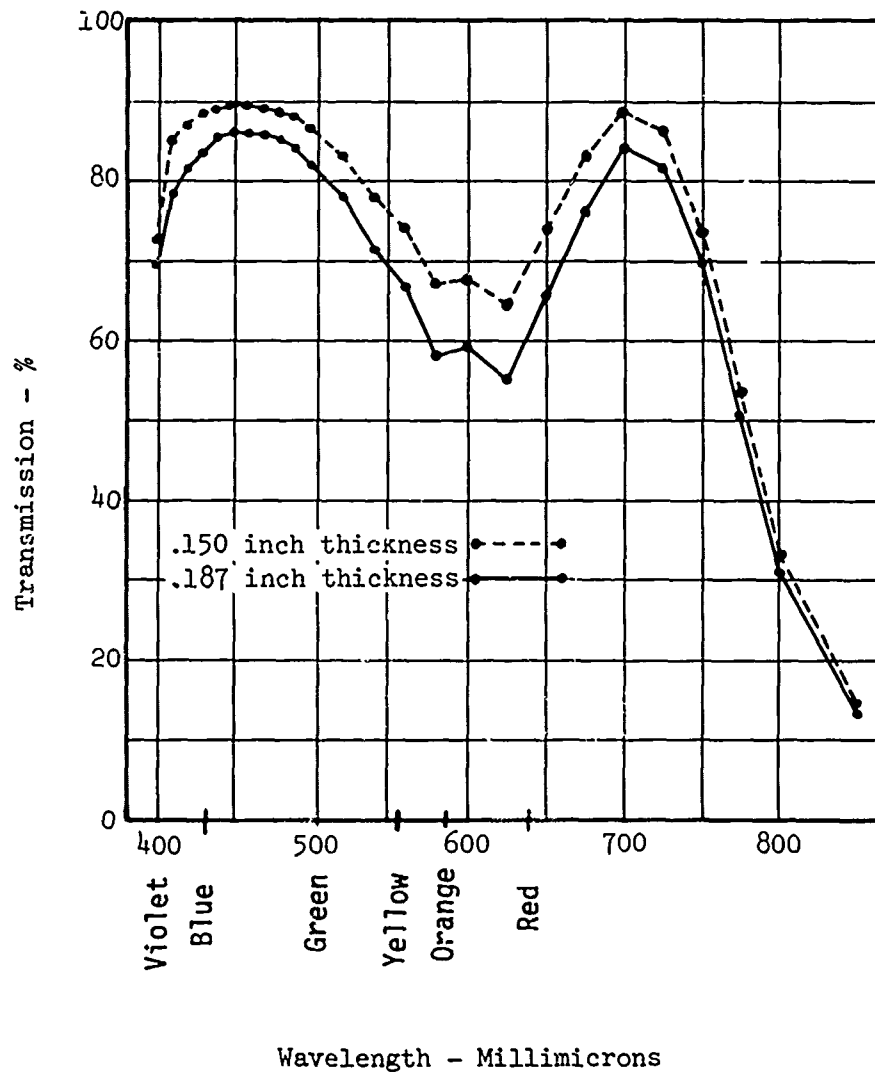
Wavelength - Millimicrons
Averaged Spectral Transmittance is 27%

Figure 4-8. Spectral Transmittance for Green/Grey Acrylic Plastic.

Pilots generally find such windows comfortable during flight in clear weather but complain when ambient light is reduced. Therefore, when good overhead visibility is required as part of a helicopter mission, tinted roof windows become undesirable, and an alternate means of reducing the intensity of incident sunlight, such as tinted helmet visors, is suggested.

Figure 4-9 shows a light transmission curve for a blue-tinted acrylic that has been used in a helicopter windshield and canopy to reduce cockpit heat loads caused by solar radiation. Due to its absorption and transmission characteristics, a pilot would be less able to see the red warning lights of other aircraft through this material, especially in marginal visual flight regulation (VFR) conditions. Furthermore, it is a physiological fact that blue light is scattered more in the eye than longer wavelengths,

and that the eye is myopic for blue light. Thus, the blue-tinted transparency would tend to distort a pilot's depth perception so that objects would seem to be farther away than reality.



Data from Ref. 3

Figure 4-9. Spectral Transmittance of Visible Wavelengths for Blue Acrylic Plastic.

4.6 Minor Optical Defects

During the manufacture and processing of transparent materials, imperfections, such as bubbles or foreign matter, can become imbedded within the material. At normal viewing distances (1 to 3 ft), particles smaller than 0.005 inch are not visible. Larger defects can be detected by the eye and mistaken for distant air traffic, which is an obvious distraction to air crews. Unfortunately, there is little quantitative data available on this subject, and standards are based on historical values used in material specifications.

The following are representative of maximum limits:

- a) Any defects under .032 inch shall be disregarded. The quantity is not limited to number, unless they form a tight pattern which would interfere with normal vision.
- b) Seeds, bubbles, small cullet, and dust particles from .032 to .093 inch in maximum dimension with no more than four of these within a 6-inch-diameter area.
- c) There shall be no defects greater than .093 inch in maximum dimension in the daylight opening of the transparency.
- d) Defects over .063 inch are not allowed within 2 inches of each other.
- e) Lint, very fine hair, fibers, and similar inclusions up to 3 inches in length are permissible provided they do not impair, obscure, or reduce visibility.
- f) The total number of optical defects for the applicable panel size and thickness shall not exceed the sum of the totals permitted by specification MIL-P-5425, MIL-P-8184, MIL-P-25690, MIL-G-35667, or MIL-P-83310 for the individual glass or plastic plies plus the allowable number specified in Table 4-3 for each interlayer.

TABLE 4-3. ALLOWABLE MINOR DEFECTS IN EACH INTERLAYER

Area of Daylight Opening (sq ft)	Maximum Number of Minor Defects per 0.120 Inch or Fraction Thereof in Interlayer Thickness
-------------------------------------	--

0.00 through 4.00	4
4.01 through 6.00	6
6.01 through 8.00	9
8.01 through 10.00	12
10.00 through 15.00	19
15.01 through 20.00	26
Over 20.00	As Specified

4.7 Cracks

Transparencies that are designed with redundant load paths or materials that possess good fracture toughness can suffer cracking and still maintain structural integrity. In such cases, the decision to abort a mission is based on residual visibility through the cracks, assuming that the fear of imminent cave-in does not take precedence.

A sparse crack pattern such as that shown in Figure 4-10, although disconcerting, does not interfere significantly with vision, whereas a dense pattern similar to that shown in Figure 4-11 can obliterate visibility. For glass, crack density is a function of temper, thickness, and stress intensity.

The effect of crack density is illustrated in Figure 4-12, where the time required to identify figures is plotted against particle density. From this data, 1,000 particles per square foot is considered a threshold for satisfactory vision.

The angle of incidence is important because, as the angle is increased, the spaces between the cracks are reduced and more of the lines of sight must pass through the edges of the cracks, which creates prismatic deviations that reduce visibility. This effect is illustrated in Figure 4-13.

4.8 Reflections

All transparent materials reflect light. External sun reflections from windows create glint which can reveal otherwise undetected helicopters to enemy forces during combat. Internal cockpit reflections are distracting to flight crews and can hinder safe flight.

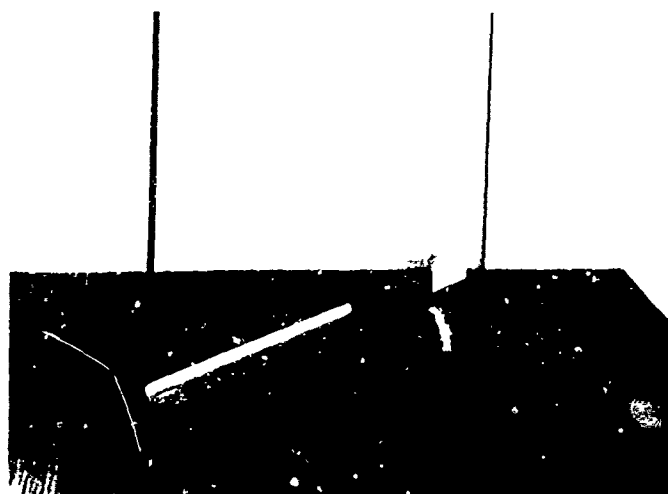


Figure 4-10. Sparse Crack Pattern.



Figure 4-11. Dense Crack Pattern.

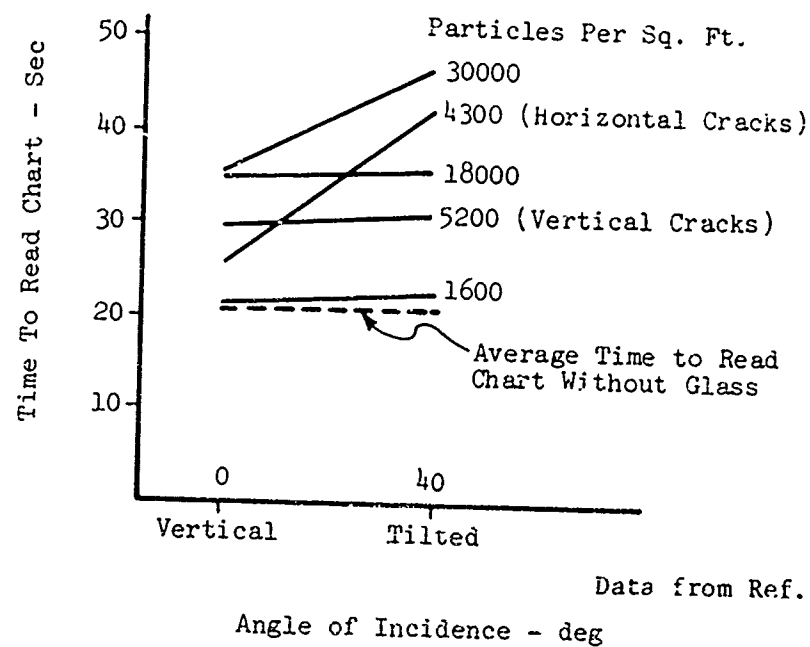


Figure 4-12. Effect of Crack Density on Visual Response.

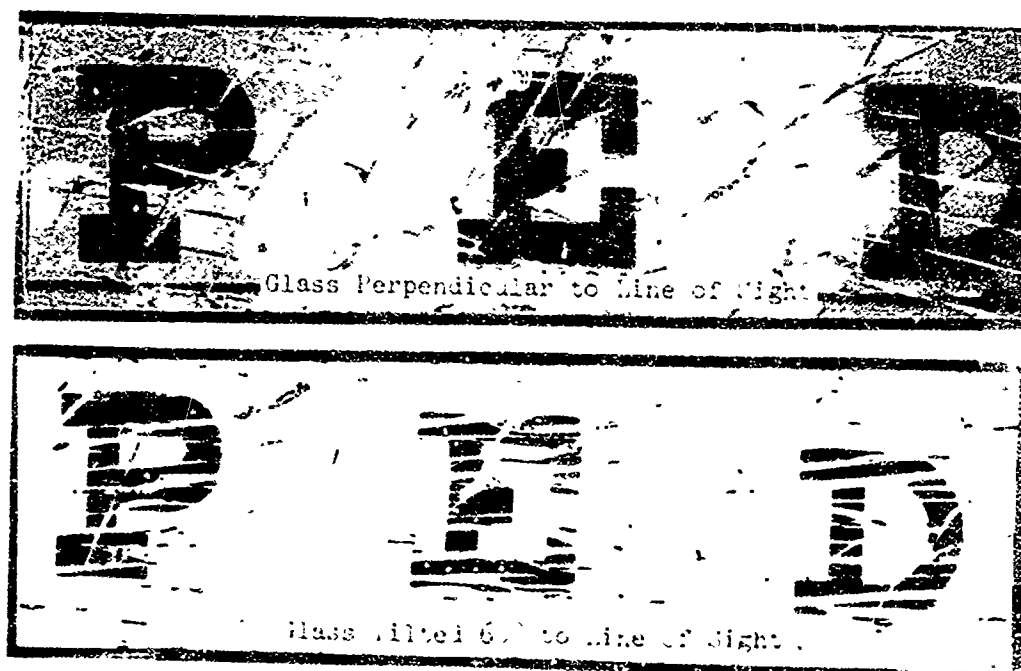


Figure 4-13. Horizontal Cracking vs. Angle of Incidence.

In bright daylight, windshield and window reflections are rarely discernable by pilots. However, in darkness, when the intensity of reflected interior lights is considerably greater than the intensity of the ambient outside light, reflected images become visible.

The images reflected from flat transparencies are sharper than the images reflected from curved transparencies. At night the reflected images from the flat panels cause difficulty in distinguishing the difference between real and reflected objects.

Reflections of interior lights can be prevented by suitable shields or by orienting transparencies to reflect light away from the crew. These concepts are illustrated in Figure 4-14 and follow from the law of reflection, which states that the angle of incidence is equal to the angle of reflection. The latter technique may sometimes create a conflict with the geometry needed to reduce external glints, and trade-offs may be required.

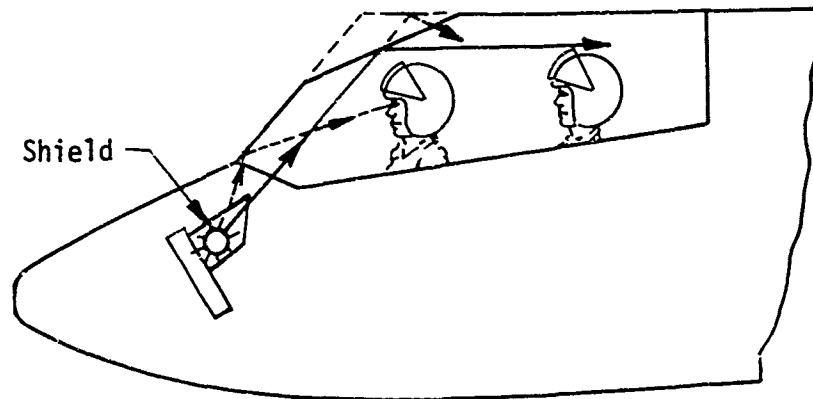


Figure 4-14. Transparency Oriented to Reflect Instrument Lights Away From Rear Pilot.

Reflection problems due to interior light sources are normally resolved during lighting mockup studies.

Exterior light sources are more difficult to control because offending light can come from virtually any direction. Figure 4-15 shows how rays of light from an exterior source below the helicopter can enter through one window and reflect off another into the pilot's eye. The pilot would not necessarily know where it was coming from, since the light would appear to be in front of the windshield. Night curtains are one means of preventing distracting light from entering cockpits through lower windows, but this method has obvious disadvantages in restricting visibility. Proper window placement is the more effective method.

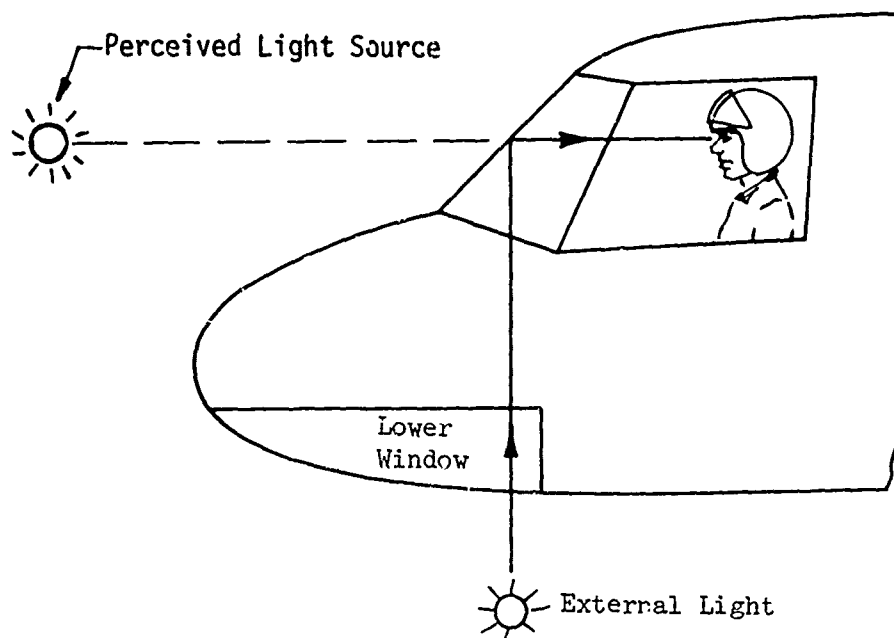


Figure 4-15. Windshield Reflections From Light Entering Cockpit Through Lower Window.

4.9 Multiple Images

Multiple images are another type of distracting reflection that is particularly troublesome at night. For example, if a windshield design is prone to form multiple images, a pilot viewing runway lights through it at night will have difficulty in discerning the real lights from the reflected lights.

The phenomenon occurs because some light is always reflected from surfaces separating transparent materials of dissimilar indices of refraction. Thus, for the monolithic transparency shown in Figure 4-16, there are two surfaces that will reflect light. For laminated transparencies containing conductive coatings, there will be reflections from the coating as well as the inner and outer surfaces (Figure 4-17).

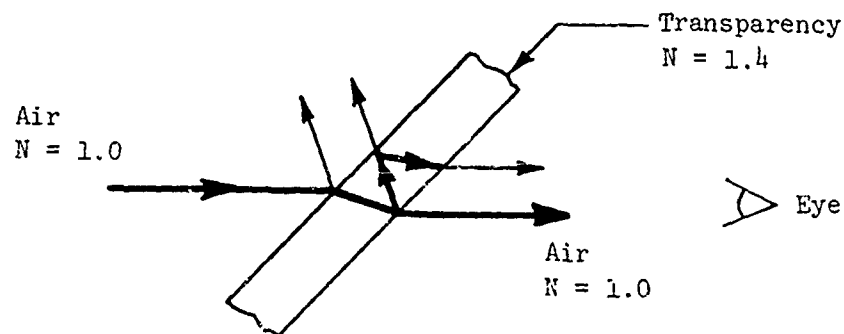


Figure 4-16. Multiple Reflections From Monolithic Transparency.

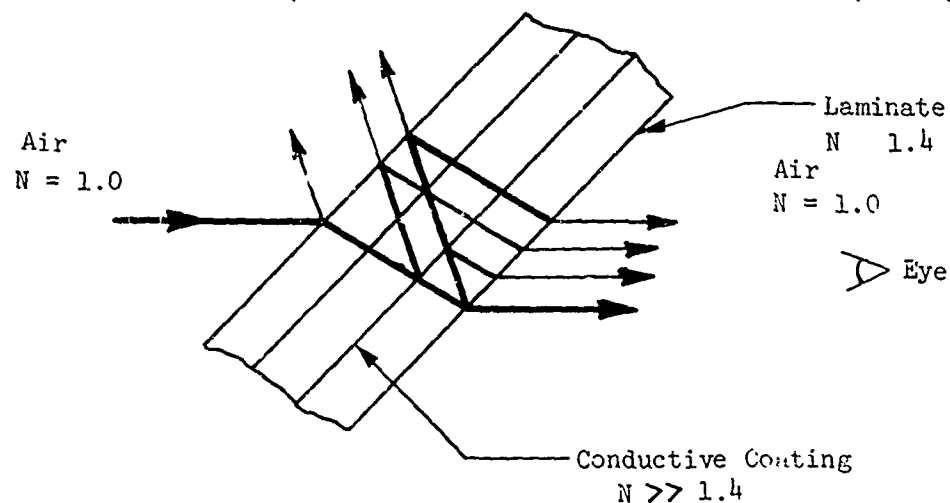


Figure 4-17. Multiple Reflections From Laminated Transparency With Conductive Coating.

The reflections from the interface between interlayer and face ply will be insignificant, providing the indices of refraction for the two materials are close to each other.

The worst multiple images occur in double-glazed installations, as shown in Figure 4-18. Here, the air gap is a major source of the reflections because of the great difference in index of refraction between it and the facing and the large distance between reflecting surfaces.

Multiple images are minimized in designs having low angles of incidence and short distances between the reflecting surfaces.

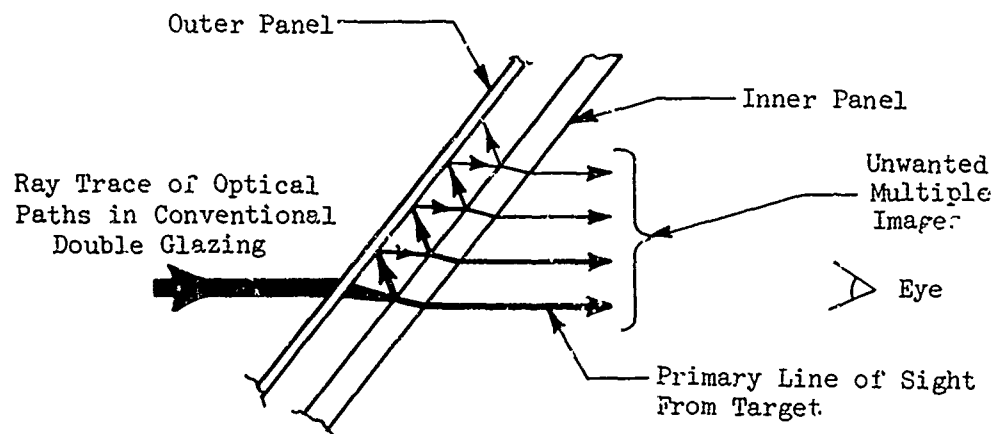


Figure 4-18. The Origin of Multiple Reflections in Double Glazing.

4.10 Antireflective Coatings

Antireflective coatings conforming to specifications MIL-C-675A and MIL-C-1480A are used in optical instruments, cameras, and instrument cover glasses to attenuate unwanted reflections. Yet these coatings have not been adapted to helicopter transparencies despite their obvious advantages. Some of the reasons are listed below:

1. Prohibitively high application costs.
2. Easily damaged from normal maintenance and aggressive environments.
3. Blemishes stand out on such coatings.
4. Application of MIL-SPEC coating requires high processing temperatures.

An understanding of the fundamental physics of thin films is helpful for appreciating the delicacy and precision required by this method of reducing reflections.

A thin film of antireflective coating reduces reflections by a mechanism involving the destructive interference of light waves. In Figure 4-19, light reflection from a thin film is shown, with dimensions greatly exaggerated for clarity. Some of the incident light is reflected from the surfaces of the substrate and the coating material. In order to have the two reflections cancel each other, the light waves must be 180° out of phase with each

other. This will occur if the distance along the path ABC (see Figure 4-19) is equal to a half wavelength of the incident light or if the coating thickness is approximately one-quarter wavelength. Visible light has wavelengths from 0.4 to 0.7 micron, which means the thickness of the film must be in the order of 0.1 micron to be antireflective. It should also be noted that a simple one-quarter wave coating will only be totally effective for a specific wavelength, at a specific angle of incidence, and at the surface to which it is applied.

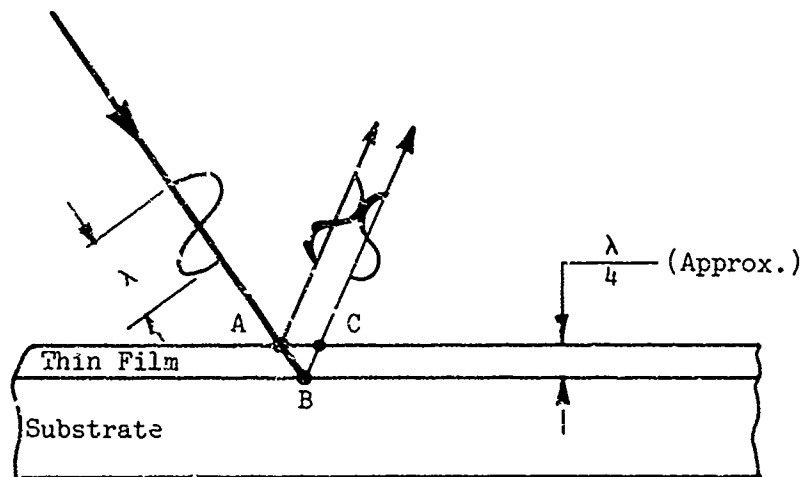


Figure 4-19. Destructive Interference of Reflected Light.

In actual practice, an antireflection film may involve several layers of coatings, working in conjunction with each other to provide optimum characteristics for a broader spectrum of conditions. Figure 4-20 illustrates a typical reflectance curve for a high-efficiency antiglare coating that was evaluated on an acrylic helicopter windshield. The reflectance values in the curve were measured at normal incidence and may be compared to the values of uncoated acrylic and electrical conductive coatings which have average visible light reflectances ranging between 4% and 15%. The reflectance from each surface of bare acrylic is 4%. Figure 4-21 shows visible light reflectance for two types of coatings as a function of electrical resistivity.

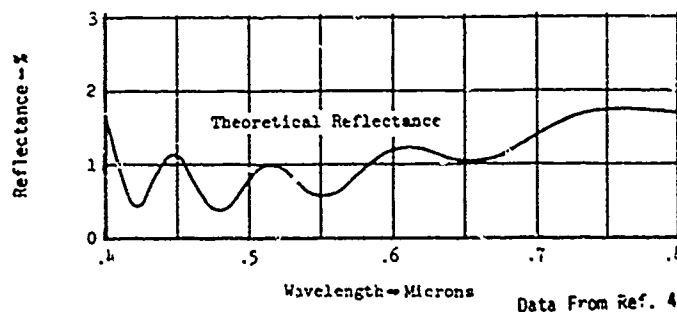
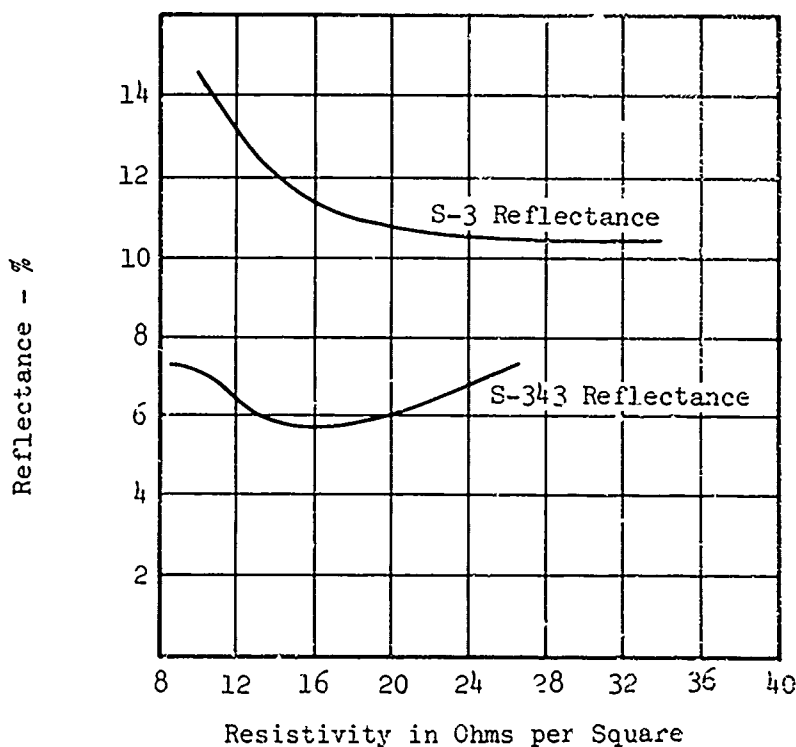


Figure 4-20. Reflectance Curve of a Typical Antireflective Coating.



Data From Ref. 5

Figure 4-21. Visible Light Reflectance versus Resistivity of Sierracote Metallic Coatings.

4.11 Head-Up Display

Head-Up Display (HUD) systems used for target acquisition and tracking require that associated transparencies be of superior optical quality in order to minimize sighting errors and related problems. This requirement is applicable to the following types of HUD systems used on helicopters: fixed HUD as shown in Figure 4-22 or movable HUD (helmet mounted) as shown in Figure 4-23.

The fixed HUD contains a transparent plate onto which symbology and/or a reticle is projected. The reticle is normally collimated so that it appears to be at an infinite distance. Sighting is accomplished by viewing the target through the reticle.

Movable helmet-mounted HUDs are typically used for missile guidance and control of slewable gun turrets. Sighting is accomplished in two ways: (1) direct vision through a collimated reticle projected onto a transparent helmet-mounted display, or (2) direct vision used in conjunction with imagery obtained from a remote TV camera and projected onto the helmet display.

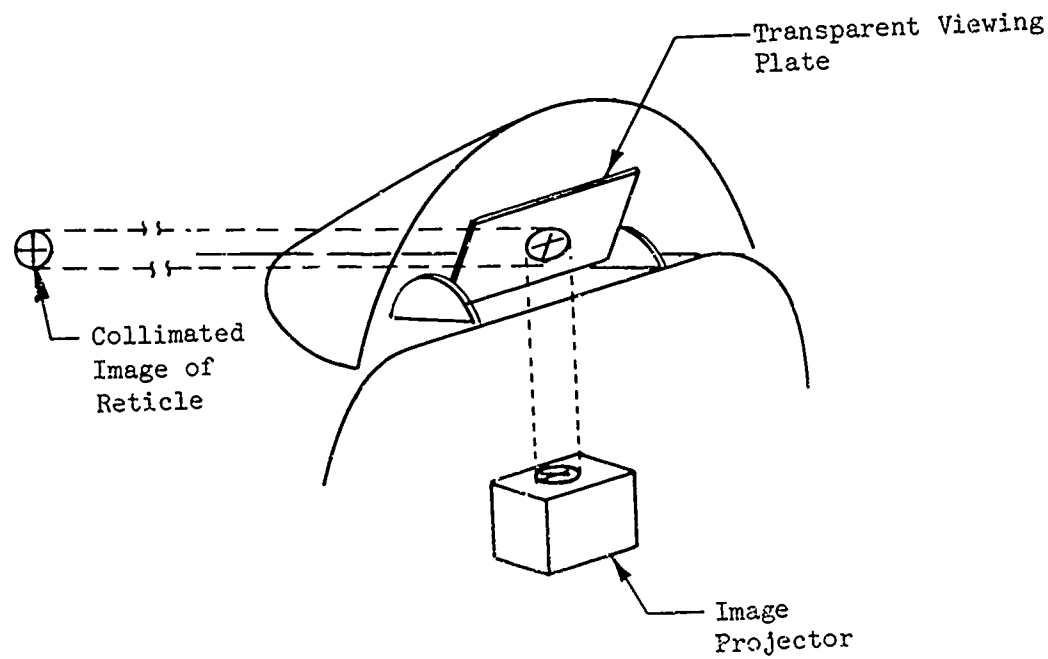


Figure 4-22. Fixed-Head Up Display.

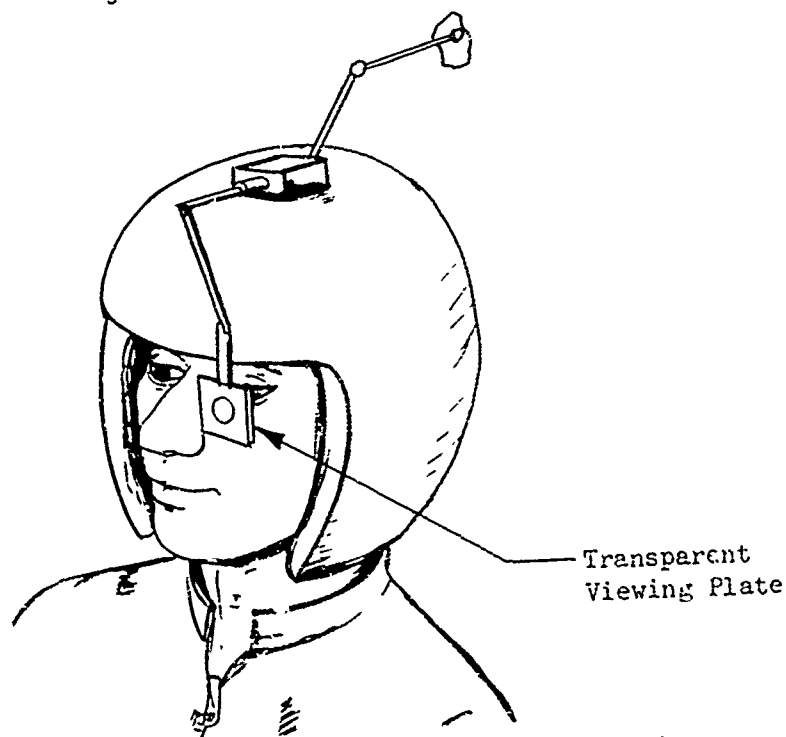


Figure 4-23. Movable Helmet-Mounted Display.

Common to all of the preceding systems is the ability of the pilot or gunner to look through the display and see the actual scene or target in full view. Thus, the optical path from the target through the HUD to the eye must also pass through a windshield or other transparency and can be affected by transparency curvature or wedginess.

4.11.1 Effects of Optical Deviation on HUD System

In order to achieve a given accuracy with a weapon system, tolerances or allowances must be established for all variables within the system. One of the most important variables is optical deviation of vision in that portion of a transparency falling within the zone scanned by the sighting reticle. This optical deviation in line of sight will cause targets to appear displaced from their true positions as shown in Figure 4-24. To emphasize the consequence of such errors, a deviation of 10 minutes of an arc is equivalent to an apparent target shift of 9 feet at a range of 1,000 yards, which is certain to reduce the probability of hitting the target.

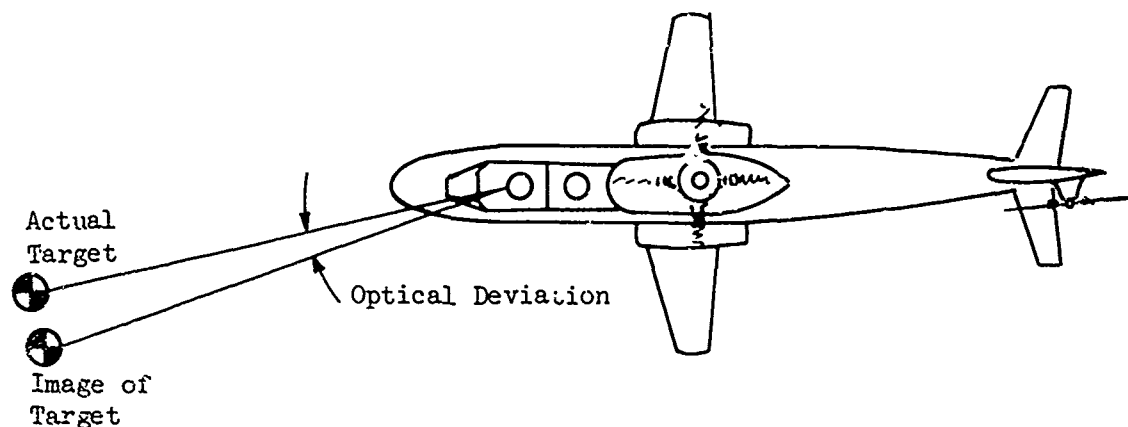


Figure 4-24. Target Displacement Resulting From Optical Deviation.

Some deviation can be tolerated in systems using a fixed HUD by boresighting the weapon or by optical compensation within the HUD. However, the optical deviations of the lines of sight for a movable HUD scanning through a curved transparency vary depending upon the direction the HUD is aimed (see Figure 4-25). These deviations cannot be effectively nulled except by locating the gunner's eye at the center of curvature so that all lines of sight are along radii, and, therefore, are perpendicular to the surface.

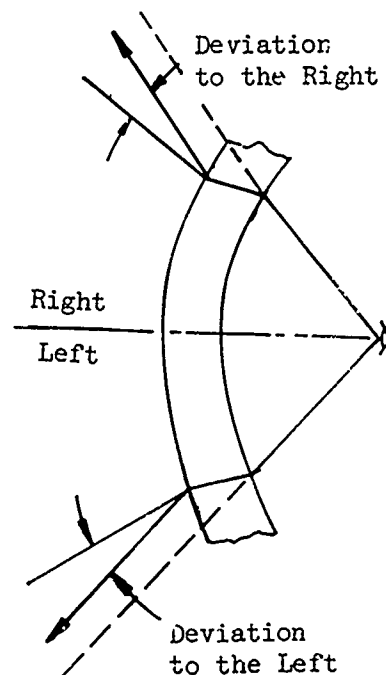


Figure 4-25. Deviation is a Function of Direction for a Curved Transparency.

Any changes of deviation introduce another undesirable effect: binocular parallax. The visual effects of this are shown in Figure 4-26. In this figure, the eyes must align their optical axes in order to view an outside object normally. The pilot readily adapts to small magnitudes of misalignment or parallax (1-5 mr) and observes a high acuity target image. The unacceptable situation arises when an aiming reticle is introduced. Reticles are normally collimated so that they appear to be at an infinite distance. With this kind of collimation, all rays originating from any point on the reticle are parallel and will enter each eye from the same direction (dotted lines in Figure 4-26).

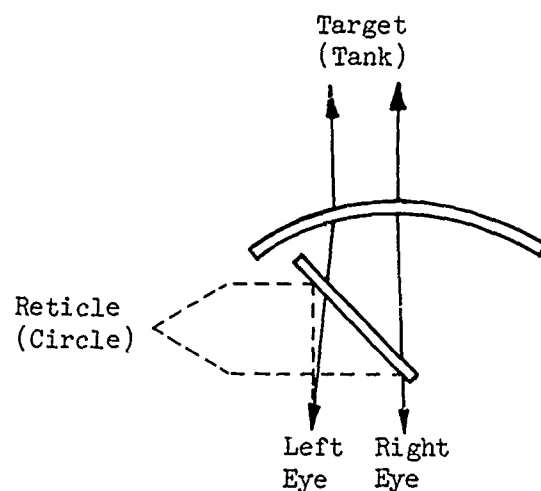


Figure 4-26. Lines of Sight Through a Curved Windshield.

If one considers the combined reticle/target image on the retina of each eye, the situation shown in Figure 4-27 is observed. The right eye sees the target properly centered within the reticle while the left eye sees the reticle well to the left of the target. The brain will interpret this situation in either of two ways. It will either adjust the eyes to bring the reticles in coincidence and see two targets, or it will do the converse, causing one target to be seen with two reticles. These two conditions are shown in Figure 4-27.

The brain will normally cause the image with the most spatial detail to be brought into registration; i.e., one target and two reticles. When the reticle appears by itself, such as against the sky, it is brought into registration, but the moment anything with more spatial detail appears, the eyes will shift to favor the target. This shifting of eye alignment is distracting and fatiguing, and can cause errors in target acquisition.

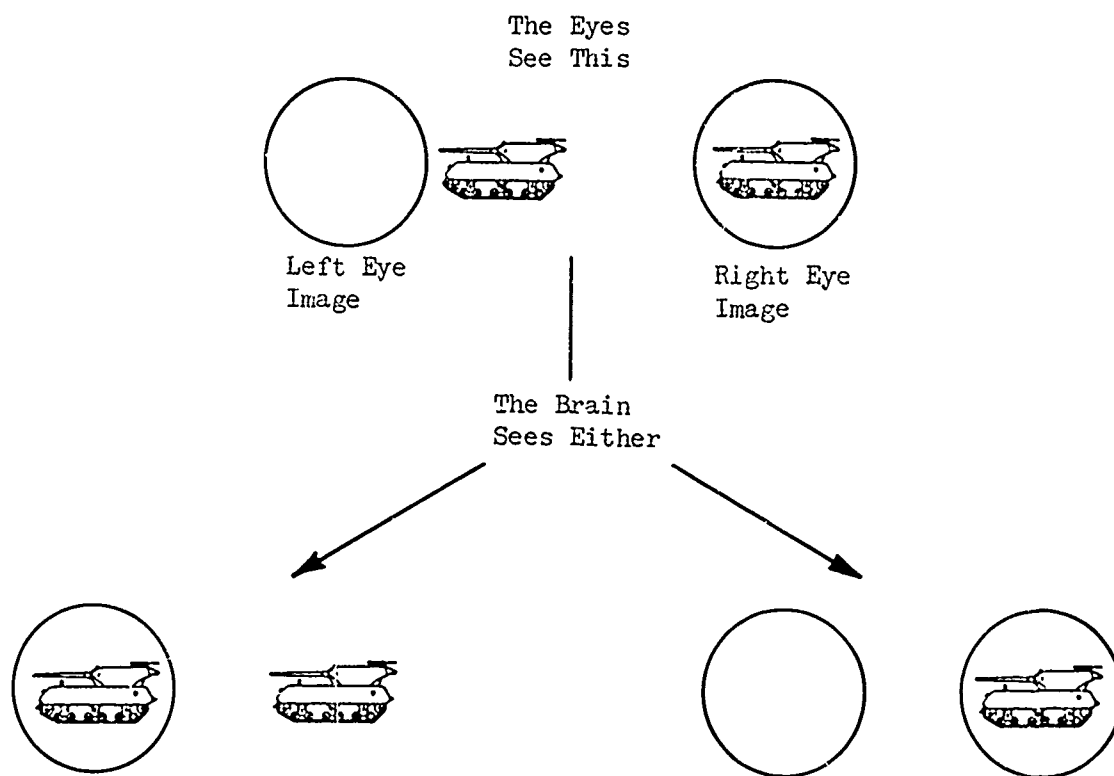


Figure 4-27. The Visual Parallax Problem.

4.12 Analysis of Optical Deviation

Optical deviation is caused by transparency curvature or wedginess. The deviation resulting from curvature is fixed by the transparency configuration (geometry and thickness) and will always be present regardless of the optical quality of the part. Deviation resulting from transparency wedginess is a function of manufacturing quality and is algebraically additive to values resulting from curvature. Thus, deviation in a flat panel is solely based on manufacturing tolerances, whereas a curved panel has, in addition, an increment of deviation that is a function of shape, thickness, and angle of incidence.

For a curved panel, the fixed component of deviation can be determined analytically. Analysis is necessary for two reasons:

- (1) to determine quality control standards that are achievable (i.e., deviations not less than the amount fixed by curvature) and
 - (2) to determine optimum sight positions and windshield shapes.
- The latter reason dictates that the analysis be performed early in the design stages, since aircraft shape and crew placement are difficult to change later.

Expressions for calculating deviation are based on the law of refraction, presented here as equation 4-1.

$$\sin \theta = N_2 \sin \phi \quad (4-1)$$

where N is the index of refraction, and the angles are as defined in Figure 4-28.

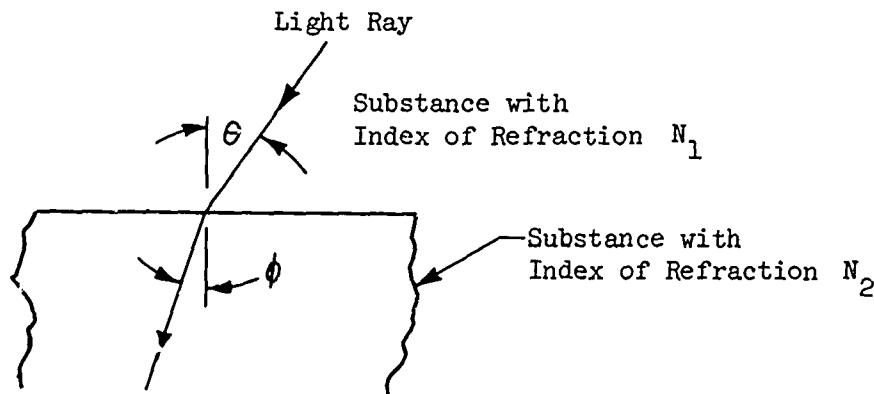


Figure 4-28. Refraction of Light.

For air, N is equal to one.

Equation 4-2 can be used to calculate the deviation in line of sight through a cylindrically curved transparent panel of uniform thickness.

$$\psi = \theta - \sin^{-1} \left(\frac{R \sin \theta}{R + t} \right) - \sin^{-1} \left(\frac{\sin \theta}{N} \right) + \sin^{-1} \left(\frac{R \sin \theta}{N(R + t)} \right) \quad (4-2)$$

where N is the index of refraction, and the remaining symbols are as defined in Figure 4-29. Equation 4-2 is valid only for panels where the cross section is circular in a plane, perpendicular to the line of sight. For three-dimensional problems where lines of sight do not intersect circular cross sections, similar equations may be derived; however, the task is more efficiently accomplished with the aid of a computer.

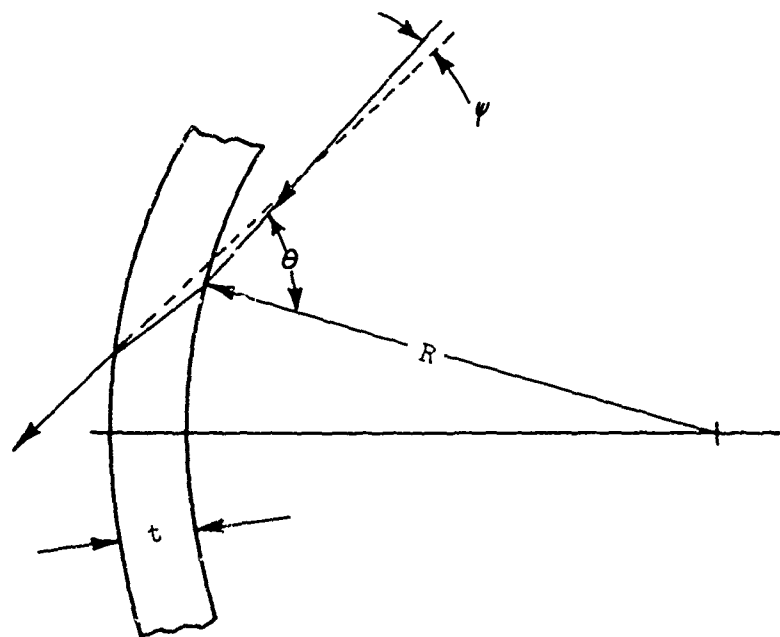


Figure 4-29. Geometrical Representation of the Deviation of a Line of Sight Through a Cylindrically Curved Transparent Panel of Uniform Thickness.

References

1. Grether, W. F., "Optical Factors in Aircraft Windshield Design as Related to Pilot Visual Performance," AMRL-TR-73-57, Aerospace Medical Research Laboratory, Wright-Patterson Air Force Base, Ohio, July 1973.
2. Kay, B. F., Sikorsky Aircraft Division, "Design, Test, and Acceptance Criteria for Helicopter Transparent Enclosures," USARTL-TR-78-26, (AVRADCOM), Applied Technology, Laboratory U. S. Army Air Mobility Research and Technology Laboratories Fort Eustis, Va.,
3. Crosley, J. K., "Tinted Windscreens in U. S. Army Aircraft," USAAERU Report No. 68-7, U. S. Army Aeromedical Research Unit, Fort Rucker, Ala., Mar. 1968.
4. Lundren, G. A., Optical Coating Laboratory, Inc., "A Coating for Helicopter Canopies," AFML-TR-73-126, Air Force Materials Laboratory, Wright-Patterson Air Force Base, Ohio, June 1973.
5. Wiser, G. L., The Sierracin Corp., "New Materials in Aircraft Windshields," 700802, Society of Automotive Engineers, New York, N. Y., Oct. 1970.

Bibliography

Grom, R. V., and Marshall, R. R., "Degradation Limits of Plastic Windshields in Service," FAA-ADS-57, Federal Aviation Agency, Nov. 1965.

Grether, W. F., and Muich, C. J., "The Effect of Transparent Windows on Human Visual Capabilities," WADC-TR-65-212, Air Force Materials Laboratory, Wright-Patterson Air Force Base, Ohio, Sept. 1965.

Atkin, H. P., and McQuilkin, F. T., North American Aviation, Inc., "Material and Design Studies for the Transparent Areas of a M2.65 Supersonic Transport Aircraft," WADC-TR-65-212, Air Force Materials Laboratory, Wright-Patterson Air Force Base, Ohio, Sept. 1965.

Halloway, R. A., "Survey of Optical Test Procedures for Aircraft Transparencies," LR-23711, Lockheed California Company, Sept. 1970, AD-887715.

Islinger, J. S., Armour Research Foundation, "Engineering Design Factors for Laminated Aircraft Windshields, Part 2," WADC-TR-53-99, Wright Air Development Center, Wright-Patterson Air Force Base, Ohio, Apr. 1954.

Cook, L. M., et al, PPG Industries, Inc., "Development of Design, Test, and Acceptance Criteria for Army Helicopter Transparent Enclosures," USAAMRDL-TR-73-65, U. S. Army Air Mobility Research and Development Laboratory, Fort Eustis, Va., Sept. 1973, AD 772936.

James, H. C., et al, Goodyear Aerospace Corp., "Design, Test, and Acceptance Criteria for Army Helicopter Transparent Enclosures," USAAMRDL-TR-73-19, U. S. Army Air Mobility Research and Development Laboratory, Fort Eustis, Va., May 1973, AD-767242.

Hassard, R. S., Goodyear Aerospace Corp., "Plastics for Aerospace Vehicles, Part II, Transparent Glazing Materials," MIL-HDBK-17A, Part II (Proposed Revision), Air Force Materials Laboratory, Wright-Patterson Air Force Base, Ohio, Jan. 1973.

Corney, N. L., Ministry of Defense, U.K., "Optical Requirements for Aircraft Transparencies," AFML-TR-73-126, Air Force Materials Laboratory, Wright-Patterson Air Force Base, Ohio, June 1973.

Gibbs, B. D., British European Airways, "Transparency Development in Civil Airline Operation," AFML-TR-73-126, Air Force Materials Laboratory, Wright-Patterson Air Force Base, Ohio, June 1973.

Fisher, R. W., McDonnell Aircraft Company, "Correction of Optical Deviation in Curved Windshields," AFML-TR-73-126, Air Force Materials Laboratory, Wright-Patterson Air Force Base, Ohio, June 1973.

Wulfech, J. W., et al, Tufts University, "Vision in Military Aircraft," WADC-TR-58-399, Wright Air Development Center, Wright-Patterson Air Force Base, Ohio, Nov. 1958.

Corney, N. S., and Shaw, W., Ministry of Defense, U.K., "The Specification of Optical Requirements for Aircraft Transparencies," A72-27003, Society of British Aircraft Companies, London, England, June 1971.

"Optical Considerations - Transparent Enclosures," TB-73-104, Swedlow, Inc., Garden Grove, Calif., Mar. 1973.

Pinson, E. A., and Chapanis, A., Air Technical Service Command, "Visual Factors in the Design of Military Aircraft," Aviation Medicine, Apr. 1946.

Provines, W. F., and Kislin, B., "Transparencies Used in Military Aviation and their Effects on Vision," Journal of the American Optometric Association, Jan. 1971.

Sears, F. W., and Zomansky, M. W., "University Physics," Addison-Wesley Publishing Co, Reading, Mass., Mar. 1965.

Kohler, H., "Mathematical Method of Calculating the Optical Characteristics of Cone-Shaped Cockpit Windscreens," Aircraft Engineering, June 1973.

Watson, J.D.L., "The Effects of Tinted Plexiglass on Visibility in the AH-1G Cobra Aircraft," Naval Postgraduate School, Apr. 1970, AD 709405,

Daniels, P. B., "Antireflective Coatings for Aircraft Windshields and Windows," TEM-K3-4055, Sikorsky Aircraft Division, Stratford, Conn., Mar. 1973.

Rancourt, J. D. Optical Coating Laboratory, "Thin Film Coatings on Plastic Substrates". AFML-TR-76-54, Air Force Materials Laboratory, Wright Patterson Air Force, Ohio, Apr. 1976.

Arnold, J. R., "Army Preliminary Evaluation YAH-1Q Helicopter with a Flat Plate Canopy," USAAEFA-75-18, Army Aviation Engineering Flight Activity, Edwards Air Force Base, Calif., Aug. 1975.

"Plexiglass Handbook for Aircraft Engineers," PL-26a, Rohm & Haas Co., Philadelphia, Pa., Oct. 1962.

Lawrence, J. H., Douglas Aircraft Co., "Windshield Technology Demonstrator Program," AFFDL-TR-77-1, Air Force Flight Dynamics Laboratory, Wright-Patterson Air Force Base, Ohio, Sept. 1977.

Beck, R. I. et al, Douglas Aircraft Co., "Standardized Windshield Fabrication Specification," AFFDL-TR-77-97, Air Force Flight Dynamic Laboratory, Wright-Patterson Air Force Base, Ohio, Oct. 1977.

5.0

RADAR CROSS SECTION REDUCTION

Glass and plastic cockpit enclosures are transparent to microwave energy, thereby allowing the flat metal surfaces inside the cockpit to become a major source of radar reflection. If the radar beam can be prevented from entering the cockpit, the nose-on radar cross section (RCS) can be greatly reduced. This may be accomplished by reflection or absorption.

5.1 Reflection

RCS will be reduced if the radar beam is reflected in a direction other than back to the radar antenna. This can be best accomplished by sloping the transparencies at an angle other than normal to the radar, and adding a conductive medium that will reflect the radar beam. Transparent, electrically conductive thin films and wire meshes are suitable for this purpose. However, if the transparency is likely to become oriented perpendicular to the radar beam as a result of aircraft attitude, it will give a strong return to the radar receiver. Under such conditions, the echo from a transparency with double curvature will be less than the echo from a flat panel of equivalent area.

Conducting films on aircraft windshields are also used for anti-icing by passing an electrical current through the film to heat the glass or plastic. These conductive films can be designed to serve a dual purpose: reflecting radar and heating. In such cases, three factors are involved in determining the resistivity of the films: light transmission, radar reflectance, and power dissipation.

Special considerations are required for three-phase electrical systems. Three-phase, alternating-current electrical systems use deletion lines to divide the heating film into sections. These deletion lines, which are narrow uncoated strips, can increase the RCS by allowing the radar to enter the cockpit and should be evaluated accordingly.

5.2 Radar Reflecting Properties of Transparent Materials

To obtain radar reflections of 90% or more, it is necessary for the surface resistance of the conducting film to be 10 ohms per square or less. With film on the interior side of the transparency, some of the radar energy is absorbed, due to cancellation effects, at or near a resonant frequency, depending on the thickness of the transparency. This may permit the use of thinner films with greater light transmissions. Wire grid samples (.002-inch copper spaced at .100 inch) were found to have radar reflection characteristics equivalent to coated samples but with higher light transmission (Reference 1).

Measurements of the radar reflection characteristics of thin conducting films are shown in Table 5-1 as attenuation factors, K_r . This data was obtained as follows: The radar echo from a 12 in. flat metal plate aligned normal to radar beams of various frequencies was measured, and the power received from the metal plate was designated P_m . The

echos received from glass samples, also 12 in², with conducting films applied were measured, and the power received from the glass sample was designated P_i . The ratio P_i/P_m is given in decibels, so that:

$$K_r = 10 \text{ Log } (P_i/P_m)$$

The relationship between K_r and percent reflectance is shown in Figure 5-1.

TABLE 5-1. RADAR ATTENUATION CHARACTERISTICS OF TRANSPARENT MATERIALS

Radar Frequency	K_r (db down from 12-in ² metal plate)...			
	3 GHz	4.5 GHz	8 GHz	10 GHz
1/4-inch plain glass	3	3	7.75	15
Tin-oxide coat, glass side exposed, @				
10 ohms/square	0.5	0.5	0	0.75
20 ohms/square	0.75	1.25	2.0	1.25
30 ohms/square	1.5	1.5	2.0	2.5
50 ohms/square	1.25	1.5	3.5	3.0
.002-inch copper wire grid 0.10-inch spacing, on one side of 1/4-inch glass, glass side exposed	1.0	1.75	2.5	2.25
0.005-inch wire grid between two 1/4-inch glass plates with 1/16-inch spacing	2.0	1.1	0.25	1.0
0.002-inch wire grid between two 1/8-inch glass plates with .10-inch spacing	1.0	5.0	6.25	1.75

Data from Ref. 1.

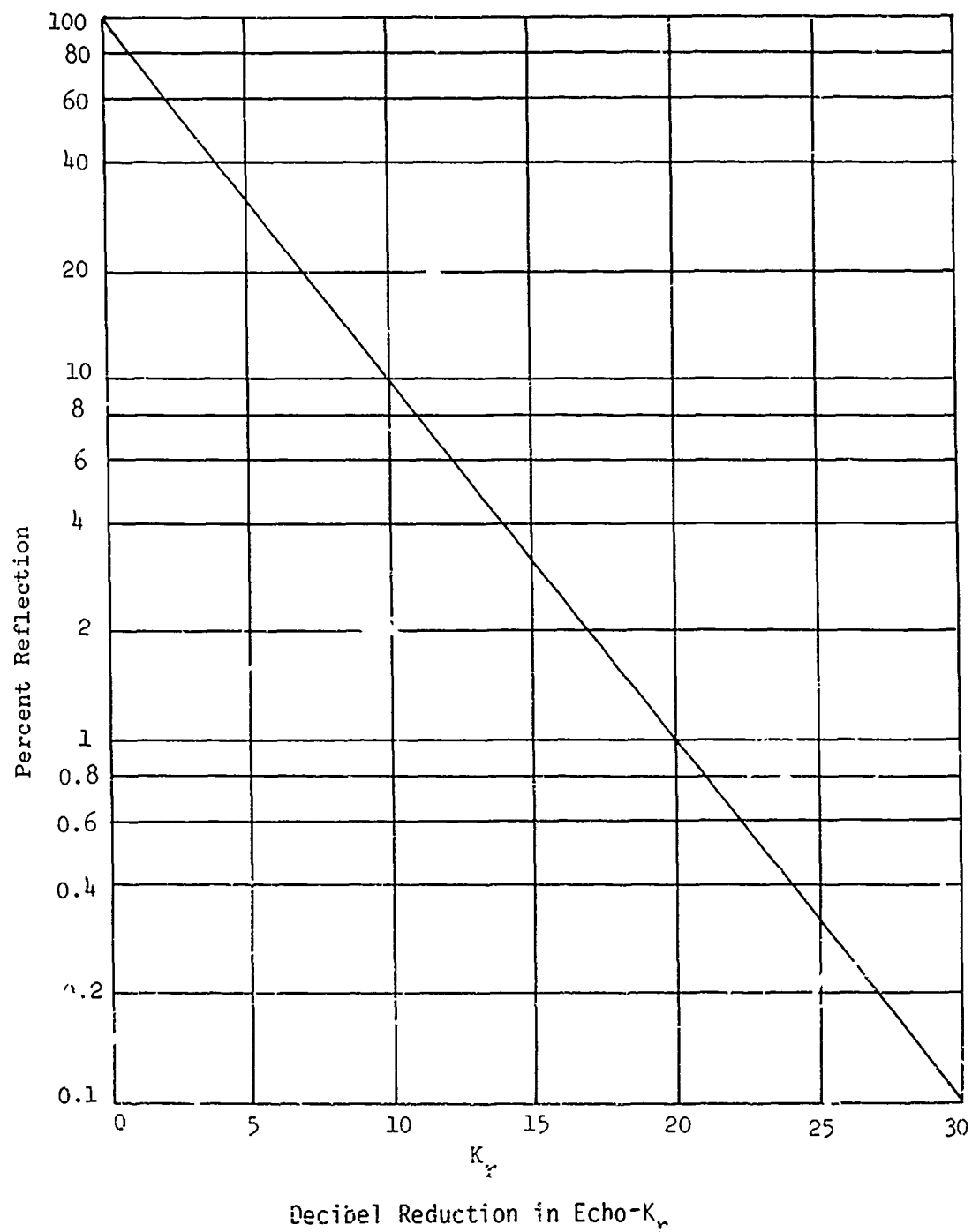


Figure 5-1. Relationship Between Percent Reflection and Decibel Reduction in Echo.

5.3 Absorption

- RCS reduction through absorption would be possible if a material could be developed which is transparent to light and absorbs radar frequencies. This idea has been investigated by Dawson (Reference 2). It involved using a double-walled canopy with a suitable liquid placed between the walls to absorb radar energy. Another technique involves matching the impedance of a dielectric layer and conductive thin film to that of free space, which reduces the reflections.

References

1. Mann, M. J., "Radar Reflection of Transparent Materials", AFML-TR-65-212, Air Force Materials Laboratory, Wright-Patterson Air Force Base, Ohio Sept. 1965.
2. Dawson, T. W. G., "Radar Camouflage Techniques for Aircraft and Finned Missiles," Royal Aircraft Establishment Report No. Rad. 289, Farnborough, Oct. 1960, SECRET.

Bibliography

"Reduction of Detection of Army Aircraft by Radar," TRECOM Technical Report 63-25, Cornell Aeronautical Laboratory, Inc., U.S. Army Transportation Research Command, Ft. Eustis, Va. Mar. 1963, SECRET.

Bahret, W. F., and Price, E. L., "Radio-Frequency and Optical Properties of Thin Metallic Films," AFAL-TR-66-260, Nov. 1966, CONFIDENTIAL.

Foreman, D. E., and Gall, E. S., Calspan Corporation, "Cockpit RCS Reduction," presented at the Radar Camouflage Symposium, Air Force Wright Aeronautical Laboratories, Wright-Patterson Air Force Base, Ohio, Oct. 1975, SECRET.

Lawrence, J. H. Douglas Aircraft Co., "Windshield Technology Demonstrator Program," AFFDL-TR-77-1, Air Force Flight Dynamics Laboratory, Wright-Patterson Air Force Base, Ohio, Sept. 1977.

Jettisonable hatches are required for emergency egress by the flight crew and occupants of helicopters. A logical location for such hatches is in the transparent enclosure, since it is secondary structure. This eliminates the need for additional cutouts in the primary structure.

Two basic egress systems are discussed below: mechanical and pyrotechnic.

6.1 Mechanical Systems

Mechanically operated escape hatches typically contain windows mounted to rigid frames which contain jettison features. The transparency interface for this type of hatch is limited to the mounting of the transparency to its frame, and is discussed more fully in Chapter 22, Transparency Supports, and Chapter 23, Edge Attachments. Additional guidance relative to size, placement, and operational requirements may be found in Reference 1.

Rubber extrusion mountings as shown in Figure 6-1 sometimes permit fixed windows to become "kickout" emergency exits. That is, when the rubber extrusion does not have to support the more than about 100 pounds total load, a sharp blow at an edge or corner of the window can be used to disengage the window from the extrusion. Accurate knowledge of the applied loads and the control of the retention force is extremely critical because, if retention forces become too great, the panel cannot be physically kicked out. "Kickout" windows can only be considered a backup for emergency exits. They should not be considered for primary emergency exits because they require physical force for operation, which bars their use by incapacitated personnel. Additional information on rubber extrusion is contained in Chapter 23, Edge Attachments.

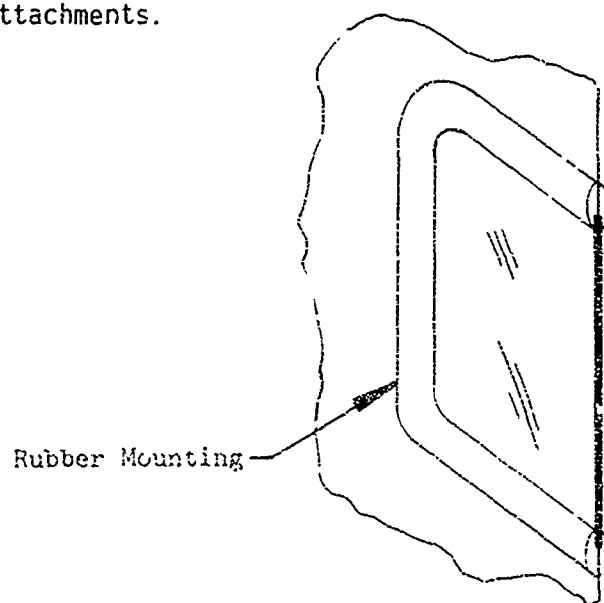


Figure 6-1. Separable Rubber Extrusion Mounting.

6.2 Pyrotechnic Systems

Cutting transparent enclosures by means of linear explosive charges is a relatively new method for the rapid removal of transparencies in emergency situations. Explosive cutting systems, unlike mechanical release systems, cannot be jammed as a result of postcrash fuselage distortions. Figure 6-2 illustrates the concept and shows a test firing of an AH-1 Cobra escape system.

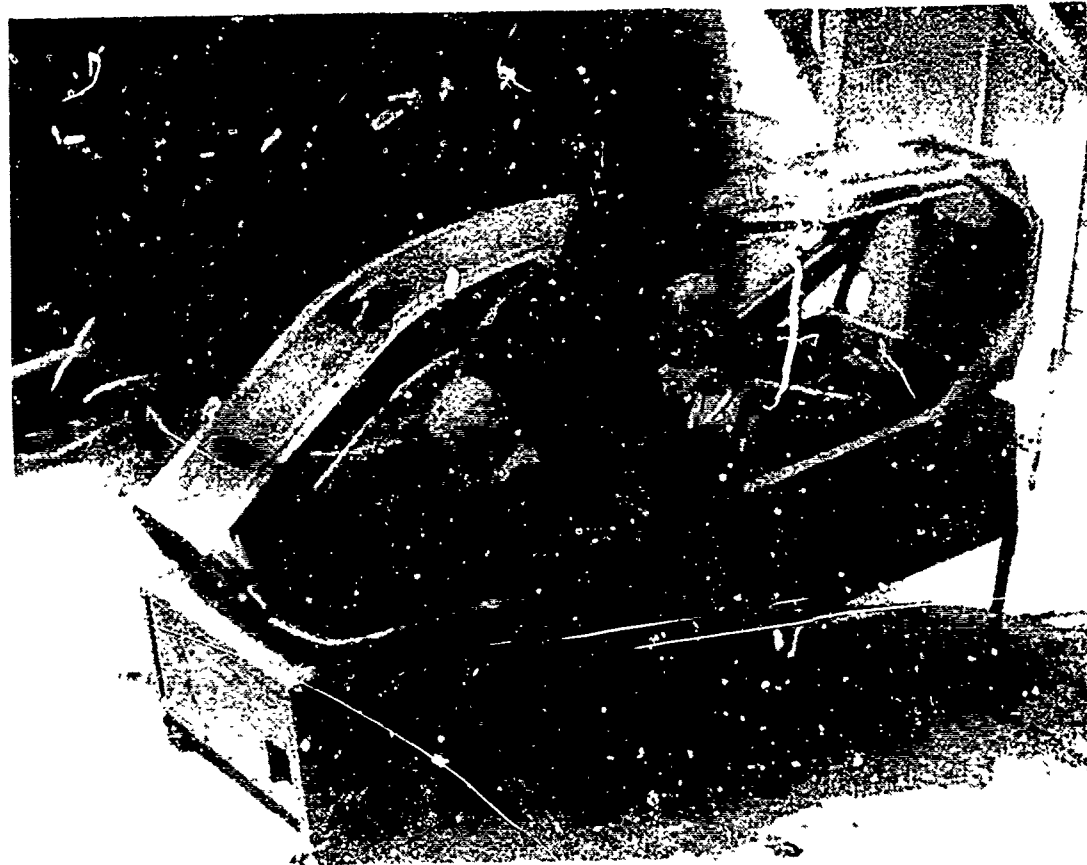


Figure 6-2. Test Firing of an AH-1 Cobra Escape System.

In its simplest form an explosive cutting system consists of a loop of a linear explosive charge placed along the perimeter of a transparency and connected to a suitable detonating device. A linear explosive is a continuous, small-diameter column of explosive charge. The explosive used is not dimensionally stable in its high-purity linear form, and it is normally surrounded by a sheath, which may be metal, plastic, or woven textile filaments. The explosive reaction occurs at a rate of 20,000 ft/sec or greater.

By placing the explosive cord in direct contact with the surface to be cut, a crack is induced during detonation. The explosive force transfers momentum to the crack, causing it to propagate through the material as shown in Figure 6-3. Since this mechanism depends on transverse crack propagation through the material, the cut will follow the internal stress planes of the material. For stretched acrylic, it is common to see sharp-edged cuts with the surface of the cuts inclined 30° to the plane of the material.

The basic design goal of an explosive cutting system is to insure reliable cutting capability with a minimum charge level. Minimum charge level will facilitate containment of blast effects and shrapnel; however, a slight "overkill" should be provided to accommodate normal manufacturing tolerance.

Monolithic and laminated plastics in the thicknesses normally used for helicopter transparent enclosures may be cut with linear explosive charges. These materials can be classified as either shock sensitive or shock resistant. Acrylic is shock sensitive and can be cut with a mild detonation fuse held in contact with the surface of the panel. Polycarbonate is extremely shock resistant and must be cut with special linear shaped charges. The linear shaped charge is geometrically configured to concentrate the blast effect and has greater cutting capacity.

Interlayers used in laminated transparencies are highly shock resistant and can effectively isolate the outer ply of the laminate from the blast shock. Even if the explosive charge is placed near the edge so that the shock would be transmitted through the edge member to fracture the outer ply, the interlayer would remain intact, as shown in Figure 6-4. For this reason, it is preferable to sever the edge members to avoid the interlayer altogether.

The cutting system can be designed so that both ends of the explosive charge terminate at a single point. Thus, detonation occurs at both ends of the charge simultaneously, thereby providing inherent redundancy.

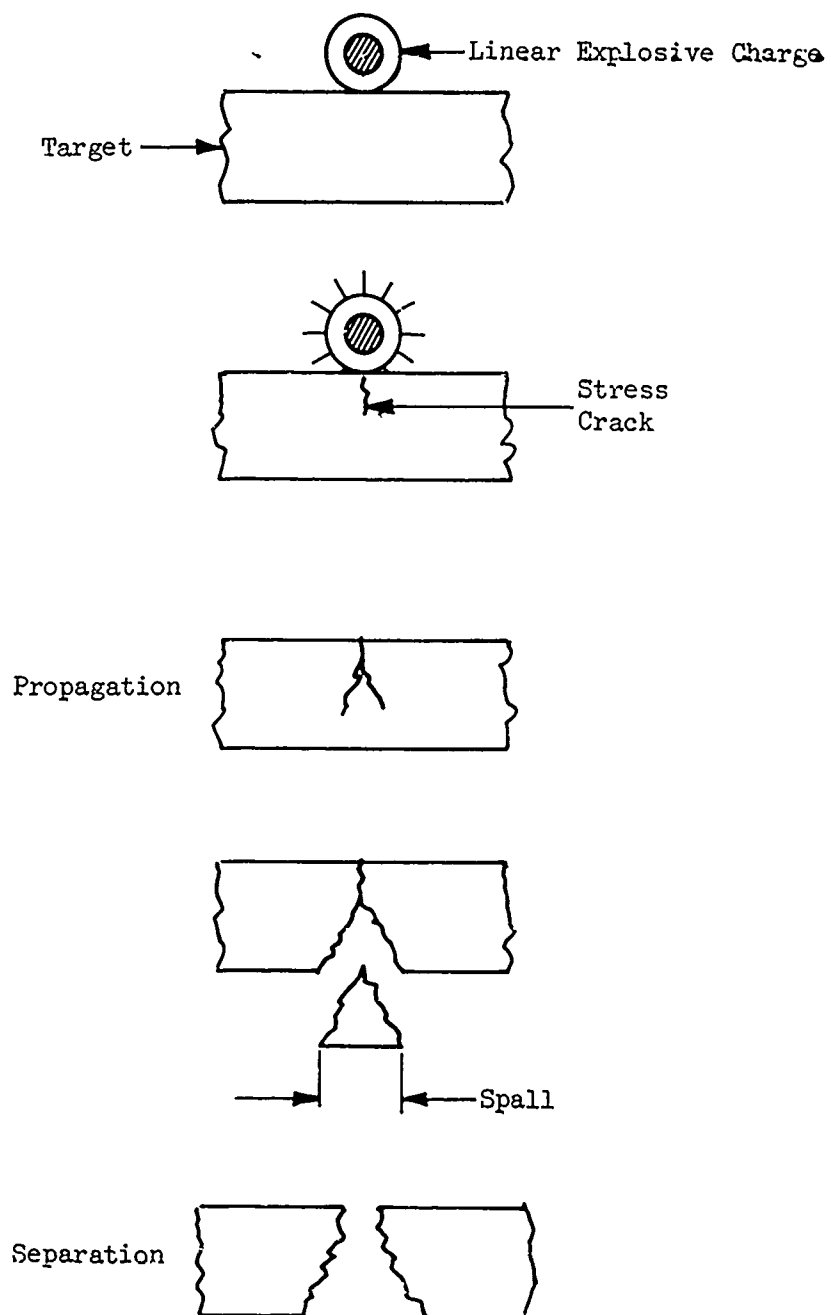


Figure 6-3. Cutting Sequence for Linear Explosive Charges.

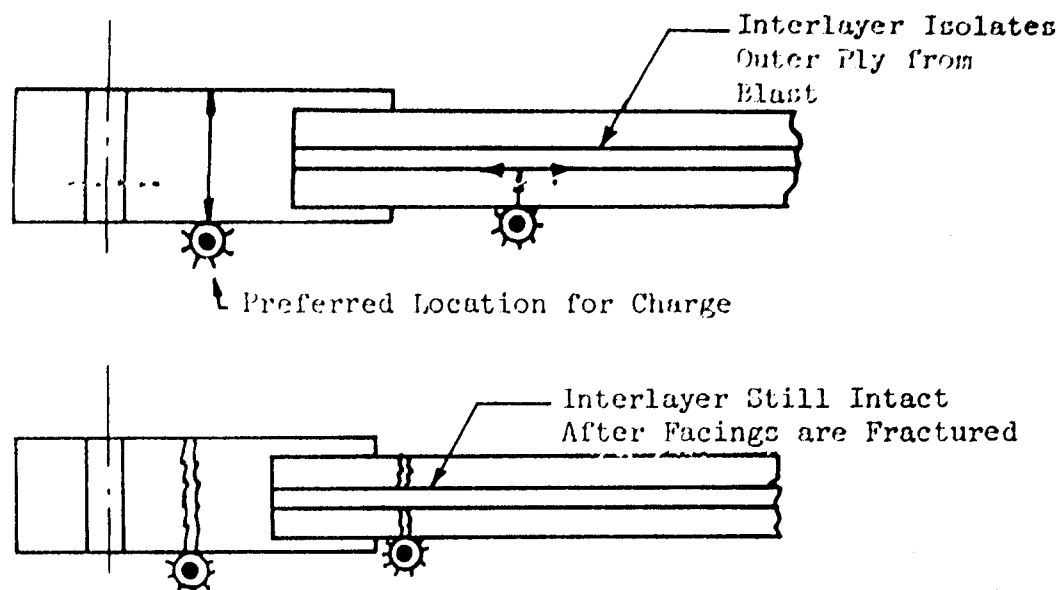


Figure 6-4. Explosive Cutting of Laminated Transparencies.

6.3 Containment of Explosive Charge

A linear explosive charge for cutting applications is held rigidly in place by a holder, which is alternately referred to as a blast retainer, charge holder, or backup strip. The holder has three purposes: to protect the explosive charge from physical damage, to hold the charge in the proper position, and to contain the back blast and shrapnel.

The normal procedure is to attenuate the blast with a compressible material such as silicone rubber. An extruded strip is designed to hold the charge, position it with respect to the surface, and seal it from moisture. The thickness and shape of the extrusion are determined by the charge level and type of explosive element. The extruded strip and explosive element are fitted into a rigid holder, which is preformed to the required panel configuration. The holder may be aluminum, steel, or any of the shock-resistant plastic constructions used for edge members. While the physical size of the explosive charge rarely exceeds .250 inch for transparency cutting, the holder is normally at least 1 inch in width; the holder is the element of the system that reduces the visible area of the transparent panel. Therefore, it is highly desirable to hide as much of the holder as possible behind the edge member, or better yet, to integrate it directly into the edging design.

The combination of the linear explosive, blast attenuator, and charge holder is called a cutting assembly. Figure 6-5 shows the cutting assembly installation used on the Sikorsky S-72 helicopter. This installation uses a 3-grain/foot charge and weighs slightly more than 0.2 pound per linear foot.

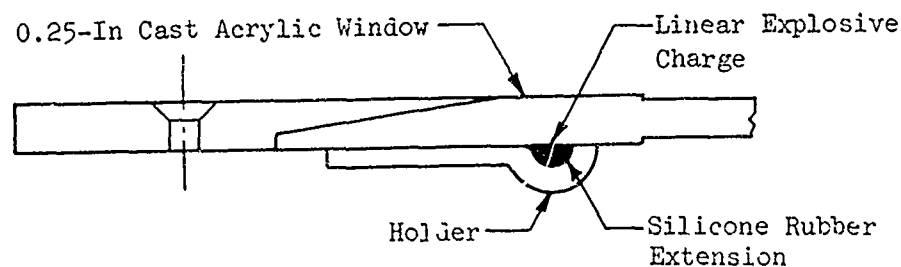


Figure 6-5. Sikorsky S-72 Cutting Assembly.

6.4 Ballistic Initiation

In the interest of design simplicity and reliability, mechanically operated detonators are preferred to electrical devices. Electrical devices are unfavorable because they require a power source independent of the aircraft electrical system to insure function after a crash, and they require special shielding and safety features to prevent unintentional triggering from electromagnetic sources.

If the detonating device is remote from the transparency, explosive transfer lines are used to interconnect the detonator with the explosive charge. Detonators may be installed at crew stations and on the outside of the aircraft for postcrash rescue. When external detonators are employed, they should be placed away from the transparency to prevent fragments from the shattered transparency from injuring rescue personnel.

6.5 System Safety

As with any explosive device, system safety is of paramount importance. For this reason, development testing is required to verify performance and also to insure operator safety. The following elements of safety must be demonstrated for each new design application:

1. Preclusion of inadvertent firing
2. Noninjurious noise level
3. Containment of explosive effects
4. Nontoxic explosive by-products
5. Ejection of debris away from occupants
6. Prevention of jagged, sharp edges that could cause injury during egress.

Reference

1. Isenberg, S. A., "Explosive Cutting of Transparent Enclosures," Technical Bulletin 74-4, Teledyne McCormick Selph, Hollister, Calif., June 1974.

Bibliography

Hudson, G. T., Hawker Siddeley Aviation Ltd., "Escape Through Aircraft Transparencies," Optical Transparency Symposium, London, June 1971.

Dynamic Science "Crashsurvival Design Guide", USAAMRDL-TR-71-22, U. S. Army Air Mobility Research and Development Laboratory, Ft. Eustis, Va., Oct. 1971, AD-733358.

Bemeat, NASA, "Rotor Systems Research Aircraft Canopy Explosive Severance," Franklin Institute Research Laboratories, Philadelphia, Pa., Sept. 1976.

Current operational doctrine for Army helicopters specifies nap-of-the-earth (NOE) flight in a combat area with the intent of preserving a complete radar and visual mask between the target and the helicopter. The aural signature is behind mask at standoff range, and the ambient noise level at the observer location in a tank-versus-helicopter situation makes aural detection unlikely. Radar is ineffective when the aircraft remains behind mask or within ground clutter, and moving-target fire-control radar is used reluctantly for fear of exposing the user's location. After arriving at the target area, tactics call for the scout or the attack helicopter to popup, retaining a terrain background, and to acquire the target. The helicopter becomes most vulnerable when line of sight with the target is established. The key to increased survivability lies in denying or delaying visual detection of the helicopter by the ground observer when the line-of-sight condition is reached.

Sun glint, or reflection, from the transparent enclosure is one of the most frequently cited visual cues used by ground observers for detecting low-flying helicopters, especially at ranges beyond 1 kilometer. This section provides engineering information (design and analytical) which can be used to minimize the glint signatures of transparent enclosures.

7.1 Zone of Interest

The zone in which glints are of interest is shown in Figure 7-1. The ground region is shaded and includes all areas beyond a ground range of 1 kilometer, since within the 1 kilometer range the helicopter is generally visible to the naked eye without the aid of glint. The altitude is assumed to be 100 feet since NOE tactics call for the helicopter to be as close to the terrain as possible except for pop-up maneuvers during engagement of the enemy and not to present a silhouette against the sky.

The zone of interest can be related to the helicopter as a region contained between angles of 90° and 91.75° subtended from and revolved about the helicopter's vertical axis, as shown in Figure 7-2. However, this zone should be expanded by about 10 degrees to accommodate uneven terrain. In addition, aircraft attitude changes in pitch and roll must also be considered.

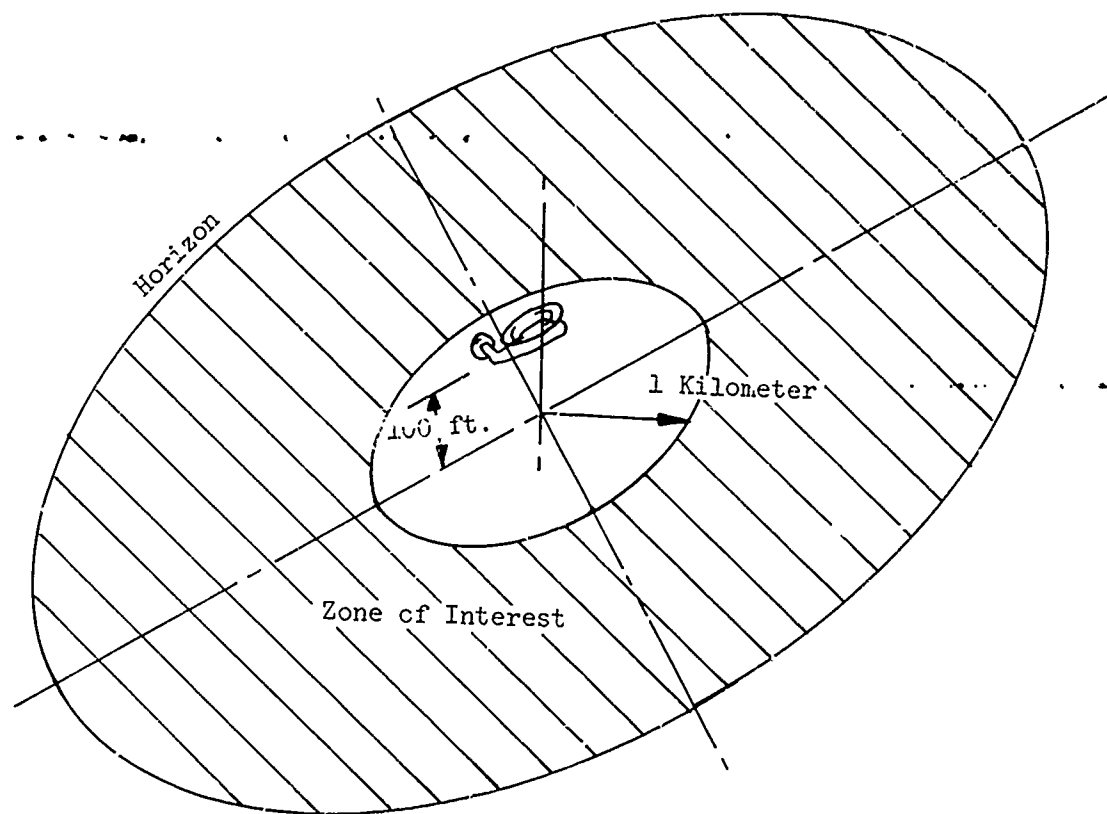


Figure 7-1. Zone of Interest for Glint Detection of Low Flying Helicopters.

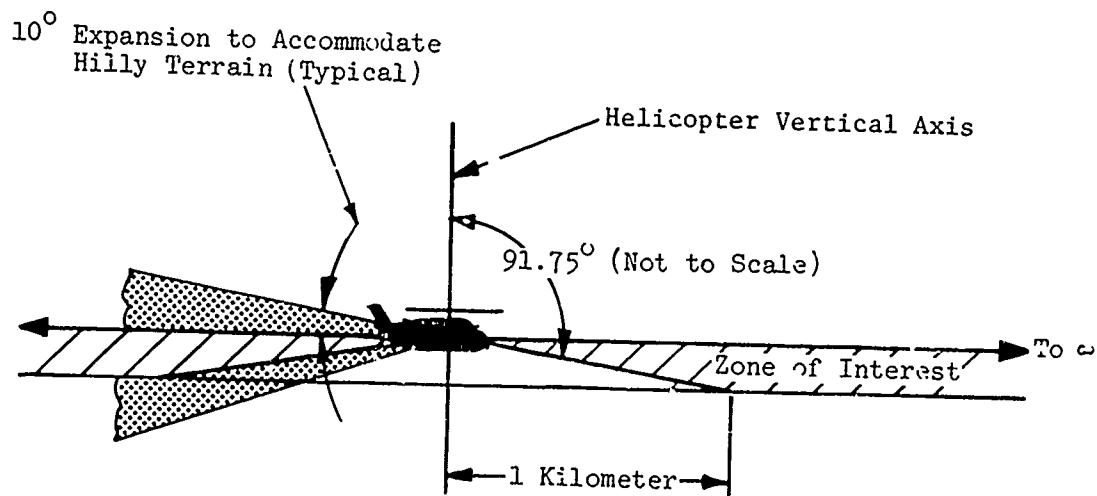


Figure 7-2. Zone of Interest for Glint Detection as Related to the Helicopter.

7.2 Sun Positions

The sun positions of interest are dependent upon geographic location. Table 7-1 shows the percentage of time that the sun spends at different elevations between the latitudes of 20° and 60° north. For this geographic region, sun elevations from 0° to 65° would be of primary interest since sun elevations above 65° occur less than 4% of the time. Sun azimuth positions are random since the helicopter can be oriented in any direction.

TABLE 7-1. SUN ELEVATION OCCURRENCE FOR 20° to 60° NORTH
LATITUDE LOCATIONS

Sun Elevations (Degrees)	Percentage of Occurrence
0 - 5	8.78
5 -10	9.28
10 -15	9.22
15 -20	9.04
20 -25	8.77
25 -30	8.43
30 -35	8.01
35 -40	7.52
40 -45	6.95
45 -50	6.29
50 -55	5.05
55 -60	3.96
60 -65	3.04
65 -70	2.26
70 -75	1.59
75 -80	1.03
80 -85	.58
85 -90	.20

Data from Reference 1.

7.3 Glint Detection

An awareness of the factors controlling visual detection of objects is necessary to enable engineers to analyze and design low-glint helicopters. The basic parameters that govern whether or not a stationary object can be seen are:

- Target size
- Target distance
- Background illumination
- Brightness contrast
- Atmospheric attenuation
- Foveal and peripheral visual perception of the observer

These parameters are related in a nonlinear manner, as shown in Figure 7-3. Target size and distance to target are coupled in the figure by presenting the visual angle subtended from the observer's eye to the extremities of the target. The curves show that, for a given target size, the background illumination required for detection increases as the contrast ratio decreases. Contrast ratio is expressed as a percentage and is equal to $\Delta B/B \times 100$, where ΔB is the difference in illuminance between target and background, and B is the illuminance of the background. The contrast ratio is also subject to atmospheric attenuation. This attenuation can be related to the meteorological visibility by the following expression obtained from Ref. 6:

$$C_A = ce^{-3.912R/V}$$

where C_A = attenuated contrast ratio (%)

c = inherent contrast ratio (%)

R = range to target (miles)

V = meteorological visibility (miles)

To provide a perspective on the range of conditions possible, Figure 7-4 shows luminance for various conditions of natural illumination.

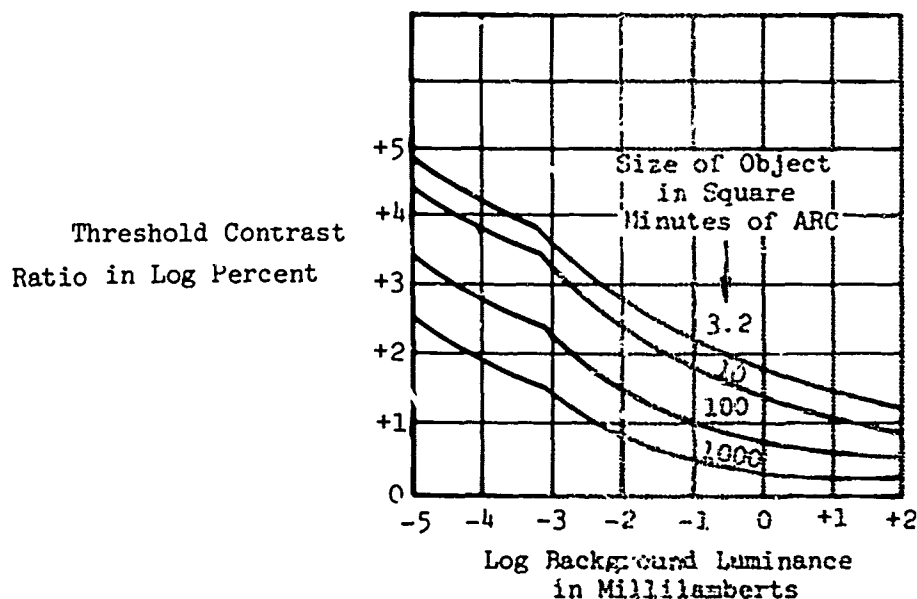
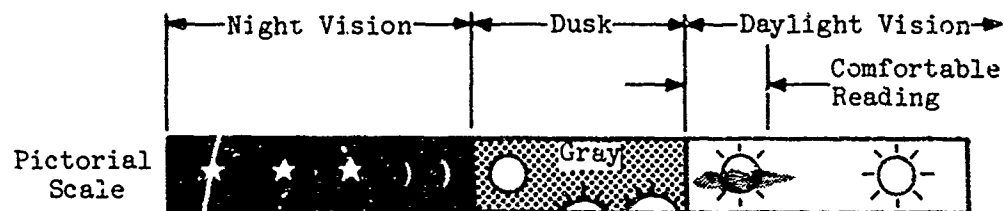
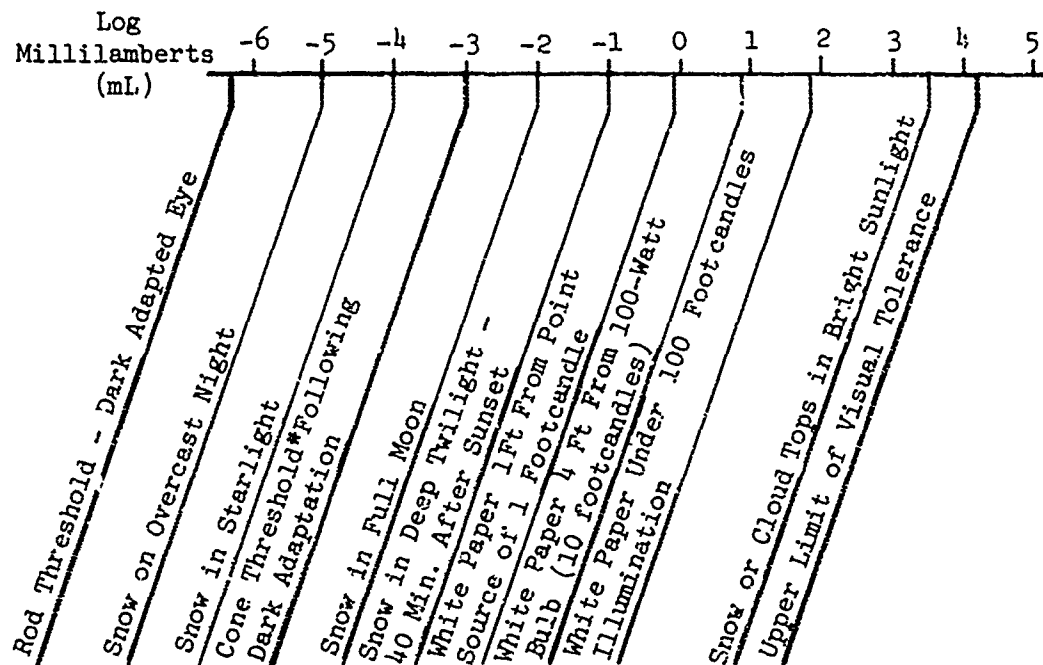


Figure 7-3. Contrast Discrimination Curve. Data From Ref. 2



Data from Ref. 2



Threshold is brightness level at which an object can just be seen

Figure 7-4. Range of Possible Lighting Conditions.

7.4 Sun Glint

The sun can be 10 times brighter than the surrounding sky and 100 times brighter than surrounding terrain. When even a small percentage of this sun brightness is reflected by a transparency, it is brighter than anything else on the horizon and deserves primary consideration when evaluating glint. The brightness of the sun is dependent upon geographic position, time of day, season of year, and local weather conditions. Likewise, background illumination depends additionally on the reflectance of the background medium, which can be sky, snow, trees, rock, etc., and the presence or absence of shadows from topography or clouds.

7.5 Glint Signature

Sun glints obey Snell's law of reflection, which provides that the angle of incidence is equal to the angle of reflection. Thus, if the observer and the sun are located so that the line of sight from each to the surface in question is at the same angle to the surface but on opposite sides of the normal, the observer will see the reflection of the sun on the surface (see Figure 7-5). This is called specular reflection, and in the case of glass or transparent plastic, the amount of light reflected is a function of angle of incidence. For example, at normal incidence, approximately 4% of the incident light is reflected, whereas at 80° obliquity approximately 25% of the incident light is reflected.

The sun subtends a visual angle of $1/2^\circ$ to the earth. This means that for ranges where glint is of interest, i.e., greater than 1 kilometer, the sun will appear larger than most helicopter transparencies, and its reflection will appear to cover the entire surface of the transparency, providing it is flat, as shown in Figure 7-6.

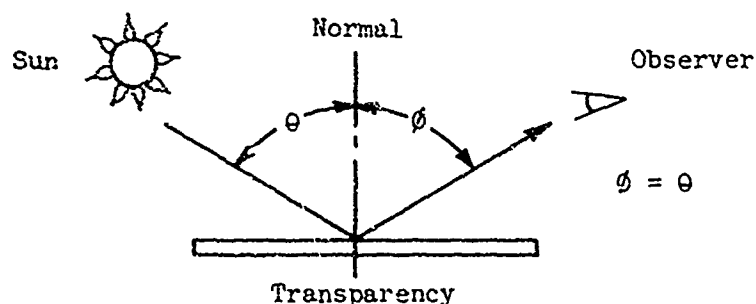


Figure 7-5. Snell's Law of Reflection.

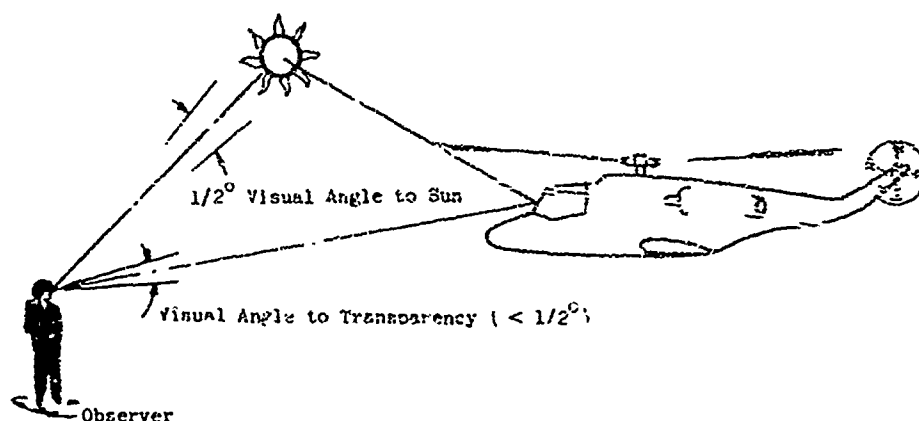


Figure 7-6. Visual Angle to Transparency and Sun.

In the case of curved reflecting surfaces, the glint signature is dispersed over a wider angle, as shown in Figure 7-7. However, only a portion of the curved transparency is effective in reflecting the sun's rays to an observer, and most of the light is scattered away from the observer. The size of this effective area is limited such that the visual angle from the transparency to the sun cannot exceed $1/2^\circ$ (see Figure 7-8).

7.6 Glint Signature Evaluation

Glint signatures from helicopter transparencies can be determined experimentally or analytically. In the experimental technique, the following method may be used.

7.6.1 Experimental Glint Signature Determination

Determination of canopy sun-glint signatures is performed using a scale model of the aircraft being studied, a simulated sun source, and provisions for observing and recording glint patterns. A typical test facility, shown in Figure 7-9, contains these necessary elements:

- | | |
|------------------------------|--------------------------|
| • Aircraft model | • Viewing-screen support |
| • Model-mounting fixture | • Sun simulator |
| • Translucent viewing screen | • Sun-simulator support |

Construction details are described in Reference 3.

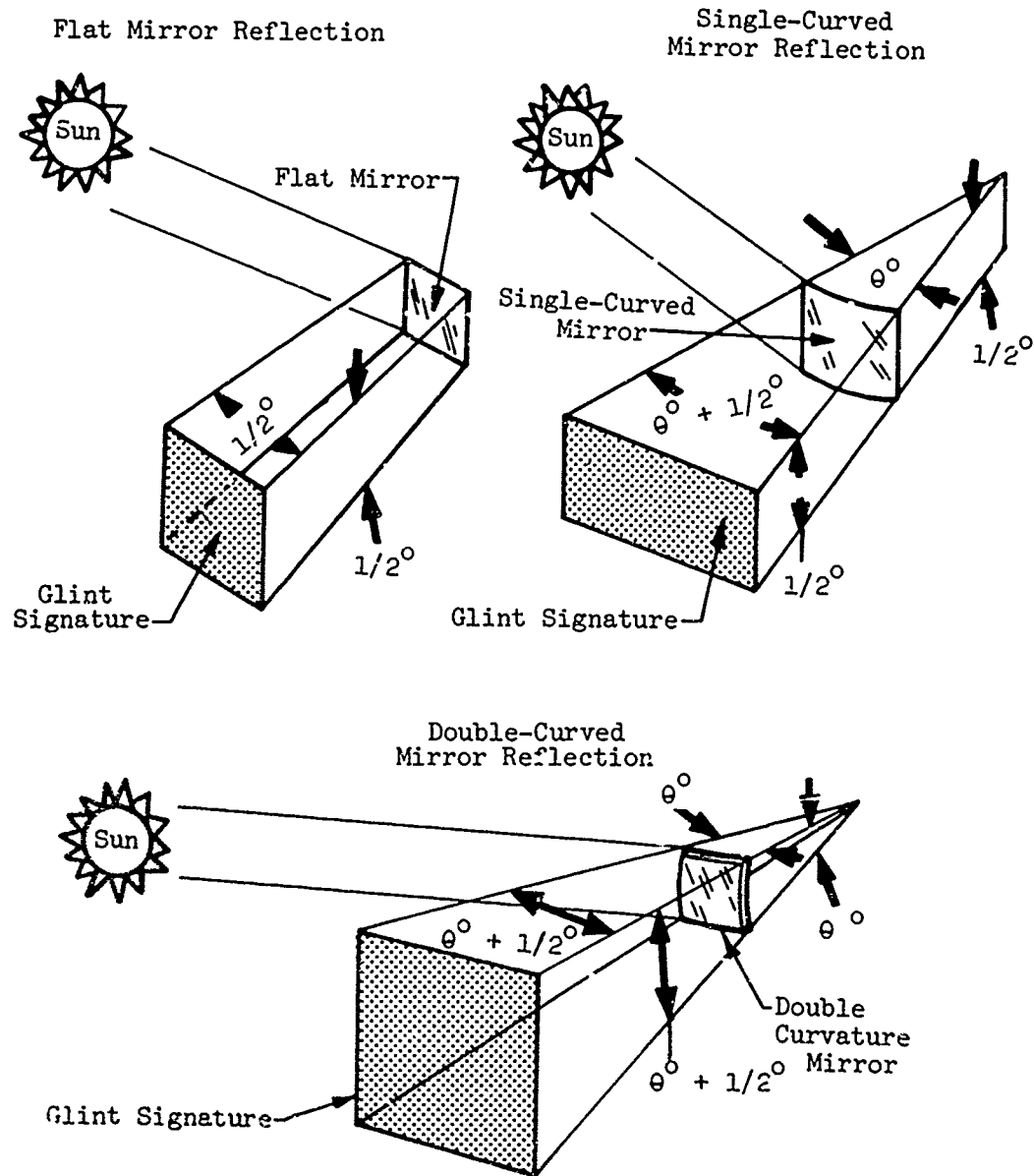


Figure 7-7. Sun Reflections From Surfaces of Different Curvature.

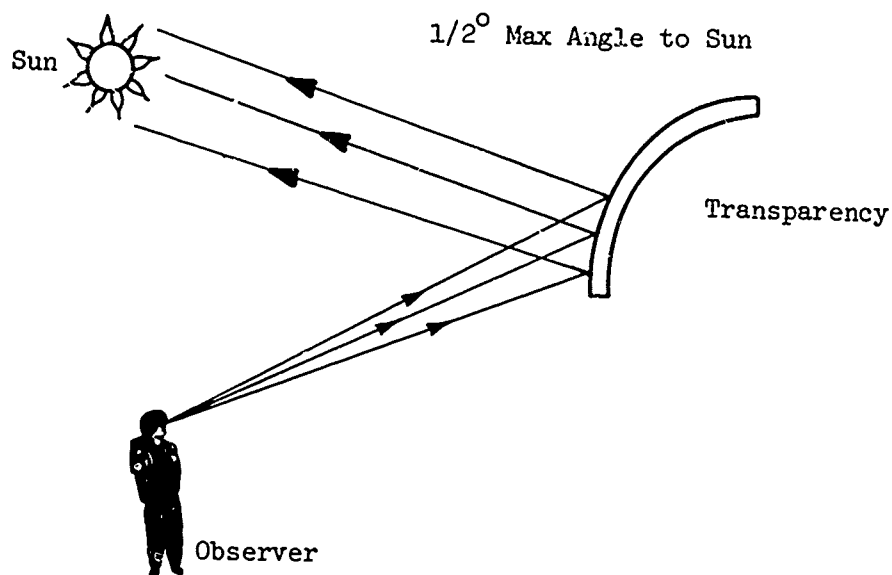


Figure 7-8. Effective Area of Reflection for Curved Transparencies.

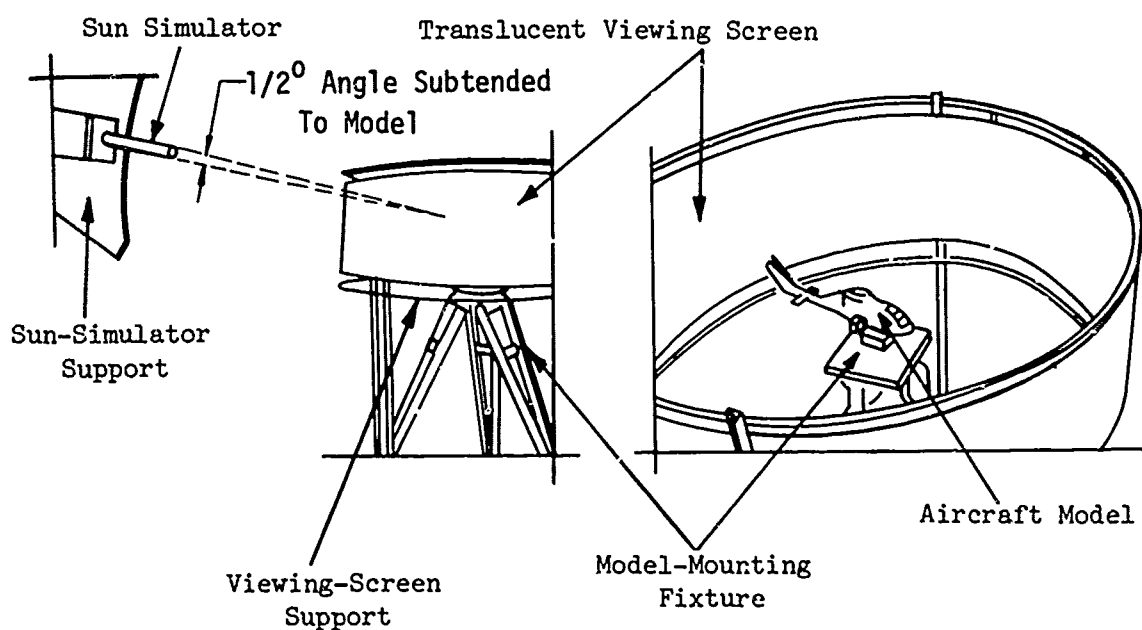


Figure 7-9. Test Setup for Determining Canopy Sun-Glint Signature.

7.6.1.1 Experimental Procedure

The model is mounted with the center of gravity of the aircraft on the nominal rotation axis of the mounting fixture. The model is raised or lowered until the centerline of the sun-simulator axis at an elevation angle of 0 degrees passes through the nominal eye level of a pilot seated within the aircraft. This position is marked as the 0-degree line on the viewing screen. The sun simulator is then positioned at the desired test elevation angle. The aircraft is positioned with its nose pointed at the sun simulator and its waterline parallel to the viewing screen support base. The room lights are extinguished to improve visibility, and all glints visible on the viewing screen are outlined with a marking pen. The model is then rotated to the right 20 degrees and the glint-outlining process is repeated. The sequence of rotating the model 20 degrees and marking sun glints is repeated until the model has completed 360 degrees of rotation. For aircraft that possess left-right symmetry, a 180-degree rotation of the model is sufficient. For other sun-elevation angles, the screen is replaced, the sun-elevation angle is changed, and the procedure is repeated.

7.6.1.2 Display Format

Figure 7-10 is a top view of the test setup shown in Figure 7-9. As indicated, the sun is fixed and always located along the 0-degree azimuth. Any observer's position can then be defined uniquely in terms of an azimuth and elevation measured relative to the aircraft's rotational axis and referenced to the sun's position. Aircraft headings are also referenced to the sun's direction and are measured positive to the right. If canopy sun glints are marked on the screen, then the outlines of the sun glints on the screen define the azimuths and elevations where sun glints can be seen for each aircraft heading. If the viewing screen is opened at the 180-degree azimuth and flattened with the outside of the screen face up, there is a panoramic display of the sun glints produced by the aircraft for the set of heading angles selected. This display defines all possible observer locations where sun glint may be seen. By specifying the markings on the flattened viewing screen, a standard display format for test data can be obtained. Figure 7-11 is a standard display developed in just this way which contains the following elements:

- A. Sun-elevation angle and aircraft pitch and roll attitude.

- B. Scale ranging from 0 to -180 and 0 to 180 degrees of azimuth referenced to the direction of the sun. The display is viewed as an opened right circular cylinder with 0 degrees being in the direction of the sun and the angles increasing positively to the right and negatively to the left as seen from the inside of the cylinder. The cylinder axis is vertical.
- C. Analyst-specified band of potential observer elevations with respect to the aircraft.
- D. Canopy sun-glint signatures, together with the aircraft heading, with respect to the sun that produced them. If the canopy sun-glint signature is so extensive that rotating the aircraft causes considerable overlapping, a single heading may be selected for each display.

7.6.1.3 Probability of Sun Glint

For each display, the probability of a glint existing within the observer elevation band may be computed. The probability of glint is defined as the fraction of the panorama between the upper and lower observer elevation limits that is swept by the canopy sun glint as the aircraft is rotated 360 degrees in heading. Measurements of the extents of glints are made in degrees, using the sun as the reference point (0°). A swept area is counted only once. For example, if the area between 60 degrees and 90 degrees with respect to the sun and 0 degrees and 10 degrees of observer elevation angle is the position of a glint when the aircraft is heading at either 20 degrees or 340 degrees, the fact that there is an overlap is ignored in the computation. For the limits shown on Figure 7-11, $360 \text{ degrees} \times 20 \text{ degrees} = 7,200 \text{ degrees}^2$ total area. The sun glint sweeps over $305 \text{ degrees} \times 15 \text{ degrees} = 4,575 \text{ degrees}^2$. The probability of glint is therefore $4,575/7,200 = 0.6354$.

Note that this probability applies only to the existence of glints within a zone of interest. It is not a probability for detection, since glint intensity, background illumination and visual angle are not involved in the calculations.

7.6.2 Analytical Procedure for the Determination of Glint Signature

Vector analysis techniques utilizing surface normals and sun position vectors can be used to calculate glint signatures. Such procedures require the aid of a computer to facilitate the numerous calculations involved. Typical computer programs for this purpose are described in References 1 and 2. Inputs for these programs include a mathematical definition of the transparency shapes, and sun and observer positions (azimuth and elevation) relative to the aircraft.

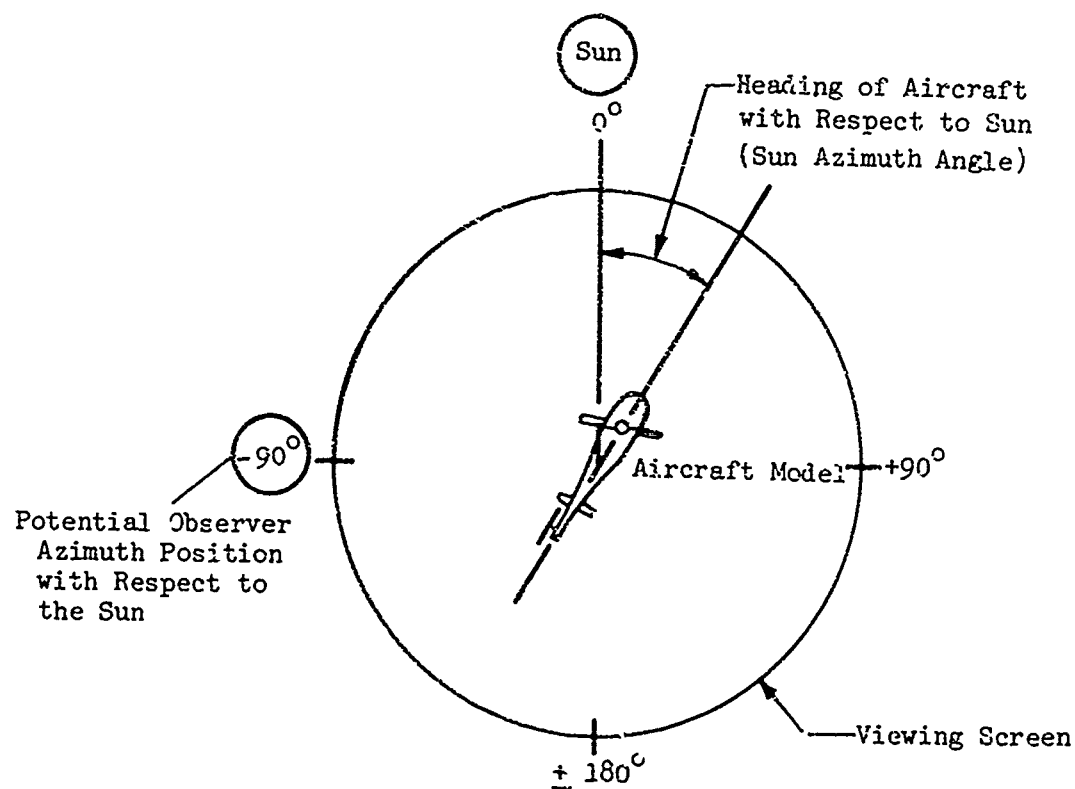


Figure 7-10. Top View of Experiment Setup.

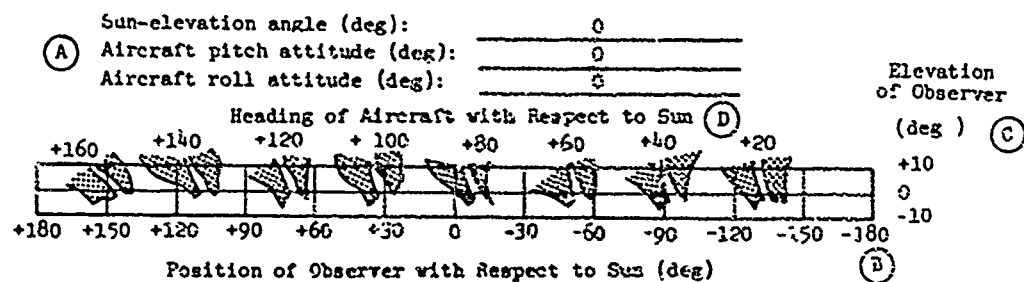


Figure 7-11. Standard Format for Presenting Canopy Sun-Glint Signature.

7.6.2.1 Geometric Relationships

Flat-surfaced transparent enclosures are more effective in reducing glint signatures than curved transparent enclosures of equivalent area. This is because the glint signature from flat shapes is much smaller. For example, considering sun elevations of 5 degrees to 65 degrees, the area swept by glint by a standard curve AH-1 canopy is between 63% and 98% of the total area, whereas for the same sun positions, the maximum area swept by glint by a flat AH-1 canopy does not exceed 7% of the total area. The increased glint intensity from flat panels is apparently of secondary importance since detection studies using helicopters equipped with both curved and flat canopies have shown the flat panels to be less detectable.

Even with flat panels, glint cannot be entirely eliminated. There will always be a combination of sun azimuth and elevation positions that will produce offending glints. For example, in Figure 7-12, given a sun elevation of 40 degrees, an azimuth position of 0 degrees (I_1) will cause a reflected ray (R_1) to emanate above the region of interest. However, for the same elevation when the sun ray azimuth (I_2) is at 180 degrees, the reflected ray (R_2) is below the region of interest. Hence, for some sun ray azimuth between 0 degrees and 180 degrees, the reflected ray vector must sweep through the region of interest.

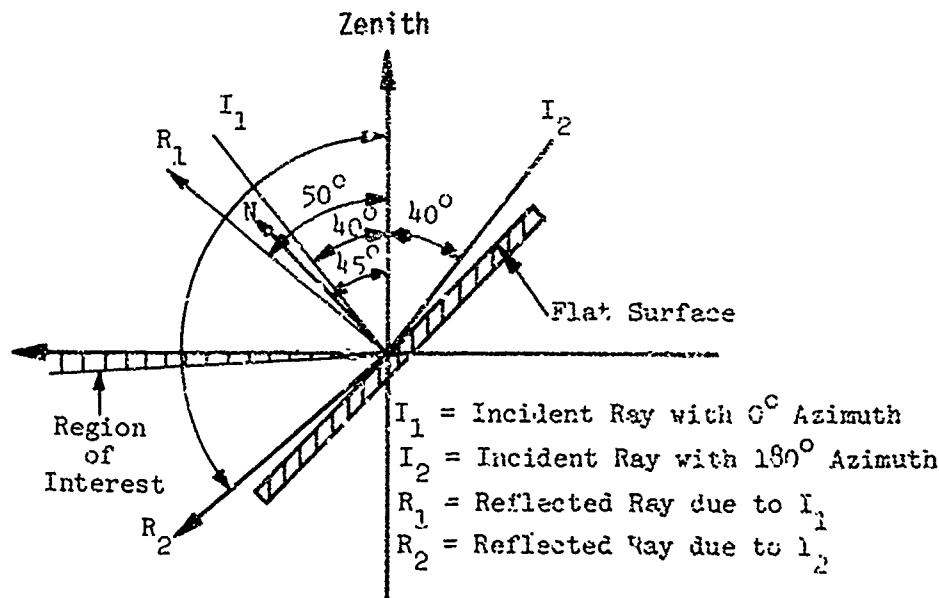


Figure 7-12 Illustration of Window Reflections.

For the basic canopy shape illustrated in Figure 7-13, Figures 7-14 and 7-15 show the combinations of sun azimuth and elevations that will produce offending glints for various window positions. For these curves, offending rays are those rays that fall 1 degree below a horizontal plane.

It is important to note that Figure 7-14 could have been plotted for sun-ray azimuths for 360 degrees to 180 degrees and the curves would have the same form. For example, when the window elevation is 45 degrees and the sun elevation is 65 degrees, a sun azimuth of 270 degrees would cause a reflected vector with 91 degrees zenith. In other words, the sun azimuths which cause glints in the region of interest are symmetrical with respect to the longitudinal axis of the helicopter.

Figure 7-15 corresponds to Figure 7-14 and illustrates the azimuth of the reflected vector when the reflected vector is in the region of interest for a given window elevation and a given sun elevation. Note that for all the cases considered, the reflected vector emanates toward the front of the aircraft, beginning with small azimuth for high suns and increasing in azimuth as the sun gets lower in the sky. For example, when the window elevation is 45 degrees and the sun vector elevation is 40 degrees, the reflected vector has an azimuth of -44 degrees and a zenith of 91 degrees.

Figures 7-16 and 7-17 represent the same type of data for the top windows as Figures 7-14 and 7-15 do for the front sloped window. Figures 7-18 and 7-19 represent the same type of data for the side windows.

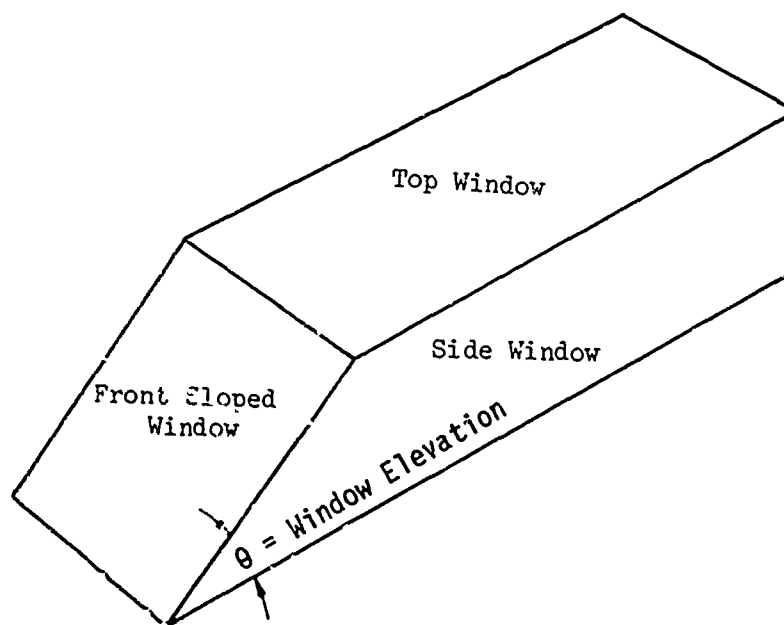
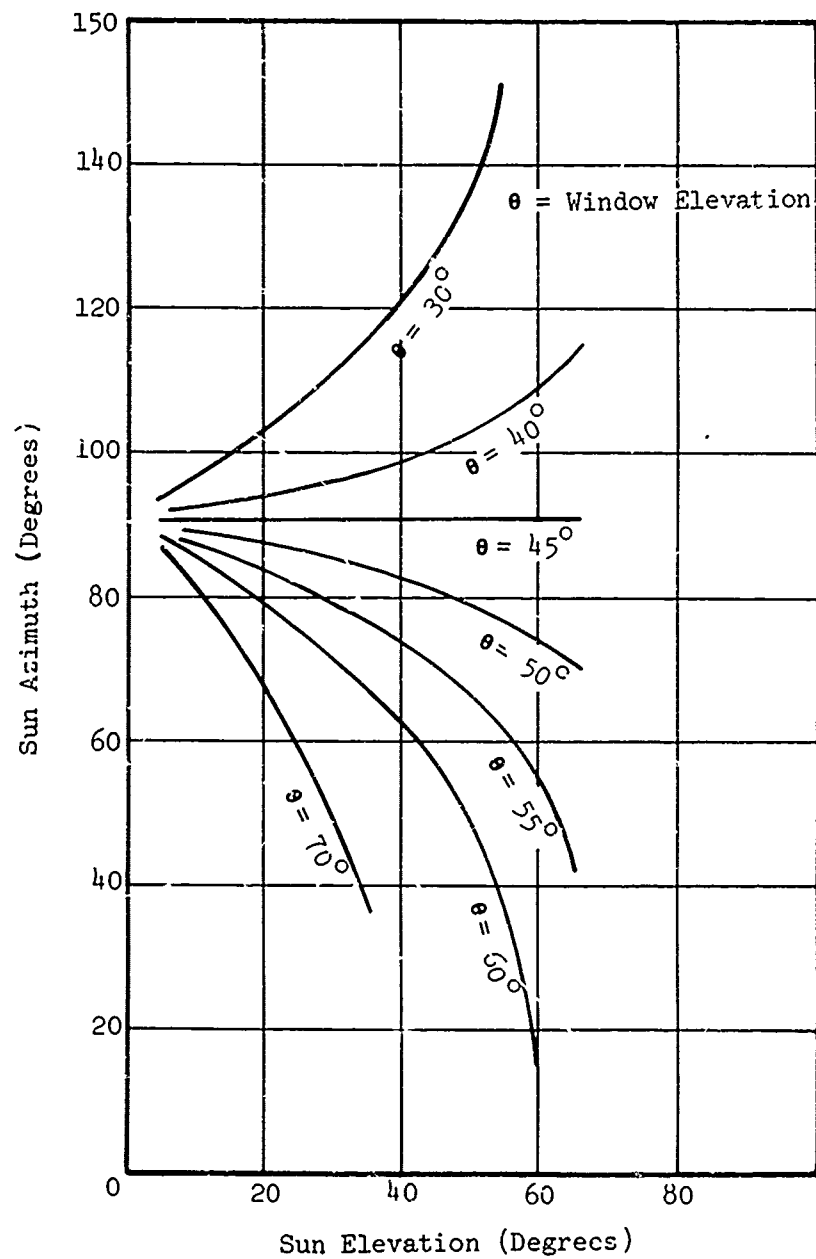
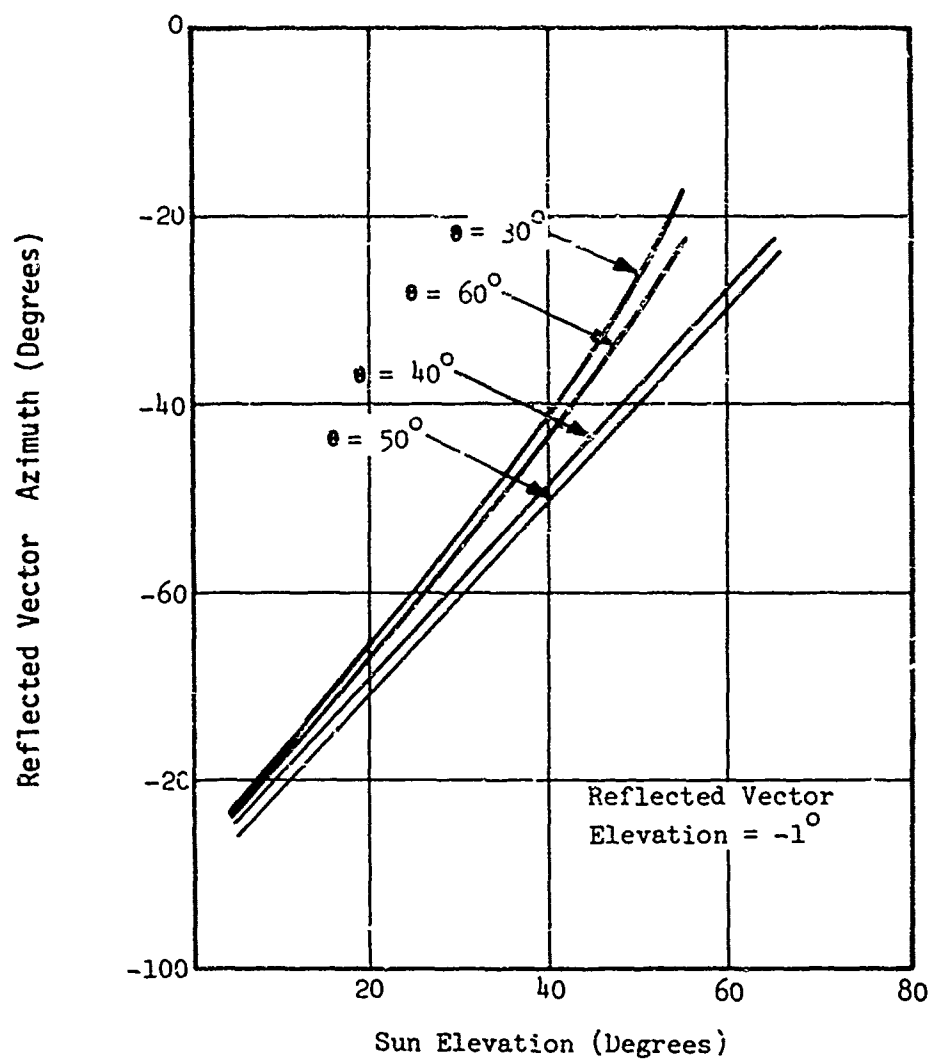


Figure 7-13. Basic Canopy Shape.



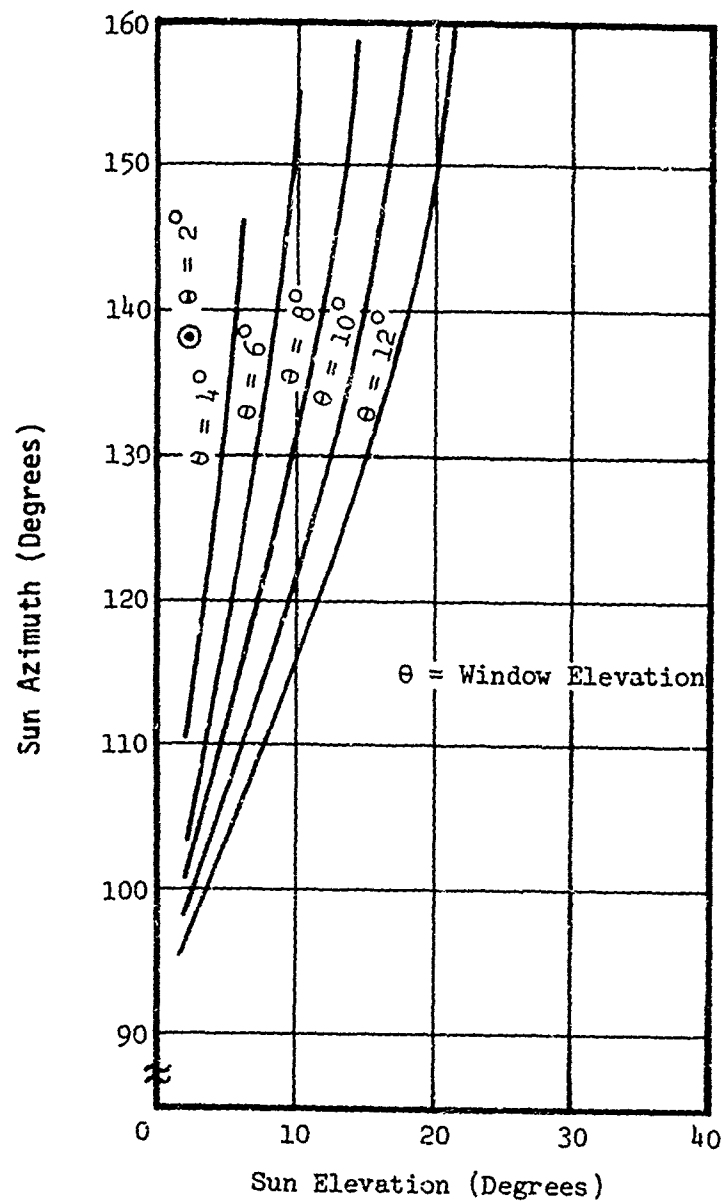
Data from Ref. 4

Figure 7-14. Offending Sun Positions for Various Elevations of Front Sloped Window.



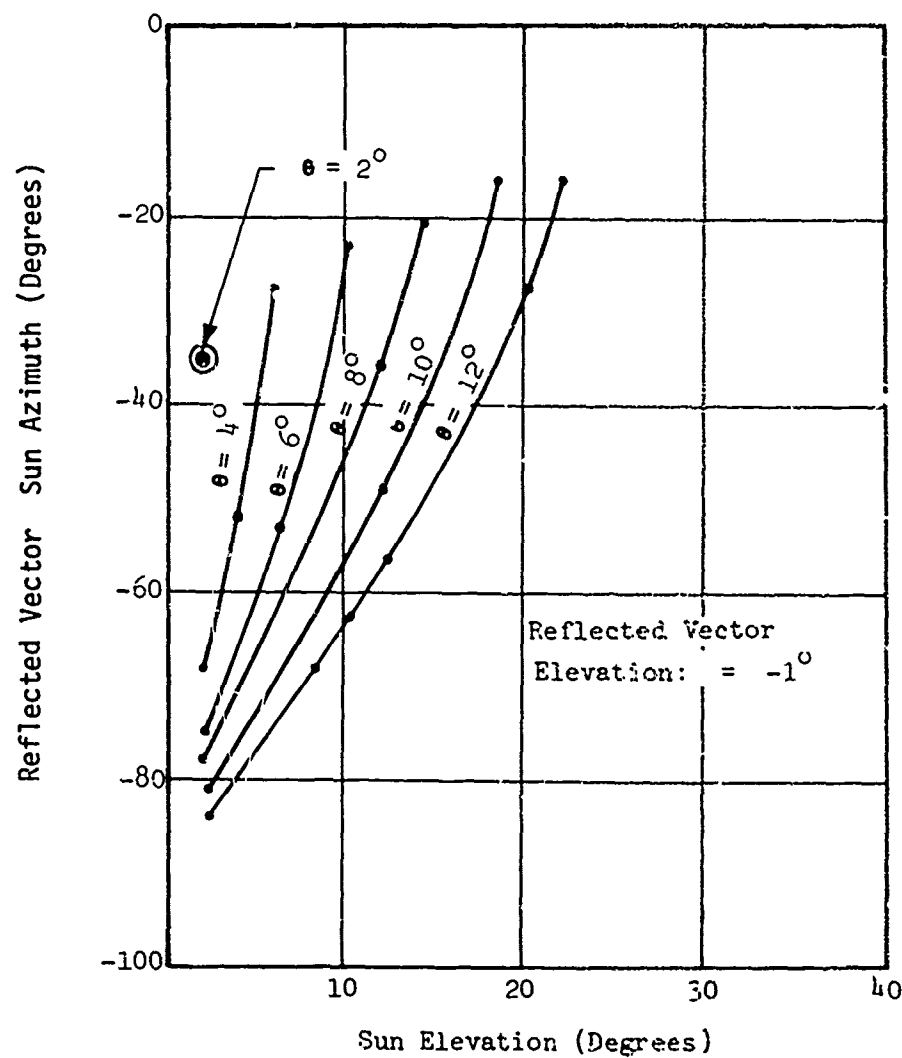
Data From Ref. 4

Figure 7-15. Reflected Vectors That Correspond to the Offending Sun Positions in Figure 7-14.



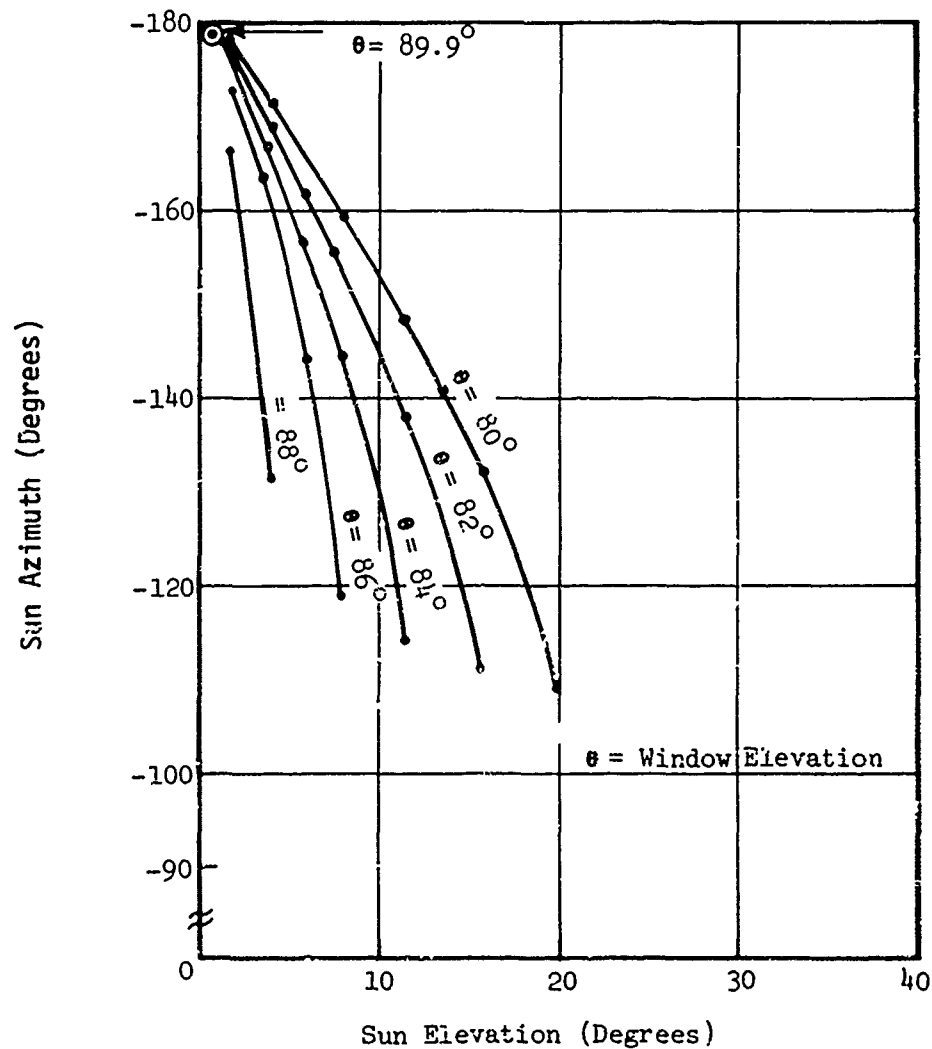
Data From Ref. 4

Figure 7-16. Offending Sun Positions for Various Elevations of Top Window.



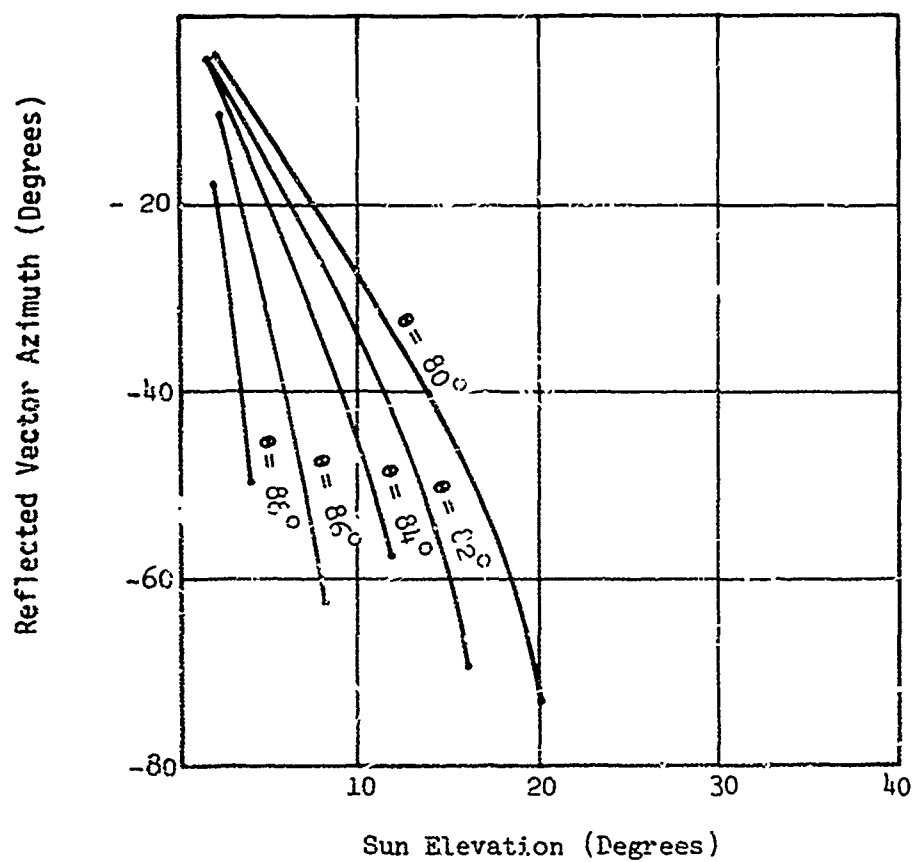
Data From Ref. 4

Figure 7-17. Reflected Vectors That Correspond to the Offending Sun Positions in Figure 7-16.



Data From Ref. 4

Figure 7-18. Offending Sun Positions for Various Elevations of the Side Windows.



Data From Ref. 4

Figure 7-19. Reflected Vectors That Correspond to the Offending Sun Positions in Figure 7-18.

Figures 7-14 through 7-19 can be used to predict the positions of glints on the ground for a variety of canopy designs that have the basic form shown in Figure 7-13. Also, a very important point is that, for any glint on the ground, the sun position which caused that glint can be located for a given window elevation.

7.7 Glint Countermeasures

From the preceding discussion it is apparent that geometry alone cannot totally eliminate glint, although favorable reflection patterns can be achieved by this method. For example, outward canting of vertical transparencies is effective at low altitudes since all sun rays are directed downward short of the 1-kilometer zone of interest, as shown in Figure 7-20. However, this advantage can be negated by sun rays entering the cockpit through another window and reflecting off the inboard surface, although clutter within the cockpit provides some masking from this effect.

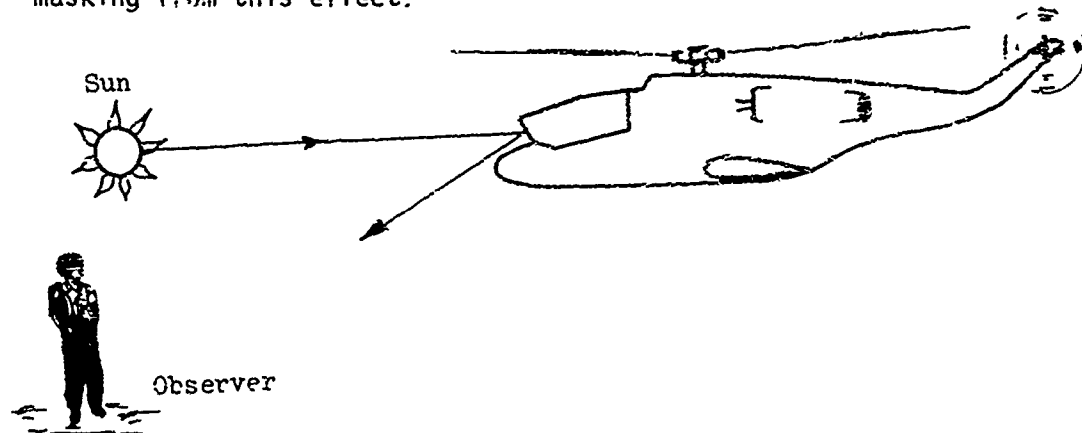


Figure 7-20. Downward Reflections From an Outward Canted Window.

Baffles or fences provide another means to attenuate glint signatures. As shown in Figure 7-21, these fences are mounted externally and either preclude the incidence of some offending sun rays or block other offending sun rays from reflecting in certain directions. Careful placement of baffles in conjunction with flat transparencies can virtually eliminate cockpit glint as a source of detection, although there are certain inherent disadvantages to this method, such as restricting visibility and increasing aerodynamic drag.

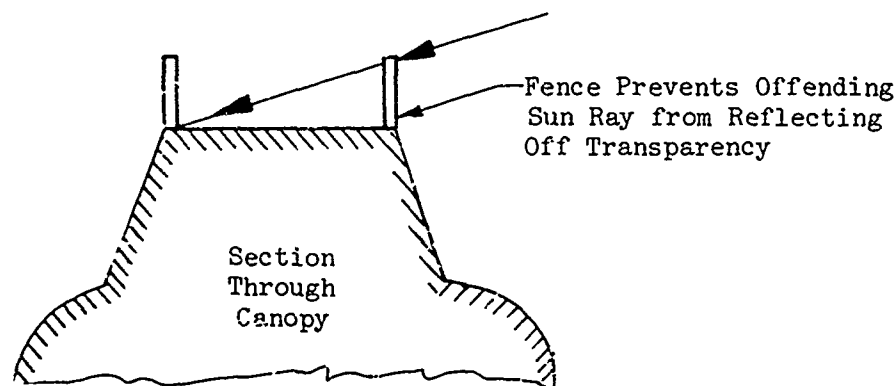


Figure 7-21. Reflection Control With Fences.

Antireflective coatings are frequently considered as solutions to glint problems. These coatings reduce the intensity of reflected light by a factor of about four at specified incidence angles. However, under conditions of very bright sunlight, this reduction is not necessarily great enough to prevent detection in the zones of interest. In addition, attenuation is optimized for a narrow range of incidence angles, which for practical purposes does not exceed 60 degrees. Beyond this range, the coatings become even less effective.

In an evaluation of the detectability characteristics of an AH-1 helicopter canopy with an antireflective coating, a series of tests described in Reference 5 showed that there was no significant difference in either detection range or total angle of glint between the coated canopy and the standard uncoated configuration.

References

1. Daumit, R. H., et al, Westinghouse Defense and Electronics Systems Center, "Cobra Glint Model AH-1G," LWL-CR-06P72B, U. S. Army Land Warfare Laboratory, Aberdeen Proving Ground, Md., Mar. 1974.
2. Wulfeck, J. W., et al, Tufts University, "Vision in Military Aircraft," WADC-TR-58-399, Wright Air Development Center, Wright-Patterson Air Force Base, Ohio, Nov. 1958.
3. Gundling, D. R., and White, F., Boeing Vertol Company, "Canopy Sun Glint Evaluation and Display Standard," USAAMRDL-TR-75-42, U. S. Army Air Mobility Research and Development Laboratory, Fort Eustis, Va., Oct. 1975, AD A0181079.
4. Daumit, R. H., and Kiesel, J. B., Westinghouse Defense and Electronics Systems Center, "Cobra Window Design Analysis and Noglare Canopy Design," LWL-CR-06P72, U. S. Army Land Warfare Laboratory, Aberdeen Proving Ground, Md., Mar. 1974.
5. Martin E. L., and Uliano, G. L., "Helicopter Disguise Evaluation," MASSTER Test No. 1029, Modern Army Selected Systems Test Evaluation and Review, Fort Hood, Tex., Oct. 1972.
6. Blewitt, S. J., Boeing Vertol Company, "Investigation of Helicopter Visual Detection," USAAMRDL-TR-74-72, U. S. Army Air Mobility Research and Development Laboratory, Fort Eustis, Va., Sept. 1974, AD B000297L.

Bibliography

Lundgren, G. A., Optical Coating Laboratory, Inc., "A Coating for Helicopter Canopies," AFML-TR-73-126, Air Force Materials Laboratory, Wright-Patterson Air Force Base, Ohio, Feb. 1973.

The capability of flying in adverse weather has become a common design requirement for military helicopters. A major problem is the presence of supercooled water droplets in clouds at ambient temperatures below freezing. When the supercooled water droplets are disturbed by an aircraft, the droplets will impinge and may freeze on unheated areas such as transparencies. The resultant ice buildup can obscure vision through the transparency. Therefore, all transparent areas essential to the mission must be maintained clear of external ice.

Due to weight, power, and cost constraints, it is seldom possible to heat the entire transparent enclosure, and heating is frequently limited to main windshields, as shown in Figure 8-1. Partial heating of localized areas of a windshield is sometimes used for emergency capability, although this technique usually results in restricted vision.



Figure 8-1. Anti-Icing of Main Windshields.

8.1 Definitions and Conditions

The following terms are used to define the various means of maintaining clear vision through transparencies in icing conditions.

Anti-icing - Anti-icing is the prevention of ice buildup by the process of either evaporating the impinging water, or melting it so that it may run off or run back and freeze on a noncritical area. Heated aircraft windshields do not normally vaporize the water. Anti-ice protection is provided by maintaining the windshield outer surface above $+35^{\circ}$.

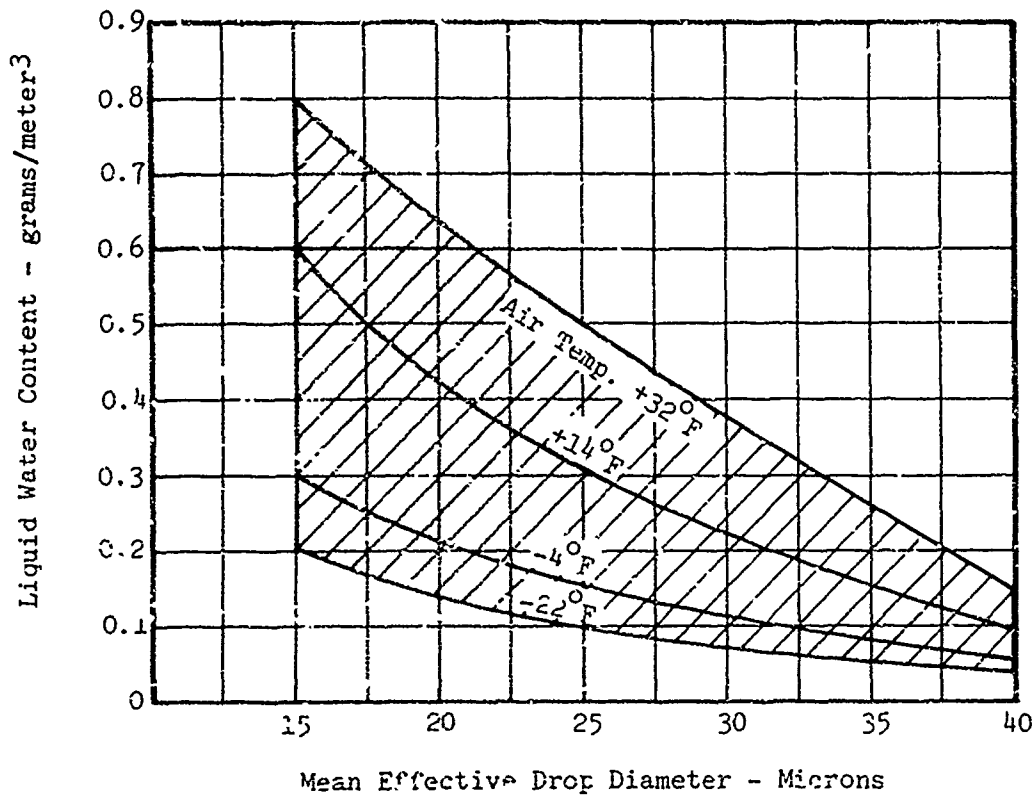
Deicing - Deicing is the periodic shedding of ice by mechanically or thermally destroying the bond between the ice and the protected surface. The ice shed by deicing may damage aft-mounted engines, components and rotors. However, the most important deficiency is the restriction on visibility during periods in which the ice is allowed to accumulate on windshields.

Defogging - Defogging is the removal of moisture and vapor on the interior surface on the windshield. This is normally accomplished by maintaining the surface temperature above the surrounding air dew point. The dew point is the temperature at which water vapor begins to condense out of air that is being cooled.

Design Icing Conditions - Windshield design icing/fogging conditions are directly related to the liquid water content of the air, the mean water droplet size, the ambient air temperature, and the local air velocity and surface geometry. The selection of specific environmental design criteria may be found in customer requirements, MIL-T-5842A, or Federal Aircraft Regulation FAR 25, Appendix C.

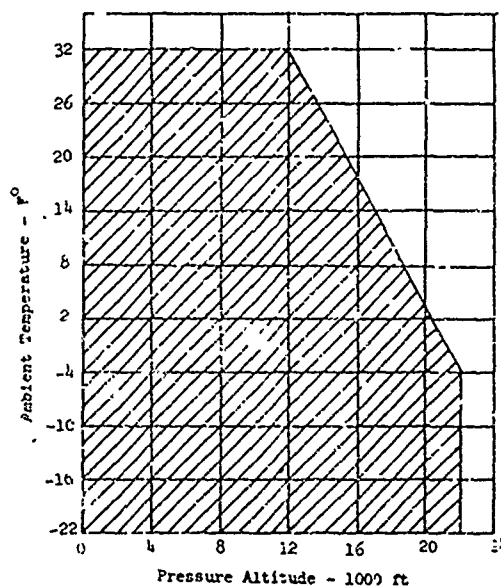
Continuous Icing Conditions - Continuous icing conditions occur during flight in extended (stratiform) cloud cover, and apply to a pressure altitude range from sea level to 22,000 feet. The intensity of continuous atmospheric icing conditions is defined by the variables of the cloud liquid water content, the mean effective diameter of the cloud droplets, and the ambient air temperature. Maximum values and the relationship between these three variables are shown in Figure 8-2 for a standard horizontal distance of 17.4 nautical miles. The limiting icing envelope in terms of altitude and temperature is given in Figure 8-3. The relationship of cloud liquid water content with drop diameter and altitude is determined from Figures 8-2 and 8-3. The cloud liquid water content for continuous maximum icing conditions of any horizontal extent is determined by the value of liquid water content of Figure 8-2 multiplied by the appropriate factor from Figure 8-4.

Horizontal distance of
17.4 Nautical Miles



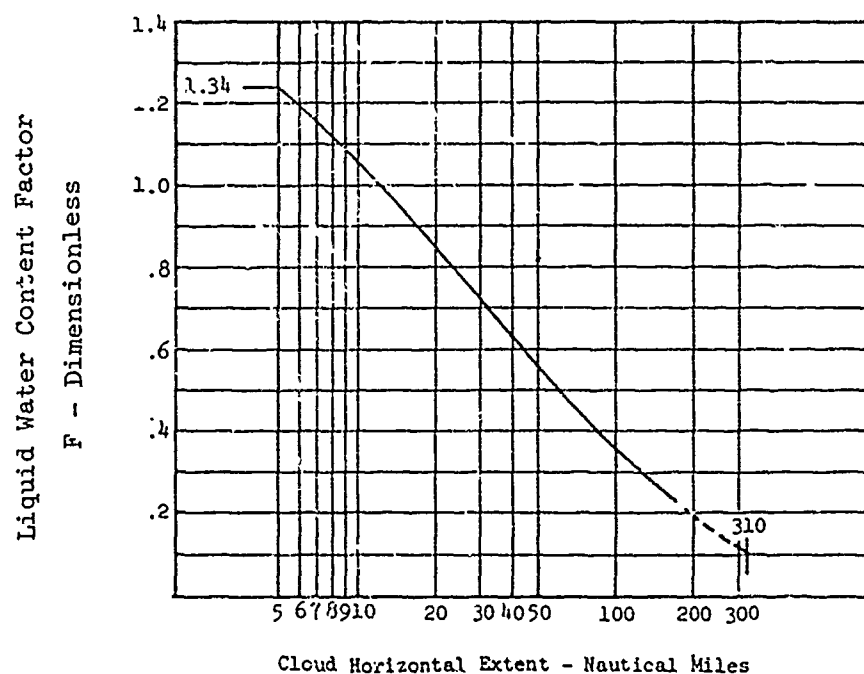
Data From Ref. 1

Figure 8-2. Continuous (Stratiform Clouds) Atmospheric Icing Conditions, Liquid Water Content Versus Mean Effective Drop Diameter.



Data from Ref. 1

Figure 8-3. Continuous (Stratiform Clouds) Atmospheric Icing Conditions. Ambient Temperature Versus Pressure Altitude.



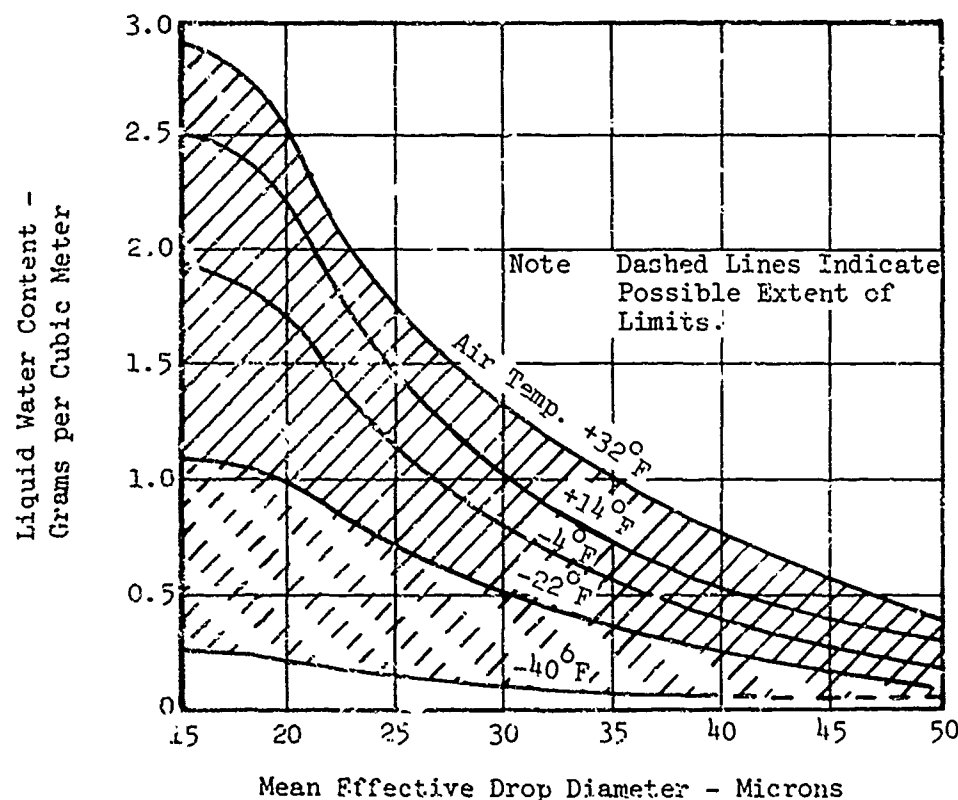
Data From Ref. 1

Figure 8-4. Continuous (Stratiform Clouds) Atmospheric Icing Conditions, Liquid Water Content Factor Versus Cloud Horizontal Distance.

Intermittent Icing Conditions

Intermittent icing conditions occur during flight in cumuliform clouds and can be more intense than conditions to be found in continuous stratiform clouds. The condition applies to pressure altitudes ranging from 4000 to 22,000 feet.

The intensity of intermittent atmospheric icing conditions is defined by the variables of the cloud liquid water content, the mean effective diameter of the cloud droplets, and the ambient air temperature. Maximum values and the relationship between these three variables are shown in Figure 8-5 for a standard horizontal distance of 2.6 nautical miles. The limiting icing envelope in terms of altitude and temperature is given in Figure 8-6. The relationship of cloud liquid water content with drop diameter and altitude is determined from Figures 8-5 and 8-6. The cloud's liquid water content for intermittent maximum icing of any horizontal extent is determined by the value of cloud liquid water content of Figure 8-5 multiplied by the appropriate factor in Figure 8-7.



Data From Ref. 1

Figure 8-5. Intermittent (Cumuliform Clouds) Atmospheric Icing Conditions, Liquid Water Content Versus Mean Effective Drop Diameter.

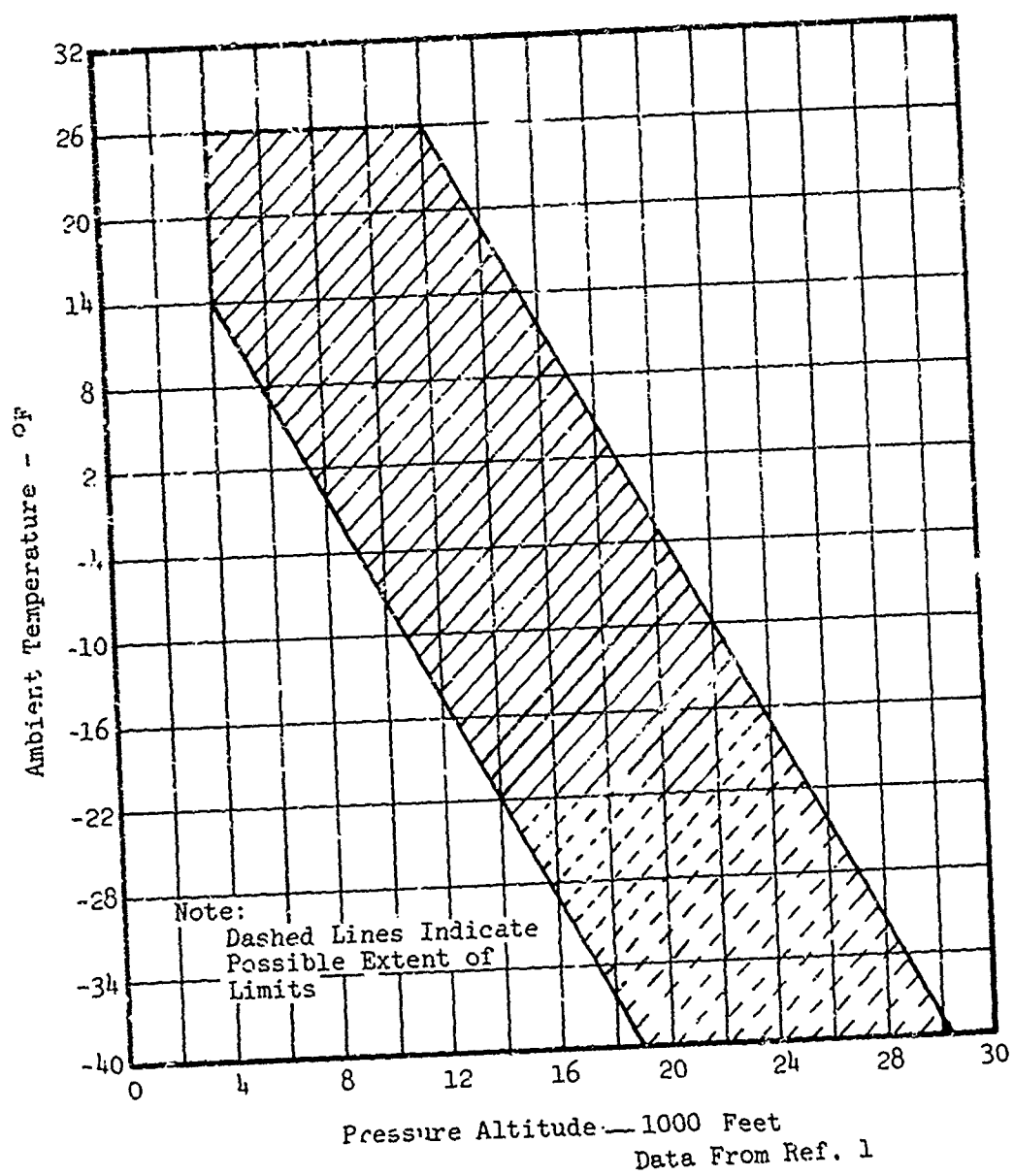


Figure 8-6. Intermittent (Cumuliform Clouds) Atmospheric Icing Conditions, Ambient Temperature Versus Pressure Altitude.

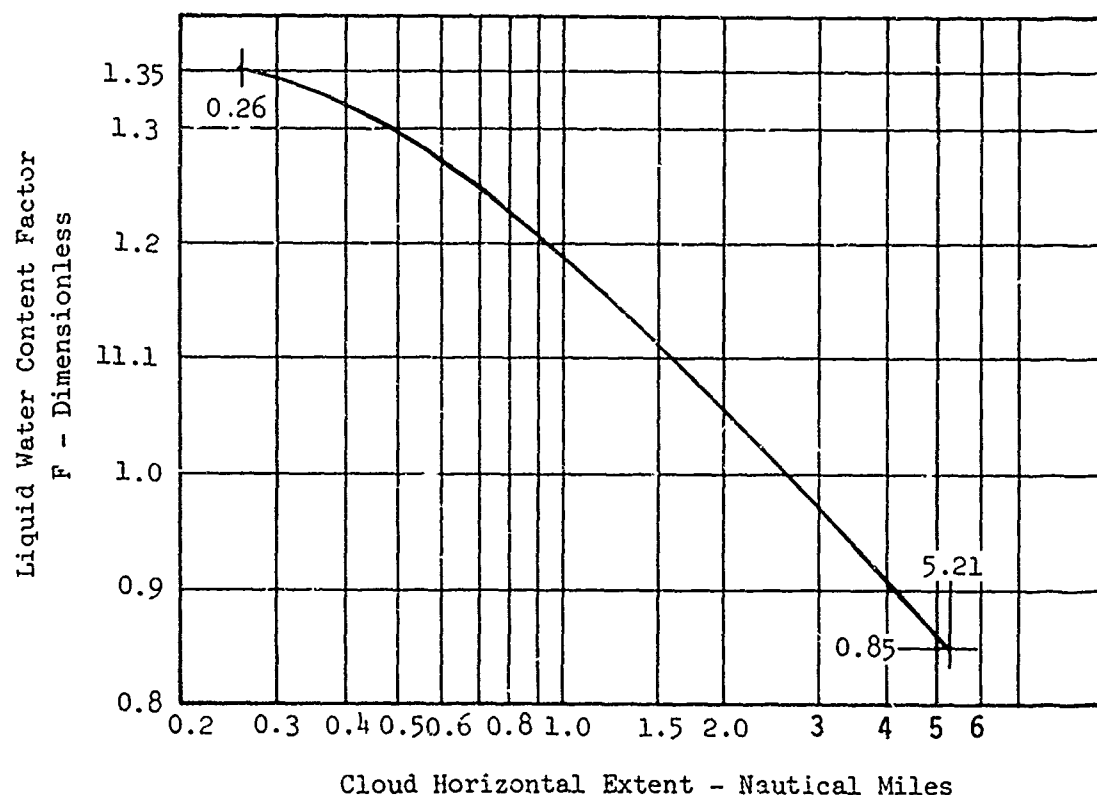


Figure 8-7. Intermittent (Cumuliform Clouds) Atmospheric Icing Conditions, Liquid Water Content Factor Versus Cloud Horizontal Extent. Data From Ref. 1

8.2 Heat Requirements

Power requirements for heated windshields are normally obtained from MIL-T-5842. For helicopters, these power densities have been found to be adequate if not somewhat conservative. Pertinent requirements from that specification are excerpted below.

The heating requirements shall be met during all conditions, including engine warm-up, taxiing, takeoff, and touchdown, up to the normal cruising speed of the aircraft in order to maintain an exterior windshield surface temperature of 35°F. Under these conditions, the anti-icing system shall be capable of supplying sufficient heat to all points of the exterior surface of the windshield to meet the requirements of the curve shown in Figure 8-8. Anti-ice heating can be accomplished by hot air or electrically conductive coatings.

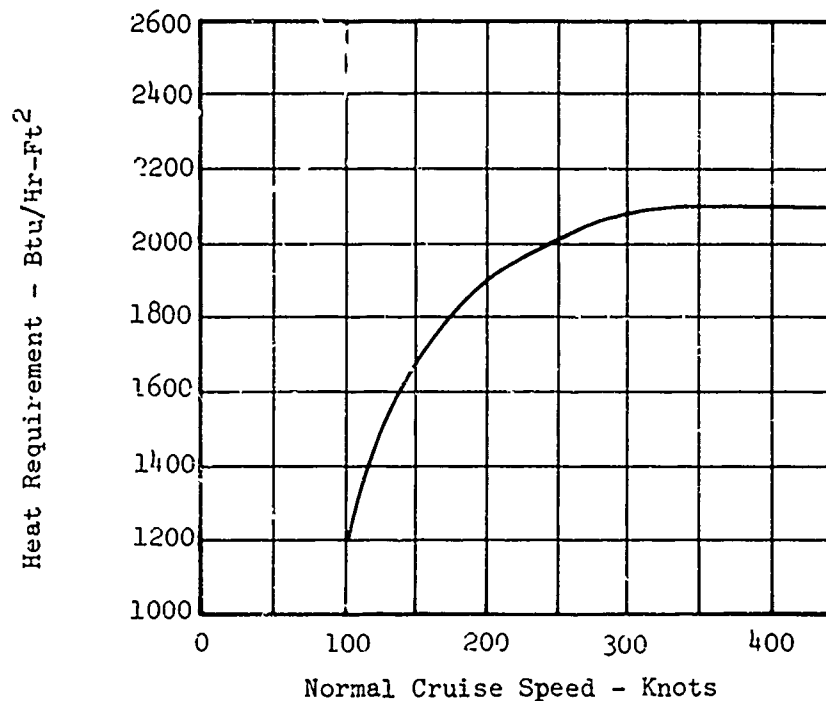


Figure 8-8. Windshield Heating Requirements as Defined by MIL-T-5842A.

8.3 Analysis of Heat Requirements

Analytical calculations provide an alternate, more detailed evaluation of the total unit heat flow requirement to that obtained from the MIL-T-5842 curve.

The establishment of a general solution for the total heat flux of a heated, anti-iced windshield includes the following possible modes of heat transfer:

Convective loss, q_c , direct heat transfer to the ambient outside atmosphere

Evaporative heat loss, q_e , outside heat transfer to vaporizing surface water.

Sensible heat loss, q_w , outside heat transfer to impinging liquid water

Radiation loss, q_r , outside radiation to space

The total outside windshield heat flux, q_o , Btu/(hr - ft²) is therefore:

$$q_o = q_c + q_e + q_w + q_r \quad (8-1)$$

In typical windshield heat analyses, the radiation losses are regarded as negligible and that term is frequently omitted from the analysis.

The total required windshield heat flux is the sum of the outside, q_o , and inside, q_i , heat fluxes (see Figure 8-9).

$$q_t = q_o + q_i \quad (8-2)$$

A parametric definition of each term is provided in the discussion that follows.

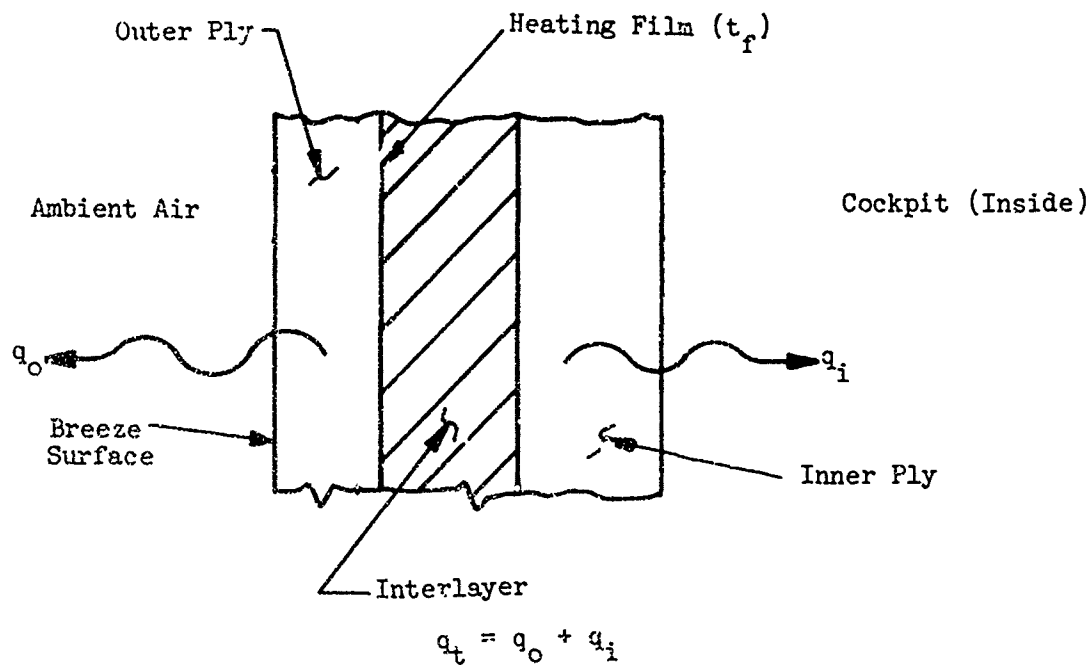


Figure 8-9. A Model of a Windshield's Transverse Heat Flow.

8.3.1 Convective Outside Flux

Heat transfer to the atmosphere consumes a relatively large amount of a windshield's total heat output. This heat loss occurs by convention and is quantified by the following equation:

$$q_c = h_c \left(t_s - \left(t_o + \frac{R_f}{2gJ c_p} v^2 \right) \right) \quad (8-3 \text{ from Ref.2})$$

where

q_c = convective outside heat flux, Btu/(hr - ft²)

h_c = convective outside or breeze surface heat transfer coefficient, Btu/(hr - ft² - °F).

Refer to Nomogram, Figure 8-10 for specific values of h_c .

t_s = outside windshield surface temperature (usually 35°F)

t_o = ambient outside air temperature, °F

See Figure 8-3 and/or Figure 8-6 for range of possible values.

V = local velocity over windshield, ft/sec

Usually assumed to equal aircraft velocity.

J = work equivalent of heat = 778.15 (ft - lb)/Btu

g = gravitational constant = 32.17 ft/sec²

c_p = specific heat = 0.24 Btu/lb for air

R_f = recovery factor = $(P_r)^{1/3} = 0.9$

P_r = Prandtl number

8.3.2 Evaporative Outside Heat Flux

The presence of liquid water is a necessity in an icing encounter. The windshield's outer surface will be partially wet and somewhat warmer than the surrounding moisture-bearing atmosphere. This results in mass transfer and hence an evaporative heat flux, q_e .

$$q_e = 2.91 L_s h_c w \frac{P_{ws} - P_{wo}}{P_B} \quad \text{(8-4) from Ref. 3 and 4}$$

where

L_s = latent heat of vaporization of water at the windshield surface temperature, Btu/lb.

L_s = 1074.1 Btu/lb at $t_s = 35^\circ\text{F}$. Other values of L_s may be obtained from steam tables, Reference 6.

h_c = convective outside heat transfer coefficient in Btu/(Hr - ft² - °F). Refer to nomogram, Figure 8-10 for specific values.

w = surface wetness factor, dimensionless. The surface wetness factor varies between 0 and 1. It has a value of 1 for a completely wet surface and a value of 0 for a completely dry surface.

P_{ws} = vapor pressure of saturated water at the windshield surface temperature, lb/ft².

P_{ws} = 14.39 lb/ft² at $t_s = 35^\circ\text{F}$. Other values of P_{ws} may be obtained from Table 8-1.

P_{wo} = vapor pressure of saturated water at ambient air temperature lb/ft². Refer to Table 8-1 for specific values.

P_B = atmospheric (barometric) pressure corresponding to the flight altitude, lb/ft². Refer to Table 8-2 for specific values.

NOTE: Equation 8-4 is based on the assumption that P_B is much larger than P_w .

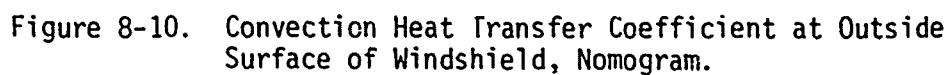


TABLE 8-1. TEMPERATURE VERSUS VAPOR PRESSURE OF SATURATED AIR

Temperature (t_o) (°F)	Vapor Pressure of Saturated Vapor (P_{ws} ; P_{wo}) Absolute Pressure (lb/ft ²)
-40	0.2736
-30	0.5040
-20	0.8928
-10	1.5552
0	2.6654
+10	4.4496
+20	7.2720
+30	11.6350
+35	14.3900
+40	17.5248
+50	25.6470

Data from Ref. 5

TABLE 8-2. ALTITUDE VERSUS BAROMETRIC PRESSURE

Altitude (ft)	Barometric Pressure, P_B (lb/ft ²)
0	2116
1000	2041
2000	1968
3000	1897
4000	1828
5000	1761
6000	1696
7000	1633
8000	1572
9000	1513
10000	1456
11000	1400
12000	1346
13000	1294
14000	1244
15000	1195

Data from Ref. 6

8.3.3 Sensible Outside Heat Flux

The heat flux associated with catching the liquid water at the atmospheric temperature and warming it to the windshield surface temperature by direct heat transfer is termed sensible heat flux. The equation includes the kinetic energy available from the impinging water.

$$q_w = .225 E_m (\text{Sine } \theta) (\text{Cosine } \phi) U (\text{LWC}) C_{Pw} \left(t_s - t_o + \frac{v^2}{2gJC_p \text{ water}} \right) \quad (8-5) \text{ from Ref. 3}$$

where

q_w = sensible outside heat flux, Btu/(hr - ft²)

t_s = temperature of the outside surface of windshield, °F

$$\frac{1}{2gJC_p \text{ water}} = 2 \times 10^{-5} \text{ ft}^2/(\text{sec}^2 - ^\circ\text{F})$$

t_o = ambient outside air temperature, °F

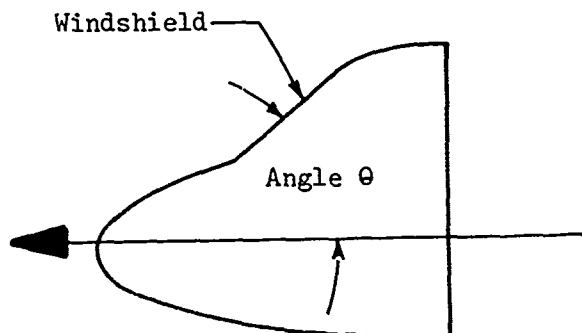
See Figure 8-3 or Figure 8-6 for the range of possible values.

V = local velocity over windshield, ft/sec

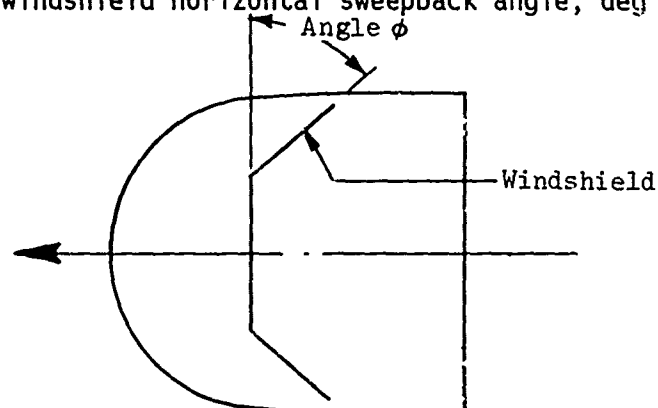
Usually assumed to equal aircraft velocity.

U = free-stream velocity, ft/sec

Angle θ = windshield vertical sweepback angle, deg



Angle ϕ = windshield horizontal sweepback angle, deg



LWC = liquid water content, gm/m³.

Specific values may be obtained from Figure 8-2 for continuous maximum icing conditions where $0.1 < (LWC) < 0.8$ or Figure 8-5 for intermittent maximum icing conditions where $0.1 < (LWC) < 2.9$.

C_{pw} = specific heat of water = 1.0 Btu/(lb - °F).

E_m = windshield droplet collection efficiency, dimensionless.
This term is a measure of how many supercooled droplets in a given approach area actually impinge on the windshield surface and may be related mathematically to Figure 8-11 as follows:

$$E_m = \frac{\text{Number of droplets in } \Delta y \text{ hitting windshield}}{\text{Number of droplets in } \Delta y \text{ approaching windshield}} \quad (8-6)$$

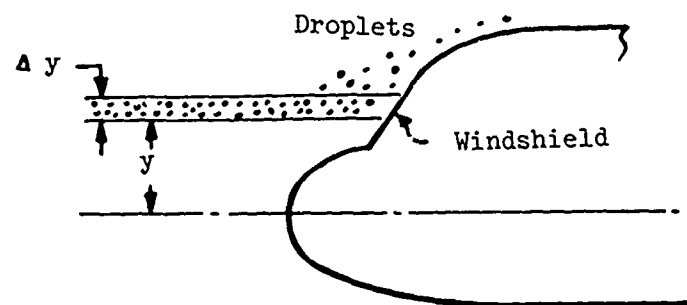


Figure 8-11. Physical Significance of Collection Efficiency.

The collection efficiency may be obtained as a function of the Reynolds number and a dimensionless inertia factor, K , from Equations 8-7 and 8-8 or Figure 8-12.

$$E_m = e^D \quad (8-7)$$

$$D = \frac{-\left(\frac{151}{K^2 + 150} + 0.267 + 0.225 R_N^{0.28}\right)\left(1.02 - \frac{180}{250 + R_N}\right)}{(K - 0.15)^{.74}} \quad (8-8)$$

where

R_N = free-stream Reynolds number, dimensionless

K = inertia parameter, dimensionless

and

$$R_N = \frac{2apV}{\mu} \quad (8-9)$$

where

a = droplet radius, ft

Specific values for a may be obtained from Figure 8-2 for continuous maximum icing conditions and Figure 8-5 for intermittent maximum icing conditions.

NOTE: 1 micron = 3.281×10^{-6} feet

μ = absolute viscosity of air, lb/(ft - sec). Specific values of μ may be obtained from Table 8-3.

and

$$\rho = \frac{P_B}{53.35 T_0} \quad (8-10)$$

where

P_B = barometric pressure corresponding to flight altitude, lb/ft^2
Refer to Table 8-2 for specific values.

T_O = absolute ambient air temperature, degrees Rankine

$$(T_O = t_O + 460)$$

ρ = density of air, lb/ft^3

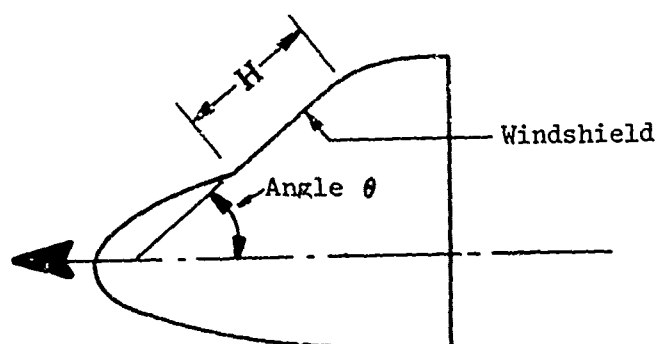
and

$$K = \frac{2\rho_w a^2 v}{9\mu (\sin \theta) H} \quad (8-11)$$

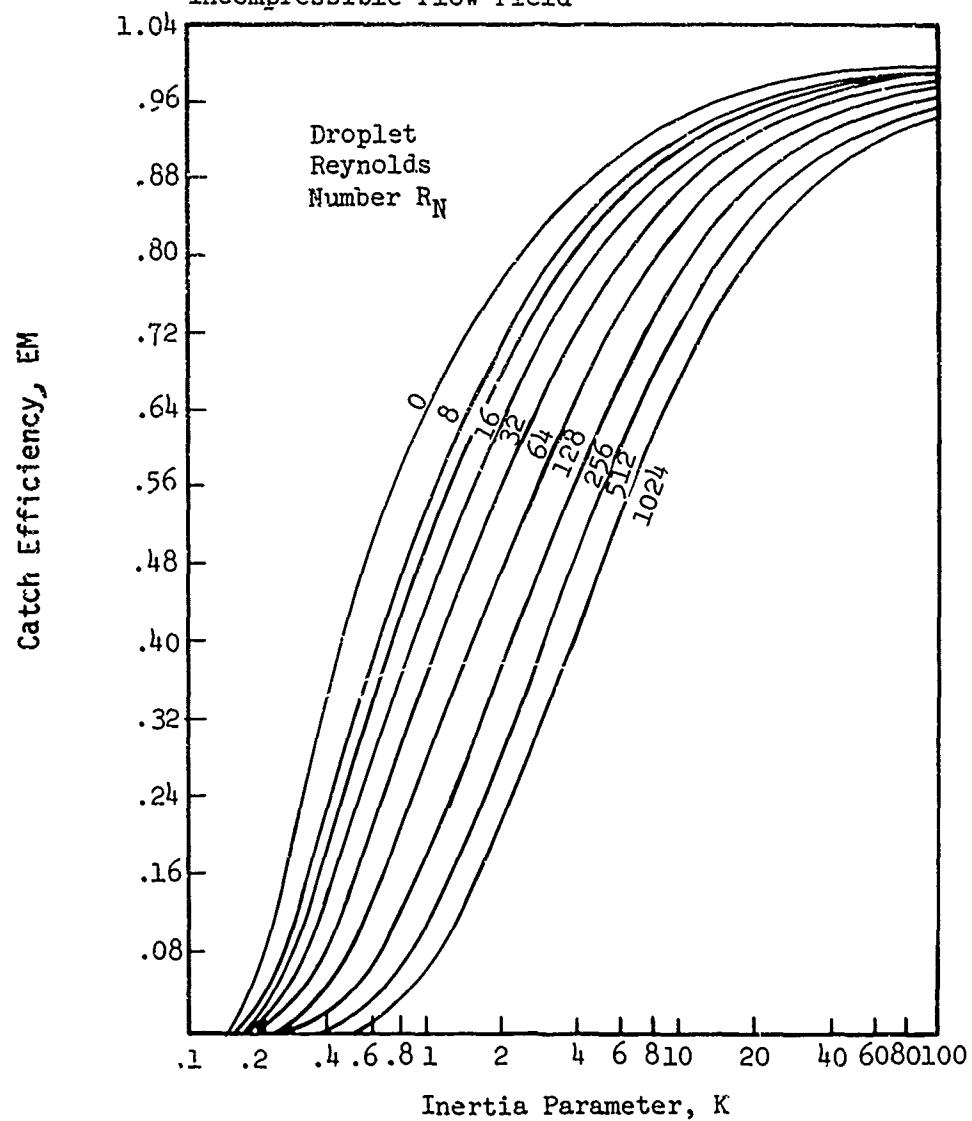
where

ρ_w = density of water = 62.4 lb/ft^3

H = vertical length of windshield



Average Catch Efficiency of Water Droplets on a
Rectangular Half Body in a Two-Dimensional
Incompressible Flow Field



Data From Ref. 3

Figure 8-12. Curve of Droplet Catch Efficiency.

TABLE 8-3. TEMPERATURE VERSUS ABSOLUTE VISCOSITY OF AIR

Temperature (t_o) $^{\circ}F$	Absolute Viscosity of Air (μ) lb/(ft - Sec)
-50	99.74×10^{-7}
-25	104.57×10^{-7}
0	108.75×10^{-7}
+25	113.57×10^{-7}
+50	118.40×10^{-7}

Data from Ref. 6

8.3.4 Radiation Outside Heat Flux

The basic equation for the unit heat loss at the windshield outer surface due to radiation is expressed by:

$$q_r = \delta \epsilon (T_s^4 - T_o^4) F_r \quad (8-12) \text{ from Ref. 7}$$

where

δ = Stefan-Boltzmann constant, which equals
 $0.173 \times 10^{-8} \text{ Btu}/(\text{hr} - \text{ft}^2 - ^{\circ}R^4)$.

ϵ = emissivity of windshield, which is assumed to be glass
and has a value of .94, Ref. 6.

T_o = absolute ambient outside air temperature, degrees Rankine.

See Figure 8-3 or Figure 8-6 for range of possible values.

T_s = absolute outside windshield surface temperature, degrees Rankine. Usually $35^{\circ}F + 460 = 495^{\circ}R$.

F_r = radiation shape factor. Assume = 1.0.

8.4 Temperature Uniformity

Temperature uniformity across the surface of a heated windshield is necessary to prevent hot spots that cause material breakdowns and cold spots that impair anti-ice or defog capability. Hot spots and cold spots are regions of local temperature variation resulting from nonuniform thickness (and therefore, heating) of the electrically conductive film. Thermal gradients in heated windshields also cause optical distortion and mechanical strains that affect structural integrity.

Typical windshield anti-icing systems cycle power on and off between limits of approximately 80° F and 100° F. A wide spread between on-off points is necessary to accommodate the tolerances of the temperature sensing elements and the electrical controller. In addition, the switching temperatures must be considered nominal values that are applicable only at the windshield temperature sensor location and that vary across the surface of the windshield.

Therefore, limits on temperature uniformity must be established which relate hot spots and cold spots to the sensor (control point) temperature.

8.4.1 Power Constant Equations

Temperature uniformity limits for heated windshields are defined by means of power constant equations. Power constant equations relate the ratio of local power dissipation, which is directly proportional to the transverse temperature gradient, at any two points on a windshield surface to a specified constant.

The power constant relationships are derived from the basic heat transfer equation:

$$Q = \frac{\Delta T}{R} \quad (8-13)$$

where

Q = heat flow

ΔT = total temperature gradient between the windshield heating film and ambient air

R = thermal resistance (conductive and convective) between the windshield heating film and ambient air along the path of heat flow

The following conditions are assumed to apply.

1. Heat flow is steady state.
2. External heat transfer coefficients are uniform.
3. Thermal resistance does not change with temperature.
4. Electrical resistivity of the heating film is independent of temperature.
5. All electrical power is converted to heat.

Therefore, at a steady state condition, R and Q will be constant for a given windshield:

$$RQ = \Delta T = \text{constant} \quad (8-14)$$

And for any two points on the windshield surface, the ratio of temperature gradients will also be constant.

$$\frac{R_1 Q_1}{R_2 Q_2} = \frac{T_1}{T_2} = \text{constant} = K \quad (8-15)$$

The temperatures that are of significant interest are:

T_H = hottest point on the windshield heating film ($^{\circ}\text{F}$)

T_L = coldest point on the windshield heating film ($^{\circ}\text{F}$)

T_{CH} = highest permissible temperature at the temperature sensor location

T_{CL} = lowest permissible temperature at the temperature sensor location

T_o = external ambient temperature

T_{CH} and T_{CL} are control points since power regulation is based on temperatures measured at those locations. The hottest temperature on the windshield heating film as well as the coldest temperature can be related to the control point temperature by a substitution in equation (8-15).

$$K_H = \frac{T_H - T_o}{T_{CH} - T_o} \quad (8-16)$$

where

K_H = hot-spot power constant

$$K_L = \frac{T_L - T_o}{T_{CL} - T_o} \quad (8-17)$$

where

K_L = cold-spot power constant

Equations 8-16 and 8-17 are used to calculate power constants for quality control purposes. The control point temperatures, T_{CH} and T_{CL} , are the highest and lowest temperatures at which the power is respectively switched off and on. The maximum hot-spot temperature, T_H , is a function of material properties and usually falls in a range between 150°F and 200°F. The minimum cold-spot temperature, T_L , is the lowest heating film temperature needed to maintain surface temperatures above freezing or dew point values. It is obtained from the windshield thermal design analysis.

It should be noted that as T_o , the ambient temperature, is lowered, the transverse thermal gradient increases. For example, at 70°F ambient temperature, if the hottest point on the windshield is 100°F and the control point is 90°F,

$$K_H = \frac{100 - 70}{90 - 70} = \frac{30}{20} = 1.5$$

Then, at -65°F, the hottest point for the same control-point temperature (90°F) would be

$$T_H = 1.5 (90 + 65) - 65 = 167.5^\circ\text{F}.$$

Thus, the ambient temperature used to establish the power constants should be the lowest temperature at which the operation of the equipment is required. For calculating hot spots, this would be -65°F, and for calculating cold spots this would be -22°F, the lowest temperature at which liquid water is found.

Equation 8-16 is plotted for various values of K in Figure 8-13.

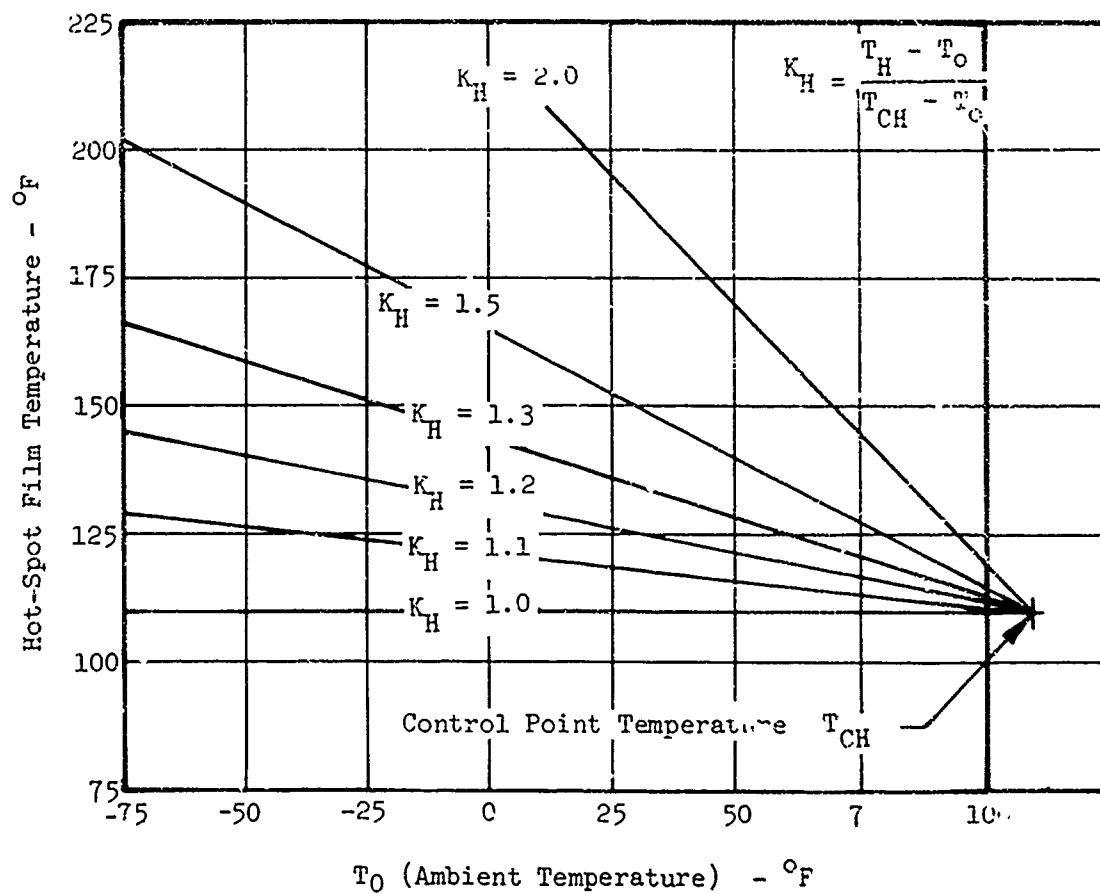


Figure 8-13. Hot-Spot Film Temperature Versus Ambient Air Temperature.

8.4.2 Effects of Nonuniform Airflow

The effects of nonuniform airflow over the exterior surface of a heated windshield cause variations in the local convective heat transfer coefficient and hence in the surface temperature. The local air velocity over the windshield surface is related to the free-stream velocity by equation 8-18, with the local convective coefficient (velocity function) and temperature given by equation 8-19.

$$V_L = V_\infty \sqrt{1 - C_p} \quad (8-18)$$

where

V_L = local velocity, mph

V_∞ = free-stream velocity, mph

C_p = local pressure coefficient, dimensionless
(Usually obtained from wind tunnel test data)

$$\frac{t_{f1} - t_\infty}{t_{f2} - t_\infty} = \frac{1 + \frac{h_1 \Delta x}{K}}{\frac{h_2 \Delta x}{K}}$$

where

t_f = temperature of windshield heating film, $^{\circ}\text{F}$

t_∞ = ambient temperature of free stream, $^{\circ}\text{F}$

Δx = windshield thickness, in

K = windshield thermal conductivity, $\frac{\text{Btu} \cdot \text{in}}{\text{hr} \cdot \text{ft}^2 \cdot ^{\circ}\text{F}}$

h = convective heat transfer coefficient, $\frac{\text{Btu}}{\text{hr} \cdot \text{ft}^2 \cdot ^{\circ}\text{F}}$

and subscripts 1 and 2 represent discrete locations on the windshield surface.

The following example shows the variations in temperature at two points on the windshield surface for a typical configuration as shown in Figure 8-14.

Given: $V_\infty = 150 \text{ mph}$
 $C_{p1} = 0.7$ Altitude = 2000 ft
 $C_{p2} = 0.45$

$$\Delta X = 0.1 \text{ in}$$

$$K = 7.14 \text{ Btu-in /hr} - ^\circ\text{F}$$

$$t_\infty = -4 ^\circ\text{F}$$

$$t_{f2} = 110 ^\circ\text{F}$$

$$V_L = V_\infty \sqrt{1 - C_p} \quad (8-18)$$

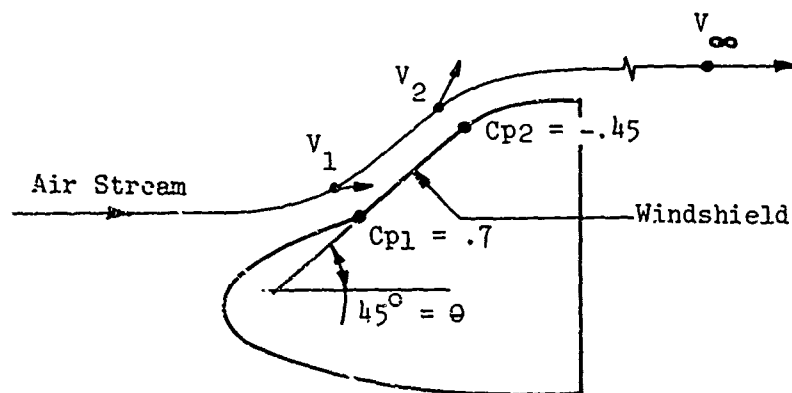


Figure 8-14. Variation in Airspeed at Windshield Surface

For V_{L1}

$$V_{L1} = 150 \sqrt{1 - .7} = 82 \text{ mph}$$

For V_{L2}

$$V_{L2} = 150 \sqrt{1 + .45} = 181 \text{ mph}$$

V_{L1} represents the slower moving air at the bottom of the windshield and V_{L2} the faster moving air at the top of the windshield. Using Figure 8-10, the corresponding values for convective heat transfer coefficients are 12 and 22.5 Btu/hr-ft² respectively. Assuming the heating-film temperature at point 2 is 110°F, the temperature at point 1 will be:

$$\frac{t_{f2} - t_\infty}{t_{f1} - t_\infty} = \frac{1 + \frac{h_2 \Delta x}{K}}{1 + \frac{h_1 \Delta x}{K}} \quad (8-19)$$

$$t_{f1} = \left(\frac{1 + \frac{22.5 (.1)}{7.14}}{1 + \frac{12 (.1)}{7.14}} \right) (110 + 4) = 128^{\circ}\text{F}$$

Thus, if the temperature sensor, set at 110°F , was located at the top of the windshield, the bottom of the windshield would automatically become a hot spot. This can be minimized by providing temperature sensors at both locations and averaging their signals to the power controller.

8.5 Temperature Sensor Location

Temperature sensing elements (TSE) are used to monitor windshield temperatures and, in conjunction with a power controller, determine when to switch power on and off. The TSE should be located as close to the heating film as possible to minimize thermal lag, as shown in Figure 8-15.

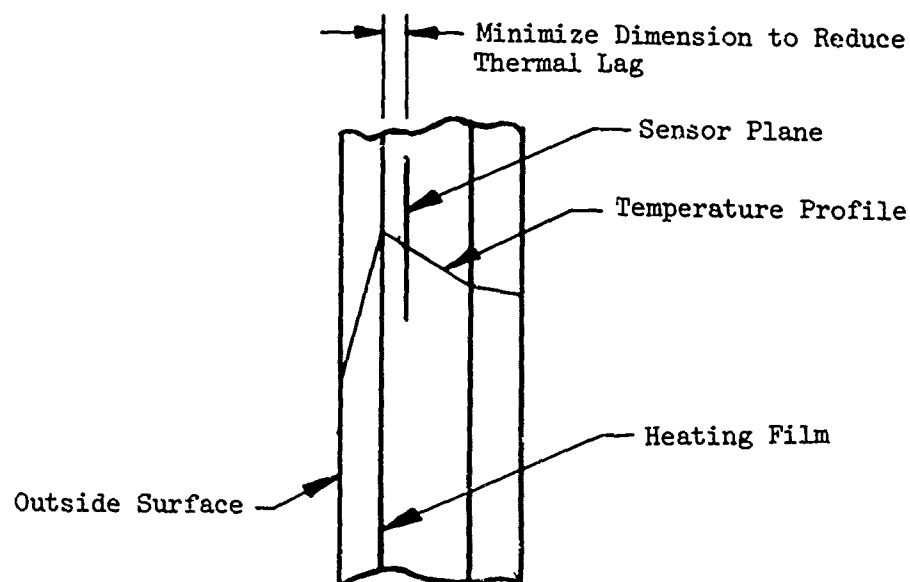


Figure 8-15. Transverse Temperature Sensor Location.

The sensor is located along the windshield perimeter and its location is usually allowed to vary within a specified zone. This permits the windshield manufacturer to place the sensor in the most favorable location with regard to hot spots and cold spots.

For example, with an ambient temperature of 50°F , the hot-spot and cold-spot power constants for the temperature sensor location shown in Figure 8-16 would be:

$$K_H = \frac{T_H - T_0}{T_{CH} - T_0}$$

$$K_L = \frac{T_L - T_0}{T_{CL} - T_0}$$

$$K_H = \frac{130 - 50}{120 - 50} = 1.14$$

$$K_L = \frac{105 - 50}{120 - 50} = .78$$

Moving the temperature sensor closer to the hot spot would reduce K_H but increase K_L , and moving the temperature sensor closer to the cold spot would improve K_L but increase K_H .

Ambient Temperature = 50°F

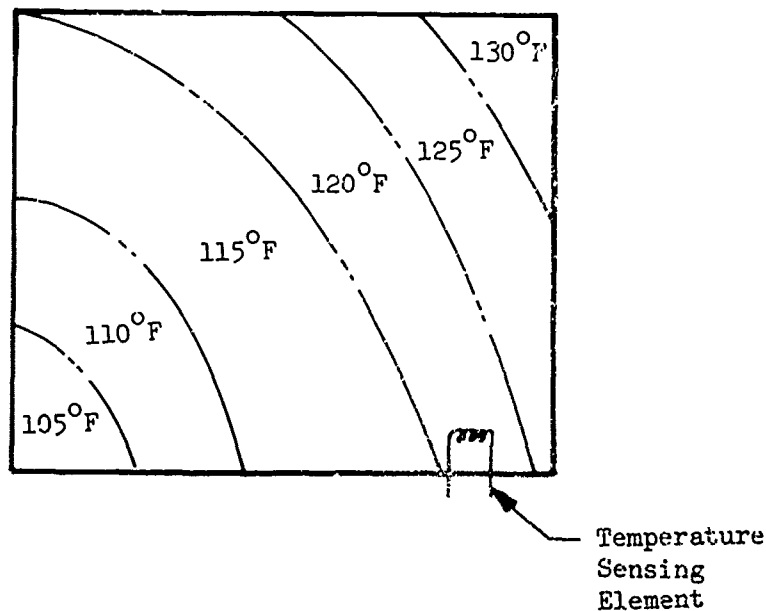


Figure 8-16. Temperature Sensor Location Relative to Hot and Cold Spots.

8.6 Sample Problem

The following sample problem has been included to further define the computational procedure for windshield thermal design and to provide results that show the relative importance of the four modes of heat transfer considered.

Given the following set of conditions:

Cruise speed	$s = 150$ knots
Windshield outer surface temperature	$t_s = + 35^{\circ}\text{F}$
Cockpit temperature	$t_i = + 40^{\circ}\text{F}$
Altitude	10,000 ft
Windshield vertical sweepback angle	$\theta = 45^{\circ}$
Windshield height	$H = 2.5$ ft
Windshield horizontal sweepback angle	$\theta' = 30^{\circ}$

Weather Conditions:

Intermittent icing

Ambient air temperature $t_o = -4^{\circ}\text{F}$, which is compatible with curve shown in Figure 8-6 for an altitude of 10,000 ft.

Mean effective drop diameter 30 microns

Therefore, from Figure 8-5 $\text{LWC} = .8 \text{ grams/meter}^3$

Horizontal extent of clouds 2 miles

From Figure 8-7 $F = 1.05$ and $\text{LWC} = .8 \times 1.05 = .84 \text{ grams/meter}^3$

The total heat flux may be obtained directly from the MIL-T-5842 curve, Figure 8-8 for a cruise speed of 150 knots.

$$q_t = 1700 \text{ Btu}/(\text{hr} - \text{ft}^2)$$

The computation of each heat flux mode is performed below for comparative purposes.

$$q_o = q_c + q_e + q_w + q_r \quad (8-1)$$

Convective Outside Heat Flux

$$q_c = h_c \left(t_s - \frac{(t_o + R_f V^2)}{2gJC_p} \right) \quad (8-3)$$

$$S = 150 \text{ knots} \times 1.151 \frac{\text{mph}}{\text{knot}} = 173 \text{ mph}$$

From Figure 8-10

$$h_c = 18 \text{ Btu}/(\text{hr} - \text{ft}^2)$$

$$V = 150 \text{ knots} \times 1.688 \frac{\text{ft}/\text{sec}}{\text{knot}} = 253 \text{ ft}/\text{sec}$$

$$q_c = 22 \left(35 - \frac{(-4 + .9 (253)^2)}{2(32.17)(778.16)(.24)} \right)$$

$$q_c = 616 \text{ Btu}/(\text{hr}-\text{ft}^2)$$

Evaporative Outside Heat Flux

$$q_e = 2.91 L_s h_c w \frac{P_{ws} - P_{wo}}{P_B} \quad (8-4)$$

$$L_s = 1074.1 \text{ Btu}/\text{lb} \text{ at } t_o = 35^\circ\text{F}$$

$$h_c = 18 \text{ Btu}/(\text{hr}-\text{ft}^2 - ^\circ\text{F})$$

$$w = 1.0$$

$$P_{ws} = 14.39 \text{ lb}/\text{ft}^2 \text{ at } t_o = 35^\circ\text{F}$$

$$P_{wo} = 2.22 \text{ lb}/\text{ft}^2 \text{ from Table 8-1 at } -4^\circ\text{F}$$

$$P_B = 1456 \text{ lb}/\text{ft}^2 \text{ from Table 8-2 at 10,000 ft}$$

$$q_e = (2.91) (1074.1) (18) (1.0) \frac{14.39 - 2.22}{1456}$$

$$q_e = 470 \text{ Btu}/(\text{hr}-\text{ft}^2)$$

$$q_w = .225 E_m (\sin \theta) (\cos \phi) U(LWC) C_{pw} \left(t_s - t_o + \frac{v^2}{2gJC_{p \text{ water}}} \right) \quad (8-5)$$

$$E_m = e^D$$

$$D = \frac{-\left(\frac{151}{K^2 + 150} + 0.267 + 0.225 R_N^{0.28}\right) \left(1.02 - \frac{180}{250 + R_N}\right)}{(K - 0.15)^{.74}} \quad (8-8)$$

$$R_N = \frac{2a\rho V}{\mu}$$

$$a = 30 \frac{\text{microns}}{2} \times 3.281 \times 10^{-6} \frac{\text{ft}}{\text{microns}} = 4.92 \times 10^{-5} \text{ft}$$

$$\rho = \frac{P_B}{53.35 T_o} \quad (8-10)$$

$$T_o = t_o + 460 = -4 + 460 = 456^\circ R$$

$$p = \frac{1456}{53.35(456)} = .060 \text{ lb/ft}^2$$

$$\text{From Table 8-3, } \mu = 108.8 \times 10^{-7} \text{ lb/ft-sec}$$

$$R_N = \frac{2(4.92 \times 10^{-5})(.060)(253)}{108.1 \times 10^{-7}} = 138.2$$

$$K = \frac{2\rho_w a^2 v}{9\mu (\sin \theta) H}$$

$$K = \frac{2(62.4)(4.92 \times 10^{-5})^2(253)}{9(108.8 \times 10^{-7})(.707)(2.5)} = .445$$

$$D = \frac{-\left(\frac{151}{(.445)^2 + 150} + 0.267 + 0.225(138)^{0.28}\right) \left(1.02 - \frac{180}{250 + 138}\right)}{(.445 - 0.15)^{.74}}$$

$$D = -2.97$$

$$E_m = e^{-2.97} = .051$$

The value of E_m , as taken from Figure 8-12, is approximately the same.

Continuing,

$$q_w = .225(.051)(.707)(.866)(253)(.84)(1.0)(35+4+(253)^2(2 \times 10^{-5})) \\ = 60 \text{ Btu/(hr-ft}^2\text{)}$$

Radiation outside heat flux

$$q_r = \delta \epsilon (T_s^4 - T_o^4) F_r \\ q_r = (0.173 \times 10^{-10}) (.94)(.95^4 - .456^4) = 27.30 \text{ Btu/(hr-ft}^2\text{)}$$

Total outside required windshield heat flux

$$q_o = q_c + q_e + q_w + q_r = 616 + 470 + 60 + 27 = 1173 \text{ Btu/hr-ft}^2$$

8.7 Windshield Temperature Profile

Prior to determining the heat flux to the cockpit interior, the windshield heating-film temperature must be determined. The procedure for calculating the minimum heating-film temperature is summarized below.

Given a windshield cross section as shown in Figure 8-17, the temperature rise between the outer surface and the heating film is calculated from the thermal resistance of the outer ply.

$$t_f - t_s = q_o \frac{x}{k} \quad (8-20)$$

where

t_s = surface temperature, $^{\circ}\text{F}$

t_f = film temperature, $^{\circ}\text{F}$

x = outer ply thickness, in.

k = thermal conductivity, $\frac{\text{Btu-in.}}{\text{ft}^2\text{-hr-}^{\circ}\text{F}}$

q_o = heat available, $\text{Btu/(hr-ft}^2\text{)}$

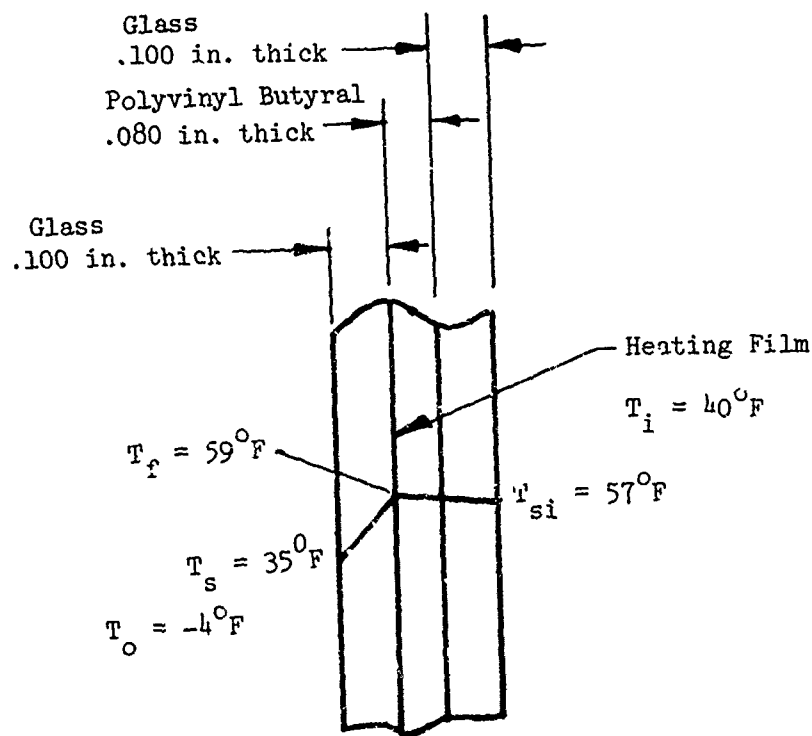


Figure 8-17. Windshield Cross Section and Temperature Profile.

$$k = 7.14 \frac{\text{Btu-in.}}{\text{ft}^2\text{-hr-}^{\circ}\text{F}} \quad \text{for glass}$$

$$t_f = 1700 \left(\frac{0.100}{7.14} \right) + 35 = 59^{\circ}\text{F}$$

This is the minimum heating film temperature required for anti-icing. It is used to establish the power controller-turn-on temperature and also the lower limits for the temperature uniformity power constants.

8.7.1 Interior Heat Flux

The heat flux into the cockpit is given by the conductive equation for q_i :

$$q_i = \frac{t_f - t_i}{\frac{1}{h_{ci}} + \sum \frac{\Delta x}{k}} \quad (8-21)$$

where

t_f = heater film temperature, $^{\circ}\text{F}$

t_i = cockpit temperature, $^{\circ}\text{F}$

h_{ci} = convection inside surface heat transfer coefficient
(typically $h_{ci} = 2.0 \text{ Btu}/(\text{hr-ft}^2 - ^{\circ}\text{F})$)

Δx = thickness, in.

k = thermal conductivity, $(\text{Btu-in})/(\text{ft}^2\text{-hr-}^{\circ}\text{F})$

Using

$t_i = 40^{\circ}$ and $t_f = 59^{\circ}\text{F}$ as previously developed, the cockpit side heat is calculated:

$$k = 1.5 \frac{\text{Btu-in}}{\text{ft}^2\text{-hr-}^{\circ}\text{F}} \quad \text{for PVB}$$

$$k = 7.4 \frac{\text{Btu-in}}{\text{ft}^2\text{-hr-}^{\circ}\text{F}} \quad \text{for glass}$$

$$q_i = \frac{59 - 40}{\frac{1}{2.0} + \frac{(.08)}{1.5} + \frac{(.10)}{7.14}} = 33.5 \text{ Btu}/(\text{hr-ft}^2)$$

The temperature of the cockpit side of the windshield would be:

$$t_{si} = \frac{q_i}{h_{ci}} + t_i$$

$$t_{si} = \frac{33.5}{2} + 40 = 57^{\circ}\text{F}$$

8.7.1.1 Total Heat Demand

The total minimum power for the windshield is then given by q . This power is provided by the windshield heater film at the low end of its manufacturing tolerance.

$$q_t = q_o + q_i = 1171 + 33 = 1204 \text{ Btu}/(\text{hr-ft}^2)$$

8.8 Defogging Requirements

Assuming the windshield heating system is also required to provide defogging capability, the interior surface must be maintained above the cockpit dew point.

The procedure used to calculate the dew point temperature is shown in example form.

The example shall assume that water vapor is introduced by 14 cabin occupants at the rate of 0.5 lb/hr per occupant. The cabin ventilation system brings in fresh air at the rate of 2500 lb/hr. The air is assumed to be initially saturated at -4°F and is heated to a cockpit ambient temperature of 40°F .

The aircraft specific humidity is given by:

$$M_{si} = \frac{M_o W_v + N(M)(7000)}{W_v} \quad (8-22)$$

where M_{si} = internal air specific humidity, $\frac{\text{grains water}}{\text{pound air}}$
 M_o = external air specific humidity, $\frac{\text{grains water}}{\text{pound air}}$

Obtain specific values from psychrometric charts as shown in Figures 8-18 and 8-19.

W_v = ventilation rate, pounds of air per hour

N = number of occupants

M = occupant moisture increment, $\frac{\text{pounds water}}{\text{hour}}$

Then: M_o = 4 grains/lb at -4°F from Figure 8-18

$$M_{si} = \frac{4(2500) + 14(.5)(7000)}{2500} = 23.6 \frac{\text{grains}}{\text{lb}}$$

From the psychrometric chart in Figure 8-18, the dew-point temperature corresponding to the internal specific humidity of 23.6 grains/lb is then 30°F , which is well below the windshield's internal surface temperature of 57°F . Therefore, the surface will remain fog-free.

However, critical antifog requirements usually occur during hot, humid conditions when the dew-point temperatures are above ambient temperatures. For example, consider the following conditions:

$$t_o = 80^{\circ}\text{F}$$

$$t_i = 80^{\circ}\text{F}$$

relative humidity = 100%

14 cabin occupants

ventilation airflow = 2500 lb/hr.

From Figure 8-19, $M_o = 156$ grains/lb.

$$M_{si} = \frac{156(2500) + 14(.5)(7000)}{2500} = 175.6 \text{ grains/lb.}$$

From the psychrometric chart, Figure 8-19, the dew-point temperature corresponding to the internal specific humidity of 175.6 grains/lb is 83.5°F . In order to prevent condensation, the interior surface must be maintained at a temperature above the dew point at, say, 85°F .

Then the internal heat flux is

$$q_i = h_{ci} (t_{si} - t_i)$$

$$q_i = 2.(85 - 80) = 10 \text{ Btu/(hr - ft}^2\text{)}$$

and the heating film temperature becomes

$$t_f = q_i \frac{\Delta X}{k} + t_s$$

$$t_f = 10 \left(\frac{.08}{1.5} + \frac{.10}{7.14} \right) + 85 = 86^{\circ}\text{F}$$

Thus, for effective defogging, under hot, humid conditions the minimum heating film switch-on temperature must be substantially greater than the value determined for anti-icing.

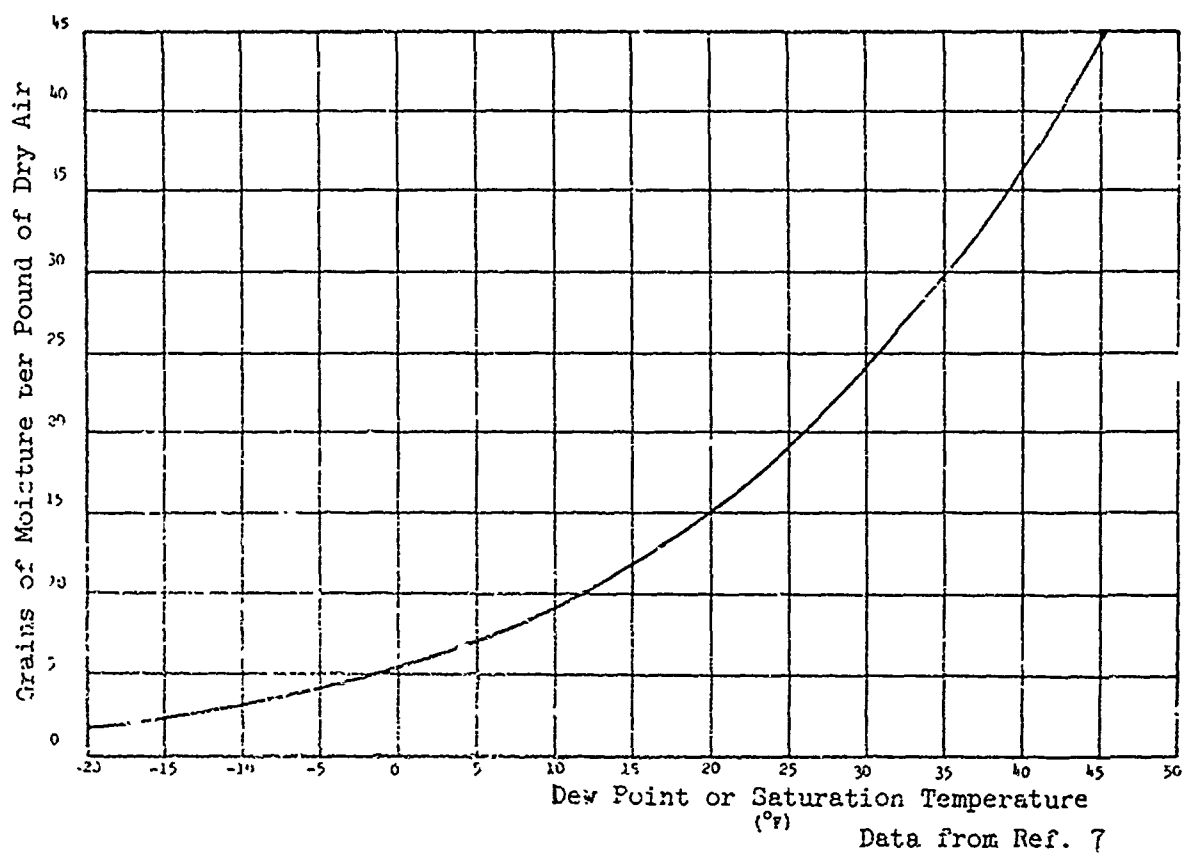
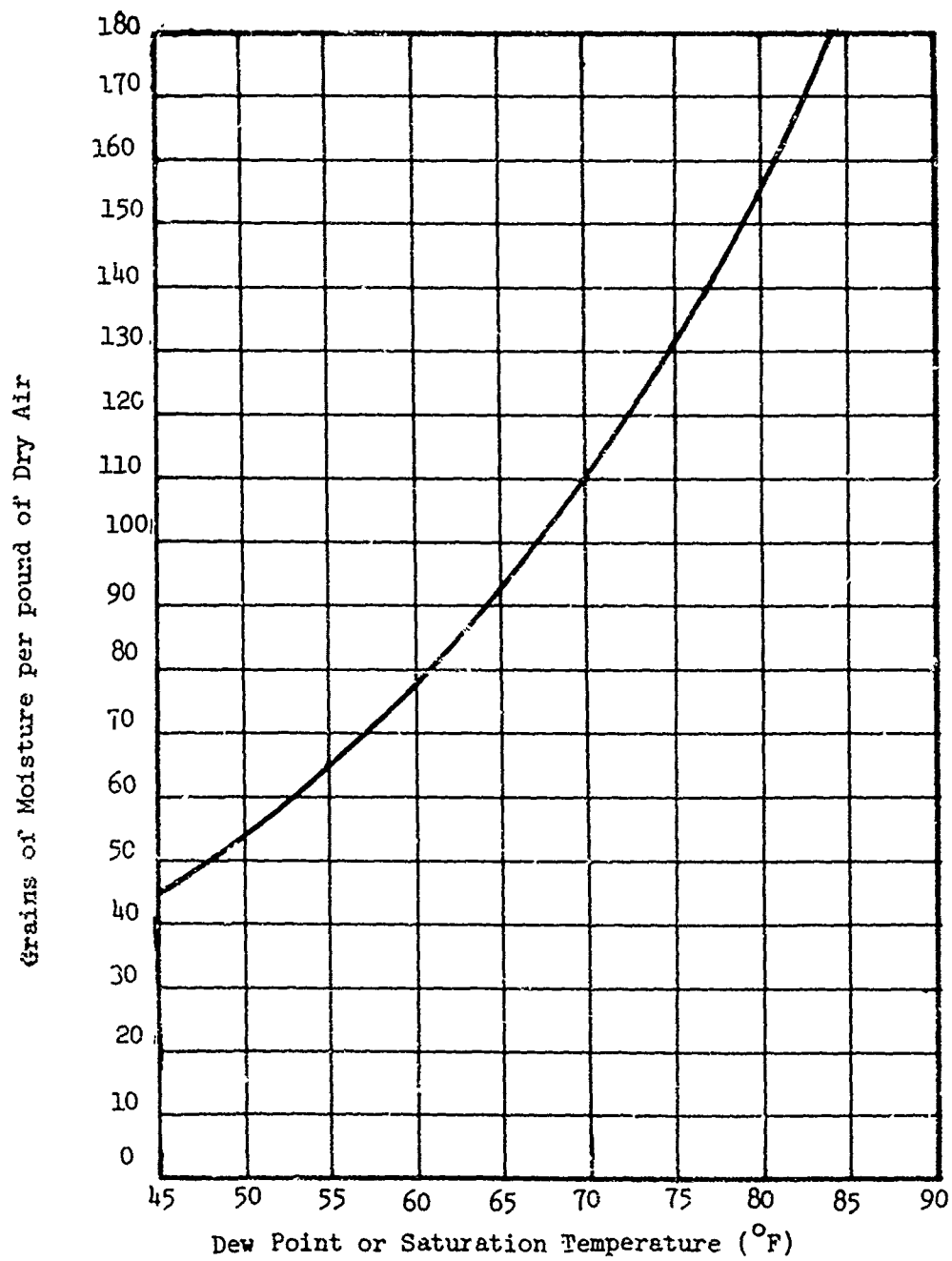


Figure 8-18. Psychrometric Chart for Obtaining the Dew Point at Temperatures Below 50°F.



Data From Ref. 7

Figure 8-19. Psychrometric Chart for Obtaining the Dew Point at Normal Temperatures.

8.9 Time to Warm Up

The time required to heat the windshield outer surface to 35°F for anti-icing should be kept to a minimum to preclude an accumulation of ice during flight into an icing situation. The time interval can be calculated with the aid of Figure 8-20 by assuming that all heat flows toward the outer ply and normal to the windshield.

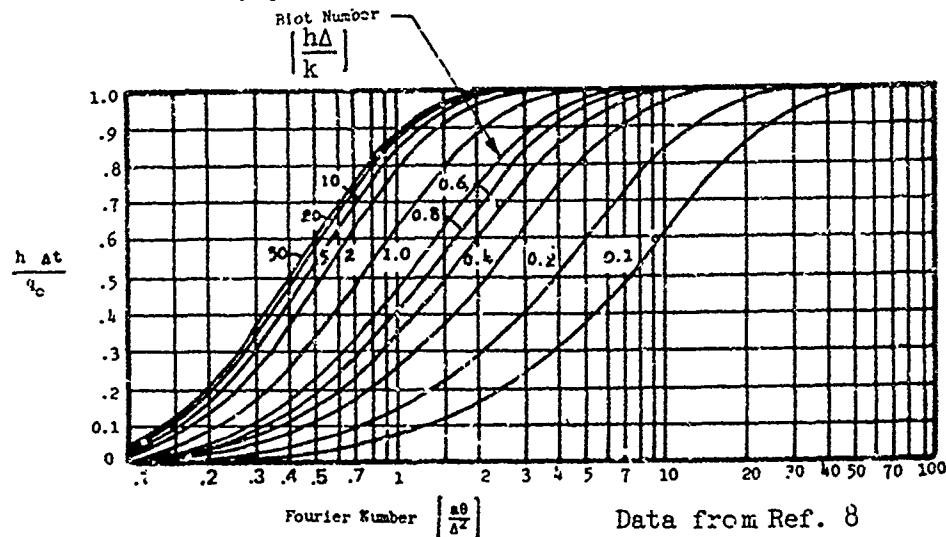


Figure 8-20. Biot and Fourier Relationships for Transient Heat Transfer Problems.

An analysis is presented to show a typical warmup calculation. The following data is given.

Aircraft speed	150 knots
h , external convective heat transfer coefficient	18 Btu/(hr-ft ² -°F)
Outside ambient air temperature	-4°F
Outside windshield surface temperature	10°F
Δ , thickness of outer glass ply	0.10 in.
q_0 , heat flux	1700 Btu/(hr-ft ²)
ρ , density of outer glass ply	152 lb/ft ³
c_p , specific heat of glass	.20 Btu/(lb-°F)
k , thermal conductivity of glass	7.14 $\frac{\text{Btu-in.}}{\text{ft}^2\text{-hr-°F}}$
a , thermal diffusivity $\frac{k}{\rho c_p}$.019 ft ² /hr

To use the curve, the Biot number, Fourier number, and dimensionless term A are calculated:

$$\text{Biot number} = \frac{h\Delta}{k} = \frac{18(.10)}{7.14} = .252$$

$$\text{Fourier number} = \frac{a\theta}{\Delta^2} = \frac{(.019)\theta(144)}{(.10)^2} = 288 \theta$$

$$A = \frac{h \Delta t}{q_0} = \frac{18(35 - 10)}{1700} = .264$$

where

θ = time to warm up, hours

Δt = temperature rise of outside windshield surface, $^{\circ}\text{F}$

From the curve, Fourier number = 1.6

$$288 \theta = 1.6$$

$$\theta = .0056 \text{ hours} = 20 \text{ seconds}$$

8.10 Hot Air Jet Blast

Windshield anti-icing is normally achieved through the use of heated windshields. The free moisture remaining on the windshield must be removed to provide clear windshield vision. The hot air jet blast water removal system shown in Figure 8-21 is an alternative to windshield wipers and can be used to fulfill the anti-ice requirement as well. The hot air jet blast system operates on the principle of directing a high temperature, high velocity airstream across the windshield surface, thus deflecting and evaporating moisture from the windshield surface. The jet blast is obtained from engine compressor bleed air and is activated on demand, minimizing the resultant engine performance penalty.

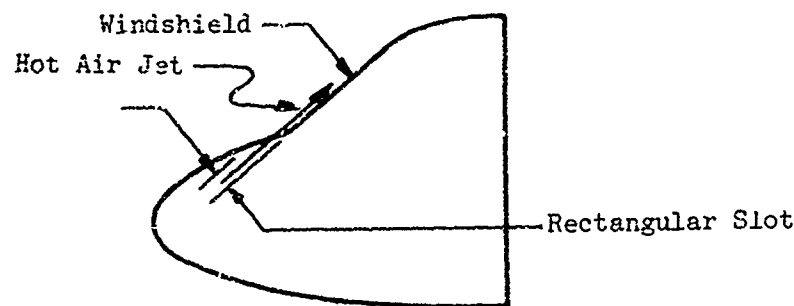


Figure 8-21. Hot Air Jet Anti-Ice System.

The air from the jet blast system is sufficiently warm as it leaves the nozzle located at the base of the windshield to maintain the surface temperature above the freezing point of water. However, the temperature decreases very rapidly as the air flows across the windshield. The complexity of the interaction of the hot air jet and the cold air stream makes it necessary to resort to empirical methods for predicting the jet temperature and velocity. Reference 9 provides data showing the relationship between jet blast velocity, weight flow and temperature for several visibility conditions and nozzle configurations. The data allows the designer to determine parametric relationships involved in obtaining good visibility. Purely analytical relationships are also available in Reference 3.

Some typical performance data for the windshield configuration shown in Figure 8-22 is plotted in Figure 8-23. The windshield surface temperature is shown as a function of distance from the nozzle in Figure 8-24 for a velocity of 829 ft/sec. The nozzle was a thin, continuous rectangular slot located at the base of the windshield and oriented so that the lower edge discharging the air was flush with the windshield surface.

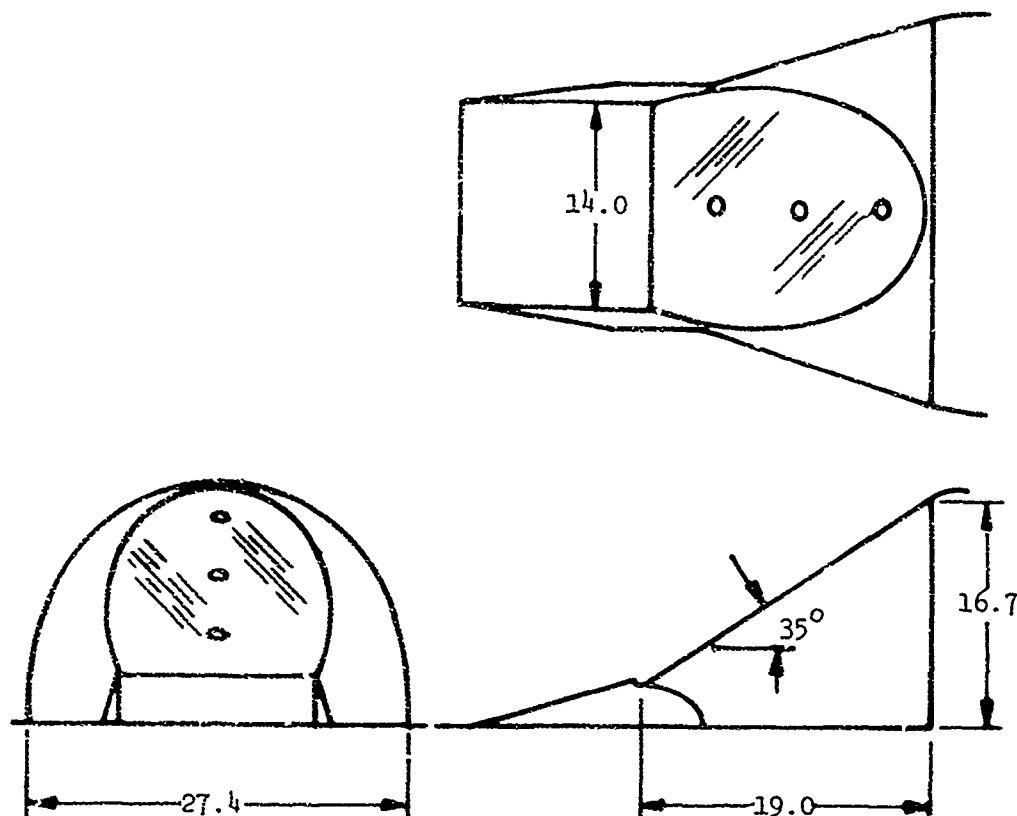
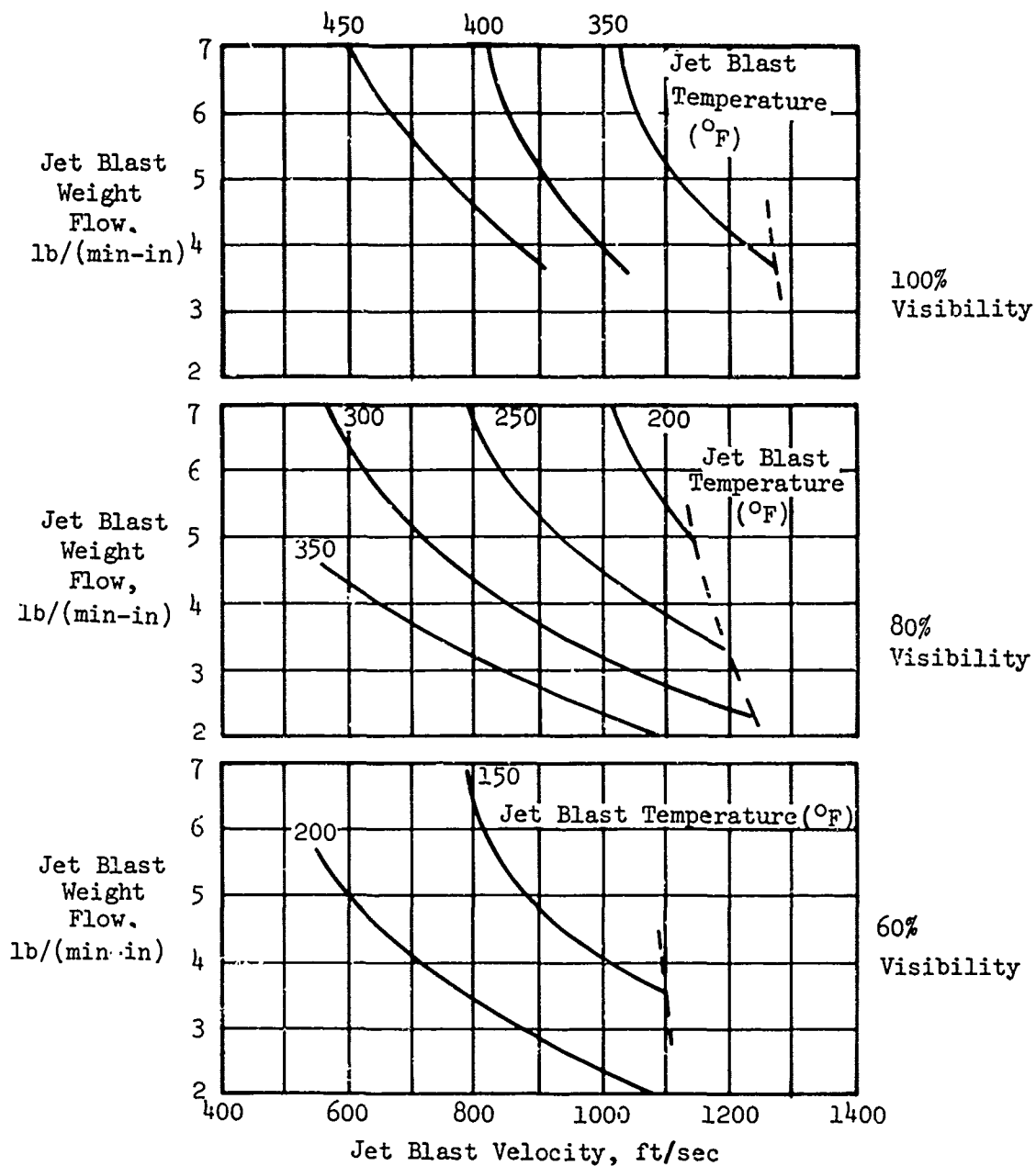


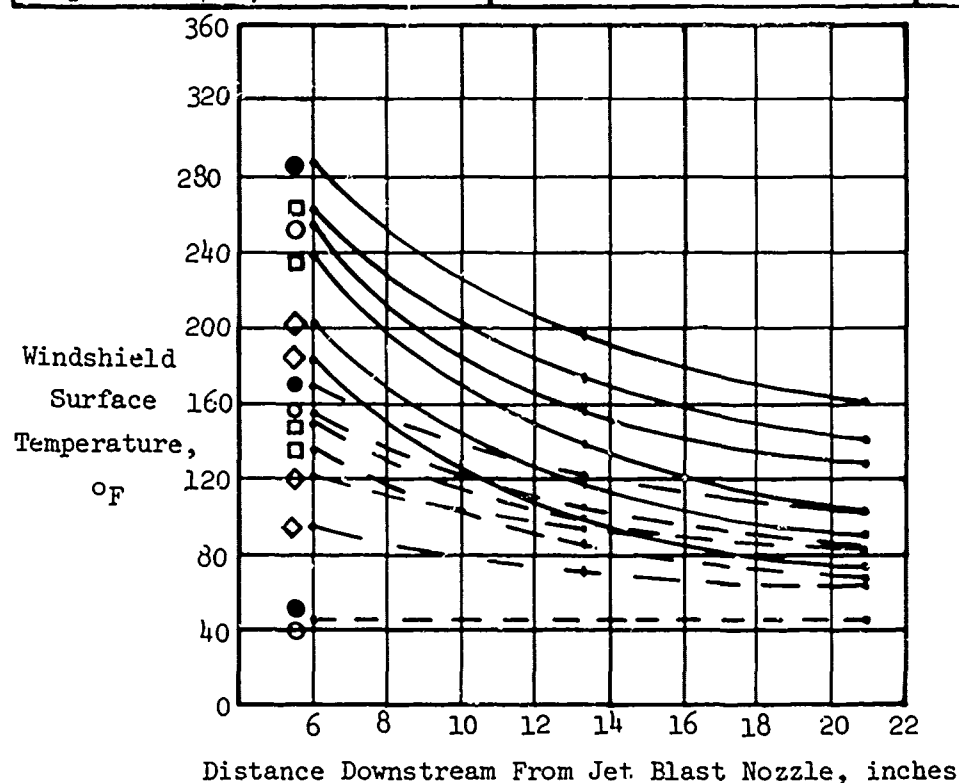
Figure 8-22. 35°F, Flat Windshield and Canopy.



Data from Ref. 9

Figure 8-23. Relationship Between Jet Blast Velocity, Weight Flow, and Temperature Under Heavy Rain Conditions at 140 Knots.

Symbols					
Jet Blast	————	450	Jet Blast Weight	○ 7.0	Rain ○ On ● Off
Temperature (°F)	———	400	Flow (lb/ min-in)	□ 4.5	
	---	50		◇ 2.0	



Data from Ref. 9

Figure 8-24. Windshield Surface Temperature as a Function of Air Temperature and Distance From Nozzle Under Moderate Rain Conditions at 140 Knots.

References

1. FAR Part 25, Airworthiness Standards: Transport Category Airplanes. Federal Aviation Administration Regulations, Department of Transportation.
2. Islinger, J. S., Armor Research Foundation, "Engineering Design Factors for Laminated Aircraft Windshields," WADC Technical Report 53-99 Part I, Wright Air Development Center, Apr, 1954.
3. Letton, G. C., Aeronautical Systems Division, "An Analytical Investigation of Aircraft Windshield Anti-Icing Systems," AFML Technical Report TR-73-126, Air Force Materials Laboratory, Wright-Patterson Air Force Base, Ohio, June 1973.
4. Dendy, N. C., and Nienow, S. G., PPG Industries, "Anti-Icing, De-Icing, De-Fogging Considerations for Helicopter Transparent Enclosures," Rotary Wing Icing Symposium - Summary Report Volume III; USAAEFA Project No. 74-77, Edwards Air Force Base, Calif., June 1974.
5. Keenan, J. H., and Keyes, F. G., "Thermodynamic Properties of Steam," Wiley, 1936.
6. "SAE Aerospace Applied Thermodynamics Manual," Compiled and Published by the Society of Automotive Engineers, Inc., AC-9 Committee, Aircraft Environmental Systems, 1969.
7. Burgess, H. J., and Lewis, S. "Air Conditioning and Refrigeration," International Textbook Company, Scranton, Pa., 1950.
8. Mikhaylov, M. D., "Transient Temperature Fields in Shells," NASA TTF- 552.
9. Meline, H. R., and Smith, I. D., Research Inc., "Design Manual for Windshield Jet Air Blast Rain and Ice Removal," WADC Technical Report 58-444, Wright Air Development Center, Ohio, Nov. 1958.

Bibliography

Lawrence, J. H., Douglas Aircraft Co, "Windshield Technology Demonstration Program," AFFDL-TR-77-1, Air Force Flight Dynamics Laboratory, Wright-Patterson Air Force Base, Ohio, Sept. 1977.

9.0

ELECTRICAL HEATING SYSTEMS

Electrical resistance heating is one of the most common methods for preventing ice buildup on aircraft windshields. Electrical power is converted to heat by applying a voltage to a conductive film or series of fine wires embedded within the transparency. This section provides guidance for the design and control of electrical windshield heating systems.

9.1 Heated Area

Heated areas should be as nearly rectangular in shape as possible while meeting visibility requirements for icing or fogging conditions. Other shapes may necessitate graded resistance coatings that are more difficult to manufacture and can result in uneven heating. Rectangular heated areas simplify the design, fabrication, and quality control operations with consequent cost savings and reductions of defects.

9.2 Bus-Bar Spacing

For a given power density, the bus-bar spacing affects the relationship between power supply voltage and the conductive surface resistivity as shown in equation 9-1.

$$P = \frac{V^2}{rL^2} \quad (9-1)$$

where

P = power density, watts/in²
V = applied voltage, volts
r = resistivity, ohms/square
L = bus-bar spacing, in

Large heated areas with wide separated bus-bars require thick, low resistance coatings that have high light transmission losses. This can be avoided by the use of power transformers to step up the supply voltage, but the weight penalty is severe.

9.3 Nominal Voltage

The electrical power supply for windshield heating will normally be three-phase, 400 Hz at a nominal voltage of 115/200 volts rms. The performance characteristics for this power are in accordance with the limits of MIL-STD-704A, Category B, which refers to the power at the input terminals of the equipment (in the case of windshield heating systems, at the temperature controller). An additional voltage drop may occur between the controller input and the windshield itself. For modern solid-state controllers the additional voltage drop will be up to 2 volts rms line-to-neutral, or 3 volts rms line-to-line.

In special cases, when the heated area is very large, higher voltages may be required. The transformers or autotransformers required to step up the voltage must then be part of the windshield heating system. Such nonstandard voltages should be avoided because of the weight and cost penalties involved:

In other cases, when the aircraft has a prime direct current (dc) electric power system, it may be necessary to use 28V dc supplies. For this low voltage, heating films become very thick, which reduces light transmission. With existing materials, the lowest practical surface resistivity for a heating film is about 3 ohms per square. Therefore, unless an alternative imbedded wire heating system or power transformers are used to step up the supply voltage, the dc systems are normally restricted to small areas of coverage.

The characteristics of the dc power will be in accordance with MIL-STD-704A, Category B.

9.4 Phase Configuration

Windshield heating equipment shall conform to the requirements of MIL-STD-704A. This standard calls for three-phase loading for all loads exceeding 500 volt-amperes, and when practicable, for smaller loads. Each windshield must contain its own three-phase power elements. It is normally unacceptable to use separate single-phased windshields where each one is connected to a different phase of the aircraft power supply, because the temperature controllers will switch the power on at different times, resulting in an unbalanced phase loading.

Windshield loads may be configured for Y or delta type connections in order to provide the most convenient phase voltage. In Figure 9-1 the Y configuration provides 115V ac to each heated section, while the delta connection applies 200 V ac.

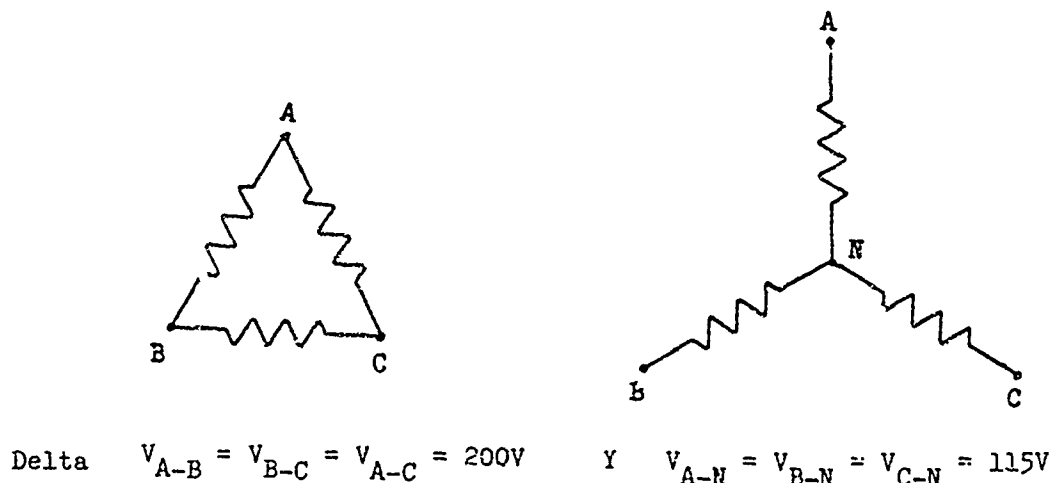


Figure 9-1. Comparison of Y and Delta Electrical Systems.

9.5 Phase Resistance and Applicable Tolerance

The phase resistance, also known as the bus-to-bus resistance, must be controlled to ensure that the minimum required power density can be achieved. The highest permissible resistance is selected so that the resulting minimum average power density is adequate to achieve the anti-icing function. Procedures for calculating power density requirements are given in the Anti-Icing section of this manual. These requirements are given in Btu/ft² - hr and must be multiplied by 2.04×10^{-3} to obtain watts/in².

Allowance should be made in the calculation for the lowest supply voltage, allowing for the drop at the temperature controller.

$$\text{Thus, } R_{\max} = \frac{(V_{\min})^2}{W_{\min} A}$$

where V_{\min} is the lowest supply voltage (volts)

W_{\min} is the minimum average power density (watts/in²)

A is the heated area (in²)

and R_{\max} is the maximum allowable resistance at the operating temperature of the conducting element (ohms).

The lowest permissible resistance is determined by the accuracy of the fabrication process, which is normally in the range of $\pm 10\%$ to $\pm 15\%$ at room temperature (70 to 75°F). The tolerance range should be as small as possible to prevent unnecessarily high peak power demands on the helicopter's electric power system and temperature controller.

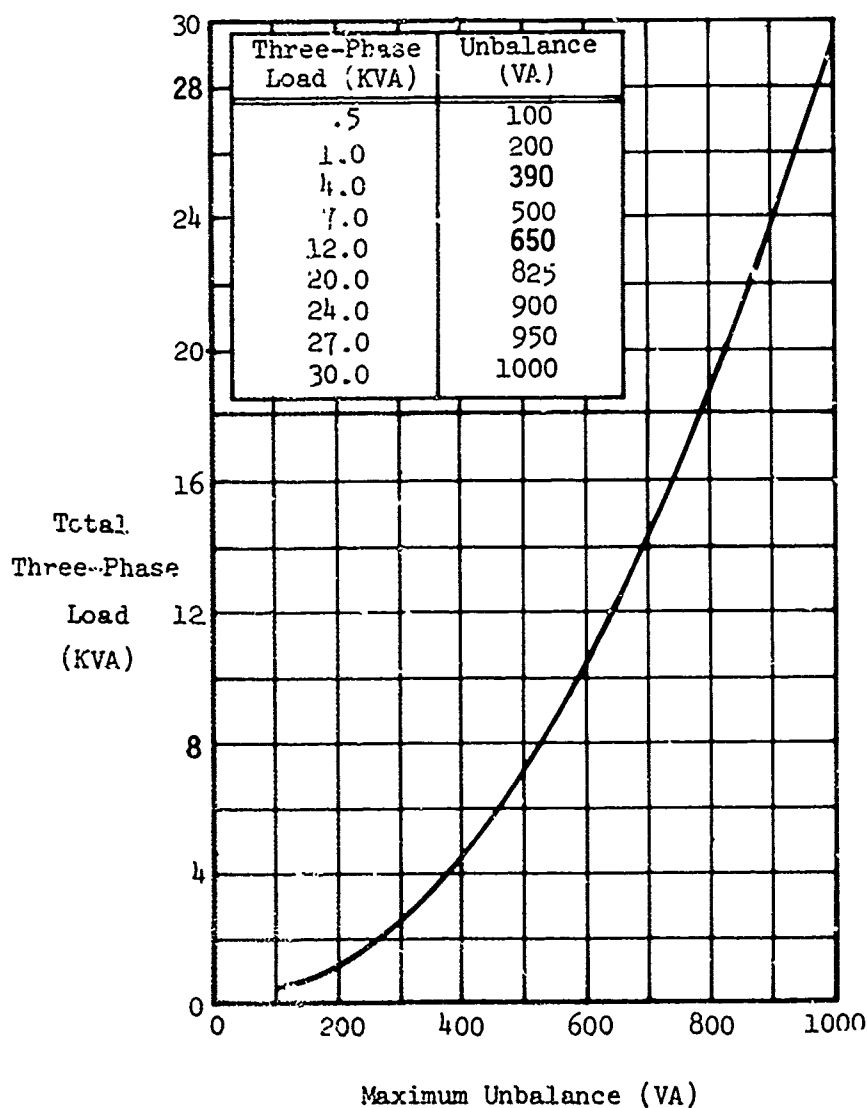
9.6 Permissible Phase Loading Unbalance

The variation of resistance between phases of a three-phase heating system shall be controlled to meet the requirements of MIL-STD-704A for phase loading unbalance. This standard requires that the volt-ampere difference between the highest and lowest phase loading values shall be less than the limits specified in Figure 9-2. Balanced phase voltages may be assumed for this calculation. For windshields drawing less than 3.5 kilowatts, this requirement will be met by phase resistances that are within $\pm 15\%$ of the nominal value.

Excessive variations in the resistance of the phases will lead to nonuniform heating of the windshield. Temperature uniformity requirements and their relation to power dissipation are discussed in the Anti-Icing section of this manual.

9.7 Electrical Terminations

Electrical terminations for the power bus-bar and for the temperature sensors can be of several types. The most common is a terminal block having threaded holes for each connection. This type has given satisfactory service when securely bonded to the transparency, although some malfunctions have occurred due to poor bonds. A cover plate can be used over the terminations, or the live leads can be covered by a rubber boot that is part of the wire termination assembly. Self leads (pigtails) connected to the airframe-mounted terminal blocks have also been used but have a disadvantage in that a broken or damaged wire necessitates the removal and replacement of the transparency.



Data From Ref. 1

Figure 9-2. Unbalance Limits for Three-Phase Utilization Equipment.

Consideration should be given in new designs to the use of terminal junction modules similar to those specified in MIL-T-81714. The junction modules feature an environmental sealing capability, and the airframe wire is terminated in a crimp contact using the same tools as aircraft connectors. The possibility of a poor or open contact is reduced because the wire terminal is locked in position, requiring no loose components, such as lockwashers.

Figure 9-3 shows the screw-type and junction module termination.

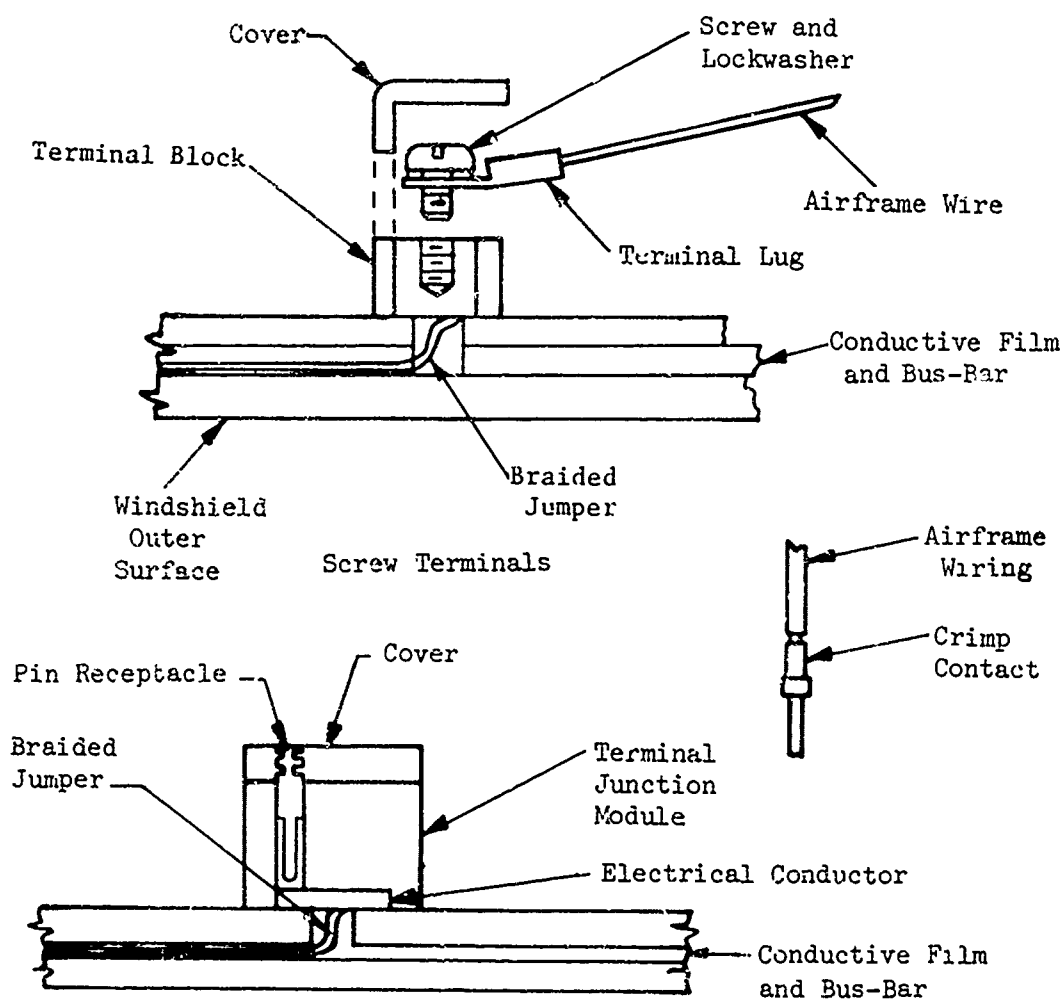


Figure 9-3. Windshield Electrical Terminals.

A common arrangement of bus-bars in a three-phase heated windshield is shown in Figure 9-4. Four power terminals are required, even though two of them are connected to the same phase. Two additional terminals are required for each temperature sensing element. The termination for the sensor should be configured so that the wiring cannot be cross connected with the power wiring. This can be done through use of different size screw threads for threaded terminals or different contact sizes for terminal junction blocks. Terminals are conveniently located in the corners where their effect on visibility is least noticeable. All terminals must be numbered to identify the connections required to airframe wiring. Figure 3-4 also shows the deletion lines that provide insulation between the adjacent heated phases, by leaving gaps 0.03 to 0.10 inch wide in the conductive film.

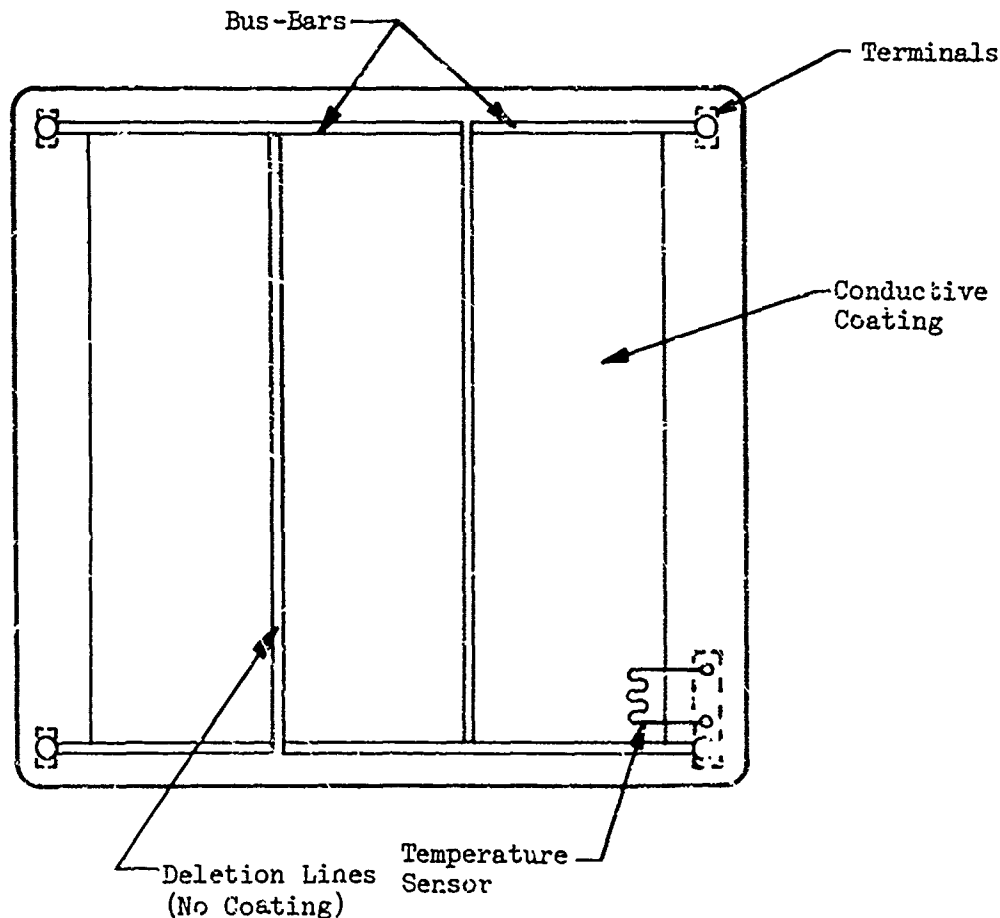


Figure 9-4. Bus-Bars and Terminals for Three-Phase Electrically Heated Windshield.

9.8 Temperature Sensing Elements

A fixed power level for windshield heat is impractical because a power density that will prevent ice formation under the worst conditions of temperature and aircraft speed will result in severe overheating in less extreme conditions. It is normal, therefore, to employ a temperature control system that responds to signals from one or more temperature sensors embedded in the windshield. The usual practice is to provide a single sensor and a controller that shuts off power if the sensor or its leads become open or short circuited.

A second sensor may be mounted in the windshield and used as an over-temperature detector that either warns the crew or automatically turns off the electric power. In some cases, an extra sensor is provided to permit continued use of a windshield with a failed sensor.

Multiple sensors are also used when it is expected that the temperature distribution over the windshield surface will be nonuniform. This condition may be anticipated if the windshield curvature or outline shape makes the control of conductive coating thickness difficult, or if variable or extremely uneven heat losses may occur in flight. When multiple sensors are used, they are connected in parallel so that the power controller responds to the average output and thus to the approximate average temperature of the sensors. In cases where uniform heating is difficult to achieve, sensor locations may be determined on the basis of tests on individual units. The location must also satisfy the requirements for power constants as discussed in the Anti-Icing section of this handbook.

Wire filament temperature sensors suitable for helicopter windshields are commercially available and have given satisfactory service. They consist of fine resistance wire formed into grids and mounted in thin transparent plastic sheets, with areas up to about one square inch. They can be mounted very close to the conductive coating, and this, together with their low thermal inertia, minimizes thermal lag. The sensor resistance increases with temperature as shown on Figure 9-5, which also indicates a typical tolerance band. Thermistors are also suitable as sensors in interlayers thick enough to accommodate them, but they suffer from increased thermal lags because of their greater masses.

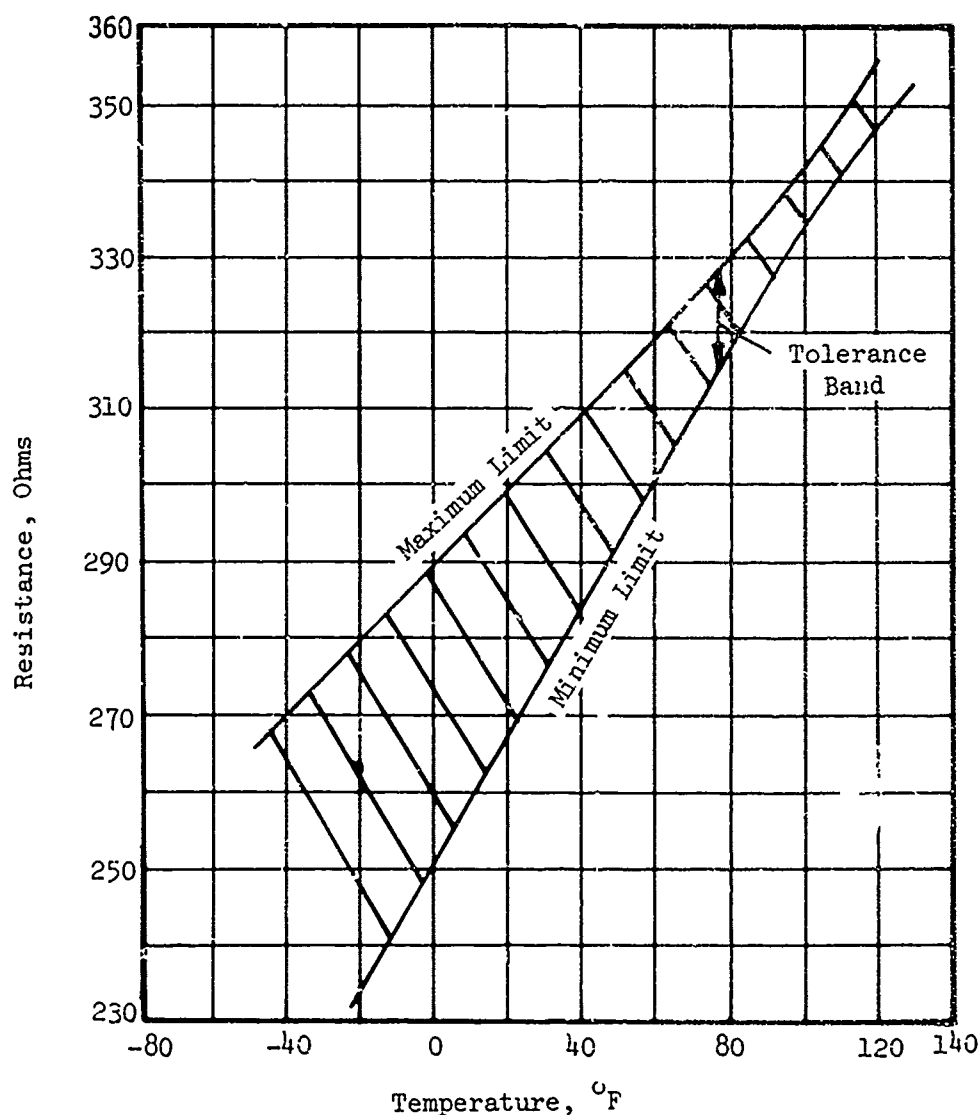


Figure 9-5. Typical Sensor Resistance/Temperature Characteristics.

9.9 Temperature Controller Switch Points

The temperature at which power is switched on and off is determined by considering the maximum heating film temperature to which the windshield materials can be exposed and subtracting from that temperature the various tolerances within the system.

Table 9-1 shows a typical error analysis used to determine the maximum "hot-spot" temperature. A similar analysis can be performed to predict the minimum "cold-spot" temperature, using the switch-on point of the controller.

9.10 Power Control Modes

Power can be applied to the windshield by an on-off controller or a controller with a stepped or continuously variable power output. The latter types can be programmed to provide gradual warm-up from cold, to minimize the thermal shock on the windshield. The three modes of operation are displayed graphically on Figure 9-6.

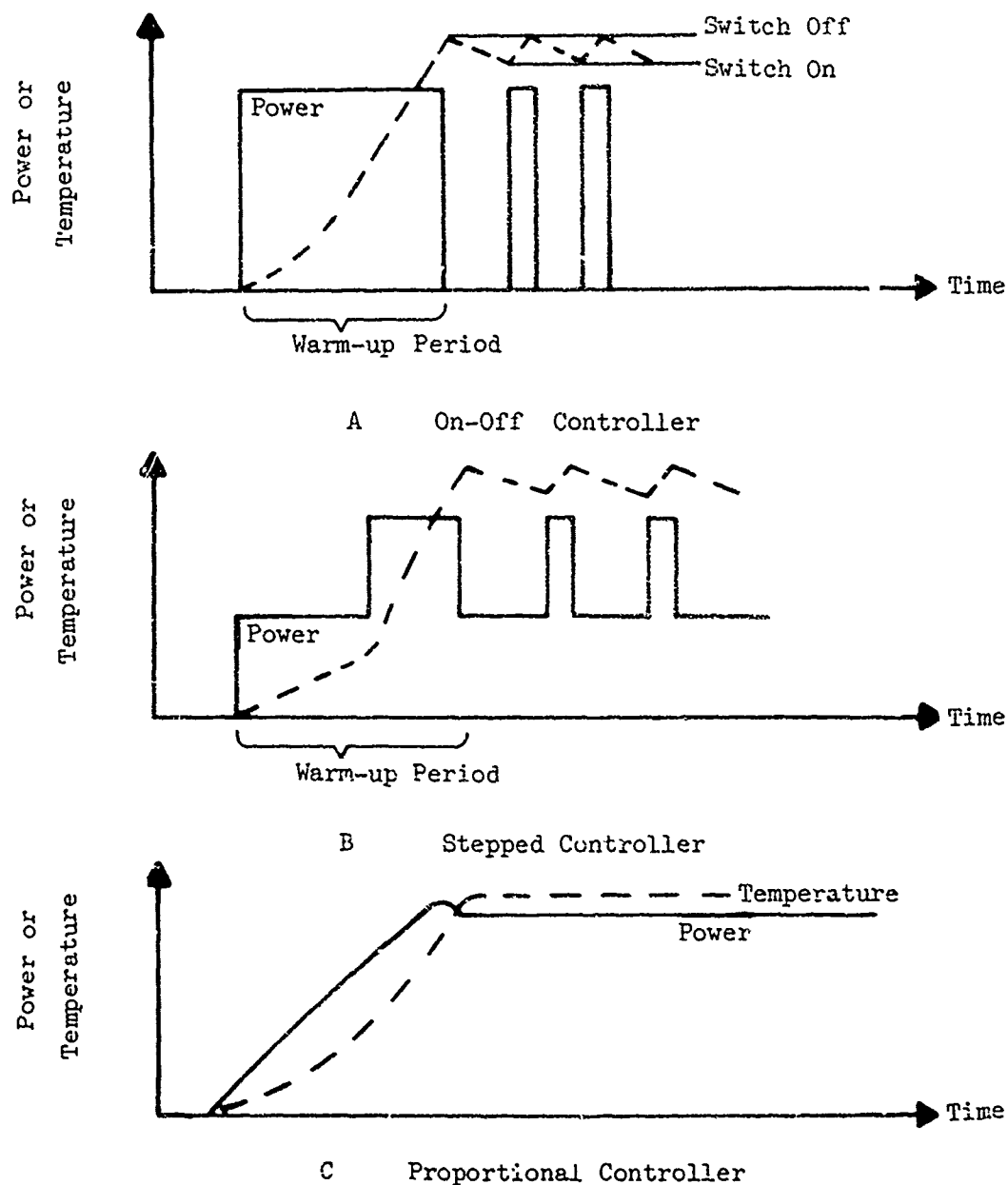


Figure 9-6. Power Modes for Windshield Temperature Controllers.

TABLE 9-1. TYPICAL TOLERANCE ANALYSIS FOR TEMPERATURE SWITCH-OFF POINT

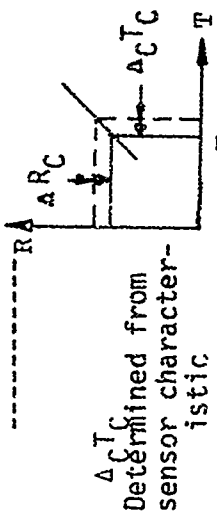
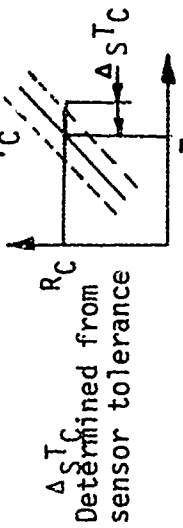
Factor Contributing to Maximum "Hot-Spot" Temperature	Source of Error	Method of Calculation
T_C (Nominal control temperature)	None (Design Point)	
$+ \Delta_C T_C$ (Change in control temperature T_C due to tolerance on controller switching point)	Controller switches off at $R_C - \Delta R_C$	 <p>$\Delta_C T_C$ Determined from sensor characteristic</p>
$+ \Delta_S T_C$ (Change in control temperature T_C due to tolerance on sensor resistance at T_C)	Sensor tolerance band	 <p>$\Delta_S T_C$ Determined from sensor tolerance</p>
$+ \Delta_L T_C$	Sensor thermal lag error	System design should ensure these errors are negligible by locating sensor close to heater and limiting sensor current.
$- \Delta_H T_C$	Sensor self heating	

TABLE 9-1. TYPICAL TOLERANCE ANALYSIS FOR TEMPERATURE SWITCH-OFF POINT (cont.)

Factor Contributing to Maximum "Hot-Spot" Temperature	Source of Error	Method of Calculation
$+ \Delta_k T_H$ $(T_H = \text{Temperature at hottest spot on heating film})$	Nonuniformity of heating as defined by K-factor	Calculate From: $K_H = \frac{T_H - T_0}{T_C - T_0}$ Use: T_0 Min. ambient T_C Max. control temperature including errors
$+ \Delta_M T_H$	Margin for variation in convective heat transfer coefficient	K_H from windshield specification Airflow characteristics determined from wind tunnel data

The benefits of the gradual warm-up procedure are not well established, and the approach is not often used because of the cost and weight penalties for the power controller.

The differential between the turn-on and turn-off points (shown in Figure 9-6) is selected by a compromise between conflicting requirements. A low differential is desirable to maintain the average temperature as high as possible without overheating at the hot spot. Since the rate of cooling after the power shutoff is determined only by thermodynamic factors, a very low differential leads to a high cycling rate that can cause voltage modulation of the power supply and reduce the life of contacts in a relay-type power controller. Experience has shown that a differential of 5 to 10°F gives acceptable results. Systems with solid-state power controllers are not life-limited by the cycling rate and a lower differential can be used.

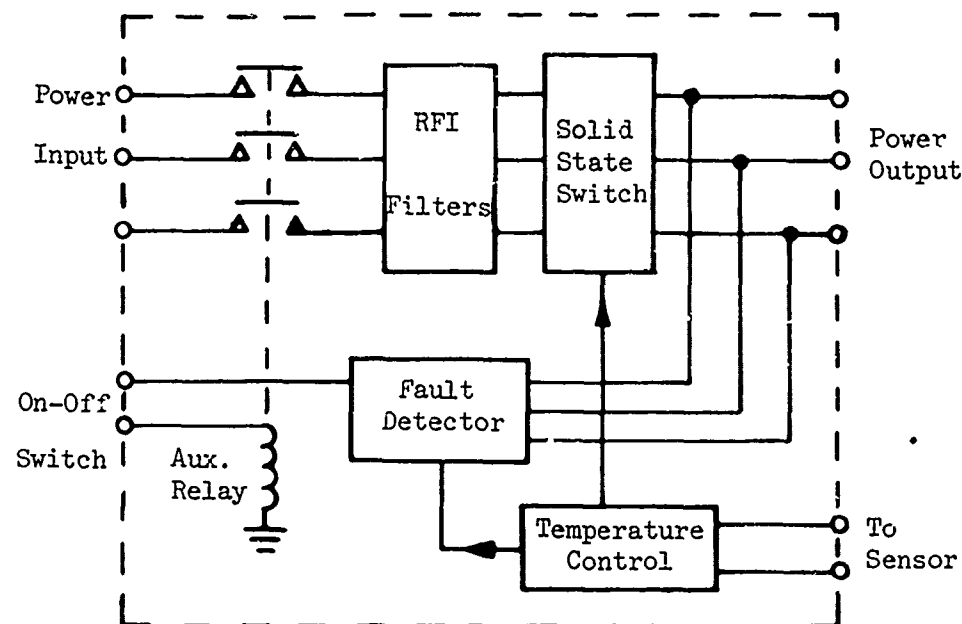
All three types of power controllers can respond to a multiposition switch to produce intermediate levels of power. MIL-T-5842 requires a three-position switch (off-low-high) for anti-icing systems. The reduced average power can be controlled by switching a bias resistor into the controller's circuit in response to the temperature sensor, so that the temperature is regulated at the intermediate level selected. Figure 9-7 shows a block diagram of a typical windshield heating system and power controller.

9.11 Fault Protection

It is obviously desirable to prevent damage to a transparency from overheating due to failure in the temperature sensing system or in the power controller. Protection against this failure mode can be provided with relatively little added complexity. For a system with a single temperature sensor, protection is provided in the controller by shutting off the output power if the sensor or its leads become open or short circuited. Similar protection can be achieved by adding an overheat detection sensor operating on a separate control circuit in the power controller.

Solid state power controllers using silicon-controlled rectifiers (SCR) or triacs as power switches have many advantages over relay-type power switches, including improved life and reduced radio frequency interference (RFI). However, they are more likely to malfunction in the power-on condition than are relays, as a result of short-circuited semiconductors. It is therefore recommended that an auxiliary relay be included in the power controller that will open if the output becomes uncontrolled. This can be accomplished as explained below.

The fault detector circuit shown in Figure 9-7 compares the switch



Block Diagram of Power Controller with Auxiliary Relay

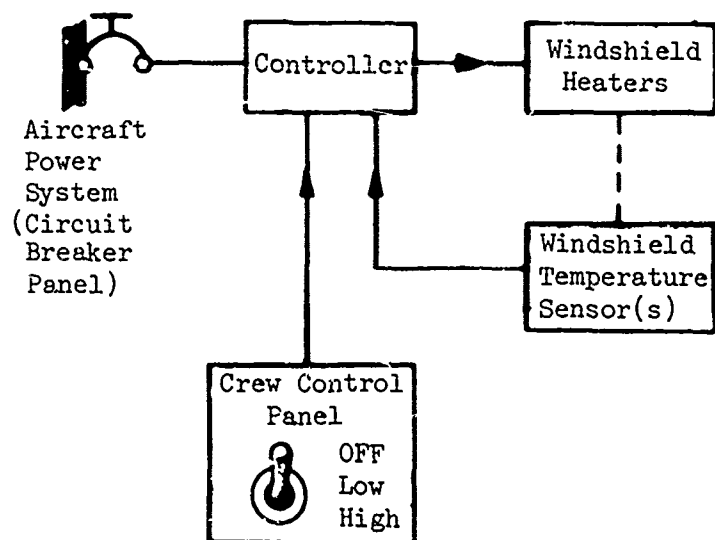


Figure 9-7. Block Diagram of Typical Windshield Heating System.

command signal to the power output and opens the relay coil circuit if the circuit is on when commanded to be off. The inclusion of the relay does not significantly reduce the life of the controller because in normal operation it does not switch the power current. If the relay is connected and controlled as shown, it is open when the crew control switch is off, so that power is not applied to the RFI filters or semiconductors when the system is not in use. Filter capacitors will have longer lives, and the chance of the semiconductor being damaged by unusual spikes or surges from the power supply is reduced.

9.12 Weight of Electrical Provisions

The electrical provisions for a heated windshield include the power controller, the circuit breakers, switches, and the interconnecting wiring. The power controller for each windshield will usually weigh between 2 and 3 lbs, depending on the power rating and protection features incorporated. The circuit breakers and control switch with mounting provisions will have a total weight of approximately 0.5 lb per windshield. The wiring weight will range between 0.02 lb/ft for each windshield system less than 2 kilowatts, and 0.05 lb/ft for 6 kilowatt systems. In most helicopters, the wiring run from the distribution area (circuit-breaker panel) to the controller and on to the windshield will be less than 15 feet.

There is also a weight penalty in the electric power generation system since the generators must be sized to provide additional power. The influence of windshield anti-icing on overall electric power system weight cannot be adequately defined by a simple factor of lb/KW load, since the presence or absence of anti-icing loads is a major factor in electrical system basic design. However, 3 lb/KW may be used as a general guide for the electrical system weight penalty for helicopters with prime AC power systems, when windshield heating is a required load for mission completion.

Reference

1. MIL-STD-704A, "Electric Power, Characteristics and Utilization of."

Bibliography

Miller, P. A., Sierracin Corporation, "Anti-Icing Aspects of Helicopter Windshields Design," Published by Sierracin Corp., Sylmar, Calif., 1972.

MIL-T-81714, "Terminal Junction Systems, General Specification for."

James, H. C., at el, Goodyear Aerospace Corp., "Design, Test, and Acceptance Criteria for Army Helicopter Transparent Enclosures," USAAMRDL-TR-73-19, U. S. Army Air Mobility, Research and Development Laboratory, Fort Eustis, Va., May 1973, AD 767242.

MIL-B-5087, "Bonding, Electrical and Lightning Protection for Aerospace Systems."

MIL-T-5842, "Areas, Anti-Icing, Defrosting and Defogging Systems, General Specification for."

Lawrence, J. H., Douglas Aircraft Co., "Windshield Technology Demonstrator," AFFDL-TR-77-1, Air Force Materials Laboratory, Wright-Patterson Air Force Base, Ohio, Sept. 1977.

10.0

RAIN REMOVAL SYSTEMS

Windshield wipers, electrically or hydraulically driven, form the mainstay of helicopter rain removal systems. When used with washer systems, they can remove salt spray and insect deposits from the windshield.

Jet air blast systems have replaced windshield wipers on high-performance aircraft where wipers lose much of their effectiveness. In this system, high-temperature, high-velocity air, bled from the engine compressor, is blown across the windshield to deflect and evaporate moisture from the surface.

Chemical rain repellents are also employed, but usually only to supplement one of the other two systems. Two types of repellents are in use. The first is semipermanent and is applied while the aircraft is on the ground. The second, a newer development, is a liquid that can be applied in-flight and enhances water-repellancy temporarily.

10.1 Rain Intensities

A rain removal system should operate effectively over a range of conditions likely to be encountered in service. Different possible rain conditions are given in Table 9-1. The capability to clear a windshield during excessive rain, 1.6 inches per hour, is normally chosen as a practical upper limit for a wiper system. During cloudburst conditions wipers have only limited capabilities.

TABLE 10-1. RAIN INTENSITIES AND VISIBILITY

Rain Classification	Rain Intensity (in/hr)	Droplet Diameter (microns)	Water Content (mg/m ³)	Visibility	
				Nautical miles	Statute miles
Clear	-	-	0.00	-	-
Fog	-	10	6.00	-	-
Mist	0.002	100	55.5	-	-
Drizzle	0.1	200	92.6	-	-
Light Rain	0.4	450	138.9	7.5	8.62
Moderate Rain	0.16	1000	277.8	2.7	3.11
Heavy Rain	0.59	1500	833.3	0.93	1.07
Excessive Rain	1.6	2100	1851.9	0.49	0.56
Cloudburst	4.0 to	3000	4000	0.25	0.29
	50.0	-	35000	-	-

Data from Ref 1.

10.2 Windshield Wipers

Most all-weather helicopters employ windshield wipers as their primary rain removal system. Wipers are very effective in the low speed envelope within which rotary-wing aircraft operate. At higher speeds, wipers tend to lift off the windshields and lose much of their effectiveness. This tendency can be remedied by the incorporation of aerodynamic blade deflectors that use the high-speed airstream to help hold the wiper blade in contact with the windshield. An example of a deflector built into the blade holder of a wiper system is shown in Figure 9-1. Incorporation of heavier springs in wiper arm assemblies has the disadvantage of increasing blade pressure on the windshield at all aircraft speeds. Any increase in blade pressure over a recommended value of approximately .5 pound per linear inch of blade can lead to abrasion problems and excessive drag loads on the wiper.

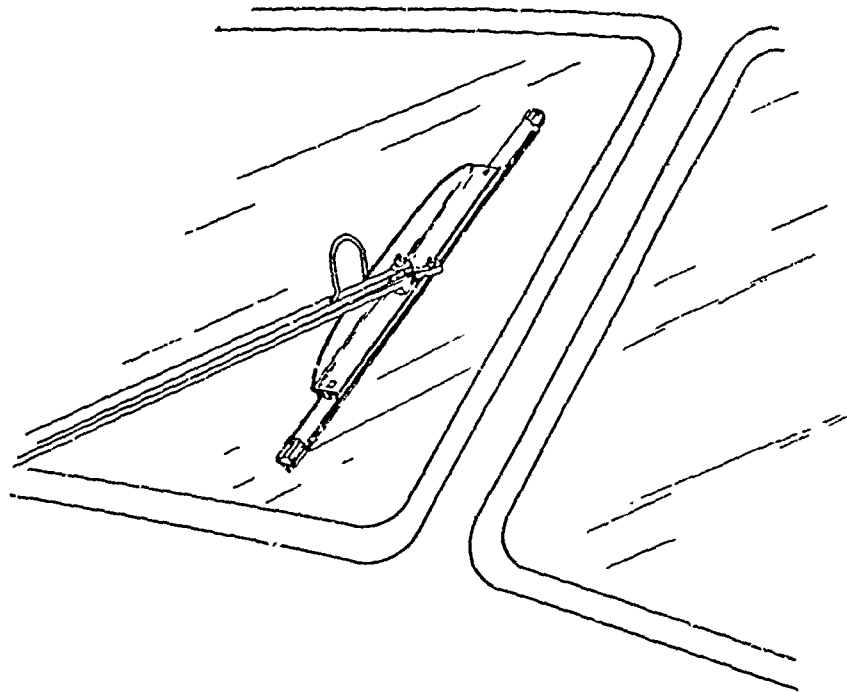


Figure 10-1. Windshield Wiper With Aerodynamic Deflector.

The direction of water flow across a windshield is usually upward and outboard. Therefore, the wiper axis should be located near the lower inboard corner of the windshield to reduce the mechanical effort required. A wiper pivoting about the lower outboard corner will oppose the air and water stream on the downward stroke, and in addition, the water will follow the wiper blade closely on the upward stroke, reducing the wiper's effectiveness. The latter problem can sometimes be overcome by the use of deflectors at the base of the windshield to draw off the water pushed down by the blade, although deflectors will increase the system's drag.

When not in operation, wipers should be parked vertically to avoid accumulating dirt and debris. A parking position on the windshield post has an advantage in that the blade will not obstruct the pilot's view.

The general specification for airplane windshield wipers, MIL-W-7233A, specifies a minimum sweep speed of 160 strokes per minute. However, experience has shown that helicopters, with their relatively lower airspeeds and hence reduced raindrop impingement, can satisfactorily clear the required 1.6 inches of rain per hour at 160 strokes per minute and do not require higher speed position. High speeds are not recommended since wipers become noisy at high sweep speeds. A stroke is defined as the motion of the wiper blade sweep from one extreme position to the other.

The suggested minimum wiper cleared area of a windshield, from Reference 2, is a section 10 degrees up to 15 degrees down and between 15 degrees left and 15 degrees right, or an equivalent area. Angles are taken from the pilot's design eye position with respect to a horizontal plane and a vertical plane parallel to the aircraft's longitudinal axis.

10.3 Jet Air Blast

Jet air blast systems offer two distinct advantages over wipers that could make them desirable systems for particular helicopter applications.

Jet air blast eliminates abrasion problems common to plastic windshields and also provides an inherent anti-icing capability in addition to rain removal. A complete discussion of jet air blast systems is included in the Anti-Icing section of this handbook.

10.4 Rain Repellents

A rain repellent, applied as a thin film on the surface of a windshield, increases the windshield's surface tension. As a result of the higher surface tension, water will not adhere to the glass and beads up into droplets. These droplets have small contact areas with the surface and large areas exposed to the air stream, and are therefore easily blown off the windshield. The area between droplets remains dry and clear, as can be seen in Figure 10-2. Used in conjunction with windshield wipers, cloudburst conditions can even be coped with.

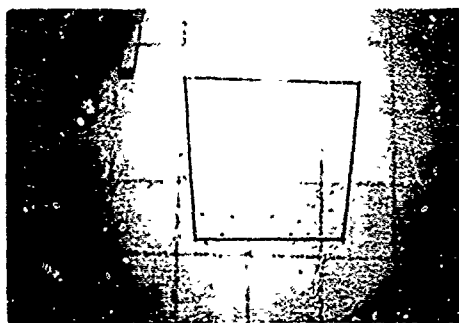


Figure 10-2. View of Grid Through Sample Windshield Under Simulated Rainfall of 3 Inches per Hour. Center Section Treated With a Chemical Rain Repellent.

The exact composition of a chemical rain repellent is usually a commercial secret, but silicone titanate copolymers, disilane compounds, and fluorochemicals have all been used. Some repellents are suitable for glass and plastic windshields, while others are specifically intended for use with one type or the other. Plastic windshields are naturally water-repellent when clean, so the improvement attained is usually less marked than with glass.

Operationally, rain repellents are of two types: those applied to the windshield by hand, on the ground, and those sprayed onto the windshield as required during flight through rain. The choice between hand-applied or in-flight-applied repellent depends upon the role of the aircraft.

Manual application of rain repellents is time-consuming and the period of effectiveness limited. Reapplication depends upon weather conditions and aircraft usage, but typically is necessary every 25 flying hours or 3 weeks. Since the repellent film is transparent and undetectable in clear weather, there is always the possibility of neglecting to renew the film prior to actual need. This means the actual need for a rain repellent has to be anticipated prior to flight, and the film checked and replenished if necessary. Some operators prefer

in-flight application systems since these eliminate the necessity for arranging routine applications when the aircraft is away from base. However, in the Armed Services, routine application of a hand-applied repellent is more easily controlled, and there has not yet been a strong demand for in-flight application systems.

Both types of rain repellent have the added advantages that salt spray and insect debris adhere less to treated surfaces and the buildup of ice deposits is also retarded. Their primary drawback, which is preventing more widespread use, is that they are not effective in light rain. Also, some compounds will produce a haze that will degrade vision when applied to a dry or only slightly wet windshield.

10.5 Systems Comparison

The relative advantages and disadvantages of the rain clearance systems are summarized in Table 10-2.

TABLE 2. RAIN REMOVAL SYSTEMS COMPARISON

Type	Description	Advantages	Disadvantages	Weight/Cost
Windshield wipers	Electromechanical, MIL-W-7233 applies.	Effective in moderate to heavy rain at low speeds. Good reliability. Efficient for large areas. With washer can remove salt spray and sect deposits.	Can scratch plastic. Aerodynamic drag penalty. Good only to heavy rain intensity. Lose effectiveness at high speed. Interfere with vision. Can be noisy at high wiping rates.	Low weight/ Low cost
Jet air blast	Engine bleed air-blown over windshields. WADC TR 58-444 is an acceptable design guide.	Effective in heavy rain. Good for anti-icing. Good at high aircraft speeds.	Engine performance penalty. Small area of coverage.	High weight/ High initial cost
In-flight-applied rain repellent	Liquid dispensed on windshield that repels water. MIL-R-83055 and MIL-R-83056 apply.	Effective in excessive rain. Excellent at high aircraft speeds. Use only when necessary.	Maintenance on refills. Dispensing system necessary. Not effective in light rain or low speeds.	Low weight/ Low cost
Ground-applied rain repellent	Applied to windshield on ground by hand. MIL-W-6882 applies.	Can be used on any aircraft. Effective in excessive rain. Excellent at high aircraft speeds.	Short effective life. Not effective in light rain or at low speeds.	Very low weight Very low cost

References

1. Hassard, S., Goodyear Aerospace Corp., "Plastics for Aerospace Vehicles, Part II Transparent Glazing Materials," MIL-HDBK-17A, Part II, Air Force Materials Laboratory, Wright-Patterson Air Force Base, Ohio, Jan. 1973.
2. "Pilot Visibility from the Flight Deck Design Objectives for Commercial Transport Aircraft," AS 580A, Society of Automotive Engineers, Inc., New York, Oct. 1958.

Bibliography

Booker, J. D., "Aircraft Windscreen Rain Clearance - A Review," TR70122, Royal Aircraft Establishment, Farnborough, England, July 1970.

Matusovich, C., "Chemical Rain Repellents for Windshield Application," TRR-6201, Sikorsky Aircraft Div., United Technologies Corp., Stratford, Conn., Apr. 1965.

Meline, H. R., and Smith, I. D., Research, Inc., "Design Manual for Windshield Jet Air Blast Rain and Ice Removal," WADC TR-58-444, Wright Air Development Center, Dayton Ohio, Nov. 1958.

Savio, A.M., and Nantz, D.S., "Service Tests of Chemical Rain Repellents," WADC TR 56-385, Wright Air Development Center, Dayton Ohio, Sept. 1956.

Wright, Ernest E., "Liquid Rain Repellents for Aircraft Windshields," AFML TR 65-212, Air Force Materials Laboratory, Wright-Patterson Air Force Base, Ohio, Sept. 1965.

"Boeing Rain Repellent Development for Aircraft Windscreens," Boeing Co., Renton, Wash., 1964.

"Operational Test and Evaluation, Helicopter Windshield Rain Repellent," MAC OT&E 3-1-68, Military Airlift Command, Scott Air Force Base, Ill., Nov. 1969.

The helicopter has played an increasingly important role in modern warfare. Expanded combat area mission requirements have exposed the helicopter to greater levels of hostile fire. Helicopters used for search and rescue, attack, or other close-proximity missions are outfitted with high-performance opaque armor to reduce vulnerability. This armor protects critical aircraft components and has also been built into aircrew seats. Unfortunately, the transparent glazings required for helicopter operation represent very large areas of ballistic vulnerability. Only limited quantities of opaque armor covering the vulnerable glazing areas can be tolerated without impairing visibility. Because of visibility requirements, the pilot's head is virtually unprotected, resulting in a large percentage of combat wounds occurring in the head and neck area.

A solution to maintaining high levels of visibility while reducing ballistic vulnerability is the incorporation of transparent armor. However, the weight and spatial accommodation required to add transparent armor were prohibitive. For these reasons, the selection of helicopter glazing materials for ballistic properties had been limited primarily to consideration of relative spall resistance.

Recent advances in the state of the art have made transparent armor a more practical alternative for protection against small arms fire and fragmentary explosives.

11.1 Threat Specification

Design of transparent armor begins with an analysis of the threat environment in which the aircraft is expected to operate and the specification of the threats that the armor must defeat. The threat level must be specified in order to design armor that will be adequate and lightweight. The threat level involves types of projectiles used in tactical areas, their probable muzzle velocities, the altitude and attitude of the aircraft when entering the ballistic environment, and the position of the transparent armor in relation to the direction of threat. From this information, the velocities and obliquities of certain expected types of ammunition can be determined at the point of impact on the armor. Table 11-1 identifies some typical threats and their range-velocity relationships.

The ballistic protection limit of a panel for a specific threat and obliquity is given as a velocity. Typically chosen for a design protection limit is V_{50} , the velocity at which a projectile has a 50% chance of effecting a complete penetration of the armor. The V_{50} of a panel is determined by ballistic test. V_{50} is calculated as the average of four fair impact velocities comprising the two lowest velocities resulting in complete penetration and the two highest velocities resulting in partial penetration of the armor. A maximum spread of 150 feet per second is allowed between the highest and lowest velocities employed in the calculation.

A complete penetration is defined as having occurred when the bullet core or core fragments completely penetrate the armor being tested or when a 0.020-inch-thick sheet of cellulose acetate mounted parallel to and 6 inches behind the armor is cut or opened by the bullet core, core fragments, or pieces of the armor. Any fair impact that is not a complete penetration is considered a partial penetration. A fair impact occurs when an unyawed projectile strikes an unsupported area of the ballistic test sample at a location where there is at least 6 inches of undamaged material in any direction around the point of impact.

11.2 Transparent Armor Materials

The ballistic properties of traditional helicopter glazing materials and glass/plastic composites are summarized below.

11.2.1 Monolithic Plastics

Acrylic does not offer ballistic defeat capability at any reasonable thickness.

Polycarbonate (MIL-P-83310) has better ballistic properties than any of the acrylic materials. It does not offer significant ballistic defeat capability at reasonable thickness, but the nonspalling characteristics are very good. The material exhibits unusual toughness and effectively resists crack propagation. Projectile penetration often results in a hole smaller than the projectile with minimal glazing material removal. Polycarbonate has been extensively used as the backing ply of high-performance glass/plastic composite armor.

11.2.2 Laminated Plastics

Laminated plastics do not offer ballistic defeat capabilities at reasonable areal densities, although a laminated system utilizing a brittle acrylic facing and a ductile polycarbonate backing can exhibit ballistic resistance up to 45% higher than the polycarbonate alone.

For example, under ballistic impact of a .22-caliber, 17-grain, fragment-simulating projectile (FSP), acrylic behaves in a brittle fashion and undergoes cracking and spallation. Polycarbonate, on the other hand, is ductile, does not spall, and fails in shear.

The ballistic performance of clamped acrylic/polycarbonate laminates over a range of relative compositions is shown in Figure 11-1. The extreme left of the figure shows the ballistic resistance of 100% acrylic with $V_{50} = 1040$ feet per second. At the extreme right is the ballistic resistance of 100% polycarbonate, $V_{50} = 1100$ feet per second.

TABLE 11-1. RANGE VELOCITY CHARACTERISTICS,
KINETIC ENERGY (SOLID CORE) AMMUNITION

Target Distance Yards	Remaining Velocity (ft/sec) At Specific Distance					
	Cal .30 Ball M2	Cal .30 AP M2	Cal .50 AP M2 (45" Barrel)	14.5mm API-B32 Soviet	20mm AP M75	23mm API-T BZT Soviet
0	2800	2760	2940	3280	2620	3280
100	2565	2560	2800	3130	2455	3120
200	2325	2360	2680	3000	2320	2975
300	2090	2165	2560	2870	2170	2830
400	1865	1985	2445	2750	2050	2690
500	1650	1800	2320	2630	1920	2560
600	1450	1640	2220	2520	1800	2420
700	1270	1490	2100	2410	1695	2290
800	1125	1340	1990	2310	1590	2160
900	1010	1220	1880	2200	1500	2030
1000	940	1130	1780	2100	1400	1910

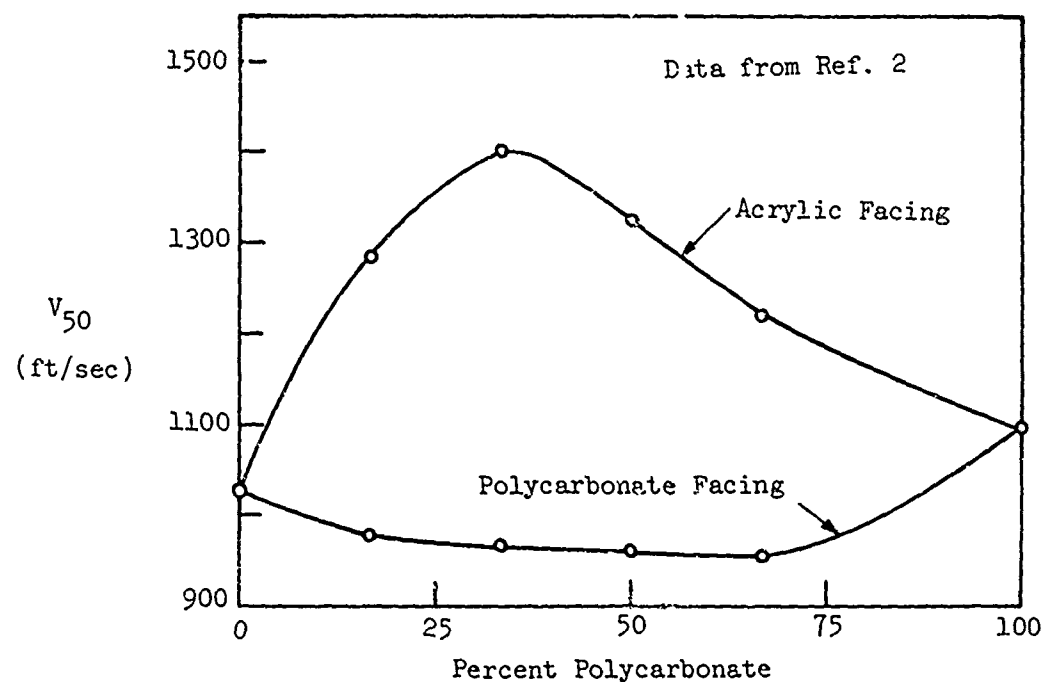


Figure 11-1. Ballistic Behavior of 38 oz/sq ft Acrylic-Polycarbonate Laminates (17-Grain Fragment Simulators).

It was found that a clamped system with the acrylic facing the incoming threat showed a higher ballistic resistance than either material alone. A clamped system with the polycarbonate toward the incoming threat showed a lower ballistic resistance than either material alone.

These results can be explained by examining the failure mechanisms of the two materials. The brittle acrylic facing shattered and spread the impact over a wide area. The ductile polycarbonate backing then served to absorb the impact and prevent the facing material from spalling. However, with the more ductile polycarbonate facing toward the incoming threat, the impact was not spread so efficiently and the brittle acrylic backing had a tendency to spall. Hence, the polycarbonate-faced system exhibited a poorer ballistic resistance.

In order to be useful in aircraft applications, the laminates must be bonded, either thermally or by an adhesive interlayer. It was found that the thermal bonding of the two layers or the use of a brittle adhesive interlayer degraded the ballistic resistance of the system by causing brittle failure and spallation of the polycarbonate backing. However, the use of a flexible adhesive interlayer enhanced the ballistic resistance between 15 and 45% over that of polycarbonate alone.

11.2.3 Laminated Glass

This material (MIL-G-5485C) has a density of approximately 13 pounds per square foot per inch of thickness. As can be seen in Figure 11-2, the weight penalty associated with providing adequate protection for large transparent areas could become prohibitive. Backside spalling is a problem also associated with laminated glass armor and can be very severe if the glazing is overpowered and penetrated. Post-hit visibility will also be poor if fully tempered small dice-glass is used.

11.2.4 Laminated Glass/Plastic

Glass/plastic composites offer the highest performance-to-weight ratios of any currently available transparent armor materials. The glass/plastic armors utilize borosilicate or soda-lime glass as the hard facing layer. A polycarbonate backing ply is bonded to the glass with a cast-in-place or sheet interlayer.

The basic principles of armor design require that the kinetic energy of impact be diverted, converted into heat, and absorbed. Diversion is accomplished by the hard glass facing material, which shatters on impact. This brittle type of failure spreads the impact over a large area of the armor. The hard face also tends to break up the projectile and throw it sideways. The backing plastic material acts as a spall shield. It absorbs the residual energies and contains the fragments of both the projectile and the face sheet. Additional layers may be added as required to defeat higher caliber threats.

Promise of further performance gains is indicated by development work in magnesium-oxide and aluminum-oxide transparent ceramic facing materials. These high-hardness materials offer improved ballistic properties, particularly when protection is required against armor-piercing ordnance.

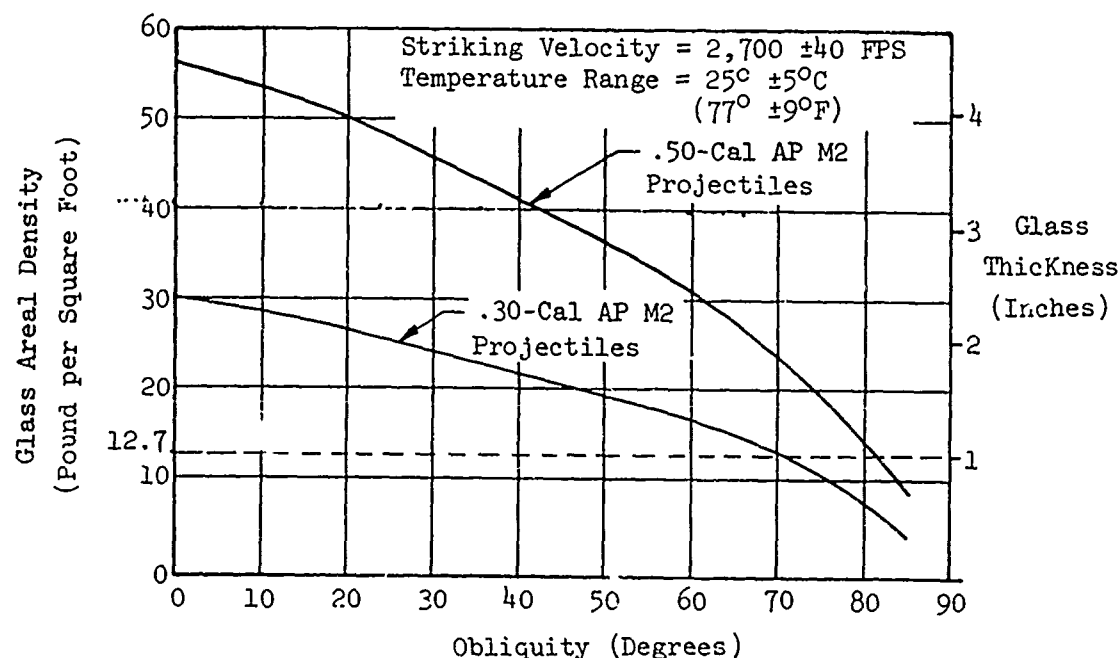


Figure 11-2. Abilities of .30-Caliber and .50-Caliber Projectiles to Penetrate Bullet-Resistant Glass, MIL-G-5485C.

11.3 Fragment Penetration Resistance

Fragment-simulating projectiles (FSP's), as their name implies, simulate fragments from explosive projectiles. They are used extensively in the testing, evaluating, and rating of lightweight armor materials.

Transparent armor systems can be designed to defeat the fragments of a 23mm HEI (high explosive incendiary) projectile detonating in close proximity to the armor panel. Specific performance characteristics for various configurations are given in classified reports such as Ref. 1, 3, 4, 5, 6, and 7.

11.4 Installation

Transparent armor should be installed so that the edges of the armor are rigidly supported to insure the transmission of energy to the supporting frame. Otherwise, the armor may be pushed aside so that the projectile may pass through.

A simple and effective mounting technique is to contain the transparency's edges in a channel-section frame. Clip angles or brackets

are welded or riveted to the frame at the corners for attachment to the supporting structure as shown in Figure 11-3.

An alternate mounting technique would be the bonding and bolting of attachment brackets to the corners of the armor panel. However, this method does not retain segments of a damaged panel as well as the channel-mounted design does. Consideration should also be given to the design of redundant load paths, so that the loss of a single attachment does not render the armor panel ineffective.

Ballistic impact loads are complex and difficult to calculate with any degree of certainty. An armor mounting scheme should therefore be substantiated by actual test firings.

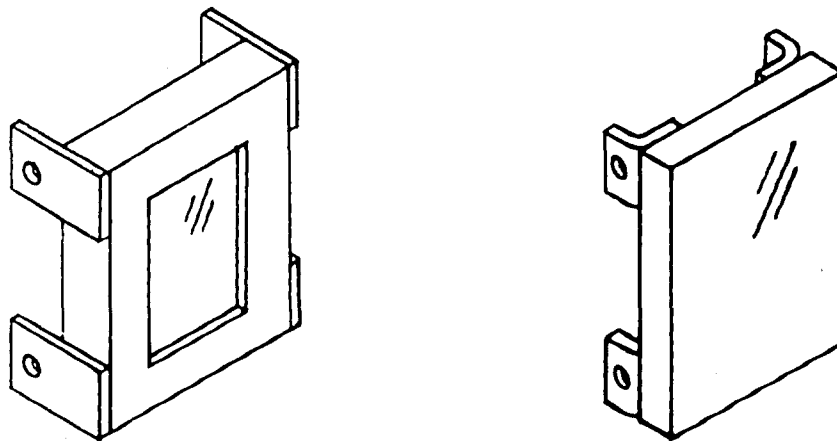


Figure 11-3. Transparent Armor Mounting Brackets.

References

1. Mascianica, F. S., "Ballistic Technology of Lightweight Armor - 1973," AMMRC TR 73-47, Army Materials and Mechanics Research Center, Watertown, Mass., Nov. 1973, CONFIDENTIAL.
2. Illinger, J. L., and Lewis, R. W., Army Materials and Mechanics Research Center, "Effect of Adhesive on the Impact Resistance of Laminated Plastics for Windshield Applications," AFML TR 73-126, Air Force Materials Laboratory, Wright-Patterson Air Force Base, Ohio, June 1973.
3. Layden, J. E., Goodyear Aerospace Corp., "Analysis and Design of Lightweight Transparent Armor Material for the Protection of Army Aircrews," USAAMRDL TR 71-49, U. S. Army Air Mobility Research and Development Laboratory, Fort Eustis, Va., Jan. 1972, AD 523449L, CONFIDENTIAL.
4. Littell, H. E., Jr., Pittsburgh Plate Glass "Transparent Armor Shields," AMMRC CR 71-12, Army Materials and Mechanics Research Center, Watertown, Mass., Aug. 1971, RESTRICTED.
5. Parsons, G. R., and Frost, R. H., "Ballistic Performance of Transparent Materials against Fragment Simulating Projectiles and the Soviet 23MM HEI-T Projectiles," AMMRC TR 75-24, Army Materials and Mechanics Research Center, Watertown, Mass., Nov. 1975, CONFIDENTIAL.
6. Shorr, N., and Littlell, H. E., Jr., Pittsburgh Plate Glass, "Ancillary Properties for Transparent Armor," AMMRC CR 69-03(f), Army Materials and Mechanics Research Center, Watertown, Mass., May 1969, RESTRICTED.
7. Shorr, N., and Littlell, H. E., Jr., Pittsburgh Plate Glass, "Transparent Armor (Glass - Plastic Composite)," AMMRC CR 69-06, Army Materials and Mechanics Research Center, Watertown, Mass., May 1969, RESTRICTED.

Bibliography

Hassard, R. S., Goodyear Aerospace Corp., MIL-HDBK-17A, Part II, "Plastics for Aerospace Vehicles, Part II Transparent Glazing Materials," Air Force Materials Laboratory, Wright-Patterson Air Force Base, Ohio, Jan. 1973.

James, H. C., Ingelse, A. O., and Huyett, R., Goodyear Aerospace Corp., "Design, Test, and Acceptance Criteria for Army Helicopter Transparent Enclosures," USAAMRDL-TR-73-19, U. S. Army Air Mobility Research and Development Laboratory Fort Eustis, Va., May 1973, AD 767242.

Lewis, R. W., and Parsons, G. R., "Ballistic Performance of Transparent Materials for Eye Protection," AMMRC TR 72-36, Army Materials and Mechanics Research Center, Watertown, Mass., Nov. 1972, CONFIDENTIAL.

Royland, M. E., and Lewis, R. W., "Development of Transparent Polymers for Armor," AMMRC TR 72-23, Army Materials and Mechanics Research Center, Watertown, Mass., July 1972.

Aircraft and Defense Manual, Libbey-Owens-Ford Co., Toledo, Ohio, June 1969.

Lovelace Foundation for Medical Education and Research, "Biological Effects of Plexiglass Fragments", BRL CR 143, Mar. 1974, CONFIDENTIAL.

MIL-A-46108A, "Armor: Transparent, Glass Plastic Laminates," May 1972.

MIL-G-5485C, "Glass: Laminated, Flat, Bullet Resistant," Apr. 1971.

12.0

SPALL DESIGN REQUIREMENTS

Spall consists of many small fragments that are produced and ejected when a material is impacted by a projectile or shock wave. Transparencies, which necessarily enclose large portions of the crew-occupied helicopter areas, are particularly susceptible to spallation.

Data compiled during the hostilities in the Republic of Vietnam indicated that spall from the transparencies of U. S. Army helicopters posed a significant hazard to the aircrews and passengers. This spall was generated primarily by small arms fire impacting on the aircraft cast-acrylic transparencies. Although spall rarely caused permanent injury, it nonetheless hindered aircraft operations.

The areas of the body most vulnerable to spall wounding are those which are not protected by clothing - the head, neck, hands, and arms. In particular, the eyes must be protected by visors or goggles; even the smallest of spall fragments hitting an eye can temporarily incapacitate a pilot and have serious consequences.

12.1 Wound Criteria

Figure 12-1 shows combinations of fragment mass and velocity that can lacerate or penetrate the skin. The curve was derived from several wounding models and empirical data. A fragment whose mass and velocity describe a point below the threshold line has less than a 5 percent chance of causing a wound. The curve may, therefore, be considered as a conservative standard for evaluating the spall resistance of candidate transparent materials.

In order to utilize such a wound criteria, one must know the spall characteristics - fragment quantities, sizes, and velocities - associated with different combinations of threats and targets. Numerous tests have been conducted to ascertain these characteristics and will be discussed.

12.2 Mechanisms of Spall

Spallation is associated with stress-wave phenomena in the target material. When a projectile strikes a solid target at a high speed, a shock wave is generated that becomes spherical in shape after a short period of time. The shock decays in strength as it propagates through the target and ultimately becomes a compressive elastic wave.

When the stress wave encounters the inside surface of a transparency, it is reflected as a tensile stress wave. If the reflected wave exceeds the dynamic tensile strength of the material, fracture planes will form parallel to the target surface, and spall will be generated. Spallation may occur at both the impact and exit faces.

The spallation mechanism becomes more complex when one considers a laminated target structure. At each material interface, the shock wave will be both reflected and transmitted. The relative strength of the waves will depend upon the ratio of the material's acoustic impedances. In general, material combinations with higher acoustic impedance ratios (and higher transmitted shocks as a result) appear to suffer greater amounts of possibly higher velocities of backface spall. Acoustic impedance is the product of the material density and the velocity of sound in the material.

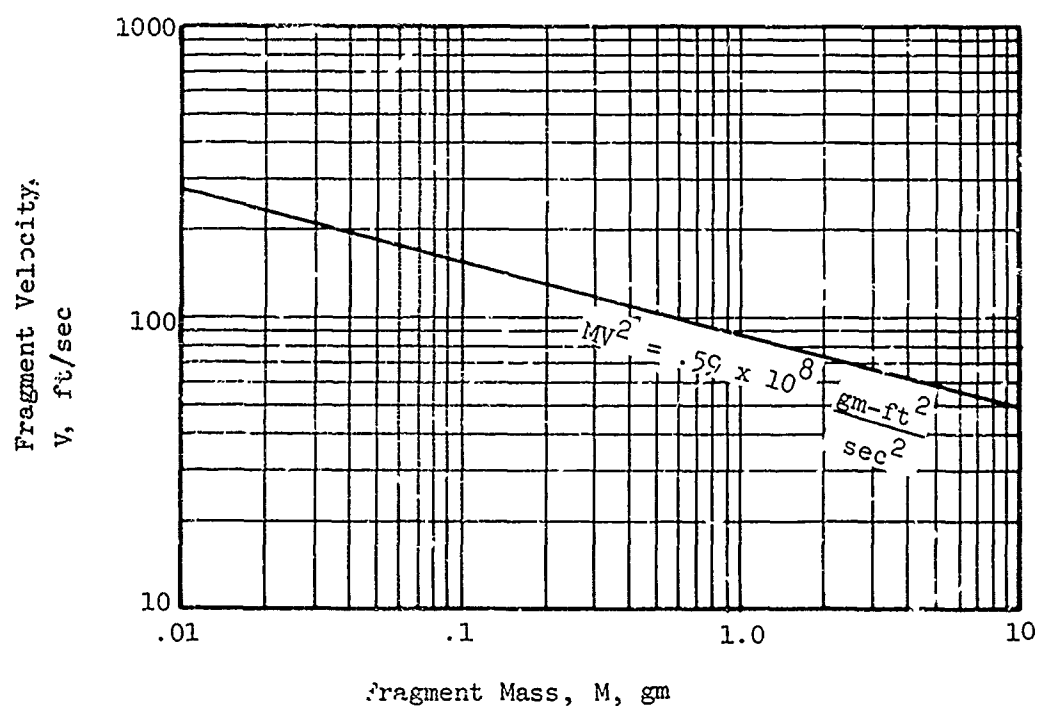


Figure 12-1. Wounding Model, Skin Laceration by Glass Fragments.

12.3 Major Parameters Influencing Spallation

A number of parameters have been identified that have significant effects on spallation. For spall produced by ballistic impact, these parameters may be grouped into three categories:

- 1) impact conditions
- 2) projectile parameters
- 3) target parameters

12.4 Impact Conditions

Impact conditions are those parameters that result from the relative motion of the projectile and the target. These are impact velocity and obliquity.

Impact velocity is an important parameter for determining the amount of material removed from a target during impact. Studies have shown that a target will eject the largest amount (and mass) of material when the projectile velocity is slightly above the ballistic penetration limit; the spall may consist of a few large chunks. Projectiles with higher velocities will produce more intense impact stresses, which in turn, produce smaller, more numerous fragments.

Impact obliquity is defined as the angle between the projectile's flight path and a normal to the target surface. At velocities near the ballistic penetration limit, projectile impacts at 0° obliquity will produce the greatest amount of spall. As the impact velocity increases, increasing obliquity will also produce greater spall, up to the angle at which the projectile will ricochet and not penetrate the target.

12.5 Projectile Parameters

Projectile parameters include projectile size, type, and shape.

With all other factors being equal, larger projectiles will produce greater target damage and more spall.

Projectile shape is also significant in predicting spall characteristics. A blunt-nose projectile under normal impact may penetrate the target with a shearing action that restricts target damage to a hole that is the diameter of the projectile. An ogive-nose projectile, on the other hand, will have its impact concentrated in a much smaller area. The wedge action of the shape will induce in-plane stresses, further damaging the target. Projectile shape is not so significant when impacts occur at oblique angles.

12.6 Target Parameters

Target parameters are thickness, material, and structural configuration. Thickness is the target parameter that directly affects impact conditions. Thin targets will receive small holes while sufficiently thick targets will sustain a dent or crater. Thicknesses in between these limits will suffer various sizes and types of damage, depending on the ratio of target thickness to projectile diameter. The basic thickness effect is such that thicker sections tend to limit local deformations, such as petalling or denting, and to increase spallation. This increased spallation may be due to the fact that the thicker sections allow far more shock interaction before the projectile completes penetration.

The choice of target materials is, of course, critical. Material parameters expected to be significant include strength, hardness, fracture, toughness, elastic modulus, and other physical factors such as density. No satisfactory model has yet been established, and therefore experimental data is the means for evaluation. The spallation characteristics of several transparency candidate materials will be discussed.

Structural configuration includes such factors as physical composition (monolithic, laminated), method of manufacture (cast, stretched, bonded), dimensional relationships (curvature, planform), and edge attachment fixity (simple, free, fixed support). The first two considerations are addressed under Material Characteristics. There is little empirical data on the last two, and they are considered to be relatively insignificant in determining target damage.

12.7 Material Characteristics

The threat environment in which a helicopter must operate is a condition given to the designer. He, therefore, has little control over the impact or projectile parameters. In attempting to reduce spallation to acceptable levels, he can best control the target transparency parameters, which includes the selection of materials with low-spall characteristics.

Numerous tests have been conducted to determine the spallation characteristics of various materials. The results of one series of ballistic tests, that were performed in conjunction with the preparation of this handbook, will be described.

Five materials selected as representative of current-generation helicopter transparencies were tested. Specimens of each material were impacted with .30-caliber ball and AP ammunition at velocities and obliquities that had been predetermined to inflict the maximum damage. An aluminum foil witness sheet located behind the specimen demonstrated spall damage and distribution.

12.7.1 Monolithic Polycarbonate

After impact, polycarbonate has excellent residual visibility. No surface cracks occur and the entry hole closes up to become smaller than the round itself (Figure 12-2). The polycarbonate spall causes little damage to a witness sheet. One or two particles generally make minute penetrations of the sheet within 2 inches from the impact position. A typical polycarbonate witness sheet pattern is shown in Figure 12-3.

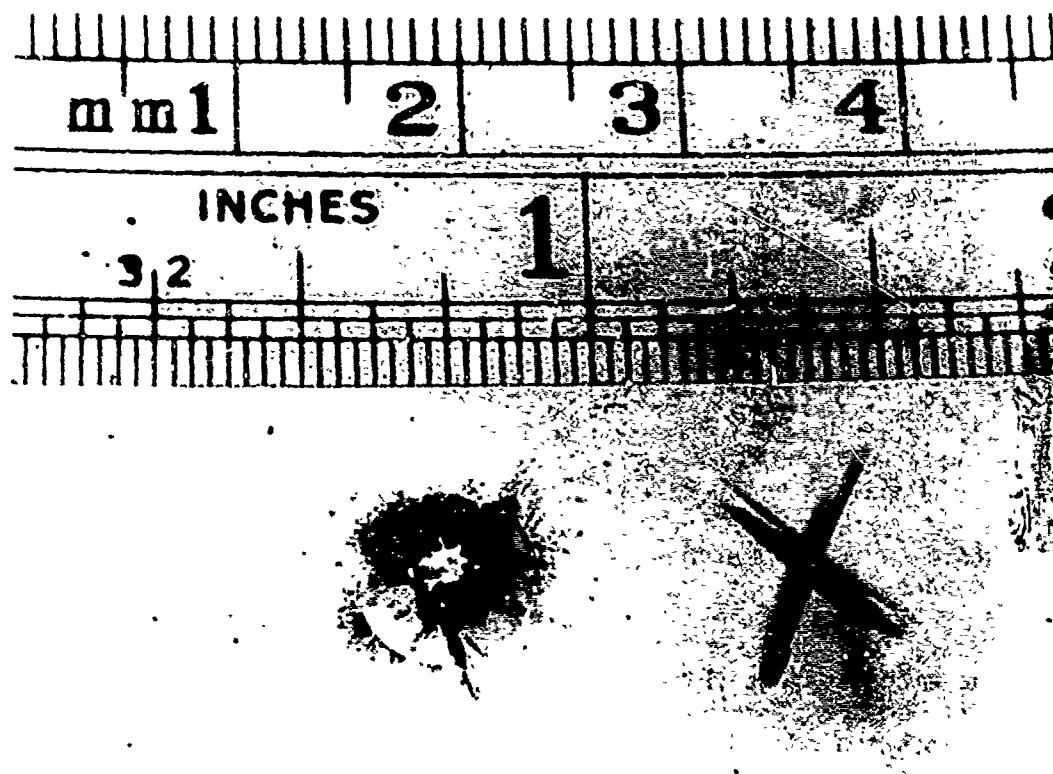


Figure 12-2. Monolithic .080-Inch-Thick Polycarbonate Specimen After .30-Caliber Ball Ballistic Impact.



Figure 12-3. Spall Penetration of Witness Sheet for Polycarbonate.

12.7.2 Monolithic Stretched Acrylic

After impact, stretched acrylic also has excellent residual visibility. Penetration is only the round diameter. Fine radial cracks, less than $\frac{1}{2}$ inch long, are characteristic (see Figure 12-4).

The witness sheet (Figure 12-5) shows a few small penetrations and a large number of dents, within 5 inches of the impact center. The spall fragments produced are uniformly small and blunt (see Figure 12-6).



Figure 12-4. Monolithic .080-Inch-Thick Stretched Acrylic Specimen After .30-Caliber Ball Ballistic Impact.



Figure 12-5. Spall Penetration of Witness Sheet for Stretched Acrylic.

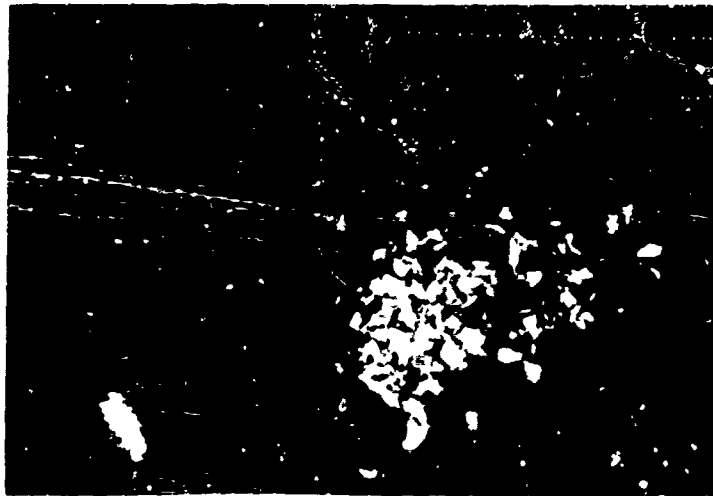


Figure 12-6. Spall Produced by .30-Caliber Ball Ballistic Impact on Stretched Acrylic.

12.7.3 Monolithic Cast Acrylic

Penetration holes are equal to the diameter of the test round. Damage is confined to a 3-inch diameter for .080-inch sheets, as shown in Figure 12-7. The 0.187-inch plate sustains more surface cracking, as shown in Figure 12-8.

Spall from cast acrylic specimens cause several penetrations in a compact area of the witness sheet with approximately an equal number of dents in the same area. The 0.187-inch material exhibits the same pattern, but has slightly larger penetrations. A typical witness sheet for the cast acrylic is shown in Figure 12-9.

The cast acrylic spall fragments (Figure 12-10) are larger and more jagged than those for the stretched acrylic.

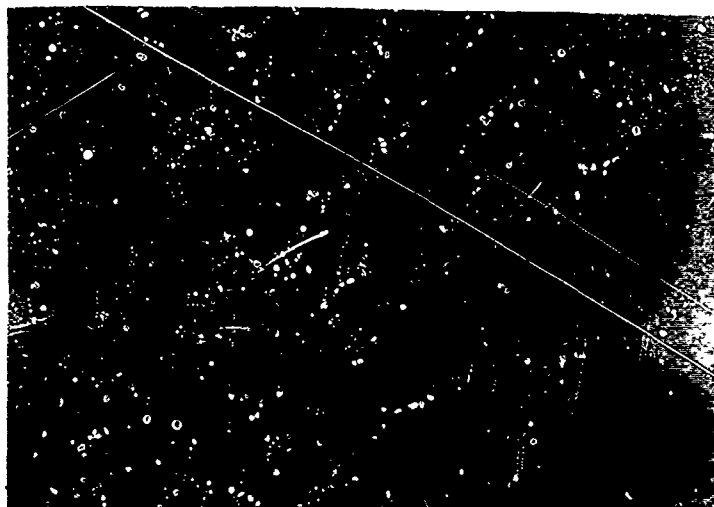


Figure 12-7. 0.080-Inch-Thick Cast Acrylic Specimen After .30-Caliber Ball Ballistic Impact.



Figure 12-8. 0.187-Inch-Thick Cast Acrylic Specimen After .30-Caliber Ball Ballistic Impact.

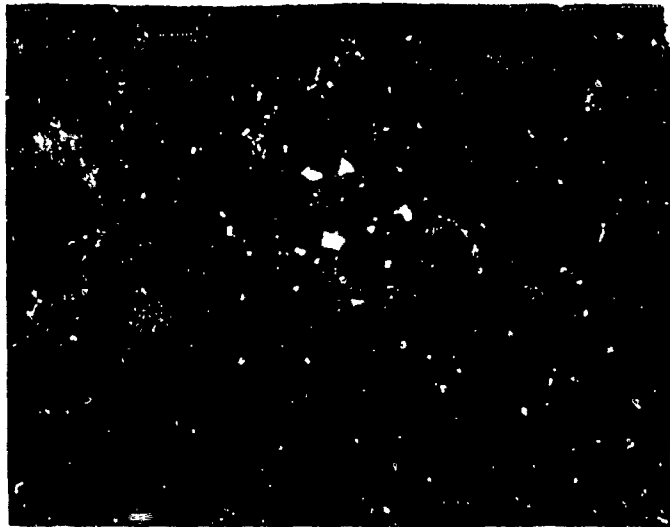


Figure 12-9. Spall Penetration of Witness Sheet for Cast Acrylic.



Figure 12-10. Spall Produced by .30-Caliber Ball Ballistic Impact on Cast Acrylic.

12.7.4 Glass-Acrylic Laminate

Glass-acrylic laminates suffer considerable post-impact surface damage. When struck at a 60° angle of obliquity to the normal, the damage pattern tends to be oblong. The entry hole is small and the soft interlayer tends to close the hole. An area 2-3 inches across is diced with fine radial cracks extending several inches from the impact, as shown in Figure 12-11. The laminate pictured had an .085-in glass face ply, an .075-in. PVB interlayer, and an .080-in. stretched acrylic innerply.

A typical witness sheet for the above strike is shown in Figure 12-12. Damage area is oblong and closely covered with a mixture of dents and penetrations, most being less than a quarter of an inch long. The larger penetrations tend to be nearer to the point of impact. The glass-acrylic spall showed a wide variation in size, as can be seen in Figure 12-13.

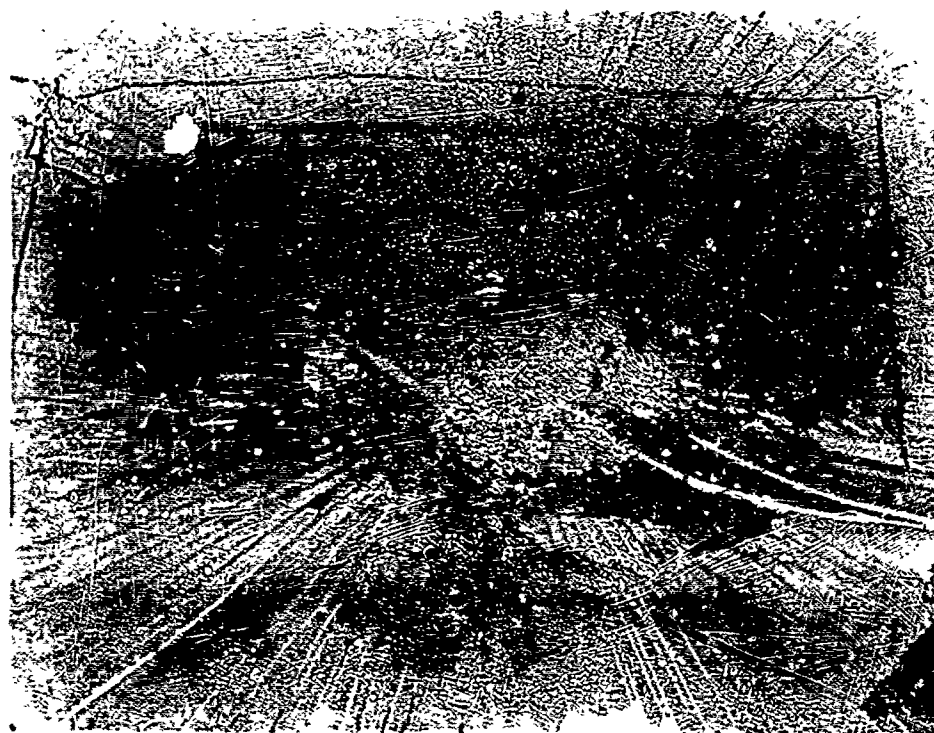


Figure 12-11. Glass-Acrylic Laminated Specimen After .30-Caliber Ball Ballistic Impact.

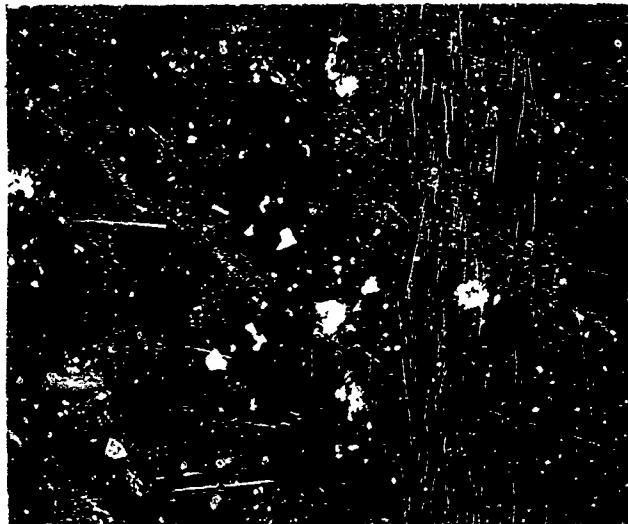


Figure 12-12. Spall Penetration of Witness Sheet for Glass-Acrylic Laminates.

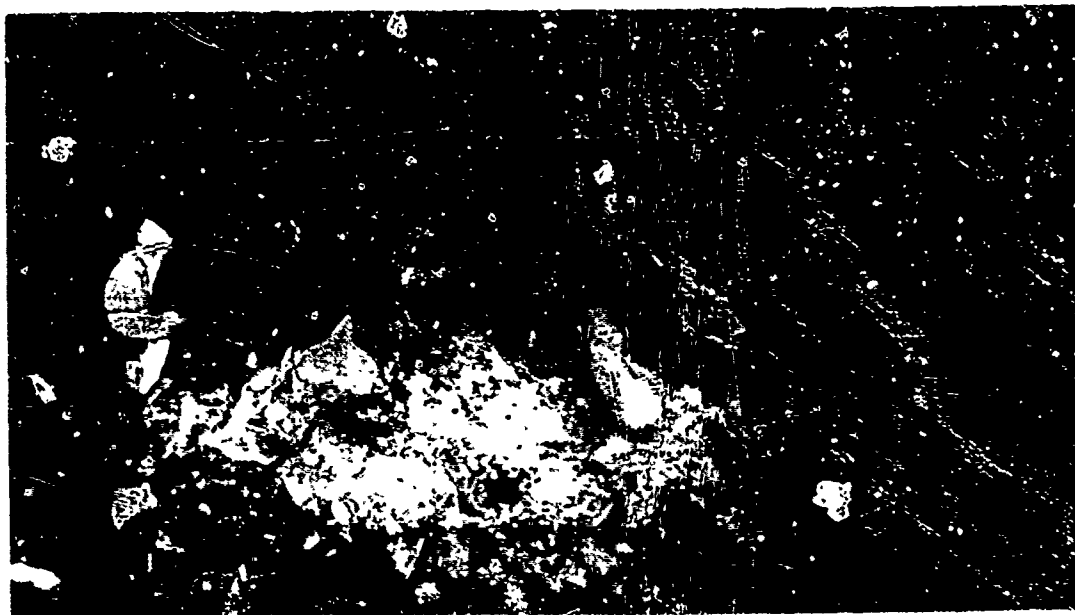


Figure 12-13. Spall Produced by .30-Caliber Ball Ballistic Impact on Glass-Acrylic Laminates.

12.7.5 Laminated Glass

Glass-glass laminates sustain considerably more surface damage than monolithic plastic specimens. Entry holes are from 1 to 2 inches across, as shown in Figure 12-14. The laminate pictured had .095 glass facings and an .085 PVB interlayer. The pulverized areas are oblong because of the obliquity between the projectile path and the specimen.

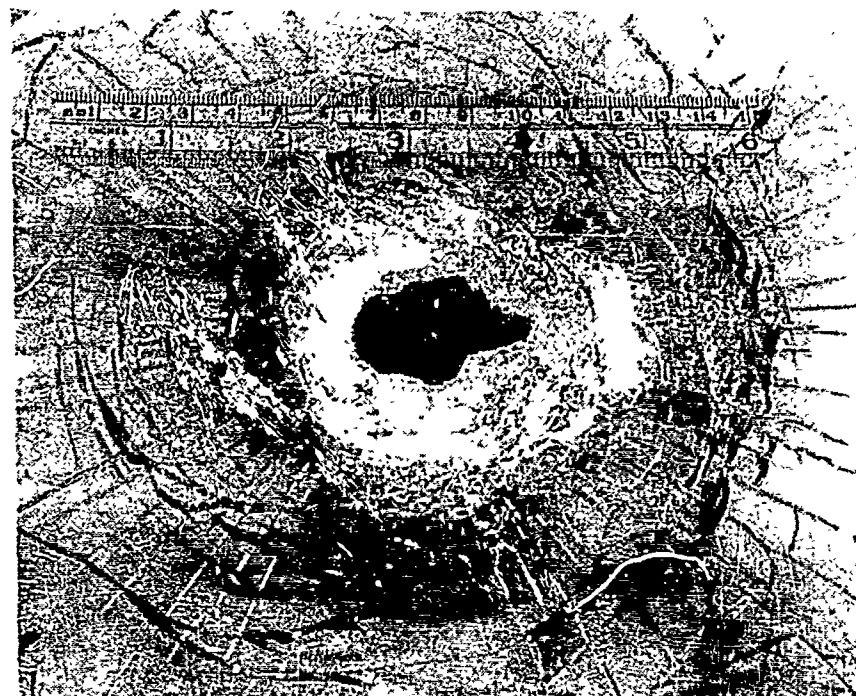


Figure 12-14. Laminated Glass Specimen After .30-Caliber Ball Ballistic Impact.

Witness sheets for glass-glass laminates suffer extensive damage. Large pieces of interlayer, weighing at least two grams and at least 1.5 inches in diameter, are blown free from the laminate. One of these fragments can be seen in Figure 12-15. Although these fragments are capable of tearing large holes in the foil, they are soft and pose a minimum wounding hazard. In addition, a large number of smaller penetrations occur within a 14 by 10-inch area, the most severe being in the immediate vicinity of the ballistic impact. A typical penetration pattern is shown in Figure 12-16. It should be noted that the purpose of the witness sheets is to determine the spall penetration patterns, and not severity of spall.

Figure 12-17 shows spall from a laminated glass specimen. A wide variation in size is apparent.

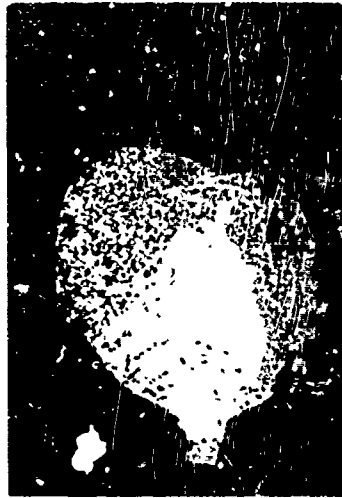


Figure 12-15. Polyvinyl-Butyral Interlayer Fragment From a Laminated Glass Specimen.

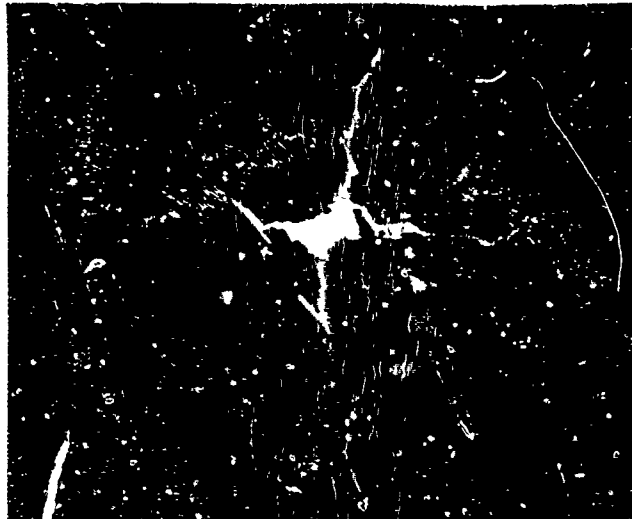


Figure 12-16. Spall Penetration of Witness Sheet for Laminated Glass Specimen.



Figure 12-17. Spall Produced by .30-Caliber Ball Ballistic Impact on Laminated Glass.

12.8 Spall Fragment Energy

During the aforementioned ballistic tests the spall generated was weighed and velocities calculated. This fragment mass and velocity data is presented in Figure 12-18, superimposed on the skin laceration wounding model previously discussed. The large fragments of the PVB interlayer have not been included in the data as they were considered incapable of lacerating the skin and were inappropriate for the model.

The laminated transparencies have the worst performance. Both the glass-acrylic and all-glass combinations produce a wide range of fragments, the most severe of which exceed the wounding threshold.

The fragments from the cast-acrylic transparencies are more closely grouped in mass and velocity. A significant number of these exceed the wounding threshold.

The stretched acrylic and polycarbonate transparencies do not produce fragments which exceed the wounding threshold. Polycarbonate spall is almost nonexistent.

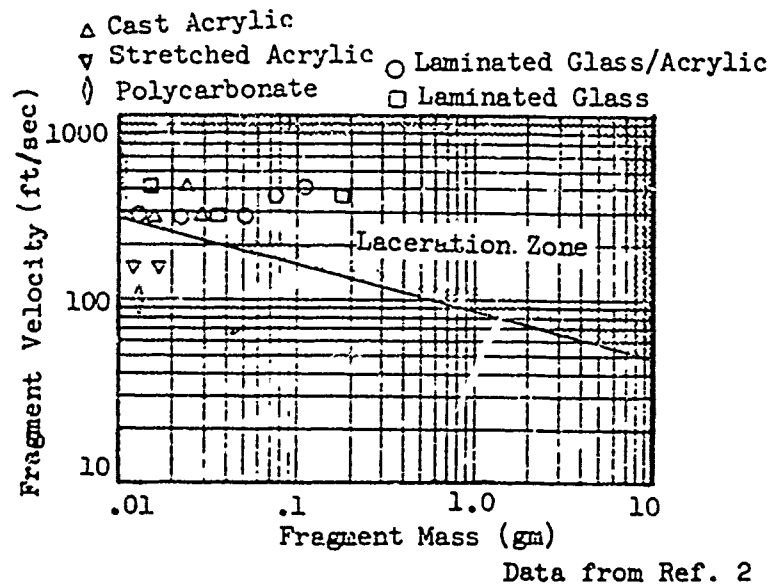


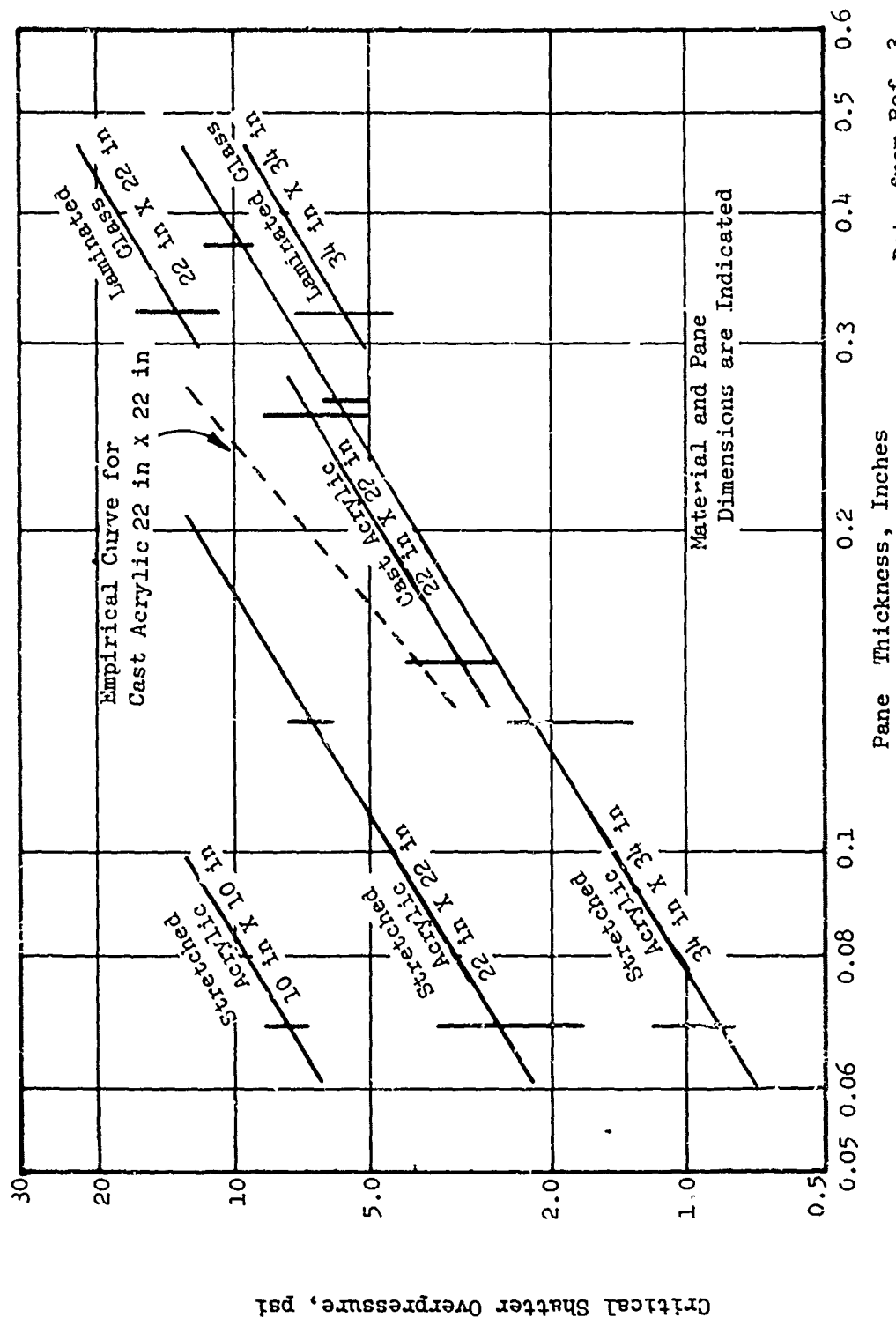
Figure 12-18. Spall Data Compared to Wounding Threshold.

12.9 Blast Overpressure Hazards

Spallation may also be caused by shock waves from high explosives impinging on a transparency. Under these circumstances, the important parameters are those that describe the impinging shock. These would include peak overpressure and duration of the positive phase of the shock.

Studies utilizing airblasts and shock tubes have shown overpressure to be the most important of these parameters. Any particular configuration will have a critical shatter pressure called overpressure below which shattering will not occur. Figure 12-19 gives the thickness required for panels of cast acrylic, stretched acrylic, and laminated glass to survive a shock without shattering. Situations described by points above the line of interest (overpressure exceeds critical shatter overpressure) will result in the shattering of the transparency. Points below the line will not.

The vertical lines on the chart indicate the spread of actual test data. The lines of critical shatter overpressure for particular materials and panel sizes are approximations that have been fitted by eye to the data.



Data from Ref. 3

Figure 12-19. Critical Shatter Overpressure (Reflected) for Common Transparent Materials (Vertical lines correspond to the range of uncertainty of the data).

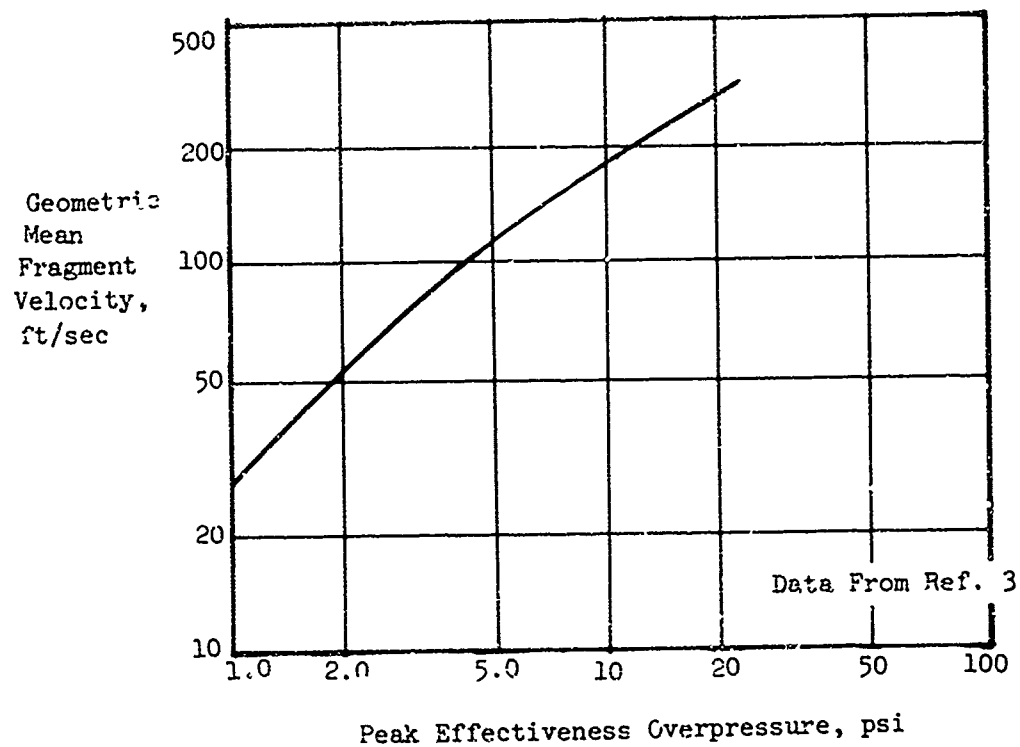
Shocks near the critical shatter overpressure tend to produce large fragments. Shock tests of laminated glass panels have dislodged heavy segments weighing up to 80% of the panel weight with velocities between 140 and 240 feet per second. These could cause blunt-body trauma.

Fragment size tends to decrease and fragment numbers tend to increase as overpressure is increased. These tendencies can be seen in the data of Table 12-1 which was developed utilizing UH-1 helicopters parked at varying distances from a 500-ton TNT airblast. All helicopters were positioned with their noses toward the blast. This data and Figure 12-20 show the tendency of higher overpressures to produce higher mean fragment velocities. Longer shock duration will also result in higher fragment velocities.

TABLE 12-1. FRAGMENT DATA FROM UH-1 HELICOPTERS EXPOSED TO 500-TON TNT AIRBLASTS

Ground Range (ft)	Peak Overpressure (psi)	Number of Fragments in Crew Section	Mean Fragment Mass (gms)	Mean Fragment Velocity (ft/sec)
1400	5.0	45	2.92	100
1700	3.5	37	6.92	76.1
2285	2.3	9	8.46	52.8
3590	1.2	2	33.4	18.2

Data from Ref. 4



NOTE: The Measured velocities have been scaled to correspond to 1/8-inch-thick stretched or cast acrylic panes exposed to a long-duration blast wave.

Figure 12-20. Geometric Mean of the Fragment Velocity Versus the Peak Effective Overpressure.

References

1. Kolsky, "Stress Waves in Solids, "Dover Publications Inc., N. Y.
2. Kay, B. F., "Design, Test and Acceptance Criteria for Army Army Helicopter Transparent Enclosures," USARTL-TR-78-26, Sikorsky Aircraft Div. United Technologies, Stratford, Conn., Applied Technology Laboratory, U. S. Army Research and Technology Laboratories-(AVRADCOM) Fort Eustis, Va.
3. Lovelace Foundation for Medical Education and Research, "Characteristics of Plexiglass Fragments from Windows Broken by Airblast," BRL-CR-146, Aberdeen Proving Ground, Md., Mar. 1974.
4. Lovelace Foundation for Medical Education and Research, "Blast Effects on Helicopter Plexiglass Windows," BRL CR 142, Aberdeen Proving Ground, Md., Mar. 1974, CONFIDENTIAL.

Bibliography

Bernier, R. G., and Smith, H. C., "U. S. Army Casualties Aboard Aircraft in the Republic of Vietnam (1962 through 1967)," BRL MR2030, U. S. Army Ballistic Research Laboratories, Aberdeen Proving Ground, Md., Mar. 1970, CONFIDENTIAL.

Burch, G. T., Jr., and Avery, J. G., The Boeing Company, "An Aircraft Structural Combat Damage Model - Volume 1, Final Report," AFFDL-TR-70-115, Vol. I, Wright-Patterson Air Force Base, Ohio, Nov. 1970.

Clough, and Lieblein, McMillan, A. R., Lewis Research Center, and General Motors Corporation, "Dimple, Spall, and Perforation Characteristics in Aluminum, Columbium, and Steel Plates Under Hypervelocity Impact," NASA tn-d-3468, National Aeronautics and Space Administration, Washington, D. C., June 1966.

Degnan, W. G., "On the Penetration Dynamics of Non-Deforming Projectiles in Filamentary Composites," Sikorsky Aircraft Div., United Technologies Corp., Stratford, Conn., Mar. 1976.

Feinstein, D. I., "Personnel Casualty Study," IITRI Report J6067, IIT Institute, Chicago, Ill., July 1968.

Johnson, Orlando T., "Ballistic Tests of Prototype CH-47 Windshields," AMXRD-BVL, Aberdeen Proving Ground, Md., May 1970.

Malick, D., et al, Falcon Research and Development Co., "U. S. Army Casualties Aboard Aircraft in the Republic of Vietnam (1968 through 1970)," BRL CR 257, Aberdeen Proving Ground, Md., Aug. 1975, CONFIDENTIAL.

McDonald, C., and Huyett, A., Goodyear Aerospace Corp., "UH-1 Ballistic and Bird Impact Test Study," AMMRC CTR 75-7, Army Materials and Mechanics Research Center, Watertown, Mass., Apr. 1975.

Parsons, R., and Frost, H., "Ballistic Performance of Transparent Materials against Fragment-Simulating Projectiles and the Soviet 23 MM HEI-T Projectiles," AMMRC TR 75-24, Army Materials and Mechanics Research Center, Watertown, Mass., Nov. 1975, CONFIDENTIAL.

Plumer, J. R., "Development of Scratch - and Spall-Resistant Windshields," AMMRC TR 74-19, Army Materials and Mechanics Research Center, Watertown Mass., Aug. 1974.

Stefancin, T. R., "Helicopter Windshield Design Improvement Program," ER-72-006A, Sierracin Corp., Sylmar, Calif., July 1972.

White, C. S., et al, Lovelace Foundation for Medical Education and Research, "The Environmental Medical Aspects of Nuclear Blast," DASA 1341, Nov. 1962.

"Plexiglass Handbook for Aircraft Engineers," Rohm and Haas Co., Philadelphia, Pa., 1951

In-flight collision with birds represents a hazard to all types of aircraft. The energy that must be absorbed from a 4-pound bird colliding with an aircraft at 136 mph is approximately 10,000 ft-lbs. This can lead to serious consequences, such as the penetration of the windshields and the incapacitation of the flight crew. Even if the bird does not penetrate the windshield, considerable backside spall can be emitted, and visibility can be substantially reduced.

Figures 13-1 and 13-2 show the results of bird-strike tests on two types of UH-1 windshields. Figure 13-1 shows the remains of a standard 0.25-in.-thick cast-acrylic windshield after being struck by a 4-pound bird at 122 knots. Figure 13-2 shows a glass-faced windshield after being struck by a 4-pound bird at 92 knots.

In spite of the hazard, relatively few serious incidents involving bird strikes on helicopter windshields have been reported. This may be attributed to the low airspeeds which permit both the birds as well as the helicopters to avoid collisions. Furthermore, existing helicopter windshields are capable of defeating impacts by 4-pound birds up to speeds around 100 mph, and impacts by smaller birds at even higher speeds. Nevertheless, with a trend toward higher airspeeds and nap-of-the-earth missions, birdproofing could become a requirement for future helicopters.

13.1 Bird Hazards

As might be expected, the hazard of in-flight collision with birds is most intense at the altitudes normally flown by helicopters: 80 to 90 percent of all bird strikes occur below 3,000 foot altitude.

Studies have shown that birds weighing less than 4 pounds constitute over 90% of all bird strikes. The 4-pound bird has been used as a standard for FAA certification of birdproof windshields, and there have been no catastrophic failures due to bird strikes on transparencies designed to this criterion.

13.2 Methods for Defeating Bird Strikes

There are two basic methods used to prevent colliding birds from penetrating cockpit transparencies: bagging and bouncing. Bird bagging is possible if the transparency can undergo substantial elongation without tearing. The combination of high load and large deformation results in high energy absorption, and the bird may be stopped prior to entering the cockpit. Windshields utilizing thick interlayers rely on this method to provide bird impact resistance, which is illustrated in Figure 13-3.

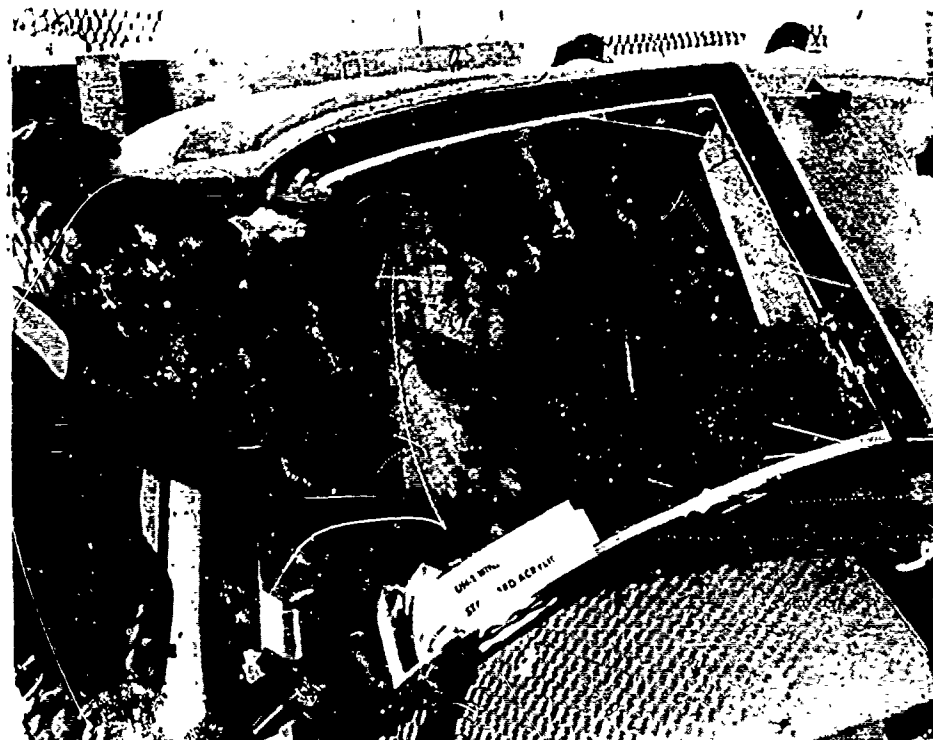


Figure 13-1. Bird Impact Damage at 122 Knots, Acrylic Windshield.



Figure 13-2. Bird Impact Damage at 92 Knots, Glass-Faced Windshield.

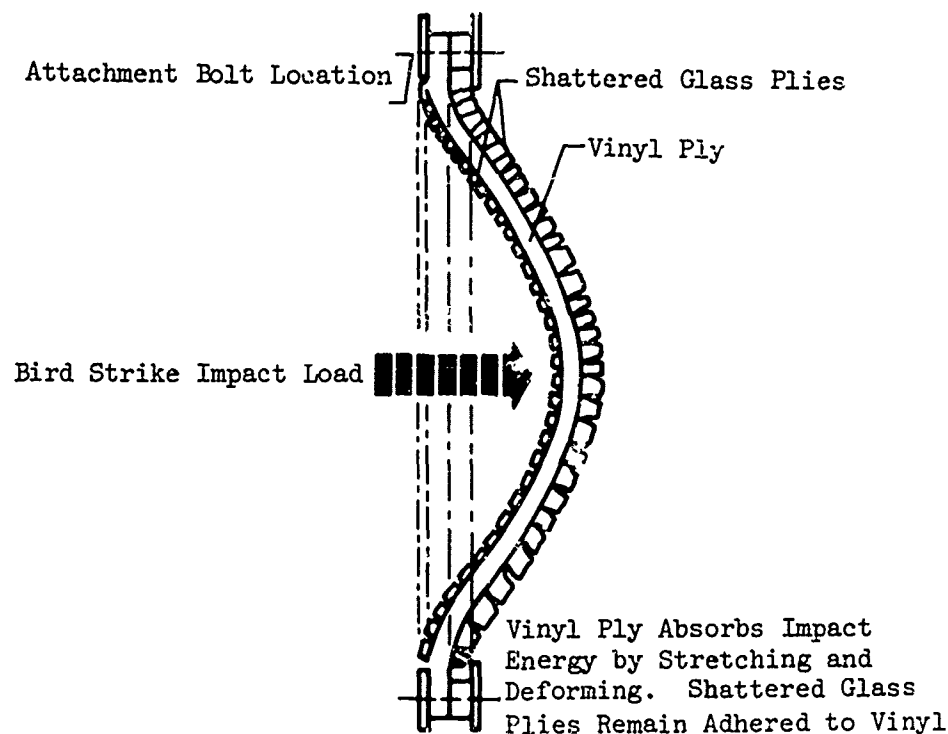


Figure 13-3. Manner in Which a Birdproof Windshield Panel Resists a Bird Strike.

Bird bouncing is more of a brute force approach, reacting bird impact forces by plate bending action. Here, structural deformations are minimal, and most of the energy is dissipated by crushing or splattering the bird. The bird bouncing technique is normally used only on large transport airplanes and is generally unsuitable for helicopters because of the weight penalties involved.

Windshields with inboard surfaces fabricated from glass tend to generate spall when impacted at high speeds. This spall can be attenuated by thin-plastic or low-tempered-glass shields laminated to the glass surface as shown in Figure 13-4, or by changing the inner ply of the laminate to a plastic material.

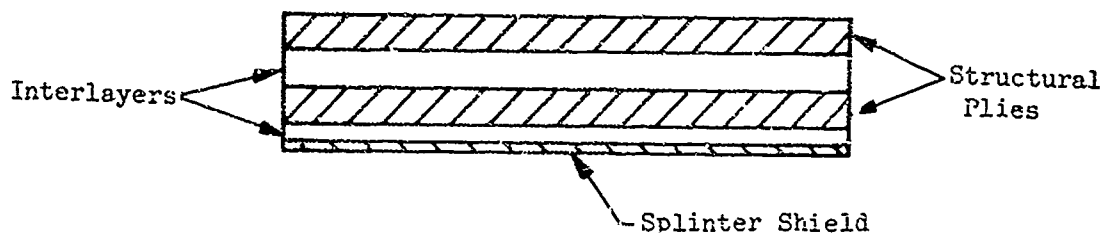


Figure 13-4. Safety Shield Laminated to Inboard Surface of Windshield to Reduce Spall.

13.3 Bird-Strike Capabilities of Transparent Materials

The ability of a windshield to resist bird impact depends on many variables, among which are the following:

- Windshield material properties
- Windshield thickness
- Weight and speed of the bird
- Trajectory relative to the transparency
- Windshield shape, size and contour (minor effects)
- Temperature of the transparency
- Rigidity of attachment to the airframe
- Airframe rigidity

Over the years, a great deal of quantitative data has been accumulated concerning the response of transparent materials to bird impact. Most of this data has been collected from tests conducted on flat specimens mounted in rigid fixtures. Empirical equations have been derived from this data that are useful for preliminary design purposes. However, the equations do not consider all of the important variables and therefore cannot be used for design substantiation. The only acceptable method to substantiate bird resistance is by tests conducted on full-size cockpit assemblies.

The basic analytical expressions for bird-resistant windshields are summarized below. These empirical equations provide an estimate of windshield thickness necessary to defeat bird strikes under varying conditions of impact. Using superposition, these equations can also be used to provide a very rough estimate of the penetration resistance of laminated composite windshields. Detailed explanations describing the conditions for which these equations were derived are contained in References 1 through 4.

a. Glass

From Reference 1 for fully tempered monolithic glass:

$$t = 0.136(1 - 0.348 \cos \alpha) e^{\frac{V \cos \alpha}{87.3}} \quad (13-1)$$

where bird weight = 4 pounds
 α = windshield sweepback angle, degrees
 (See Figure 13-5)
 e = constant = 2.71828
 t = total thickness of all structural plies,
 inches
 V = velocity, mph

From Reference 2 for thermally toughened glass:

$$t = \frac{V(\cos \alpha)(W)^{1/2}}{400} \quad (13-2)$$

where W = bird weight, pounds

and for ten-twenty glass:

$$t = \frac{V(\cos \alpha)(W)^{1/2}}{520} \quad (13-3)$$

From Reference 3:

$$t^{3/2} = \frac{.00105V^2W^{2/3}(\sin \beta)\lambda}{C} \quad (13-4)$$

or, if all the plies are not the same,

$$(t)^{3/2} = \left(\frac{t_1 C_1 + t_2 C_2 + \dots}{t} \right) = .00105V^2W^{2/3}(\sin \beta)\lambda \quad (13-5)$$

where the subscripts designate individual plies and the coefficients are:

β = bird impact angle, degrees (See Figure 13-5)
 λ = contour coefficient
 λ = 1.0 for transparencies similar to transport aircraft
 windshields
 λ = 0.92 to 1.1 for small flat windshields
 C = 107 for annealed glass

$C = 194$ for semitempered glass
 $C = 268$ for tempered glass
 $C = 275$ for Saint Gobain special tempered glass
 $C = 210$ to 360 for chemically strengthened glass

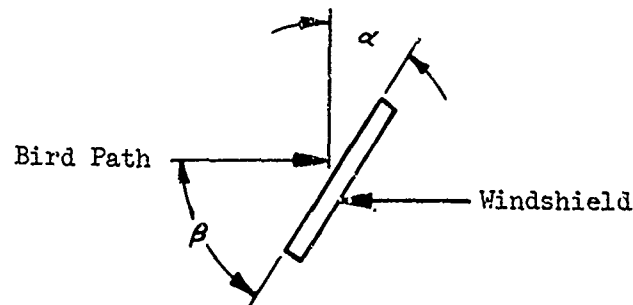


Figure 13-5. Windshield Sweepback Angle.

b. Polyvinyl Butyral Interlayers (20% plasticized)

From Reference 1:

$$t = 0.0498e^{\left(\frac{V}{180}\right)} \quad (13-6)$$

where

Bird weight = 4 pounds
 Windshield slope = 40° - 46°
 Interlayer temperature = 80°F

c. Stretched Acrylic

From Reference 2, for windows with clamped edges:

$$t = \left(\frac{V(\cos \alpha)W^{1/2}}{470} \right)^{3/2} \quad (13-7)$$

and from Reference 3:

$$t = \left((6.5 \times 10^{-6}) v_w^{2/3} (\sin \beta)_\lambda \right)^{1/2} \quad (13-8)$$

where

- λ = a contour coefficient
- λ = 1.0 for transparencies similar to transport aircraft windshields
- λ = 0.5 for transparencies similar to side windshields of fighters
- λ = 0.35 for transparencies similar to wraparound fighter windshields

d. As-Cast Acrylic

From Reference 3 for flat transport aircraft windshields:

$$t = \left((6.53 \times 10^{-6}) v_w^{2/3} (\sin \beta) \right)^{1/2} \quad (13-9)$$

and for curved windshields (radius of curvature = 25 to 35 inches):

$$t = \left((2.25 \times 10^{-6}) v_w^{4/3} (\sin \beta) \right)^{1/2} \quad (13-10)$$

Figures 13-6 and 13-7 compare the predicted penetration velocity versus total ply thickness for a number of the above expressions. Figure 13-6 is for glass materials, and Figure 13-7 is for plastic materials. The curve for polycarbonate is for optically treated material. Penetration velocity for this material is substantially lower than the penetration velocity of as-received polycarbonate as a result of the press-polishing process used to improve the optical quality.

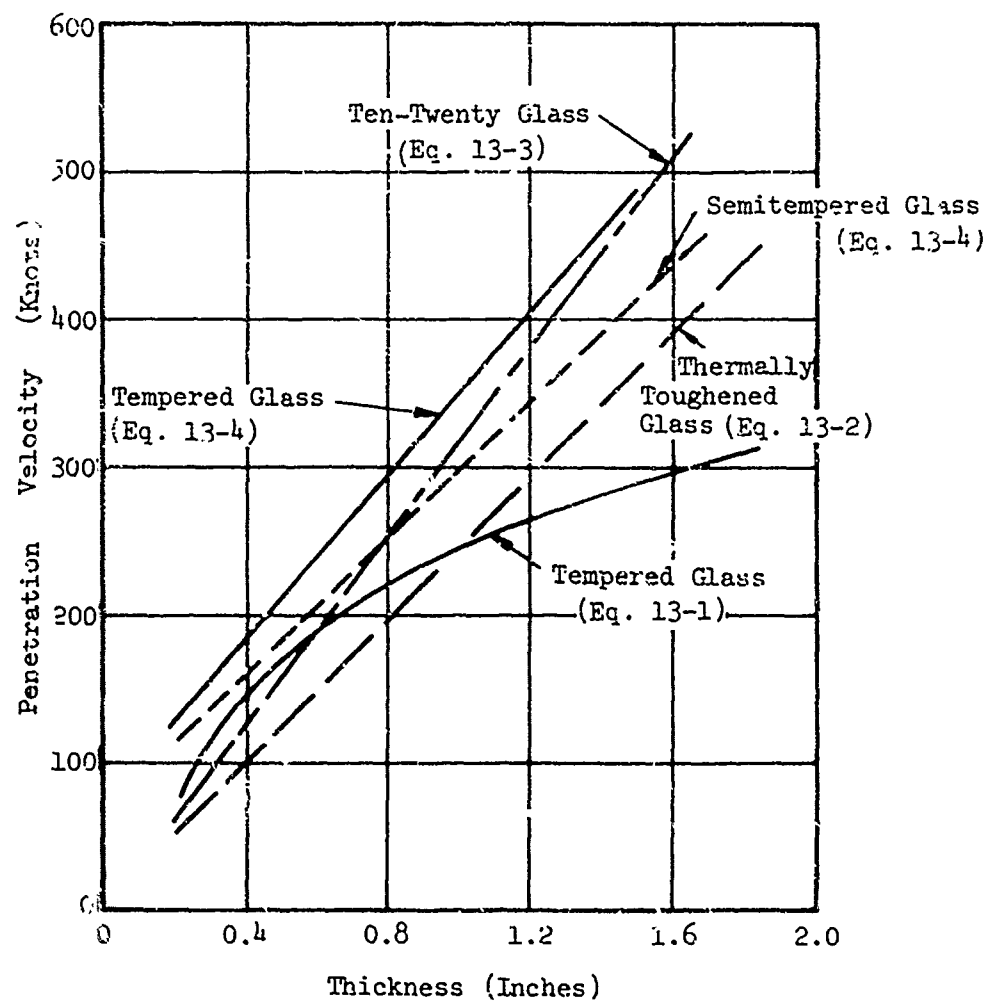


Figure 13-6. Velocities of 4-lb Birds for Penetration of Flat Glass Windshields at 45-Degree Impact Angles.

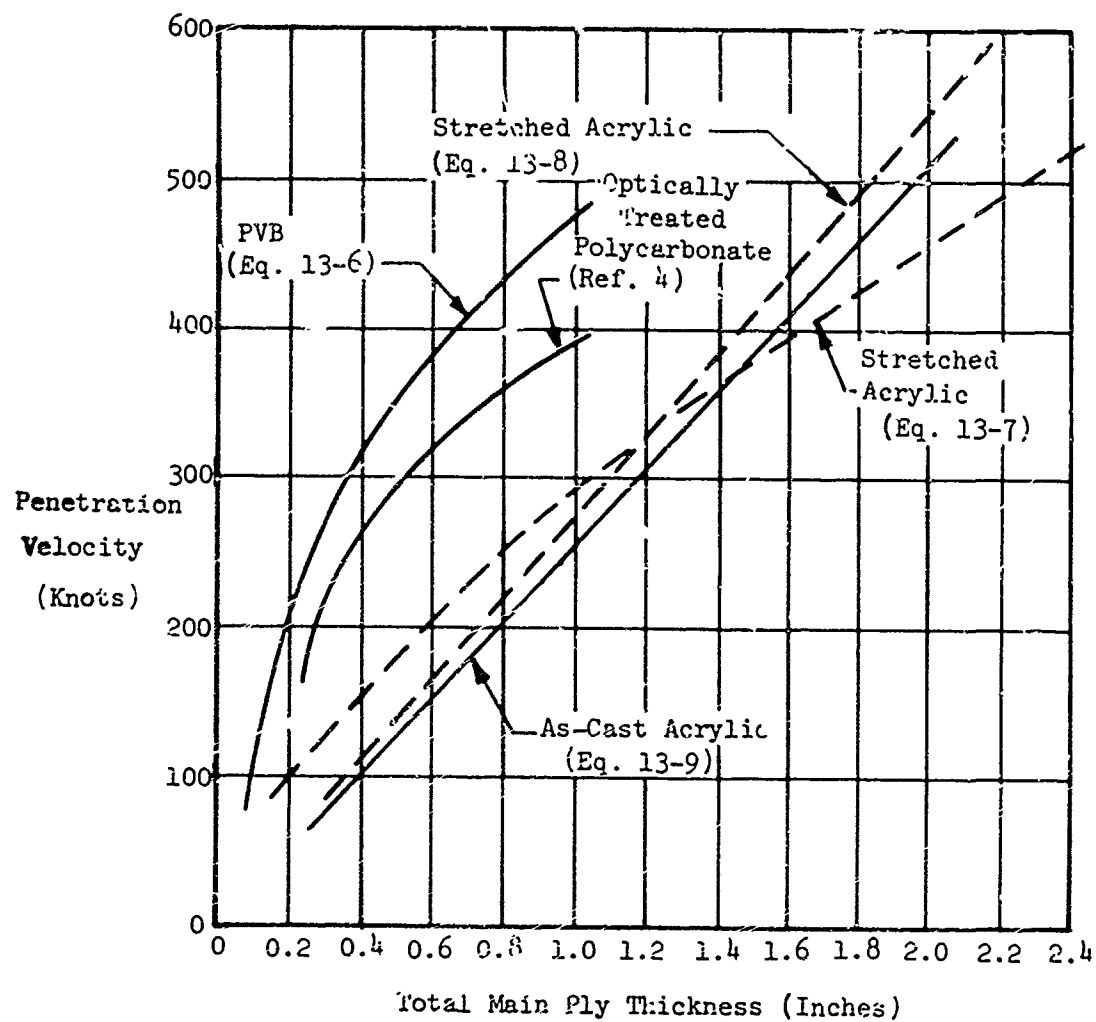


Figure 13-7. Velocities of 4-lb Birds for Penetration of Flat Plastic Windshields at 45-Degree Impact Angles.

The angle used in these calculations, 45 degrees, is within the range of angles used by all the investigators in developing their expressions. It is evident that the theories predict penetration velocities that vary considerably for the same materials, which indicates the need for testing new configurations.

13.3.1 Laminates

The velocities required to penetrate laminates are higher than those for monolithic panels of the same total structural ply thickness. Penetration velocities can be increased up to about 30% by this method.

The penetration velocities for polycarbonate panels with fusion-bonded cast-acrylic faces are approximately the same as those for panels made entirely of cast-acrylic, and fusion bonding is therefore considered inefficient.

Abrasion-resistant hardcoats applied to one or both surfaces of a polycarbonate panel also appear to cause decreases in the penetration velocity, based on limited testing.

13.4 Bird Weight Relationships

Penetration velocities for different bird weights can be related by assuming that the specific kinetic energy level remains constant. Thus, if the penetration velocity is known for a specific bird weight, penetration velocities for other bird weights can be found using this relationship:

$$V = V_k \frac{W_k}{W}^{1/2} \quad (13-11)$$

where V = penetration velocity

W = bird weight

and the subscript k indicates known values.

13.5 Angle of Incidence

Generally, bird penetration velocity decreases as a function of the cosine of the windshield slope. An exception to this rule occurs for flexible materials where impact is at the aft edge of the panel. In such cases, the bird tends to pocket into the transparency as it stretches. Because of the proximity of structural members to the rear, the carcass cannot slide off the sloped panel. Under such circumstances, the penetration velocity is to a large degree independent of the windshield angle.

13.6 Temperature

Material temperature significantly affects the penetration velocity of plastic glazings. The penetration velocity is usually maximum near room temperature and lower at both higher and lower temperatures. This effect is most severe for polyvinyl butyral (PVB) interlayers, as shown in Figure 13-8.

Windshields incorporating PVB as a birdproofing medium require heating systems to maintain the vinyl's temperature during operation in cold environments.

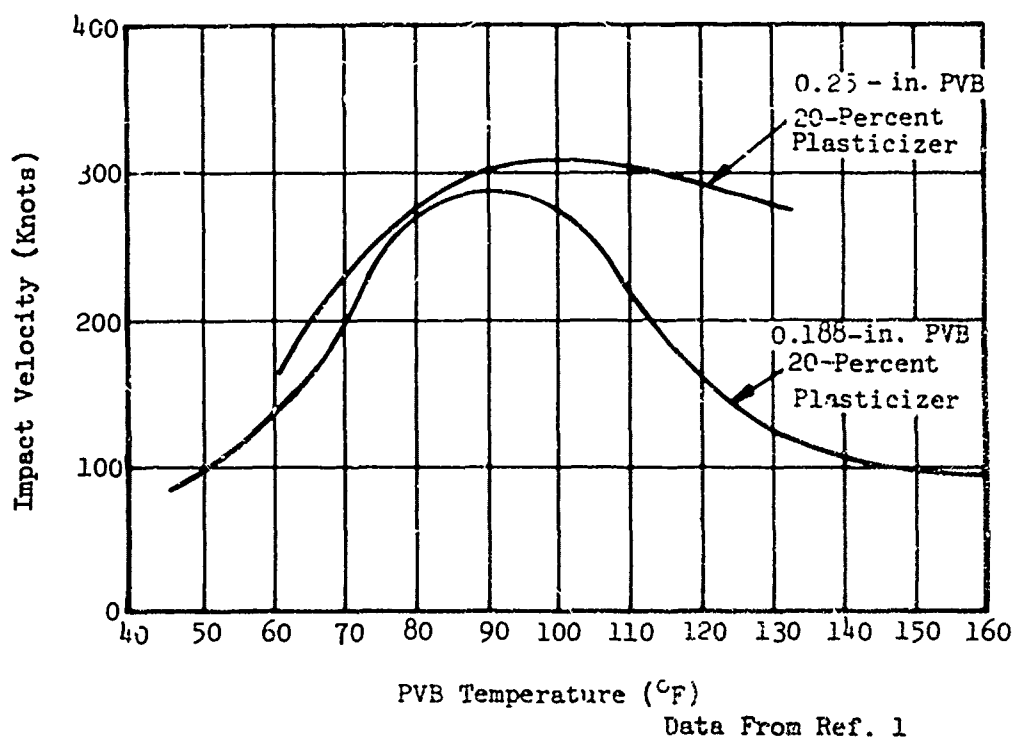


Figure 13-8. Effect of PVB Temperature on Penetration Velocity.

13.7 Panel Size and Curvature

Penetration velocity is in general independent of panel size or plan-form shape. The exception is for very small panels which are too small to permit energy absorption via stretching, or for which edge effects predominate.

Curved transparencies are ordinarily stiffer than equivalent flat transparencies. This added stiffness restricts the ability of the panel to assume membrane shapes and therefore has a deleterious effect on the bird impact resistance of the thin windshields typically used on helicopters. However, for thicker panels such as armor windows or pressurized airplane windows, where bird-strike resistance is accomplished by bending, the reverse is true; curvature is beneficial.

13.8 Impact Location

The location of the impact point can have a considerable effect on the penetration velocity of a windshield. Central areas generally require higher penetration velocities than border areas. Edge impacts cause high localized loads, leading to shearing and tension failures. Edge members can cause local pocketing of the bird carcass and prevent it from sliding off the panel, which results in higher impact forces.

13.9 Edge Attachments

In general, test results have shown that the edge attachment of bolted-in panels constitutes the most critical part of the installation with regard to impact strength; the method of transmitting tensile and shear stresses from the panel into the airframe is of primary importance.

Laminated panels that rely on interlayer stretching for birdproofing require inserts imbedded within the interlayer to transmit edge loads. For PVB interlayers, 2024 aluminum inserts need not be greater than $1/6$ of the interlayer thickness for interlayers that are less than 0.188 inch thick, and not greater than $1/5$ of the interlayer thickness for interlayers that are greater than 0.250 inch thick. With regard to the width of the insert strip, it has been found that satisfactory results are obtained if the insert extends at least 0.25 inch between the two facings, as shown in Figure 13-9. If the strip does not extend between both faces in this manner the plastic interlayer is very likely to shear along the inside edge of the strip.

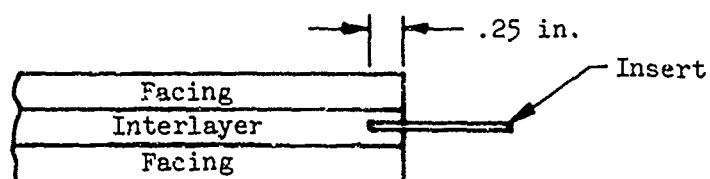


Figure 13-5. Edge Insert for Laminated Windshields.

Particular care must be exercised in designing edge reinforcement for stretched acrylic and polycarbonate materials to avoid abrupt changes in cross section. Otherwise, the resultant stress concentrations can substantially reduce impact resistance.

It is generally agreed that clamped edges provide higher penetration velocities than bolted edges because they allow more panel movement and reduce stress concentrations at the edges. However, when bolted attachments are used, closely spaced small bolts provide more uniform support than widely spaced large bolts. In Reference 1 it was found that bolt size and distance between fasteners should provide strength equivalent to a 2-inch spacing of No. 10 steel bolts (100,000 psi heat treat) for a 0.125-inch PVB interlayer thickness and a 1-inch spacing of identical bolts for a 0.25-inch interlayer thickness.

13.10 Bird Impact Forces

Bird impact forces are dependent on the elastic and inelastic effects of the impacting body and wave propagation response of the windshield and structure. For this reason, static analyses that assume no structural deformation are extremely conservative and yield results that can only be approached, but never reached. Equation 13-12 from Reference 5 is typical of relationships that do not account for structural deformation.

$$F = .705 W^{2/3} (V^2) \quad (13-12)$$

where F = peak impact force, assuming sinusoidal variations (pounds)

W = bird weight (pounds)

V = velocity (knots)

13.11 Structural Stiffness

The general rigidity and energy absorbing characteristics of the windshield supporting structure have considerable effects on the strength exhibited by the windshield panel. A structure that is highly elastic apparently causes lower forces to develop in the panel with less tendency for panel failure. Uniformity of structural rigidity around the panel also appears advantageous.

Heavy reinforcement of a cockpit structure is not necessary for bird collision resistance except in very light structures. The determination of whether or not special reinforcements are required is made in conjunction with bird impact development tests.

13.12 Openable Hatches

Openable hatches and clearview panels forward of the flight crew have considerably more rearward slope than windshields, and birdproofing requirements are somewhat lessened. However, when impacted, fluid substances from the bird carcass tend to force their way into the opening between the frame and window, creating tremendous hydraulic pressure. This action can disengage or fail retaining latches and hinges, allowing the window to be ejected into the cockpit with considerable force. The window may become a flying missile. This phenomenon highlights the fact that the clearview window requires special attention in the design of secure closure devices.

13.13 Bird Impact Testing

The preceding sections of this chapter have described the many variables that influence bird impact resistance. It was shown that analysis, at best, can only approximate the response of transparent enclosures to bird impact. For example, comparison of data from tests conducted on flat polycarbonate panels and data from tests conducted on actual UH-1 helicopter installations using the same material show the penetration velocity of the installation to be lower by about 30 knots. Other aircraft installations have demonstrated improved performances when compared to specimen tests. Therefore, it becomes apparent that the only method to substantiate bird-strike integrity is by testing actual installations.

There are several government and private test facilities in the United States and Canada equipped to perform bird impact tests. Most of these facilities use a setup similar to that shown in Figure 13-10. The principal features are a compressed air source and storage tank, a quick-opening valve and breech section for loading, a large smooth-bore barrel, and timing gates. The birds are usually freshly killed chickens which are launched in special sabots to fit within the cannon. A sabot stripper removes the sabot prior to impact. High-speed photography is often used to analyze and record the mechanics of failures when they occur and to aid in the evaluation of fragmentation.

Tests should be conducted on representative, full-size structures to verify the following:

1. Spall shall not cause injury to the flight crew.
2. Visibility shall not be reduced more than 50%.
3. Structural damage shall not be cause for aborting the mission.
4. Solid portions of the bird shall not enter the cockpit and cause injury to the crew or prevent them from performing their normal duty.
5. Jettisonable hatches and latching mechanisms shall not be damaged to the extent that crew escape is restricted.

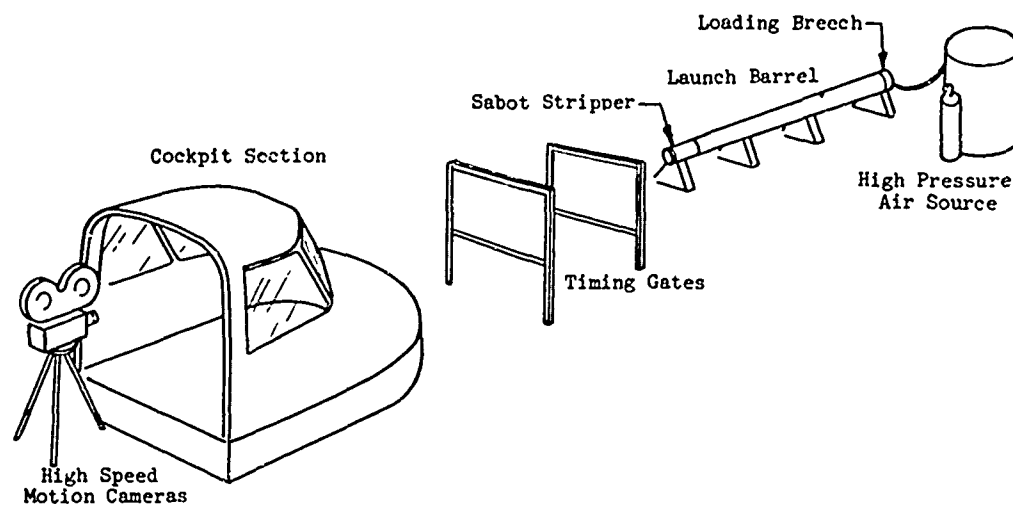


Figure 13-10. Bird Impact Test Facility.

The number of tests to be performed is determined by the specific aircraft installation. As a minimum, the following tests are necessary unless otherwise substantiated by similarity and analysis:

1. Each transparency located in the front of the helicopter or those transparencies located where critical fragmentation would injure the flight crew shall be tested.
2. The transparencies shall be tested under the most extreme temperature conditions likely to occur in operation.
3. Impacts shall be at points of maximum deflection and greatest stiffness - usually the center and edge of the panel.
4. Each transparency support member shall be tested at its center and at its intersections with adjacent structure.
5. Openable hatches with edges ahead of the pilot shall be tested.

References

1. Kengas, P., and Pigman, G., "Development of Aircraft Windshields to Resist Impact with Birds in Flight, Part II," Technical Development Report No. 74, Civil Aeronautics Administration, Indianapolis, Ind., Feb. 1950.
2. Mott, M. N., Hawker Siddeley Aviation, Ltd., "Experimental Investigation into the Bird Impact Resistance of Flat Windscreen Panels with Clamped Edges," AFML-TR-73-126, Air Force Materials Laboratory, Wright-Patterson Air Force Base, Ohio, June 1973.
3. Poullain, G., Clamagirand, Avions Marcel Dassault, "Windscreen to Resist Bird Strikes," A72-27014, Society of British Aircraft Companies, London England, June 1971.
4. Ingelese, A. O., et al, Goodyear Aerospace Corp., "Bird Strike Capabilities of Transparent Aircraft Windshield Materials," AFML-TR-74-234, Air Force Materials Laboratory, Wright-Patterson Air Force Base, Ohio, Dec. 1974.
5. Lawrence, J. H., Douglas Aircraft Co., "Windshield Bird Strike Structure Design Criteria," AFFDL-TR-73-103, Air Force Flight Dynamics Laboratory, Wright-Patterson Air Force Base, Ohio, Oct. 1973.

Bibliography

McDonald, W. C., Goodyear Aerospace Corp., "UH-1 Ballistic and Bird Impact Study," AMMRC-CTR-75-7, Army Materials and Mechanics Research Center, Watertown, Mass., Apr. 1975.

Somers, J., Federal Aviation Agency, "Certification Requirements for the Windshields of Civil Transport Aircraft," WADC-TR-65-212, Air Force Materials Laboratory, Wright-Patterson Air Force Base, Ohio, Sept. 1965.

Somers, J., "A Study of the Bird Impact Resistance of Windshields for High Performance Transport Aircraft," ADS-8, Federal Aviation Agency, Washington D. C., Mar. 1964.

Cook, L.M., et al, PPG Industries, "Development of Design, Test, and Acceptance Criteria for Army Helicopter Transparent Enclosures," USAAMRDL-TR-73-65, U. S. Army Mobility Research and Development Laboratory, Fort Eustis, Va., Sept. 1973, AD 772936.

Hassard, R. S., Goodyear Aerospace Corp., "Plastics for Aerospace Vehicles, Part II Transparent Glazing Materials," MIL-HDBK-17A, Part II (Proposed Revision), Air Force Materials Laboratory, Wright-Patterson Air Force Base, Ohio, Jan. 1973.

"Sikorsky RSRA Helicopter Program, Bird Shooting at National Research Council," PPG Industries, Huntsville, Ala., Aug. 1974.

Noonan, J. W., "Progress in Bird Impact Test Program for Windshields of Small Light Aircraft," ST-178, National Aeronautical Establishment, Ottawa, Canada, Dec. 1973.

Kengas, P., and Pigman, G. L., "Development of Aircraft Windshields to Resist Impact with Birds in Flight, Part III," Civil Aeronautics Administration, Indianapolis, Ind., Mar. 1950.

Sanders, E. J., ARO Inc., "The AEDC Bird Impact Test Facility," AFML-TR-73-126, Air Force Materials Laboratory, Wright-Patterson Air Force Base, Ohio, June 1973.

Peterson, R. L., and Barber, J. P., "Bird Impact Forces in Aircraft Windshield Design," AFFDL-TR-75-150, Air Force Flight Dynamics Laboratory, Wright-Patterson Air Force Base, Ohio, Mar. 1975.

Jansen, W. R., "Analysis of Shock-Absorbing Concepts for Birdproof Windshields of Advanced Air Force Vehicles," AFFDL-TR-74-155, Air Force Flight Dynamics Laboratory, Wright-Patterson Air Force Base, Ohio, Feb. 1976.

Barber, J. P., Wilbeck, J. S., University of Dayton, "Characterization of Bird Impacts on a Rigid Plate: Part I," AFFDL-TR-75-5, Air Force Flight Dynamics Laboratory, Wright-Patterson Air Force Base, Ohio, Jan. 1975.

Halpin, J. C., Griffin, J., Aeronautical Systems Div., "An Analytical Methodology for Defining the Bird Strike Requirements for Aircraft Crew Enclosures," Conference on Aerospace Transparent Materials and Enclosures, Long Beach, Calif., Apr. 1978.

Roberts, W. G., Triplex Safety Glass Co., Ltd., "Development and Application of Thin High Strength Glass," Conference on Aerospace Transparent Materials and Enclosures, Long Beach, Calif., Apr. 1978.

Historically, helicopters have rarely been struck by lightning, having only recently become truly all-weather vehicles. In the past few years, at least one fatal accident and a number of incidents have focused attention on the need to upgrade the lightning protection of helicopters. Complete protection of an aerial vehicle against lightning must ensure that there is no serious structural damage, no fuel system explosion, no electrical system failure, and of course, no shock hazard for the crew.

The requirements for lightning protection of helicopter transparencies must be seen in the context of the overall crew compartment design. The ideal form of lightning protection consists of a complete, continuous, conductive shell of such low resistance that lightning currents flowing from end to end do not produce dangerously high voltages. A cockpit enclosure having metal frames, metal skin, and transparencies with a highly conductive external coating would be the best approximation to the ideal. A coating grounded to the airframe would also avoid any problems with static electricity while assisting in the reduction of radar cross-section. Unfortunately, no coating material is available as yet that has sufficiently low resistance, adequate light transmission, and durability. The resistivity of the coating would probably need to be less than one ohm per square. See Chapter 19 for definition of resistivity terms.

However, adequate lightning protection can usually be obtained by other, practical means. If the pilots are surrounded by a cage of closely spaced conductors, they will be protected not only from direct lightning strikes but also from any serious shock hazard due to so-called "streamering". The cage structure can be formed by the cockpit main frames and the perimeter frames of the transparencies or doors, if they are metal and grounded to the airframe. There is no definitive theoretical criterion to determine the adequacy of protection of a cage-type structure, so that the best means of evaluating a design is by tests on a mockup cockpit, or a scale model, in a suitably equipped high voltage laboratory. As a preliminary design guide, the following has been developed from the requirements of MIL-B-5087, which were stated for the type of canopy used on jet fighter aircraft.

"The lightning protection afforded by a cage system will be adequate if the crew cannot be touched through the spaces between the conductive members of the apex of a cone of 120° included angle." The application of this guide to a cockpit design is illustrated in Figure 14-1, but it should be extended to cover any movements the crew may perform during operation of the helicopter. In the example shown, the pilot's helmet can be touched by the cone, and therefore, he may be vulnerable to streaming induced by a high voltage electric field. Protection should be provided by relocating metal frames to the locations Marked A or by a grounded metal strip running fore and aft over his head. The strip can

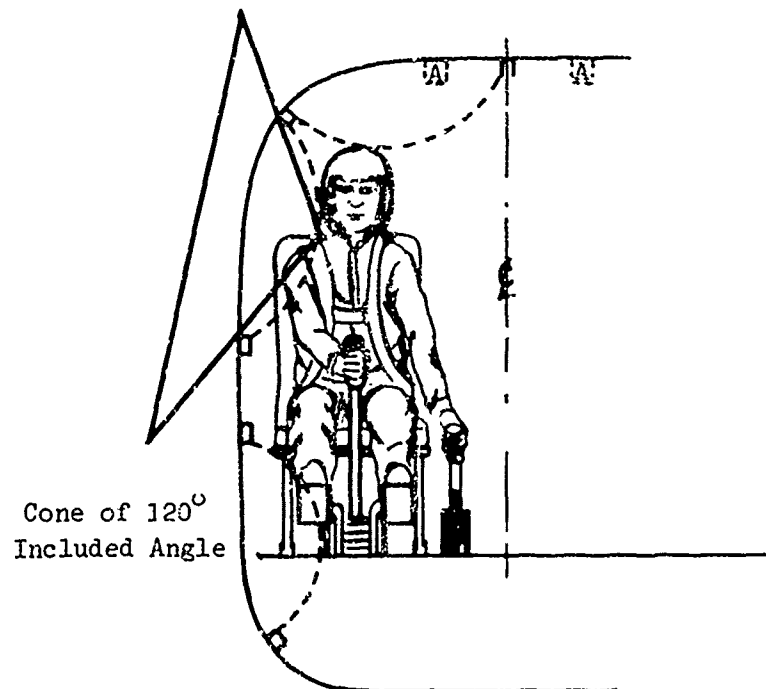
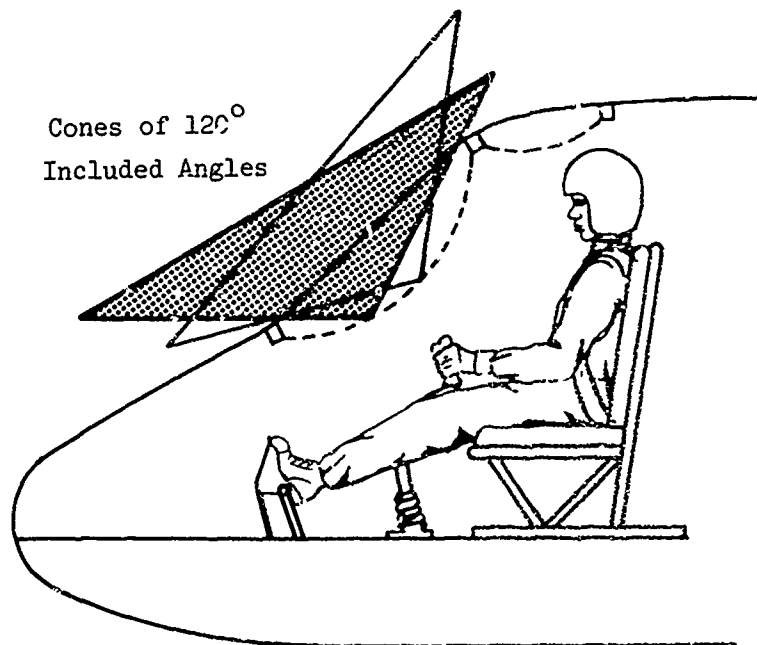


Figure 14-1. Crew Protection by Cockpit Frames.

be inside or outside of the transparency and can be narrow enough to avoid any significant interference with vision. Reference 1 requires that the cross-sectional area of an external conductor be at least 33,100 circular mils if made of aluminum or 20,820 mils if made of copper. The corresponding figures for internal conductors are 10,380 mils and 6,530 mils.

Shock hazard to the crew can also be introduced if any ungrounded conductor is mounted in a transparency (or a nonconducting skin area) in such a way that it can lead a lightning strike or streamer into the enclosure. A common example is the outside air temperature gauge (OAT). Figure 14-2 shows a typical OAT gauge mounting and how a streamer can be induced by a pilot's hand as he reaches to operate an overhead control. Grounding the gauge to the airframe will eliminate this hazard.

Damage to a windshield or to the aircraft's electrical system can occur if a streamer occurs between the conductive heating elements. Spike transients induced in the electric power system can damage semiconductor equipment and lead to equipment malfunctions, or even loss of the main generating system.

In the absence of a suitable conductive coating material, protection is best achieved by requiring that the flashover voltage from any point on the windshield to ground shall be lower than the breakdown voltage from the surface to the internal conducting elements. This protection against the penetration of the insulating layers should be verified by tests using a high voltage electrode at several positions near the outer surface. Suitable test methods are described in Reference 2.

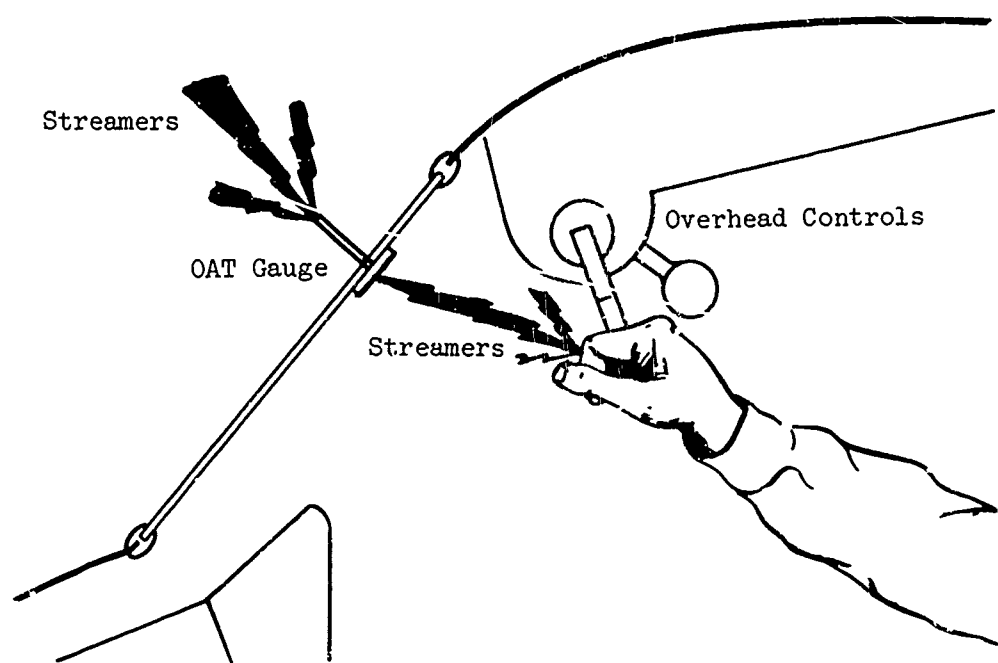


Figure 14-2. Shock Hazard due to Ungrounded Outside Air Temperature Gauge.

References

1. MIL-B-5087, "Bonding, Electrical, and Lightning Protection for Aerospace Systems."
2. Aston, R., Gorton, R., and Weinstock, G. L., McDonnell Aircraft Company, "Lightning Protection Techniques for Large Canopies on High Speed Aircraft," Technical Report AFAL-TR-49, Published by Air Force Systems Command, Jan. 1972.

Bibliography

James, H. C., et al, Goodyear Aerospace Corp., "Design, Test, and Acceptance Criteria for Army Helicopter Transparent Enclosures," USAAMRDL-TR-73-19, U. S. Army Air Mobility Research and Development Laboratory, Fort Eustis, Va., May 1973, AD 767242.

Bartman, H. M., and Chopin, M. H., Air Force Avionics Laboratory, "Design of the Helicopter for the Lightning Environment," Report No. SW 70-11, Published by American Helicopter Society, Nov. 1970.

Lawrence, J. H., Douglas Aircraft Co., "Windshield Technology Demonstrator Program," AFFDL-TR-77-1, Air Force Flight Dynamics Laboratory, Wright-Patterson Air Force Base, Ohio, Sept. 1977.

Twomey, R. C., Douglas Aircraft Co., "Effects of Laboratory Simulated Precipitation Static Electricity and Swept Stroke Lightning on Aircraft Windshield Subsystems," AFFDL-TR-76-75, Air Force Flight Dynamics Laboratory, Wright-Patterson Air Force Base, Ohio, July 1976.

Twomey, R. C., Douglas Aircraft Co., "Precipitation Static Electricity and Swept-Stroke Lightning Effects on Aircraft Transparency Coatings," Air Force Flight Dynamics Laboratory Wright-Patterson Air Force Base, Ohio, Dec. 1977.

Electrically insulated sections of an aircraft that are subjected to impingement of airflow carrying dust or precipitation particles acquire static surface charges that can result in very high voltages. If the rate of accumulation of charge is high enough and the dissipation due to conduction over the surface and through the air is low enough, the voltage will reach a level where insulation breakdown or surface flash-over can occur.

Surface flashovers resulting from static electrification of a transparency can cause impairment of the crew's vision during night operations, radio frequency interference due to high frequency components of the arcing, and damage to solid-state control components in an electrical heating system due to induced spike transients. Insulation breakdown and punctures of the outer layer of a windshield can shatter the glass or lead to delamination.

The above problems have been known to occur on fixed-wing aircraft for many years because high-speed flight tends to produce high charging rates. Static electricity is not usually considered a problem for helicopter windshields because of the lower air velocities involved. However, unexplained malfunctions of temperature controllers occur that suggest the possibility of static-related damage modes. This damage may occur when a helicopter hovers over a dry, dusty area; in such conditions, radio frequency interference (RFI) generated by corona discharge from the helicopter's extremities and by spark discharges from other parts could mask any noise contribution that may originate on transparencies.

It is interesting to note that one of the methods employed to check static electrification effects on airplane windshields is to blow dust-laden air onto the surface. It is therefore considered possible that damage can occur to heated windshields on helicopters as a result of static electricity.

Protection can be provided against dielectric puncture if the surface flashover voltage from any point on the outer surface is lower than the breakdown voltage to internal conducting parts, such as heating layers or embedded temperature sensors. This criterion is more stringent if an embedded-wire heating element is used, because the fine wires cause local concentrations of electrical charge, and thicker insulating layers are then required to prevent insulation breakdown.

A transparency with a glass outer surface can be treated with indium oxide, stannous oxide or some other proprietary material to give a surface resistivity below 1 megohm per square - low enough to alleviate any problems due to electrification. The oxides are fused into the surface of the glass so the coating is fairly resistant to degradation by erosion and abrasion. There is no known coating material for plastic surfaces that can withstand the abrasion and erosion effects of

windshield wipers, cleaning, and weather. In such cases, the criterion stated above of requiring the surface flashover voltage to be lower than the dielectric breakdown level should be applied, and the temperature control circuits should be protected from transients induced by the discharges by means of spike/surge suppressors.

Fixed-wing aircraft operators have reported that ground maintenance personnel have received serious shocks because of the static charges stored on windshield surfaces. The oxide coatings for glass surfaces will remove this hazard if the coating has a discharge path to the airframe. The charge can be removed from plastic surfaces by flushing with water, or proprietary antistatic compounds can be applied. Antistatic coatings must be reapplied frequently to maintain their effectiveness.

Coatings for the surface that are required for static charge dissipation (1 kilohm to 1 megohm per square) have a negligible effect on the light transmission of a transparency, and will assist in preventing insulation breakdown due to streamers in the high electric fields of a thunderstorm. (See Chapter 19 for definitions of resistivity.)

Bibliography

James, H. C., et al, Goodyear Aerospace Corp., "Design Test, and Acceptance Criteria for Army Helicopter Transparent Enclosures" USAAMRDL-TR-73-19, U. S. Army Air Mobility Research and Development Laboratory, Fort Eustis, Va., May 1973, AD 767242.

Sharp, P. J., Lucas Aerospace Ltd., "Transparencies for European Aerospace, The Problems and Future Trends," AFML-TR-73-126, Air Force Materials Laboratory, Wright-Patterson Air Force Base, Ohio, June 1973.

Twomey, R. C., Douglas Aircraft Co., "Effects of Laboratory Simulated Precipitation Static Electricity and Swept Stroke Lightning on Aircraft Windshield Subsystems," AFFDL-TR-76-75, Air Force Flight Dynamics Laboratory, Wright-Patterson Air Force, Ohio, July 1976.

Christine, P., Boeing Military Airplane Div., "Windshield Design for Military Aircraft, Conference on Aerospace Transparent Materials and Enclosures, Long Beach, Calif, Apr. 1978.

Lawrence, J. H., Douglas Aircraft Co. "Windshield Technology Demonstrator Program," AFFDL-TR-77-1, Air Force Flight Dynamics Laboratory, Wright-Patterson Air Force Base, Ohio, Sept 1977.

Twomey, R. C. Douglas Aircraft Co., "Precipitation Static Electricity and Swept Stroke Lightning Effects on Aircraft Transparency Coatings," Air Force Flight Dynamics Laboratory, Wright-Patterson Air Force Base, Ohio, Dec. 1977.

This section contains descriptions and physical properties of the common transparent materials used for glazing helicopters. Only the properties that are important to design are covered. A more comprehensive tabulation of transparent material properties can be found in Part II of MIL-HDBK-17A, "Plastics for Aerospace Vehicles, Part II, Transparent Glazing Materials."

Helicopter transparencies may be either monolithic or laminated. Monolithic designs are generally thermoformed plastic materials. Laminated designs consist of plastic or glass sheets joined by transparent adhesives or interlayers. Materials suitable for laminated or monolithic construction are described in this section.

Physical and mechanical properties for transparent materials have been extracted from available literature, and the data has not been substantiated to the same extent as the familiar aircraft metallic elements. As a result, transparent material properties presented here can only be considered typical values unless controlled by specification.

Most transparent materials are extremely sensitive to changes in ambient temperature and ultraviolet radiation. These factors must be considered during design, and standard condition properties must be adjusted accordingly. Past experience and rigorous qualification testing are as important in transparency engineering as strictly analytical verifications.

16.1 Proprietary Products

Many transparent materials are available only as proprietary products and are not covered by Government specification. This is particularly true of interlayer materials. In the following material descriptions, proprietary items are noted as they exist commercially. The determination of their properties and their availability or suitability for an intended application should be made by contacting the suppliers.

The mention of any trade name or proprietary product in this handbook does not constitute an endorsement, nor does it imply that it is the only product available possessing the prescribed characteristics.

16.2 Acrylic Plastic

Acrylic plastic is an unplasticized, ultraviolet-absorbing polymethyl methacrylate available in several formulations for helicopter applications. The material is produced as thermoplastic sheet and is optically clear in its natural form. To date this is the most common material used for helicopter glazing. Physical properties of acrylics are temperature dependent and are also subject to change by other environmental conditions.

16.2.1 Heat-Resistant Cast Acrylic Sheet, MIL-P-5425

This material, also known commercially as Plexiglas II HVA, Trademark Rohm & Haas Co., Philadelphia, Pa., is noted for excellent thermoformability and machinability though it has largely been superseded by MIL-P-8184, Modified Acrylic Sheet, and MIL-P-25690, Stretched Modified Acrylic Sheet. MIL-P-5425 acrylic can be procured in a variety of tints and hues for special applications.

16.2.2 Modified Acrylic Sheet, MIL-P-8184

This cast-acrylic sheet, also known as Plexiglas 55, Trademark Rohm & Haas Co., Philadelphia, Pa., has slightly higher heat resistance and better craze and solvent resistance than the MIL-P-5425. The cast acrylics are not suited for installations using bolted or riveted attachments.

16.2.3 Stretched Modified Acrylic Sheet, MIL-P-25690

Stretched acrylic plastic is produced by reorienting the long polymer chains that make up MIL-P-8184 to significantly improve resistance to crack propagation and stress-solvent crazing. In fact, stress-solvent crazing for stretched acrylics is virtually nonexistent. Elongation to failure is also drastically increased, from 4% for the as-cast acrylic to 16% after stretching, which results in an approximate threefold increase in impact strength.

The stretching operation is conducted by heating slabs of MIL-P-8184 to approximately 300°F and then pulling uniformly on all edges until it has become 65 to 70% longer and its thickness has been reduced to approximately 1/3 of its original value. The sheet is then ground and polished to impart the necessary optical quality and thickness control. As a result of this processing, stretched acrylic is more expensive to manufacture than the cast variety.

The stretching process also degrades some properties of the basic cast acrylic. If stretched acrylic is heated above 220°F, it begins to revert to its as-cast dimensions. This limits the temperatures at which it may be formed, and special forming methods must be used to contour parts. Shear strength parallel to the surface is also lower for stretched acrylic than for cast acrylic.

16.3 Polycarbonate Sheet, MIL-P-83310

Polycarbonate is a relatively new material, which is finding applications in aircraft transparent enclosures. Polycarbonates for aircraft use are produced under the trade name of Lexan SL-2000-111, by the General Electric Company. However, this material requires postprocessing in order to meet the optical requirements of MIL-P-83310.

The most outstanding advantage of polycarbonate is its exceptional toughness and impact resistance. Ballistic damage tolerance is also considered excellent, and the material can be used to advantage in transparent armor and spall-shield applications.

Polycarbonate has very poor resistance to chemical attack and is susceptible to stress-solvent crazing. Common alcohols and aliphatics routinely employed in aircraft operation and maintenance can cause severe degradation. Polycarbonate also has very poor abrasion resistance. Protective hardcoatings are frequently employed to improve these deficiencies.

Polycarbonate in its natural form has a slight yellow straw-colored tint, and frequently blue colorants are added to the resin to neutralize the color.

16.4 Glass, Monolithic, Aircraft-Glazing, MIL-G-25667

Glass is an extremely hard, durable, transparent material. Glass is approximately 20 times stiffer than transparent plastic materials and completely obeys Hooke's Law, exhibiting no yielding up to its point of failure, and is therefore categorized as a brittle material. Because of this lack of ductility, glass must be laminated when used in transparent enclosures to avoid catastrophic failure.

Although there are literally thousands of glass formulations possible, the materials generally used on helicopters are Type I commercial soda-lime float or polished plate glass, MIL-G-25667, and Type V chemically strengthened glass, MIL-G-25667.

In the plate process, a heated viscous glass is fed from a melting tank into alehr containing water-cooled rollers to form a continuous ribbon of glass sheet. This sheet is then fed between twin grinders to impart the necessary flatness and surface finish.

In the float glass process, melted glass is fed onto a bed of molten tin. Because the tin is kept in a liquid state and is denser than glass, the floating sheet formed on the surface will be limited in flatness and parallelism only by the curvature of the earth and surface tension forces at the edge of the bath. Plate glass is initially weaker than float glass since the mechanical grinding process does not produce as smooth a surface finish as the "fire-polished" float process. However, the strength difference, due to microscopic surface cracks in the plate glass, is minimized after either glass has received normal service wear.

16.4.1 Glass Tempering

Annealed glass has an intrinsic tensile strength of approximately 6000 psi that may be increased to over 50,000 psi by tempering. The tempering may be accomplished by either thermal or chemical means. In the thermal tempering process, the glass is heated to a temperature close to its softening point and then cooled rapidly by a cooling air blast. The sudden cooling of the glass product at high temperature introduces a temperature gradient between the surface and the core that is practically without mechanical stress, since the glass is soft enough to yield. The glass is then cooled down, bringing the surface to room temperature while the core remains hot. As the core continues to cool, the glass becomes rigid and cannot yield, and stress is induced so that the core is in tension and the outer surface is in compression. The resulting parabolic stress distribution through the cross section is illustrated in Figure 16-1.

Chemical tempering produces a similar stress distribution, as illustrated in Figure 16-2, but by a completely different mechanism. In this process, annealed flat or formed glass is immersed in a molten alkali-nitrate-salt bath for a specified time. During this period, small alkali ions near the surface of the glass are replaced by larger alkali ions from the salt bath. The resultant crowding of the larger ions at the surface induces compressive stress that must be held in equilibrium by tension in the central region.

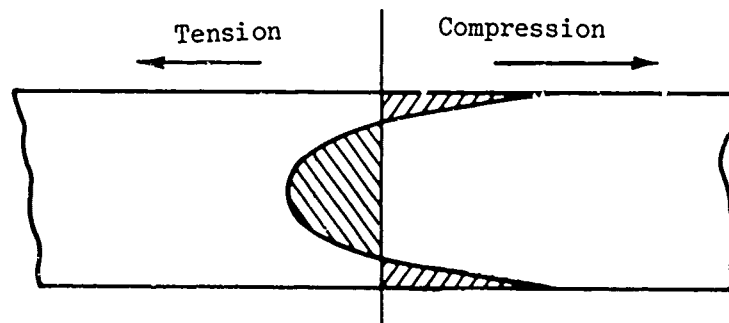


Figure 16-1. Thermal Tempered Glass Residual Stress Distribution.

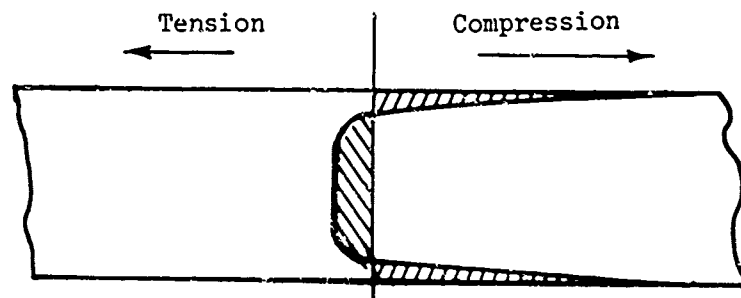


Figure 16-2. Chemical Tempered Glass Residual Stress Distribution.

Several unique characteristics depend on this stress distribution. Glass always fails in tension, never in compression or shear. For structural failure to occur in glass, the applied stress must exceed both the annealed glass strength plus the residual surface compressive stress. The compressive surface stress or case can range in depth from 10% to 20% of the material thickness. This depth is reduced when the glass is loaded in flexure.

Since most of the strength of tempered glass is in the thin region of compression, any scratches or surface cracks, however shallow, can have deleterious effects on the material strength. It is inevitable that surface flaws will occur in service or during handling, and it is for this reason that abraded or reduced-strength properties are customarily used for the design of glass components.

Once tempered, glass will shatter if cut, trimmed, drilled, or otherwise altered. This phenomenon occurs when the surface compressive layer is penetrated, thus disturbing the equilibrium of the internal stresses. The level and control of the tempering process are also determining factors in fracture or dicing patterns. Generally, the higher the temper, the smaller the size of the glass particles.

16.5 Thermosetting Polyester, MIL-P-8257

The abrasion resistance of this polyester material is superior to that of acrylic or polycarbonate. However, notch sensitivity, poor impact properties, and low strength have relegated the material to non-structural applications such as outer facings on laminated windshields.

16.6 Standard Gauges

Standard gauges and thickness tolerances for the common transparent materials are presented in Tables 16-1 through 16-4. Actual availability of these sizes is subject to commercial conditions, and suppliers should be contacted early, during the design stage, for confirmation of availability.

16.7 Physical Properties

A summary of the physical properties of the common transparent materials is presented in Tables 16-5 and 16-6. Separate tables are used to present glass and plastic properties because the characteristics of these materials are sufficiently different to render certain properties unique to each class of materials. In general, the values listed are short-term, room-temperature properties. Many of these properties are dependent upon the environment, the duration of loading, and the test method. Some of the factors that could influence singular value properties are discussed in the subsequent section on mechanical properties of transparent glazing materials.

TABLE 16-1. STANDARD THICKNESSES AND TOLERANCES OF
CAST ACRYLIC SHEET (MIL-P-8184 and MIL-P-5425)

Nominal Thickness (in.)	Tolerance (in.)		
	Sheets up to and including 36 by 60 and 40 by 50 in.	Sheets larger than 36 by 60 or 40 by 50 to and includ- ing 53 by 80 and 60 by 72 in.	Sheets larger than 53 by 80 and 60 by 72 to and includ- ing 72 by 90 and 67 by 102 in.
.060	$\pm .012$	--	--
.080	$\pm .012$	$\pm .020$	--
.100	$\pm .012$	$\pm .020$	--
.125	$\pm .015$	$\pm .020$	$\pm .030$
.150	$\pm .017$	$\pm .020$	$\pm .030$
.187	$\pm .020$	$\pm .023$	$\pm .030$
.220	$\pm .023$	$\pm .025$	$\pm .030$
.250	$\pm .025$	$\pm .030$	$\pm .035$
.312	$\pm .030$	$\pm .035$	$\pm .040$
.375	$\pm .035$	$\pm .040$	$\pm .045$
.417	$\pm .040$	$\pm .045$	$\pm .045$
.500	$\pm .040$	$\pm .045$	$\pm .050$
.625	$\pm .050$	$\pm .050$	$\pm .060$
.750	$\pm .050$	$\pm .050$	$\pm .065$
.875	$\pm .050$	$\pm .050$	$\pm .070$
1.000	$\pm .050$	$\pm .050$	$\pm .075$

MIL-P-25690 stretched acrylic is obtained by biaxially stretching MIL-P-8184 acrylic. The actual thickness of the stretched sheet shall be the nominal thickness $\pm 10\%$ for thicknesses of .250 inch and above, and $\pm .020$ inch tolerance for all thicknesses of .250 inch.

TABLE 16-2. STANDARD THICKNESSES
AND TOLERANCES OF MIL-P-8257
THERMOSETTING PLASTIC SHEET

Nominal Thickness (in)	Tolerance (in)
.060	$\pm .010$
.080	$\pm .010$
.100	$\pm .010$
.125	$\pm .013$
.150	$\pm .015$
.187	$\pm .019$
.220	$\pm .022$
.250	$\pm .025$
.312	$\pm .031$
.375	$\pm .038$
.417	$\pm .042$
.500	$\pm .050$
.750	$\pm .060$

TABLE 16-3. STANDARD THICKNESSES
AND TOLERANCES OF MIL-P-83310
POLYCARBONATE SHEET

Nominal Thickness (in)	Tolerance (in)
.060	$\pm .006$
.080	$\pm .008$
.100	$\pm .009$
.125	$\pm .010$
.187	$\pm .015$
.250	$\pm .020$
.375	$\pm .030$
.500	$\pm .040$
.750	$\pm .050$
1.000	$\pm .050$
-	-
-	-
-	-

TABLE 16-4. STANDARD THICKNESSES AND TOLERANCES
OF MIL-G-25667 GLASS

Nominal Thickness (in.)	Tolerance (in.)	Commercial Designation
.050		(Cnemcor 0319)*
.085		(Chemcor 0401)*
.095	$\pm .005$	(Herculite I)**
.110		(Herculite II)**
.125	$\pm .016$	
.187	$\pm .016$	
.203	$\pm .032$	
.250	$\pm .032$	
.375	$\pm .032$	
.500	$\pm .032$	
.625	$\pm .032$	
.750	$\pm .032$	
.875	$\pm .032$	
1.00	$\pm .032$	
1.25	$\pm .032$	

*Corning Glass Works, Corning, New York

**PPG Industries, Huntsville, Alabama

TABLE 16-5. PROPERTIES OF PLASTIC TRANSPARENT MATERIALS

Property	Units	MIL-P-5425 Cast Acrylic	MIL-P-8184 Modified Cast Acrylic	MIL-P-25690 Stretched Acrylic	MIL-P-83310 Polycarbonate	MIL-P-825/ Polyester
Poisson's Ratio	-	0.35	0.35	0.35	0.37	-
Tensile Strength	ksi	9.8-10.5	10.5-11.0	11.5-11.9	9-11.5	8.0-10.0
Ult. Elongation	%	4.9-6.4	6.7	42	75	-
Tensile Modulus	psi x 10 ⁵	4.5-4.6	4.5-4.7	4.5-4.9	3-3.5	-
Compr. Strength	ksi	18.0	19.0	17.0	12.5	30
Flex. Strength	ksi	16.0	16.0	16.0-17.5	10.3-13.5	12-20
Flex. Modulus	psi x 10 ⁵	4.5	4.5	5.0	3.2-3.5	5.0-5.5
Shear Strength	ksi	9.0-10.0	9.5-10.0	9.0	12-18	5.4
Izod Impact (Notched)	ft-lb in	0.3-0.99	0.31-0.45	1.5-3.0	14-17.5	0.2-0.43
Izod Impact (Unnotched)	ft-lb in	1.5-3.0	1.41-4.55	9-10	78	1.8-2.5
Rockwell Hardness	M	92	93-96	92-97	3.47	103
Coef. of Therm. Expansion	in/in °F x 10 ⁵	4.1	4.1	3.5	3.47	55-70
Density	lb/in ³	.043	.043	.043	.043	.043-.046
Therm. Conductivity	Btu-in ft ² -hr-°F	1.31-1.7	1.2-1.55	1.15	1.35	1.56
Specific Heat	Btu-lb-°F	0.35	0.35	0.35	0.28	-
Heat Deflection Temp. @264psi	°F	204-205	219	212	265-290	150-176
Flammability	in/min	1.5-2.5	1-1.5	1-1.5	self extg.	1.0-2.0
Refractive Index	-	1.491	1.496	1.495	1.581	1.52
Transmittance	%	91	91	91	88-91	70-89
Haze	%	1.0	1.0	1.0	1.0	3
Fracture Toughness	lb ^{3/2} /in	1200	1300	2600	5300	-
K-Value	ksi	-	-	14.0	7.4	-
Bearing Strength	ksi	-	-	-	0.18	-
Water Absorption (24 hours)	%	0.2	0.2	-	-	-

Data from Ref. 1,4,5

TABLE 16-6. PROPERTIES OF GLASS

Property	Units	Annealed Soda Lime	Semitempered Soda Lime	MIL-P-25667 Chemical Strengthened (Chemcor 0401)
Poisson's Ratio	-	0.22		
Flex Strength (Abraded)	ksi	6.9	13.4	
Flexural Strength	ksi	11.3	21.1	17.2 average
Flexural Modulus	psi	10.5×10^6	10.3×10^6	10.74×10^6
Coef of thermal expansion	$\frac{\text{in/in}}{^\circ\text{F}}$	47.2×10^{-7}	47.2×10^{-7}	48.9×10^{-7}
Density	lb/in^3	.091	.091	.084
Thermal Conductivity	$\frac{\text{Btu-in}}{\text{ft}^2\text{-sec-}^\circ\text{F}}$	6.5	6.5	7.1
Specific Heat	$\text{Btu/lb-}^\circ\text{F}$	0.185	0.185	0.192
Strain Point	$^\circ\text{F}$	959	959	1065
Flammability	-	non-burning	non-burning	non-burning
Refractive Index	-	1.518	1.518	1.506
Transmittance	%	85	85	85
Haze	%	1	1	1

Data from Ref. 1,6.

16.8 Mechanical Properties

The responses of transparent materials to environmental and structural loading are very different from those of common materials used in aircraft construction, and thus warrant special comment. Whereas the static strength of a metal structure is usually based on the material's ultimate or yield strength, additional considerations are necessary to provide adequate service life for transparent structures. These special factors are discussed below.

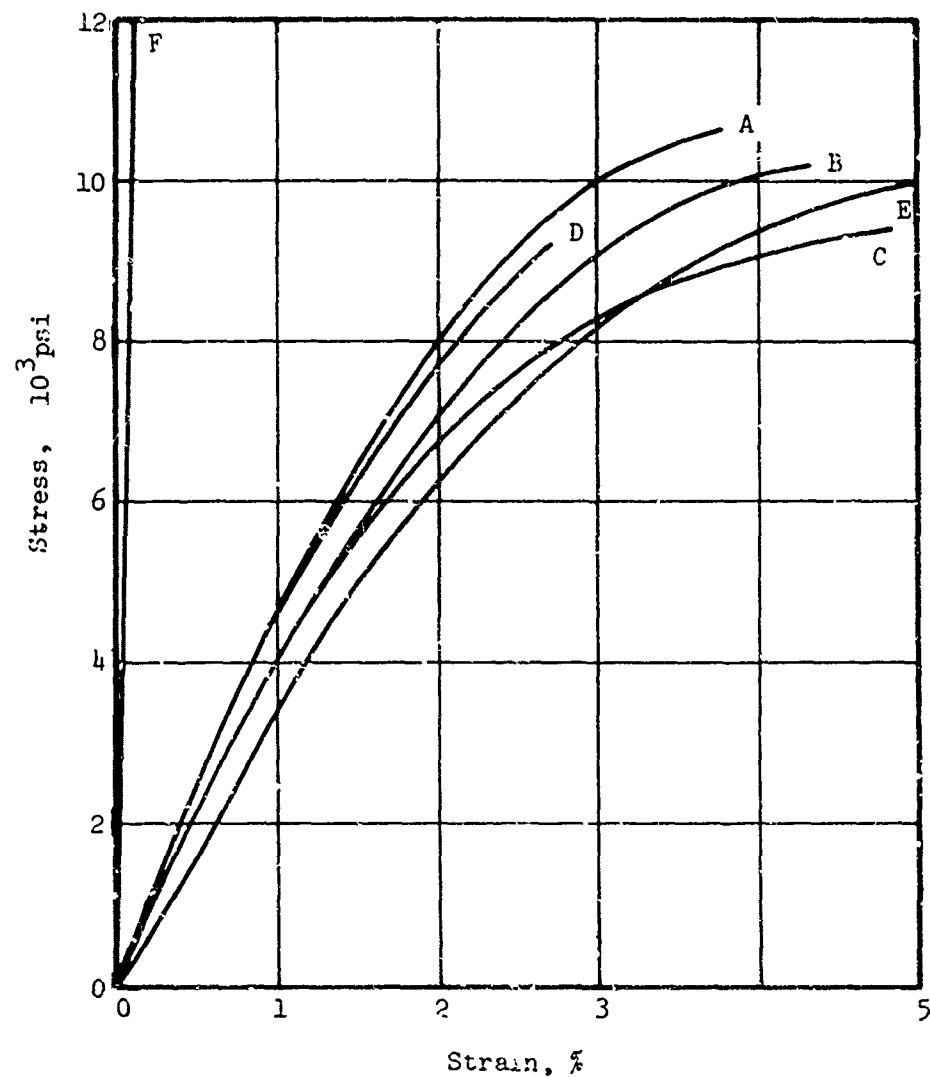
16.8.1 Tensile Strength

Short-term stress-strain curves for several common transparent materials are plotted in Figure 16-3. Typically, the minimum strength for transparent plastics is obtained when the load is applied slowly, in the order of 0.2 in/minute or less, since higher loading rates tend to be more indicative of impact strength than static strength. Material thickness is also a factor, with thin materials generally exhibiting higher strength.

The tensile strength of glass is measured as modulus of rupture in bending because it is a very brittle material and difficult to test in tension. Verification of glass strength is accomplished by either proof loading or optical measurement of birefringent lines. Reduced allowables for design purposes should be based on the following factors.

16.8.2 Temperature Effects

The strengths of all transparent materials except glass are severely affected by normal temperature variations. In Figures 16-4 through 16-8, the wide variations of tensile strength and the modulus of elasticity between high and low temperatures are shown for five different plastic materials. The materials are considerably weaker at high temperatures than at room temperature, and they are stronger and stiffer at low temperature than at room temperature.



- A MIL-P-8257 Thermosetting Polyester
- B MIL-P-8184 Modified Acrylic
- C MIL-P-5425 Heat Resistant Acrylic
- D MIL-P-25690 Stretched Acrylic
- E MIL-P-83310* Polycarbonate
- F MIL-G-25667 Glass

Data from Ref. 1

*Dried 18 Hr at +26; Deg F Before Testing

Figure 16-3. Tensile Stress-Strain Curves for Some Transparent Glazing Materials at Room Temperature.

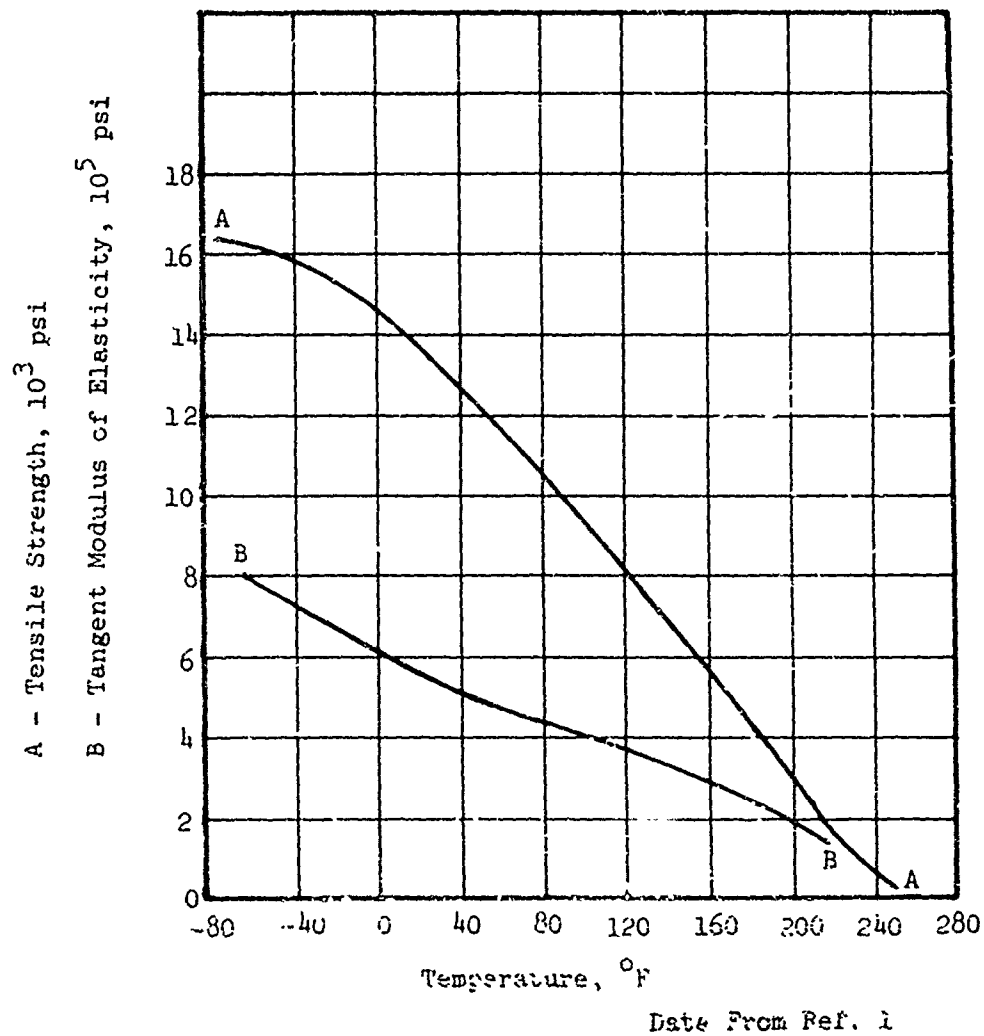


Figure 16-4. Effect of Temperature on Tensile Properties (Short-Time Test) of MIL-P-2184 Cast Acrylic Material.

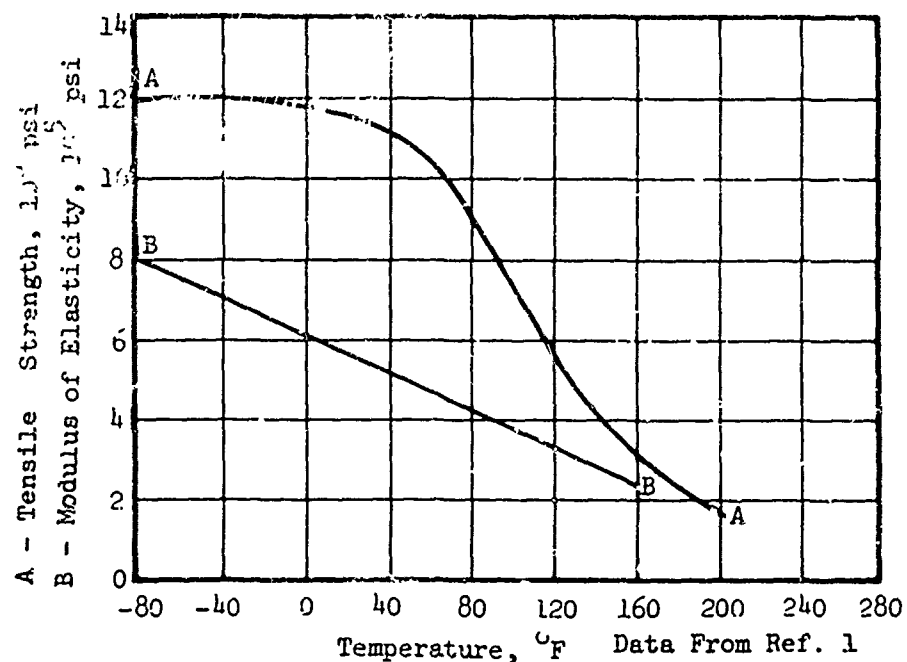


Figure 16-5. Effect of Temperature on Tensile Properties (Short-Time Test) of MIL-P-8257 Thermosetting Polyester Material.

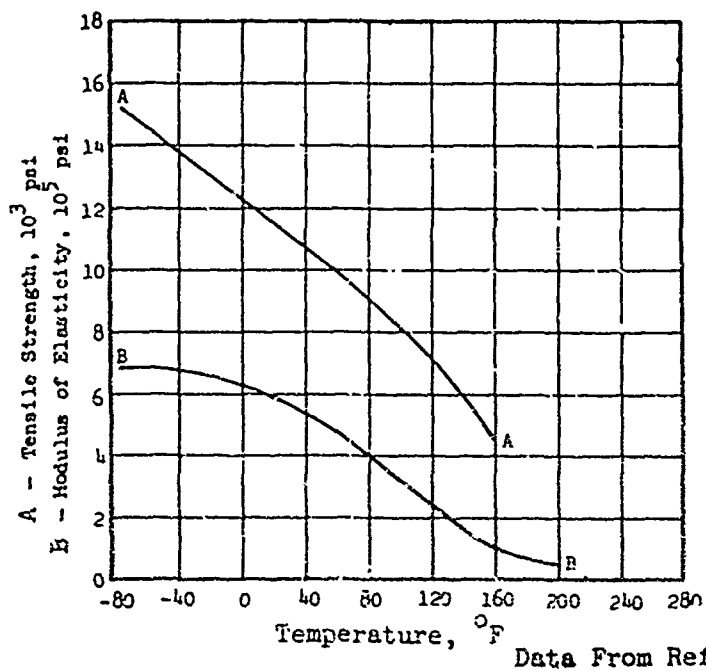


Figure 16-6. Effect of Temperature on Tensile Properties (Short-Time Test) of MIL-P-5425 Cast Acrylic Material.

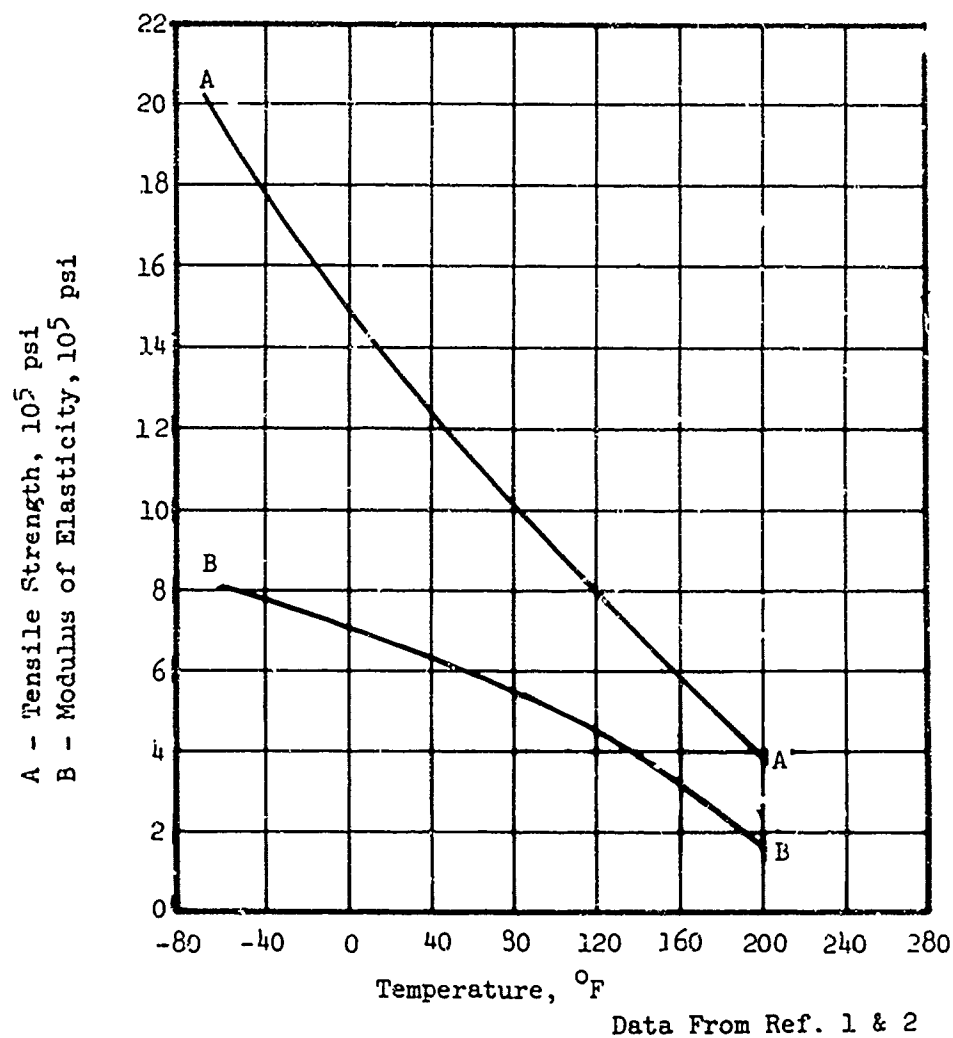


Figure 16-7. Effect of Temperature on Tensile Properties (Short-Time Test) of MIL-P-25690 Stretched Acrylic Material.

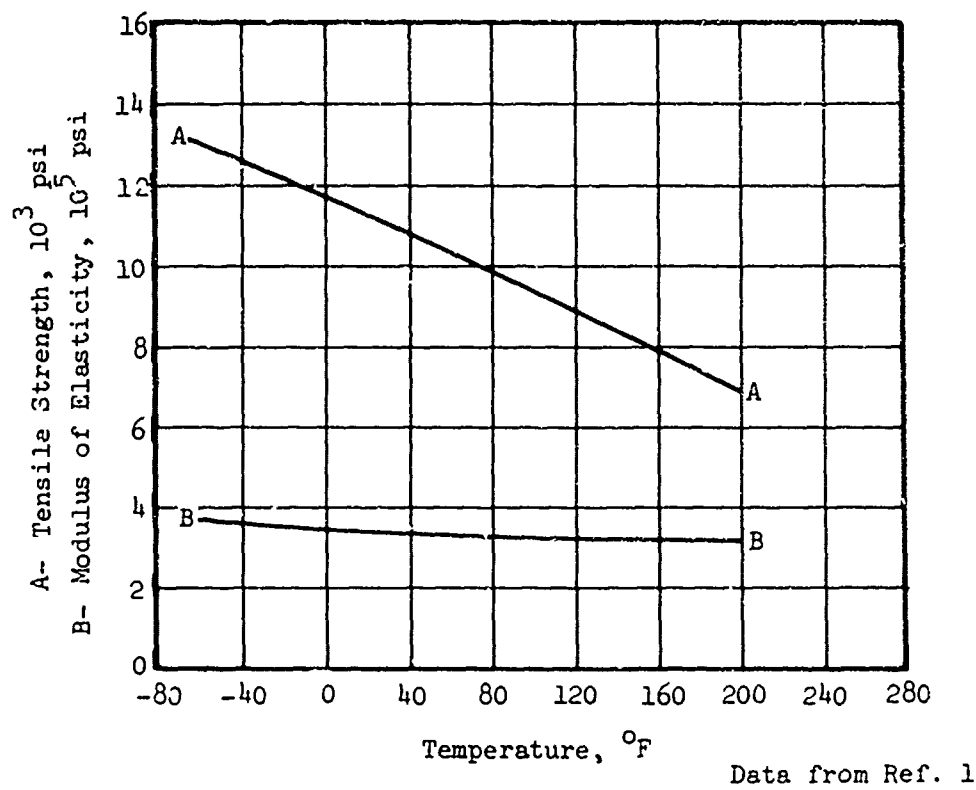


Figure 16-8. Effect of Temperature on Tensile Properties (Short-Time Test) of MIL-P-83310 Polycarbonate Material.

16.8.3 Duration of Loading Effects

Long-term loading will have deleterious effects on most transparent materials. Glass is subject to static fatigue, while thermoplastics suffer from stress-crazing or creep rupture.

Figure 16-9 illustrates the deterioration of static strength with time for plastic materials. Figure 16-10 shows the time to craze for both cast and stretched acrylic. The stress levels in this curve will be even lower at elevated temperatures.

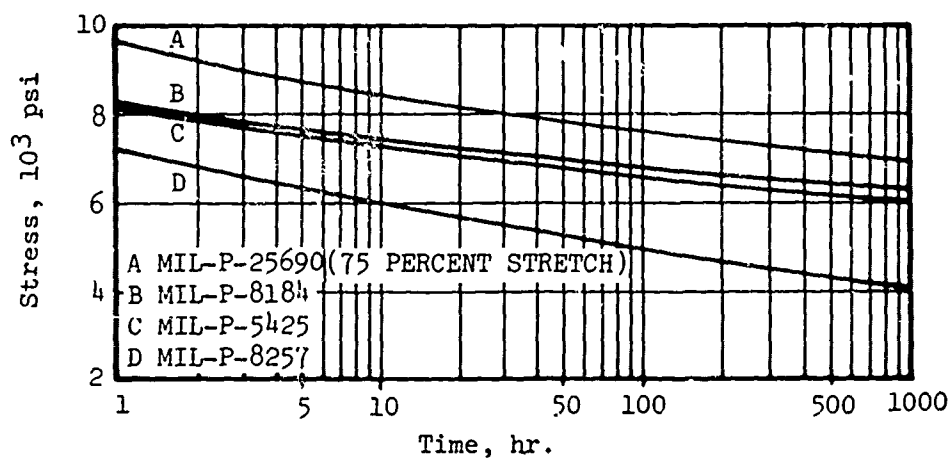
Glass exhibits static fatigue (time dependent loss in strength) in a humid environment while under tensile load. The effect of sustained loading on the breaking strength of annealed sheet glass is shown in Figure 16-11. The effect is cumulative.

16.8.4 Fatigue

Transparent plastic materials are subject to loss of strength from repeated application of structural loading. A set of flexural fatigue curves for acrylic plastic is presented in Figure 16-12.

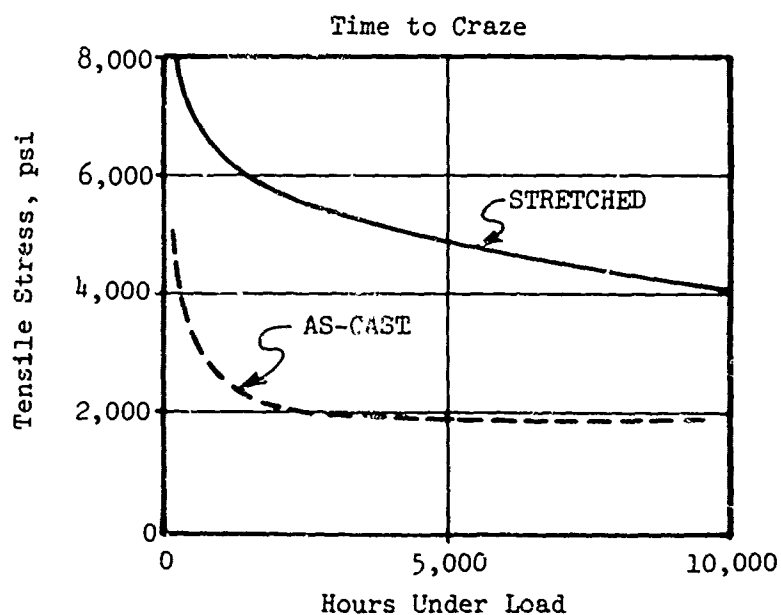
16.8.5 Surface Finish

Acrylic plastics and polycarbonates are susceptible to crazing. Crazing may be defined as a network of fine cracks or fissures on the surface of the part, which are only several thousandths of an inch in depth. Stress concentration will occur at the base of the cracks and will affect structural strength. Crazing of cast acrylic is particularly damaging, and crazing cracks 0.006 inch deep resulted in a 30% loss in tensile strength of MIL-P-5425 in one investigation. In contrast, stretched acrylic suffered only a 10% loss of original strength when severely crazed to a depth of .030 inch. While polycarbonate is also susceptible to crazing damage, its effect on static strength has not been documented, although it does have a very pronounced effect in reducing impact strength.



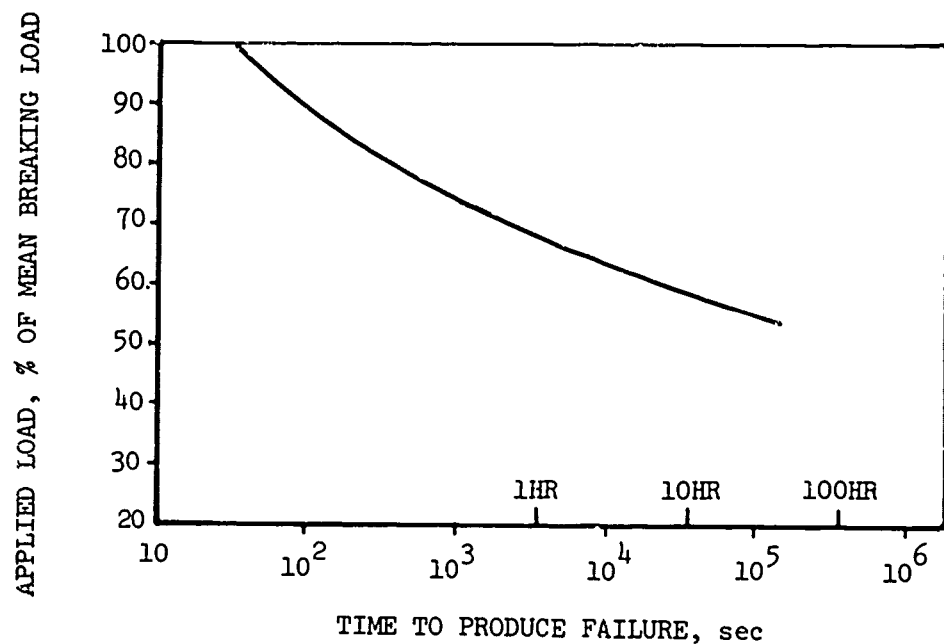
Data from Ref. 1

Figure 16-9. Effect of Duration of Loading on the Tensile Rupture Behavior of Plastic Glazing Materials at 80°F.



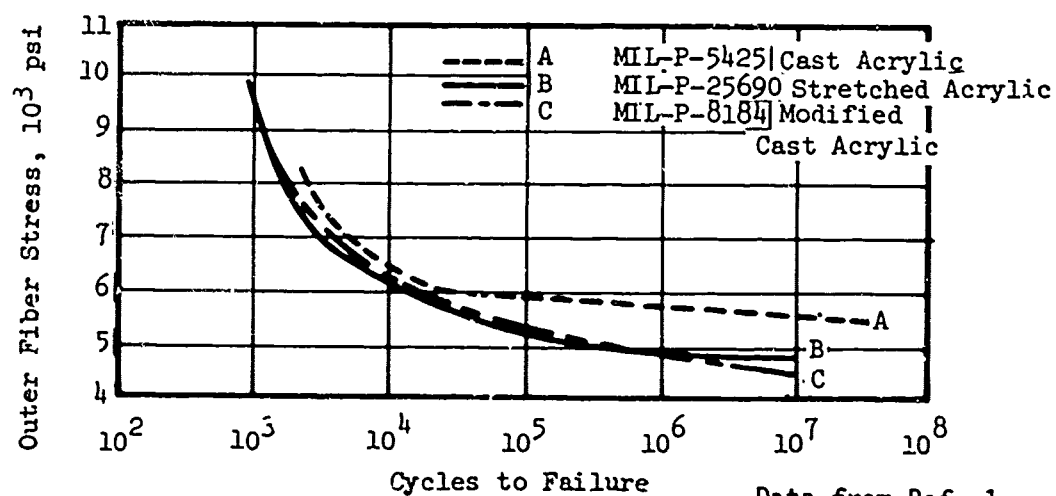
Data From Ref. 3

Figure 16-10. Crazing of Plexiglas 55 Under Continuous Tensile Stress While Exposed to Natural Weather.



Data from Ref. 1

Figure 16-11. The Effect of Sustained Loading on the Breaking Strength of Annealed Glass.



Data from Ref. 1

Figure 16-12. Flexural Fatigue Curves for 0.250-Inch-Thick Plastic Glazing Materials at Room Temperature.

16.8.6 Notch Sensitivity

The notch sensitivity of the common transparent materials is very low in comparison to familiar metals used in aircraft construction. Fracture due to notch sensitivity occurs because of stress concentration at flaws such as nicks, scratches, star fractures, and machining or tool marks. K-value or crack propagation resistance is the energy required to propagate a crack of defined area; the test procedure used for measuring this data is defined in specification MIL-P-25690.

Because of an infinite variety of defects, and the impracticality of applying the Izod and K-value results directly, this information is useful only for determining the relative ranking of different materials. Table 16-7 compares crack propagation values for common transparent materials with 2024-T3 aluminum.

TABLE 16-7. RELATIVE CRACK PROPAGATION RESISTANCE OF VARIOUS MATERIALS

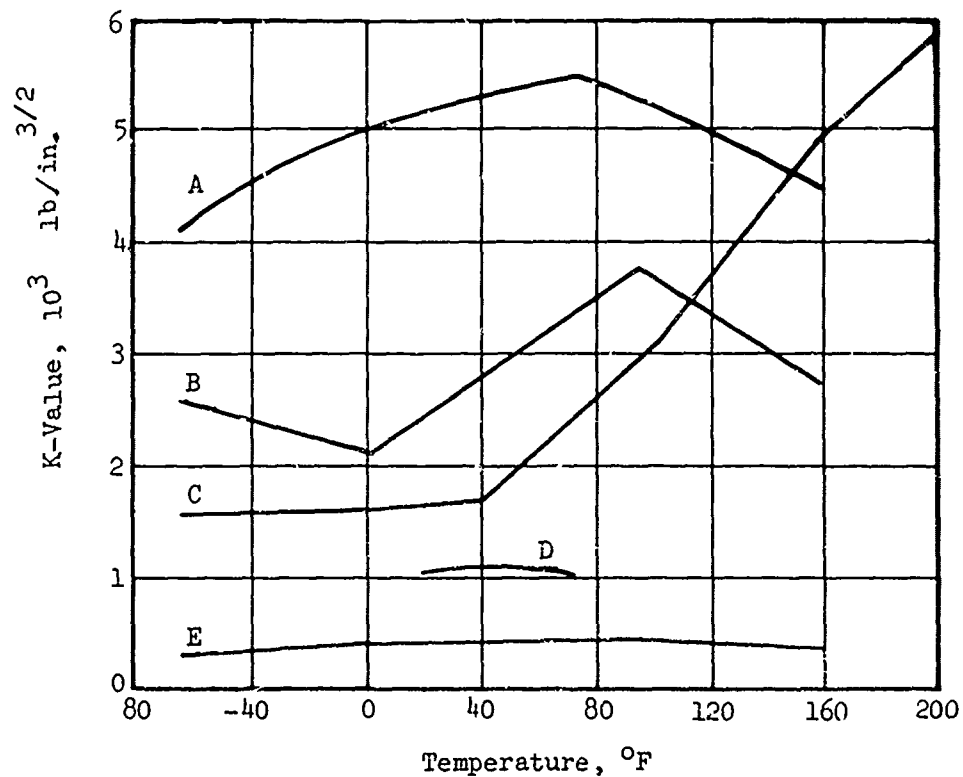
Material	K-Value $(10^{31b})^{3/2}$ in
2024-T3 Aluminum	63.2
MIL-P-83310 Polycarbonate	5.3
MIL-P-25690 Stretched Acrylic	3.2
MIL-P-5425 Cast Acrylic	1.2
MIL-P-8257 Polyester	0.4
MIL-P-8184 Cast Acrylic	1.3
Glass, in air	0.3

K-values are temperature dependent for plastic materials. This relationship is illustrated in Figure 16-13.

Glass and MIL-P-8257 polyester are considered to have such a poor notch sensitivity that they are not normally used for monolithic applications and must be laminated to preclude shattering from foreign object or service-induced damage. Tests have shown that star fractures can reduce tensile and bending strengths to only 20% of their original values for polyester.

Cast acrylics are also highly sensitive to notch defects and have low crack-propagation resistance. Significant reduction in both impact and flexural strength can result from deep sharp-edged nicks or scratches. The notch sensitivity of acrylic is greatly decreased and the resistance to crack propagation greatly improved by stretching, and the stretched material has thus found widespread acceptance for general applications.

- A Swedlow Processed Polycarbonate Sheet
- B MIL-P-5425 Cast Acrylic
- C MIL-P-25690 (68% Stretch) Stretched Acrylic
- D MIL-P-8184 Modified Cast Acrylic
- E MIL-P-8257 Polyester



Data from Ref. 1

Figure 16-13. Effect of Temperature on the K-Value of Glazing Materials.

MIL-P-83310 polycarbonate has good notch sensitivity and resistance to crack propagation except after exposure to ultraviolet radiation for extended periods. Reduction in notched Izod strength of 50% has been observed for polycarbonate after six months of weathering. Polycarbonate also exhibits a transition from being a ductile material to being a brittle material when the thickness is increased above 0.140 to 0.180 inch, as measured by impact tests.

16.8.7 Bearing Strength

Bearing strength in Table 16-5 was presented for only two materials, MIL-P-25690 stretched acrylic and MIL-P-83310 polycarbonate, because the other transparent materials listed have such poor notch sensitivity that they are not suited for applications using mechanical fasteners, for which this data is applicable. The values listed are for 4% hole elongation measured at room temperatures.

Bearing strength for polycarbonate remains relatively constant up to 160°F; however, the bearing strength for stretched acrylic drops to 6000 psi at that temperature.

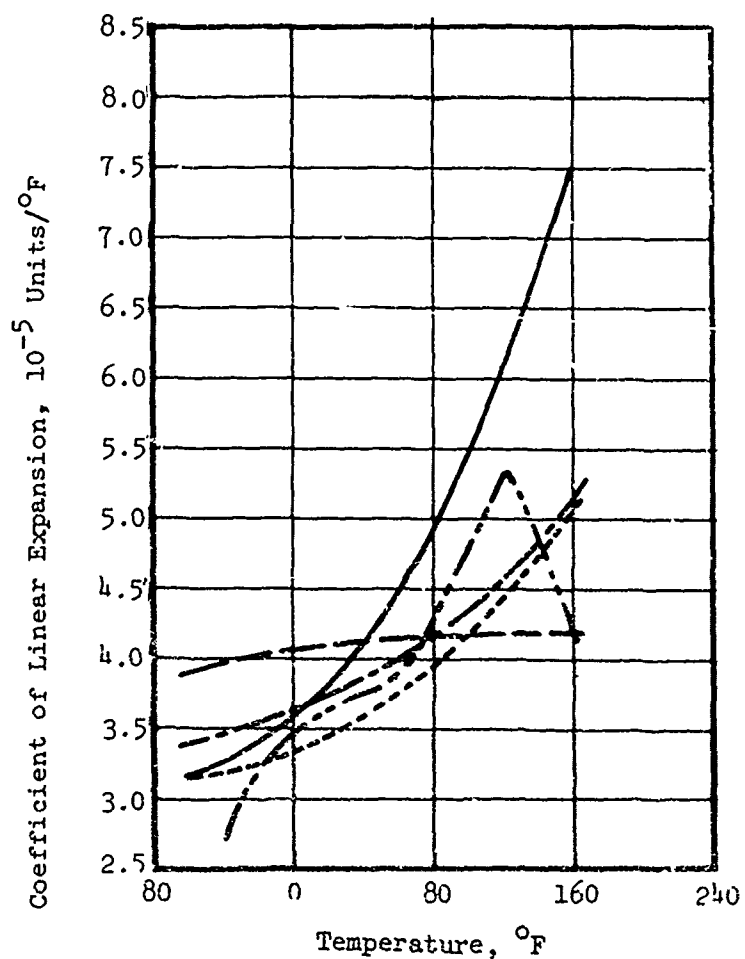
16.8.8 Thermal Expansion

The coefficients of thermal expansion for several transparent materials are shown in Figure 16-14. With the exception of glass and polycarbonate, the coefficients of thermal expansion for transparent materials are temperature dependent. For MIL-P-25690 stretched acrylic at temperatures above 200°F, thermal relaxation occurs and the material starts to shrink back to its original, unstretched state.

These curves are useful for determining the amount of expansion or contraction of transparent materials relative to structure or other transparent materials in laminated panels or assemblies.

16.9 Design Allowables

There are many conditions that can and do occur in service to cause mechanical properties of transparent materials to deteriorate from their original values. These conditions include the environment, repeated load application, and foreign object damage, and are impossible to avoid. Therefore, it is considered prudent to reduce allowable material strength properties for design purposes to insure adequate service life.



--- MII-P-5425 Cast Acrylic
 --- MIL - P -8184 Modified Cast Acrylic
 --- MIL-P-8257 Polyester
 --- MIL-P- 25690 (Swedlow) Stretched Acrylic
 --- Polycarbonate, Lexan 9030-2

Data From Ref. 1 & 2

Figure 16-14. Coefficient of Linear Expansion Versus Temperature for Various Transparent Glazing Materials.

The values in Table 16-8 are listed as typical working or limit stresses that can be used for helicopter transparent-enclosure design and should be adjusted for specific applications. It should be noted that, although the allowable stresses for some plastic materials are low in comparison with their ultimate strengths, the plastic materials have low moduli of elasticity, and deflection considerations would ordinarily govern the design to preclude the use of higher operating stresses.

TABLE 16-8. ALLOWABLE TENSILE STRESSES FOR HELICOPTER TRANSPARENT ENCLOSURES

Material	Tensile Limit Stresses (psi)	Criteria
MIL-P-5425 Cast Acrylic	800	Crazing threshold
MIL-P-8184 Modified Cast Acrylic	1500	Crazing threshold
MIL-P-25690 Stretched Acrylic	4000	Crazing threshold
MIL-P-83310 Polycarbonate (Coated)	6000	2/3 of Ultimate Strength
MIL-P-83310 Polycarbonate (Uncoated)	1500	Crazing threshold
Semitempered glass	4500*	2/3 of long term abraded strength
Chemically tempered glass	undetermined	Abraded strength unknown

* Modulus of rupture in bending

16.10 Material Attributes

A matrix summarizing advantages and disadvantages of each of the common transparent glazing materials is presented in Table 16-9.

TABLE 16-9. SUMMARY OF TRANSPARENT GLAZING MATERIAL ATTRIBUTES

Material	Advantages	Disadvantages
MIL-P-5425 Cast Acrylic	<ol style="list-style-type: none"> 1. Excellent formability 2. Surface restoration is possible 	<ol style="list-style-type: none"> 1. Very poor resistance to stress-solvent crazing 2. Poor crack propagation resistance 3. Poor abrasion resistance
MIL-P-8184 Modified Cast Acrylic	<ol style="list-style-type: none"> 1. Excellent formability 2. Surface restoration is possible 	<ol style="list-style-type: none"> 1. Poor resistance to stress-solvent crazing 2. Poor crack propagation resistance 3. Poor abrasion resistance
MIL-P-8257 Polyester Sheet	<ol style="list-style-type: none"> 1. Moderate abrasion resistance 2. Good solvent resistance 	<ol style="list-style-type: none"> 1. Very poor notch and impact resistance 2. Contour forming limitations 3. Low strength at high temperature 4. Not recommended for monolithic applications

TABLE 16-9. SUMMARY OF TRANSPARENT GLAZING MATERIAL ATTRIBUTES
(cont'd)

Material	Advantages	Disadvantages
MIL-P-83310 Polycarbonate Sheet	<ol style="list-style-type: none"> 1. Excellent toughness and crack propagation resistance 2. Excellent high temperature properties 3. Flame retardant 4. Very ductile 5. Excellent ballistic properties 	<ol style="list-style-type: none"> 1. Very poor abrasion resistance 2. Low resistance to stress-solvent crazing 3. Long-term physical properties not fully evaluated
MIL-P-25690 Stretched Acrylic	<ol style="list-style-type: none"> 1. Good crack propagation resistance 2. Good stress-solvent resistance 3. High ductility 4. Surface can be restored 5. Good ballistic properties 	<ol style="list-style-type: none"> 1. Poor abrasion resistance 2. Subject to creep at high temperatures 3. More expensive than cast acrylic 4. Low shear strength parallel to the surface
MIL-P-25667 Glass	<ol style="list-style-type: none"> 1. Excellent abrasion resistance 2. Excellent optical properties 3. Impervious to chemical attack 4. Does not deteriorate from aging 	<ol style="list-style-type: none"> 1. Low strength-to-weight ratio 2. Contour forming limitations 3. Very poor notch sensitivity and crack propagation resistance 4. Very brittle

References

1. Hassard, R. S., Goodyear Aerospace Corp., "Plastics for Aerospace Vehicles, Part II Transparent Glazing Materials," MIL-HDBK-17A, Part II (Proposed Revision), Air Force Materials Laboratory, Wright-Patterson Air Force Base, Ohio, Jan. 1973.
2. "Typical Physical Properties of Swedlow Stretched Acrylic (MIL-D-25090) Sheet-Swedlow Type 3505," MP-3-100, Swedlow Inc., Garden Grove, Calif., Apr. 1973.
3. Foster, L. E., Lockheed Aircraft Corp., "Progress Report on the use of Stretched Acrylic at Lockheed," WADC-TR-57-421, Wright Air Development Center, Dayton, Ohio, Oct. 1957, AD142021.
4. James, H. C., et al, Goodyear Aerospace Corp., "Design Test, and Acceptance Criteria for Army Helicopter Transparent Enclosures," USAAMRDL-TR-73-19, U. S. Army Air Mobility Research and Development Laboratory, Ft. Eustis, Va., May 1973, AD 767242.
5. Cook, L. M., et al, PPG Industries, "Development of Design, Test, and Acceptance Criteria for Army Helicopter Transparent Enclosures," USAAMRDL TR-73-65, U. S. Army Air Mobility Research and Development Laboratory, Ft. Eustis, Va., Sept. 1973, AD 772936.
6. Data Sheet, Corning Code 0401, Corning Glass Works, Corning, New York
7. "Typical Physical Properties of Swedlow Processed Polycarbonate Sheet," MP-3-107, Swedlow Inc., Garden Grove, Calif., Apr. 1973.

Bibliography

Shaver, Dr. D. W., Corning Glass Works, "Glass for High Temperature Applications in Aircraft," WADC-TR-421, Wright Air Development Center, Dayton, Ohio, Oct. 1957, AD 142021.

Habrer, C. H., National Bureau of Standards "Elevated Temperature Properties of Glasses," WADC-TR-57-421, Wright Air Development Center, Dayton, Ohio, Oct. 1957, AD 142021.

Mochel, E. L., Corning Glass Works, "Strong Glass," WADC-TR-65-212, Air Force Materials Laboratory, Wright-Patterson Air Force Base, Ohio, Sept. 1965, AD 47343.

Robinson, J., Whitaker Corp., "Glass Edge Attachment and Seal Design Criteria," WADC-TR-212, Air Force Materials Laboratory, Wright-Patterson Air Force Base, Ohio, Sept. 1965, AD 74343.

Cully, D. C., Goodyear Aerospace Corp., "Factors to Consider in Designing Stretched Acrylic Aircraft Transparencies," WADC-TR-65-212, Air Force Materials Laboratory, Wright-Patterson Air Force Base, Ohio, AD 47343.

Hayashida, K., et al, "Rationale for Windshield Glass System Specification Requirements for Shuttle Orbiter," NASA CR-112209, Space Division, North American Rockwell, Oct. 1972.

Husman, G. E., "Environmental Data and Machining Techniques of Polycarbonates," AFML-TR-73-126, Air Force Materials Laboratory, Wright-Patterson Air Force Base, Ohio, AD 769344.

Mahaffey, J. E., Rockwell International, "Material Evaluation B-1 Crew Module Windshield and Windows," AFML-TR-73-126, Air Force Materials Laboratory, Wright-Patterson Air Force Base, Ohio, AD 769344.

Malty, Jr., R. E., Libby Owens Ford, "Plate Versus Float Glass in Aircraft Transparencies," AFML-TR-73-126, Air Force Materials Laboratory, Wright-Patterson Air Force Base, Ohio, AD 769344.

Miller, W. A., "Aircraft Transparency Applications of Polycarbonates," Sierracin Corporation, Sylmar, Calif., June 1971.

Wiser, G. L., "Sierracin Glass/Plastic Composite Windshields," Sierracin Corporation, Sylmar, Calif., June 1969.

Wiser, G. L., Sierracin Corp., "New Materials in Aircraft Windshields," National Aeronautics and Space Engineering and Manufacturing Meeting, Los Angeles, Calif., Society of Automotive Engineers, New York, Oct. 1970.

"Plexiglas Handbook for Aircraft Engineering," Rohm & Haas Co., Philadelphia, Pa., 1952.

Hassard, R. S., Goodyear Aerospace Corp., "Design Criteria-Transparent Polycarbonate Plastic Sheet," AFML-TR-72-117, Air Force Materials Laboratory, Wright-Patterson Air Force Base, Ohio, Aug. 1972.

Caird, D. W., General Electric Corp., "Prevention of Fracture in BPA-Polycarbonate Structures," AFML-TR-76-54, Air Force Materials Laboratory, Wright-Patterson Air Force Base, Ohio, Apr. 1976.

Miska, H. A., Corning Glass Works, "Understanding the Basis of Chemically Strengthened Glass," Materials Engineering, June 1976.

Lawrence, J. H., Douglas Aircraft Co., "Windshield Technology Demonstrator Program," AFFDL-TR-77-1, Air Force Flight Dynamics Laboratory, Wright-Patterson Air Force Base, Ohio, Sept. 1977.

Interlayers are transparent adhesives used to bond the individual component plies together in laminated transparent assemblies. Laminating is used for the following purposes:

- a. To join dissimilar transparent materials in order to create a hybrid with properties superior to those of its constituents.
- b. To imbed electrical heating systems in the assembly.
- c. To provide a flexible medium to improve shatter and impact characteristics.
- d. To form multiple ply laminates for special applications such as transparent armor.

Currently available interlayers are proprietary products not covered by Government specifications. Hence, a particular interlayer may have limited availability. Manufacturing methods for lamination and processing may also be proprietary. Engineers should bear this in mind when preparing design specifications and should work closely with the appropriate suppliers to obtain current material data.

The materials described in this section include some of the more common interlayers used for helicopter transparencies. The important variables are as follows:

Tensile and shear strength versus temperature
Elongation versus temperature
Adhesive strength
Environmental resistance
Thermal conductivity and specific heat
Coefficient of thermal expansion
Chemical compatibility with substrate
Producibility

The relationship between physical properties and temperature for interlayers is most important since values change drastically over a normal operating temperature range.

17.1 Interlayer Forms

Plastic interlayers are available in two forms: sheet and liquid resin. Polyvinyl butyral and ethylene terpolymer are normally supplied in sheets, 0.015 inch or 0.025 inch thick, while silicone and polyurethane varieties are liquid "cast-in-place" (CIP) resins. Most transparency manufacturers can produce laminates using either sheets or cast-in-place interlayers; however, aside from material properties, preferences are strongly influenced by producibility and cost.

Sheet interlayers are in general easier to use, and vacuum bag techniques can frequently be employed during lamination. CIP interlayers require more sophisticated tooling to maintain thickness and parallelism. However, this enables the interlayer to fill in local depression or tapered thickness variations on the interlayer side of the facing. Careful controls are also required for CIP interlayers to prevent the formation of bubbles or voids within the cured interlayer. Therefore, the minimum thickness commonly accepted for cast-in-place interlayers is 0.100 inch, while sheet interlayer thickness as low as 0.060 inch is possible.

17.2 Polyvinyl Butyral

Polyvinyl butyral (PVB) has been the most widely used, general-purpose interlayer material for laminating transparent materials in the aircraft and automotive industries. For glass laminates, about 20 parts of triethylene glycol di-2-ethyl butyral plasticizer (3GH) are used per hundred parts of resin. Additional plasticizer is required for plastic laminates to improve the thermal compatibility of interlayer and facings, and 37.5 parts of dibutyl is used per hundred parts of resin.

PVB has excellent toughness at room temperature and for years has served as a medium to birdproof windshields on fixed-wing aircraft. Its adhesion to glass is so great that when tested to destruction, glass failure often occurs prior to bond failure.

PVB also has severe limitations. These include a tendency to produce bubbles when exposed to temperatures above 200°F for extended periods of time. Moisture penetration will damage PVB and is one of the major causes of delamination. The temperature coefficient of expansion of PVB is approximately thirty times as great as that of glass, and as PVB hardens at low temperatures, special design techniques must be employed to preclude service problems. PVB is also chemically incompatible with polycarbonates, and special tie coats or primers are employed if the two materials are used together.

Room temperature properties for PVB are shown in Table 17-1. Mechanical properties of PVB are drastically affected by temperature. At low temperatures PVB is a brittle material with considerable strength and rigidity, while at high temperatures, it behaves almost as a viscous fluid and has virtually no strength. The variations of modulus of elasticity, ultimate strength, and elongation properties are shown in Figures 17-1, 17-2, and 17-3.

TABLE 17-1. ROOM TEMPERATURE PROPERTIES OF POLYVINYL BUTYRAL

Density (lb/in ³)	.039
Index of Refraction	1.483
Light Transmission (%)	87 (.075 inch thick)
Haze (%)	1 (.075 inch thick)
Thermal Conductivity (Btu/(hr-ft ² - °F - in))	1.5
Specific Heat (cal/(cm-°F))	0.35
Coefficient of Expansion (units/°F)	21.2 x 10 ⁻⁵
Tensile Strength (psi)	570
Ultimate Elongation (%)	350
Poisson's Ratio	0.46

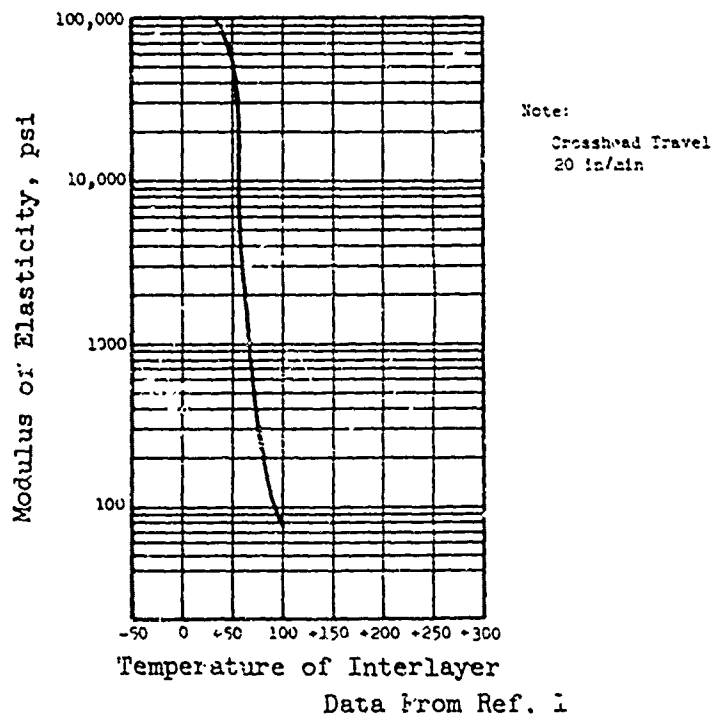


Figure 17-1. Tensile Modulus of Polyvinyl Butyral (PVB) Interlayer.

17.3 Ethylene Terpolymer

Ethylene terpolymer (ETP) was developed as an optimum adhesive interlayer sheet for glass polycarbonate laminates. Other interlayers such as polyvinyl butyral are unsuitable for use in transparent polycarbonate laminates without special tie coats or primers. A limited amount of testing conducted on glass-polycarbonate laminates has demonstrated the integrity of the adhesive during ballistic impact at room temperature.

Physical properties of ethylene terpolymer have not been fully evaluated, and only limited data is available. Comparisons of tensile strength and tensile elongation for ethylene terpolymer (ETP) versus polyvinyl butyral (PVB) are shown in Figures 17-2 and 17-3.

17.4 Silicone-Base Interlayers

Silicone-base interlayers are extremely flexible materials that were developed to accommodate the large expansion differential between glass and plastic without excessive stress buildup. The material has excellent high-temperature properties and maintains very uniform physical properties throughout a wide range of temperatures. Tensile strength and elongation characteristics versus temperature are shown in Figures 17-2 and 17-3.

SS52725 (HT) is a representative, cast-in-place, silicone-base interlayer produced by Swedlow, Inc. This material has demonstrated superior resistance to SO₂ attack, which caused severe degradation of earlier silicone interlayers. Room temperature physical properties for SS5272Y (HT) are presented in Table 17-2.

TABLE 17-2. ROOM TEMPERATURE PROPERTIES OF SWEDLOW SS5272Y (HT)
SILICONE-BASE INTERLAYER

Density (lb/in ³)	.037
Index of Refraction	1.409
Light Transmission (%)	89
Haze (%)	1.0
Thermal Conductivity (Btu/(hr-ft ² -°F-in))	0.988
Specific Heat (cal/(cm ³ -°F))	0.31
Coef. of Thermal Expansion (units/°F)	21.2 x 10 ⁻⁵
Tensile Strength (psi)	570
Ultimate Elongation (%)	400

Data from Ref. 1

17.5 Polyurethane-Base Interlayers

The transparent urethanes are the most recent of interlayer materials. They are characterized by good tear strength and relatively high tensile strength. PPG 112, produced by PPG Industries, is a polyurethane-base interlayer.

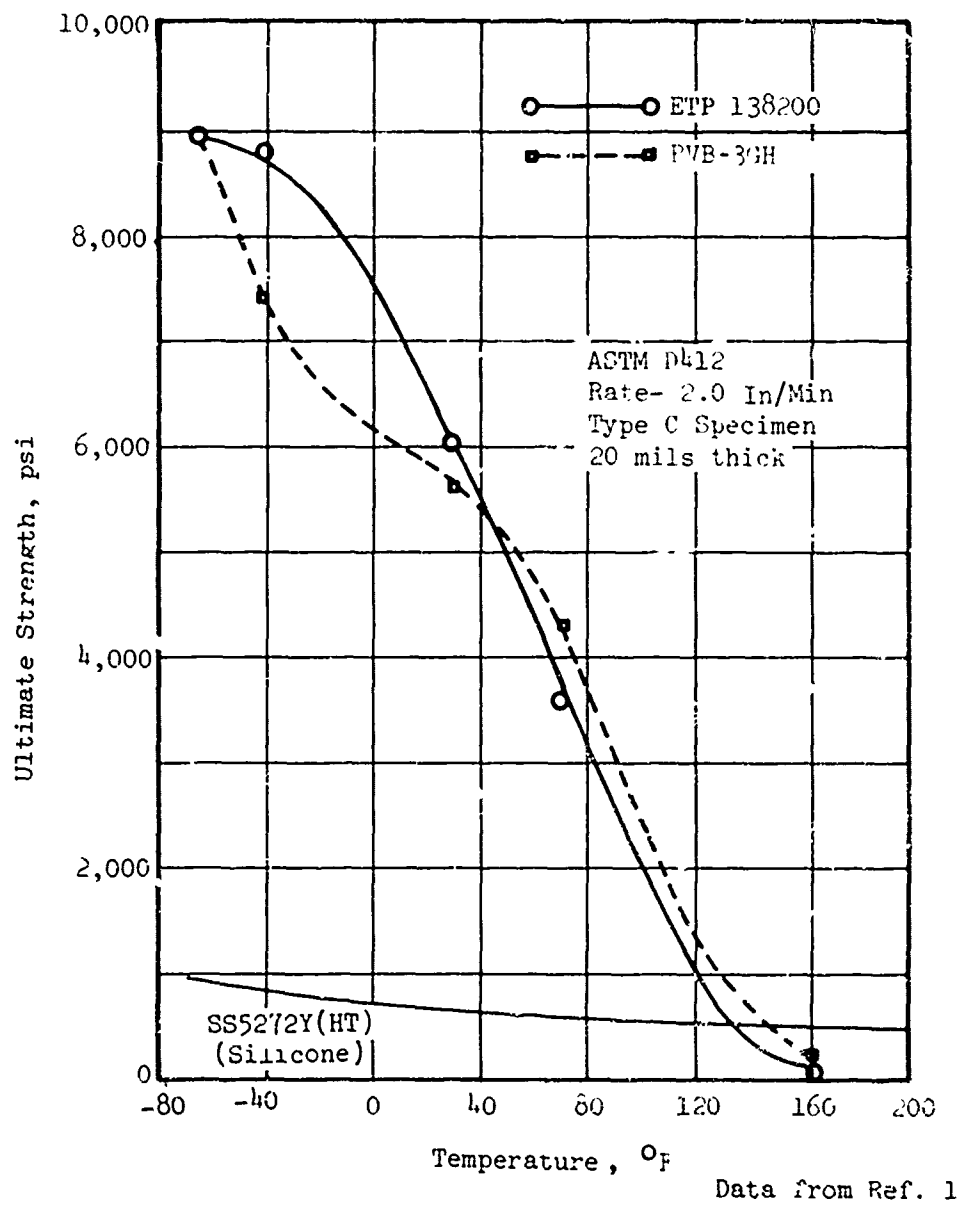


Figure 17-2. Ultimate Strength Versus Temperature for ETP, SS52724 (HT) and PVB-3GH.

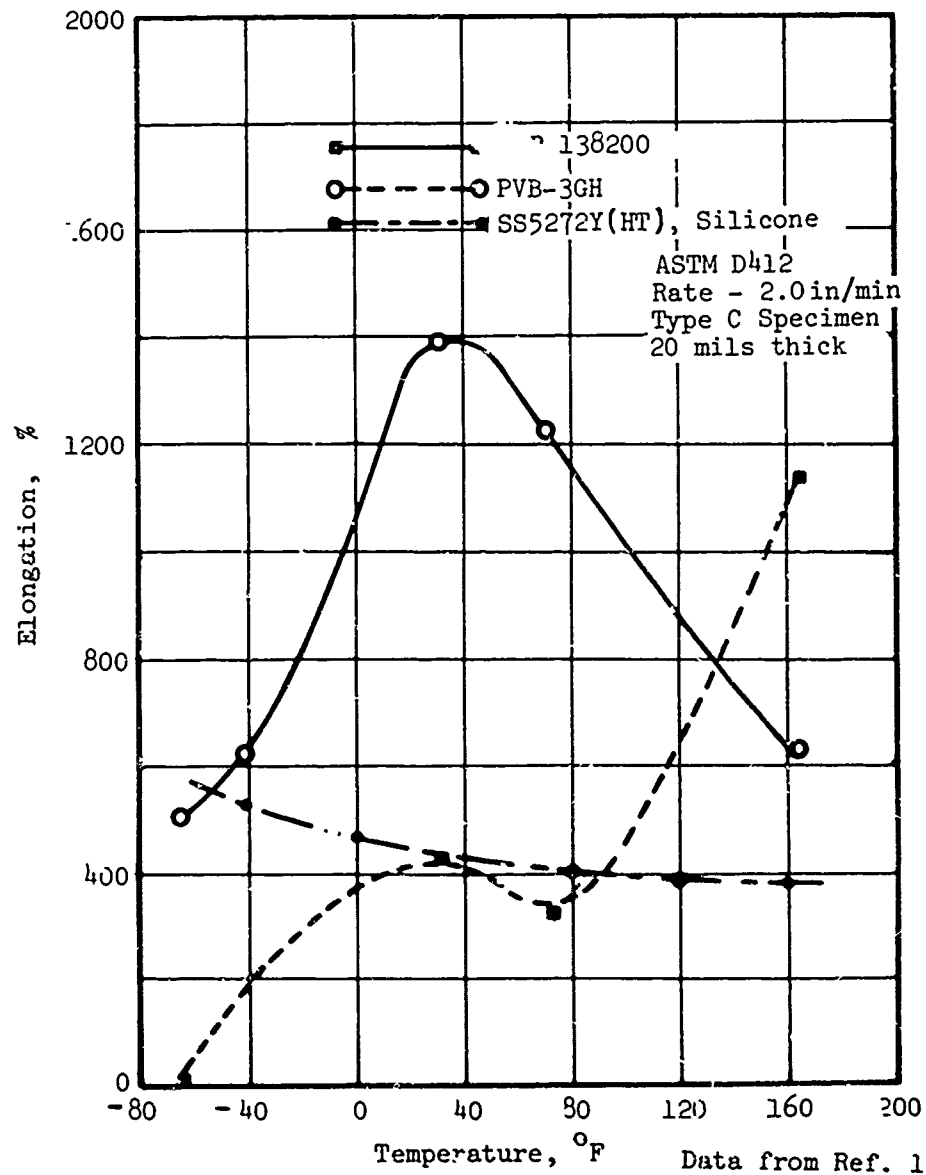


Figure 17-3. Tensile Elongation Characteristics of ETP, SS5272Y (HT) and PVB-3GH as a Function of Temperature.

Reference

1. Hassard, R. S., Goodyear Aerospace Corp., "Plastics for Aerospace Vehicles, Part II Transparent Glazing Materials," MIL-HDBK-17A, Part II (Proposed Revision), Air Force Materials Laboratory, Wright-Patterson Air Force Base, Ohio, Jan. 1973.

Bibliography

Ball, G. L., "A Thermoplastic Transparent Adhesive for Bonding Polycarbonate to Glass," AMMRC-CR-71-10, Army Materials and Mechanics Research Center, Watertown, Mass., July 1971.

Yamaguchi, W., Swedlow Inc., "High Performance Cast-In-Place Interlayer," WADC-TR-65-212, Air Force Materials Laboratory, Wright-Patterson Air Force Base, Ohio, Sept. 1965.

Digger, K. M., "Design of High Temperature Aircraft Windows," WADC-TR-65-212, Air Force Materials Laboratory, Wright-Patterson Air Force Base, Ohio, Sept. 1965.

Wiser, G. L., Sierracin Corp., "Interlayers and Laminating," WADC-TR-65-212, Air Force Materials Laboratory, Wright-Patterson Air Force Base, Ohio, Sept. 1965.

Mahaffey, J. E., Rockwell International Corp., "Materials Evaluation B-1 Crew Module Windshield and Windows," AFML-TR-73-126, Air Force Materials Laboratory, Wright-Patterson Air Force Base, Ohio, June 1973.

Bickford, G., The Boeing Co., "Interlayer Needs for Subsonic Windshields," AFML-TR-73-126, Air Force Materials Laboratory, Wright-Patterson Air Force Base, Ohio, June 1973.

Coatings are an attractive means to selectively alter physical characteristics of transparent materials.

They are categorized by function or intended usage, and are normally applied as proprietary processes. Identification is typically by vendor code and usage; for example, Universal 123 antireflective coating. Government specifications or generic material classification are normally not used.

Certain physical characteristics of coatings must be known to enable the designer to establish reasonable performance specifications. The data presented herein will be helpful in this regard, and more detailed information can be obtained directly from the processors.

The coatings that have potential applications to helicopter transparent enclosures are summarized below.

18.1 Antireflective Coatings

The function of an antireflective coating is to attenuate the light reflected from a transparency. Applications include the reduction of external glint and internal cockpit reflections. Antireflective coatings were discussed in more detail in the Optical Factors section of this handbook.

18.2 Radar Cross Section Reduction Coatings

A radar reflective coating is a metallic, conductive coating that is applied to a transparency in order to reflect a radar beam away from the cockpit cavity. Radar cross section reduction treatment is necessary for some types of combat helicopters in order to avoid detection by hostile radar. Section 5.0 of this handbook is devoted to radar reflective coatings.

18.3 Electromagnetic Radiation Protective Coatings

Electromagnetic radiation protection may be necessary for shielding the flight crew when powerful, radiating avionics equipment is carried on board the helicopter. Treatment is essentially the same as for radar cross section reduction coatings.

18.4 Abrasion-Resistant Coatings

An abrasion-resistant coating, or hardcoat, may be applied to a soft plastic surface to enhance the material's tolerance to abrasion. A comprehensive discussion on hardcoating is included in the Abrasion section of this handbook.

18.5 Rain Dispersion Coatings

Rain dispersion coatings reduce the surface tension between water and transparencies, thereby causing the water to form beads or small droplets to enhance visibility in rain. A comprehensive discussion of rain repellents is included in the Rain Removal Systems section.

18.6 Static Dissipation Coatings

Static dissipation coatings are used to prevent static electricity buildup on the exterior surfaces of transparencies. This phenomenon is discussed in the Static Electricity section of this handbook.

18.7 Electrical Heating Films

These films are thin, virtually transparent, metallic or metallic oxide, electrical-resistive coatings used as heating mediums for some anti-ice and anti-fog transparencies. The thickness of a film is typically measured in angstrom units (10^{-9} meter). The films are virtually transparent to directly transmitted light but are visible in reflected light with characteristic color patterns that are determined by thickness.

Two distinctly different coating systems are used for this function. Pyrolytic applications use tin oxide or similar alloys, which are applied to a glass substrate at around 1000°F. This temperature is near the softening point of glass and is normally accomplished in conjunction with forming and tempering processes. The process is only applicable to thermally tempered glass and cannot be used on chemically tempered glass or plastic. Although other metallic alloys, such as indium oxide, have now been developed that can be applied to tempered glass at about 500°F, vacuum deposition techniques must be used for plastic materials. Gold is one of the materials traditionally used in this process. The gold may be used as part of a coating stack that incorporates metal-oxide film on either side of the gold. These stacks act to modify conduction, thus changing the resistivity limits. They also optically "antireflect" the gold. Also used in conjunction with conductive coatings are base coats, top coats, and primers. These additional film elements are required in order to enhance adhesion, to mask substrate surface scratches, and to offer processing protection to the conductive film.

The coating materials differ in electrical resistivity and light transmission. Film characteristics, such as thickness, transmittance, and reflectance, are normally related to resistivity.

18.8 Coating Resistivity

Resistivity for electrically conductive coatings is measured in terms

of ohms per square. This is a nondimensional measurement and applies to any size of square. That is, the number of ohms remains the same regardless of the area, be it square inches or square miles. This can be explained by considering a square element of coating such as that shown in Figure 18-1. The electrical resistance to a current flowing in the direction shown is directly proportional to the length and inversely proportional to the width and thickness of the element.

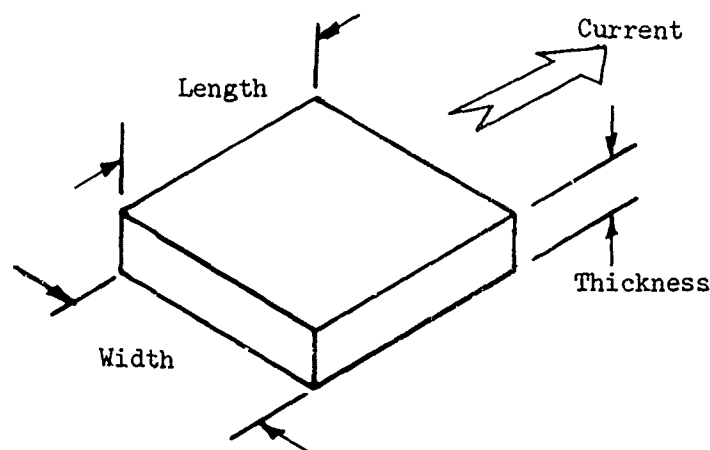


Figure 18-1. Resistivity of a Square Shape.

The resistance will not change if the area of the square is increased or decreased while the thickness is held constant because any change in resistance due to increasing or decreasing the length of the square is exactly offset by a corresponding increase or decrease in width. Varying coating thickness, then, is the means of controlling resistance.

The resistivity of any coated rectangular panel is the value of the bus-to-bus resistance, expressed in ohms, divided by the number of squares whose sides are equal in length to the bus bar's width that will fit into the panel. In equation form:

$$r = RW/L \quad (18-1)$$

where

r	=	resistivity (ohms/square)
R	=	bus to bus resistance (ohms)
L	=	bus-bar spacing
W	=	bus-bar width

Two examples of this calculation are shown in Figure 18-2. For irregular panels, such as trapezoids and rhomboids, or panels with curved edges, the resistivity must be varied over the surface area if a uniform power dissipation is required. For simple tapered panels, the resistivity variation can be calculated using voltage, power, and geometry relationships, whereas complex shapes require either analog computer or laboratory development techniques (electrolytic plotting tank) to establish proper patterns. In general, nonrectangular shapes requiring gradient coatings are more difficult to manufacture with consistency than uniformly coated panels.

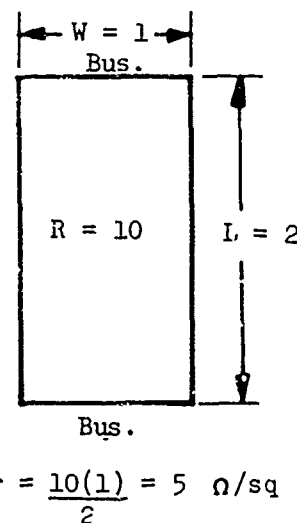
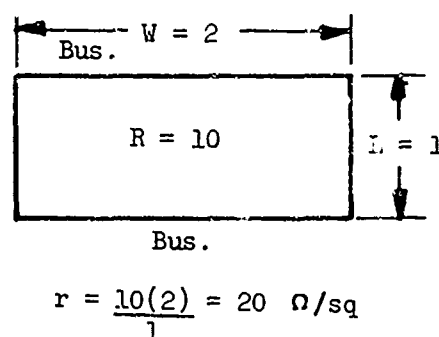


Figure 18-2. Sample Resistivity Calculations.

Application of electrically conductive coatings may be accomplished on flat or curved panels. For curved panels, it is preferable to apply the coating to the concave surface. The typical bus-to-bus resistance tolerance for coated panels is $\pm 15\%$.

The approximate range of resistivities for some currently available coatings is shown in Table 18-1. The manner in which coating resistivity effects light transmittance is shown for a typical coating in Figure 18-3.

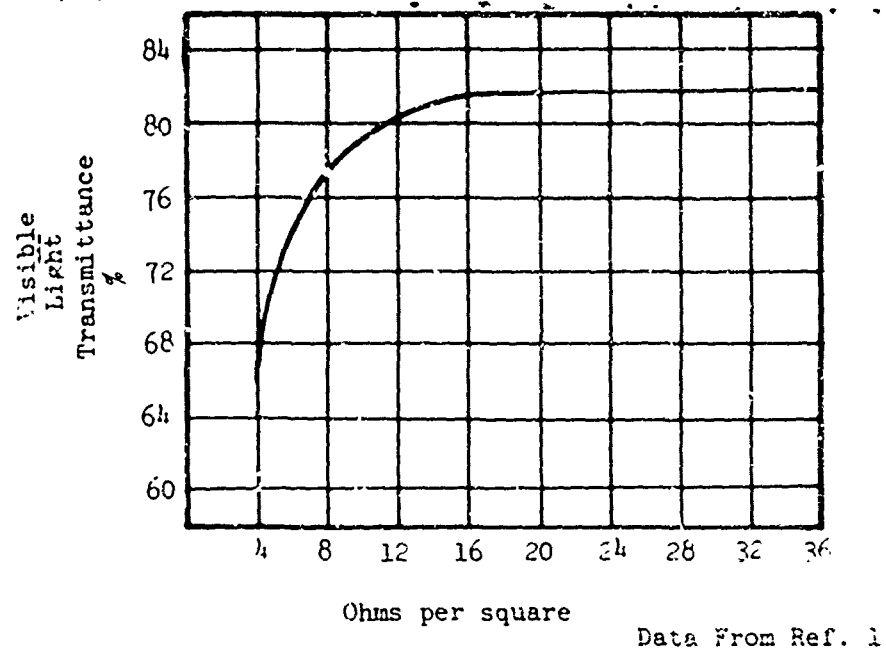


Figure 18-3. Light Transmission Versus Resistivity, Sierracin S-343 Coating.

TABLE 18-1. COATING RESISTIVITY

Coating	Resistivity Range (Ohms/Square)
Tin Oxide	20-250
Sierracin S-3	8- 30
Sierracin S-343	3- 30
Triplex Hyviz*	6-100
Swedlow SS-6295	8- 25
Nesatron Glass*	10-1000

Data from Ref. 3,4,5,6,7

*Trademark - Triplex Safety Glass Co., Ltd.
 **Trademark - PPG Industries

18.9 Solar and Infrared Shielding

Reflective coatings may be used to reduce the amount of heat generated in a helicopter from solar radiation. On small helicopters, solar radiation can cause about half of the total heat load, and attenuation of this incident energy can be of significant advantage in lowering interior temperatures and may permit the size of the environmental control system to be reduced.

The spectrum of solar radiation is shown in Figure 18-4. The distribution of radiant energy is approximately 8% ultraviolet, 45% visible light, and 45% infrared. The ideal solar shield would transmit no less than 70% of the visible light and reflect 100% of the UV and IR radiation. This is in contrast to tinted plastics, which merely prevent the transmission of certain colors and hence restrict a very limited amount of energy from being transmitted. The visible color spectrum is shown in Figure 18-5. For heat rejection purposes, reflectance is considered preferable to absorption since absorbed energy causes heating of the material and subsequent partial transfer of this heat into the aircraft by reradiation, convection, and conduction.

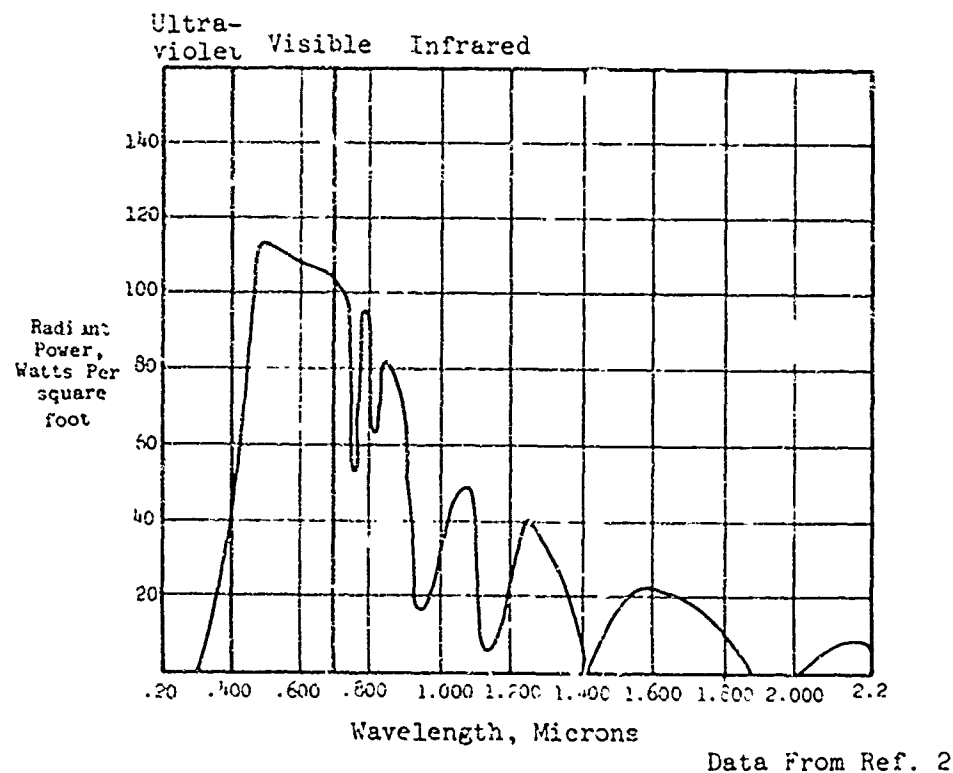


Figure 18-4. Spectral Distribution of Solar Radiant Power at Sea Level Perpendicular to the Sun's Rays.

A curve showing percent of terrestrial solar transmittance for wavelengths between .395 microns and 2.55 microns versus visible light transmittance of a Sierracin S-343A coating is shown in Figure 18-6.

One consequence of increased reflectance that must be considered is an undesirable mirror-like appearance of the coating that can accentuate cockpit glare or external glint signatures. For comparison, glass has a visible reflectance of 4%.

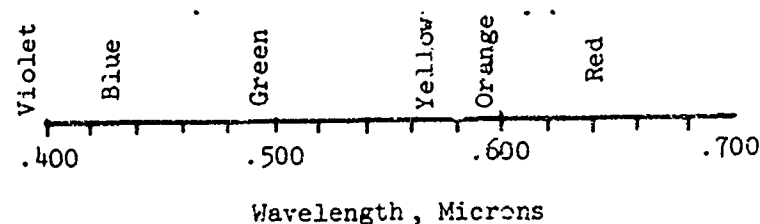
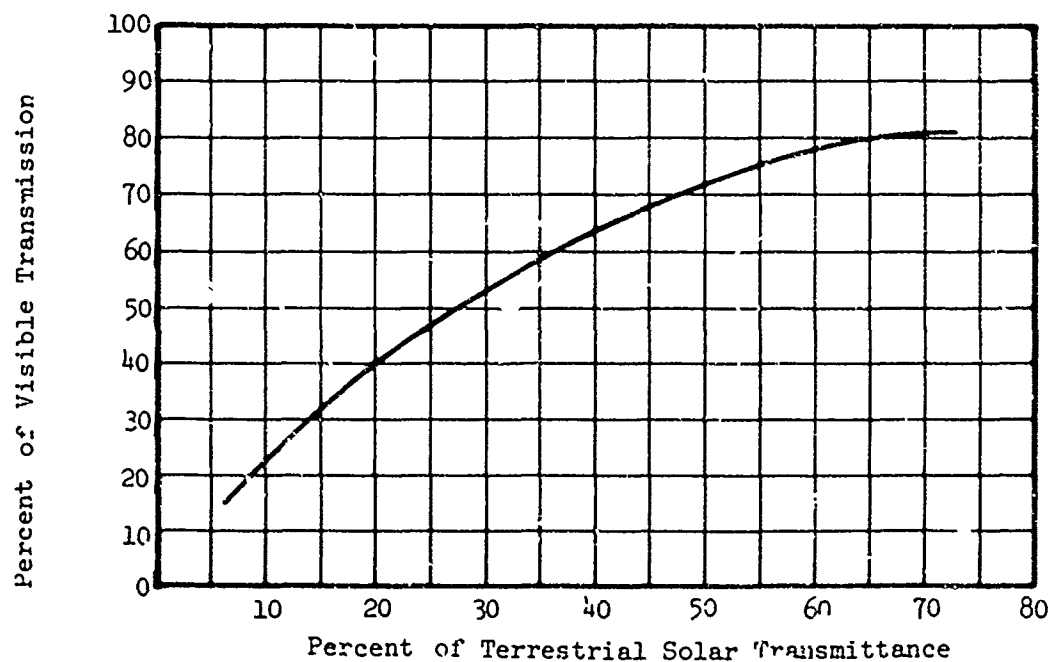


Figure 18-5. Visible Light Spectrum.



Data From Ref. 1

Figure 18-6. Shielding of Solar Radiation for Sierracin S-343A Coating.

References

1. Bright, C. I., "Solar Shielding Performance of Sierracin Coating," RD-13-71, Sierracin Corp., Sylmar, Calif., Jan. 1971.
2. Forthyns, W. E., "Smithsonian Physical Tables," Smithsonian Institute, Washington, D. C., 1959.
3. Slatky, J. E., "The Properties of Sierracote," WADC-TR-57-421, Wright Air Development Center, Wright-Patterson Air Force Base, Ohio.
4. Grove, D. R., "Coatings on Transparent Materials for Aerospace Enclosures. A Summary of the State-of-the-Art," WADC-TR-65-212, Air Force Materials Laboratory, Wright-Patterson Air Force Base, Ohio.
5. King, R. D., Triplex Safety Glass Ltd., "Triplex Hyviz - A High Light Transmission and Electrically Conducting Film for Aircraft Windscreen," Aircraft Engineering, Apr. 1972.
6. "Vacuum Deposited Thin Films," TB-73-200, Swedlow, Inc., Garden Grove, Calif., Mar. 1973.
7. "Nesatron Glass," PPG Industries, PPS n-2, Huntsville, Ala.

Bibliography

Hassard, R. S., Goodyear Aerospace Corp., "Plastics for Aerospace Vehicle Part II Transparent Glazing Materials," MIL-HDBK-17A, Part II (Proposed Revision), Air Force Materials Laboratory, Wright-Patterson Air Force Base, Ohio, Jan. 1973.

Miller, P. A., "Anti-Icing Aspects of Helicopter Windshield Design," Sierracin Corp., Sylmar, Calif., May 1972.

"Transmittance and Exposure Stability of Colorless Plexiglas Cast Sheet," PL-53h, Rohm & Haas Co., Philadelphia, Pa., June 1973.

Nixon, G., Swedlow Inc., "Vacuum Deposited Electrically Conductive Coating Design," AFML-TR-73-126, Air Force Materials Laboratory, Wright-Patterson Air Force Base, Ohio, June 1973.

Shelton, R. C., Swedlow, Inc., "Development of the Windshield for the B-1 Aircraft," AFML-TR-76-54, Air Force Materials Laboratory, Wright-Patterson Air Force Base, Ohio, Apr. 1976.

Lawrence, J. H., Douglas Aircraft Co., "Windshield Technology Demonstrator Program," AFFDL-TR-77-1, Air Force Flight Dynamics Laboratory Wright-Patterson Air Force Base, Ohio, Sept. 1977.

19.1 Weathering

Exposure to natural elements promotes the degradation of certain types of transparent materials. The elements that cause degradation, either singly or in combination, are sunlight, temperature, moisture, wind and atmospheric-borne abrasives and contaminants. Of these, the most damaging factor is the ultraviolet portion of sunlight. Ultraviolet radiation causes photochemical reactions in some materials that alter physical properties. Exposure to high temperatures can cause slow evaporation of plasticizers, which ultimately embrittles the material. These effects are cumulative.

Glass does not deteriorate from exposure to natural weathering, while most plastic materials are affected to varying degrees.

Mechanical strength properties of acrylic and polycarbonate materials are only slightly degraded by exposure to natural weathering, although significant reductions in izod strength have been noted for polycarbonate. Likewise, optical clarity, as measured by visible light transmittance, and haze are also affected. Haze in acrylic and polycarbonate materials can be expected to increase one or two percent after prolonged exposure. Yellowing of polycarbonate also becomes apparent after six months to a year of exposure to ultraviolet light.

Abrasion-resistant coatings are particularly susceptible to deterioration from exposure to the combination of high temperature, high humidity and sunlight. Failure mechanisms differ with coating type and substrate. The following failure modes have been observed after accelerated weathering tests on different hardcoat materials.

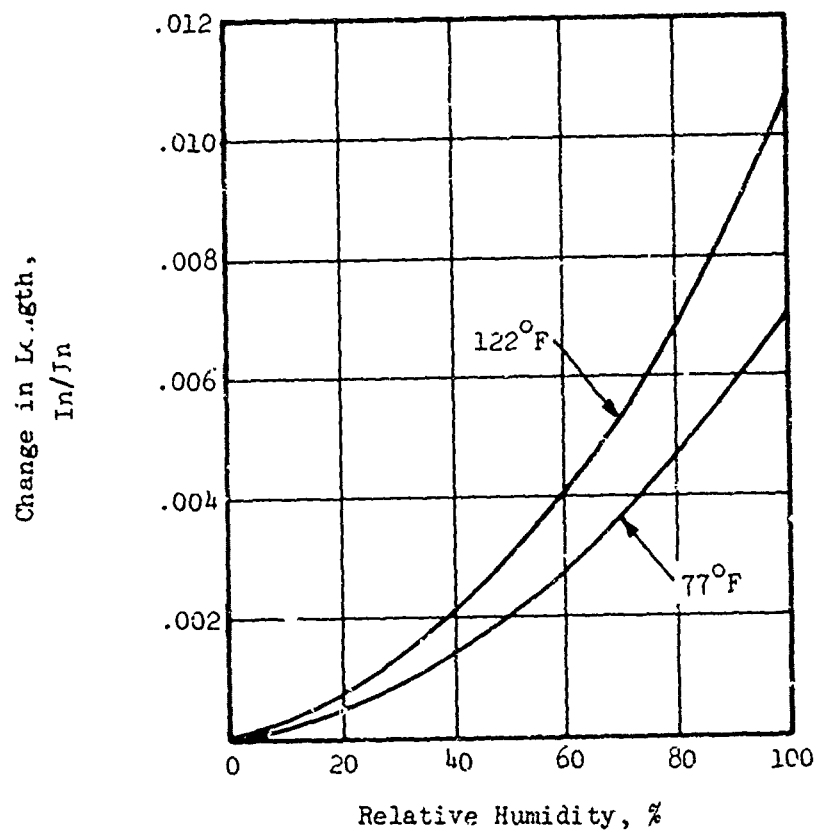
- a) Loss of adhesion
- b) Cracking of the hardcoat
- c) Clouding or excessive haze
- d) Loss of abrasion resistance

19.2 Moisture

Acrylic, polyester, and polycarbonate materials are hygroscopic materials and can absorb moisture to the extent shown in Table 16-5. While this absorption has negligible effects on the mechanical properties of the material, two of the side effects may be of interest.

After prolonged exposure to high humidity at elevated temperatures, moisture can permeate hygroscopic facings on laminated panels to ultimately reach the interlayer. This moisture can lead to delamination for certain types of interlayer materials unless suitable barrier coats or other preventative measures are employed.

The other noteworthy effect of moisture absorption is the expansion or the contraction of the material. These dimensional changes occur in a manner similar to thermal expansion except that the changes do not occur instantaneously, but require several days to reach equilibrium. When changing from one equilibrium condition to another, if the humidity change is small (10% to 30% relative humidity differential) the major part of the dimensional change will occur within 15 to 30 days. If the humidity change is large (60 percent relative humidity differential), two months or longer may be required to reestablish dimensional equilibrium. The sizes of these dimensional changes are of the same magnitudes as those encountered during thermal expansion. Figure 19-1 shows the rate of humidity expansion versus relative humidity for Plexiglass 55.



Data From Ref. 1

Figure 19-1. Humidity Expansion of Plexiglass 55.

19.3 Chemical Resistance

The chemical resistance of transparent materials is of interest because of the potential for damage due to contact with fluids and vapors associated with helicopter maintenance and operations. The damage attributed to chemical attack can take the form of crazing, clouding, or the dissolving of material. Stress-solvent crazing is a typical failure mode in which the material, when stressed in tension, will develop crazing in the presence of certain chemicals. Time to craze, chemical concentration, and stress level are all interrelated variables for this phenomenon.

Glass is essentially unaffected by most chemicals encountered in helicopter operations, while plastic materials are susceptible to chemical attack in varying degrees.

Acrylic is unaffected by most inorganic solutions, mineral and animal oils, and low concentrations of alcohol. Oxidizing acids affect the material only in high concentrations. Lower esters, aromatic hydrocarbons, phenols, aryl halides, aliphatic acids, and alkyl polyhalides usually have solvent actions.

Polycarbonate has very poor chemical resistance to many substances found in an aircraft environment. The material has good resistance at room temperature to water, dilute inorganic and organic acids, solutions of neutral and acid salts, vegetable oils, aliphatic hydrocarbons, ethers, and alcohols. But polycarbonate is readily dissolved by certain halogenated solvents such as methylene chloride, dichlorethane, and chloroform. Plasticization and crystallization can result from contact with partial solvents such as low molecular-weight aldehydes and ethers, ketones, esters, aromatic hydrocarbons, and perchlorinated hydrocarbons. The material may be partially or completely destroyed by alkali, alkali salts, amines, or ozone.

Polycarbonate's low tolerance to chemical attack can be substantially improved by protective coatings. Typically, such coatings are those used to enhance abrasion resistance.

Cast polyester is more resistant to chemical attack than either acrylic or polycarbonate. The material has good stress-solvent crazing properties when tested with isopropyl alcohol or lacquer thinner.

A tabulation showing some of the common chemicals that can damage plastic glazing materials is shown in Table 19-1.

TABLE 19-1. CHEMICALS THAT CAN DAMAGE PLASTIC GLAZING MATERIALS

Solvent	MIL-P-5425 Cast Acrylic	MIL-P-8184 Modified Cast Acrylic	MIL-P-8257 Polyester	MIL-P-25690 Stretched Acrylic	MIL-P-83310 Polycarbonate
Isopropyl Alcohol	X	X	0	X	0
Methyl Ethyl Ketone	X	X	0	X	X
Toluene	X	X	0	X	X
Acetone	X	X	X	Y	X
Lacquer Thinner	X	X	*	X	X
Strong Acids	X	X	*	X	X
Esters	X	X	*	*	X
Hydraulic Fluid	*	*	*	*	X
JP-4 Jet Fuel	*	*	*	*	X

Data from References 2, 3

X = Will attack

0 - No reaction

* - No data

References

1. "Thermal and Differential Bowing," PL-72e, Rohm and Haas Co., Philadelphia, Pa.
2. Hassard, R. S., Goodyear Aerospace Corp., "Plastics for Aerospace Vehicles Part II Transparent Glazing Materials," MIL-HDBK-17A, Part II (Proposed Revision), Air Force Materials Laboratory, Wright-Patterson Air Force Base, Ohio, Jan. 1973.
3. James, H. C., et al, Goodyear Aerospace Corp., "Design, Test and Acceptance Criteria for Army Helicopter Transparent Enclosures," USSAAMP:DL-TR-73-19, U. S. Army Air Mobility Research and Development Laboratory, Ft. Eustis, Va., May 1973, AD 767242.

Bibliography

Hassard, R. S., Goodyear Aerospace Corp., "Design Criteria Transparent Polycarbonate Sheet," AFML-TR-72-117, Air Force Materials Laboratory, Wright-Patterson Air Force Base, Ohio, Aug. 1972.

Voss, D. L., Sierracin Corp., "Protective Coatings," AFML-TR-73-126, Air Force Materials Laboratory, Wright-Patterson Air Force Base, Ohio, June 1973.

"Plexiglas Design & Fabrication Data," PL-229L, Rohm & Haas Co., Philadelphia, Pa.

Wiser, G. L., Sierracin Corp., "New Materials in Aircraft Windshields," 700862 Society of Automotive Engineers, Oct. 1970.

McDonald, W. C., and Huyett, R. A., Goodyear Aerospace Corp., "Window Contoured Glass/Plastic Transparent Armor for the UH-1D Helicopter," AMMRC-CTR-75-12, Army Materials and Mechanics Research Center, Watertown, Mass., May 1975.

ABRASION

Field service has demonstrated that the most prevalent problem with Army helicopter windshields is abrasion and the resultant loss of transparency. Abrasion damage is caused by rubbing or particle impingement, and occurs in a number of different ways, some of which are enumerated below.

Windshield wipers are one of the main causes of abrasion because of their propensity to oscillate with abrasive particles trapped between their blades and the windshield surface. Figure 20-1 shows a severe example of the type of damage that results from windshield wipers used in conjunction with plastic-faced windshields.



Figure 20-1. Windshield Wiper Abrasion Damage.

Other forms of rubbing abrasion are random in nature and include improper cleaning techniques and contact with hard objects.

Blowing sand and dust found in sandstorms or induced by rotor downwash are the more aggressive forms of impingement abrasion. Hail and ice crystals will not normally damage helicopter transparencies because of relatively low impingement velocities. However, specialized coatings applied to exterior surfaces are subject to attack by these elements and, in some cases, can even be eroded by rain or water from high pressure hoses used to wash aircraft.

20.1 Effects of Abrasion

The most pronounced effect of abrasion is the change in reflected light. Random abrasion, such as the scratches and gouges in Figure 20-2, may be considered generally distracting to flight crews. The intensity of scratches in transparent materials can be quantified by comparison to specially prepared scratch specimens. ASTM-F428 Glass Scratch Standards are available for this purpose.



Figure 20-2. Random Scratching of Transparent Plastic.

When the surface damage becomes widespread, consisting of many closely spaced fine scratches, pits or surface indentations, the surface will scatter or diffuse transmitted light, which can then be quantified by haze measurement.

Structural integrity and impact resistance are also degraded by the presence of scratches. However, the loss in strength is normally compensated for by reducing the allowable stresses used for design.

20.2 Abrasion Resistance

Commonly used aircraft glazing materials are ranked in order of their abrasion resistances and surface hardnesses in Table 20-1. The Mohs' hardness values are based on the ability of a material to scratch or be scratched by certain standard materials listed on the Mohs' scale. For example, a relatively soft mineral such as pure copper, which has a value of 3.0 on the Mohs' scale, would be capable of scratching acrylic, whereas hardened steel (Mohs' > 6) would be required to scratch glass.

TABLE 20-1. RANKING OF TRANSPARENT MATERIALS FOR ABRASION RESISTANCE

Rank	Material	Mohs' Scale Hardness
1	Glass	6
2	Polyester (CR-39)*	3.25
3	Acrylic	2.25
4	Polycarbonate	2.0

* Trademark - PPG Industries Data from Reference 1

20.3 Abrasion Protection

The low abrasion resistance of plastic materials can be improved through the use of protective coverings. The most effective protection is obtained by laminating a glass facing over the plastic. This function requires a minimum of 0.085 inch of glass. The resulting composite will be considerably heavier and more complex than equivalent strength monolithic plastic; therefore, this type of construction is useful only for applications that would require laminated construction for other reasons, such as for windshield heating.

Lightweight abrasion protection is possible through the use of organic polymer coatings. These hardcoats are proprietary formulations, and are applied by suppliers using processes such as flow or dip coating. Typical coating thicknesses range from 0.002 to 0.004 inch, and their Mohs' hardnesses generally do not exceed 3.5.

Light transmission through a coated panel is slightly improved due to the favorable refractive indexes of typical coatings and the covering of minute scratches in the substrate. In addition, resistance to chemical attack is usually enhanced by these hardcoats, a trait that is particularly important for polycarbonate materials. On the debit side: hardcoats are not field repairable, and attempts to blend or smooth surface scratches will result in more pronounced blemishes.

20.4 Operational Durability

The hardness of a material is only one criterion for determining its susceptibility to abrasion. Wear also depends on the following characteristics:

- Ductility and elasticity of the substrate material
- Type of abrading medium
- Frictional forces between the abrasive and the transparency
- Thickness of coating

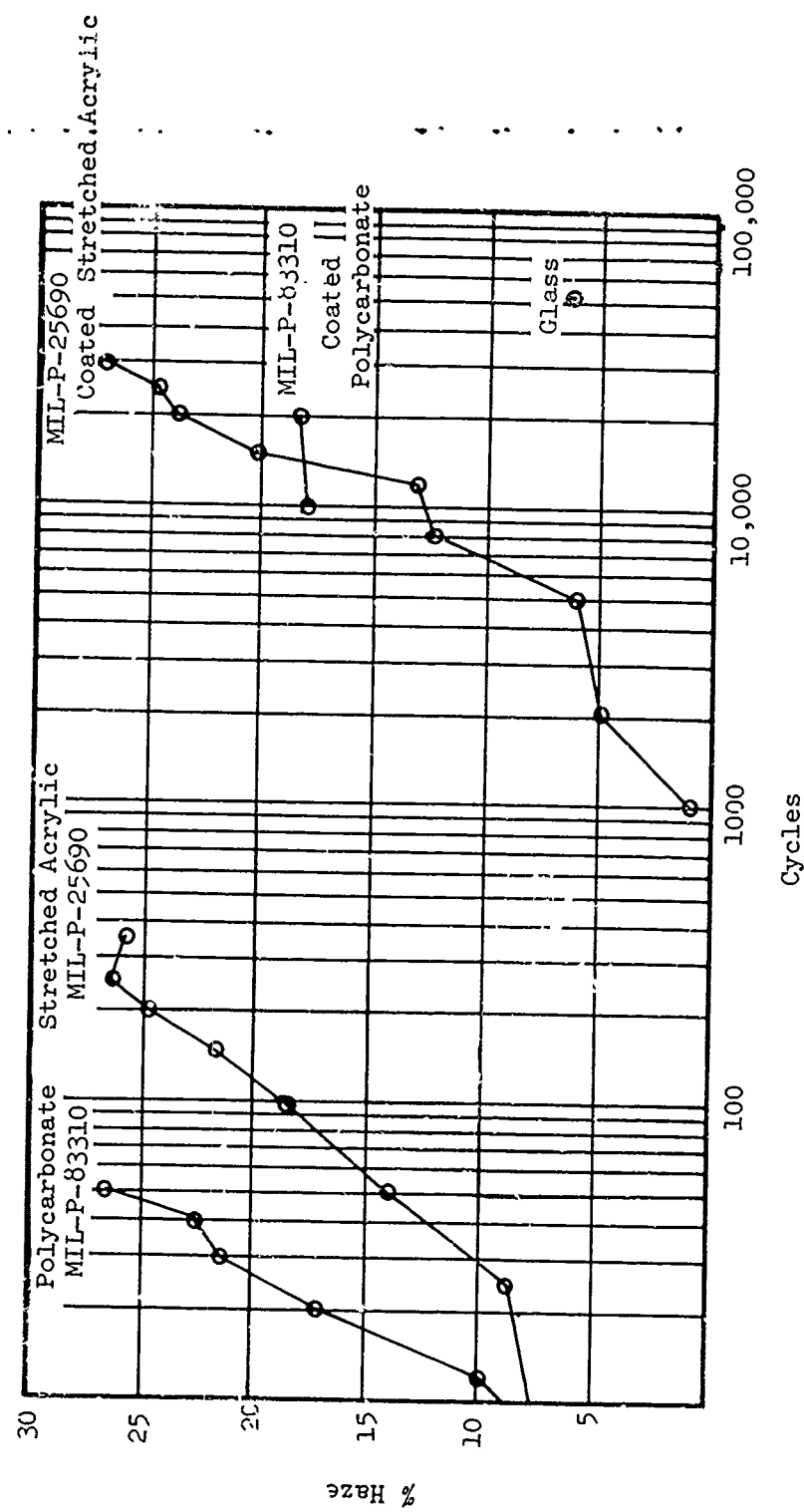
The effects of these parameters on wear characteristics can only be obtained by testing. In order to be meaningful, data for ranking abrasion resistance of transparent materials should be obtained from tests that simulate conditions representative of the actual service environment. For helicopters, this includes primarily windshield wiper action, hand wiping by crew, and sand impingement. Unfortunately, uniform test standards to simulate these do not exist, and test methods vary considerably throughout industry. In addition, the test methods that do exist yield considerable scatter in test results, partially due to test procedures, and partially due to the nature of the abrading phenomena. For these reasons, it is difficult to confidently compare data obtained from different sources or to use such data for projecting actual service lives.

Windshield wiper test data is presented in Figure 20-3 that shows the deterioration of optical quality due to windshield wiper operation on dirty windshields. This test method, which is described in detail in the Qualification Tests section of this handbook, uses an abrasive slurry to simulate the effects of dirt. However, it should be noted that the test data was obtained with the wipers operated at 100 cycles per minute, whereas the recommended test method specifies 160 cycles per minute. Windshield wiper testing is recommended for evaluating durability of windshield materials.

The dry rubbing abrasion data presented in Figure 20-4 is representative of the type of damage caused by wiping transparencies with dirty rags. This test method is also described in detail in the Qualification Tests section of this handbook, and is recommended for use as a means to compare the abrasion resistance of different materials.

As evidenced by this test data, glass material is shown to be vastly superior to hardcoated plastics, and is virtually unaffected by windshield wiper or other cleaning operations.

Figure 20-5 shows test data from a falling sand test that was conducted in accordance with ASTM-D-673-70, which measures the effect of impingement by silicon carbide abrasive particles. Here, after prolonged exposure, hardcoated materials show performance superior to glass, thus indicating that, for some abrading mediums, a certain amount of ductility is desirable.



Data From Ref. 2

Figure 20-3. Windshield Wiper Abrasion Test Results.

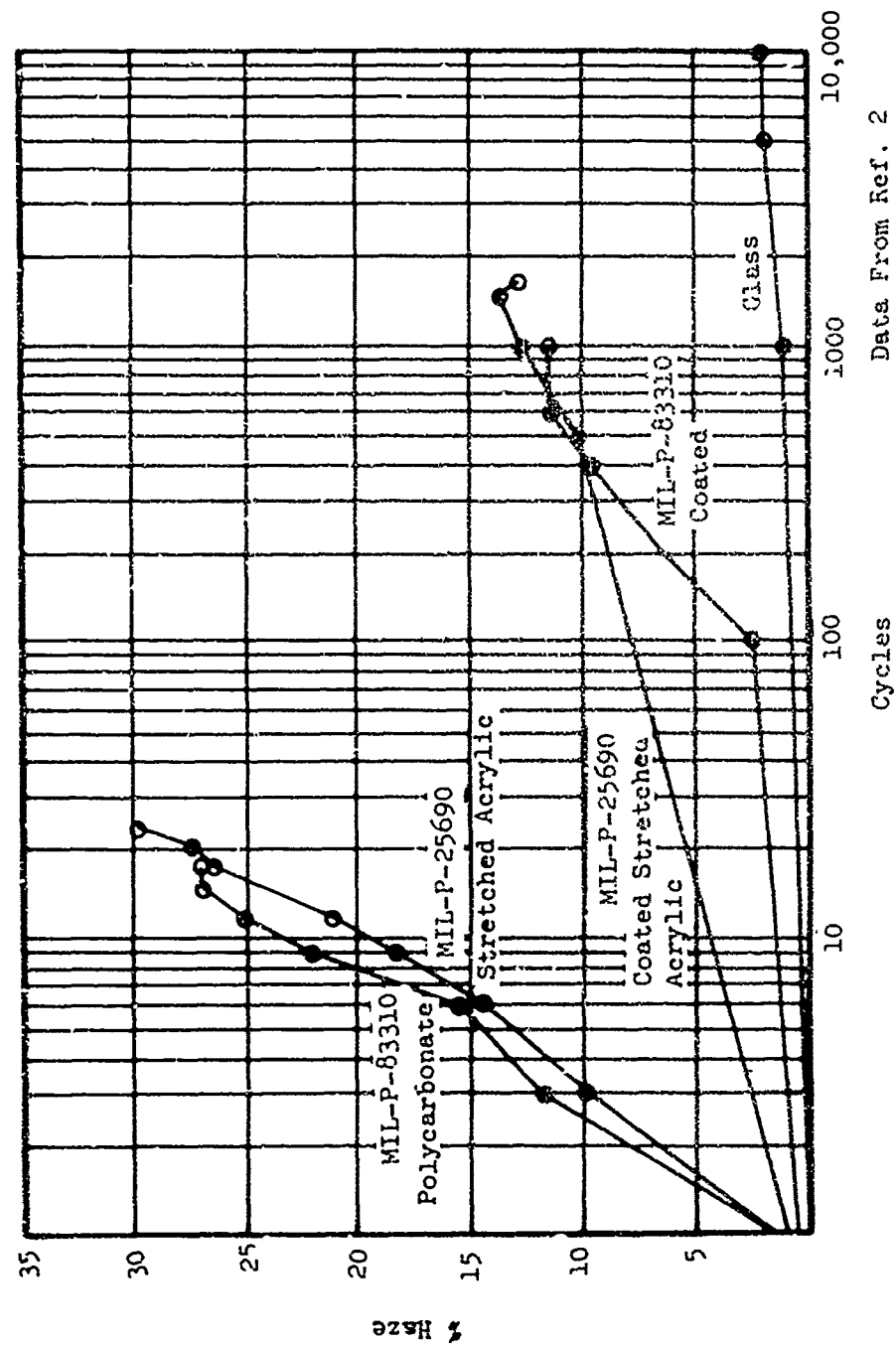
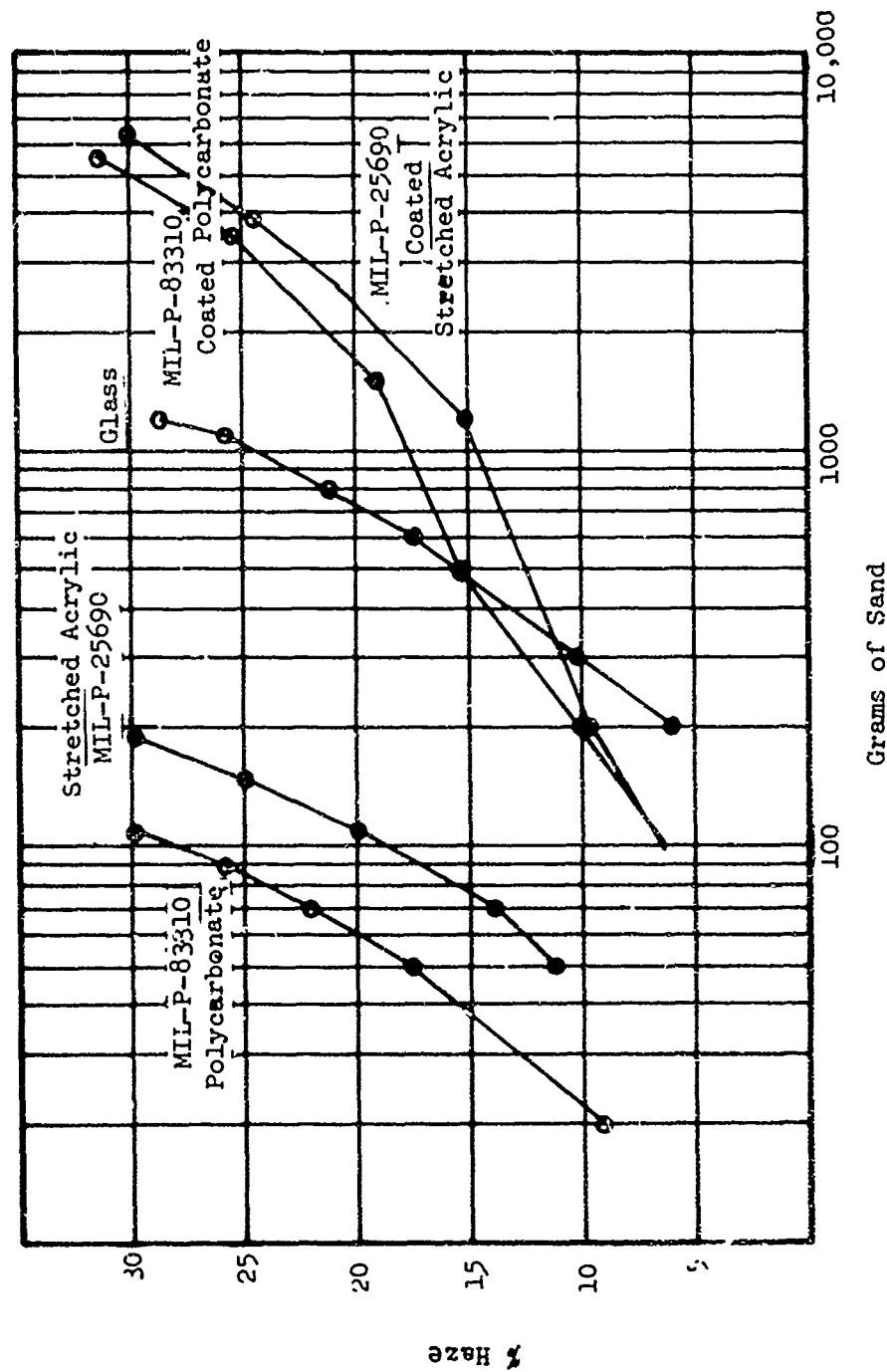


Figure 20-4. Dry Rubbing Abrasion Test Results.



Data From Ref. 2

Figure 20-5. Falling Sand Test Results.

Correlation of the falling sand test to actual service experience is difficult because this wear mode is rare in comparison to other forms of abrasion. However, some estimation of the severity of the test can be obtained by calculating the flux of the impinging sand particles and comparing it to Army specifications for density of blowing sand, which is 0.1 gm/ft^3 . Using this approach, 1 gram of falling sand can be roughly equated to 4 minutes' exposure to blowing sand at 7.5 mph.

To further put this data into perspective, an increase in haze of 10% was measured for the stretched acrylic material after exposure to 50 gm of falling sand, which might be likened to 3 hours' exposure to dense blowing sand. When one considers that a sand storm can induce higher impingement velocities, not to mention the flight speed through the storm, the hazard can be fully appreciated. Note that the kinetic energy of the impinging particles is proportional to the square of their velocities. It is felt that the reason impingement abrasion damage to helicopter transparencies has not been documented as a serious problem is that there has been only minimal exposure to conducive environments. In addition, the ASTM 673-70 test abrasive, silicon carbide, is harder than silicon dioxide common sand, which tended to increase the amount of haze experienced in the test.

20.5 Abrasion Resistant Hardcoats

The application of hardcoats to acrylic and polycarbonate can significantly improve their tolerances to abrasion. However, the variations in effectiveness are considerable between different formulations and processes. For example, the data in Table 20-2 shows this relative performance, as measured by increase in haze level, of 13 coating/substrate combinations after 2,000 cycles of windshield wiper abrasion testing. It should be noted that this tabulation is by no means complete and is presented only for illustrative purposes. Coating suppliers are continuously improving and modifying formulations, and they should be consulted during material evaluation studies to obtain current information.

TABLE 20-2. HAZE LEVEL AFTER 2,000 CYCLES OF WINDSHIELD WIPER
ABRASION FOR VARIOUS HARDCOATED MATERIALS

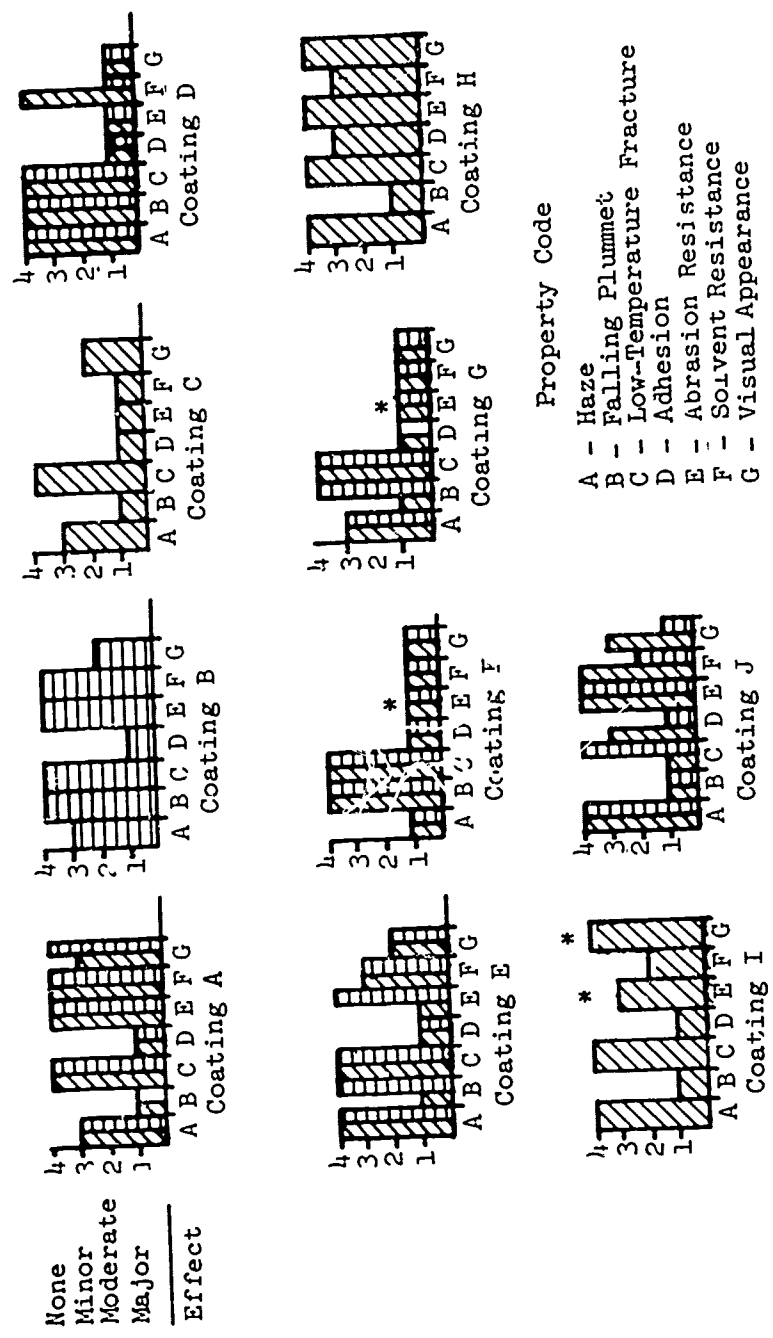
Substrate	Coating	Supplier	Haze (%)
MIL-P-5425 Cast Acrylic	Abcite	Dupont	6.9
MIL-P-5425 Cast Acrylic	Armor Clad	Symbolic Display	9.7
MIL-P-25690 Stretched Acrylic	SS-6426ARC	Swedlow	7.9
Acrylic, as cast	311	Sierracin	12
Polycarbonate	Abcite	Dupont	3.9
Polycarbonate	Abcite	Goodyear	5.9
Polycarbonate	#100-35	Astro Research	28.0
Polycarbonate	ESB	ESB Corp.	19.4
Polycarbonate	MR-4000	General Electric	34.00
Polycarbonate	Mobay	Mobay Chemical	24.2
Polycarbonate	SS-6432	Swedlow	13.4
Polycarbonate	Texstar	Sierracin	8.1

Data from Ref. 4

In addition to abrasion resistance, hardcoats must also be capable of resisting the same aggressive environments to which the helicopter is exposed without suffering deleterious effects. This point is extremely important, since noncompliance can render the cure worse than the disease.

To illustrate, Figure 20-6 shows the effects of nine months of exposure to outdoor weathering on 10 different materials coated on polycarbonate substrates. The figure shows that all of the coatings evaluated suffered some loss of adhesion. In addition, other properties, such as haze, impact resistance, abrasion resistance, solvent resistance and visual appearance, showed varying levels of degradation. Coated acrylic has somewhat better resistance to weathering than coated polycarbonate.

Temperature, humidity, and ultraviolet radiation may be singled out as the most damaging components of natural weathering. Temperature extremes give rise to large thermal strains in acrylic and polycarbonate, and unless the coating is sufficiently ductile to accommodate such strain, coating failure, such as cracking and loss of adhesion, will result. Ultraviolet radiation and humidity can promote photo-chemical reactions affecting physical properties as well as adhesion. In this regard, coatings applied to the interior transparency surfaces benefit from ultraviolet filtering through the substrate and suffer less degradation.



Legend:

Arizona Exposure

Florida Exposure

* Estimated

Data from Ref. 3

Figure 20-6. Effects of Outdoor Weathering on Coatings (45° Inclination Facing South, Nine-Month Exposure).

References

1. Marks, A. M., Marks Polarized Corp., "Superhard Transparent Coatings," USAAMRDL-TR-75-22, U. S. Army Air Mobility Research and Development Laboratory, Fort Eustis, Va., Apr. 1975, AD A010388.
2. Kay, B. F., Sikorsky Aircraft Division, "Design, Test, and Acceptance Criteria for Army Helicopter Transparent Enclosures," USARTL-TR-78-26 (AVRADCOM) Applied Technology Laboratory, U. S. Army Research and Technology Laboratories, Fort Eustis, Va., 1976.
3. Wintermute, G. E., et al, Goodyear Aerospace Corp., "Environmental Resistance of Coated and Laminated Polycarbonate Transparencies," ARML-TR-76-54, Air Force Materials Laboratory, Wright-Patterson Air Force Base, Ohio, Apr. 1971.
4. Plumer, J. R., "Development of Scratch- and Spall-Resistant Windshields," AMMRC-TR-74-19, Army Materials and Mechanics Research Center, Watertown, Mass., Aug. 1974.

Bibliography

Hassard, R. S., Goodyear Aerospace Corp., "Design Criteria - Transparent Polycarbonate Sheet," ARML-TR-72-117, Air Force Materials Laboratory, Wright-Patterson Air Force Base, Ohio, Aug. 1972.

James, H. C., et al, Goodyear Aerospace Corp., "Design, Test, and Acceptance Criteria for Army Helicopter Transparent Enclosures," USAAMRDL-TR-73-19, U. S. Army Air Mobility Research and Development Laboratory, Fort Eustis, Va., May 1973, AD 767242.

Hassard, R. S., Goodyear Aerospace Corp., "Plastics for Aerospace Vehicles, Part II, Transparent Glazing Materials," MIL-HDBK-17A, Part II (Proposed Revision), Air Force Materials Laboratory, Wright-Patterson Air Force Base, Ohio, Jan. 1973.

McNaughton, I. I., Ministry of Defense, U. K., "Hail Impact on Aircraft Transparencies," AFML-TR-73-126, Air Force Materials Laboratory, Wright-Patterson Air Force Base, Ohio, June 1973.

Tarnopol, M. S., PPG Industries, Inc., "PPG Salt Blast Abrader for Aircraft Plastic Windshields," AFML-73-126, Air Force Materials Laboratory, Wright-Patterson Air Force Base, Ohio, June 1973.

Voss, D. L., Sierracin Corp., "Protective Coatings," AFML-TR-73-126, Air Force Materials Laboratory, Wright-Patterson Air Force Base, Ohio, June 1973.

"Lucite AR Abrasion Resistant Sheet," A-99511, E. I. DuPont De Nemours & Co., Wilmington, Del., June 1974.

Miller, W. A., Sierracin Corp., "Aircraft Transparency Applications of Polycarbonates," Society of British Aircraft Companies, London, England, June 1971.

Fisher, K. J., "Windshield Wiper Tests on Plastic-Faced FAR Part 25 Windshield," ER-73-017, Sierracin Corp., Sylmar, Calif., Dec. 1973.

Knighton, J. L., "Sierracin HC-2 Protective Coating," ER-71-013, Sierracin Corp., Sylmar, Calif., Nov. 1971.

Schmitt, G. F., Air Force Materials Laboratory, "Rain Droplet Erosion Effects on Transparent Plastic Material," SAMPE Journal, Mar.-Apr. 1974.

"Tough New Composites: Plastics Faced with Glass Microsheet," Machine Design, July 1975.

Voss, D. L., Sierracin Corp., Sylmar, Calif., "Polycarbonate Protection," AFML-TR-76-54, Air Force Materials Laboratory, Wright-Patterson Air Force Base, Ohio, Apr. 1976.

McGarvey, J. H., and Kay, B. F., Sikorsky Aircraft Division, "Design and Development of Helicopter Transparent Enclosures," AFML-TR-76-54, Air Force Materials Laboratory, Wright-Patterson Air Force Base, Ohio, Apr. 1976.

Mahaffey, J. E., PPG Industries, Inc., "Abrasion Testing of Transparent Plastics," Conference on Aerospace Transparent Materials and Enclosures, Long Beach, Calif., Apr. 1978.

Impact characteristics of transparent materials are related to safety and crashworthiness because breakage due to any cause poses a hazard to personnel.

21.1 Material Response to Low Energy Impacts

Standard test data from small-scale izod tests is not easily related to safety criteria, although the data is useful for comparison. Instead, studies of shatter resistance and fracture characteristics use steel balls and darts dropped from a specified height. An impact energy of 20 foot-pounds has been arbitrarily chosen as being representative of foreign object damage (FOD) hazards. This energy level is also sufficient to enable characterization of material shattering effects.

In Reference 1, a series of tests are described wherein a spherically tipped steel dart was used to evaluate the performance of common transparent materials. Test panels were 2 foot square, and subjected to 20 ft-lb impacts. The impact characteristics of the different materials tested are described below.

Polycarbonate and .250 cast acrylic specimens are not damaged by falling dart impacts.

Stretched acrylic panels are undamaged at room and high (150°F) temperature impacts, but at low (-65°F) temperature, the stretched acrylic specimens crack as shown in Figure 21-1. The transverse crack propagation in this material follows stress planes created by the stretching process. This results in fracture edges forming oblique planes. Figure 21-2 shows further detail of a fracture surface of a stretched acrylic sheet.

Laminated glass panels exhibit large numbers of long, fine, radial cracks similar to those seen in Figure 21-3. The panel depicted has .095 semitempered soda lime glass facings and an .075 PVB interlayer. The tendency of the glass to shatter would be unacceptable were it not for the plastic interlayer that retains the glass fragments.

Impacts on laminated glass-acrylic panels also produce a large number of cracks. As with laminated glass, the interlayer serves to hold the fragments of the facing materials.

.080 and .125 cast acrylic panels exhibit the lowest impact strength and are completely penetrated by the 20 ft-lb impact. The dart generally makes a clean entry, leaving radial cracks that close on themselves. Wedge-shaped segments break loose, as shown in Figure 21-4.



Figure 21-1. 0.080-Inch Stretched Acrylic After Low Temperature Dart Impact.

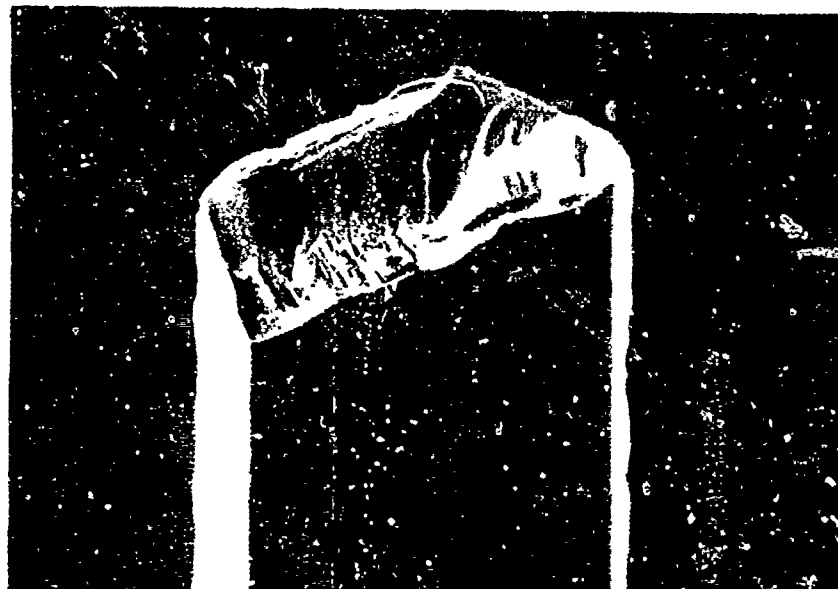


Figure 21 2. Stretched Acrylic Fracture Surface.

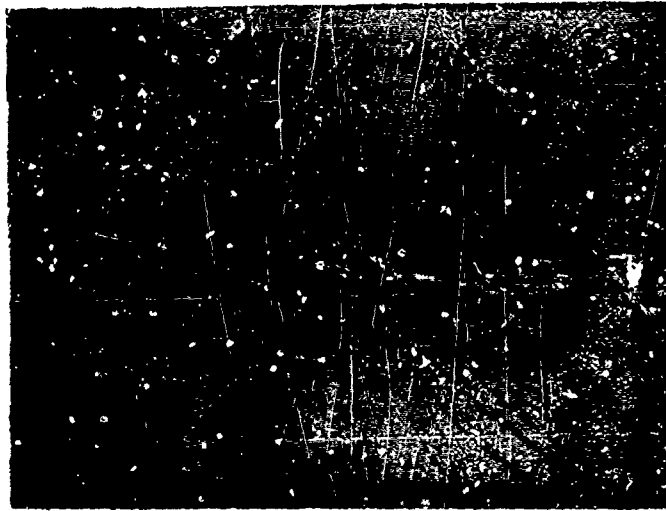


Figure 21-3. Glass-Glass Laminate After Room Temperature Dart Impact.

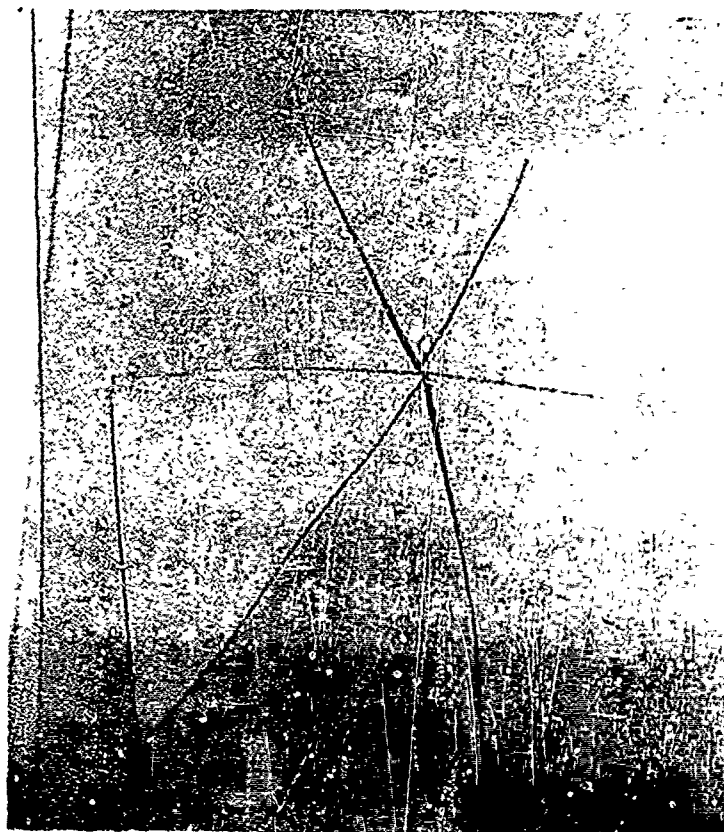


Figure 21-4. 0.080-Inch Cast Acrylic After Room Temperature Dart Impact.

21.2 Temperature and Interlayer Effects on Laminates

The data in Table 21-1 clearly shows the temperature dependence of the impact strength of glass laminated with PVB interlayer. Steel balls were dropped onto laminated glass specimens held at 0°, 75° and 120° F. The critical distance recorded was that height of drop which produced failure of 50 percent of at least 20 specimens. Specimens were judged failures when a hole or continuous tear in the plastic interlayer exceeded 1-1/2 inches. In all cases, performance was best at 75° and worst at 0°. This variation of impact strength with temperature establishes the need to perform impact tests on materials at the temperature extremes to which they will be exposed.

Two more trends are easily seen in the data of Table 21-1: (1) for similar impact conditions, tempered plate glass outperformed plate glass, and (2) impact resistance is directly related to interlayer thickness.

21.3 Fail Safety

After fracture, a transparency should retain enough residual strength to support the operational loads placed upon it. This requirement must be substantiated by tests. For example, a series of tests, described below, were run to determine the residual strengths of the common transparent materials.

A flat, 2-foot-square specimen of each material was penetrated by a .30-caliber round. The entry hole was sealed by a soft rubber gasket and the enclosed volume behind the specimen evacuated to simulate aerodynamic unloading. Laminated glass and glass-acrylic specimens with .075 PVB interlayers were subjected to a pressure differential of 1 psi. Monolithic specimens of .080-in. cast acrylic, stretched acrylic, and polycarbonate were tested at .25 psi, and a .187-in. cast-acrylic specimen was tested at .5 psi. This loading was maintained for 1 minute in order to determine any time-dependent effects.

All of the materials tested had enough residual strength after ballistic penetration to react the simulated aerodynamic loads.

Another study has pointed out the importance of the transparency retention system (Reference 3). A loosely clamped system can allow excessive deflections and the transparency can slip out of its retainer. All structural integrity will then be lost.

TABLE 21-1. EFFECTS OF TEMPERATURE ON IMPACT STRENGTH OF LAMINATED GLASS (PLASTIC INTERLAYER) -
POLYVINYL BUTYRAL CONTAINING 28% DIBUTYL SEBACATE)

Glass Components Used	Plastic Interlayer Thickness (in.)	Weight Steel Ball (lb)	Critical Distance (ft)		
			0°F	75°F	120°F
.109 in. plates	0.015	1/2	18	Greater than 33-1/2	20
.109 in. tempered plates	0.015	1/4	22	Greater than 33-1/2	27
.109 in. plates	0.015	2	2 1/4	5-1/2	4-1/2
.109 in. tempered plates	0.015	2	5-1/2	8	7
.109 in. plates	0.030	2	7-1/2	22	11
.109 in. tempered plates	0.030	2	10	33	15
.109 in. plates	0.045	2	12	Greater than 33	33
.109 in. tempered plates	0.045	2	21	Greater than 33	33

Data from Reference 2

References

1. Kay, B. F., Sikorsky Aircraft Division, "Design, Test, and Acceptance Criteria for Army Helicopter Transparent Enclosures," USARTL-TR-78-26 Applied Technology Laboratory, U. S. Army Research and Technology Laboratories, (AVRADCOM), Ft. Eustis, Va.
2. Hassard, R. S., Goodyear Aerospace Corp., "Plastics for Aerospace Vehicles, Part II Transparent Glazing Materials," MIL-HDBK-17A, Part II, (Proposed Revision) Air Force Materials Laboratory, Wright-Patterson Air Force Base, Ohio, Jan. 1973.
3. Stefancin, T. R., "Helicopter Windshield Design Improvement Program", ER-72-006A, Sierracin Corp., Sylmar, Calif., July 1972.

Bibliography

Pickard, J., Triplex Safety Glass Co., Ltd., "Reduced Laceration from a New Laminated Windshield," Fifth International Technical Conference on Experimental Safety Vehicles, London, June 1974.

Plumat, E., and Glaverbel, S. A., "Today's Innovations and Military Uses in Glass Techniques," Lecture delivered at N.A.T.O., Oct. 1968.

Riley, J. L., "Stretched Acrylic Canopy Program," WADC TR 57-421, Wright Air Development Center, Dayton, Ohio, July 1957.

PPG Industries, "Performance Tests under Simulated Environmental Conditions for Sikorsky YUH-60A Pilot and Copilot Windshield," QTR-1110-01, Oct. 1975.

United States of America Standards Institute, "Safety Code for Safety Glazing Materials for Glazing Motor Vehicles Operating on Land Highways," U.S.A.S. Z26.1-1966 (R 1973), July 1966.

22.0

TRANSPARENCY SUPPORTS

Structural members used to divide transparent enclosures into sections can be classified as primary, secondary, and tertiary structures. The definitions used in this context are as follows

22.1 Primary Structures

These members, in addition to dividing or supporting transparencies, also contribute to the overall bending strength of the fuselage by reacting ground and flight loads. The loads in these elements are based in great part on conditions unrelated to the transparent installation, and they must be sized accordingly.

Ordinarily, the cross section of a primary structure is optimized for weight. This procedure must be modified for members that pass through the pilot's primary field of view. In such cases, the most compact design is desirable and a trade-off between weight and obstruction to vision is in order.

22.2 Secondary Structures

Secondary structures in the cockpit enclosure do not significantly contribute to overall fuselage strength and are used only as framing to support windshields, windows, hatches and doors.

Airloads generally cause these members to be loaded in bending, which creates the need for beam-like structures. Simple channel, Z and I sections may be used as shown in Figure 22-1. When the support is curved or passes through regions where contour changes or when stability is critical, box sections may be required. Box sections are also used to provide torsional rigidity and stiffness for transverse and inplane loads that are applied to close-out members adjacent to cut-outs. Figure 22-2 shows typical box beams. These hollow structural members also offer possibilities for simplifying hot air defog systems by taking advantage of their natural shapes to form integral air ducts.

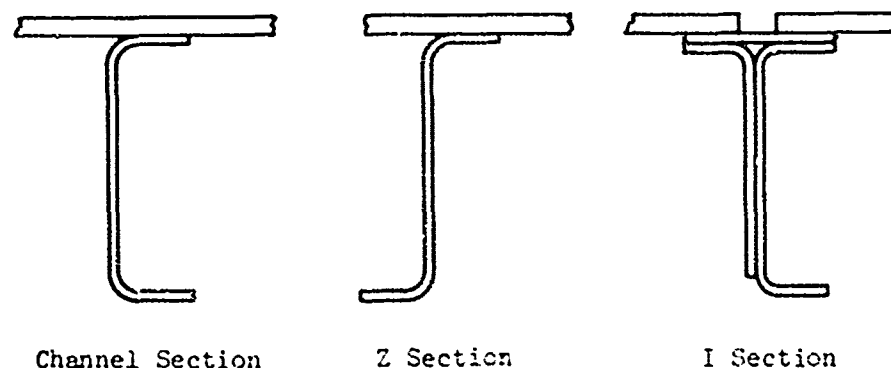


Figure 22-1. Typical Framing Members.

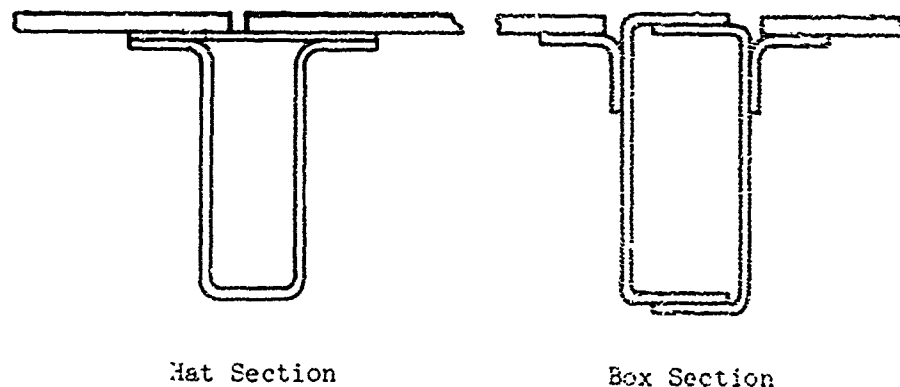


Figure 22-2. Typical Box Members.

Design of transparency support members is a compromise between the conflicting demands of size, stiffness and weight. It is desirable that members be made as small as possible to minimize obstruction of vision. Stiffness is required to prevent excessive secondary stresses in transparencies due to support deflections. These deflections will be the result of both directly applied loading (i.e., pressure loads) and loads induced by airframe flexure. In Reference 1 it was shown that stresses induced in a utility helicopter windshield as a result of airframe wracking during high-g maneuvers could be equal in magnitude to the maximum stresses from pressure loading alone. Similar high local stress producing conditions occur at locations adjacent to door hinges and stops when the structure is too flexible to withstand door slam loads.

In some cases it is not practical for a support member to provide complete restraint for all transparencies. For example, in Figure 22-3 pressure loads applied to the upper eyebrow window create bending and torsion in the upper sill between points A and B. If the upper sill were expected to support the load by itself, an inordinately heavy member might be required. However, the front windshield can be made to share the load by virtue of its inherent in-plane stiffness, and the strength requirements of the sill can be reduced substantially. This design technique can frequently be used to advantage, but caution is necessary to avoid designs where the failure of one member could result in the loss of the complete cockpit enclosure. Damage tolerance is mandatory for this type of construction, along with fail-safe substantiating analysis.

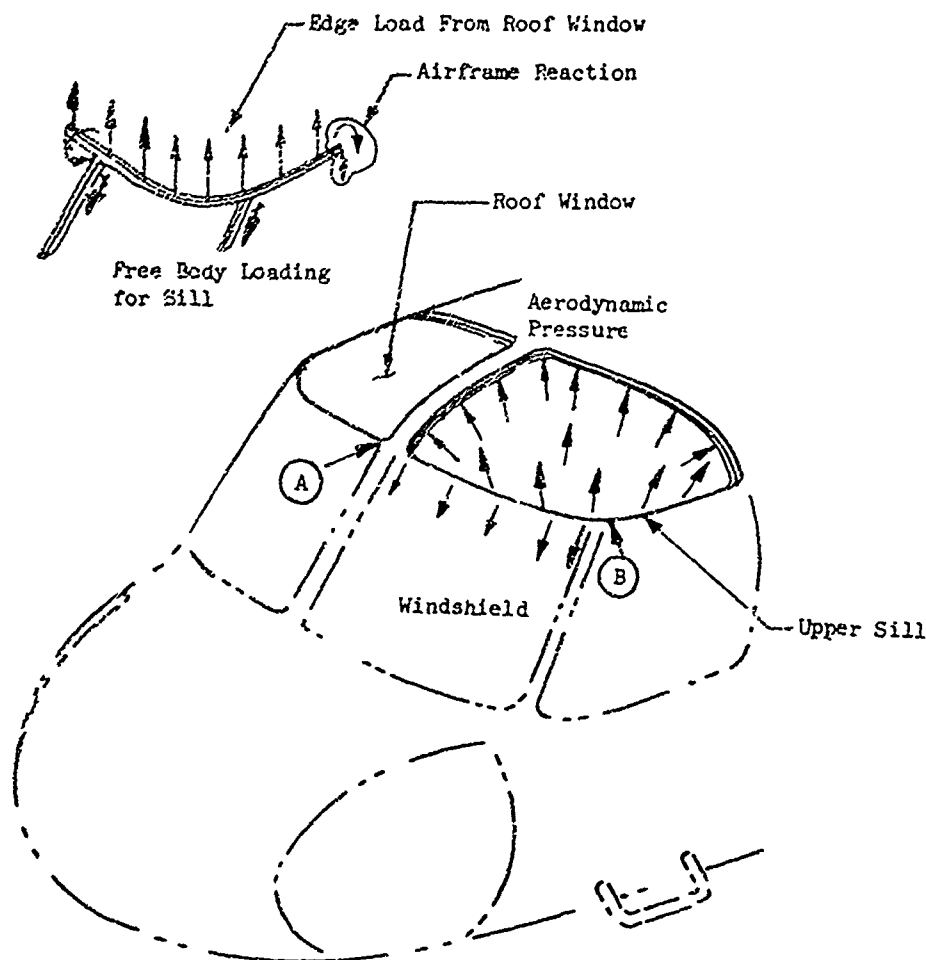


Figure 22-3. Windshield In-Plane Stiffness Supports Roof Window.

22.3 Tertiary Structures

This class of structures includes stiffening members used only to limit deflections or to support miscellaneous items or equipment. Structural requirements for reinforcing members are not as stringent as for primary or secondary structures. As a result, configurations and materials that are normally considered nonstructural may be satisfactory for these functions.

Stiffeners fabricated from transparent materials are good examples of how the physical presence of stiffening members can be diminished, although it should be noted that such parts rarely possess good optical clarity and are usually considered to be translucent. Another advantage of this design approach is the minimization of the thermal mismatch and joining problems. Figures 22-4 and 22-5 show examples of simple rib designs fabricated from transparent materials.



Figure 22-4. Formed Hat Section Ribs on Door Window.

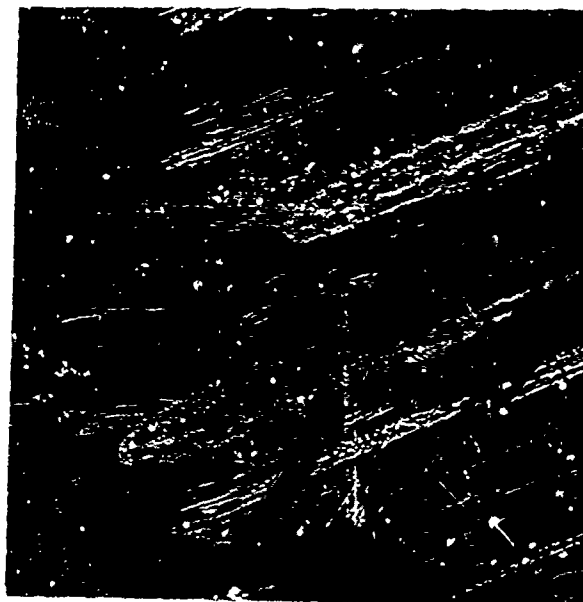


Figure 22-5. Soldi Acrylic Reinforcements on Sliding Window.

Reference

1. Kay, B. F., Sikorsky Aircraft Division, "Design, Test, and Acceptance Criteria for Army Helicopter Transparent Enclosures," USARTL-TR-78-26, Applied Technology Laboratory, U. S. Army Research and Technology Laboratories, (AVRADCOM), Fort Eustis, Va.

Edge reinforcements are required when mechanical fasteners are used to install certain transparency materials. The necessity for an edge reinforcement, as well as the type of reinforcement required, is a function of the substrate material.

23.1 Monolithic Panels

Edge reinforcements are not normally required for monolithic polycarbonate or stretched acrylic materials. Fasteners may be installed through holes drilled along the edge of the panels providing there is adequate edge distance, usually 2.5 to 3.0 times the diameter of the hole. For stretched acrylic, it has been shown that edge reinforcement can actually have a deleterious effect on strength. This occurs because the edge reinforcement creates stress raisers along the boundary of the reinforcement. In addition, it has been found that, during storage, cracks along the edges, parallel to the surface, can appear in stretched acrylic when the plastic contains over 1.6% moisture and is subsequently exposed to low humidity. An edge attachment with a coefficient of thermal expansion different from the parent material will cause the cracks to propagate as shown in Figure 23-1.

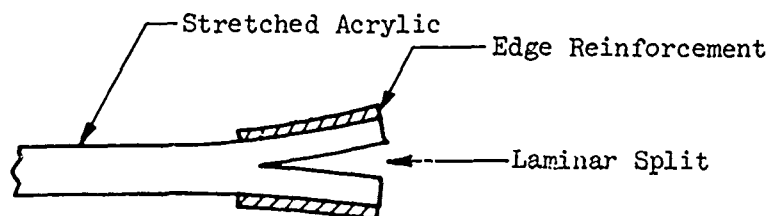


Figure 23-1. Laminar Splitting of Stretched Acrylic.

Holes are not normally drilled through cast acrylic because of the material's low notch sensitivity. When direct mechanical fasteners are to be used, a suitable edge reinforcement is necessary. Reinforced plastic impregnates are often used for this purpose. Impregnated edge attachments can be cured in place when the resin cure temperature is below the softening point of the acrylic (200°F). However, this can be a messy operation, and post-bonded prefabricated strips may be a preferable method of assembly.

Figure 23-2 shows four different types of edge reinforcements that are suitable for use on cast-acrylic helicopter transparencies. Extended edge reinforcements are preferable to bolt-through designs since the holes do not go through the acrylic. The bottom design features flexible, laminated straps bonded to the acrylic that offer an advantage in that contour mismatches between the transparency and the airframe can be readily accommodated.

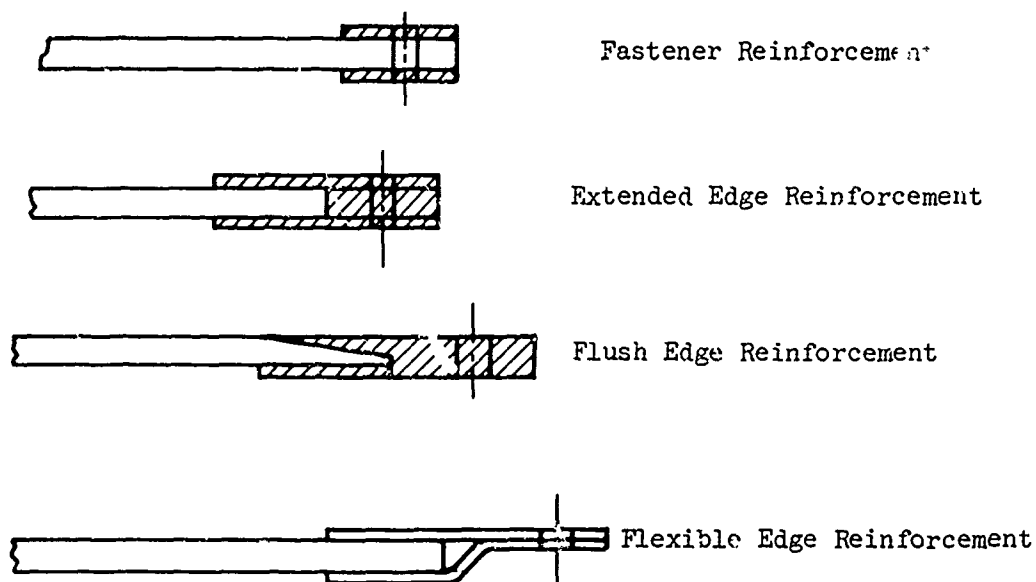


Figure 23-2. Cast Acrylic Edge Reinforcements.

23.2 Laminated Panels

There is a wide variety of edge treatments available for laminated transparencies; the choice of a specific configuration is based on the material and other design considerations. Figure 23-3 shows the range of design possibilities.

Type A, B, and C configurations have attachment holes drilled directly through the base ply, which therefore restricts their usage to polycarbonate or stretched acrylic. The increased thickness provided by the reinforcement in type A provides greater fastener bearing area and also helps to stiffen the edge between fasteners, necessary for transmitting clamping pressure to sealing gaskets. A disadvantage of the Type A design is the possibility that moisture will penetrate through the sealant area due to rotation of the edge attachment during structural loading. Also, a thermal expansion differential between dissimilar base and face plies can cause a crevice to open in the sealant, rendering it ineffective. Type B and C designs overcome the seal deficiency by overlapping the face ply. The overlapping joint can be strictly for sealing or, depending on materials and adhesives employed, can be structural.

Type D and E configurations are frequently employed with glass laminates. The straps used in configuration E provide retention by virtue of the mechanical overlap when stiff straps are used, or by an adhesive joint when flexible straps are used. The single strap design in Type D is commonly used with glass laminates using polyvinyl butyral interlayers.

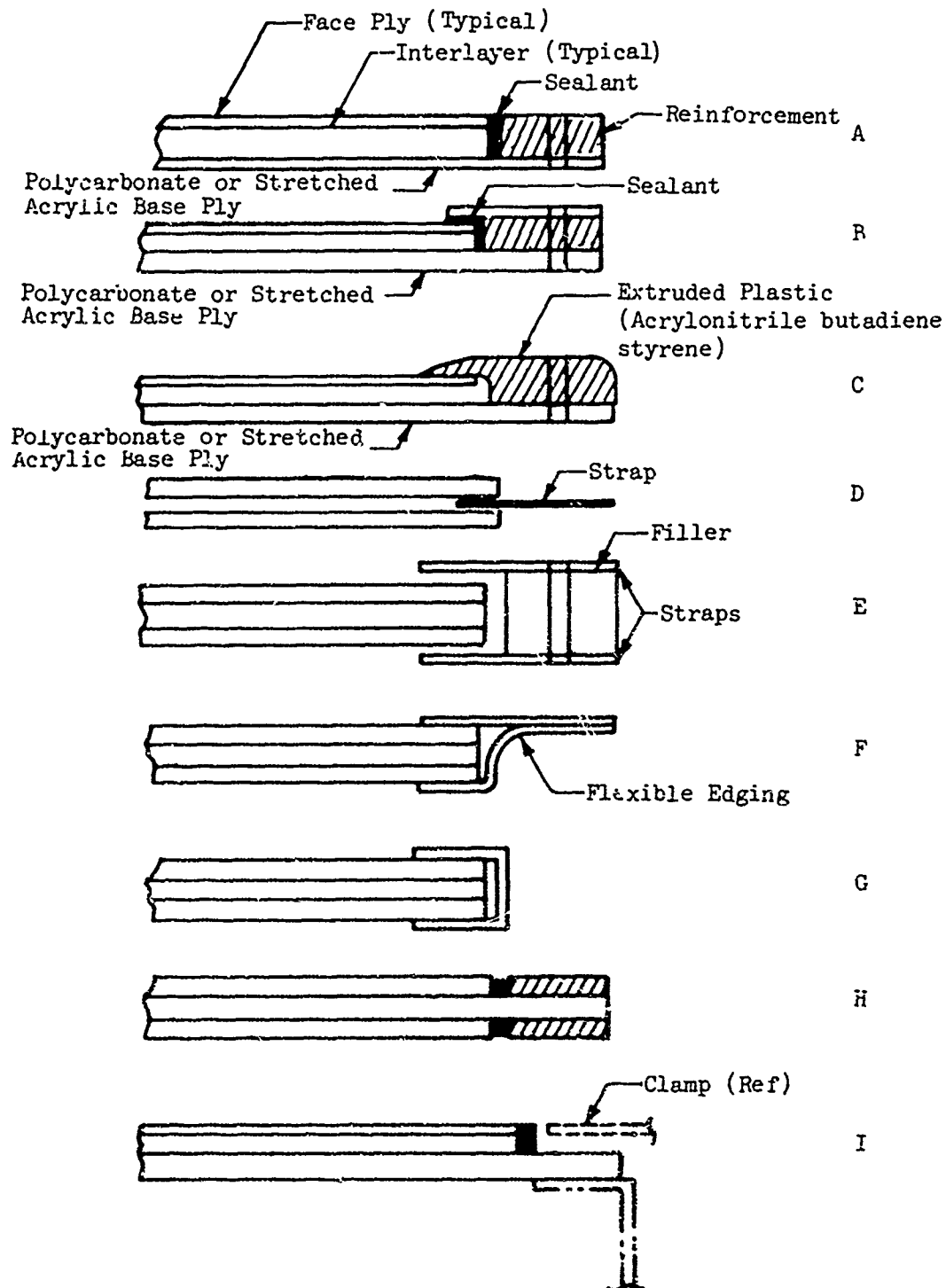


Figure 23-3. Laminated Transparency Edge Configurations.

Straps may be metal or fiberglass and are usually .020 to .040 inch thick. The strap offers flexibility for edge rotation and is very effective in providing fail-safety capability by virtue of its direct shear connection to the interlayer (the fail-safe medium).

The edging of Type F is intended to provide a flexible joint that can be used to compensate for contour mismatches. Flexible reinforced fabrics are most effective for this purpose.

Type G edging is intended for designs that are clamped in place rather than bolted in place and functions primarily as a barrier to prevent moisture penetration into the interlayers. This design is most appropriate for thick, laminated, transparent-armor panels.

Type H is an extended interlayer design in which the only structural tie to the airframe is through the interlayer. Its main advantage is its flexibility. In order to meet strength requirements, however, this design is only suitable for windshields incorporating thick interlayers.

Type I uses a stiff inner ply intended for flush clamp retention to the airframe.

Additional variations are, of course, possible by combining the features of one design with those of another or by developing entirely new designs.

23.3 Flushness

There are several factors that influence the choice of whether or not to use flush reinforcements. Table 23-1 lists advantages for both configurations.

TABLE 23-1. FACTORS AFFECTING FLUSHNESS OF EDGE REINFORCEMENTS FOR LAMINATED WINDSHIELDS

Advantages of Flush Reinforcement	Advantages of Protruding Reinforcement
1. Aerodynamic cleanliness	1. More positive edge sealing
2. Level surface facilitates the scraping of accumulated snow and ice	2. Direct load path to outer ply
3. Smooth surface to park windshield wipers	

23.4 Slip Planes

Slip planes are sometimes used along the edges of laminated assemblies to reduce or prevent bonding of the interlayers to the face plies. This practice is necessary for certain geometric configurations using glass and polyvinyl butyral (PVB) because, at low temperatures, large differences in thermal contraction rates between the PVB and glass create high stresses. These stresses can be so high along the edges, where the PVB clings tenaciously to the glass, that chips are pulled from the glass. To prevent glass edge chipping, a parting medium or slip plane is added between the interlayer and the glass to move the peak stresses inboard, away from the edge, where a smoother surface free of stress concentrations exists (see Figure 23-4).

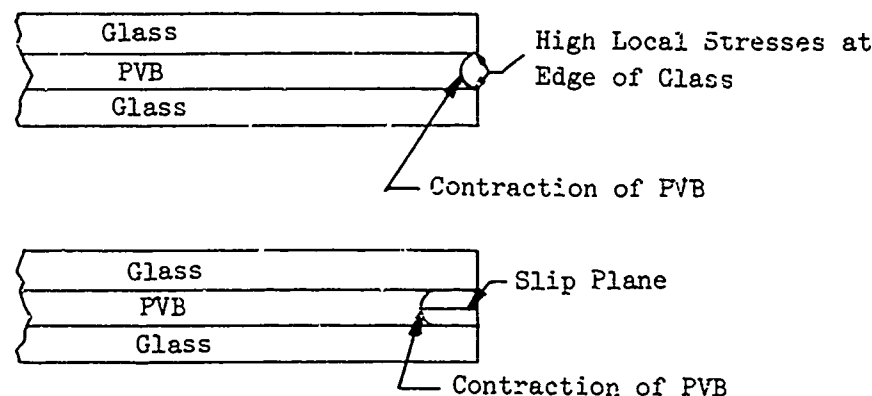


Figure 23-4. Function of Slip Planes.

23.5 Joint Stiffness

A major consideration in the design of edge reinforcements is joint stiffness. A certain amount of flexibility is desirable to accommodate manufacturing tolerances without developing stresses in the transparency and to provide structural isolation from airframe loads. Tailored joint stiffness is achieved by controlling either geometry or material properties, or both.

Figure 23-5 illustrates the effects of different geometries on edge rotational stiffness. Configuration A is naturally stiff by virtue of its thickness and couple distance between the straps. Configuration B is naturally flexible by virtue of its limber shape. Configuration C utilizes a sealant or adhesive to allow rotation of the transparency within the edge attachment.

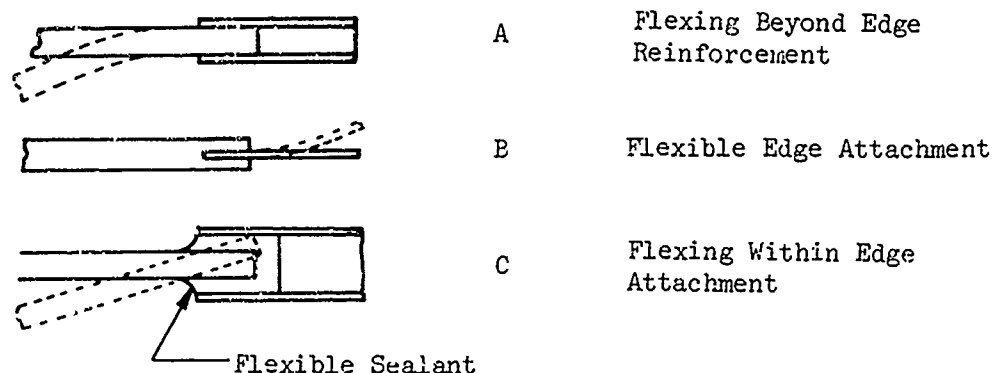


Figure 23-5. Edge Rotational Stiffness.

Certain combinations of geometry and materials used in extended base-ply designs can allow delamination-promoting peel stress to develop as a result of edge rotation, as shown in Figure 23-6. While it is difficult to analytically predict these cleavage stresses, a measure of interlayer cleavage strength can be gained through the use of data in Table 23-2. Laminates were tested as shown in Figure 23-7. A load was then applied to the extended base ply until delamination occurred. The resulting test data should be considered conservative and representative of an extreme since the outer ply was completely restrained from flexing, which would normally relieve some of the interlayer stress.

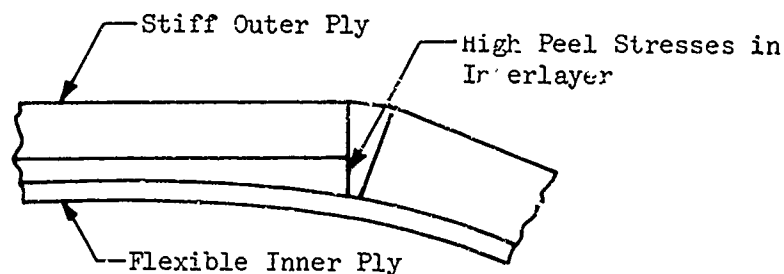


Figure 23-6. Peel Stresses Due to Edge Rotation

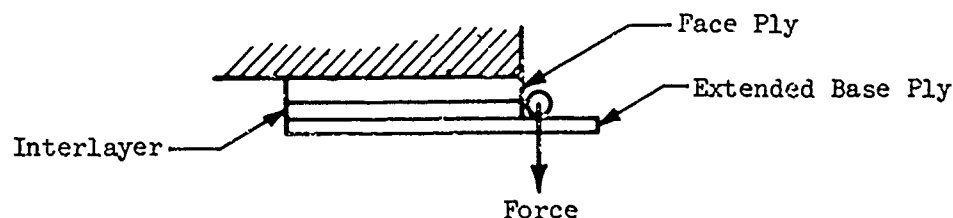


Figure 23-7. Cleavage Test Setup.

TABLE 24-2. CLEAVAGE STRENGTHS OF VARIOUS LAMINATES

Base Ply	Thickness (in.)	Interlayer	Thickness (in.)	Coating	Face Ply	Cleavage Strength (lb/in.)	Temp. (°F)
Stretched Acrylic MIL-P-25690	.150	PVB 38 pph DBS	.075	Sierracin 303	Polyester CR-39	62	70
Stretched Acrylic MIL-P-25690	.150	PVB 38 pph DBS	.075	Sierracin 303	Polyester CR-39	33	-65
Stretched Acrylic MIL-P-25690	.150	PVB 38 pph DBS	.075	Sierracin 303	Polyester CR-39	25	125
Stretched Acrylic MIL-P-25690	.080	PVB 38 pph DBS	.075	Sierracin 303	Chemcor 401	28	70
Stretched Acrylic MIL-P-25690	.080	PVB 38 pph DBS	.075	Sierracin 303	Chemcor 301	13	-65
Stretched Acrylic MIL-P-25690	.080	PVB 38 pph DBS	.075	Sierracin 303	Chemcor 401	14	125
Polycarbonate 9030-112	.063	Ethylene Terpolymer	.075	Sierracin 303	Chemcor 401	60	70
Polycarbonate 9030-112	.063	Ethylene Terpolymer	.075	Sierracin 303	Chemcor 401	18	-65
Polycarbonate 9030-112	.063	Ethylene Terpolymer	.075	Sierracin 303	Chemcor 401	17	125
Stretched Acrylic MIL-P-25690	.080	PVB 38 pph DBS	.075	None	Chemcor 401	84	70
Stretched Acrylic MIL-P-25690	.080	PVB 38 pph DBS	.075	None	Chemcor 401	30	-65
Stretched Acrylic MIL-P-25690	.080	PVB 38 pph DBS	.075	None	Chemcor 401	36	125

Data from Reference 1

23.6 Adhesives

Adhesives for bonding edge reinforcements can be either rigid epoxies or flexible elastomeric compounds. The high-strength adhesives can develop shear strengths in the order of 1000 psi, and while flexible elastomeric adhesives are much lower in strength, they do offer benefits, such as high elongations to failure.

The wide range of potential adherent combinations and design conditions makes it impractical to recommend specific adhesive materials. An adhesive would therefore be selected after careful evaluation of the following physical properties:

- Chemical compatibility with adherents
- Shear strength
- Peel strength
- Temperature sensitivity
- Environmental resistance
- Ultimate elongation
- Cure cycle
- Working characteristics

Typically, the space available for overlapping adherents in bond joint, must be kept small to minimize intrusion into the visual field. Because of the small overlap dimension, stress concentrations have a pronounced effect on joint strength. Figure 23-8 shows how strain in a scarfed joint between two parts of identical stiffness causes the stress to peak at either end of the joint. For the more common nonsymmetrical joints, eccentricities between layers will introduce additional stress concentrations. Further, increasing the width of the joint beyond a certain point does little to increase overall strength, since most of the load is still transferred at the edges, and the central region of the joint remains virtually unstressed. Thus, accurate analytical predictions of joint stresses are difficult to obtain at best, and adhesive joint strengths should be verified by specimen tests whenever possible.

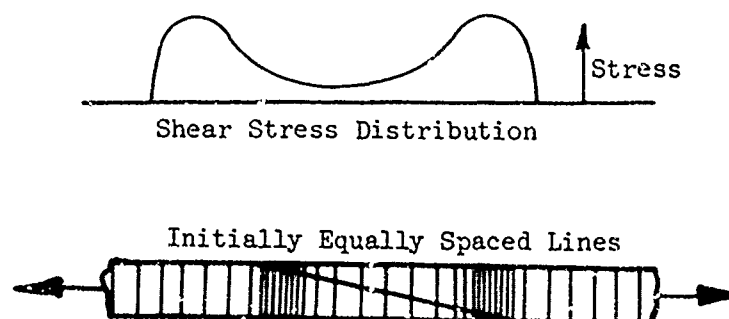


Figure 23-8. Stress Distribution in a Scarfed Adhesive Joint.

23.7 Reinforcement Materials

Edge reinforcement materials should have strength properties as good or better than those of the materials they are expected to reinforce. This requirement should not present any problem because most transparent materials have low strengths in comparison to common structural metal, plastic, and reinforced-fabric materials. Reinforced fabrics suitable for edge attachments include fiberglass (glass), nylon (a polyamide), orlon (acrylic) and dacron (polyester) impregnated with acrylic, polyester or epoxy resins. Stainless-steel wire mesh impregnated with resin offers an additional possibility. Extruded Acrylonitrile Butadiene Styrene (ABS) has also been used to advantage because of inherent low-cost production characteristics.

The materials selected for edge attachments should have thermal expansion rates compatible with the transparent material and low modulus of elasticity to minimize thermal stresses resulting from different thermal expansion coefficients. Table 23-3 lists the coefficients of thermal expansion at room temperature for common transparent materials and potential reinforcing materials.

For electrically heated windshields, edge attachment materials having low thermal conductivity are desirable. Edge attachments possessing good insulating qualities will reduce the flow of heat to the unheated airframe, thereby minimizing cold-edge effects. Cold edges create undesirable stresses in the interlayer. Such stresses are discussed in section 27, Interlayer Design Considerations.

23.8 Installation/Removal

Attachment designs can be ranked according to how easy it is to install or remove their transparencies. The following methods are listed according to difficulty, with those designs requiring the least amount of time for installation and removal appearing first:

1. Quick-release fasteners
2. Rubber molding
3. Threaded fasteners
4. Rivets
5. Adhesives

23.8.1 Quick-Release Fasteners

Quick-release fasteners such as quarter turn are useful for installations requiring rapid and frequent assembly and disassembly. Internal cockpit transparent armor that must be removed for cleaning or to facilitate maintenance is a typical example. The installation or removal with this type of fastener can usually be accomplished in seconds. However, there are disadvantages that prohibit more widespread application: the unit costs and weights for the quick-operation fasteners are higher than those for comparable screws and nuts. Also, larger mounting holes are typically required, and this necessitates wider edge attachments and larger brackets.

TABLE 23-3. COEFFICIENTS OF THERMAL EXPANSION OF TRANSPARENT
AND EDGE-ATTACHMENT MATERIALS AT ROOM TEMPERATURE

Material	Coefficient of Thermal Expansion ₅ (per °F x 10 ⁻⁵)
MIL-P-5425 Acrylic	4.1
MIL-P-8184 Acrylic	4.1
MIL-P-25690 Stretched Acrylic	3.5
MIL-P-83310 Polycarbonate	3.47
MIL-P-8257 Polyester	5.5 - 7.0
MIL-G-25667 Soda Lime Glass	0.47
MIL-G-25667 Chemically Strengthened Glass	0.48
2024 Aluminum	1.25
4130 Steel	0.63
301 Stainless Steel	0.89
6Al-4V Titanium	0.46
Nylon Acrylic	3.5
Orlon Acrylic	2.2
Dacron Acrylic	2.1
Epoxy Fiberglass (MIL-R-9300)	0.55 - 0.67
Polyester Fiberglass (MIL-R-7575)	0.78 - 0.85
Silicone Fiberglass (MIL-R-25506)	0.4 - 0.5
Phenolic Fiberglass (MIL-R-9299)	0.6 - 0.64

Data from Ref. 1,2,3,4

23.8.2 Rubber Extrusions

Two-piece rubber extrusions can be used for permanent and semipermanent glazing installations. The basic rubber extrusion, in its free state, is shown in Figure 23-9 along with a mating rubber key extrusion. When the key is inserted into the basic section, it forces the basic extrusion to close and grip both the airframe and the transparency, as illustrated in Figure 23-9. A special hook-shaped tool facilitates installation of the key.

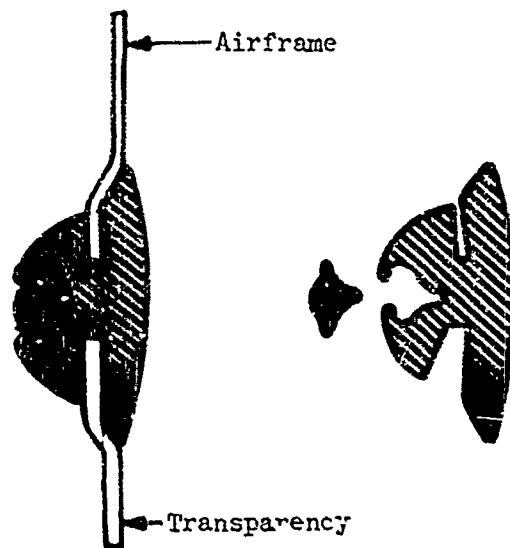


Figure 23-9. Transparency Retention via Rubber Extrusions.

Depending on the geometry and hardness characteristics of the rubber, retention forces can be tailored to meet a wide range of installation requirements. Precise control of cavity and glazing trim dimensions, as well as thickness, is required because of an extremely sensitive relationship between fit and retention force. Temperature extremes must be considered as they have a pronounced effect on rubber hardness, thus influencing retention forces. Differences in the expansion and contraction characteristics of the airframe and the glazing materials, due to temperature and humidity changes, are also extremely important. For large panels, these dimensional changes can be in the order of 1/8 inch or more. Lastly, fuselage wracking can alter cavity shapes during flight, which could adversely affect transparency retention.

A major drawback of this design is the lack of positive mechanical retention. This deficiency can be reduced by stringent quality control requirements, such as proof load testing.

23.8.3 Threaded Fasteners

Threaded fasteners (screws and nuts) are the most common method used to install glazings. A wide variety of hardware and materials are available for this purpose. Cross-head screws are preferred over slot head screws because they reduce the possibility of the screwdriver slipping from the screw head and damaging the transparency. The choice of plain nuts, captive nuts, or threaded inserts is based on the types of backup structures employed and the accessibility of the fasteners. Blind installations, where the nuts are inaccessible, are undesirable because of the difficulty in replacing fasteners damaged during maintenance.

The time required to install or remove threaded fasteners is moderate, with an average time of two minutes per fastener being typical. Total time for installation, excluding fitting and sealing, is thus dependent upon the total number of fasteners. This in turn is based on the maximum permissible fastener pitch, which is a function of the structural loading and the clamping requirements for sealing. For most general applications on helicopters, spacing between fasteners will rarely exceed 3 to 4 inches.

The torquing sequence, as well as the magnitude of torque applied to screws, is extremely important. Excessive fastener torque can create very high local stresses in the transparency. A good practice is to use at least two steps in tightening fasteners: (1) partially tighten the screws to just bring the transparency into uniform contact with its mating surface or gasket, and (2) tighten the screws to their prescribed torques. Additional incremental steps may be required, depending on fit, gasketing, or other peculiarities of individual designs. Figure 23-10 illustrates a sequence for tightening individual fasteners for installations having mismatches of contour between the transparency and the airframe. The gap is closed gradually, and the buildup of local stress at the fasteners is minimized. Also, care must be taken to avoid excessive fastener torque. A compressible gasket will allow the transparency to bend in the vicinity of a fastener. If the fastener is too tight, the transparency will fracture.

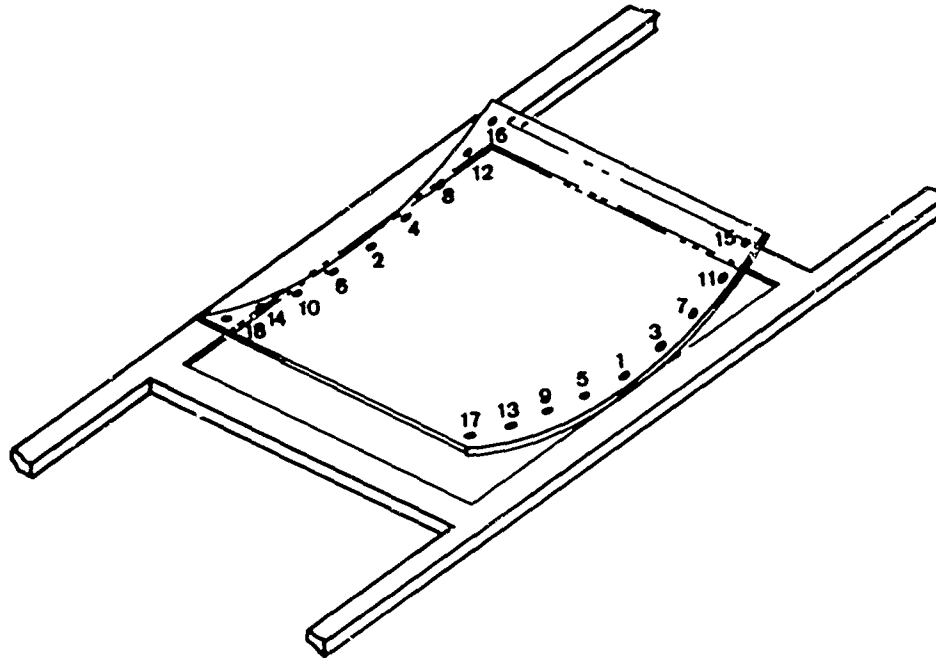


Figure 23-10. Torquing Sequence for Closing Gap Between Transparency and Support.

23.8.4 Rivets

Riveted assemblies are considered permanent installations. Disassembly entails drilling out the rivets, a time-consuming operation requiring a great deal of skill. Therefore, rivets are unsuitable for installing transparencies that may require field replacement.

Rivets may be attractive for the installation of transparencies in expendable assemblies, and offer weight and sometimes cost savings during manufacture.

Rivets can be installed directly through stretched acrylic and polycarbonate, although backing strips or washers, as shown in Figure 23-11, are desirable. All other transparent materials require edge reinforcements to prevent cracking. The rivets should be soft aluminum or have hollow points to minimize local stresses in the plastic caused by the expansion of the rivet shank during installation.

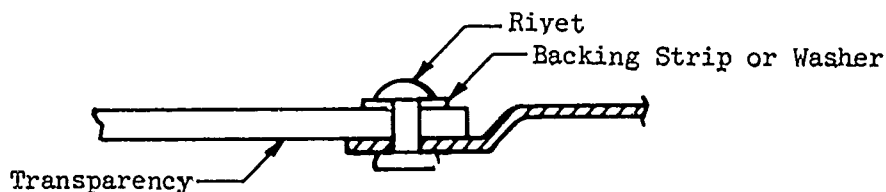


Figure 23-11. Riveted Installation.

23.8.5 Bonding

Adhesively bonded transparent installations are considered permanent. Disassembly is difficult and often results in damage to the window retainers. Accordingly, this type of construction is only useful for expendable assemblies. In such cases, savings in both weight and cost are possible because the adhesive replaces fasteners, sealants and gaskets.

23.9 Hole Size

Whenever possible, oversize fastener holes should be used in transparency installations. This will:

1. Provide isolation from in-plane airframe structural loads.
2. Permit unrestrained thermal expansion/contraction between transparency and airframe.
3. Accommodate manufacturing tolerances in hole locations.

In order to prevent frictional forces from negating the float provided by the oversize holes, it is necessary to control fastener clamping forces. This may be accomplished by prescribing fastener torque limits or by controlling clamping dimensions with spacers, as shown in Figure 23-12. The possibility for damaging transparencies by overtightening fasteners is also virtually eliminated when spacers are used.

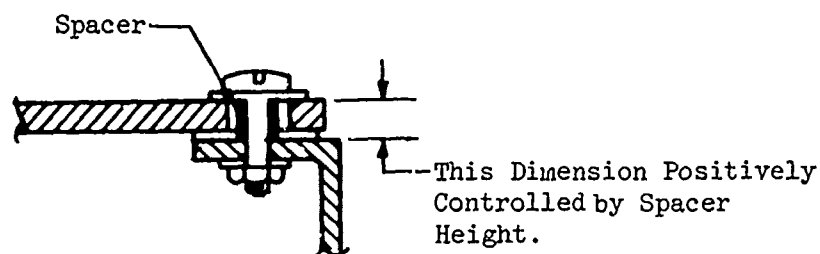


Figure 23-12. Spacer Used to Control Clamping Dimensions.

Two methods for incorporating oversize holes in installations with flush fasteners are illustrated in Figure 23-13. On the left side of the figure, all of the required radial float is accommodated by oversize holes in the structure. On the right side of the illustration, the same radial float is accommodated by smaller oversize holes in both the structure and the transparency. Dimpled washers support the screw heads above the enlarged countersunk holes.

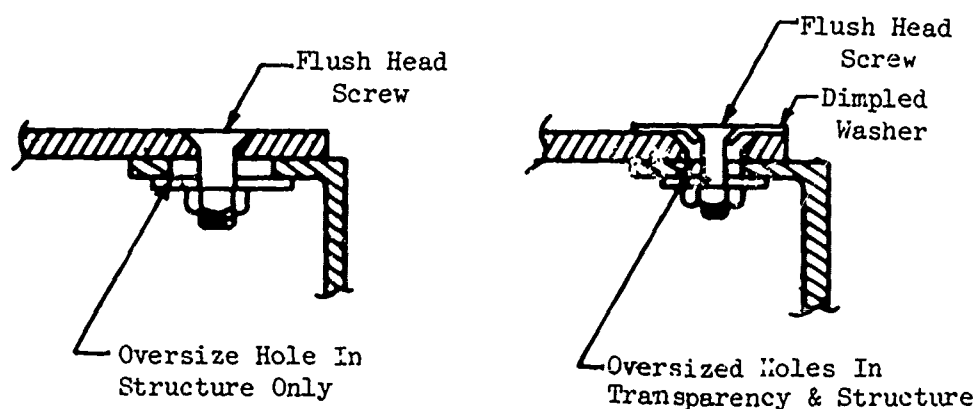


Figure 23-13. Oversized Hole Installations for Flush Fasteners.

It is important to note that there are certain design conditions for which oversize mounting holes should not be used. For example, panels that support transverse pressure loads by in-plane membrane action require relatively tight-fitting holes to react edge tension loads. Also, oversize holes cannot be used in shell-like enclosures where the structural continuity between adjacent transparent panels comprising the shell is important.

Even with tight-fitting holes, most edge attachment designs have a certain amount of inherent flexibility that will isolate the transparency from small airframe strains. To demonstrate structural isolation characteristics, tests were performed on several edge attachment designs (see Figure 23-14). These tests demonstrated that even

with relatively stiff glass laminates, less than 6% of the post member strain was transmitted to the glass. It is assumed that most of the strain is absorbed by the gasketing, fasteners, and the edge reinforcement, and does not reach the transparency itself.

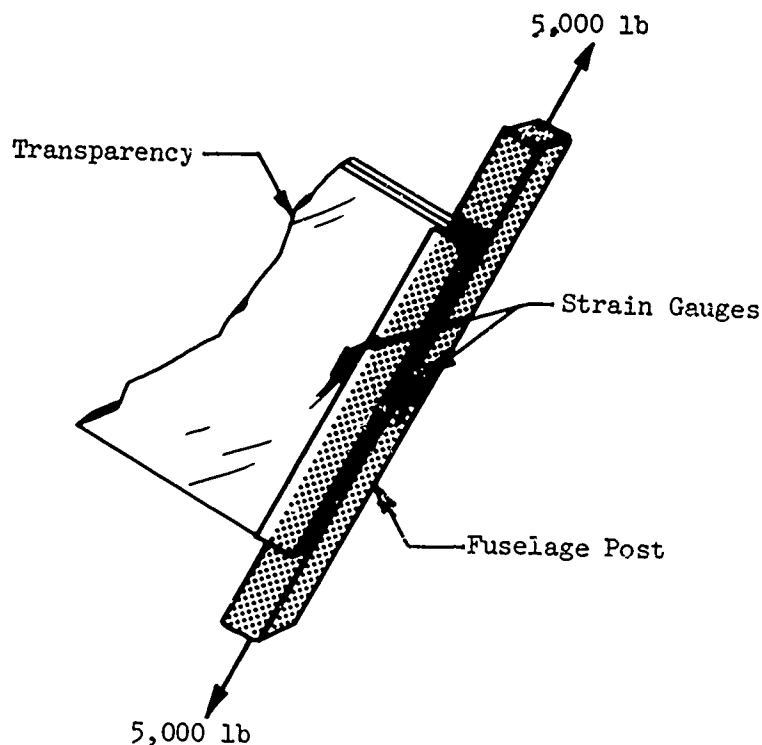


Figure 23-14. Strain Compatibility Test.

23.10 Clamped-Edge Retainers

Clamps provide an alternate method for installing transparencies where the glazing is held in place between fixed retainers and removable clamps. Figures 23-15 and 23-16 illustrate clamp-retainer designs for single- and multiple-glazed installations. For the double-glazed installation there is a potential saving in the number of fasteners required, since a single row of fasteners suffices for both glazings. The clamp itself is an additional component but can sometimes be traded off for a simplified edge reinforcement resulting from the elimination of holes through the transparency. Interchangeability is enhanced because all mounting holes are in the airframe and the clamps, and do not change when the glazing is replaced. This eliminates drilling or the need to match the holes in the airframe with those in the transparency. Also, stress concentrations in the transparency due to fasteners are eliminated, and edge support is more uniform.

Clamp retainers do not provide positive mechanical retention, particularly in the plane of the transparency itself. When in-plane edge loads are significant, as would be the case for membranes, heavy-edge retainers and backups are required to provide sufficient clamping force to prevent the transparency from pulling out. The exception is the lipped design shown in Figure 23-17.

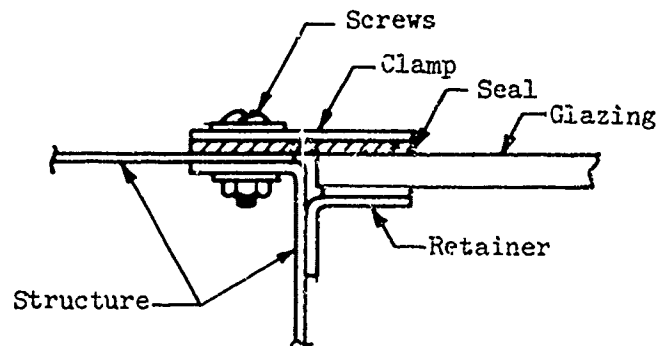


Figure 23-15. Single Glazing Clamp Retention.

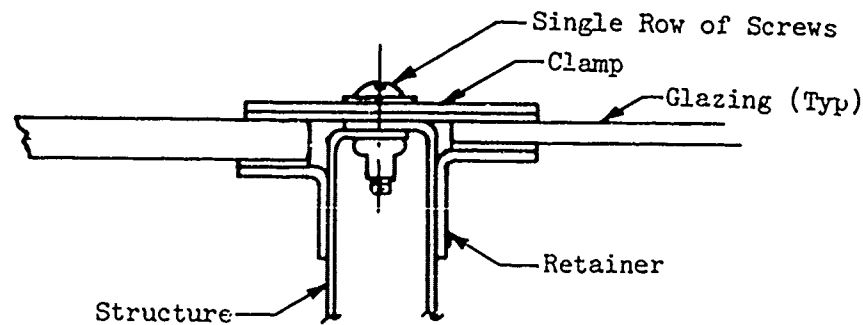


Figure 23-16. Double Glazing Clamp Retention.

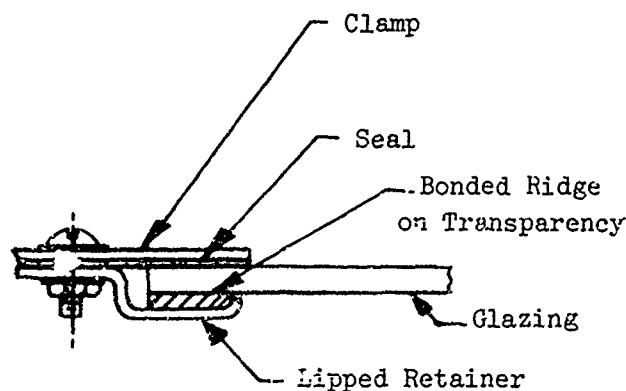


Figure 23-17. Lipped Window Retainer.

23.11 Sealing

There are two basic sealing methods employed to make transparent installations weathertight: dry seals and wet seals.

Dry seals are typified by sponge rubber gaskets that are clamped between the transparency and the airframe. The thickness and the hardness of the rubber are determined by considering the amount of clamping force available from the edge attachment. Thick soft gaskets are required for flexible edgings, while thin firm gaskets can be used with stiff edgings. Gaskets fabricated as solid-rubber moldings are generally unsuited for helicopter glazing installations, because such installations lack the joint stiffness necessary for adequate seal compression.

Other forms of dry seals applicable to helicopter transparent enclosures are hollow-bulb seals and resilient pile liners, shown in Figure 23-18. These seals require a great deal more space than do flat compression seals and are therefore more appropriate for movable installations such as hatches and doors. The hollow-bulb seals are effective over a large range of gaps and tolerances. The pile liner reduces friction in sliding applications. However, pile liners are not totally effective in driving rain, and such designs require supplemental deflection shields or drain holes.

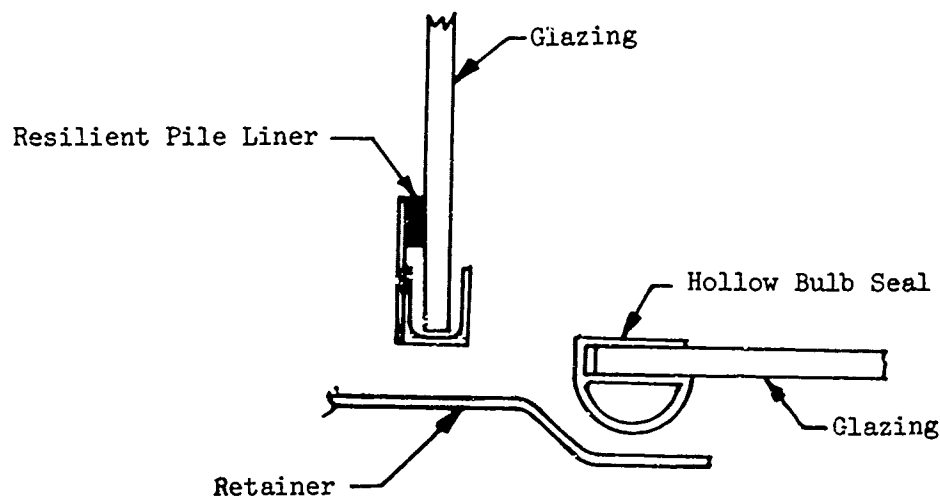


Figure 23-18. Hollow-Bulb Seal and Pile Liner.

Wet sealants include curing and noncuring compounds that are applied to the joint in a viscous or compliant state. Typically, a bed of sealant is applied to the airframe retainers so that any local surface depressions or imperfections will be filled in or covered. The transparency is then pressed into the soft sealant to achieve intimate contact along the entire joint. In some applications, sealants or similar filler materials are also used to fill gaps resulting from mismatches in contour between a transparency and an airframe.

Wet sealants are available in a tape or bead form, and also as a viscous liquid suitable for application with a caulking gun, spatula, or similar tool. Curable compounds, such as MIL-S-8802, high temperature, high adhesive sealant, cure in the same manner as adhesives and will actually bond the transparency to its supports, making replacement of the transparency difficult. Also, adhesive sealants can bond assembly fasteners in place, which further hampers removal.

Qualification of sealants should always include tests for chemical compatibility with applicable substrate materials to avoid the possibility of crazing damage to the transparency. In addition, sealants should be capable of withstanding exposure to high temperatures without excessive softening or flowing, or exposure to cold temperatures without becoming embrittled.

References

1. Kay, B. F., Sikorsky Aircraft Division, "Design, Test, and Acceptance Criteria for Army Helicopter Transparent Enclosures," USARTL-TR-78-26 Applied Technology Laboratory U. S. Army Research and Technology Laboratories Fort Eustis, Va.
2. "Strength of Metal Aircraft Elements," MIL-HDBK-5, Armed Forces Supply Support Center, Washington, D. C., Mar. 1961.
3. "Plastics for Flight Vehicles, Part I, Reinforced Plastics," MIL-HDBK-17, Armed Forces Supply Center, Washington, D. C., Nov. 1959.
4. Hassard, R. S., Goodyear Aerospace Corp., "Plastics for Aerospace Vehicles, Part II Transparent Glazing Materials," MIL-HDBK-17A, Part II (Proposed Revision), Air Force Materials Laboratory, Wright-Patterson Air Force Base, Ohio, Jan. 1973.

Bibliography

"Plexiglas Handbook for Aircraft Engineers," PL-26a, Rohm & Haas Co., Philadelphia, Pa., Dec. 1952.

Woloch, D. R., et al, "Study of Failed TA-4 Aircraft Canopies," Naval Research Laboratory, AFML-TR-73-126, Air Force Materials Laboratory, Wright-Patterson Air Force Base, Ohio, June 1973.

Mulville, D. R., et al, "Crack Formation in F-4 Aircraft Canopies, Naval Research Laboratories, AFML-TR-73-126, Air Force Materials Laboratory, Wright-Patterson Air Force Base, Ohio, June 1973.

Roberts, W. G., "The Development of Windscreen Reliability," Triplex Safety Glass Co., Ltd., Society of British Aerospace Companies Ltd., London, England, June 1971.

"Military Standardization Handbook, Adhesives," MIL-HDBK-691A, Department of Defense, Washington, D. C., May 1965.

Beaumont, P. N., and Parker, L., The Boeing Commercial Airplane Company, "Windshield Design Concepts," AFML-TR-73-126, Air Force Materials Laboratory, Wright-Patterson Air Force Base, Ohio, June 1973.

Daniels, P., "Sealing Compound, Polysulfide, Mixing and Application of," SS8654 Sikorsky Aircraft Div., Stratford, Conn., May 1961.

Morgia, J., "Window Installation, Cockpit Canopy," SS8795, Sikorsky Aircraft Div., Stratford, Conn., Sept. 1963.

INTERCHANGEABILITY

For components that are expected to require frequent replacement during their service lives (components that have mean times between overhauls that are less than airframe overhaul intervals), interchangeability is a desirable requirement. Noninterchangeable windshield installations that require drilling and trimming for installation are time consuming to replace, typically requiring 8 to 15 man-hours.

The fit requirements that govern interchangeability for transparencies are: hole location, part trim, and contour, which are functions of both design and tooling. By design, tight tolerances for part trims can be minimized by providing liberal clearances. Similarly, tolerances for hole locations can be relaxed by using oversize holes or eliminated entirely by using clamp edge retainers. However, when other design considerations prohibit large tolerances, precision tooling must be employed to control interface dimensions on both the airframe and the transparency. Master mockups like the one shown in Figure 24-1 are recommended in such cases to locate critical dimensions. From these fixtures, the necessary tooling required to fabricate the parts is made and coordinated.

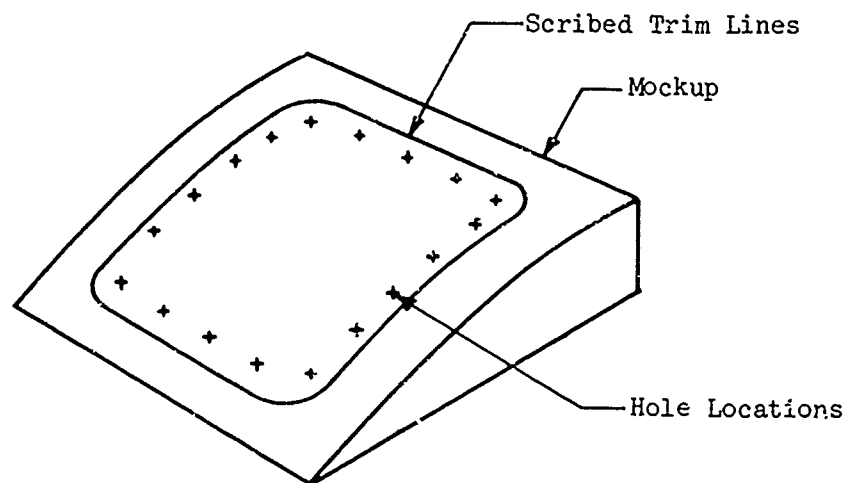


Figure 24-1. Master Mockup for Contoured Transparency.

24.1 Thermal Expansion

Differences in thermal expansions of detail parts must be considered closely to prevent severe mismatches between components in installations.

Figure 24-2 shows the strain or unit elongation due to thermal expansion for aluminum and stretched acrylic over a broad temperature range. The difference between the two curves in the figure represents the thermal expansion differential of these materials measured from a room temperature reference. This thermal expansion differential is the net change in length per unit length ($\Delta L/L$) as a function of temperature and reflects that the coefficient of thermal expansion for stretched acrylic varies with temperature.

To illustrate, consider a stretched-acrylic canopy 50 inches long that is to be installed into an aluminum structure. If the holes in the canopy and structure were predrilled at 70°F and field replacement is attempted at 32°F, the expansion differential obtained from Figure 24-2 is 120×10^{-5} in/in, or a total change in length of 0.060 inch. Obviously, if this relative contraction is not accounted for, holes will not align, and the shape will be considerably different than at room temperature. To allow for this, replacement canopies must be supplied either undrilled or with oversize holes.

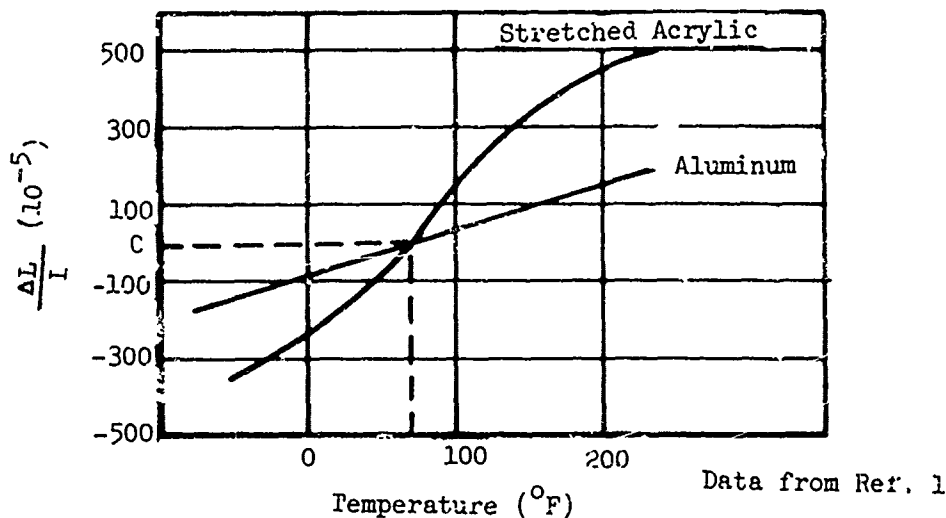


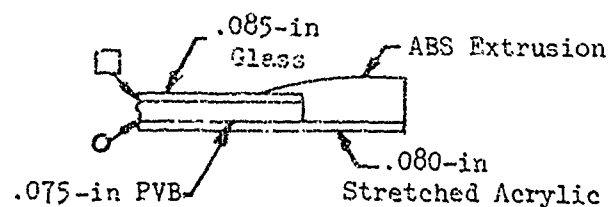
Figure 24-2. Differential Thermal Change in Length per Unit Length.

24.2 Contour Conformity

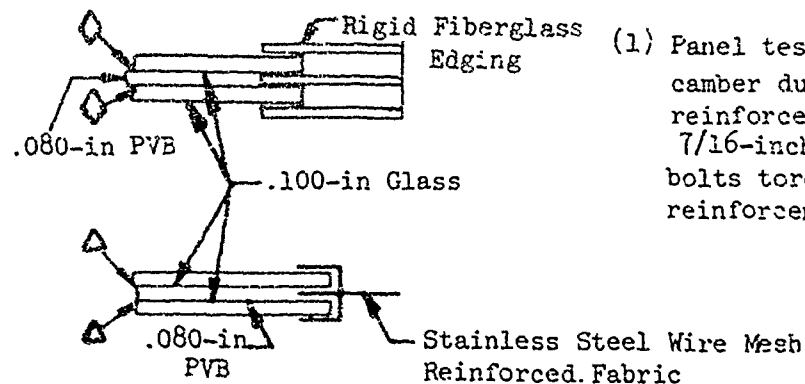
The last important dimensional consideration that affects interchangeability is contour. A close match between the airframe and the transparency contours is important in order to avoid inducing excessive stress into the transparency from installation preload. This is a subtle point and is discussed here because it is the designer's responsibility to specify the necessary features or tolerances to prevent an otherwise interchangeable panel from being preloaded excessively. Otherwise, mechanics installing transparencies will sometimes force the parts into place, excessively torquing the fasteners, thus inadvertently or unknowingly introducing high preloads, leaving little residual strength to accommodate flight loads.

Figure 24-3 shows induced stress as a function of camber or contour mismatch for three different windshield configurations. The data was derived from 24-in square test panels. From these curves, it can be seen that large induced stresses can result from relatively small contour mismatches. This is especially significant for stiff panels with rigid edgings.

It should also be noted that unsymmetrical laminated assemblies behave in a manner similar to bimetal elements; that is, they tend to change curvature with temperature changes. Glass-faced-plastic windshields fall into this category. In the unrestrained state, severe contour changes will occur over the range of temperatures (32°F to 100°F) that are considered amenable for assembly. Appropriate installation procedures must therefore be prepared for such situations.



Note



(1) Panel testing started at 3/8-inch camber due to flexibility of edge reinforcement. Test stopped at 7/16-inch camber when attachment bolts tore through fabric edge reinforcement.

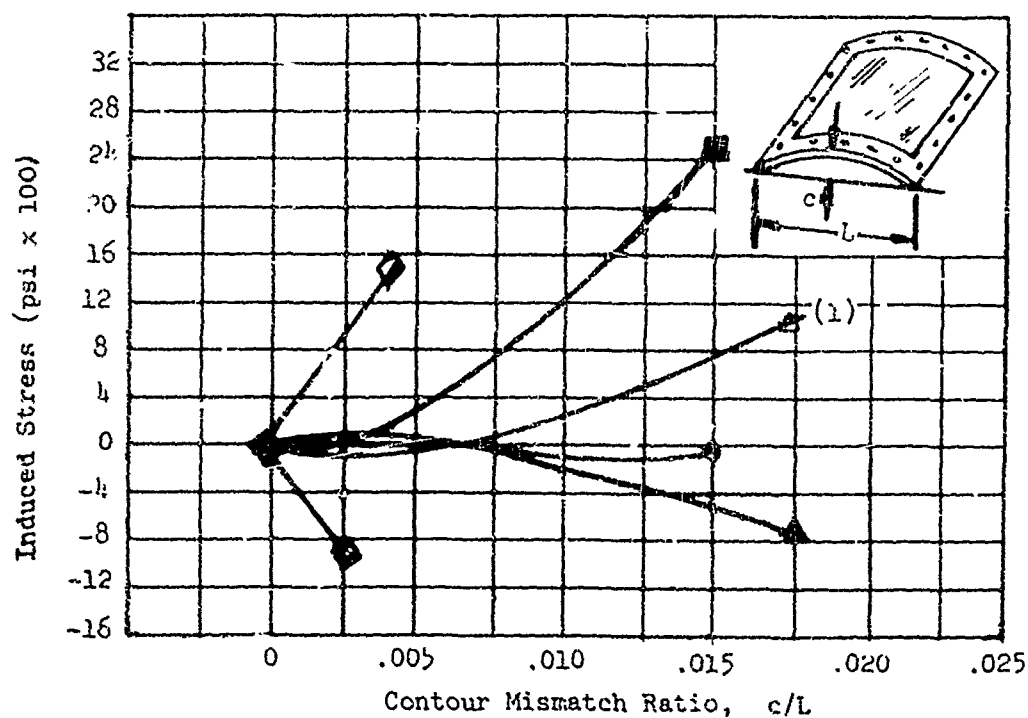


Figure 24-3. Windshield Installation Preload, Induced Stress Versus Camber.

References

1. "Aircraft Transparencies Installation," TB73-101, Swedlow Inc., Garden Grove, Calif., Mar. 1973.
2. Kay, B. F., Sikorsky Aircraft Division, "Design, Test, and Acceptance Criteria for Army Helicopter Transparent Enclosures," USARTL-TR-78-26 Applied Technology Laboratory, U. S. Army Research and Technology Laboratories, (AVRADCOM) Ft. Eustis, Va.

Bibliography

Clark, M., et al, "Identification and Analysis of Army Helicopter Reliability and Maintainability Problems and Deficiencies, Volume II, Utility Attack and Training Helicopters (UH-1, AH-1, TH-1)," USAAMRDL-TR-72-11B, U. S. Army Air Mobility Research & Development Laboratory, Ft. Eustis, Va., Apr. 1972.

There are many conditions, both mechanical and environmental, that induce stress in transparencies. In addition, laminated windshields containing integral heating elements develop complex thermal gradients that also affect the stresses in the transparency. It is important that all of these conditions be considered during design and qualification because the low strength levels of transparent materials, in comparison to conventional structural materials, can cause seemingly small stresses to have significant effects on structural integrity.

Table 25-1 summarizes the different types of loading conditions, along with descriptions of their possible effects. Some of these conditions occur simultaneously and must be combined to calculate or develop critical loading.

TABLE 25-1. LOADING CONDITIONS


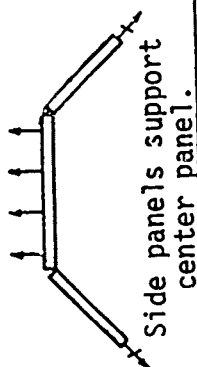
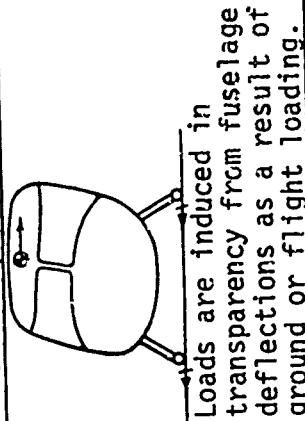
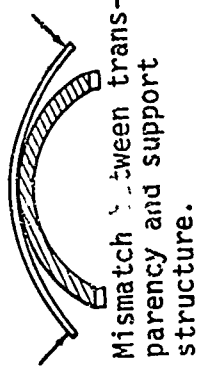
Condition	Description	Effects	Magnitude of Condition
Direct Aerodynamic Pressure		Can cause plate bending, diaphragm action or shell compression, depending on stiffness and geometry of transparency.	Can become dominant loading condition.
Indirect Aerodynamic Pressure		Can produce tension, compression, bending and shear loads, depending upon structural arrangement and pressure distributions.	Can become dominant loading condition.
Airframe Wracking		Can produce tension, compression, bending, shear or torsional loading, depending on the structural arrangement. Induced loads are inversely proportional to stiffness of the transparency.	Can become dominant loading condition.
Installation Preload		Bending stress induced into transparency. Induced loads are directly proportional to stiffness of the transparency with edging stiffness the dominant influence.	Can become dominant loading condition.

TABLE 25-1. LOADING CONDITIONS (cont.)


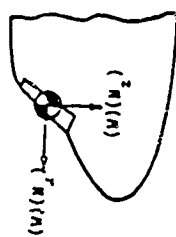

Condition	Description	Effect	Magnitude of Condition
Vibration	 <p>Resonance with main rotor blades</p>	Causes bending, diaphragm action or shell compression. Forces are functions of natural and excitation frequencies. Excessive dither becomes objectionable to flight crews. Flat panels are more susceptible to dither than curved panels.	Usually very small because excitation is low at high frequencies. Typical of panel natural frequencies.
Inertial Loads	 <p> w = Weight N_z = Vertical load factor N_x = Longitudinal load factor </p>	Plate bending, diaphragm action or shell compression. Forces are functions of areal density and local acceleration vectors.	Usually has negligible effect on transparency stress.
High Temperature	 <p>Differential thermal expansion</p>	Shear stress in interlayers of laminated panels.	Major factor affecting interlayer adhesion.

TABLE 25-1. LOADING CONDITIONS (Cont.)


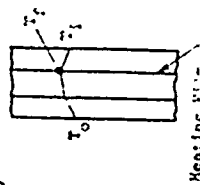
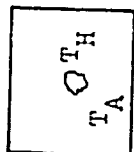
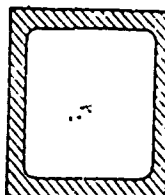

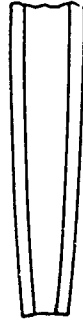
Condition	Description	Effects	Magnitude of Condition
Low Temperature	 <p>Differential thermal contraction</p>	Tension and/or shear stress in interlayers. Local tensile stress along edge of bond line. Compressive or tensile stress in facings.	Major consideration for laminates. Can become dominant loading condition.
Transverse Thermal Gradients (Heated Windshields)	 <p>Heating film</p> <p> $T_o < T_f > T_i$ T_o = outer surface temp. T_f = heating film temp. T_i = inner surface temp. </p>	Tension, compression, and bending stress in facings due to differential thermal expansion/contraction across thickness of laminate	Stresses are low to moderate.
Hot Spots (Heated Windshields)	 <p> T_H = hot spot temp. T_A = average temp. $T_H \gg T_A$ </p>	Local thermal stress in facings. High temperatures can also significantly reduce interlayer strength.	Can be significant along edges.
Cold Edges (Heated Windshields)	 <p> T_A = average temp. T_C = cold edge temp. $T_C \ll T_A$ </p>	Local thermal stress at edge of panel. Contraction and stiffening of interlayer.	Can have significant effects on interlayer stresses at edge of panel.

TABLE 25-1. LOADING CONDITIONS (concluded)

Conditions	Description	Effects	Magnitude of Condition
Manufacturing Stresses	 <p>Residual stresses can occur as a result of overheating during drilling or machining operations.</p>	Built in tensile stress along edges and at hole locations.	Usually small in magnitude.
Laminating Stresses	 <p>Preload stresses built in as a result of interlayer flow during lamination. Also heat cycle used to cure interlayer will lock in thermal stresses.</p>	Residual stresses in interlayer and facings.	Low to moderate in intensity.

The accurate prediction of component stresses and deflections is fundamental to structural engineering. For helicopter transparent enclosures, two basic methods are commonly employed: formula solutions and finite-element analyses. Formula solutions use closed-form equations with specified boundary conditions to calculate approximate values for stresses and deflections. Compromises are usually necessary with this method to account for actual constraints, interactions, and shapes not explicitly covered by the formula. For these reasons, standard formulas for stress and strain are useful only for preliminary design calculations. In contrast, finite-element analyses are far less compromised by these restrictions and therefore provide more accurate results. However, in either method, allowances should be made when applicable for the effects of creep, thermal relaxation, and hysteresis.

Analytical procedures are provided in the following sections for certain types of loading conditions to facilitate the development of new transparencies. However, it is neither practical nor advisable to attempt analytical substantiation for all of the different types of loading conditions that affect the structural integrity of transparencies, because of the complexities involved. Thus, past experience with similar designs and development testing become important considerations for new designs.

26.1 Aerodynamic Pressure Loading

Aerodynamic pressure is considered to be a primary loading condition in the analysis of helicopter transparent enclosures. However, this should not be construed to mean that pressure loading is the only, or most critical, loading condition. Nothing could be further from the truth, since in fact most transparency failures are caused by other loading conditions, which may or may not be coupled with the pressure loading.

To facilitate preliminary design, the following formulas for analyzing plates and shells for pressure loading are provided.

26.2 Flat Plates (Bending Only)

This section presents formulas for simplifying the design and analysis of flat plates.

Table 26-1 lists formulas for stresses and deflections in circular, rectangular and square plates. Numerical values for the constants K and K_1 are given in Tables 26-2, 26-3 and 26-4. K and K_1 were determined using a value of 0.3 for Poisson's ratio. Maximum stresses and deflections for these cases are at the center of the plate.

Nomenclature:

- a - outside radius of circular plate or long side of rectangular plate.
- b - side of square plate or short side of rectangular plate.
- E - modulus of elasticity.
- f_r - stress in the radial direction.
- f_t - stress in the tangential direction.
- K - a constant for determining deflections.
- K_1 - a constant for determining stresses.
- r_0 - radius of a concentric loading circle.
- t - thickness of a plate.
- W - total load applied to a plate (lb).
- w - uniformly distributed load on a plate (lb/in²).
- s - vertical deflection.

Sign Convention:

A positive stress indicates compression on the upper surface of the plate and equal tension on the lower surface. A positive deflection is downward. A negative sign indicates the reverse condition.

Limitations:

1. The plate is flat and of uniform thickness.
2. The thickness is not more than 25% of the width.
3. The maximum deflection is not more than one-half the thickness of the plate.
4. The stresses do not exceed the elastic limit of the material.
5. The material is homogeneous and isotropic.

TABLE 26-1. STRESS AND DEFLECTION FORMULAS FOR FLAT PLATES

Configuration & Loading	Maximum Stress (psi)	Maximum Deflection (in)	Case (Table)
Circular with uniform load applied	$\frac{K_1 W}{t^2}$	$\frac{K W a^2}{E t^3}$	26-2
Square or rectangular with uniform load applied	$\frac{K_1 W b^2}{t^2}$	$\frac{K W b^4}{E t^3}$	26-3
Square with uniform load over a small area of radius r_0	$\frac{K_1 W}{t^2}$	$\frac{K W b^2}{E t^3}$	26-4

Data from Ref. 1.

TABLE 26-2. STRESS AND DEFLECTION COEFFICIENTS FOR CIRCULAR PLATIS WITH UNIFORM LOAD APPLIED


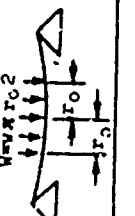
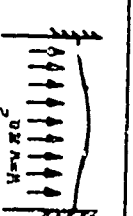
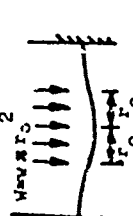
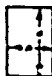
LOADING		a/b or a/r ₀									
CONFIGURATION	K and K ₁	1.2	1.4	1.6	1.8	2.0	2.5	3.0	3.5	4.0	
<p>Edges supported uniform load over entire surface</p>  <p>$W = \pi a^2$</p>	K										
	K ₁ (f _r & f _t at center)	.2214 .3939	.2214 .3939	.2214 .3939	.2214 .3939	.2214 .3939	.2214 .3939	.2214 .3939	.2214 .3939	.2214 .3939	.2214 .3939
<p>Edges supported uniform load over concentric circular area of radius r₀</p>  <p>$W = \pi r_0^2$</p>	K										
	K ₁ (f _r & f _t at center)	.2948 .5326	.3458 .6437	.3827 .7366	.4102 .8165	.4313 .8868	.4668 1.0328	.4883 1.1501	.5023 1.2482	.5120 1.3327	
<p>Edges fixed uniform load over entire surface</p>  <p>$W = \pi a^2$</p>	K										
	K ₁ (f _r & f _t at center) K ₁ (f _r at edge) K ₁ (f _t at edge)	.0543 .1552 -.2387 -.0716	.0543 .1552 -.2387 -.0716	.0543 .1552 -.2387 -.0716	.0543 .1552 -.2387 -.0716	.0543 .1552 -.2387 -.0716	.0543 .1552 -.2387 -.0716	.0543 .1552 -.2387 -.0716	.0543 .1552 -.2387 -.0716	.0543 .1552 -.2387 -.0716	.0543 .1552 -.2387 -.0716
<p>Edges fixed uniform load over concentric circular area of radius r₀</p>  <p>$W = \pi r_0^2$</p>	K										
	K ₁ (f _r & f _t at center) K ₁ (f _r at edge) K ₁ (f _t at edge)	.0766 .2209 -.3117 -.0935	.0968 .2880 -.3557 -.1067	.1137 .3523 -.3842 -.1153	.1275 .4127 -.4038 -.1211	.1389 .4690 -.4178 -.1253	.1593 .5936 -.4393 -.1318	.1726 .6992 -.4509 -.1353	.1817 .7903 -.4580 -.1374	.1682 .8702 -.4625 -.1388	

TABLE 26-3. STRESS AND DEFLECTION COEFFICIENTS FOR SQUARE OR RECTANGULAR PLATES WITH UNIFORM LOAD APPLIED

LOADING CONFIGURATION	K and K_1	a/b or a/r_0								
		1.2	1.4	1.5	1.8	2.0	2.5	3.0	3.5	4.0
All edges supported Uniform load over entire surface Rectangular Solid	K	.0624	.0788	.0924	.1031	.1114	.1246	.1314	.1352	.1375
	K_1	.3883	.4727	.5384	.5877	.6243	.6799	.7078	.7229	.7316
										
All edges fixed Uniform load over entire surface	K	.0199	.0237	.0258	.0269	.0275	.0281	.0283	.0283	.0284
	K_1 (f_b at centers of long edges)	.4137	.4618	.4821	.4910	.4952	.4987	.4996	.4998	.4999
Edges supported above and below (Corners held down) Uniform load over entire surface	K	.0443	.0443	.0443	.0443	.0443	.0443	.0443	.0443	.0443
	K_1 (f_{max} at center)	.2870	.2870	.2870	.2870	.2870	.2870	.2870	.2870	.2870

Data from Ref. 1

TABLES 26-4. STRESS AND DEFLECTION COEFFICIENTS FOR SQUARE PLATE WITH UNIFORM LOAD OVER SMALL AREA OF RADIUS

LOADING CONFIGURATION	K and K	a/b or a/r ₀								
		1.2	1.4	1.6	1.8	2.0	2.5	3.0	3.5	4.0
Edges supported above and below (Corners held down)										
1. Uniform load over small concentric circular area of radius r ₀	K	.1266	.1266	.1266	.1266	.1266	.1266	.1266	.1266	.1266
	K (at center)	.0410	.1167	.2196	.2927	.3581	.4966	.6098	.7055	.7883
2. Uniform load over small concentric circular area of radius r ₀	K	-	-	-	-	-	.0568	.0568	.0568	.0568
	K (at center)	-	-	-	-	-	.1385	.2517	.3474	.4302

Data from Ref. 1

26.3 Flat Plates (Bending with Membrane Action)

A flat transparency subjected to transverse pressure loading must be considered as a partial membrane when the deflection exceeds the thickness of the part. Such a deflection creates in-plane tension forces that provide an additional stiffening capacity over and above the plate's flexural stiffness. These tension forces must be balanced by radial tension reactions from adjacent structure if the edges are restrained, or by circumferential compression if the edges are only loosely clamped. The equations in Tables 26-5 and 26-6 can be used to calculate approximate stresses and deflections for membrane panels.

Nomenclature

a	- Length of long edge	(in)
b	- Length of short edge	(in)
f	- Total stress	(psi)
f _d	- Diaphragm stress	(psi)
r	- Outside radius of plate	(in)
t	- Thickness of plate	(in)
y	- Maximum deflection	(in)
μ	- Poisson's ratio	(dimensionless)
E	- Modulus of elasticity	(psi)

TABLE 26-5. STRESS AND DEFLECTION FORMULAS FOR CIRCULAR PLATES UNDER UNIFORM LOADS THAT PRODUCE LARGE DEFLECTIONS

Parameter	Edges Loosely Clamped	Edges Restrained
Stress at Edge	$\frac{Et^2}{r^2} \left[\frac{4}{1-\mu} \left(\frac{y}{t} \right) \right]$	$4.4E \left(\frac{yt}{r^2} \right) + .476E \left(\frac{y}{r} \right)^2$
Stress at Center	$\frac{Et^2}{r^2} \left[\frac{2}{1-\mu} \left(\frac{y}{t} \right) + \frac{1}{2} \left(\frac{y}{t} \right)^2 \right]$	$2.86E \left(\frac{yt}{r^2} \right) + .976E \left(\frac{y}{r} \right)^2$
Maximum Deflection	$\frac{16}{3(1-\mu)} \left(\frac{y}{t} \right) + \frac{6}{7} \left(\frac{y}{t} \right)^3 = \frac{wr^4}{Et^4}$	$\frac{16}{3(1-\mu)} \left[\frac{y}{t} + .488 \left(\frac{y}{t} \right)^3 \right]$ $= \frac{wr^4}{Et^4}$

Data from Ref. 2

NOTE: The first term represents the bending stress and the second term the membrane stress.

TABLE 26-6. STRESS AND DEFLECTION FORMULAS FOR RECTANGULAR PLATES UNDER UNIFORM LOADS THAT PRODUCE LARGE DEFLECTIONS
($\nu = .316$)

a/b	Edge fixity and point of max. stress	Coef.	wb^4/Et^4											
			0	12.5	25	50	75	100	125	150	175	200	250	
1.0	Loosely clamped	y/t	0	0.430	0.650	0.930	1.13	1.26	1.37	1.47	1.56	1.63	1.77	
	Center of plate	f_d^2/Et^2	0	0.70	1.60	3.00	4.60	5.00	6.10	7.00	7.95	8.60	10.20	
	Center of plate	f_b^2/Et^2	0	3.80	5.80	8.70	10.90	12.80	14.30	15.60	17.00	18.20	20.50	
1.0	Completely restrained	y/t	0	0.165	0.25	0.59	0.80	0.95	1.08	1.19	1.28	1.38	1.54	
	Center of edge	f_d^2/Et^2	0	0.070	0.22	0.75	1.35	2.00	2.70	3.30	4.00	4.60	5.90	
	Center of edge	f_b^2/Et^2	0	3.80	6.90	14.70	21.0	26.50	31.50	36.20	40.70	45.00	53.50	
	Center of plate	f_d^2/Et^2	0	0.075	0.30	0.95	1.65	2.40	3.10	3.80	4.50	5.20	6.50	
	Center of plate	f_b^2/Et^2	0	1.80	3.50	6.60	9.20	11.60	13.0	14.50	15.80	17.10	19.40	
1.5	Loosely clamped	y/t	0	0.625	0.879	1.18	1.37	1.53	1.68	1.77	1.86	1.96	2.12	
	Center of plate	f_d^2/Et^2	0	1.06	2.11	3.78	5.18	6.41	7.65	8.60	9.55	10.6	12.30	
	Center of plate	f_b^2/Et^2	0	4.48	6.81	9.92	12.95	14.22	16.0	17.50	18.90	20.30	22.80	
2 to ∞	Loosely clamped	y/t	0	0.696	0.946	1.24	1.44	1.60	1.72	1.84	1.94	2.03	2.20	
	Center of plate	f_d^2/Et^2	0	1.29	2.40	4.15	5.61	6.91	8.10	9.21	10.10	10.90	13.20	
	Center of plate	f_b^2/Et^2	0	4.87	7.16	10.30	12.60	14.60	16.40	18.00	19.40	20.90	23.50	
1.5 to ∞	Completely restrained	y/t	0	0.28	0.51	0.825	1.07	1.24	1.40	1.50	1.63	1.72	1.80	
	Center of long side	f_d^2/Et^2	0	0.20	0.66	1.90	2.20	4.35	5.40	6.50	7.50	8.50	10.30	
	Edges	f_b^2/Et^2	0	5.75	11.12	20.30	27.80	35.00	41.00	47.00	52.50	57.60	67.00	

26.4 Curved Panels

Membrane and flexural stresses in curved panels subjected to pressure loads are substantially lower than corresponding stresses in flat panels having equivalent areas. The ideal case is represented by an infinitely long circular cylinder for which circumferential and longitudinal stresses are calculated in accordance with classical pressure vessel equations:

$$f_c = \frac{pr}{t} \quad (26-1)$$

$$f_l = \frac{pr}{2t} \quad (26-2)$$

$$\delta_r = \frac{r}{E} (f_c - \mu f_l) \quad (26-3)$$

where

p = pressure loading

r = radius of cylinder

t = thickness of cylinder

f_c = circumferential stress

f_l = longitudinal stress

E = modulus of elasticity

δ_r = radial deflection

μ = Poisson's ratio

26.4.1 Deficiencies

The preceding formulas are subject to the following deficiencies:

1. Support constraints in actual installation create discontinuity stresses along the panel edges, as shown in Figure 26-1. In many cases these discontinuity stresses constitute the major portion of the total stress.
2. Helicopter transparencies with other than circular cross sections, i.e., loft conics or compound curves, support pressure loads by both membrane and bending action, which are not readily analyzed by standard formulas.

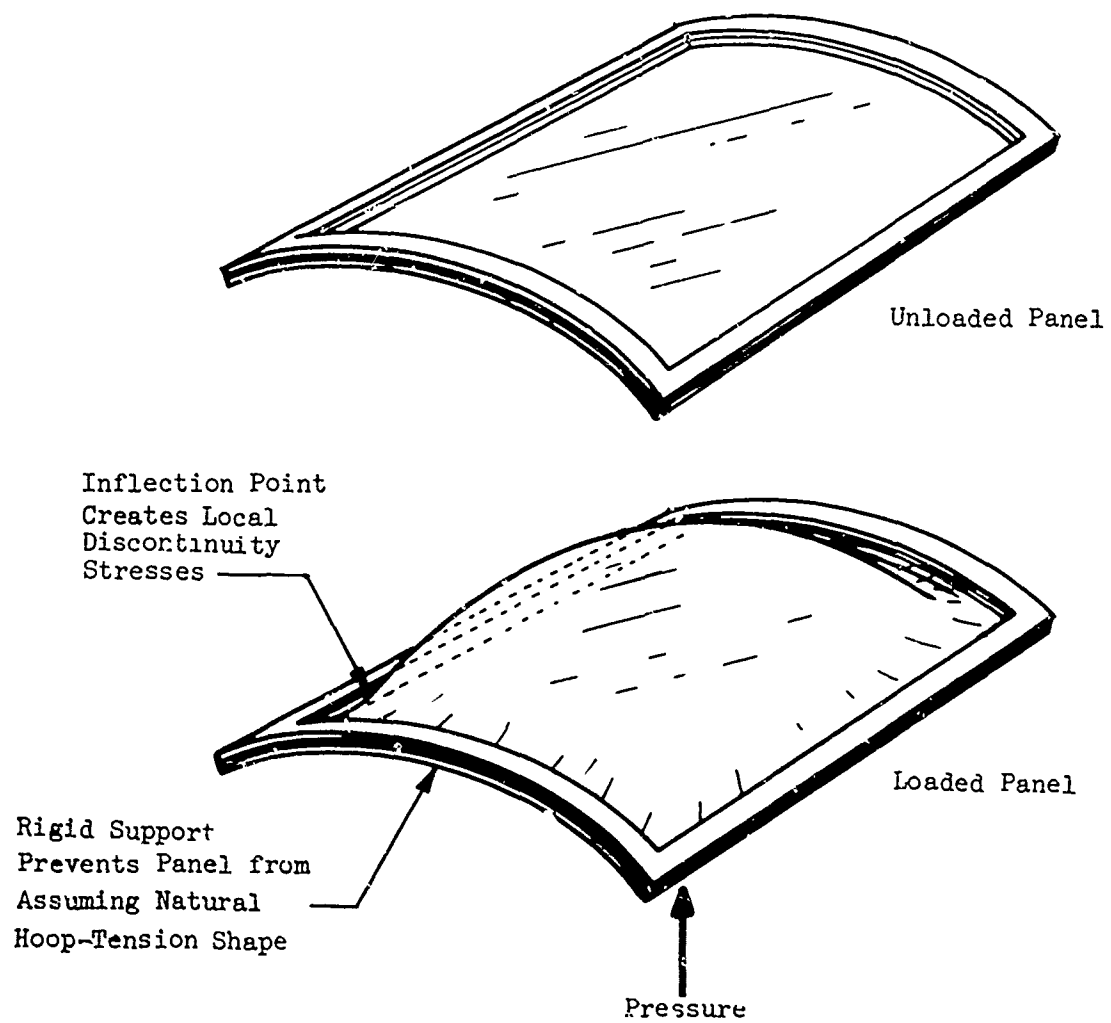


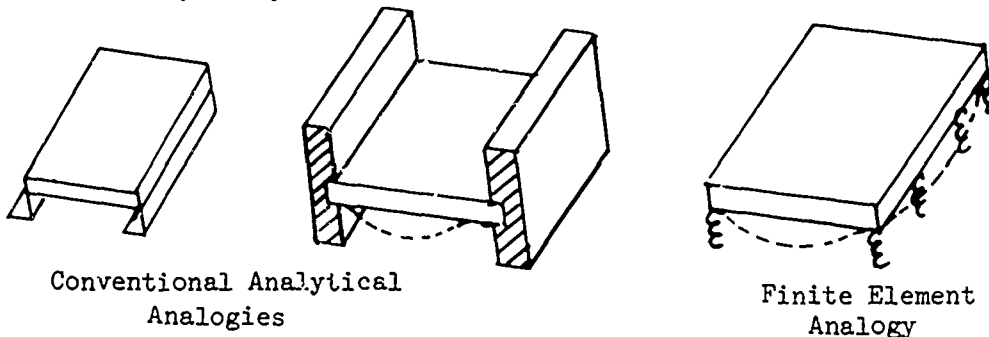
Figure 26-1. Discontinuity Stresses due to Support Constraints.

26.5 Finite-Element Structural Analysis

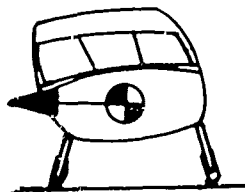
Computerized finite-element analysis provides a more accurate, detailed and less compromising method for analyzing complex structures than calculations based on formula solutions for stresses and deflections. For example, in Figure 26-2 a computer-generated stress distribution obtained by a finite-element analysis compares favorably with the results of a test conducted on a specimen loaded under similar conditions.

Finite-element analysis has significant advantages for analyzing and determining interactions for the following types of structures:

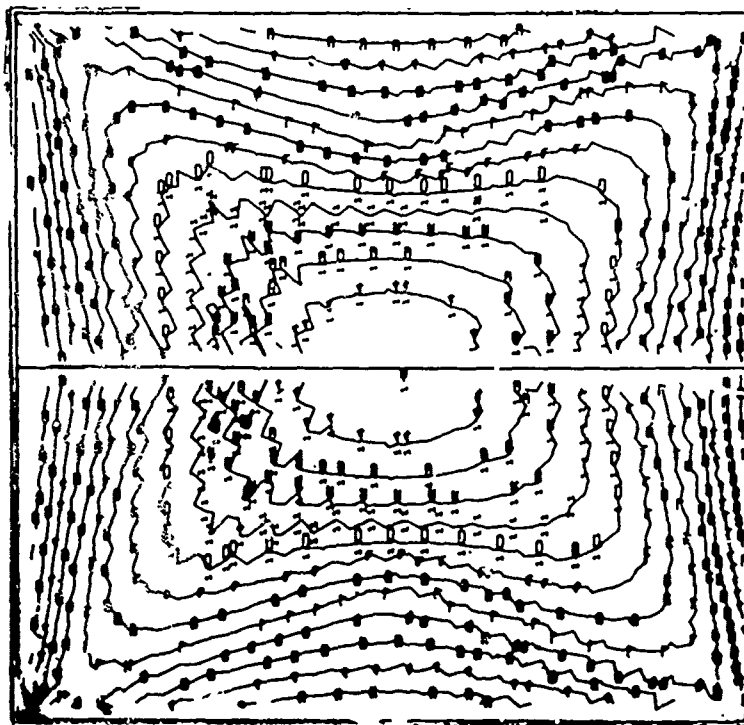
1. Transparencies mounted on elastic supports. Here, the analysis considers the effect that supporting structure deflections have on transparency stress.



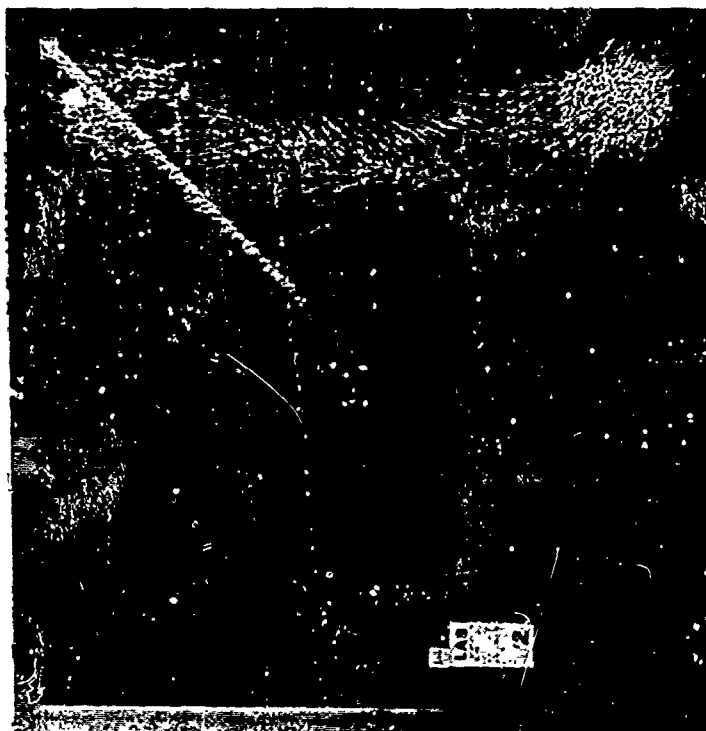
2. Transparent enclosures influenced by fuselage deformations or wracking. During flight or ground maneuvers, fuselage loads can distort transparency mountings and induce panel stress. A finite-element model of the fuselage containing the transparency can be used to determine the magnitude of these stresses.



3. Curved shells. General formulas for stress and strain apply only to flat, circular or spherical shaped panels of square, rectangular or circular planform. Unique analytical solutions are required for other shapes and are difficult to obtain. Finite-element modeling accommodates any shape by describing the surface in terms of geometric coordinates.



Computer-Generated Stress-Contour Plot

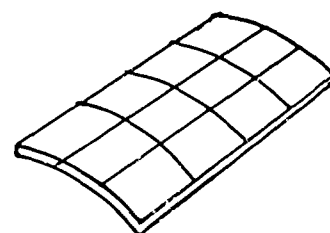


Fracture Pattern from Static Pressure Test

Figure 26-2. Stress Pattern for a Flat Windshield.

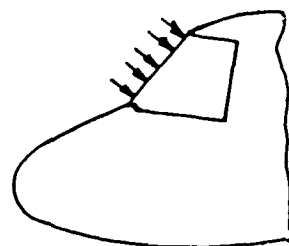


General Solutions Limited
To Common Shapes

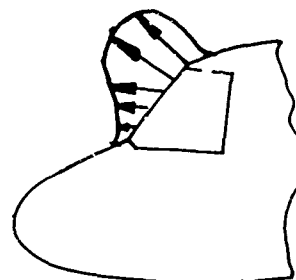


Finite-Element
Model

4. Nonuniform aerodynamic pressure distributions. Using finite-element analysis, discrete loads can be applied over a surface to represent a nonuniform pressure distribution. Conventional hand analyses are restricted to average values and tend to be conservative.



Conventional Analysis
Pressure Distribution



Pressure Distribution

Presently, existing finite-element programs are unsuitable for the analysis of transversely loaded flat plates where the load is carried partially or entirely by membrane effects. The membrane response of a flat plate subjected to pressure loading is nonlinear, and the higher-order terms that govern such relationships are not included in current programs.

26.5.1 Finite-Element Format

There are many different computer programs available for performing structural finite-element analyses. NASTRAN (NAsa STRuctural ANalysis) is one of the most widely accepted versions used in the aircraft industry. To use NASTRAN, the analyst enters a description of the structure and applied loads in a computer. The computer then provides an output consisting of a detailed listing of all internal loads, stresses, displacements, and external reactions.

A brief discussion on the use and theory of finite-element analysis is provided in the following section.

26.5.2 Finite-Element Models

A finite-element model describes a structure in terms of geometric coordinates and structural elements. The structural elements are se-

lected to simulate the actual type of structure, and individual material and geometric properties are specified for each element. Elements can represent rod, bar, shear, or plate characteristics. Rods are line elements capable of carrying axial and torsional loads. Bars are also line elements that, in addition to carrying axial and torsion loads, can react bending and shear loads. Shear elements are used to duplicate webs and skins and can take in-plane tension, compression and shear loads. Plate elements are similar to the shear elements but also have flexural stiffness.

Figure 26-3 shows a typical NASTRAN model for a helicopter nose section. In this model the windshields are composed of 200 triangular plate elements having six degrees of freedom per element. Curved surfaces are modeled by specifying coordinates of each node of each triangle. Geometry coordinates are most conveniently obtained from the analytic geometry programs used to describe an aircraft's basic contours. It is essential to have an accurate model of the structure adjacent to the transparencies because of the complex loading interactions that occur.

Laminated composite windshields must be idealized as monolithic structures because it is not practical to simulate the nonlinear coupling characteristics of the interlayers used in such panels. Equivalent properties for uncoupled laminates (least stiffness) would therefore be considered conservative for use in an analysis of direct pressure loading, whereas equivalent properties for fully coupled laminates (greatest stiffness) would be considered conservative for an analysis of forced deflections, such as airframe wracking conditions.

Prior to running a model with applied loads, the geometry inputs should be verified. A cathode ray tube (CRT) display is an effective aid in this process. As shown in Figure 26-4, the analyst can use a light pen to identify specific elements and coordinates of the model. By rotating the model about any axis on the display, missing elements, improperly connected elements, and erroneous coordinates can be readily detected.

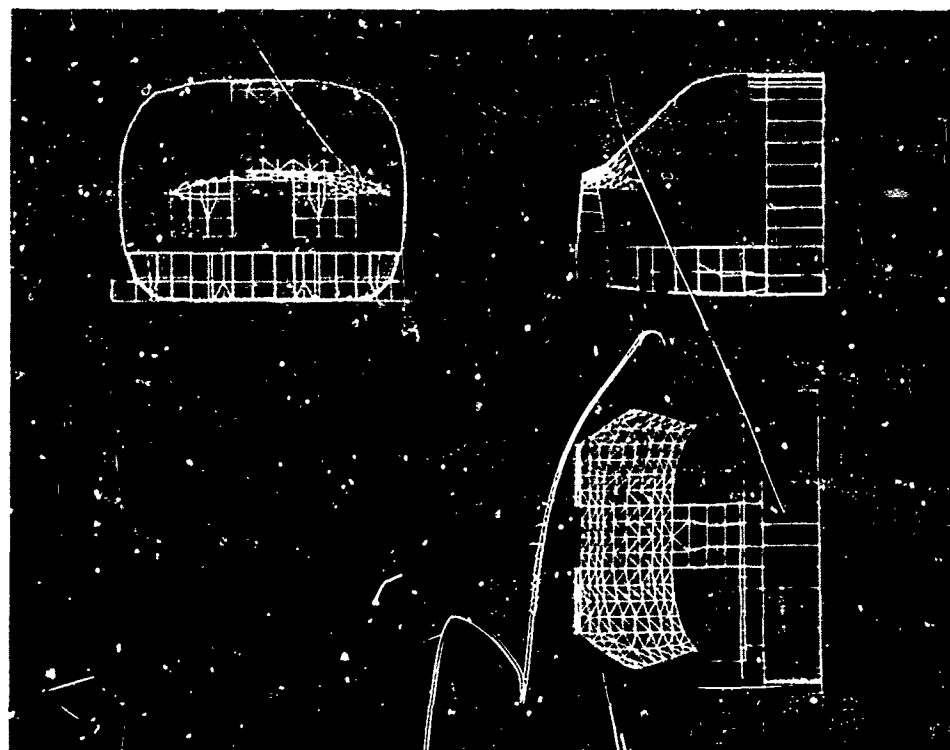


Figure 26-3. NASTRAN Model of YUH60A Nose Section.

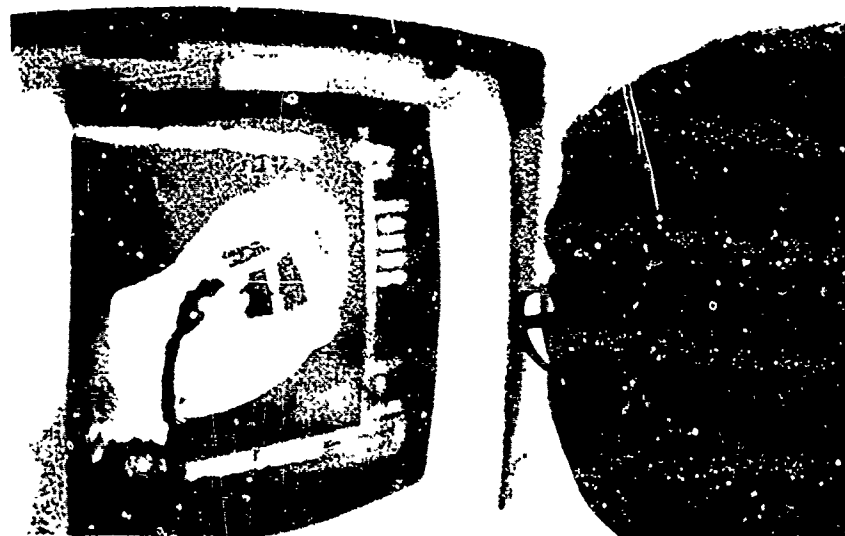


Figure 26-4. Cathode Ray Tube Display.

26.5.3 Finite-Element Theory

The displacement or stiffness method is used to calculate the forces in structural elements. This method consists of modeling a structure as a collection of finite elements that are mathematically considered to have the elastic properties of the structure they represent. These elements are connected at joints or nodes called grid points. The force-displacement equation shown below for the various connected elements is compiled by the computer program in matrix form.

$$(F) = (K) (\delta) \quad (26-4)$$

where

(K) = stiffness matrix

(δ) = displacements at node points

(F) = forces applied at node points

The nodal displacements are the unknowns in this problem, and the stiffness matrix must be inverted and multiplied by the applied load vector, which yields

$$(\delta) = (K)^{-1}(F) \quad (26-5)$$

When the displacements are known, the extension of each finite element can be found and the stresses can be determined from the stress-strain relationships of the elements.

In the development of this finite-element method for the analysis of linearly elastic structures, it is assumed that both the displacements and the strains developed in the structure are small, and that the stress-strain relationships for the material are linear. Physically, the first assumption means that, during the loading process, the geometry of the structure remains basically unchanged, so that the infinitesimal, first-order, linear strain-displacement relations may be used and so that the equations of equilibrium may be written for the undeformed structure. The second assumption can be thought of as following from the first, since the stress-strain relations for most engineering materials can be considered linear when the stresses are below the elastic limits and the displacements are small.

In some instances, these assumptions may fail because of nonlinear effects, even though the actual strains and displacements may be small and the elastic limits of the structural material are not exceeded. Nonlinear static effects are classified as material nonlinearities and geometric nonlinearities.

Material nonlinearity effects occur because the stresses are nonlinear functions of the strains, resulting from the nonlinear elastic or plastic behavior of the structural material.

Geometric nonlinear effects occur because the strains and/or displacements at the points of applied loading are nonlinear functions of the degrees of freedom used to describe the motion of the structure. That is, geometric nonlinearities occur when the loads applied to the structure are large enough to give rise to relatively large displacements. When the deflections are large, they cause significant changes in the geometry of the structure, and in such cases, the equations of equilibrium must be reformulated for the deformed configuration.

26.5.3.1 Finite-Element Capabilities for Nonlinear Problems

NASTRAN presently includes a linear static capability, a differential stiffness capability and a conservative, nonlinear material capability called piecewise linear analysis. These capabilities have not been combined.

The differential stiffness capability includes the stiffening or softening effects of static inplane loads. Thus, the differential stiffness matrix may be interpreted as an effective stiffness created by the stresses existing in the structure. This added stiffness is calculated from the geometry of and internal loads existing in the element, and is assumed to be proportional to the magnitude of the applied loads. The total stiffness of the structure is the sum of the elastic stiffness matrix and the geometric stiffness matrix.

This two-step approach is in direct contrast to iterative procedures, and because of this, the differential stiffness approach can only be expected to give accurate answers for those problems where the effects of geometric nonlinearities are not too severe.

Finally, it should be noted that, for the plate-bending element, the geometric stiffness matrices for this element are functions of only the axial or inplane loads determined from the linear solution. The changes in the axial and inplane strains due to transverse loads are considered to be higher-order effects and are ignored in the geometric stiffness matrix formulation. Physically, this means that, in the case of a perfectly flat plate with no prescribed inplane loading, membrane effects arising from transverse pressure loads cannot be predicted.

It is essential to use the differential stiffness approach in the analysis of helicopter transparent enclosures because of the relatively large displacements that occur. These displacements significantly alter the geometric matrices used for computing stresses and deflections, and must be compensated for to obtain accurate results. Differential stiffness solutions can alter the results of a linear static analysis by as much as 100%.

The piecewise linear analysis is used to solve problems involving material plasticity. In this approach, the nonlinearities of the materials are defined in the program as tabular stress-strain curves. The load is applied in small increments so that the stiffness properties of the elements can be assumed to be constant over each increment. The stiffness matrix for each increment is dependent on the current state of stress in the elements, and displacement increments and stresses are accumulated to produce the final nonlinear result.

The piecewise structural stiffness matrix must be reformulated and decomposed for each load increment. However, from the analysis standpoint, the most serious drawback is the fact that, for each load increment, the coordinates of the grid points in the undeformed state are used to calculate the element stiffness matrix. Because of this, many piecewise linear solutions are only gross approximations of the true response of the structure. However, it should be pointed out that, even if the coordinates of the grid points were updated, the solution would still be only an approximation (albeit a much better one) of the true response unless the effects of differential stiffness were included.

26.6 Thermal Stress

Analytical expressions are presented in this section to aid in estimating thermal stresses induced in heated windshields for several different conditions. These expressions are based on mathematical derivations for ideal cases and, therefore, must be considered as providing only approximations of actual stresses.

26.6.1 Temperature Gradient Across Thickness

A temperature differential across the thickness of a heated windshield exists when power is applied to the windshield heating film. The same type of temperature gradient also results from the difference in temperature between cockpit air and the outside air. This condition is illustrated in Figure 26-5.

If the windshield is unrestrained, it would assume a spherical curvature; however, since the edges are supported, thermal stresses will result, with the cold surface in tension and the hot surface in compression. The maximum stresses can be approximated by the following equation:

$$f = \frac{E \alpha \Delta T}{2(1 - \mu)} \quad (\text{from Ref. 3) (26-6)}$$

where

- f = tensile stress
- E = modulus of elasticity
- α = coefficient of thermal expansion
- ΔT = temperature gradient
- μ = Poisson's ratio

It may be noted that in most heated windshield applications the contribution of the inner ply temperature differential to the total stress is negligible. Also, the effects of the restraining moments will be shared by all plies within the laminate in proportion to their stiffnesses, which will reduce the peak stresses predicted by equation 26-6.

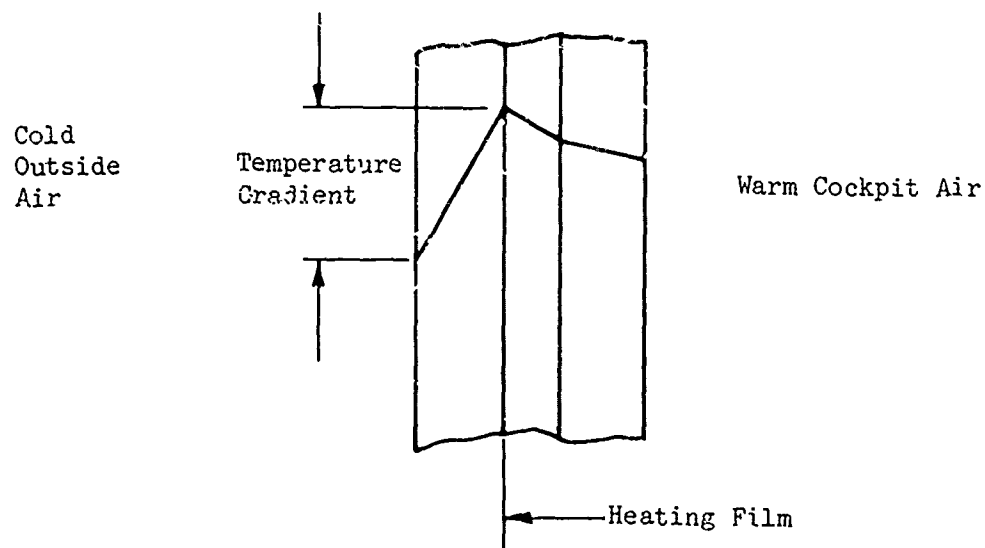


Figure 26-5. Temperature Profile of Heated Windshield.

26.6.2 Localized Hot Spots

Nonuniform heating in the conductive coating of electrically heated windshields results in regions of high temperature concentration, called hot spots. Analytical expressions for the stresses induced in the outer glass panel of the windshield by such nonuniformities are presented here.

For the purpose of the analyses, the hot spot considered is a right circular cylinder with bases coincident with the lateral faces of the transparency, as shown in Figure 26-6. Its temperature is considered constant and higher than the uniform temperature of the remainder of the plate.

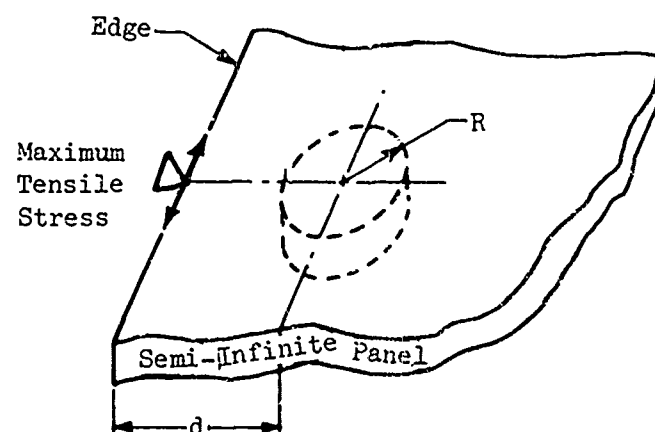


Figure 26-6. Tensile Stress at Edge of Semi-Infinite Glass Panel Produced by Cylindrical Hot Spot Located Near Edge.

For the case of a hot spot located in a semi-infinite plate, the maximum stress occurs at the edge of the plate in the position and direction indicated in Figure 26-6. This stress is given by the following equation taken from Reference 3:

$$f = 2E\alpha\Delta T_{hs} \left(\frac{R}{d}\right)^2 S \quad (26-7)$$

where T_{hs} = temperature differential between hot spot and surrounding area.

S = Hot spot temperature distribution factor.

S = 1.0 for a uniform temperature distribution yielding the maximum possible stress for any given case.

The preceding formula is useful only for gross estimations of actual stresses, because actual temperature profiles do not conform to simple geometric shapes. This is illustrated by Figure 26-7 which shows a typical thermal map of a rectangular windshield when heated.

26.6.3 Cold Edges

The edges of a heated windshield are usually somewhat cooler than the center region of the panel. Lack of edge heating and heat loss to the airframe are the predominant reasons. This condition creates tensile stresses along the edges as shown in Figure 26-8, which may be roughly estimated by equation 26-8 from Reference 3:

$$f = E\alpha\Delta T_{ce} S \quad (26-8)$$

where ΔT_{ce} = temperature differential between the central area and the cold edge.

26.6.4 Stresses due to Different Thermal Expansion Coefficients

The stresses resulting from differences in the thermal expansion or contraction of two dissimilar materials that are restrained to prevent lateral deformation, as shown in Figure 26-9, can be predicted by equation 26-9.

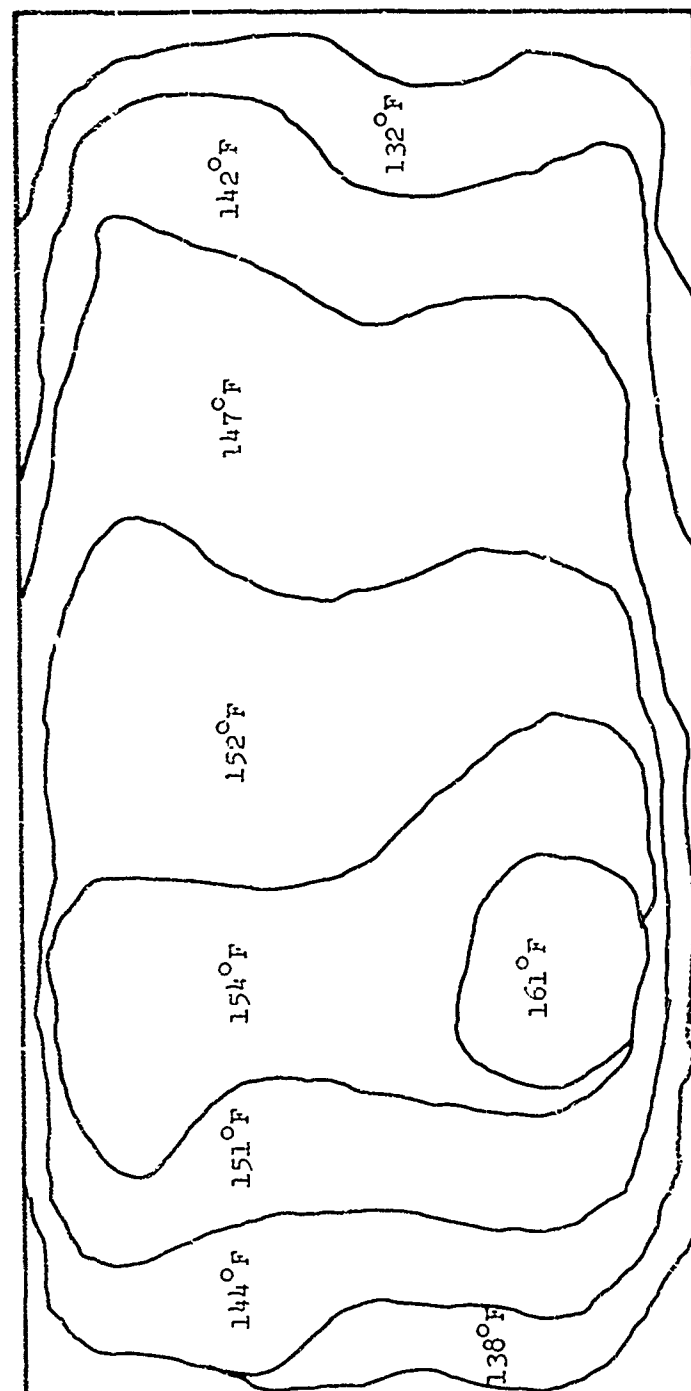


Figure 26-7. Thermal Map of Typical Rectangular Windshield.

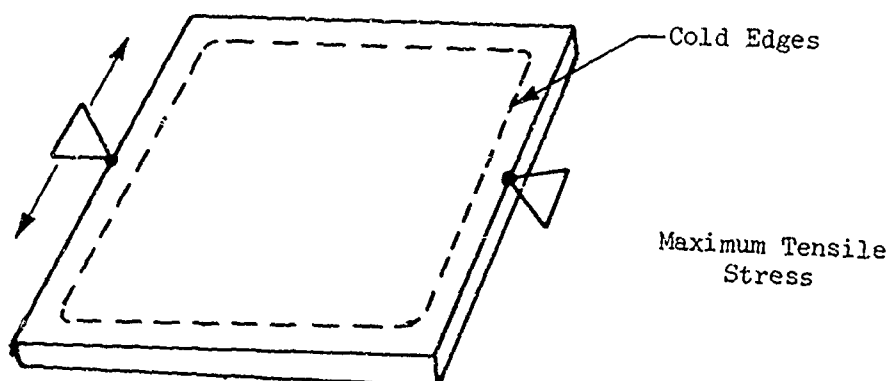


Figure 26-8. Location and Direction of Maximum Tensile Stress Induced by Cold Edges.

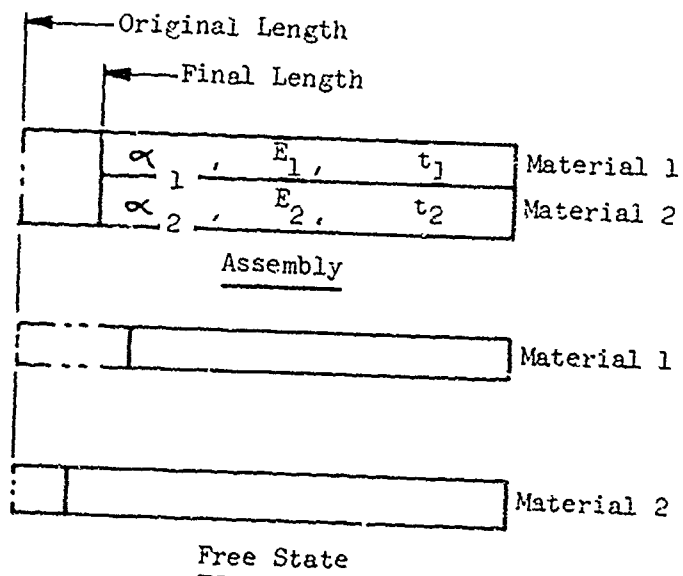


Figure 26-9. The Effect of Coupling on the Contraction of Different Materials.

$$f_1 = (\alpha_1 - \alpha_2) \Delta T_t \frac{E_1 E_2 t_2}{E_1 t_1 + E_2 t_2} \quad (26-9)$$

where α = coefficient of thermal expansion
 E = modulus of elasticity
 t = material thickness
 ΔT_t = difference between ambient temperature and temperature at which part was assembled

This equation can be used to calculate a stress that would be approached only if the two materials were rigidly coupled. In actual practice, flexible adhesives or interlayers are used to bond laminates together that allow slippage, and the thermal stresses due to expansion differences will be much lower than those predicted by equation 26-9.

The extreme condition is a very flexible interlayer that offers no coupling. Then, unrestrained thermal expansion of the facings occurs and the interlayer must absorb the difference in elongation between the two facings (see Figure 26-10). This elongation can be calculated with equation 26-10:

$$\delta = \frac{(a_1 - a_2)L \Delta T_t}{2} \quad (26-10)$$

where δ = interlayer elongation, as shown in Figure 26-10
 L = initial dimension across part as shown in Figure 26-10

It should be noted that the preceding equations can only be used to establish limits for maximum stresses. They are invalid for calculating actual stresses because of the nonlinear, temperature dependent properties of typical interlayers that influence the true stress distributions.

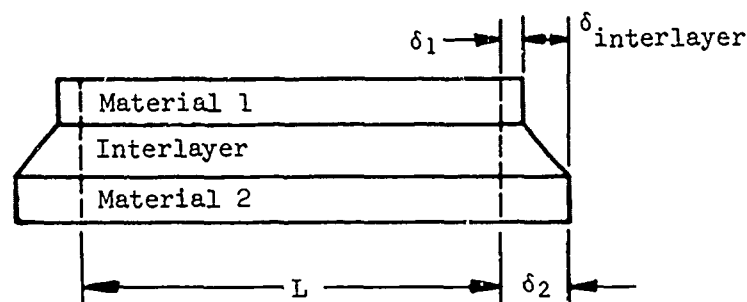


Figure 26-10. Interlayer Deformation due to Thermal Expansion Differences

26.7 Safety Factors

It is not possible to specify a general factor of safety to be used in the design of all helicopter transparent enclosures. Safety factors as high as 5.0 and 10.0 have been used for windshields in the past, although the practice of arbitrarily selecting factors much greater than 1.5 is considered unwarranted and crude.

Safety factors should be established for individual applications based on the following factors:

1. Accuracy of the analytical method used to predict stresses.
2. Consideration of coupled or combined loading conditions.
3. Reduction of allowable material stresses for environmental effects.
4. Presence of residual manufacturing stresses.
5. Possibility of service-induced flaws.
6. Variation of physical and geometric properties due to manufacturing tolerances.
7. Experience with similar designs/installations

References

1. Structures Manual, Chap. 7, Sikorsky Aircraft Division, Stratford, Conn., Jan. 1967.
2. Roark, R. J., "Formulas for Stress and Strain," Fourth Edition, McGraw Hill Book Company, New York, 1965.
3. Islinger, J.S., Armor Research Foundation, "Engineering Design Factors for Laminated Aircraft Windshields," Parts 1 and 2, WADC-TR-53-99, Wright Air Development Center, Wright-Patterson Air Force Base, Ohio, Apr. 1954.

Bibliography

Kay, B. F., Sikorsky Aircraft Division, "Design, Test, and Acceptance Criteria for Helicopter Transparent Enclosures," USARTL-TR-78-26, Applied Technology Laboratory, U. S. Army Research and Technology Laboratories, Ft. Eustis, Va.

McGarvey, J. H., and Kay, B. F., Sikorsky Aircraft Division, "Design and Development of Helicopter Transparent Enclosures," AFML-TR-76-54, Air Force Materials Laboratory, Wright-Patterson Air Force Base, Ohio, Apr. 1976.

Johnson, A. V., et al, Pittsburgh Plate Glass Company, "F-111 Transparencies - Conceptual Design," WADC-TR-65-212, Air Force Materials Laboratory, Wright-Patterson Air Force Base, Ohio, Sept. 1965.

Gallagher, R. H., "Geometrically Nonlinear Finite Element Analysis," Proceedings of the Specialty Conference of Finite Element Methods in Civil Engineering, Edited by McCutcheon, J. D., et al, June 1972.

Zienkiewicz, O. C., "The Finite Element Method in Engineering Science," McGraw Hill Publishing Company, Ltd., London, 1971.

McCormick, C. W., "NASTRAN User's Manual," MSR-39, The MacNeal Schwendler Corporation, Los Angeles, Calif., Mar. 1974.

MacNeal, R. H., "The NASTRAN Theoretical Manual," MSR-40, The MacNeal Schwendler Corporation, Los Angeles, Calif., May 1974.

Joseph, J. A., "MSC/NASTRAN Applications Manual," MSR-35, The MacNeal Schwendler Corporation, Los Angeles, Calif., Nov. 1972.

Bennet, R. D., LTV Aerospace, "NASTRAN Differential Stiffness Analysis of an Aircraft Canopy," NASA TM S-2378, National Aeronautics and Space Administration, Washington, D. C., Sept. 1971.

Lawrence, J. H., Douglas Aircraft Co., "Windshield Technology Demonstrator Program," AFFDL-TR-77-1, Air Force Flight Dynamics Laboratory, Wright-Patterson Air Force Base, Ohio, Sept. 1977.

Interlayers are considered to be nonstructural inasmuch as they are not designed to support normal flight loads. However, interlayers do become stressed as a result of differential straining that occurs between individual plies within laminated panels. This strain can be caused by thermal or mechanical forces.

Excessive interlayer strain can lead to several types of failures. The most common is delamination. Delamination occurs when the forces acting on the interlayer exceed the adhesive strength of the bond between the interlayer and facing ply. Damage to structural face plies, such as edge chipping and cracking, can also occur as a result of these forces.

The different mechanisms that affect interlayer loading, including fail-safe requirements, are discussed in the following sections. Criteria for using interlayers to resist bird impact forces are presented in the Birdproofing section of this handbook.

27.1 Thermal Expansion/Contraction Differentials

Thermal expansion/contraction differentials occur when materials with different coefficients of thermal expansion are laminated together. This condition occurs in its simplest form in symmetrical laminates where the coefficient of thermal expansion for the interlayer is typically much greater than that of the facing materials. Figure 27-1 shows how interlayer shrinkage forces develop in symmetrical laminates during cold soak. In asymmetrical composite laminates, the interlayer must also accommodate different rates of strain between facings. Figure 27-2 illustrates this condition.

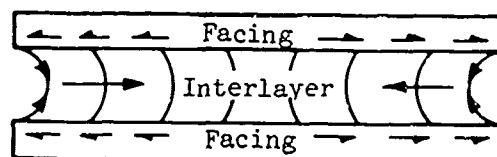


Figure 27-1. Interlayer Shrinkage Forces During Conditions of Cold Soak.

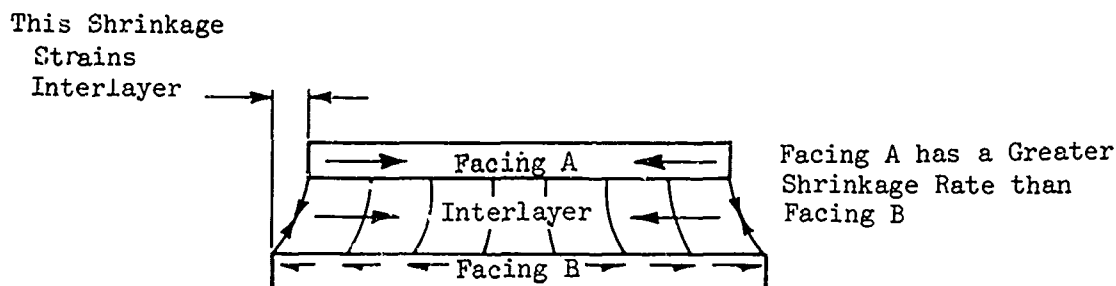


Figure 27-2. Cold Soak Forces Induced Into Unsymmetrical Laminates.

The effects of low temperature exposures are invariably more severe than those of high temperature. There are two reasons for this: First, interlayers are free of stress only at their cure temperature. The interlayer thermal strains are then proportional to thermal gradient or temperature excursion as measured from the interlayer cure temperature. Cure temperatures are generally well above 100°F. Thus, for extreme low and high environmental exposure temperatures of -65°F and 160°F, respectively, it is readily seen that at the low temperature extreme, interlayers experience the greatest thermal gradient and hence the highest thermal strains. This concept is illustrated in Figure 27-3. The second reason is that the modulus of elasticity for most interlayers increases as the temperature is lowered.

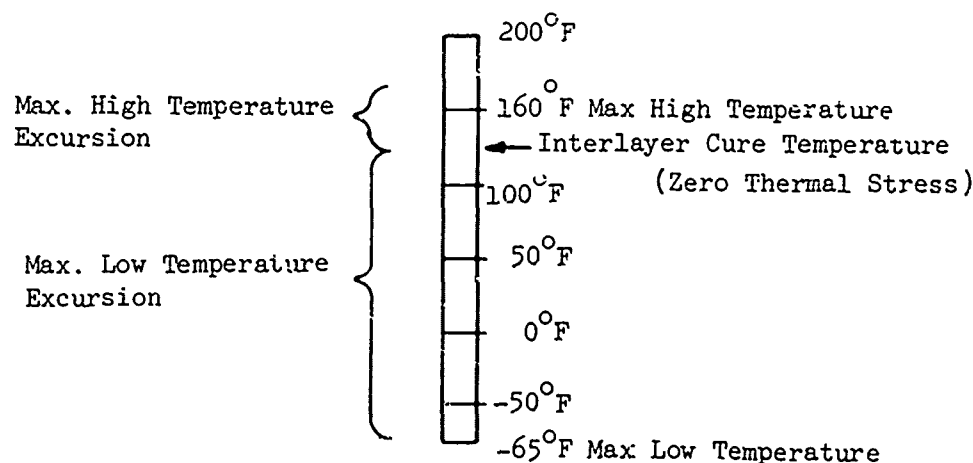


Figure 27-3. Temperature Changes Used for Establishing Thermal Stress.

Internal stress distributions resulting from thermal expansion differentials are quite complex. Figure 27-4 is a picture of a typical stress distribution for a symmetrical laminate. These results, obtained by photoelastic means, show that, under cold soak conditions, high stress concentrations occur extremely close to the edges of the laminate. Analytical methods for predicting these stresses require the use of complex, three-dimensional, nonlinear, large-displacement finite-element analyses and are considered impractical for routine design purposes. Substantiation of design integrity must therefore be based on test data.

In order to facilitate the development of new designs, empirical comparisons to existing designs can be used. To aid in this task, Table 27-1 lists the important design variables, along with brief descriptions of how they influence interlayer stresses. Table 27-2 lists representative values of facing stresses due to thermal expansion/contraction differentials for symmetrical and unsymmetrical laminates. This data applies to the configurations shown in Figure 27-5.

TABLE 27-1. FACTORS GOVERNING INTERLAYER STRESS IN LAMINATED TRANSPARENCIES FROM THERMAL EXPANSION DIFFERENTIAL

Design Variable	Relationship to Interlayer Stress
Coefficient of Thermal Expansion	Stress increases as a function of the difference in the coefficients of the constituent materials.
Interlayer Modulus	Stress increases as a function of interlayer modulus.
Interlayer Thickness	Stress decreases by increasing interlayer thickness.
Temperature Change from Interlayer Cure	Stress changes in proportion to the change in temperature as measured from the interlayer cure temperature.
Facing Stiffness (Modulus & Thickness)	Interlayer stresses will increase as a function of increasing facing stiffness.
Maximum Lineal Dimensions Across Part	The shear stress in a compliant interlayer increases as a function of component lineal dimensions.

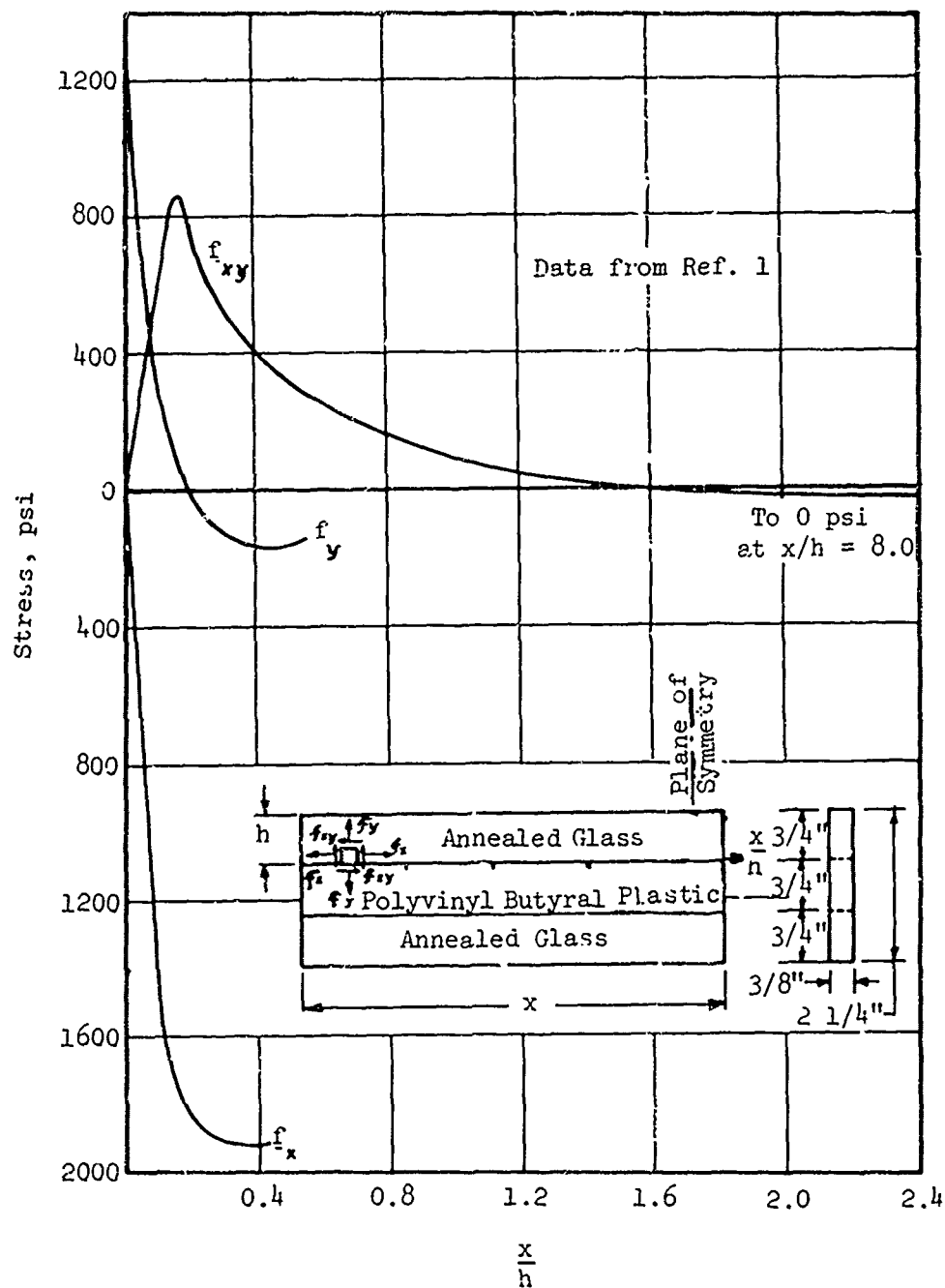


Figure 27-4. Stress Distribution Along the Glass-Plastic Interface of a Three-Ply Laminate Subjected to a Uniform Temperature of -20°F , Obtained Photoelastically.

TABLE 27-2. FACING STRESSES DUE TO DIFFERENTIAL THERMAL EXPANSION/
CONTRACTION

Configuration (See Figure 27-5)	Stress at -65°F (psi)	Stress at $+160^{\circ}\text{F}$ (psi)
Symmetrical Laminate	-2600 to -3600	300 to 1000
Unsymmetrical Laminate		
Glass ply	-9500 to -10,000	500
Acrylic ply	1,000	-200

Data from Reference 2

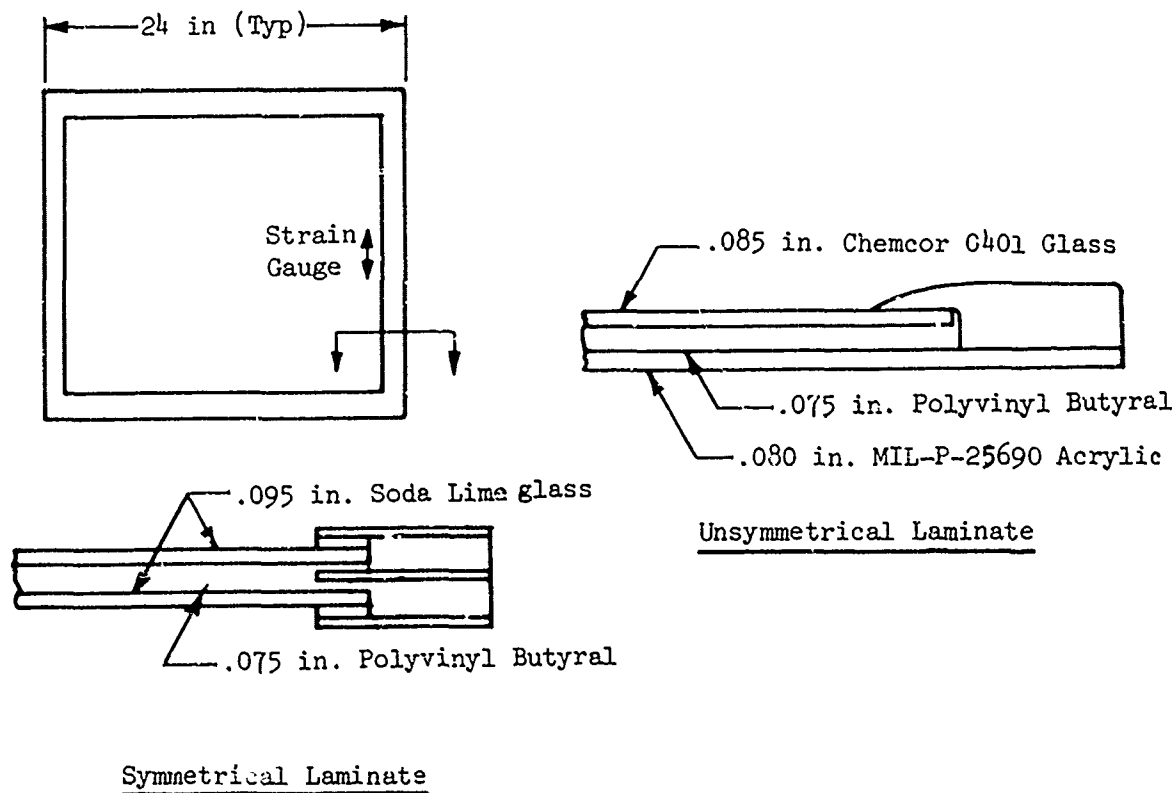


Figure 27-5. Laminates Used to Obtain Facing Stresses.

27.2 Transverse Thermal Contraction due to Cold Edges

Unless a windshield incorporates edge heating, there can be a large temperature gradient between the central heated area and the panel edges, as shown in Figure 27-6. Accompanying this temperature gradient will be a tendency for the interlayer to change its thickness. However, any change in thickness is resisted by the stiffness of the facing plies, and equilibrium is reached when the tensile forces acting over the narrow edge zone are balanced by compressive force over the central heated area. A typical stress distribution is shown in Figure 27-7.

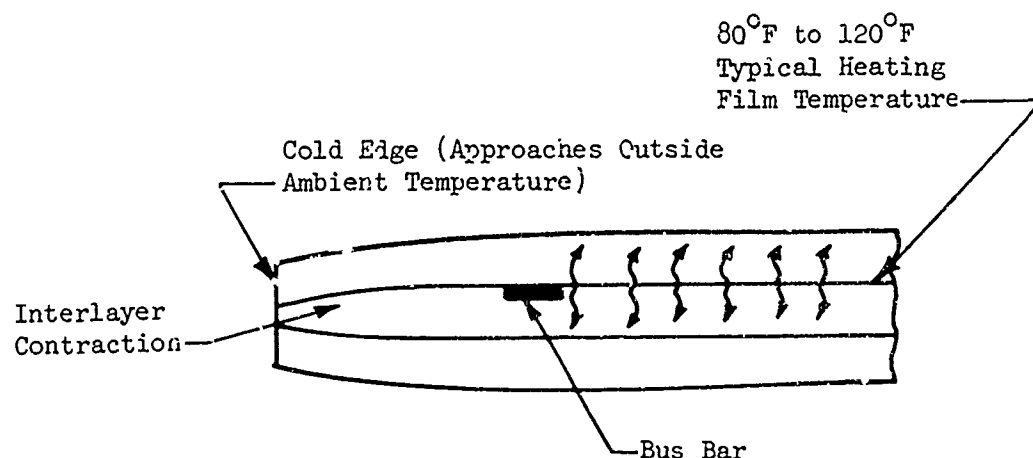


Figure 27-6. Cold Edge Contraction of Interlayer.

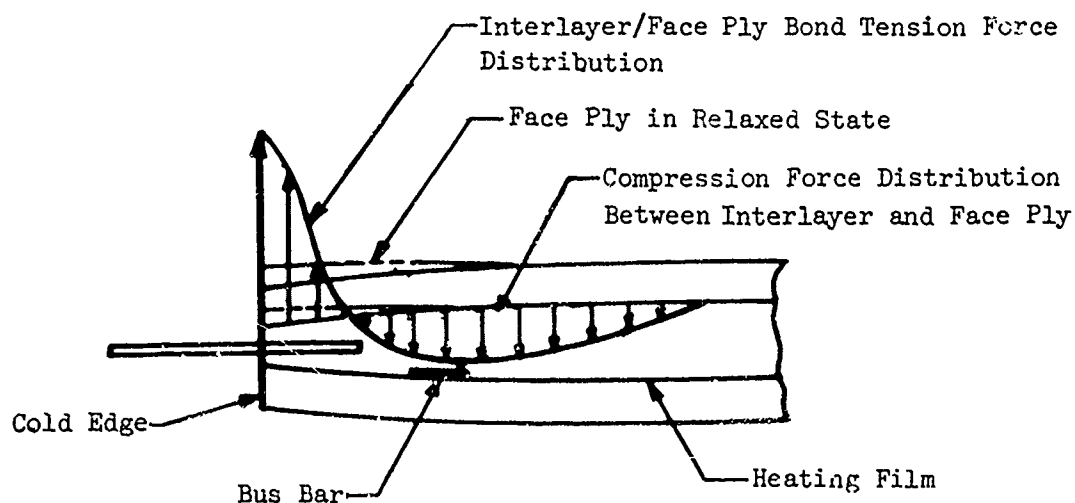


Figure 27-7. Stress Distribution due to Cold Edges.

Due to the complexity of the problem and the time- and temperature-dependent properties of the interlayer, it is virtually impossible to accurately determine these stresses. However, examination of the relevant variables is instructive. The stiffnesses of the facing plies are of primary importance, since the bending of the facing plies can substantially reduce the interlayer stresses. The interlayer forces are primarily functions of E , α , and ΔT , where E is the modulus of the interlayer at the average edge temperature, α is the expansion coefficient of the interlayer, and ΔT is the difference in temperature between the outer glass edge and the central area (mean temperature through the interlayer thickness). It is interesting to note that interlayer thickness is not a factor in the above situation.

For certain interlayers, such as polyvinyl butyral (PVB), E is in itself a function of temperature. Therefore the most effective way to minimize cold edge stress in designs using a temperature-sensitive high-modulus interlayer is to control the temperature gradients. This can be accomplished by keeping the heating element as close as possible to the edge and insulating the windshield from losses to surrounding air-frame structure. The heating film temperature should also be kept as cool as possible.

27.3 Interlayer Stress from Edge Loading

Uniform loading of individual plies within a laminate cannot be achieved with unsymmetrical edge attachments. Figures 27-8 and 27-9 illustrate how unsymmetrical edge loading, from either flexure or membrane action, produces strain in the interlayer at the panel's edge. The resultant strain is a function of the stiffness of the individual laminates and the intensity of the applied loads.

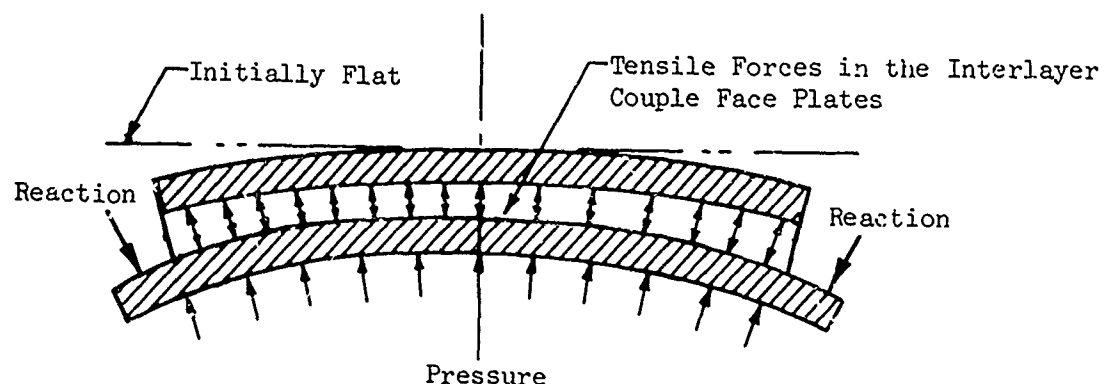


Figure 27-8. Interlayer Strain Resulting From Flexural Loading of Laminate With Staggered Edge Restraint.

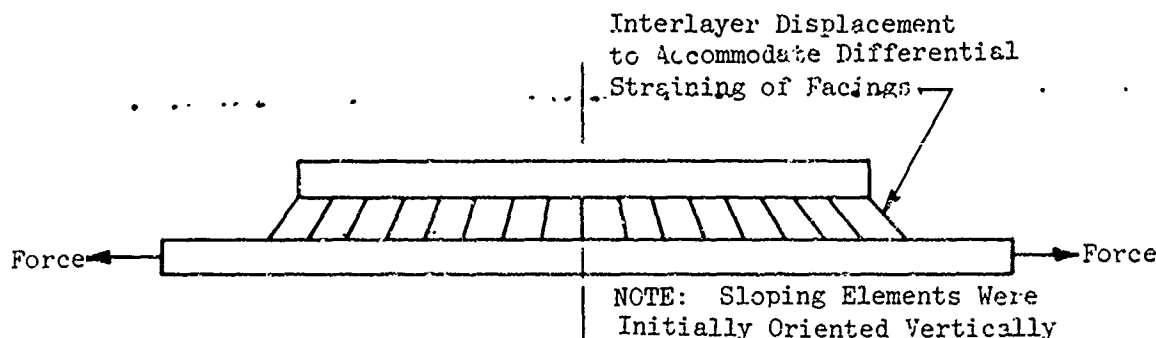
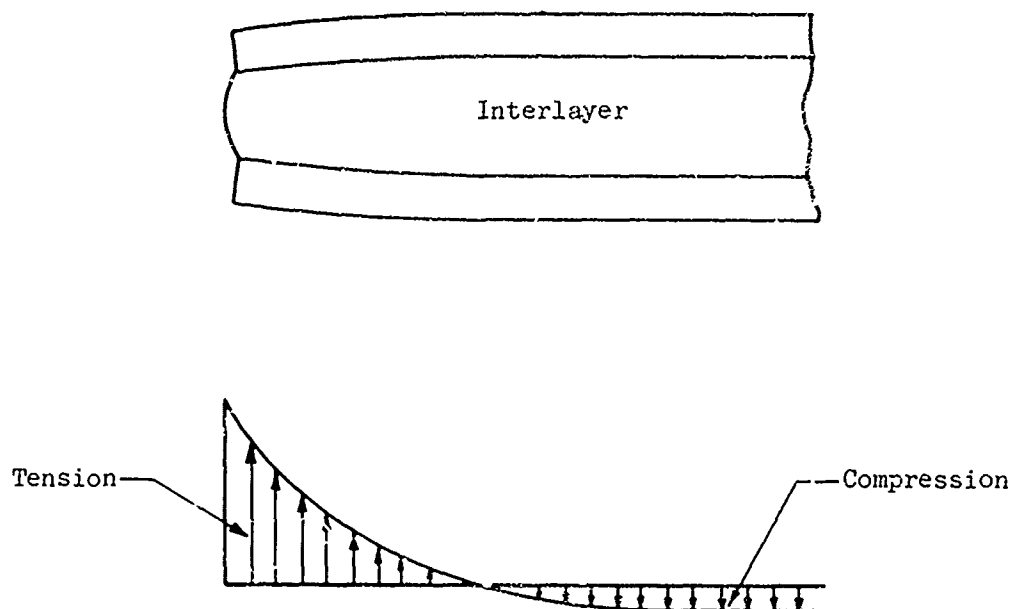


Figure 27-9. Interlayer Strain Resulting From Application of Membrane Loads to Single Ply of Laminated Assembly.

27.4 Manufacturing Stresses

During lamination it is assumed that face plies are parallel to one another. However, in actual practice the face plies may become squeezed together along the panel edges while the interlayer is being cured under pressure, as shown in Figure 27-10. When the vacuum or autoclave pressure is removed the facings tend to spring back to their original shape, which introduces residual tensile stresses in the interlayer. The key factor influencing the magnitude of these stresses is laminating process control.



Stress Distribution in Interlayer

Figure 27-10. Assembly-Induced Interlayer Bond Tension.

27.5 Structural Coupling From Interlayers

The composite bonded beams that are frequently encountered in structural practice use engineering materials having well defined elastic properties. Classical beam bending theory is applicable within the elastic range of the constituent materials. Such bonded beam plies are considered to be fully coupled; that is, each laminate carries its share of the shear and inplane forces created by the bending loads. On the other hand, the composite transparencies used in windshield and window applications use materials having both elastic and viscoelastic properties. Here, one set of plies can be considered elastic within the range of deflection and stresses of interest, with adjacent plies or layers behaving as viscous materials with extremely limited mechanical properties. Such composite beams carry practically all their loads in the main plies, with minimum support from the viscous interlayers, and are considered to be partially uncoupled. A composite beam consisting of parallel spaced plies separated by weak, nonfunctional interlayers would be considered fully uncoupled.

The section properties of fully coupled composite laminates are derived from the parallel axis theorem for moment of inertia. The resultant stiffness, derived from Equation 27-1, can be used for detailed stress and deflection calculations.

$$EI = \sum E_n I_n + \sum A_n Z_n^2 - Z \sum A_n Z_n \quad (27-1)$$

where

E = modulus of elasticity

I = moment of inertia

A = cross section area

Z = distance from base of beam to centroid of area

n = subscript for the n th lamina

Typical stress and strain distributions for a fully-coupled composite beam are as shown in Figure 27-11.

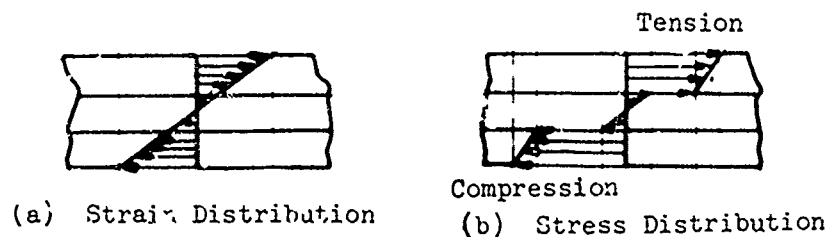


Figure 27-11. Stress and Strain Distributions in a Fully Coupled Composite Beam With Equally Stiff Face Plies.

The bending behavior of a completely uncoupled composite beam is that of a series of freely stacked plies: the leaf spring concept. Each ply acts independently and slips with respect to its neighbor as it deflects, all plies deflect identically, and individual plies take up their portion of the total load in relation to their stiffness. Accordingly, the stiffness shown in Equation 27-2 is merely the sum of the individual lamina stiffness.

$$(EI)_s = \sum_{n=1}^n E_n I_n \quad (27-2)$$

Typical stress and strain distributions, for an uncoupled beam are shown in Figure 27-12.

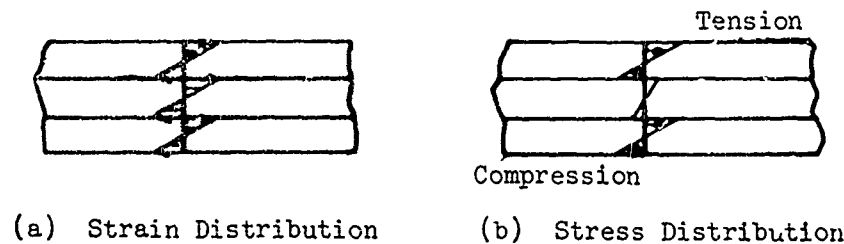


Figure 27-12. Stress and Strain Distributions in an Uncoupled Composite Beam.

Temperature plays a major role in the analysis of transparent composite structures since some of the materials have mechanical properties that vary widely within the range of operating temperatures. To illustrate this point, Figures 27-13, 27-14 and 27-15 show calculated coupled and uncoupled stiffness for three types of beams as functions of temperature. Also shown are plots of stiffness obtained from deflection test results. This data shows that at low temperatures all of the beams tested are virtually fully coupled, while at elevated temperatures they appear almost totally uncoupled. At room temperature they appear to be partially coupled.

Flexural stress and deflection calculations for pressure loading conditions will be conservative when uncoupled (minimum stiffness) section properties are used in the analyses. However, this conservatism has the following restrictions:

- 1 If there is a significant difference in stiffness between the two facings, coupling can create a strain distribution similar to that shown in Figure 27-16. Here the neutral axis remains within the stiffer facing, and interlayer coupling induces a higher strain in the more compliant facing than would occur if it were considered uncoupled.

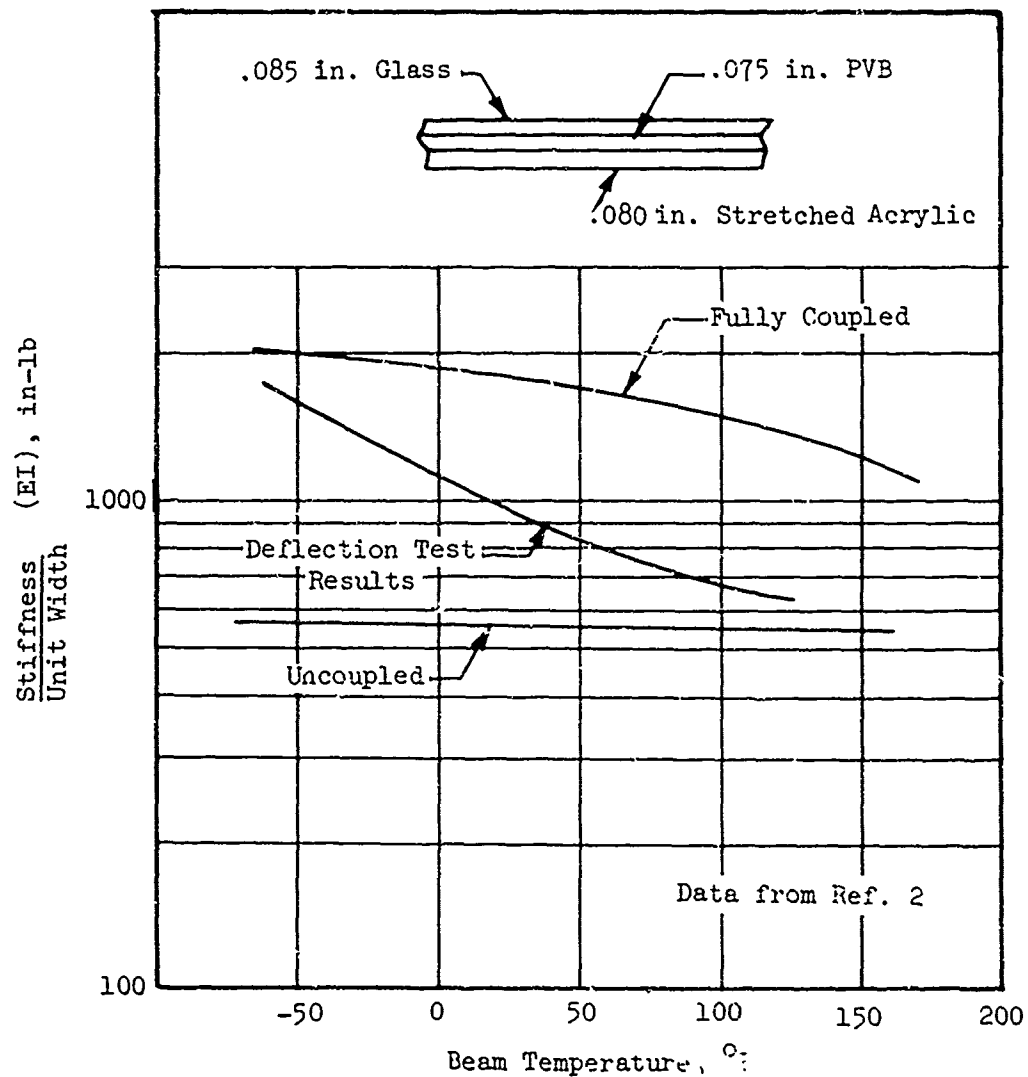
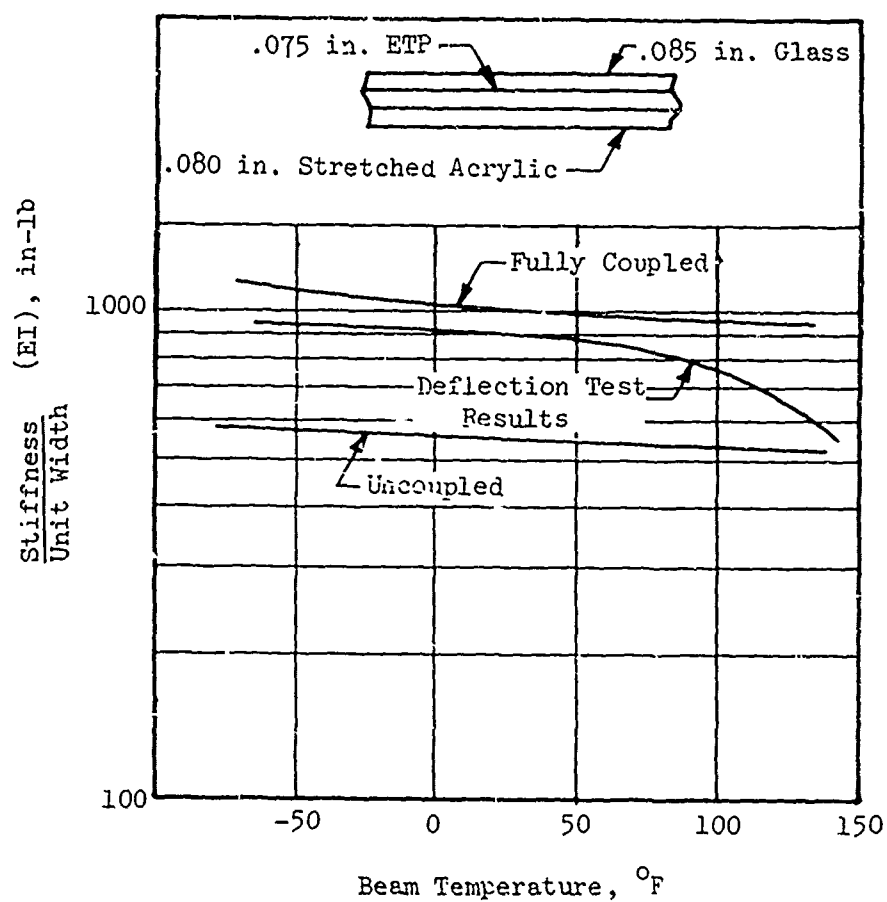


Figure 27-13. Variation of Stiffness With Temperature, Glass/Plastic Laminate With PVB Interlayer.



Data from Ref. 2

Figure 27-14. Variation of Stiffness With Temperature, Glass/Plastic Laminate With Ethylene Terpolymer Interlayer

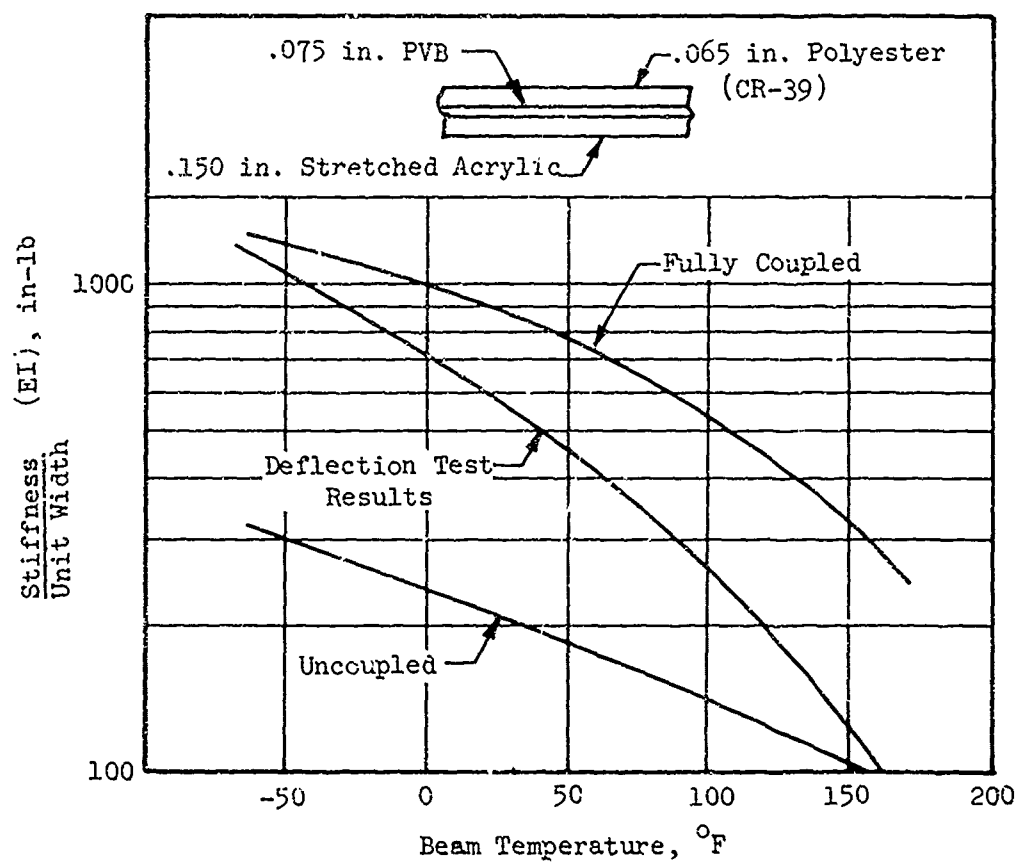


Figure 27-15. Variation of Stiffness With Temperature of Plastic Laminate.

This phenomenon is illustrated by the data in Table 27-3 which compares measured stresses to stresses that were calculated using coupled and uncoupled properties.

2. When it is desired to determine transparency stresses from fixed deflections, such as airframe wracking, the analysis should use coupled (maximum stiffness) section properties to be conservative, because for a given level of deformation or strain, stress is proportional to stiffness.

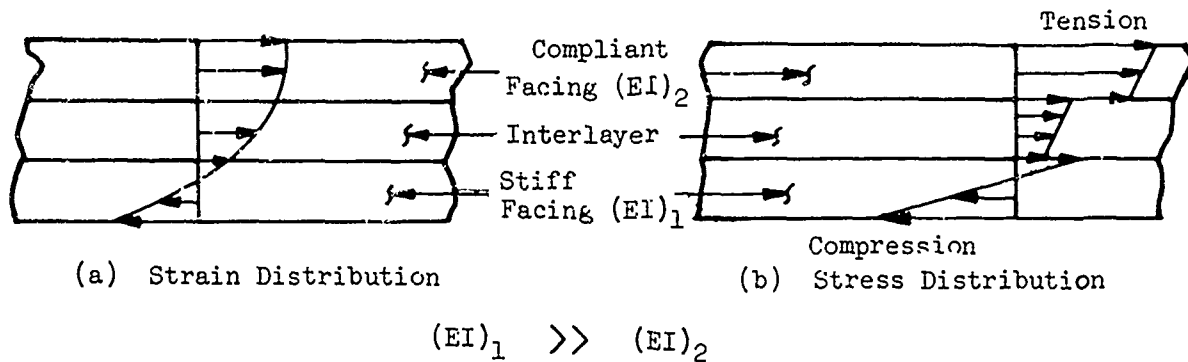


Figure 27-16. Stress and Strain Distributions in a Fully Coupled Composite Beam With Face Plies of Unequal Stiffness.

27.6 Fail-Safe Criteria for Interlayers

Design substantiation of interlayer integrity is accomplished by test because of indeterminable postfailure variables. Figure 27-18 is a photograph of a 24-inch-square glass laminate supporting pressure loading of 1 psi after fracture from ballistic penetration. The laminate had a .075-in. polyvinyl butyral interlayer and was tested at room temperature.

TABLE 27-3. COMPARISON OF STRESSES FOR COUPLED AND UNCOUPLED COMPOSITE BEAMS, FIXED DEFLECTION

Temperature (°F)	Configuration	Applied Moment (in-lb) in	Dominant Face Ply			Compliant Face Ply		
			Material	Coupled Stress (PSI)	Uncoupled Stress (PSI)	Measured Stress (PSI)	Material	Coupled Uncoupled Measured Stress Stress Stress (PSI) (PSI) (PSI)
-65	See Fig. 27-13	41.1	Glass	-10430	-31810	-12880	Acrylic	2880 2120 2980
75	See Fig. 27-13	14.5	Glass	- 4760	-11540	-10820	Acrylic	980 590 680
125	See Fig. 27-13	20.1	Glass	- 6920	-16160	-11380	Acrylic	1170 620 450
-65	See Fig. 27-14	34.1	Glass	-14825	-25890	-13770	Poly- carbonate	2040 710 1620
75	See Fig. 27-14	19.8	Glass	- 9160	-16240	-10720	Poly- carbonate	1220 400 1080
125	See Fig. 27-14	16.5	Glass	- 9120	-13540	-13240	Poly- carbonate	1010 320 860
-65	See Fig. 27-15	31.9	Acrylic	2340	5400	2230	Poly- ester	-2290 -1650 -2170
75	See Fig. 27-15	9.6	Acrylic	920	2460	1070	Poly- ester	- 490 - 550 - 800
125	See Fig. 27-15	3.5	Acrylic	360	910	770	Poly- ester	260 - 150 - 510

Data from Ref. 2

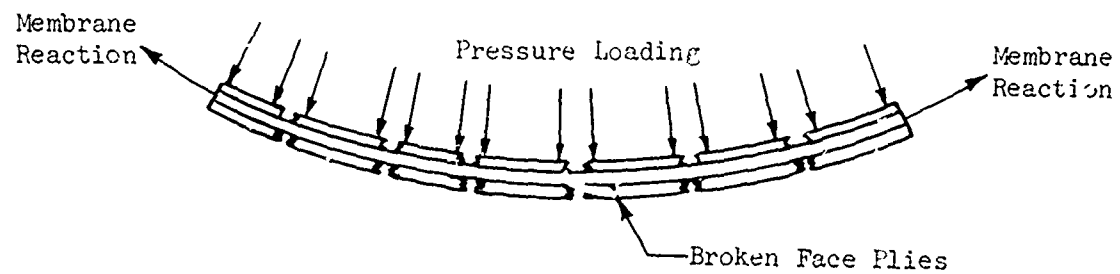


Figure 27-17. Interlayer Supports Aerodynamic Pressure Loads by Membrane Action.

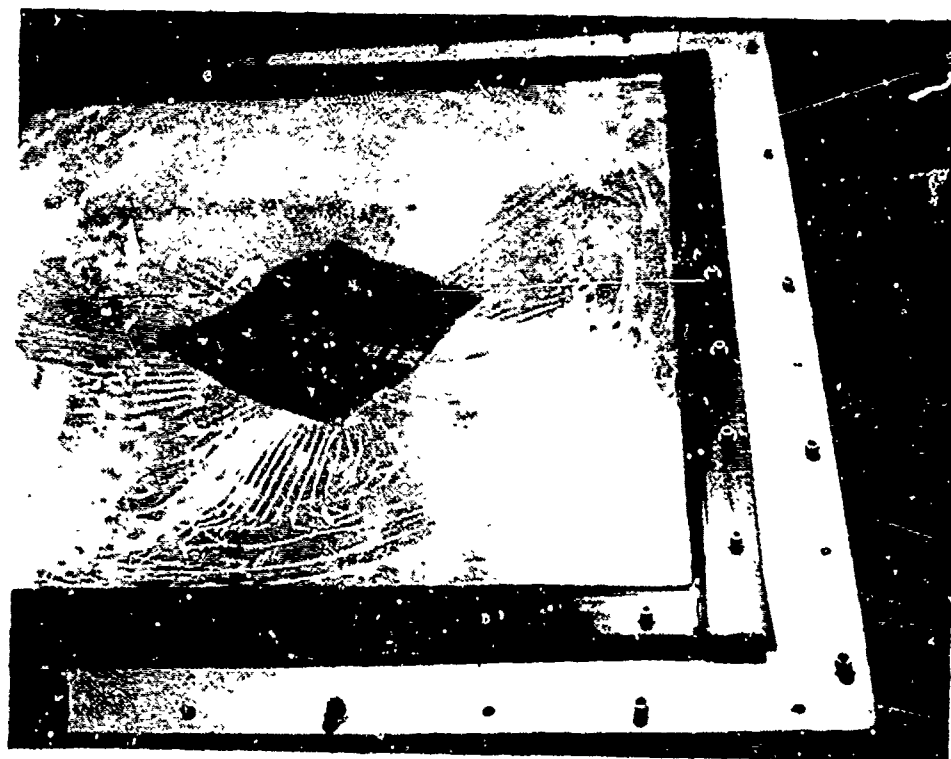


Figure 27-18. Fail-Safe Test of Fractured Glass Laminate.

27.7 Interlayer Adhesion Properties

The strength of an interlayer is highly dependent upon three variables: temperature, geometry, and substrate material. Temperatures affect the physical properties of the basic interlayer materials and are generally discussed in Section 17 of this handbook.

Geometry is important because of the nonlinear, large-displacement characteristics of most interlayers. For example, consider a typical element loaded in shear, as shown in Figure 27-19. The total displacement is seen to be made up of a shear strain component, plus a component of strain resulting from diagonal tension. This nonlinear structural response complicates analysis and also puts limitations on the use of extrapolated test data.

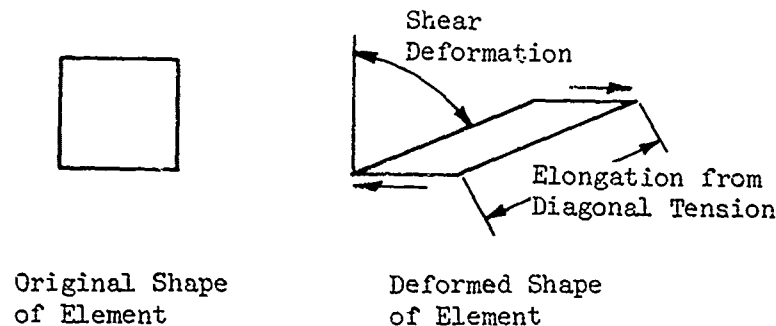


Figure 27-19. Shear Deformation of Interlayers.

The adhesive strength of an interlayer is also dependent upon the substrate material, including coatings to which it is bonded. To illustrate this dependence, Table 27-4 lists typical short-term tensile and shear strength properties for several different material combinations at high, low, and room temperatures. This data was obtained from small specimens, and appropriate caution should be used when extrapolating the results to full-scale components. Particular attention must be given to the manner in which the load is applied. For example, comparison of the tensile strength value shown in Table 27-4 with cleavage strength values from Table 23-2 reveals an order of magnitude difference in values, for an essentially tensile loading.

TABLE 27-4. TYPICAL INTERLAYER ADHESION STRENGTH PROPERTIES

Interlayer	Substrates	Temperature (°F)	Tensile Strength (psi)	Shear Strength (psi)	Secant Shear Modulus (psi)	Ult. Shear Deflection (in)
Polyvinyl Butyral, 38 PPH DBS .075-in-thick	Stretched acrylic (MIL-P-25690) polyester (CR-39) with Sierracote 303 conductive coating	-65 72 125	870 300 150	643 357 30	1150 260 31	.047 .356 .110
Polyvinyl Butyral, 38 PPH DBS .075-in-thick	Chemcor 0401 glass with Sierracote 303 conductive coating stretched acrylic (MIL-P-25690)	-65 72 125	770 390 150	517 237 28	1083 196 24	.038 .198 .152
Polyvinyl Butyral, 38 PPH, DBS .075-in-thick no coating	Chemcor 0401 glass, stretched acrylic (MIL-P-25690)	-65 72 125	770 580 240	1150 513 27	1580 495 24	.066 .126 .151
Ethylene Terpolymer NOX078 .075-in-thick polycarbonate	Chemcor 0401 glass with Sierracote 303 conductive coating	- 65 72 125	380 470 480	217 473 103	705 537 157	.024 .092 .057

Data from Ref. 2

References

1. Islinger, J. S., Armour Research Foundation, "Engineering Design Factors for Laminated Aircraft Windshields, Parts I and II," WADC-TR-53-99, Wright Air Development Center, Wright-Patterson Air Force Base, Ohio, Apr. 1954.
2. Kay, B. F., Sikorsky Aircraft Division, "Design, Test and Acceptance Criteria for Army Helicopter Transparent Enclosures," USARTL-TR-78-26, Applied Technology Laboratory U. S. Army Research and Technology Laboratories, Fort Eustis, Va.

Bibliography

Roberts, W. G., Triplex Safety Glass, Co., Ltd., "The Development of Wind-Screen Reliability," The Proceedings of the Symposium on Optical Transparencies, London, The Society of British Aerospace Companies, Ltd., June 1971.

Olson, J. B., Sierracin Corp., "Design Considerations Affecting Performance of Glass/Plastic Windshields in Airline Service," AFML-TR-73-126, Air Force Materials Laboratory, Wright-Patterson Air Force Base, Ohio, June 1973.

Beuamont, P. M., and Parker, L., The Boeing Commercial Airplane Company, "Windshield Concepts," AFML-TR-73-126, Air Force Materials Laboratory, Wright-Patterson Air Force Base, Ohio, June 1973.

Denke, P. H., Douglas Aircraft Co., "The Determination of Deflections and Stress Distribution for a Laminated Transparent Beam," AFFDL-TR-78-114, Air Force Flight Dynamics Laboratory, Wright-Patterson Air Force Base, Ohio, Nov. 1978.

Table 28-1 is a summary of mass properties for the common transparent materials. The tabulation also includes the specific stiffness and the specific strength for each material. Two values for specific strength are listed: one based on ultimate strength, and the other based on the typical reduced values that are used for design.

TABLE 28-1. DENSITIES AND SPECIFIC STRENGTHS OF TRANSPARENT MATERIALS

Material	Density (lb/in ³)	Ultimate Strength Density ₄ (in. x 10 ⁴)	Typical Design Limit Strength Density ₄ (in. x 10 ⁴)	Specific Stiffness Modulus Density ₆ (in. x 10 ⁶)
MIL-P-5425 Acrylic Sht.	.043	22.79	1.86	10.47
MIL-P-8184 Acrylic Sht.	.043	24.42	3.49	10.47
MIL-P-25690 Stretched Acrylic Sht.	.043	26.74	9.30	10.47
MIL-P-83310 Polycarbonate	.043	20.93	10.47	6.98
Semitempered Glass	.091	23.19*	4.95	113.19**
MIL-P-8257 Polyester	.043	18.60	N/A	10.46
Polyvinyl Butyral Interlayer	.039	N/A	N/A	N/A
SS5272Y(HT) Interlayer	.037	N/A	N/A	N/A

* Modulus of Rupture in Bending

**Flexural Modulus

NOTE: The preceding table is intended for reference purposes only and should never be used unilaterally to select materials for a given application. There are too many other material properties of major importance that can easily outrank weight and strength.

28.1 Weight Optimization

The most efficient method for reducing the weight of a transparency that is subjected to pressure loading is to use cylindrical or spherical shapes. This will cause the internal loading to be inplane such as hoop tension or shell compression. Conversely, the least efficient shape for supporting pressure loads is a flat panel, which supports pressure loads by bending and/or membrane action. Tests have shown even slight curvature has a pronounced effect on increasing panel strength and rigidity. Figure 28-1 shows the difference in deflection between a flat and a contoured 16-inch-diameter, 0.25-inch-thick acrylic plate. The contoured panel had an initial camber of 1 inch. The magnitudes of the stresses in the centers of the panels were proportional to the deflections over the range of pressures tested.

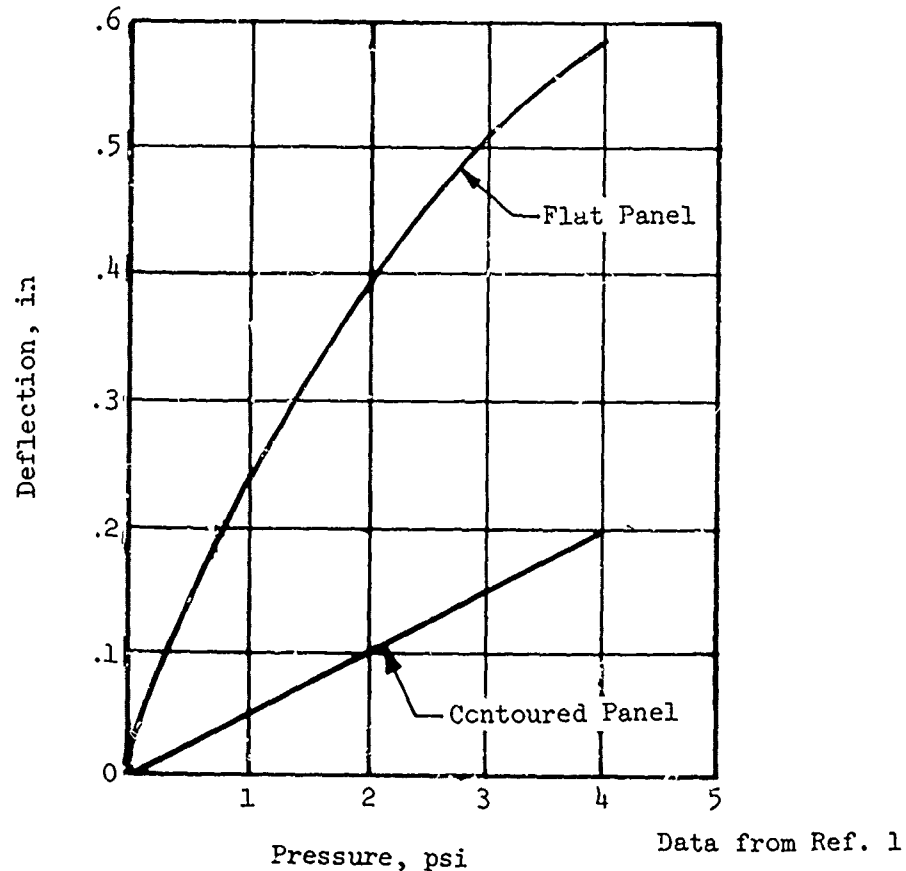


Figure 28-1. Deflection vs Pressure for Flat and Contoured 16-Inch Diameter, 1/4-Inch-Thick Acrylic Discs.

28.2 Transparency/Support Interactions

Transparency/support interactions are an important consideration in the trade-off between designs that support pressure loads by plate bending or membrane action. Membrane designs are invariably lighter than plate bending designs on a square foot basis. Membrane designs support pressure loads as diaphragms in direct tension. This tension must be balanced at the panel edges by either radial tension or circumferential compression. The membrane design edge loads are usually many times greater than the edge loads for stiffer plate-bending designs. As a result, substantial framing reinforcement is sometimes necessary for the membrane designs, which may offset savings resulting from their lower aerial weights.

The distribution between membrane and bending stresses in a panel subjected to pressure loading is a function of the pressure intensity and the panel's stiffness. Also, the magnitude of the inplane membrane stresses increase as the radius of curvature is increased. Table 28-2 lists the various types of panels and their relative aerial densities.

TABLE 28-2. COMPARATIVE WEIGHTS OF TRANSPARENCY CONFIGURATIONS.

Configuration	Predominant Stress	Aerial Density
Flat Panel	Bending	Heaviest
Flat Panel	Membrane	Intermediate
Curved Panel (Non-Circular)	Bending	Intermediate
Curved Panel (Circular)	In plane	Lightest

Reference

1. "Plexiglas Handbook for Engineers," PL-26a, Rohm and Haas Co., Philadelphia, Pa., Dec. 1952.

29.0

MANUFACTURING METHODS

A basic understanding of how transparent components are fabricated is necessary to enable designers to create efficient, cost-effective units with reasonable manufacturing tolerances. This section will describe the basic methods used to work, trim and form the common thermoplastic and glass materials.

29.1 Machinability

Acrylic and polycarbonate materials have working qualities similar to soft metals, such as brass. Standard light to medium metal or wood-working equipment, such as band saws, jig saws, routers, and milling machines, can be used for cutting. In general, machining tools are operated at high speeds with slow feed rates to minimize frictional heat buildup that could cause local softening of the material. Rough cuts are finished off by belt sanding or grinding to impart a smooth surface free of stress raisers. When undercuts are employed, a minimum fillet radius of $1/16$ in. should be used as shown in Figure 29-1 in order to minimize stress raisers.

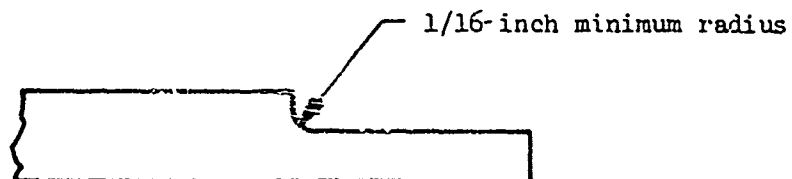


Figure 29-1. Minimum Fillet Radius for Machined Undercuts.

Polycarbonate material is extremely susceptible to stress-cracking along machined edges in the presence of contaminating environments. The contaminants can vary widely from a large number of chemicals and solvents to a high humidity at elevated temperature environments. The effect of this stress-cracking is a reduction in elongation to failure.

29.2 Drilling

Drilling of cast-acrylic materials can be accomplished successfully with twist drills commonly used for soft metals if ordinary care is observed. However, the best results can be obtained if the drills are repointed as follows: The bit should be carefully ground, free of nicks and burrs which would affect surface finish. It is particularly important that the cutting edge be dubbed-off to zero rake angle. The length of this cutting edge (and the width of the chip) can be reduced by increasing the included angle of the drill bit (see Figure 29-2). Drills with slow-spiral polished flutes should be used. Flutes should be as wide as possible. For drilling shallow or medium depth holes, no coolant is necessary. For deep holes a coolant is necessary. The lubricant and coolant for drilling plastics is a water-soluble cutting oil.

When drilling stretched acrylic, special drills should be ground and used exclusively. Standard drills will cause the hole to be oversize and distorted and chipping will be excessive. Whenever possible, a coolant should be used. The speed and feed of the drill are also critical. The drill bit included angle should be about 90° with a secondary angle approximately 0.020 inch long and 12° to 15° lip clearance. The rake should be 0° to 10° . The results of an improperly drilled hole in stretched acrylic are shown in Figure 29-3.

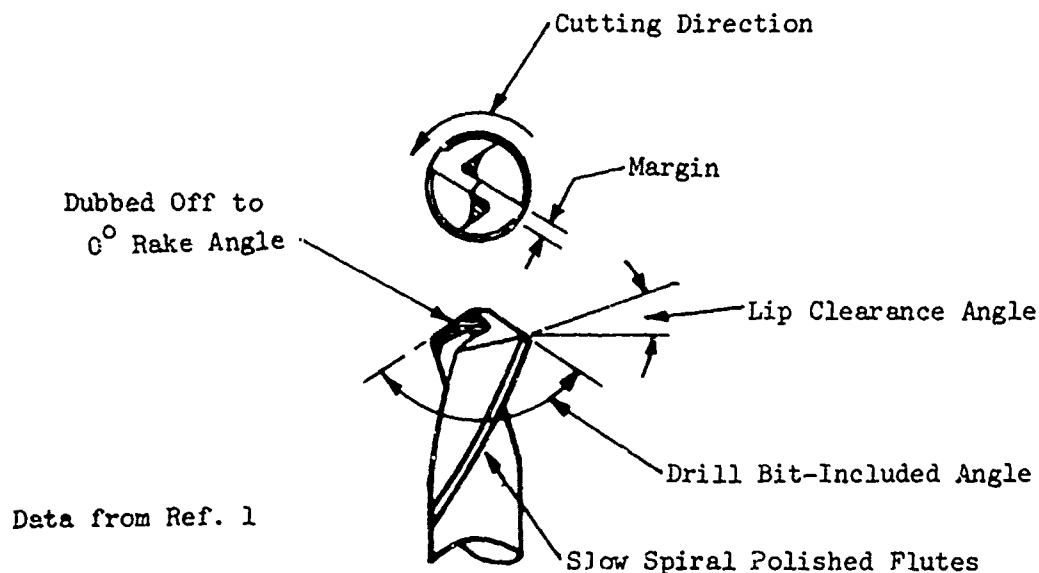


Figure 29-2. Diagram of Recommended Drill Geometry for Acrylic Plastics.

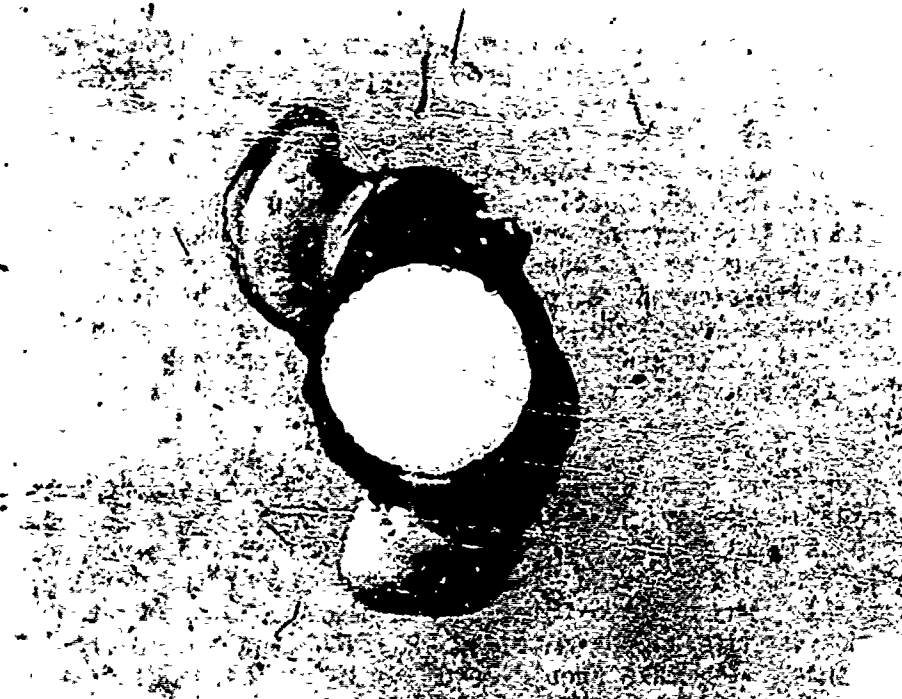


Figure 29-3. Poorly Drilled Hole in Stretched Acrylic.

Drilling structural holes in polycarbonate material is a critical process since it is difficult to prevent environmental stress-cracking. The first requirement is to keep the part cool. This is accomplished by using slow to medium cutting speeds and feed rates, and a coolant. Water is an excellent coolant; any other coolant must be checked for its compatibility with polycarbonate. The second requirement is to maintain sharp cutting edges at all times. For best results, holes should be drilled undersize and reamed by use of precision reamers in steps not exceeding 1/64 inch, to the desired size. The hole surface finish should not exceed 65 rms.

29.3 Glass

Glass, once it is tempered, cannot be cut or drilled. These operations can only be accomplished by the glass manufacturer while the material is still in the annealed state.

29.4 Forming Techniques

Transparent thermoplastic materials that have been heated until pliable can be formed to almost any shape, and on cooling, they retain the new shape, except for small contractions.

Cold forming can be accomplished within certain limits when the final contour of the part is a simple wrap shape without compound curvature. A rule-of-thumb limit for plastic materials as to the amount of curvature that may be cold framed or wrapped is: the minimum radius of curvature should not be less than 180 times the thickness of the part. Tighter bends can result in excessive preload stress than can lead to stress-crazing. The induced preload tensile stress from cold forming can be calculated using Equation 29-1. Design allowable stress for the component should be reduced by this value.

$$f = tE/2R \quad (29-1)$$

where

f = preload stress from cold forming (psi)
 t = material thickness (inches)
 E = material modulus of elasticity (psi)
 R = radius of curvature (inches)

For hot forming, transparent plastics must be heated to temperatures close to their softening points. For cast acrylics this is between 290°F and 350°F depending on the material's thickness and the type of forming to be used.

29.5 Forming Stretched Acrylic

Stretched acrylic is formed using either monotherm or duotherm stretch forming processes. The monotherm process involves the simultaneous stretching and forming of a component to the desired percent stretch and desired shape during a single relatively short heating cycle. This process is best applied to free-blown bubble configurations of circular cross section, wherein depth-of-draw requirements are outside the limits of other forming processes.

The duotherm, or warm forming, process is basically a two-stage method of forming that involves (1) stretching of flat, hot material to a flat sheet and (2) reheating the material to a temperature sufficiently high to permit relatively slow mold forming, but at the same time staying below temperatures high enough to allow significant relaxation of the stretch or weakening of the sheet. This process has been shown to be a successful means of fabricating shallow draw parts, such as windshields, cockpit side windows, and canopies, where the depth-of-draw requirements introduce minimal amounts of material elongation.

29.6 Forming Polycarbonate

Polycarbonate materials must be thoroughly dried prior to thermoforming. Failure to do so will result in bubbles forming in the sheet during the forming operation. Drying is accomplished using air circulating ovens set at about 260°F with airing times varying according to the thickness of the sheet. The actual forming operations are conducted in the 340° - 400°F range. This means that the forming apparatus should be equipped with its own heating units. The practice of having separate heating and forming devices, often used with acrylic, will rarely be feasible with polycarbonates.

29.7 Forming Methods

Drape forming is used for most two-dimensional shapes and for mild three-dimensional shapes. In this process, the sheet is heated to its proper forming temperature and then carefully draped over a contoured form so that it assumes the shape of the form. The form must be free of waviness and other variations in contour which might cause optical distortion in the formed part. Form surfaces are covered with soft flannel cloth, velvet, grease saturated felt or other suitable materials to minimize objectionable markoff.

Parts with compound curves may be formed from transparent plastic sheets by five different methods, or occasionally by combinations of methods. These methods are:

1. Stretch Forming manually or mechanically. The heated plastic sheet is stretched across a form.
2. Air Pressure Differential without Form (free-blown method - vacuum forming) - This is the most commonly used method for making aircraft canopies. The material is restrained only along its perimeter, and an air pressure differential is used to blow a natural bubble shape to a specified depth.
3. Air Pressure Differential with Female Form - When the desired contour varies radically from a true surface tension shape by having sharp changes of contour, the part may be formed by drawing it into a female form made of plaster or metal.
4. Air Pressure Differential with Male Form (snap-back method) - Another method of obtaining shapes which vary from the true surface tension shape is the snap-back method. This method uses a male mold that is inserted into a free-blown shape while it is still hot. The air pressure differential is removed, and based on the principle that elastic memory of the material will cause a tendency to resume its flat sheet form, the sheet will contract to contact the mold. This concept is illustrated in Figure 29-4.

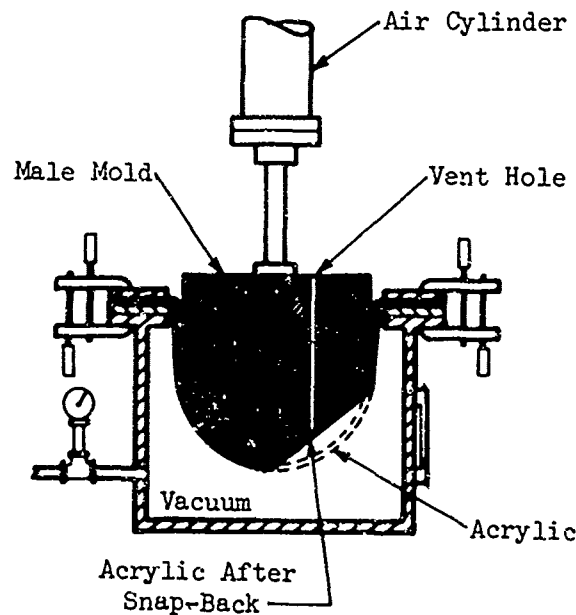


Figure 29-4. Snap-Back Forming of Acrylic Sheet.

5. Rotoforming - This method uses centrifugal force for forming transparent plastic canopies.

Stretching thins the material. Figure 29-5 can be used to estimate the ratio of the thickness of the apex to the original sheet thickness for blown spherical parts of different depths.

29.8 Forming Laminated Parts

Laminated transparent assemblies can take three basic forms: plastic laminated to plastic, glass laminated to glass, and glass laminated to plastic. Each type of construction has its own, unique method of manufacture. In general, laminated parts are manufactured with simple wrap curvature only. Compound curved parts can be made, but manufacturing problems are substantially increased.

All-plastic laminates are probably the simplest to form. The facings are joined together with an interlayer to form a flat laminate. The laminated sheet is then formed into its final shape.

Glass must be formed to its final shape prior to lamination since forming temperatures would damage the interlayer. In order to obtain matched contours, the glass facings are frequently formed as "doublets". That is, the two plies are nested on top of each other, and simultaneously heated and sag formed to their final shape. It should be noted that when glass is hot formed to a wrap shape it is usually supported only at the edges to avoid markoff. This can result in sagging between supports, and the straight-line elements of the wrapped

section will end up with slight curvatures. The contours produced using this matched set technique will be nearly identical for each ply.

Glass-plastic laminates are relatively simple to form if one of the facings can be cold formed to match the other. For example, a helicopter windshield made up of an .085-in.-thick glass ply and an .080-in.-thick stretched acrylic ply can be formed by slaving the acrylic ply to a preformed glass ply since the glass is over twenty times stiffer than the plastic. Conversely, curved windshields for transport aircraft have been produced with thin, elastic .050-in. glass slaved to thick, preformed plastic main plies.

When cold forming of dissimilar material plies cannot be accomplished, the individual plies must be formed separately to identical contours. This operation must be carried out with great precision since variations in contour between plies will create a nonuniform gap for the interlayer and will cause optical distortion if the outer surfaces of the final laminate are not parallel. Sophisticated tooling methods are needed for such applications.

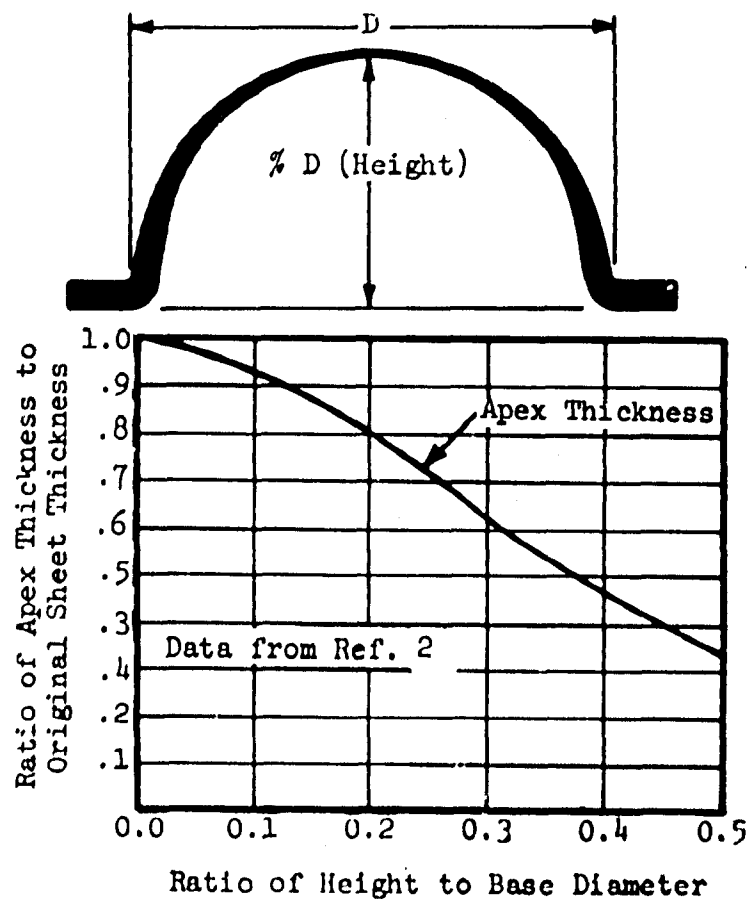


Figure 29-5. Thinning of Free-Blown Acrylic Parts.

29.9 Tolerances

Practical tolerances that can be expected for transparent components are shown in Table 29-1. These are normal tolerances and can vary considerably based on functional requirements and tooling. For curved parts it is customary to use a master tool mock-up to control trim lines, contours, hole patterns, and other interface dimensions.

TABLE 29-1. PRACTICAL TOLERANCES FOR TRANSPARENT COMPONENTS

Feature	Tolerance (inches)
Part Trim	$\pm .032$
Drilled Hole Positions	$\pm .007$
Edge Contour (plastic parts)	$\pm .032$
Edge Contour (glass parts)	$\pm .125$
Central Contour (free-formed)	$\pm .500$
Central Contour (contact-formed)	$\pm .125$

NOTE: The method of inspection to be used for contoured parts should be specified on applicable drawings.

29.10 Joining Transparent Materials - Solvent Cementing

With care and proper procedures, it is possible to obtain cemented joints of acrylic material which approximate the original plastic in strength. The cementing of transparent acrylic plastics depends on the intermingling of the two surfaces of the joint so that there is actual cohesion of the material itself (see Figure 29-6). To effect cohesion, an inorganic liquid solvent is used to soften the surfaces of the materials to be joined. With the parts in intimate contact, and allowed to cure, a cohesive bond will result. The resultant cemented joints will be translucent and will cause a local impairment of visibility.

Adhesives conforming to MIL-A-8576 should be used for bonding joints of MIL-P-5425 cast acrylic only. Use MIL-A-25055 adhesive for bonding MIL-P-8184 modified cast acrylic, and cement, Federal Specification P-S-18 for bonding MIL-P-25690 stretched acrylic. To prevent crazing, cast-acrylic materials must be annealed prior to and after cementing.

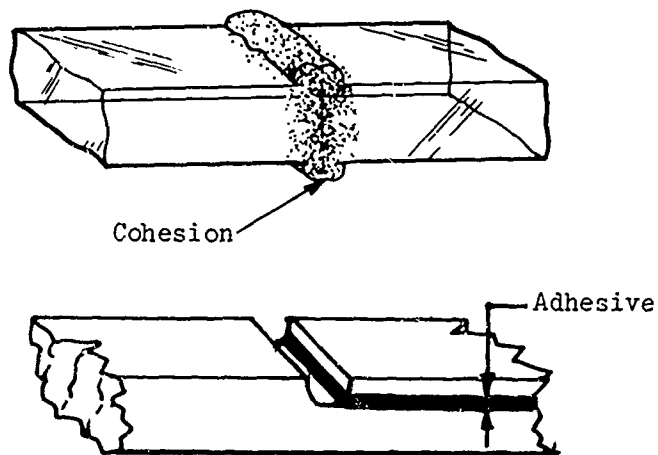


Figure 29-6. Distinction Between Cohesion and Adhesion.

Solvent cementing of polycarbonate parts may be effected by the use of either pure solvents, mixtures of solvents, or light solutions of polycarbonate and solvents. Methylene chloride is a solvent suitable for this purpose.

29.11 Adhesive Bonding

Transparent assemblies frequently use bonded joints to attach edge reinforcements, terminal blocks, seals and other detail features. These added components can be made of other plastics, metals, composites, or synthetic materials. A wide variety of adhesives may be used to attach these components, depending upon the specific application, anticipated environment, and structural loading.

When selecting the adhesives, certain factors must be considered. These include the following:

1. Adhesives containing solvents must be checked to make sure the solvents will not adversely affect the plastic substrates.
2. If a thermosetting adhesive is to be used on a plastic, its cure temperature must be below the critical softening temperature of the plastic.
3. Parts must be dried and cleaned thoroughly to obtain the highest quality bonds. Solvents used for this surface preparation must be checked for chemical compatibility with the substrate.

4. Bond strength may sometimes be improved by light sanding, sand-blasting, or vapor blasting the faying surfaces. However, this operation must be done with extreme caution to prevent the introduction of surface stress raisers.

29.12 Annealing

Proper annealing of fabricated cast-acrylic parts is one of the most effective measures to prevent crazing. Annealing consists of prolonged heating of the cast acrylic part at temperatures lower than those used for forming, followed by slow cooling. Internal stresses set up during fabrication of the article are reduced or eliminated by this treatment. This results in a part of greater dimensional stability and greater resistance to crazing. Annealing also improves the strength of cemented joints. In order to obtain these benefits, it is necessary for the annealing to be done after all other fabrication procedures, including polishing, are completed.

It is not necessary to anneal stretched acrylic material, since that material has a high inherent resistance to crazing.

Process specification for annealing can be prepared from information provided by the material suppliers.

References

1. "Fabrication, Maintenance and Repair of Transparent Plastics," (USAF) T.O. 1-1A-12, (Navy) NAVAIR 01-1A-12, U. S. Government Printing Office, Washington, D. C., Oct. 1969.
2. "Forming Plexiglas Sheet," PL-4j, Rohm and Haas Co., Philadelphia, Pa., June 1974.

Bibliography

Burkely, R. A., and Hassard R. S., Goodyear Aerospace Corp., "Factors Influencing the Choice of Processing for Stretched Transparent Enclosures," WADC-TR-5-421, Wright Air Development Center, Wright-Patterson Air Force Base, Ohio, Oct. 1957.

Hasman, G. E., and Kuhbender, R. J., "Environmental Data and Machining Techniques of Polycarbonates," AFML-TR-73-126, Air Force Materials Laboratory, Wright-Patterson Air Force Base, Ohio, June 1973.

Mahaffey, J.E., Rockwell International Corp., "Material Evaluation B-1 Crew Module Windshield and Windows," AFML-TR-73-126, Air Force Materials Laboratory, Wright-Patterson Air Force Base, Ohio, June 1973.

McDonald, W. C., and Huyette, R. A., Goodyear Aerospace Corp., "Windows Contoured, Glass/Plastic Transparent Armor for the UH-1D Helicopter", AMMRC-CTR-75-12, Army Materials and Mechanics Research Center, Watertown, Mass., May 1975.

"Cutting Plexiglas Acrylic Sheet," PL-2L, Rohm and Haas Co., Philadelphia, Pa., Sept. 1973.

"Plexiglas Sheet Annealing," PL-10i, Rohm and Haas Co., Philadelphia, Pa., June 1974.

"Machining Plexiglas Brand Acrylic Sheet," PL-3j, Rohm and Haas Co., Philadelphia, Pa., Apr. 1974.

Hassard, R. S., Goodyear Aerospace Corp., "Design Criteria - Transparent Polycarbonate Plastic Sheet," AFML-TR-72-117, Air Force Materials Laboratory, Wright-Patterson Air Force Base, Ohio, Aug. 1972.

"Fabrication Data, Lexan Polycarbonate Resins," CDC-502, General Electric Company, Pittsfield, Mass., June 1974.

"Forming Lexan Polycarbonate Film and Sheet," CDC-503-Rev.A, General Electric Co., Pittsfield, Mass., June 1974.

"Aircraft Transparencies Installation," TB-73-101, Swedlow, Inc., Garden Grove, Calif., Mar. 1973.

Coutre, R., "Acrylic Plastic Sheet, Fabrication of," SS9589, Sikorsky Aircraft Div., Stratford, Conn., Apr. 1968.

Some of the parameters affecting durability and performance of transparent enclosures cannot be analyzed with sufficient precision for design substantiation. In such cases, qualification tests are the key to product reliability. A properly structured qualification program can reveal potential service problems prior to making production deliveries. In this manner, deficiencies can be corrected early in the aircraft life cycle without the need for costly retrofitting or attribution replacement programs.

Depending upon the parameters of interest, qualification tests are conducted as material specimen tests or full-scale component tests. Qualification of some parameters is accomplished through system integration tests performed in conjunction with aircraft ground or flight tests. However, qualification of sophisticated transparencies solely on the basis of flight tests is not recommended because such tests can neither be comprehensive with regard to environmental interactions, nor demonstrate long-term durability under varying conditions.

30.1 Similarity

Qualification by similarity in lieu of testing is desirable for economic reasons. As a rule, this procedure applies only to material properties. It is not a valid alternative for tests that require full-scale components, unless it can be conclusively demonstrated that there are no significant differences between the component in question and the already qualified component.

30.2 Test Methods

Qualification test plans are developed by contractors for specific designs. The design information and criteria presented in this Handbook should be used to guide the preparation of such documents. Test criteria are presented in the "General Specification for Helicopter Transparent Enclosures" volume of this handbook, which is based on established practices and experimental data. Where applicable, standard test methods are specified and should be used if possible. Several unique tests are also described in the following sections to cover those conditions for which standard test methods are nonexistent. In addition, the American Society for Testing and Materials (ASTM) is in the process of developing and standardizing test methods for Aerospace Transparent Enclosure Materials. This effort is being conducted by ASTM Subcommittee F7.08 and includes test methods for the following parameters:

Abrasion
Chemical Attack
Distortion

Aging
Bond Integrity
Bird Impact

Hail Impact
Moisture Sensitivity
Thermal Distribution
Electrostatics

Interlayer Stability
Scratch Resistance
Toughness

30.3 Material Specimen Tests

Material specimen tests are necessary to determine the responses of transparent materials to the environmental conditions to which the helicopter will be exposed. The environments, natural and induced, that are of interest are listed below.

Ultraviolet Radiation	Humidity
Chemicals	Fungus
Abrasion	Ballistics
Flowing Water (rain, washing)	Foreign Object Damage (FOD)
Blowing Sand and Dust	Salt Spray
Fire	Temperature
Electromagnetic Radiation (Radar)	Static Electricity

The influences of these environments on common aircraft transparent materials are described in the appropriate sections of this handbook. For new products for which no data or experience has been accumulated, qualification test criteria are listed in the General Specification to determine material/environment compatibility.

To illustrate the extent to which raw materials are qualified, Table 30-1 lists qualification tests required for common aircraft transparent materials.

TABLE 30-1. QUALIFICATION TESTS FOR RAW MATERIALS

Test	Material							
	MIL-P-5425 Cast Acrylic	MIL-P-8124 Modified Acrylic	MIL-P-8257 Polyester	MIL-P-25690 Stretched Acrylic	MIL-P-83310 Polycarbonate	MIL-P-25437 Laminated Acrylic	MIL-G-25871 Laminated Glass	MIL-G-25667 Glass (Soda-Lime)
Minor Optical Defects					X			
Angular Deviation					X			
Light Transmission	X	X	X	X	X	X		X
Haze	X	X	X	X	X	X		X
Index of Refraction	X	X	X		X			
UV Transmittance	X	X			X			
Thermal Stability		X	X			X		X
Tensile Strength	X	X	X	X	X			
Elongation	X	X	X		X			
Warpage	X	X	X					
Flammability	X	X	X		X			
Specific Gravity	X	X	X		X			
Water Absorption	X	X	X					
Thermal Expansion	X	X	X		X			
Internal Strain	X	X	X		X			
Deformation Temperature		X	X	X	X			
Dimensions		X	X	X	X	X		
Thermal Deflection		X						
Crazing		X	X	X	X			
Impact Strength			X		X	X		X
Distortion				X		X		
Crack Propagation				X				
Weathering	X	X	X	X	X	X		
Shear Strength						X		
Peel Strength						X		
Fracture Resistance						X		
Thermal Shock						X		
Ballistics								X

30.4 Abrasion Tests

Existing field service has demonstrated that the most prevalent problems experienced with Army helicopter windshields are abrasion and the resultant loss of transparency. Abrasion may be caused by windshield-wiper action, impingement of sand or dust particles, or improper cleaning procedures. Laboratory simulation of these conditions is required as part of component qualification so that performance can be reasonably predicted prior to introduction to service.

Material wear characteristics depend on the abrading medium. Therefore, laboratory tests should duplicate actual conditions as closely as possible to obtain meaningful results.

The relative performances of different materials against impinging sand can be obtained from the Falling Sand Test described in ASTM-D-670-70. Windshield-wiper and cleaning abrasion require unique test methods, two variants of which are described here.

30.5 Windshield-Wiper Test

This test method simulates the effects of windshield-wiper operation on dirty windshields. The presence of an abrasive medium is necessary because soft rubber wiper blades would otherwise be incapable of abrading most windshield materials. The test fixture holds a 16-in. x 24-in. specimen windshield at a 45° incline. A windshield wiper driver arm and rubber blade (30-40 Shore Hardness) attached to an aircraft-type motor is also mounted to the test fixture, as well as a system for regulating and discharging the abrasive slurry onto the specimen at 300 ml/minute rate (see Figure 30-1).

The slurry consists of 100 grams of AC Air Cleaner Test Dust (coarse) per liter of water. A peristaltic pump is used to recirculate and apply the slurry, and vigorous stirring is required in the reservoir to prevent the abrasive from settling out.

Windshield-wiper blades are adjusted to a pressure of 0.5 pound per linear inch of blade length and operated at 160 cycles per minute unless otherwise specified. Every 12,000 cycles the windshield-wiper blades are changed and additional slurry is added as required.

Haze measurements are periodically taken at increments approximately corresponding to a 5% increase in haze. The measurements are obtained from eight locations spaced equally across the surface of the specimen.

Considerable variations in haze levels will occur with this test method. Fluctuations in readings of over 30% (haze percentage) are typical for measurements taken from the same specimen and also from specimen to specimen. Some of the factors causing the variability are inherent

to the type of abrasion, and others are related to the characteristics of the wiper blade, the flatness of the test specimen, and the wetting action of the abrasive slurry on different substrates. Nevertheless, the method does simulate actual conditions, and the variability of test results should be taken into consideration when conclusions are made.

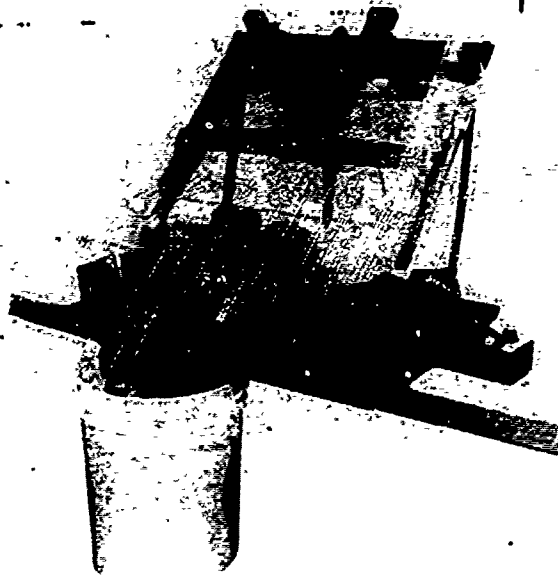


Figure 30-1. Windshield Wiper Test Apparatus.

30.6 Rubbing Abrasion Test

This test method uses a reciprocating motion abrader designed to provide a rubbing action that simulates conditions caused by dry wiping dirty transparencies.

The apparatus contains clamps to mount specimens, a motor-driven crank to impart a reciprocating motion to the abrading heads, a cycle counter, and a timer (see Figure 30-2). A 1-inch-diameter disc of 100% wool felt, 1/8-inch thick, is cemented to the abrading head and impregnated with 400-grit boron carbide. The head is weighted to produce a 1-psi pressure, and the test is run at a speed of approximately 50 cycles per minute. After each 25 cycles the abrading head is reimpregnated.

The consistency of the haze measurements obtained from this test method is approximately -10% in haze percentage points.

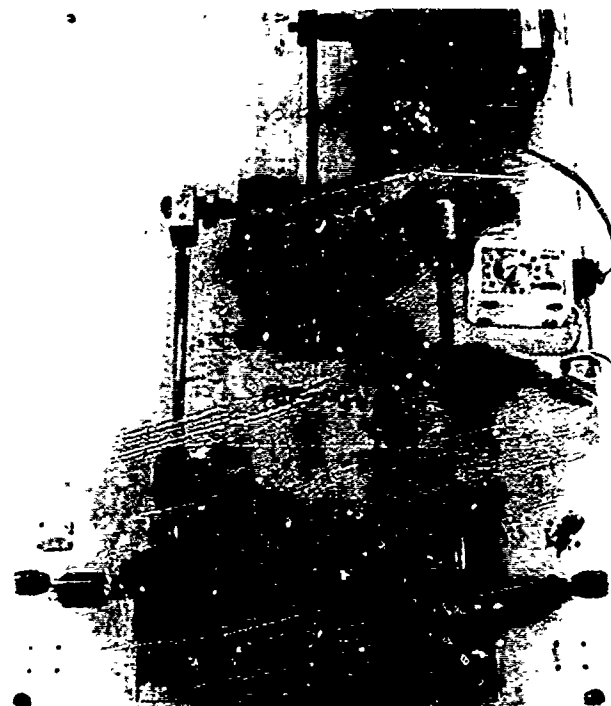


Figure 30-2. Apparatus for the Dry-Rubbing Abrasion Test.

30.7 Weathering Tests

Outdoor weathering, a degradation-promoting process, is the exposure of materials to the elements that are peculiar to a particular environment. These elements are essentially sunlight, temperature, moisture, wind, and atmospheric contaminants. Of these, one of the most important factors in the degradation of transparent materials is the ultraviolet portion of sunlight.

Solar radiation received on horizontal surfaces in the continental United States ranges between 300 and 500 Langleys per day depending upon the location. A Langley is equivalent to 3.69 Btu/ft^2 . Standardized sunshine tests, such as MIL-STD-810, Method 505, specify energy inputs of $100\text{--}140 \text{ watts/ft}^2$, which for a 24-hour period is approximately 7 times more than natural sunshine. Other accelerated weathering tests such as Federal Test Method Standard 406, Method 6024, combine ultraviolet exposure with heat and humidity to further hasten degradation. However, neither type test actually duplicates natural weather, and correlation is therefore always uncertain. The tests do serve a useful purpose for screening functions, however.

More realistic weathering tests are accomplished by exposing specimens to natural weather in regions with above average daily sunshine, such as Florida or Arizona. There are also private weathering test facilities that further increase daily solar radiation by utilizing "follow the sun" apparatuses. These devices can receive about one-third more

Langleys than stationary samples mounted at 45° incline and facing south. An additional method used to accelerate natural weathering is the Equatorial Mount with Mirrors and Acceleration (EMMA) operated by Desert Sunshine Laboratories, Phoenix, Arizona. The EMMA concentrates the intensity of solar radiation through the use of mirrors and provides a tenfold increase in radiation levels as compared to stationary mounting. This system can also be combined with a water spray to include the effects of humidity.

30.8 Component Tests

Component assembly tests are required for substantiation of the following parameters:

Bird Impact

Temperature Extremes

Structural Integrity

Fail Safety

Endurance

30.9 Birdproof Tests

Birdproof requirements are substantiated by tests in which bird carcasses are launched at full-size canopies to verify the penetration resistance of the transparencies. The rationale for such tests and the criteria for conducting the tests are presented in the Birdproofing section of this handbook.

30.10 Temperature Tests

Exposure to high and low temperature extremes is necessary for laminated transparencies to verify that thermal expansion/contraction is not a problem. These tests must be conducted on full-size transparencies because the internal stress distributions are functions of size and geometry. Optical quality can also be affected by temperature changes, particularly when anti-ice systems are energized. In such cases, dimensional changes and variations in the index of refraction can be detrimental to optical lines of sight.

30.11 Structural Integrity Tests

Structural integrity tests are necessary to verify that a transparency will meet all of the design loading conditions without structural failures. Ordinarily, such tests are necessary only for laminated windshields or other complicated configurations for which reliable methods of stress analysis do not exist.

Structural tests should include significant loading conditions (pressure, wracking, installation preload, etc.) that occur in service. The tests should be conducted in standard laboratory conditions, and also at the highest and lowest temperatures in which the aircraft will be operational. Exposure to high and low temperatures creates thermal stresses that may be additive to the stresses from mechanical loading, thereby producing more critical conditions than if either condition were tested alone. In addition, the mechanical properties of some transparent materials are also drastically affected by temperature.

To illustrate the importance of temperature in structural testing, windshield facing stresses were obtained experimentally for two different helicopter windshield configurations that were subjected to 1 psi pressure loading, -65°F cold soak, $+125^{\circ}\text{F}$ hot soak, and combinations thereof in Reference 1. These tests showed that thermal stresses were approximately equal in magnitude to pressure stresses, and the highest stresses occurred during the combined pressure-temperature tests.

30.12 Fail-Safety Tests

Windshields directly in front of the pilot should be sufficiently fail-safe so that mission abort is not necessary if a crack or bullet hole should develop in the transparency. This requirement is substantiated by demonstrating that a damaged windshield can withstand its design limit aerodynamic pressure without collapse despite a crack or bullet hole.

Aerodynamic pressure can be simulated with a vacuum/pressure chamber mounted directly to the windshield or canopy structure. It is important to provide representative edge attachments for this test since some configurations rely on the edge attachment's tensile restraint for fail-safety. Pressure can be maintained during the test by placing a soft rubber patch over the hole or crack as shown in Figure 30-3.

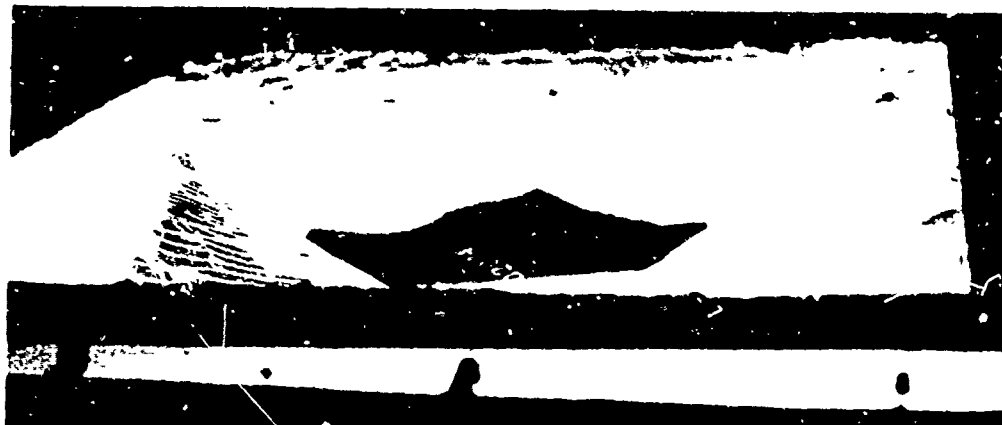


Figure 30-3. Soft Rubber Patch Maintains Pressure for Fail-Safety Test.

30.13 Integrated Endurance Test

An integrated endurance test should be conducted on all laminated windshields prior to committing the design to production to avoid costly service problems. The integrated endurance test should be conducted after all other qualification tests are completed as a final test of the windshield's quality and suitability for service. The test is designed to couple the significant loading conditions that can occur simultaneously in order to obtain a higher total stress condition and then apply those loadings cyclically to simulate the design useful life of the component. This test will detect potential design/process flaws in the laboratory, thereby permitting corrective actions to be implemented and verified in an expeditious, cost-effective manner.

30.14 Windshield Endurance Test Facility

Special test facilities are required to conduct windshield endurance tests. As a minimum, the facility should have provisions to simulate the following load and environment conditions:

1. Aerodynamic pressure differential (positive or negative).
2. Airframe wracking.
3. External ambient temperatures from -65°F to $+125^{\circ}\text{F}$.
4. Cockpit air temperatures from $+40^{\circ}\text{F}$ to $+125^{\circ}\text{F}$.
5. Sufficient airflow to permit operation of windshield heating systems at full power.
6. Cold shock representative of rapid altitude descent or sudden entry into clouds containing supercooled moisture.

Typical windshield endurance test facilities are illustrated in Figures 30-4 and 30-5. The principal components are:

1. Windshield mounting provisions duplicating the stiffness and heat transfer characteristics of the actual cockpit structure.
2. Blower, motor, and ducts to provide a circulating airflow.
3. Pressure chamber capable of applying a vacuum or pressure to the inside surface of the windshield.
4. Liquid nitrogen system for cooling.
5. Environmental condition: system.
6. Observation ports for periodic inspection of windshields.

7. Mechanical or pneumatic system to apply wracking loads.
8. Electrical power supply for a windshield anti-ice system.
9. Electrical controller to cycle electrical power to the windshield.
10. Automatic safety shutoff controls.
11. Control system for sequencing load applications.
12. Instrumentation to measure and record duct airflows, pressures, and temperatures.

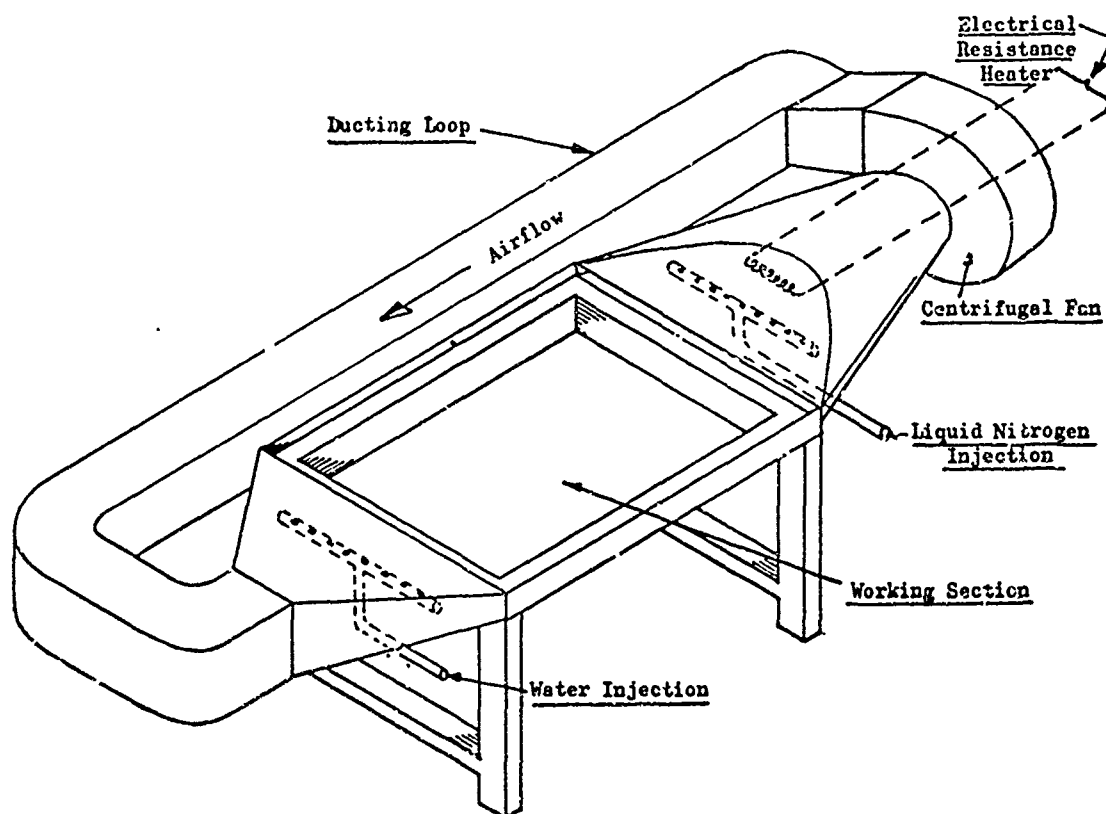


Figure 30-4. Typical Windshield Endurance Test Facility.

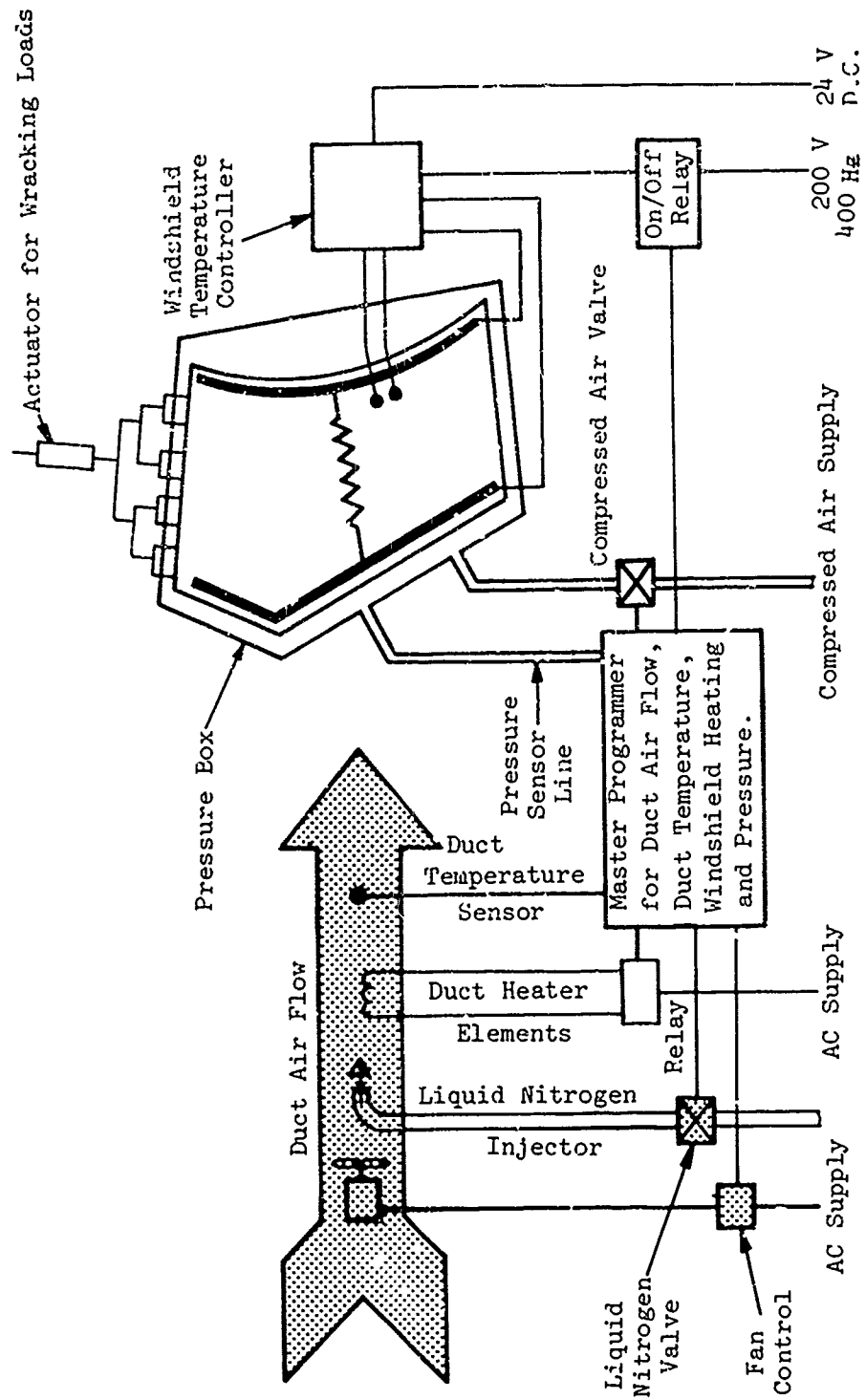


Figure 30-5. Typical Schematic Diagram of an Endurance Test Facility.

30.15 Endurance Test Load Spectrum

The objective of helicopter windshield endurance tests is to simulate service conditions on an accelerated basis. This is accomplished by condensing the time between applications of load, thus enabling several years of service to be demonstrated in a relatively short period.

In order to develop a test plan for an endurance test, a usage spectrum must be prepared and analyzed. The usage spectrum will include the significant loading conditions that affect service life. Loading combinations, magnitude, and frequency of occurrence, as well as environmental conditions, must be selected to realistically simulate operating conditions.

For test purposes, environmental conditions may be generalized, as will be described subsequently. However, the structural environment cannot be generalized and must be based on specific aircraft characteristics and mission profiles.

30.16 Environmental Conditions

The environment can degrade structural integrity through long- or short-term effects. Long-term degradation can be caused by humidity and ultraviolet radiation. If it is desired to study the long-term effects these elements will have on structural integrity, specimens should be conditioned prior to testing by prolonged exposure to such elements. The effect of flaws such as scratches and abrasions can also be evaluated by preconditioning test specimens.

The effects of temperature on the structural integrity of helicopter windshields can be considered to be short term and can be simulated during the endurance tests. Critical temperature conditions result from exposure to natural weather and the operation of windshield heating systems.

30.17 Temperature Environment from Natural Climatic Conditions

Helicopter operations are essentially conducted at low altitudes where local geographic weather conditions prevail. This means that undue conservatism would result if extreme MIL-SPEC environments (-65°F or +160°F) were assumed to occur continuously and simultaneously with all structural loading conditions. The cold and hot climate temperature distributions shown in Tables 30-2 and 30-3 are recommended.

High temperature (160°F) exposure is omitted from the hot-climate tabulation because it is not representative of flight conditions, but only ground or storage conditions. It should be noted that a severe cold climate is usually more detrimental to a transparency than a severe hot climate.

TABLE 30-2. COLD CLIMATE TEMPERATURE DISTRIBUTION

Temperature (°F)	Percent of Time
+40	45
+25	25
-25	25
-65	5

TABLE 30-3. HOT CLIMATE TEMPERATURE DISTRIBUTION

Temperature (°F)	Percent of Time
100	95
125	5

30.18 Anti-Ice Heating

Windshield anti-ice heating systems should be operated in conjunction with structural loading and adverse environment conditions to determine the effects of the interaction on reliability.

For endurance test purposes, one complete power cycle per flight may be assumed. A power cycle begins with the windshield stabilized at ambient temperatures. The windshield is energized until operational temperature is reached, as indicated by the windshield temperature sensing element. Power is then switched off, and the windshield is allowed to cool to its original ambient temperature to complete the power cycle.

30.19 Cold Shock

Cold shock occurs when an aircraft passes from dry air into clouds containing cool moisture. The impinging moisture causes a sudden cooling of the windshield, which induces thermal stresses. The thermal stresses are most severe when the temperature gradient between the windshield surface and impinging moisture is greatest. Therefore, the conditions should be imposed when the windshield is at its maximum operating temperature.

Note that the presence of liquid water is a necessity for this type of cold shock, which means that the condition is applicable only for ambient temperatures above 25°F.

The cold shock can be applied in a test by lowering the external ambient air temperature, to simulate the windshield heat demand by an amount equivalent to the sensible and evaporative heat losses that would occur from the impinging moisture. (Refer to Chapter 8 for procedures used to calculate heat loads and temperature gradients.) This method is used in lieu of introducing moisture into the airstream since it is exceedingly difficult to maintain a continuous airflow containing supercooled moisture without forming ice in the test chamber.

30.20 Structural Loading Conditions

The structural loads applied in endurance tests should be based on an analysis of ground-air-ground (GAG) cycles. The GAG cycle will contain the maximum loads that are encountered in a single flight. Since the absolute maximum load conditions do not occur every flight, a load spectrum must also be generated to show the frequency of occurrence of critical conditions.

30.21 Load Spectra

To illustrate how a load spectrum is developed, consider the case of aerodynamic pressure loading. The aerodynamic pressure load is predominantly a function of airspeed and aircraft attitude (pitch and yaw). For cargo or utility helicopters the basic mission calls for level flight at cruise speed between origin and destination, and the aerodynamic pressure GAG cycle for this condition would simply appear as shown in Figure 30-6. However, since a certain percentage of missions will be flown at airspeeds faster or slower than cruise speed, additional GAG cycles for such conditions must also be developed.

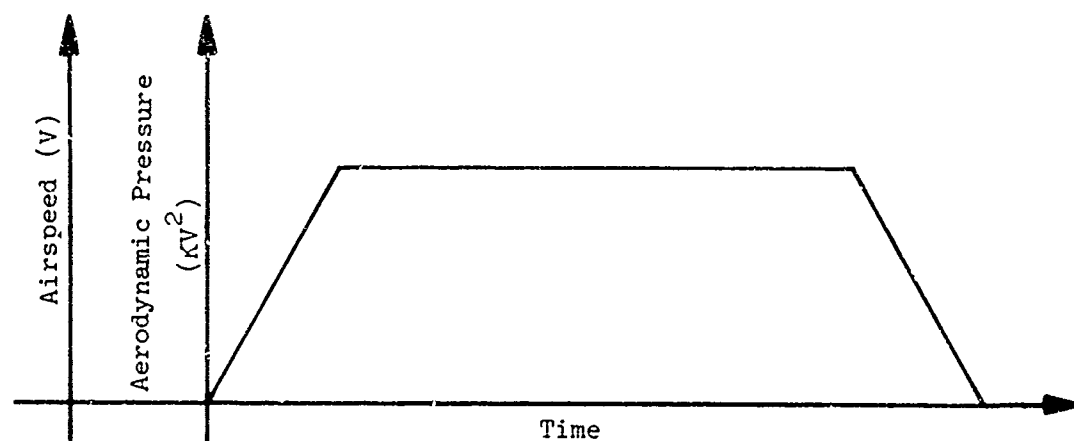


Figure 30-5. Aerodynamic Pressure Ground-Air-Ground Cycle.

The number of different GAG cycles developed is based on considerations such as the variation in load intensities and the frequency of their occurrence. For the hypothetical utility helicopter example, a spectrum showing the percentage of missions during which a given airspeed is reached might take the form shown in Figure 30-7. The schedule of load applications for endurance tests would follow the same distribution and appear as shown in Figure 30-8. If the average helicopter mission is 15 minutes, each group of 10 load applications is equivalent to 2.5 hours of flight time.

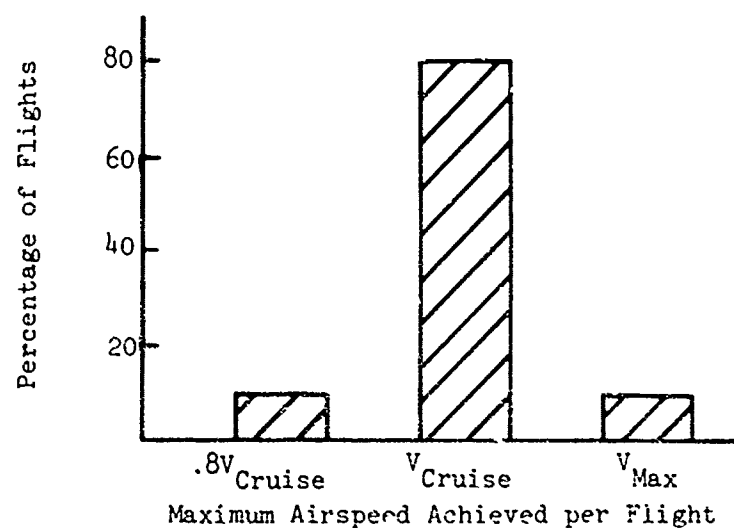


Figure 30-7. Hypothetical Distribution of Maximum Airspeed Versus Percentage of Flights.

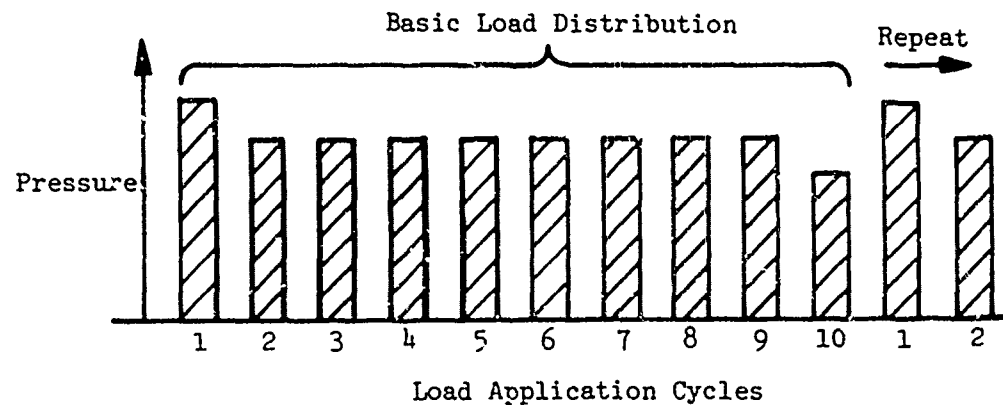


Figure 30-8. Schedule of Loading for Endurance Tests.

Thus, for a test representative of 1000 hours of flight time in a hot climate, the load application schedule is coupled with the warm climate temperature data from Table 30-3, which yields the spectrum of test cycles shown in Table 30-4.

TABLE 30-4. ENDURANCE TEST SCHEDULE (EXAMPLE)

Warm Climate (Airspeed Distribution from Figure 30-7)

No. of Load Applications	Velocity (mph)	Aerodynamic Pressure (psi)	Temperature (°F)
380	180	.75	100
95% 3040	160	.59	100
380	128	.38	100
20	180	.75	125
5% 160	160	.59	125
20	128	.38	125

Total = 4000

Notes: $v_{\text{cruise}} = 160 \text{ mph}$

1000 hours = 4000 flights

$v_{\text{max}} = 180 \text{ mph}$

Similarly, Table 30-5, shows a representative test schedule for a cold climate.

TABLE 30-5. ENDURANCE TEST SCHEDULE (EXAMPLE)

Cold Climate (Airspeed Distribution from Figure 30-7)

No. of Loads Applications	Velocity (mph)	Aerodynamic Pressure (psi)	Temperature (°F)	Cold Shock
180	180	.75	+40	yes
45% 1440	160	.59	+40	yes
180	128	.38	+40	yes
100	180	.75	+25	yes
25% 800	160	.59	+25	yes
100	128	.38	+25	yes
100	180	.75	-25	no
25% 800	160	.59	-25	no
100	128	.38	-25	no
20	180	.75	-65	no
5% 160	160	.59	-65	no
20	128	.38	-65	no

Total = 4000

Notes: v_{cruise} = 160 mph 1000 hours = 4000 flights
 v_{Max} = 180 mph

Endurance tests representative of both hot and cold climates are recommended since Army helicopters are expected to be operational worldwide regardless of climate.

30.21.1 Multiple Peak Loads

Multiple peak loads can occur during a GAG cycle. This condition occurs with Scout or Attack helicopters where the mission might include periods of loiter (hover or low speed) intermixed with periods of dash (high airspeed). The GAG cycle might then appear as shown in Figure 30-9. In addition, severe pitching and rolling may also be encountered during evasive actions or attacks. These changes in attitude affect aerodynamic pressure coefficients and therefore must also be considered in the load spectrum.

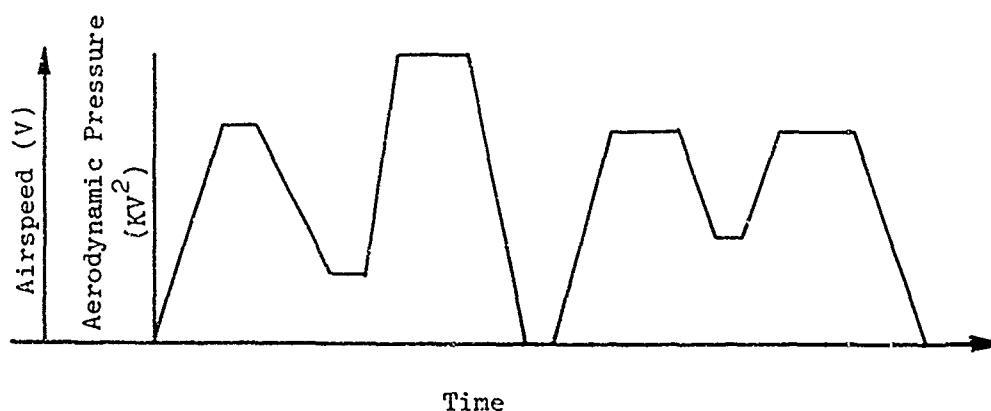


Figure 30-9. Aerodynamic Pressure During Ground-Air-Ground Cycle with Multiple Load Peaks per Flight.

30.22 Installation Preload

Maximum limits of installation preload should be simulated during endurance tests. Installation preload occurs when there is a mismatch between surface contours of the windshield and the airframe as a result of manufacturing tolerances or uneven fastener torque. This condition remains constant after the component has been installed.

Installation preload can be simulated by placing shims between the windshield and structure, or by the controlled overtightening of selected fasteners.

30.23 Miscellaneous Condition

If other flight or ground loading conditions, aside from aerodynamic pressure, are also known from stress analyses or instrumented tests to affect windshield integrity, their effects should be coupled in the load spectrum, as applicable. For example, vertical acceleration in some cases can produce racking loads that are additive to pressure loads. Thus, to consider this effect, the load spectrum might be modified as shown in Figure 30-10.

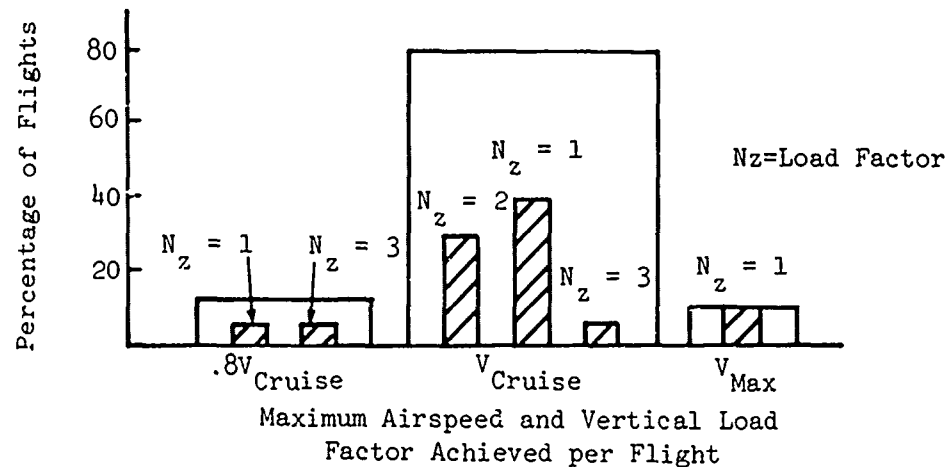


Figure 30-10. Hypothetical Distribution of Airspeed Coupled with Load Factor.

30.24 Systems Integration Tests

Certain transparency parameters are most effectively demonstrated during systems integration tests. These parameters, together with comments on typical tests, are listed in Table 30-6.

TABLE 30-6. TRANSPARENCY SYSTEMS INTEGRATION TESTS

Parameter	Comment
Anti-Ice	Demonstrated by flight-test in known icing conditions. Spray rigs or specially equipped tanker aircraft are used to create artificial icing conditions to facilitate testing (See Figure 30-11).
Rain Removal	Windshield wipers are demonstrated by flight test during light and heavy rain conditions. Jet blast rain removal systems require additional tests to demonstrate that there is sufficient airflow to clear the windshields under various engine power settings and flight conditions without overheating.
Cockpit Reflections	Internal cockpit reflections are evaluated as part of cockpit lighting mockups and flight tests.

TABLE 30-6. TRANSPARENCY SYSTEMS INTEGRATION TESTS (cont.)

Parameter	Comment
Vibration	Flight test should verify that there are no resonances to cause objects to dither when viewed through the transparencies.
Jettison of Escape Panels	Demonstrate operation during ground test.
Lightning Strikes	Need for protection is determined with scale-model tests.
Static Electricity	Rarely a problem with helicopters - Verify by flight test.
Radar Reflectivity	Evaluate radar signatures by scale-model tests.

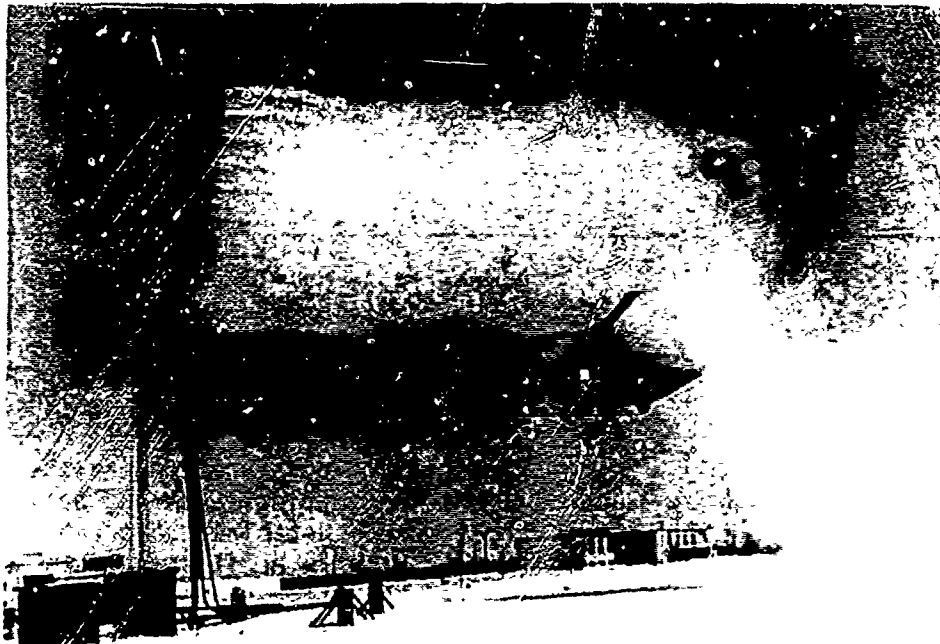


Figure 30-11. Icing Spray Rig Test.

Reference

1. Kay, B. F., Sikorsky Aircraft Division, "Design, Test and Acceptance Criteria for Helicopter Transparent Enclosures," USARTL-TR-78-26 (AVRADCOM) Applied Technology Laboratory, U. S. Army Research and Technology Laboratory, Fort Eustis, Va.

Bibliography

James, H. C., et al, Goodyear Aerospace Corp., "Design, Test and Acceptance Criteria for Army Helicopter Transparent Enclosures," USAAMRDL-TR-73-19, U. S. Army Air Mobility Research and Development Laboratories, Fort Eustis, Va., May 1973.

Cook, L. M., et al, PPG Industries, Inc., "Development of Design, Test and Acceptance Criteria for Army Helicopter Transparent Enclosures," USAAMRDL-TR-73-65, U. S. Army Air Mobility Research and Development Laboratory, Fort Eustis, Va., Sept. 1973.

Morozowicz, R., Northrop Corp., "Report on Progress of ASTM F7.08," AFML-TR-76-54, Air Force Materials Laboratory, Wright-Patterson Air Force Base, Ohio, April 1976.

Stephansin, T. R., "Helicopter Windshield Design Improvement Program," ER-72-006A, Sierracin Corp., Sylmar Calif., June 1972.

Kay, B. F., Sikorsky Aircraft Division, Stratford, Conn., "Detail Specification for Heated Windshield (Outboard-Curved)," SES-701076, Jan. 1973.

Holloway, R. U., "Survey of Optical Test Procedures for Aircraft Transparencies," LR-23771, Lockheed California Co., Sept. 1970, AD887715.

Roberts, W. G., Triplex Safety Glass Co., Ltd., "The Development of Windscreen Reliability, Proceedings of the Symposium on Optical Transparencies," London, June 1971, Society of British Aerospace Companies, Ltd., England

Campbell, L.G., Marshall, J. W., Sierracin Corp., "Windshield Flight Environment Simulator," Aircraft Air Conditioning Forum, Culver City, California Apr. 1974.

"Facilities Description," Desert Sunshine Exposure Tests, Inc., Phoenix, Arizona, Dec. 1974.

Fisher, K. J., "Preproduction Test Procedure, Performance Test Under Simulated Environmental Conditions for the Sikorsky CH-53 Composite Windshield", ETP-70-2B, Sierracin Corp., Sylmar, California, Sept. 1971.

Allen, D. C., "Performance Tests Under Simulated Environmental Conditions for Sikorsky YUH-60A Pilot and Copilot Windshield," QTR-1110-01, PPG Industries Huntsville, Ala., Oct. 1975.

Casimiro, T., "H-34 De-Icing System Test," SER-58217, Sikorsky Aircraft Division, Stratford, Conn., Mar. 1959.

Casimiro, T., "Functional Cold Weather Test of the HSS-2 Helicopter," Sikorsky Aircraft Division, Stratford, Conn., Oct. 1961.

Dowcen, J. C., et al, "Category II Icing Test of the HH-53C Helicopter," FTC-TR-71-26, Air Force Flight Test Center, Wright Patterson Air Force Base, Ohio, June 1971.

Plumer, J. R., "Development of Scratch and Spall-Resistant Windshields," AMMRC-TR-74-19, Army Materials and Mechanics Research Center, Watertown, Mass., Aug. 1974.

Wintermute, G. E., et al, Goodyear Aerospace Corp., "Environmental Resistance of Coated and Laminated Polycarbonate Transparencies," AFML-TR-76-54, Air Force Material Laboratory, Wright-Patterson Air Force Base, Ohio, Apr. 1976.

McGarvey, J. H., Kay, B. F., Sikorsky Aircraft Division, "Design and Development of Helicopter Transparent Enclosures," AFML-TR-76-54, Air Force Materials Laboratory, Wright Patterson Air Force Base, Ohio, Apr. 1976.

Olson, J. B., Sierracin Corp. Sylmar, California, "At Last a Meaningful Windshield Life Test," AFML-TR-76-54, Air Force Material Laboratory Wright-Patterson Air Force Base, Ohio, Apr. 1976.

Lawrence, J. H., Douglas Aircraft Co., "Windshield Technology Demonstrator Program," AFFDL-TR-77-1, Air Force Flight Dynamics Laboratory, Wright-Patterson Air Force Base, Ohio, Sept. 1977.

Beck, R. I., et al, Douglas Aircraft Co., "Standardized Windshield Fabrication Specification," AFFDL-TR-77-97, Air Force Flight Dynamics Laboratory, Wright-Patterson Air Force Base, Ohio, Oct. 1977.

31.0 ACCEPTANCE TESTS

Once a design has been qualified and put into production, acceptance tests are required to monitor manufacturing and processing variables that could affect performance. The following is a list of parameters that could vary between otherwise identical products:

- Dimensions
- Workmanship
- Optical Quality
- Electrical Resistance
- Dielectric Strength
- Temperature Uniformity
- Bond Strength
- Glass Temper

31.1 Acceptance Tests for Raw Materials

Raw materials, with the exception of interlayers are normally procured to military specifications. The acceptance tests that are necessary for conformity with the various material specifications are presented in Table 31-1.

31.2 Test Methods

A number of standard test methods appropriate for evaluating transparency acceptance parameters are available from several sources and are referred to in Volume B, the "General Specification for Helicopter Transparent Enclosures." In addition, the American Society for Testing and Materials (ASTM) is currently developing and standardizing test methods for Aerospace Transparent Enclosure Materials. This effort is being conducted by ASTM Subcommittee F7.08 and includes test methods for the following parameters.

- Distortion
- Interlayer Stability
- Bond Integrity
- Toughness

- Thermal Distortion
- Chemical Moisture
- Scratch
- Electrostatics

31.3 Finished Product Acceptance Tests

The General Specification for Helicopter Transparent Enclosures, Volume B of this Handbook, includes recommended acceptance criteria for finished products. This criteria is based on established practices and historical data. Historical data should also be used by manufacturers to establish sampling and frequency schedules for quality control of specific components.

TABLE 31-1. ACCEPTANCE TESTS FOR RAW MATERIALS

Test	Material									
	MIL-P-5425 Cast Acrylic	MIL-P-8184 Modified Acrylic	MIL-P-8257 Polyester	MIL-P-25690 Stretched Acrylic	MIL-P-83310 Polycarbonate	MIL-P-25374 Laminated Acrylic	MIL-G-25871 Laminated Glass	MIL-G-25667 Soda-Lime Glass	MIL-A-46108 Bullet Resistant Glass	MIL-A-46108 Glass-Plastic Transparent Armor
Minor Optical Defects	X	X	X	X		X	X	X	X	
Angular Deviation	X	X	X	X	X	X	X	X	X	X
Light Transmission	X		X	X	X	X	X		X	X
Haze	X		X	X	X	X	X			
Thermal Stability	X								X	
Tensile Strength			X					X		
Elongation			X							
Internal Strain		X	X							
Deformation Temperature	X		X	X	X					
Dimensions	X	X	X	X		X	X	X	X	
Thermal Deflection		X				X				
Impact Strength						X	X	X		
Distortion				X		X			X	X
Crack Propagation				X						
Weathering										
Shear Strength						X				
Peel Strength						X				
Fracture Resistance						X	X			
Thermal Shock						X	X			X
Flatness									X	
Humidity										X

Bibliography

James, H. C., et al, Goodyear Aerospace Corp., "Design, Test and Acceptance Criteria for Army Helicopter Transparent Enclosures," USAAMRDL-TR-73-19, U. S. Army Air Mobility Research and Development Laboratory, Fort Eustis, Va., May 1973.

Cook, L. M., et al, PPG Industries, Inc., "Development of Design, Test and Acceptance Criteria for Army Helicopter Transparent Enclosures," USAAMRDL-TR-73-65, U. S. Army Air Mobility Research and Development Laboratory, Fort Eustis, Va., Sept. 1973.

Morozowicz, R., Northrop Corp., "Report on Progress of ASTM F7.08," AFML-TR-76-54, Air Force Materials Laboratory, Wright-Patterson Air Force Base, Ohio, 1976.

Stephancin, T. R., "Helicopter Windshield Design Improvement Program," ER-72-006A, Sierracin Corp., Sylmar, California, June 1972.

Wirtanen, L. W., "Quality Plan, Acceptance Testing and Inspection Procedures Sikorsky CH-53 Glass/Plastic Composite Windshield," QR-70-156, Sierracin Corp., Sylmar California, June 1971.

Perez, R., "Windshield, Anti-Ice, Bench Test Procedure for," ATP-22431, Sikorsky Aircraft Division, Stratford, Conn., Oct. 1971.

"Windshield, Anti-Ice, Acceptance Test Procedure, H-3," ATP-22408, Sikorsky Aircraft Division Stratford, Conn.

Kay, B. F., "Detail Specification for Heated Windshield (outboard-curved) SES-701076, Sikorsky Aircraft Division, Stratford, Conn., Jan. 1973.

Nienow, L. G., "Acceptance Test Procedure YUH-60A," ATP-1110-01, PPG Industries, Huntsville, Ala., Aug. 1973.

Kay, B. F., Sikorsky Aircraft Division, "Design, Test and Acceptance Criteria for Helicopter Transparent Enclosures," USARTL-TR-78-26, Applied Technology Laboratory U. S. Army Research and Technology Laboratories, Fort Eustis, Va.

Beck, R. I., Douglas Aircraft Co., "Standardized Windshield Fabrication Specification," AFFDL-TR-77-97, Air Force Flight Dynamics Laboratory, Wright-Patterson Air Force Base, Ohio, Oct. 1977.

32.0 MAINTENANCE INSPECTION AND FAULT IDENTIFICATION

In order to provide clear vision for helicopter flight crews, proper maintenance of transparent enclosures is mandatory.

Once damaged, most transparencies cannot be repaired but require replacement. Replacement is expensive in terms of component cost, maintenance man-hours and aircraft downtime. Therefore, proper training and observance of appropriate handbook instructions for preventive maintenance will help to extend transparency service life and decrease operating expenses.

32.1 Storage

A first step toward reduced maintenance costs is the adherence to proper storage procedures.

Transparencies should be stored in cool, dry places. Protective coverings of paper, cardboard, canvas, cloth, or plastic flim should be used to prevent accumulation of surface dust. Panels should be stored on their edges.

If horizontal storage is necessary, larger panels should be placed on the bottom to eliminate overhang and subsequent creep. Care should be taken to keep foreign objects from between the panels and to avoid sliding one panel over another.

32.2 Cleaning

The cleaning of transparencies is the most common maintenance action and is accomplished daily or before every flight. Glass is more tolerant than plastic to cleaning procedures but care should still be exercised to avoid scratching. Daily maintenance consists simply of washing with clear water and drying with soft cloths. When this becomes ineffective, the following procedures may be implemented.

If the transparency has a wiper, this is first cleaned of any accumulated dust and dirt. The transparency is then wiped using a recommended cleaning compound on a clean, soft cloth of cotton flannel, outing flannel, flannelette, or a similar material. If extremely dirty, a transparency may be washed with a mild, nonabrasive detergent mixed with water. Bug specks, caked dirt, and mud should be loosened carefully by hand. The transparency should then be rinsed thoroughly and dried with a clean, damp chamois. Grease, oil and paint may be removed by using specific solvents recommended by the transparency manufacturer.

When the transparency has been washed, a thin coat of wax may be applied. After drying for several minutes, the surface can be polished to a high luster.

32.3 Precautions

Maintenance personnel should observe caution to avoid scratching transparencies with hard or sharp objects, such as rings, watches, belt buckles, and pens. Ice scrapers should never be employed to clear plastic transparencies. Handling should be limited to the transparency edges or retainers.

Care should be exercised when polishing plastic surfaces to avoid local frictional overheating as this can result in optical distortion.

Do not use gasoline, alcohol, kerosene, benzene, xylene, ketones including acetone, carbon tetrachloride fire extinguishing or de-icing fluids, lacquer thinners, aromatic hydrocarbons, ethers, glass-cleaning compounds, or other solvents on plastic transparencies unless specifically recommended by the manufacturer. These may tend to soften or craze the surface. Harmful chemicals should be listed in the appropriate manuals, or placarded in the airframe.

32.4 Inspection

Regular inspection of transparencies is necessary to determine when preventive maintenance or replacement is needed. The appropriate maintenance manuals should establish acceptance criteria, e.g. allowable depth of scratches or area of delamination and critical areas in which vision must not be impaired.

In addition to the inspection of the transparency surface, a careful examination of seals should be made. A laminated windshield assembly will have two seals around its edge when installed. An integral seal, installed by the windshield manufacturer, prevents moisture and contaminants from affecting the bonds or the heating film between transparency layers. An aerodynamic seal, which may be either pre-formed or cast-in-place, weather-seals the aircrew station from the airstream and provides the aircraft with a smooth external surface. The deterioration of either seal can lead to windshield damage requiring replacement.

32.5 Malfunctions

The categorization of failure modes facilitates problem definition and analysis. Results can then be fed back to the appropriate personnel who can implement corrective actions. The following are the most frequently encountered malfunctions.

- a. **Crazing** - Crazing is a defect common to plastic materials and consists of numerous shallow, fissure-like cracks in the surface of a transparency. Crazing may be caused by either the stress loading to which a panel is subjected or exposure to solvents. Severe crazing can ultimately lead to panel cracking and structural malfunctions. Crazing also increases panel haze and thus degrades vision. An example of light crazing is shown in Figure 32-1.

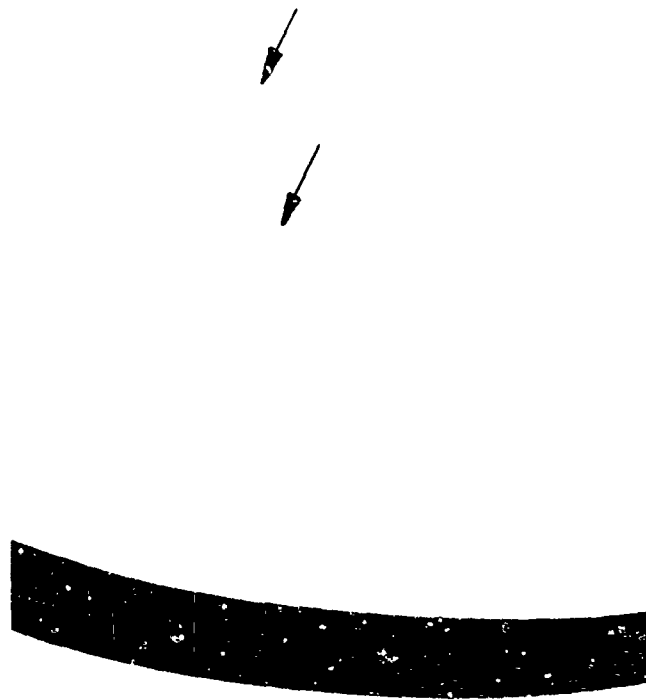


Figure 32-1. Crazed Acrylic Window.

- b. Cracking - Due to its brittle characteristics, glass is more susceptible to cracking than plastic materials. Figure 32-2 shows a laminated-glass windshield that was cracked on installation by the excessive preload used to force the windshield to match airframe contour. Plastic materials are also subject to cracking, and Figure 32-3 shows a crack which originated at a point of delamination in a laminated polyester/acrylic windshield. Transparencies are also frequently cracked by impact from foreign objects.



Figure 32-2. Laminated Glass Windshield Cracks From Excessive Installation Preload.



Figure 32-3. Crack Originating at Delamination.

- c. Scratching - Scratching is the most common cause of windshield replacement. There are countless sources of windshield scratches. To name a few: Windshield wipers, improper cleaning procedures, contact with hard objects, and even, built-in hazards. For example, the sliding window pictured in Figure 32-4 was scratched on contact with its own sill.

Plastic materials are so susceptible to abrasion that just a few strokes of dry windshield wiper can cause scratches severe enough to warrant replacement. The severe loss of vision due to windshield wiper abrasion can be seen in Figure 32-5.

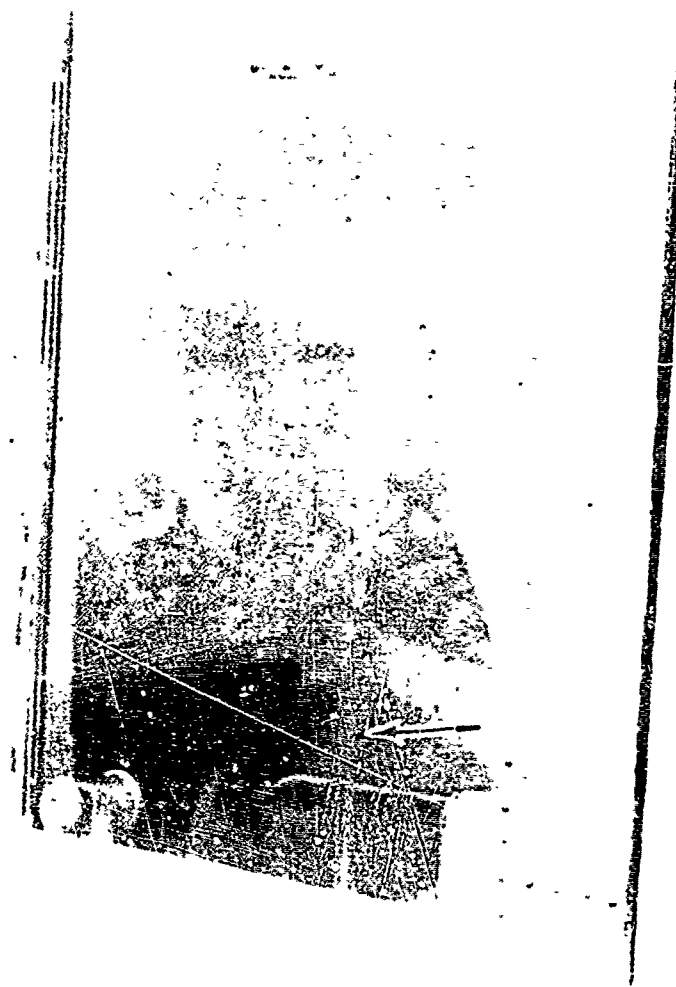


Figure 32-4. Sliding Window Scratched by Sill.

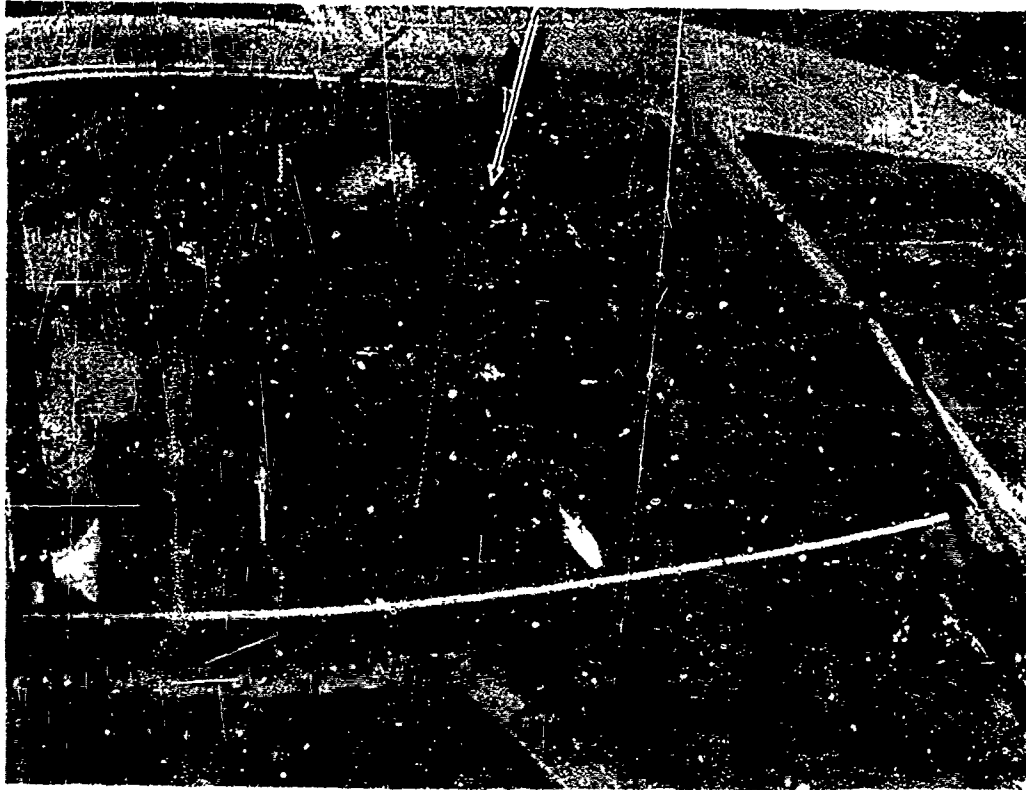


Figure 32-5. Windshield Scratched by Wiper.

- d. Delamination - Delamination is the breakdown of adhesion between the interlayer and substrate of a laminated assembly. This can occur as a result of moisture penetration or entrapment, overheating, or mechanical forces which exceed the interlayer bond strength. A delamination will produce a translucent internal surface that obscures vision. An example of this can be seen in Figure 32-6



Figure 32-6. Delamination.

- e. Bubbling - Bubbling consists of gaseous inclusions in the interlayer of a laminated windshield. These are produced by moisture or by overheating. A severe case of bubbling is shown in Figure 32-7.



Figure 32-7. Bubbles Formed in Interlayer of Laminated Windshield.

- f. Burnout - Burnout is an electrical failure of a heated windshield. It will be evidenced by charring and outgassing at the bus bar or heating film, sometimes with an adjacent area of delamination or cracking as shown in Figure 32-8. Burnout may be caused by arcing and the short-circuiting of the heating film current due to seal failure and moisture penetration.



Figure 32-8. Charred Heating Film Adjacent to Crack.

- g. Open circuits - Open circuits due to wiring breaks in heated windshields can result in partial or complete loss of power, or loss of signal from the temperature sensor. Such failures necessitate replacement if the damaged joint or component is inaccessible.
- h. Softening - Plastic transparencies may soften and flow, causing local distortion, from exposure to excessive heat, such as might occur from a jet blast rain removal system. Frictional heat from mechanical buffing and polishing can also soften plastics.
- i. Solvent Attack - Exposure of plastic materials to certain solvents can cause loss of clarity due to crazing or local clouding.
- j. Discoloration or Hazing - The long term effects of aging and solar radiation include discoloration and loss of optical clarity for certain materials.
- k. Impact Damage - Foreign object impact can produce a wide range of damage from local chipping to complete loss of structural integrity.

32.6 Repairs

Successful repairs can be made to lightly scratched plastic transparencies. Minor scratches may be polished out of a surface using a buffer and a scratch removing compound. Very little pressure is used in this procedure and the buffer is moved frequently to avoid local frictional overheating.

Deeper scratches are sanded out using a rubber (or equivalent flexible type) block and specific abrasives. The surface is kept wet and washed thoroughly between operations. The damage must be blended out over a wide area as sanding of a confined area will lead to unacceptable levels of distortion. Even so, a reworked surface cannot equal the quality of the original finish and some distortion will always result.

Transparency seals may be successfully repaired. A faulty integral seal on a laminated assembly should be removed and replaced according to the manufacturer's instructions. A faulty aerodynamic/weather seal may be repaired locally by removal and replacement of the sealant material.

Installation fasteners should not be retorqued to cure a rainwater leak. Overtorquing can cause the windshield to pick up airframe loads, warp and preload the panel, or force the interlayer to flow or distort, and it could initiate or aggravate delamination.

Cracks in monolithic plastic transparencies can sometimes be repaired by stop-drilling and cementing on a patch. As can be seen in Figure 32-9, such a patch is translucent but not transparent.

Other methods of repair, such as transparent plugs and fabric overlay patches, are described in Reference 1. These techniques are used for expediency and will degrade vision, and they should not be used in areas where vision is critical.

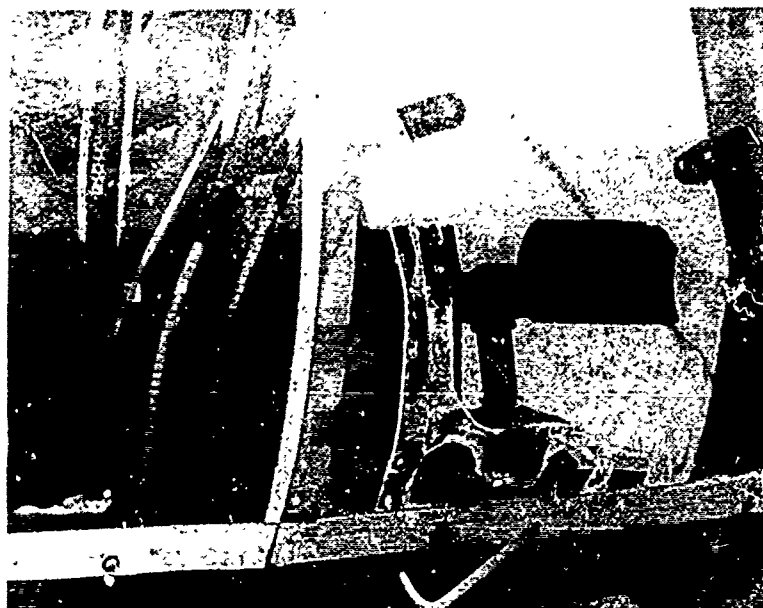


Figure 32-9. Repaired Cracks.

References

1. "Fabrication, Maintenance and Repair of Transparent Plastics", (USAF) T.O. 1-1a-12, (Navy) NAVAIR 01-1A-12, U.S. Government Printing Office, Washington, D. C., October 1969.

Bibliography

Armstrong, K. B., and Shore, D. W., "VC-10 - Investigation into Failures of Cabin Inner Windows and Cracking of Inner and Outer Windows, " EE-R-71-3 (A), British Airways, May 1971.

Clark, M. W., Krauss, W. K., and Cicotti, J. M., American Power Jet Company, "Identification and Analysis of Army Helicopter Reliability and Maintainability Problems and Deficiencies, Volume I, Introduction, Analysis, and Summary", USAAMRDL TR-72-11A, U. S. Army Air Mobility Research and Development Laboratory, Fort Eustis, Virginia, April 1972.

Clark, M. W., Krauss, W. K., and Cicotti, J. M., American Power Jet Company "Identification and Analysis of Army Helicopter Reliability and Maintainability Problems and Deficiencies, Volume II, Utility, Attack, and Training Helicopters (UH-1, AH-1, TH-1)," USAAMRDL TR 72-11B, U. S. Army Air Mobility Research and Development Laboratory, Fort Eustis, Va., April 1972.

Clark, M. W., Krauss, W. K., and Cicotti, J. M., American Power Jet Company "Identification and Analysis of Army Helicopter Reliability and Maintainability Problems and Deficiencies, Volume III, Cargo Helicopters (CH-47, CH-54)," USAAMRDL TR 72-11C, U. S. Army Air Mobility Research and Development Laboratory, Fort Eustis, Virginia, April 1972.

Clark, M. W., Krauss, W. K., and Cicotti, J. M., American Power Jet Company "Identification and Analysis of Army Helicopter Reliability and Maintainability Problems and Deficiencies, Volume IV, Light Observation Helicopters (OH-6, OH-58)," USAAMRDL TR 72-11D, U. S. Army Air Mobility Research and Development Laboratory, Fort Eustis, Virginia April 1972.

Kay, B. F., Sikorsky Aircraft Division, Design Test and Acceptance Criteria for Helicopter Transparent Enclosures" USARTL-TR-78-26, Applied Technology Laboratory, U. S. Army Research and Technology Laboratories, Fort Eustis, Va.

Tryk, H. W., "Maintenance of Sierracote Plastic Windshields". SB-62-18, Sierracin Corp., Sylmar, California, May 1964

"Aircraft and Defense Products Manual," Libbey-Owens-Ford Co., June 1969.

"Plexiglas Sheet-Maintenance", Rohm and Haas, Philadelphia, Pa., September 1974.

MIL-P-6997B(ASG), "Plastic; Working and Installation of Transparent Sheet, General Specification for", February 1958.

Couture, R., "Cleaning of Aircraft Transparent Surfaces", SS9576, Sikorsky Aircraft Division, United Technologies Corp., Stratford, Conn., March 1966.

Flone, N., "Scratch Removal, Plastic Transparent Surfaces, Procedure for" SS9577, Sikorsky Aircraft Division, United Technologies Corp., Stratford Conn., January 1967.

Lawrence, J. H., Douglas Aircraft Co., "Windshield Technology Demonstrator Program," AFFDL-TR-77-1, Air Force Flight Dynamics Laboratory, Wright-Patterson Air Force Base, Ohio, Sept. 1977.

33.0 LIFE CYCLE COSTS

The initial procurement cost of a transparency represents only a small part of its total life-cycle cost. Some of the other major cost elements are shown in the simplified life-cycle model presented in Figure 33-1. This model does not include indirect costs for transporting and stocking spare parts, routine maintenance, operational readiness, and logistics paperwork. Dollar value is assumed to be constant because it is impossible to predict the effects of economic inflation with any accuracy. As a result, life-cycle cost estimates derived from this model will be somewhat optimistic.

A grasp of the relative contributions from each element in the model can be obtained by studying the example problem shown in Figure 33-2. In the example, lifetime maintenance costs are high because the mean time between removal-replacement (MTBRR) is low in comparison to the airframe service life.

$$\text{MTBRR} = \frac{\text{Total fleet time} \times \text{number of components per aircraft}}{\text{Number of components replaced}}$$

Historical data showing a range of MTBRR's for typical transparencies are presented in Table 33-1.

TABLE 33-1. MEAN TIME BETWEEN REMOVAL-REPLACEMENT (MTBRR) FOR HELICOPTER TRANSPARENCIES

Transparency	Range of MTBRR (hours)
Heated Windshields	600 - 6000
Plastic Windshields	900 - 6000
Other Cockpit Windows	1700 - 32,000
Cabin Windows	2000 - 23,000
Fixed-Wing Transport Airplane Windshields	2000 - 7000

Data from Ref. 1, 2

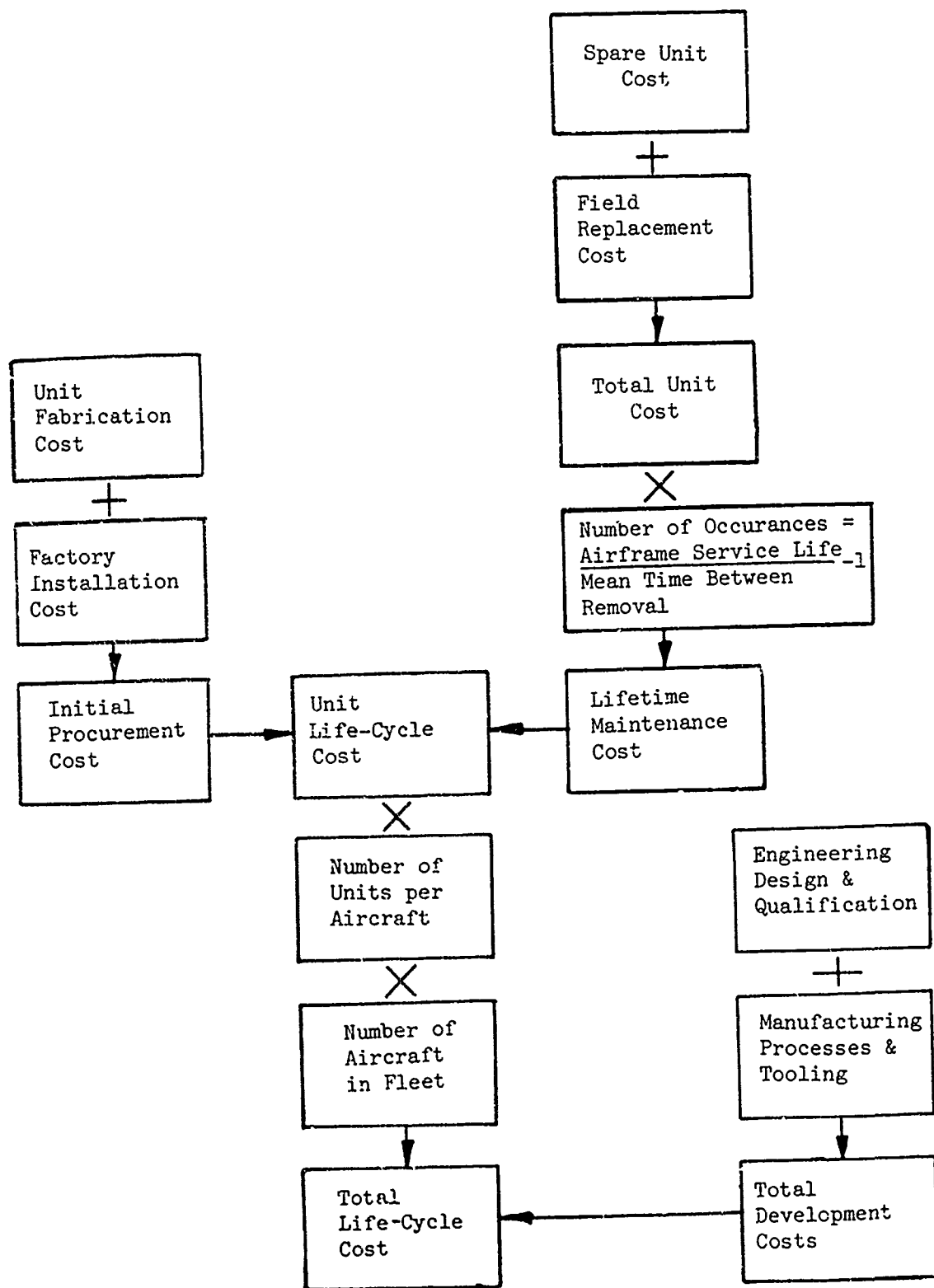


Figure 33-1. Simplified Life-Cycle Cost Model.

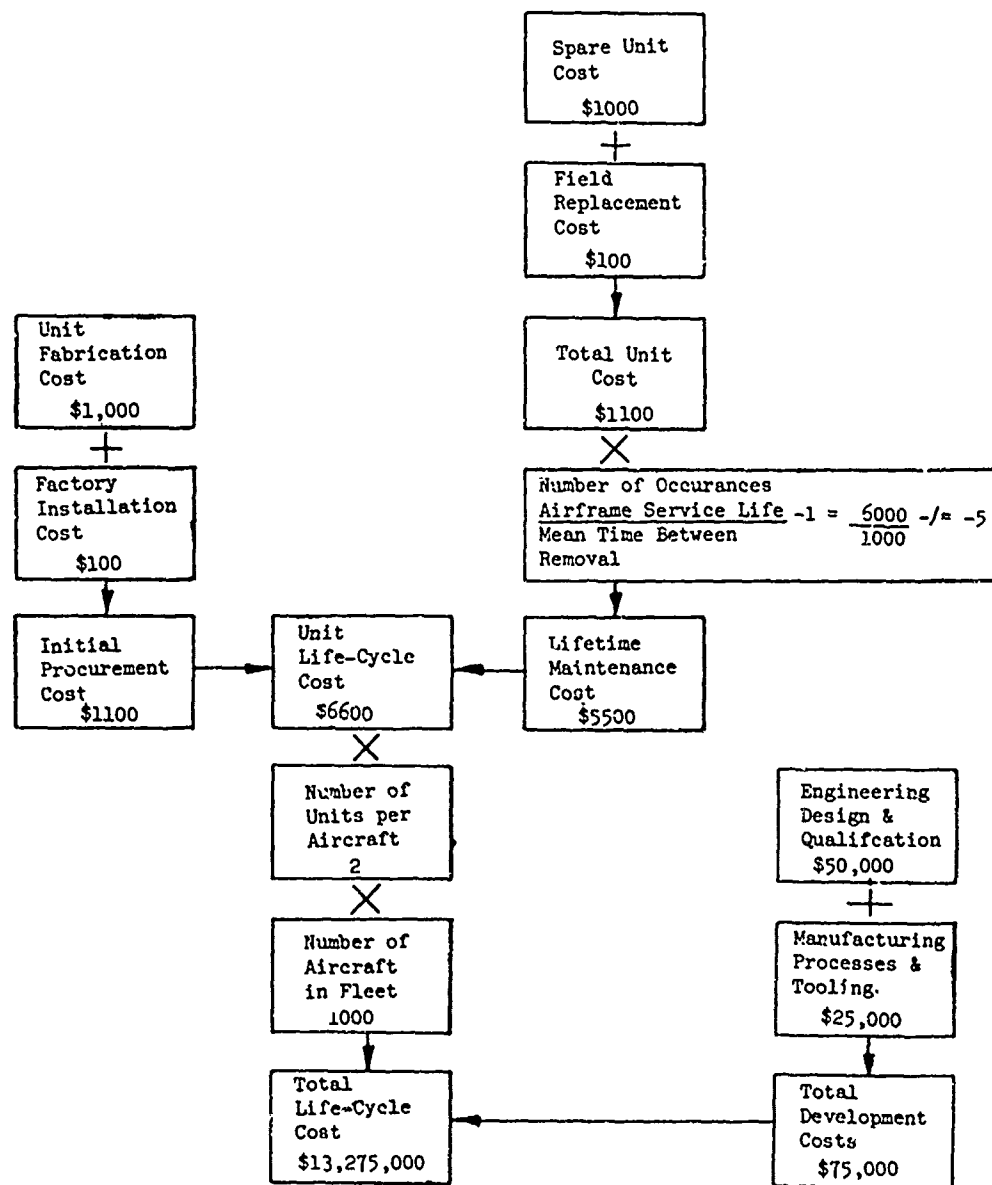


Figure 33-2. Hypothetical Life-Cycle Costs for Heated Windshields.

The wide spreads between MTBRR's in the table indicate that for certain designs or applications there is room for substantial improvement in component reliability. A comprehensive engineering development program can often substantially improve reliability without any, or very little, effect on recurring cost. This approach is highly leveraged in favor of minimizing life cycle costs. In the example problem, for instance, if an additional \$100,000 spent on development was to improve the MTBRR to 2,000 hours, the total life cycle saving would be 5.4 million dollars.

Improving MTBRR's and providing interchangeability also favorably influences aircraft operational readiness to yield additional economic benefits. As an illustration, consider the following example:

Given: Annual utilization = 500 hours

MTBRR = 1000 hours

Average time for replacement = 1-1/2 days

Number of windshields per aircraft = 2

Therefore: Number of days out of service per year = 1-1/2

Theoretically this means the helicopter is unavailable 0.5 percent of the time, and productivity will suffer accordingly. Such consequences can be greatly minimized by relatively small expenditures to provide interchangeable panels designed for rapid removal and installation.

References

1. Cook, L.M., et al, PPG Industries, Inc., "Development of Design, Acceptance, and Test Criteria for Army Helicopter Transparent Enclosures", USAAMRDL-TR-73-65, U.S. Army Air Mobility Research and Development Laboratory, Ft. Eustis, Va., Sept. 1973.
2. Olson, J.B., Sierracin Corp., "Design Considerations Affecting Performance of Glass/Plastic Windshields in Airline Service", AFML-TR-73-26, U.S. Air Force Materials Laboratory, Wright-Patterson Air Force Base, Ohio, June, 1973.

Bibliography

Lawrence, J. H., Douglas Aircraft Co., "Windshield Technology Demonstrator Program," AFFDL-TR-77-1, Air Force Flight Dynamics Laboratory, Wright-Patterson Air Force Base, Ohio, Sept. 1977.

APPENDIX A

APPLICABLE SPECIFICATION AND STANDARDS

Specifications and standards applicable to the design of helicopter transparent enclosures are listed below for reference purposes.

Federal Specifications

L-P-391C (1)	Plastic Sheets, Rods, and Tubing, Rigid Multiapplication (Methacrylate, Cast).
L-P-515A	Plastic Sheet and Plastic Rod, Thermosetting, Cast
P-P-560A	Polish, Plastic
DD-G-451C (4)	Glass, Plate, Sheet, Figured (Float, Flat for Glazing, Corrugated, Mirrors and other uses)
P-S-18	Cement

Federal Standards

Federal Test Method Standard No. 175 A - Adhesives: Methods of Testing
Federal Test Methods Standard No. 141a - Paint, Varnish, Lacquer and Related Materials, Method of Inspection.

Military Specifications

MYL-A-8576B (2)	Adhesive; Acrylic Base (for Acrylic Plastic)
MIL-A-46108A	Armor, Transparent, Laminated Glass-Faced Plastic Composite.
MIL-A-25055	Adhesive
MIL-B-5087	Bonding, Electrical and Lightning Protection for Aerospace Systems.
MIL-C-675A (3)	Coating of Glass Optical Elements (Anti-Reflection)
MIL-C-6799F (1)	Coatings, Sprayable, Strippable, Protective, Water Emulsion.
MIL-C-7439D	Coating System, Elastomeric, Rain Erosion Resistant and Rain Erosion Resistant with Antistatic Treatment for Exterior Aircraft and Missile Plastic Parts.
MIL-C-14806A (2)	Coating, Reflection Reducing, for Instrument Cover Glasses and Lighting Wedges.
MIL-C-27315A	Coating Systems, Elastomeric, Thermally Reflective and Rain Erosion Resistant.
MIL-D-16791E (3)	Detergent, General Purpose (Liquid Nonionic)
MIL-E-38453A	Environmental Control. Environmental Protection and Engine Bleed Air Systems, Aircraft and Aircraft Launched Missiles, General Specifications for
MIL-F-7179E (1)	Finishes and coatings, Protection of Aerospace Weapons Systems Structures and Parts, General Specification for
MIL-G-1366E	Glass, Window. Aerial Photographic

Military Specifications (Cont.)

MIL-G-5485C	Glass, Laminated, Flat, Bullet Resistant
MIL-G-25667B (1)	Glass, Monolithic, Aircraft Glazing
MIL-G-25871A (1)	Glass, Laminated, Aircraft Glazing
MIL-I-8500C	Interchangeability and Replaceability of Component Parts for Aerospace Vehicles.
MIL-P-116F	Preservation, Packaging, Methods of
MIL-P-5425C (4)	Plastic, Acrylic Sheet, Heat Resistant
MIL-P-5952 (1)	Plastic Areas, Transparent, Aircraft Optical Inspection of
MIL-P-6997B	Plastic, Working and Installation of Transparent Sheet, General Specification for
MIL-P-7524	Plastic Sheet, Acrylic Laminated Heat Resistant
MIL-P-8184B (1)	Plastic: Acrylic Sheet Modified
MIL-P-8257B (1)	Plastic Sheet, Thermosetting, Transparent
MIL-P-9071A	Plasticizer Content for Transparent Laminated Glazing Materials, Determination of
MIL-P-25374A (1)	Plastic Sheet, Acrylic, Modified Laminated
MIL-P-25690A (3)	Plastic, Sheets and Parts, Modified Acrylic Base, Monolithic, Crack Propagation Resistant
MIL-P-83310	Plastic Sheet Polycarbonate, Transparent
MIL-R-9300B	Resin, Epoxy, Low Pressure, Laminating
MIL-R-25506B	Resin, Silicone, Low Pressure, Laminating (ASG)
MIL-R-81261A	Rain Repellent, Glass Window and Windshield, for In-Flight Application.
MIL-R-83055	Rain Repellent, Dispensing System Aircraft Windshield, General Specification for
MIL-R-83056	Rain Repellent, In-Flight Applied, Aircraft Windshield.
MIL-S-6625A	Spray Equipment. Aircraft Windshield, Anti-Icing
MIL-S-7742B (1)	Screw Threads, Standard Optimum Selected Series, General Specification for.
MIL-S-8802	Sealing Compound, Temperature Resistant, Integral Fuel Tanks and Fuel Cell Cavities, High Adhesion
MIL-S-11030	Sealing Compound, Non-Curing, Polysulfide Base
MIL-T-5842A (1)	Transparent Areas, Anti-Icing, Defrosting and Defogging Systems, General Specification for
MIL-T-81714	Terminal Junction Systems, General Specification for
MIL-V-22272B (1)	Visors, Protective, Helmet
MIL-W-80C	Window, Observation, Acrylic Base, Antielectrostatic, Transparent (for indicating instrument).
MIL-W-6882D	Water Repellant Kits, Window and Windshield, Glass and Plastic
MIL-W-7233A	Windshield Wiper, Electric, Aircraft, General Requirements for
MIL-W-81752(AS)	Windshield Systems, Fixed Wing Aircraft-General Specification for

Military Handbooks

MIL-HDBK-17A	Plastics for Aerospace Vehicles, Part II-Transparent Glazing Materials.
MIL-HDBK-141	Military Standardization Handbook, Optical Design
MIL-HDBK-691A	Military Standardization Handbook, Adhesives
MIL-HDBK-700A	Military Standardization Handbook, Plastics
MIL-HDBK-722	Military Handbook, Glass
MIL-HDBK-725	Military Handbook, Adhesives
AMCP 706-203	Engineering Design Handbook, Helicopters, Part 3

Military Standards

MIL-STD-129F (1)	Marking for Shipment and Storage
MIL-STD-143B (1)	Specifications and Standards, Order of Precedence for the Selection of
MIL-STD-210B	Climatic Extremes for Military Aircraft
MIL-STD-721B (1)	Definitions of Effectiveness Terms for Reliability Maintainability, Human Factors and Safety
MIL-STD-704A	Electric Power, Characteristics and Utilization of
MIL-STD-794D (2)	Parts and Equipment. Procedures for Packaging of
MIL-STD-810C	Environmental Test Methods
MIL-STD-850B	Aircraft Stations Vision Requirements for Military Aircraft
MIL-STD-1241A	Optical Terms and Definitions

Miscellaneous

1-1A-12	Fabrication, Maintenance, and Repair of Transparent Plastics
AR-70-38	Research Development, Test and Evaluations of Material for Extreme Climatic Conditions
AS-580A	Pilot Visibility from the Flight Deck Design Objectives Commercial Transport Aircraft.

APPENDIX B

HELICOPTER TRANSPARENCY CONFIGURATIONS

Information pertaining to existing production helicopter transparent enclosures is useful for comparative and reference purposes. Accordingly, configuration descriptions showing gauges and materials for ten different helicopter models are presented in Figures B-1 through B-10.

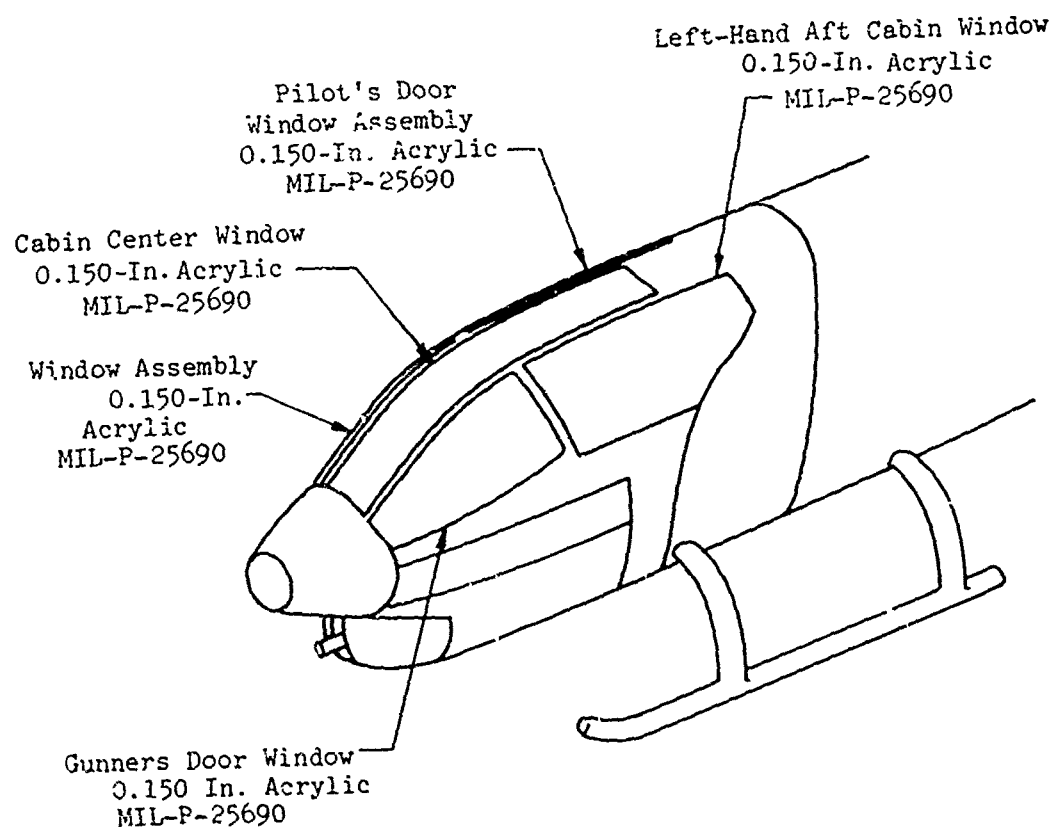


Figure B-1. AH-1 Transparencies.

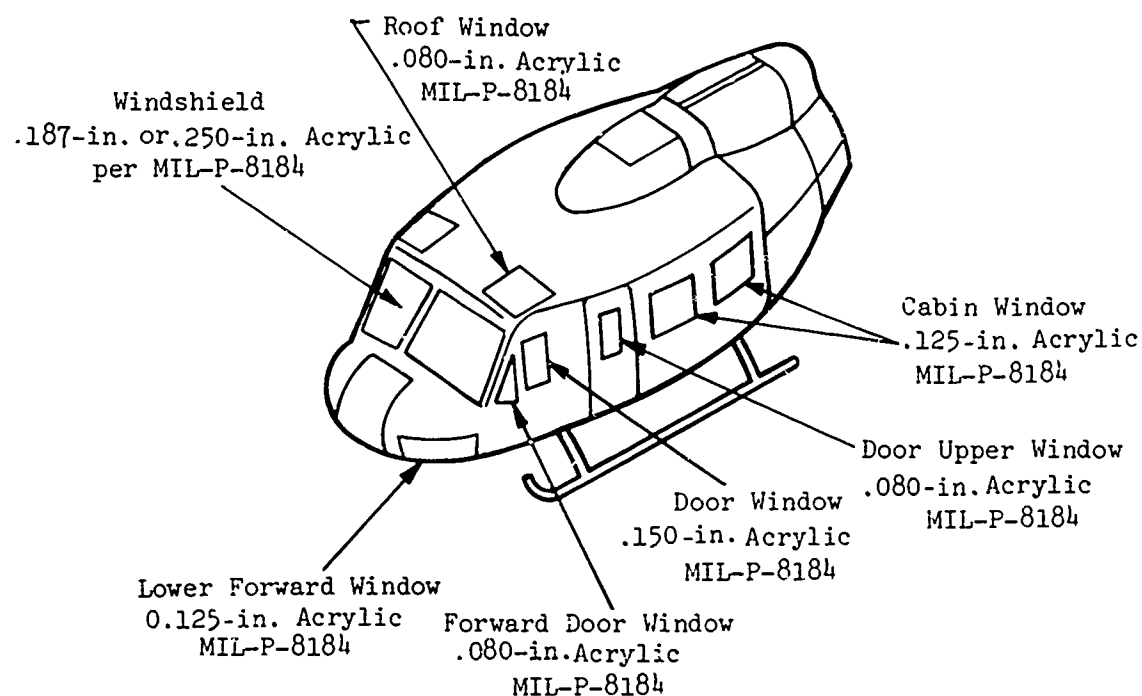


Figure B-2. UH-1 Transparencies.

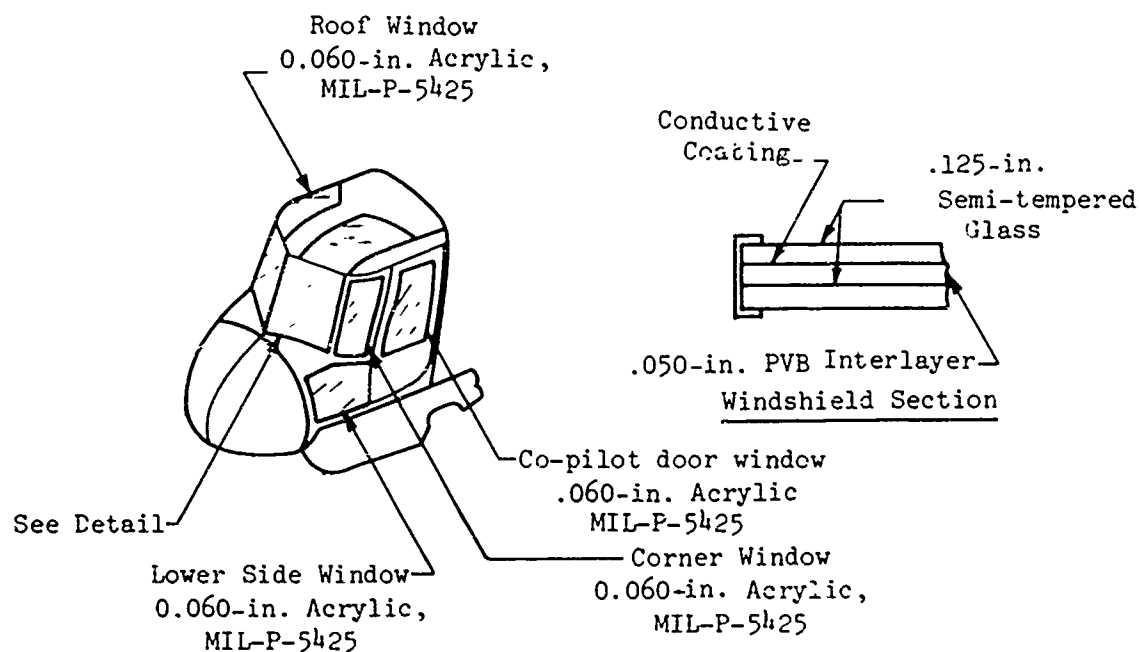


Figure B-3. H-2 Transparencies.

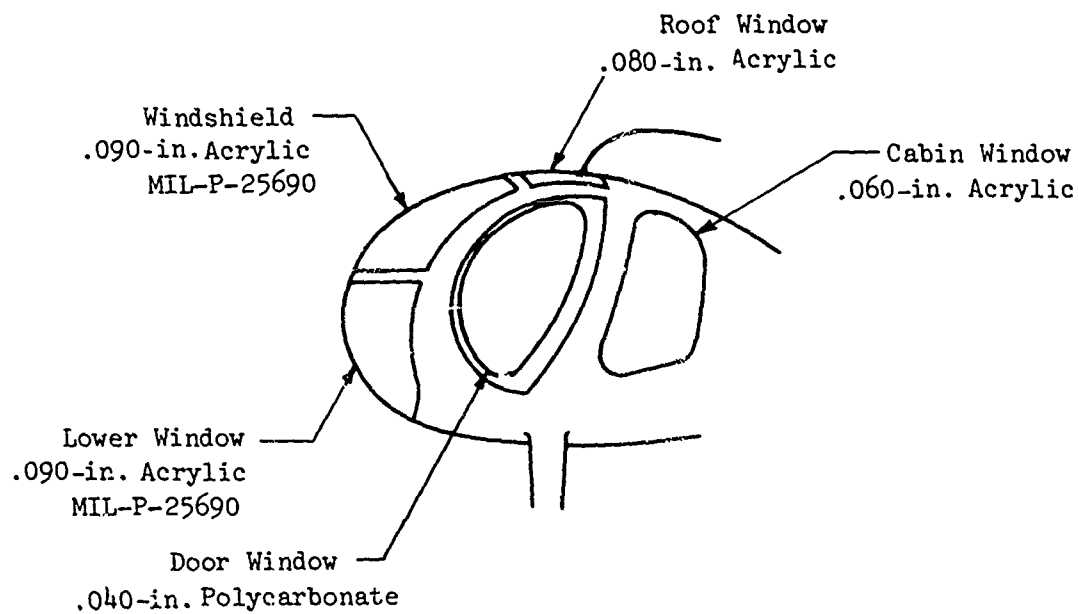


Figure B-4. OH-6 Transparencies.

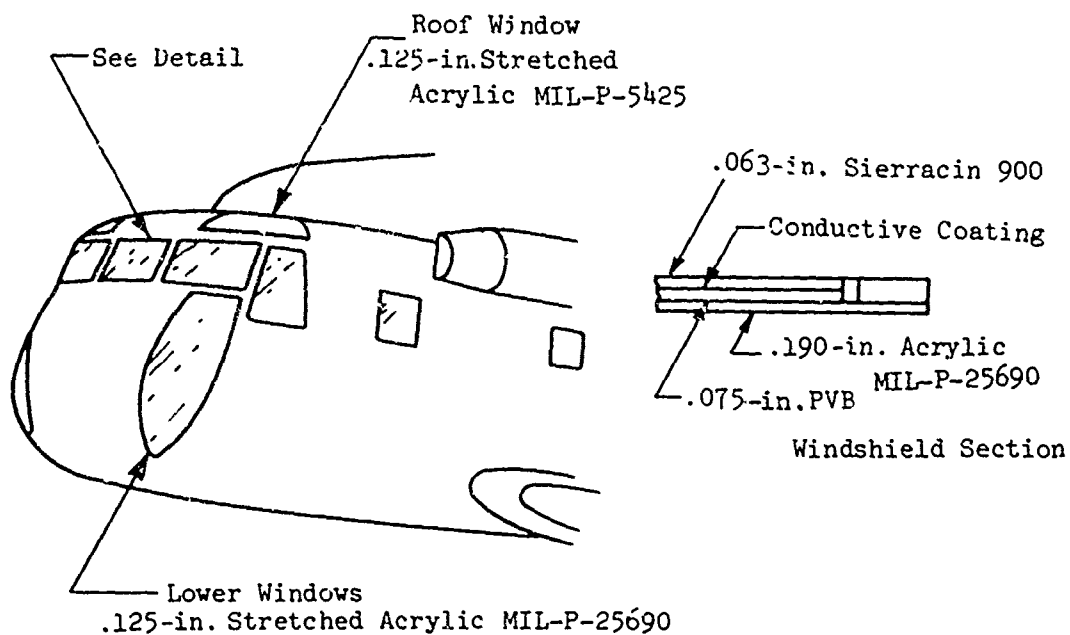


Figure B-5. CH-53 Transparencies.

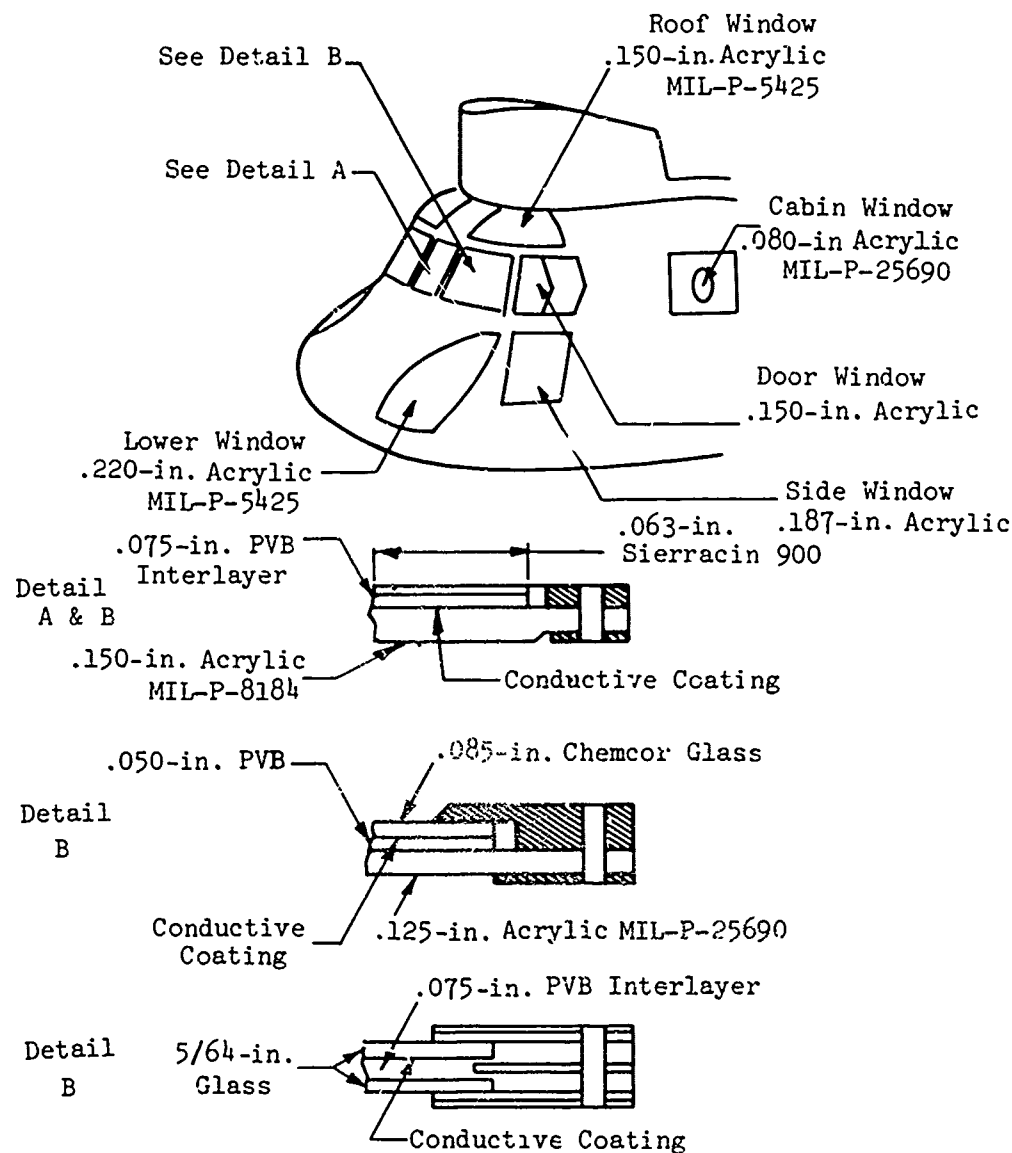


Figure B-6. CH-47 Transparencies.

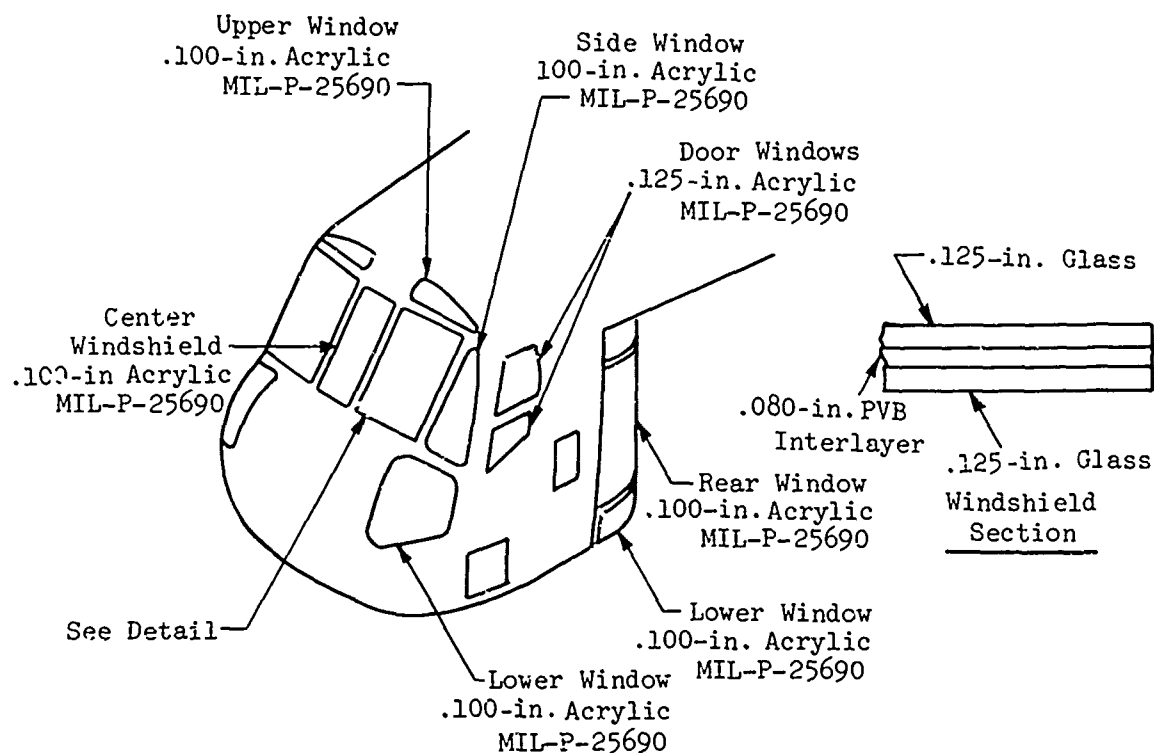


Figure B-7. CH-54 Transparencies.

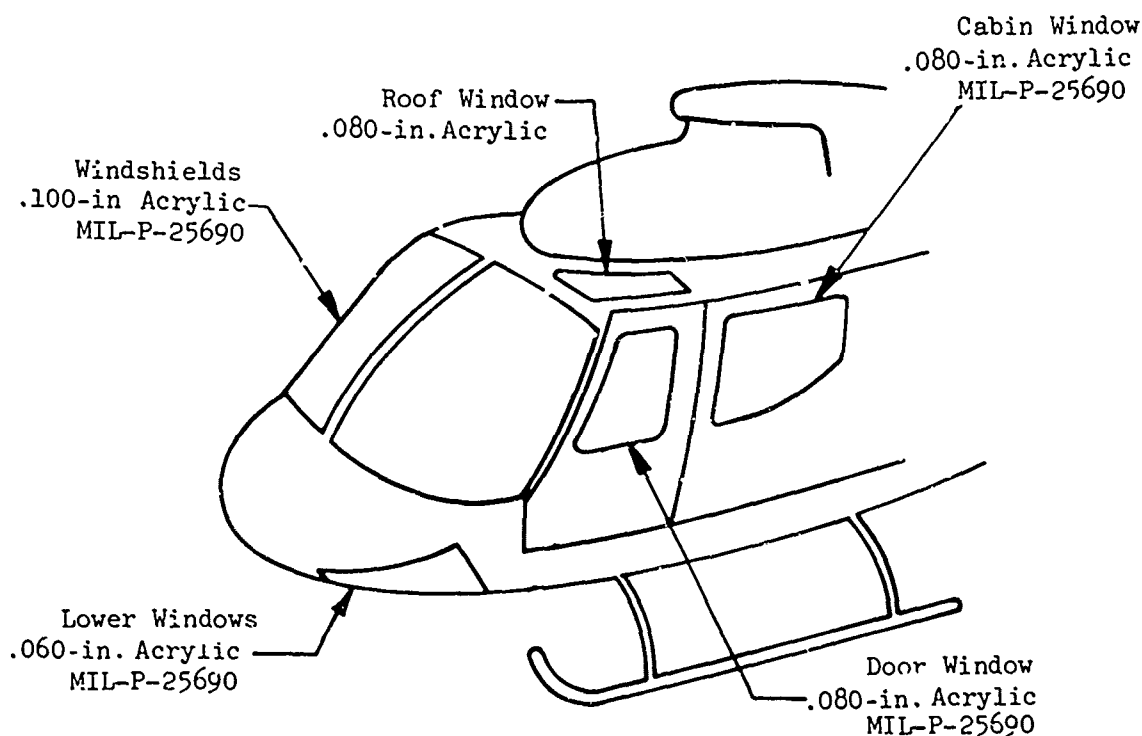
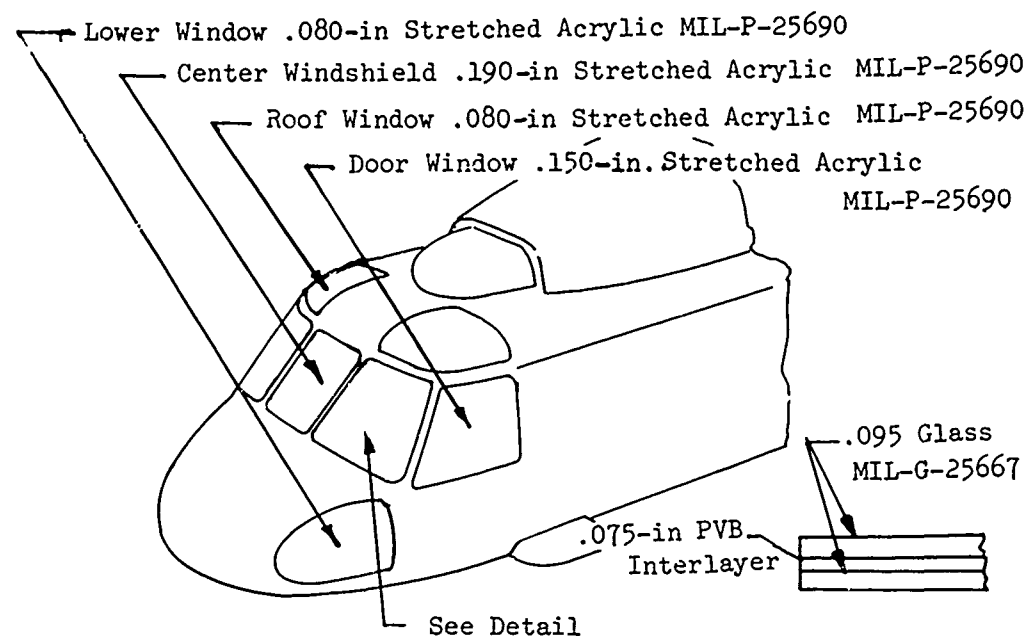


Figure B-8. OH-58 Transparencies.



Windshield Section

Figure B-9. UH-60 Transparencies.

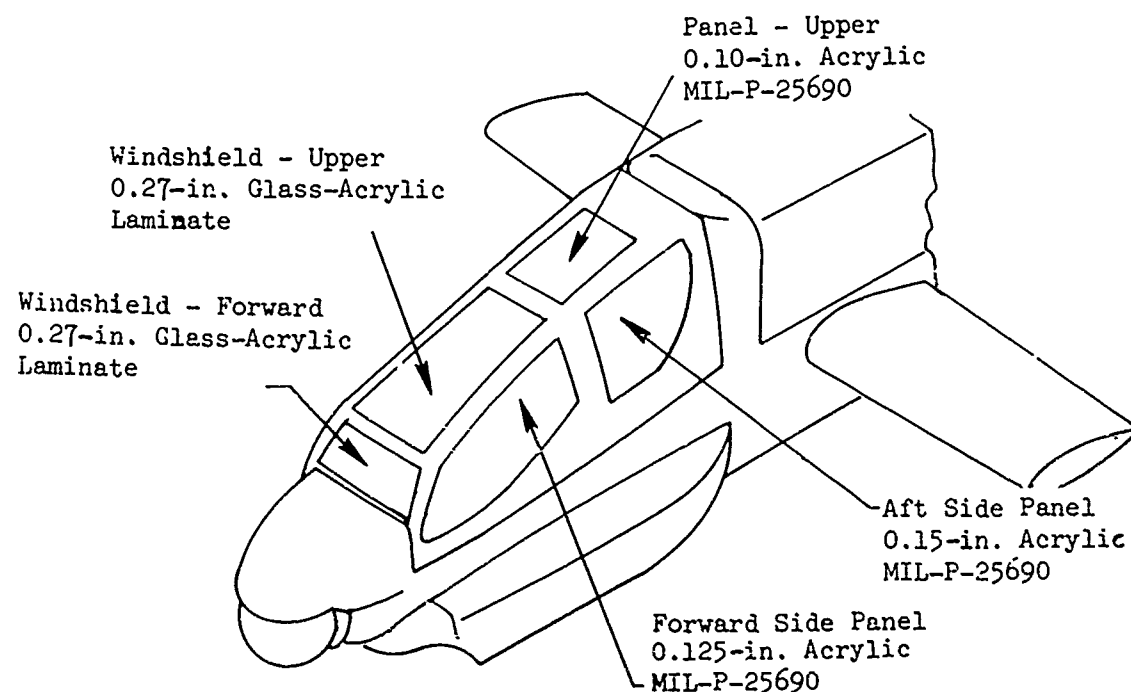


Figure B-10. YAH-64 Transparencies.

References

1. James, H.C., et al, Goodyear Aerospace Corp., "Design, Test, and Acceptance Criteria for Army Helicopter Transparent Enclosures, USAAMRDL-TR-73-19, U.S. Army Air Mobility Research and Development Laboratory, Fort Eustis, Va., May 1973, AD 767242.
2. Bok, L.M., et al, PPG Industries, Inc., "Development of Design, Test, and Acceptance Criteria for Army Helicopter Transparent Enclosures," USAAMRDL-TR-73-65, U.S. Army Air Mobility Research and Development Laboratory, Fort Eustis, Va., Sept. 1973, AD 772936.

GLOSSARY

The following is a list of definitions for terms used in this handbook and commonly associated with transparent enclosures:

Absorption - The amount of light that is neither reflected nor transmitted but is retained within the object.

Achromatic - Lacking in hue and saturation. Achromatic colors vary only in brightness, from black to white.

Acrylic Plastic - (Also known as an acrylate or a methacrylate base) Thermoplastic material produced by a complex chemical reaction of the monomeric derivatives of acrylic acid; supplied in forms of cast sheets, rods, bars, tubes, crystals and powder, transparent, opaque or a variety of colors.

Acuity, Visual - The ability of the eye to perceive form and detail in a plane perpendicular to the line of sight.

Adherend - An object bonded or to be bonded to another object by an adhesive. (See also Substrate).

Adhesion - The state in which two surfaces are held together by interfacial forces consisting of chemical or mechanical forces, or both.

Adhesive - A substance capable of holding materials together by adhesion.

Ambient - Encompassing on all sides.

Analysis - The generation, examination, and reduction of software data.

Angle of Incidence - The angle at which a line or ray strikes a surface, measured from a normal to the surface at the point of incidence.

Angular (optical) Deviation - The change in direction of a ray of light caused by incidence with a reflector or refractor. It is the angle between the direction of the incident ray and the direction of the same ray on emergence.

Annealing - A controlled heating and cooling process used to reduce internal stresses caused by previous forming or machining processes performed on glass or plastic sheet materials.

Ashing - The process of removing scratches or other surface defects from a plastic by the mild abrasive action of a pumice paste or similar material applied to the plastic surface with a rotating cloth wheel. This process, sometimes used instead of sanding, leaves a cloudy surface which may be brought to a high polish by buffing.

Azimuth - The bearing in the horizontal plane, usually expressed as an angle, and in air navigation measured clockwise from true north, grid north, or magnetic north, from $0\frac{1}{4}$ to $360\frac{1}{4}$.

Binocular Field - The field of vision of the two eyes acting conjointly.

Birefringent - A double refracting property of a transparent material which splits light rays into regions of variable intensity.

Blister - A local elevation of the surface of an adherend (somewhat resembling the shape of a blister on the human skin).

Blowins - Oil stains caused by penetration of oily substance along the edge of a laminate.

Bond - (verb) To attach materials together by adhesives; (noun) The attachment at an interface between an adhesive and an adherend. (See also Joint).

Bond Strength - The unit load (applied in tension, compression, flexure, peel, impact, cleavage, or shear) required to break an adhesive-bonded assembly, with failure occurring either within the adhesive, or at the adhesive-adherent interface.

Brightness - 1. Attribute of visual sensation determined by intensity of light radiation reaching the eye. Sometimes called lightness, tint, or value. Refers to variations along the achromatic scale of black to white.
2. Photometric measure of light emission per unit area of a luminous body or of a translucent or reflective surface, i.e., candlepower per unit area.

Bubbling - Gaseous inclusions appearing in a material.

Buffing - The process by which the ashed or sanded surface of a plastic is brought to a high polish. It usually consists of the application to the plastic surface of a polishing or "buffing" compound by means of a rotating cloth wheel.

Bus Bar - An electrical conductor used to transmit power to the edge of a thin conductive film.

Candle - Unit of light intensity. At a distance of one foot, one candle produces an illumination of one foot-candle (equivalent to one lumen per square foot) upon a surface normal to the beam.

Canopy - The transparent portion of an enclosure, exclusive of the windshield.

Cement - A substance capable of holding materials together by cohesion.

Chemical Tempering - An ion exchange process used on glass sheet that hardens the outer surfaces and places the material inside in a tensile mode. Also referred to as chemical strengthening.

CIP - Cast-in-place - A term used to identify a type of interlayer material that is poured between the transparent face sheets of a fabricated part and cured as a component part of the assembly.

Cohesion - The state in which the particles of a single substance (such as an adhesive or adherend) are held together by chemical forces.

Condensation - The formation of liquid water obtained by cooling from the gaseous state.

Conductivity - 1. The reciprocal of resistivity (electrical); 2. The time rate of heat transfer through a unit volume at a unit difference in temperature.

Copolymer - A polymer formed by the reaction of two or more different monomers.

Copolymerization - A polymerization involving two or more different monomers.

Corona - An electrical field emission surrounding a conducting body characterized by ionization of the air and often a visible glow.

Cracking - The complete separation of a structure, usually perpendicular to the surface and caused by a stress imposed on the material.

Crack Propagation Resistance - A measure of the work, other than that resulting in permanent deformation, that is absorbed per unit nominal area of crack extension, determined at the time when a creeping natural crack leaps forward. This property is sometimes called "shatter resistance" or "toughness".

Crazing - A network of fine cracks over the surface of a plastic. Crazing may be initiated by a chemical reaction with a solvent or by an applied loads. Continued load application will enlarge the cracks.

Creep - The dimensional change, with time, of a material under load, following the initial, instantaneous rapid elastic deformation.

CRT - Cathode-ray tube.

Cullets - Small, transparent glass chips that adhere to interior plastic or glass surfaces within a laminate.

Cure - To further change the physical properties of an adhesive (which has set) by chemical reaction, such as condensation, polymerization, or vulcanization.

Cushion - The soft surface layer formed on transparent plastic when immersed in a cement during soak cementing.

Dark Adaptation - The process whereby the eye attains greater sensitivity to light when placed in an illumination lower than that to which it was previously exposed.

Decibel - Log unit expressing relative levels of intensity or power.

Delamination - The breakdown of adhesion between the interlayer and the substrate of a laminated assembly.

Demonstration - The observation that the equipment meets the requirements for which it was intended under the conditions specified.

Deviation - The displacement of a beam of light as a result of its passing through a transparency at an angle; this is a function of the angle of incidence at each thickness of material and the index of refraction of the material.

Diathermanous - Highly transparent to infrared radiation.

Distortion - rapid change in angular deviation over a small area that optically distorts the portion of a true image projected through it.

Dry - To change the physical state of an adhesive by allowing solvent constituents to evaporate or become absorbed, or both.

ECM - 1. "Electronic countermeasure(s)". 2. "Electronic countermeasure mission".

Elastomer - A material which at room temperature can be stretched repeatedly to at least twice its original length, and, upon release of the stress, will immediately return to its approximate original length.

Emissivity - The heat energy radiated per unit of time from a surface to its adjacent environment, which is at a different temperature.

Enclosure - The complete transparent assembly, including canopy, edge attachments, frames, fairings, side beams and seals.

Faying Surface - That surface of an object that is bonded to another object.

Focal Length - A characteristic of a lens or other focusing optical system, being the distance from the lens where parallel light rays will meet after passing through the lens.

g - standard unit of acceleration - The acceleration due to gravity (32 ft/sec²). g is often used to represent the force on the body due to acceleration.

Glass - A transparent amorphous substance ordinarily consisting of a mixture of silicates.

Glint - A bright, reflected flash or beam of light.

Haze - Haze is that percentage of transmitted light that in passing through the specimen deviates from the incident beam by scattering.

Hue - The attribute of color determined primarily by the wavelength of light entering the eye. Spectral hues range from red through orange, yellow, green, and blue to violet.

Illuminance - The flux striking a surface, measured in lumens per unit area.

Illusion - A misinterpretation of certain elements in a given experience, so that the experience does not represent the objective situation.

Inspection - A progressive visual examination.

Intensity - 1. The quantitative attribute or value of a sensory process or unit, correlated in general with the intensity of the physical stimulus.
2. Flux per solid angle from a point source measured in lumens per steradian.

Interlayer - A transparent, flexible material used as an adhesive between plies in a laminated assembly.

Joint - A joint, plane or area of an assembly at which two or more components are held together.

Laminar Shear Strength - The shear strength parallel to the laminar plane of a composite; also, in stretched acrylic, the shear strength parallel to the principal surfaces.

Laminar Tensile Strength - Flatwise tensile strength perpendicular to the laminar planes.

Laminate - A product made by bonding together two or more materials.

Laminated Glass - A sandwich consisting of two or more layers of glass with a plastic interlayer between each pair of layers of glass.

Light - Radiant energy that arouses visual sensations.

Lint - Small bits of fabric embedded in the plastic layers or entrapped in the interlayer of a laminate.

Lumen - Unit of luminous flux: luminous flux emitted per second by a point source of one candle intensity through a solid angle of one steradian.

Luminance - The luminous emittance in one direction from an extended source, measured in lumens per unit area per steradian.

Luminous Emittance - The flux emitted in all directions from each unit area of an extended source, measured in lumens per unit area.

Luminous Flux - Analogous to rate of transfer of energy, it is the total visible energy emitted by a source per unit time.

Luminous Transmittance - The ratio of transmitted to incident light.

Mark Off - Surface imperfections produced by the transfer of mold surface defects to the component during molding and forming operations.

Masking - The process of protecting or covering a highly polished plastic surface.

Modulus of Rupture - The tensile or compressive stress, f , in the extreme fiber of a beam computed by the flexure equation $f = Mc/I$, where M is the bending moment that causes rupture, c is the distance from the neutral axis to the extreme fiber, and I is the moment of inertia of the cross-sectional area about the neutral axis.

Monocular Field - Field of vision with one eye alone.

Monolithic - Uniform throughout, as a transparency consisting of a single homogeneous ply.

Monomer - A relatively simple compound that can react to form a polymer.

MTBF - Mean Time Between Failure.

MTBRR - Mean Time Between Removal or Replacement.

Myopia - Refractive defect of certain eyes in which the focal point of the relaxed lens is in front of the retina.

Notch Sensitivity - The ratio of the unnotched and the notched strengths of a material.

Perception - The awareness of external objects, qualities, or relations, that ensues directly upon sensory processes.

Photometer - An optical device that utilizes equations of brilliance to permit the measurement of a photometric quantity, such as candle power, illumination, or brightness.

Photometry - The measurement of visible radiation on the basis of its effect upon the eye under standard conditions and usually involving an adjustment of two contiguous parts of the visual field, either to identify or to determine a minimal difference.

Photopic - Vision under illumination sufficient to permit the discrimination of colors. Sometimes called daylight vision.

Plastic - A material that contains as an essential ingredient an organic substance of high molecular weight, that is solid in its finished state, and that at some stage in its manufacture or in its processing into finished article, can be shaped by flow.

Plastic Streaks - Surface irregularities in the plastic filler that appear as faint streaks in a laminated product.

Plasticity - A property of a material that permits permanent and continuous deformation without rupture, upon the application of a force that exceeds the yield value of the material.

Plasticizer - A chemical agent incorporated in a material to increase its flexibility, workability, or ductility.

Plexiglas - Trade name for acrylic plastic manufactured by the Rohm & Haas Company.

Polarizer - An optical device or film whose crystalline or molecular orientation tends to allow transmission of light in parallel planes and attenuate all other components of random light.

Polycarbonates - A family of polymers of which only the "bisphenol A" type is considered for structural aircraft glazing.

Polymer - A large molecule of high molecular weight, formed by the reaction of simple molecules (monomers), either by polymerization (addition polymer) or by polycondensation (condensation polymer). (When two or more monomers are involved, the product is called a copolymer). A polymer can usually be represented by a chain of repeating structural units.

Polymerization - A chemical reaction in which the molecules of a monomer link together to form a polymer without releasing any other substance; when two or more monomers are involved, called copolymerization.

Primer - A coating applied to a surface to improve the performance of a bond.

PVB - Polyvinyl Butyral.

Reflectance - The ratio of luminous flux reflected from a surface to the luminous flux striking it.

Reflection - The return of a wave from a surface it encounters to the medium from which it came.

Refraction - A change in the angle of propagation of a wave that occurs when it passes from one transparent medium to another of different density or elasticity.

Refractive Index - A numerical expression indicating the degree to which the path of light or radiant energy is bent in passing from one transparent medium into another.

Resin - Any of a class of solid or semisolid organic products of natural or synthetic origin, that are insoluble in water and generally of high molecular weight, and have no definite melting point and no tendency to crystallize.

Rubber - Any of a number of elastomeric compounds.

Sag Forming - A process used for forming glass sheet by reheating it to a sufficient degree of flexibility for bending over a mold shape.

Saturation (Color) - The extent to which a chromatic color differs from a gray of the same brightness, measured on an arbitrary scale from 0% to 100% (where 0% is gray).

Scratch - A sharp, penetrating surface defect in glass or plastic caused by an abrasive material.

Shatter Resistance - See Crack Propagation Resistance, Toughness.

Set - To convert an adhesive into a fixed or hardened state by chemical action (such as condensation, polymerization, oxidation, vulcanization, gelation, and hydration) or by physical action (such as evaporation of volatile constituents).

Slip Forming - A method of forming three-dimensional parts in which thinning out is reduced by allowing the excess plastic sheeting to slip through the clamping rings while the sheet is being stretched during forming.

Snap-Back Forming - A method of forming based on the tendency of transparent plastic sheets to return to their flat sheet form as long as they are hot.

Solvent - Any liquid that attacks and dissolves certain solids with which it comes in contact.

Solvent Cement - A solvent or mixture of solvents that softens a plastic so that two or more pieces may be bonded.

Star Fracture - A minute radial craze usually originating from an inclusion, bubble or other microscopic defect. Can be detected by a bright pinpoint reflection in oblique light.

Stop Drill - The process of drilling holes at the extremities of cracks to stop the propagation of the crack.

Strain Point (Glass) - That temperature at which the internal stresses in a glass are substantially relieved in about four hours. Also, that temperature at which glass has a viscosity of $10^{14.5}$ poises.

Streamering - An electrical field emission characterized by fork-like glows in the presence of a high potential difference.

Stretching - Stretching a heated plastic sheet either in two perpendicular directions or in all directions in the plane of the sheet to improve the physical properties throughout reorientation of the molecules.

Substrate - A material on which an adhesive or similar substance is spread for any purpose, such as bonding or coating; a broader term than adherend.

Surface Resistivity - A nondimensional number in ohms/square which is used to classify the thickness of metallic coatings with relation to their electrical resistances.

Target Acquisition Signature - The shape and intensity of a returned radar signal which identifies an aircraft.

Temper - A thermal or chemical process by which a glass panel is pre-stressed, placing the surface in compression and core in tension. This results in increased strength.

Test - The verification of equipment performance through the measurement, observation, and recording of results.

Thermal Tempering - A process of heating glass to near its softening point and rapidly cooling it under rigorous control to increase its strength.

Thermoplastic - A plastic that upon being heated, becomes soft and pliable, and that will harden when cooled.

Thermosetting - A plastic that can be heated and molded only once.

Thinner - A volatile liquid added to an adhesive to modify the consistency or other working properties of the adhesive.

"Tin Float" - A process in which the glass is floated on molten tin at a sufficient temperature to heat polish the bottom surface while the upper surface is flame polished.

Toughness - A measure of a material's ability to absorb energy before fracture.

Transmission - The passage of light (energy) through an object or medium.

Transmittance - The ratio of transmitted luminous flux to incident luminous flux (expressed as a percentage).

Transparency - Any structural portion of an aircraft allowing clear vision while protecting the inside of the aircraft from the surrounding environment.

Uniaxial Stretching - A process used in the manufacture of certain films that also makes them birefringent by virtue of the molecular orientation.

Useful Life - The projected service life of a component, after which scheduled replacement is expected to be required.

Vents - Cracks in glass plates that do not so open as to make a rough surface or cause glass to fall away.

Visual Angle - The angle subtended by an object of vision at the nodal point of the eye.

Visual Field - That part of space that can be seen when head and eyes are motionless, or the totality of visual stimuli that act upon the unmoving eye at a given moment.

V₅₀ Protection Ballistic Limit - A measure of the effectiveness of an armor panel: that velocity at which a specified projectile has a 50% change of penetrating the panel.

Warm Forming - A process in which stretched acrylic is formed at less than its deformation temperature in order to prevent relaxation to its original unstretched dimensions and properties.

Waviness - A wave-like unevenness or out-of-plane area in the surface of a plastic.

Wavelength - The distance travelled by an electromagnetic wave during the interval covered by a cycle.

Windscreen - (British) a windshield.

Windshield - A pane or surface area of glass or other transparent material ahead of the cockpit or in front of the pilot's cabin affording protection from the wind and allowing forward vision.